Isolation and Structure Elucidation of Bioactive Secondary Metabolites from Mongolian Medicinal Plants

(Isolierung und Strukturaufklärung von biologisch aktiven Naturstoffen aus mongolischen Arzneipflanzen)

Inaugural-Dissertation
zur
Erlangung des Doktorgrades
der Mathematisch-Naturwissenschaftlichen Fakultät
der Heinrich-Heine-Universität Düsseldorf

Vorgelegt von

Yao Wang

aus Peking, V. R. China

Düsseldorf, 2009

Aus dem Institut für Pharmazeutische Biologie und Biotechnologie
der Heinrich-Heine Universität Düsseldorf

Gedruckt mit der Genehmigung der
Mathematisch-Naturwissenschaftlichen Fakultät der
Heinrich-Heine-Universität Düsseldorf

Referent: Prof. Dr. Peter Proksch
Koreferent: Prof. Dr. Wenhan Lin
Koreferent: PD Dr. Günter Schmahl

Tag der mündlichen Prüfung: 10. 07. 2009

Erklärung

Hiermit erkläre ich ehrenwörtlich, dass ich die vorliegende Dissertation mit dem Titel ″Isolierung und Strukturaufklärung von biologisch aktiven Naturstoffen aus mongolischen Arzneipflanzen″ selbständig angefertigt und keine anderen als die angegebenen Quellen und Hilfsmittel benutzt habe. Ich habe diese Dissertation in gleicher oder ähnlicher Form in keinem anderen Prüfungsverfahren vorgelegt. Außerdem erkläre ich, daß ich bisher noch keine weiteren akademischen Grade erworben oder zu erwerben versucht habe.

Düsseldorf, den 26. 05. 2009

Yao Wang

Acknowledgements

First of all I would like to express my heartfelt gratitude to my supervisor **Prof. Dr. Peter Proksch**, for offering me the remarkable opportunity to join his research group and to be his PhD student. I sincerely appreciate his genial supervision, admirable guidance, and valuable support for my study in Düsseldorf.

I am deeply indebted to **Prof. Dr. Wenhan Lin** for bringing me into the field of natural product chemistry and introducing me to Prof. Proksch. Thank him for his constructive discussions, expert suggestions and continuous encouragement.

I would like to expess my special appreciation to **Dr. RuAngelie Edrada-Ebel** for all the knowledge and techniques she taught me, as well as for her precious help and patient direction. Without her I could not make the study so far.

I am grateful to **Dr. Victor Wray** (Helmholtz Centre for Infection Research), for the distinguished NMR measurements and his crucial opinion on the structure elucitation of the isolated compounds.

I would like to acknowledge **PD Dr. Wim Wätjen** and **Dr. Yvonni Chovolou** (Institut für Toxikologie) for the cytotoxicity tests and successful collaboration, as well as **Mr. Sven Ruhl** and **Mr. Christian Limper** for their determinations of bioassays. My thankfulness is also to **Prof. Dr. Werner E. G. Müller** (University of Mainz) for his cytotoxic assay.

I am thankful to **Dr. Jandirk Sendker** for his generous help on the LC-MS measurement and for sharing his expertise. I would like to thank **Dr. Rainer Ebel** for his valuable comments on my study and the unforgettable free time that I spent with him.

I would like to express my acknowledgment to **Dr. W. Peters** and his coworkers (Institut für Anorganische und Strukturchemie) for the NMR measurements. My thanks are also to **Dr. Helmut Keck** and **Dr. Peter Tommes** (Institut für Anorganische und Strukturchemie) for the EI-MS and

GC-MS determinations.

I am grateful to **PD Dr. Günter Schmahl** for being my co-referee and for estimating my PhD study.

I would like to thank **Prof. Dr. Nanzad Tsevegsuren** (National University of Mongolia) and **Prof. Dr. Yijia Lou** (Zhejing University) for the collection of the plant materials and the nice collaboration.

My thankfulness is to **Prof. Dr. Manfred Braun** (Institut für Organische und Makromolekulare Chemie I) for his important advice and amiable help.

I would like to express my big appreciation to **Mrs. Julia Kjer** for helping me to get through my life in Germany and for her amiable help in translating german documents especially the german parts of this thesis. I am grateful to **Dr. Sofia Ortlepp** for graciously taking care of me and for instructing everything to me since I started my study. Thank them for the pleased conversations and for making me feel like a family in 26.23.U1.25.

I am indebted to **Mrs. Mareike Thiel** and **Mr. Claudia Eckelskemper** for their kindness and for the help of administration.

I am grateful to the technical staff **Mrs. Waltraud Schlag**, **Mrs. Katrin Rohde** for their geniality and for supplying laboratory materials. My thanks are also to **Mrs. Miljanovic Simone**, **Mr. Klaus Dieter Jansen**, **Mrs. Eva Müller** and **Mrs. Goldbach-Gecke Heike** for their help.

I would like to thank **Dr. Annika Putz** for her enjoyable discussion and for the nice lab atmosphere. I am thankful to **Dr. Nadine Weber** for her clemency and for sharing her experience with regard to this study.

I am acknowledged to **Dr Hongbing Liu** and **Dr. Xiang Li** for teaching me the isolation and structure elucidation knowledge and for sharing the pleasure time.

I would like to extend my thankfulness to all of my former colleagues: **Dr. Anke Suckow-Schnitker**, **Mr. Arnulf Diesel**, **Dr. Mirko Bayer**, **Mr. Frank Riebe**, **Dr. Amal Hassan** (Egypt), **Dr. Ine Dewi Indriani Diesel** (Indonesia), **Dr. Triana Hertiani** (Indonesia), **Dr. Abimbola Sowemimo** (Nigeria), **Mrs. Clécia Freitas-Richard** (Brazil), **Dr. Yudi Rusman** (Indonesia), **Mr. Edi Wahyu Sri Mulyono** (Indonesia), **Dr. Duong Ngoc Tu** (Vietnam), **Dr. Mohaned Ashour** (Egypt), **Dr. Claudia Torre**, **Mr. Ehab Moustafa** (Egypt), **Dr. Ashraf Hamed** (Egypt) and **Mr Sabry Younes** (Egypt) for their kind help and the multicultural atmosphere.

I would also like to thank my present colleagues in Düsseldorf: **Dr. Debbab Abdessamad**, **Mr. Elsayed Sherif**, **Mr. Yaming Zhou**, **Mrs. Wera Hauschild, Mr. Bartosz Lipowicz**, **Mr. David Rönsberg**, **Mr. Weaam Ebrahim, Mr. Mustapha El Amrani** and **Mrs. Barbara Kalisch** for their help.

I am grateful to **Dr. Cui Shi** for her affability and the enjoyable moments that we spent together. My acknowledgment is also to **Dr. Ke Ma** and **Mrs Aiying Ma** for their interesting discussion.

I would like to thank **Prof. Dr. Shuming Li** and his group for their kindness, generous help and good working atmosphere. I am thankful to **Prof. Dr. Claus Paßreiter** for his safety instruction.

I am indebted to **Dr. Yoen Ok Roth** and **Dr. Dr. Eckhard H. Roth** for their clemency and nice talks, as well as for offering me to work in Bio-Mar.

My special gratitude is to my parents for their advice and understand, and for always being there to support and encourage me to finish this study.

To all of you, thank you very much!

Zusammenfassung

Naturstoffe, womit Metabolite des Sekundärstoffwechsels gemeint sind, stellen die größte Quelle an chemischer Diversität als Ausgangsprodukte für die Entwicklung neuer Pharmazeutika dar. Traditionell den Hauptanteil in der medizinischen Anwendung tragen Pflanzenextrakte. Dennoch sind bisher nur wenige mongolische Arzneipflanzen, die dem einzigartigen mongolischen Ökosystem entstammen, phytochemisch untersucht.

Das Thema der vorliegenden Arbeit war die Isolierung und Strukturaufkläung der Sekundärmetabolite von Arzneipflanzen und die darauf folgende Untersuchung der pharmakologischen Wirksamkeit. Zur Auftrennung und Aufreinigung der Reinsubstanzen aus den Extrakten kamen unterschiedliche moderne Chromatographiesysteme zur Anwendung. Die Strukturaufklärung erfolgte auf der Basis intensiver ein- und zweidimensionaler NMR und massenspektrometrischer Daten.

Zwei mongolische Arzneipflanzen (*Scorzonera radiata* und *Dianthus versicolor*) sowie eine chinesische Arzneipflanze (*Psoralea corylifolia*) wurden als biologische Quellen für die Bearbeitung im Rahmen dieser Dissertation ausgewählt. Die isolierten Reinsubstanzen aus diesen Pflanzen sind in Tabelle 5.1 zusammengefasst. Einige der Naturstoffe zeigten viel versprechende biologische Aktivitäten und werden für weitere pharmakologische Untersuchungen in Betracht gezogen.

Scorzonera radiata

Die mongolische Arzneipflanze Scorzonera radiata wurde in der Gegend um Ulan Bator in der Mongolei gesammelt. Chromatographische Aufreinigung des Extrakts aus oberirdischen Teilen der Pflanze erbrachte fünf neue Dihydrostilbene, zwei neue Flavonoide, ein neues Chinasäurederivat sowie zwanzig bekannte Naturstoffe, darunter acht Chinasäurederivate, vier Flavonoide, zwei Cumarinderivate, fünf einfache Benzoesäurederivate und ein Monoterpenglykosid. Scorzodihydrostilbenes A–E und die isolierten Chinasäurederivate zeigten im DPPH Assay antioxidative Eigenschaften. Die antioxidativen Aktivitäten der Scorzodihydrostilbene A und E waren stärker als die des bekannten antioxidativen, natürlich vorkommenden Stilbens Resveratrol.

Keine dieser Substanzen zeigte Zytotoxizität gegenüber den Tumorzelllinien H4IIE und L5178Y oder Inhibierung von 24 ausgesuchten Proteinkinasen. Nach Hydrolyse der Dihydrostilbenderivate hemmte das Aglykon von Scorzodihydrostilbene A (ASDSA) das Überleben von Rattenleberzellen der Zelllinie H4IIE. Nach Stimulation durch unterschiedliche Konzentrationen von TNF-α erhöhte ASDSA außerdem konzentrationsabhängig die durch TNF-α vermittelte Zytotoxizität von H4IIE Zellen.

Dianthus versicolor

Die mongolische Arzneipflanze *Dianthus versicolor* wurde in der Region um Ulan Bator in der Mongolei gesammelt. Der methanolische Extrakt der oberirdischen teile der Pflanze lieferte sieben bekannte Inhaltsstoffe, zwei Lignane, vier Triterpene und ein Steroid. Die untersuchten Substanzen entwickelten leichte Zytotoxizität gegen die L5178Y Zelllinie und 24 Proteinkinasen.

Psoralea corylifolia

Samen der Pflanze *Psoralea corylifolia* wurden nach chromatographischer Aufreinigung drei Cumarine, darunter zwei neue, 7,2′,4′-trihydroxy-3-arylcumarin und Psoracumestan, sechzehn bekannte prenylierte Flavonoide und ein Meroterpen gewonnen. Die isolierten Metabolite wurden auf ihre Zytotoxizität gegenüber H4IIE, Hct-116 und C6 Zelllinien sowie antioxidative Eigenschaften im TEAC Assay hin untersucht. Auf Basis dieser Ergebnisse wurden Struktur-Wirkungs-Beziehungen ermittelt. Die aktiven Naturstoffe wurden weiterhin untersucht auf ihr apoptotischen und nekrotischen Charakter, um den Wirkmechanismus näher zu beleuchten Des weiteren wurden einige Metabolite auf ihre Inhibierung auf Proteinkinasen überprüft.

Table of contents

1. Introduction

1.1. The significance of the study

1.1.1. Importance of medicinal plants in drug discovery

Plants have been used as the essential element of traditional medicine systems to serve people all over the world for thousands of years [Samuelsson, 2004]. An evaluation of the World Health Organization validated that these ethical medical systems continue to play an important role in the primary health care of about 80% of the world's residents [Farnsworth *et al.*, 1985]. Globally, at least 119 compounds derived from 90 plant species can be considered as important drugs. 74% of these substances were found by the chemical studies through the isolation of the bioactive compounds from plants used in traditional medicine [Newman *et al.*, 2000].

In the early nineteenth century, isolating the active compounds from extracts was involved for the use of medicinal plants [Kinghorn, 2001]. Up to the 30's of last century, a series of natural products isolated from plants became clinical agents and a number of that is still in use today [Kong *et al.*, 2003]. More recently, isolation and characterization of pharmacologically active compounds from medicinal plants for drug discovery continue and become more efficient by applying the new technologies.

Nowadays there is a renewed interest in investigating plants for medically useful compounds, with some of the leading pharmaceutical and research institutions involved in this search. More than 50% of the 25 best-selling drugs worldwide were related directly to natural products. In 1990's, 61% of anticancer agents approved were natural products and their derivatives [Cragg *et al.*, 1997]. In the same period, among the projects performed by the top twenty international pharmaceutical companies, more than 80% of the compounds involved were from microorganisms and natural products. Moreover, approximately 40% of the projects at the clinical test and pre-clinical test stage were correlated to natural products [Liu, 2000].

1.1.2. Plant natural products as drugs

Drug discovery from medicinal plants led to the isolation of early drugs, such as quinine from *Cinchona* bark, morphine and codeine from the opium poppy, and digoxin from *Digitalis* leaves, in addition to atropine and scopolamine from the family *Solanaceae*, some of which are still in clinical use [Kong *et al.*, 2003; Butler, 2004]. Plant natural products exhibit the major impact as templates or direct treatment in the treatment of cancers and anti-infective aspects [Newman *et al.*, 2000].

Artemisinin is a sesquiterpene endoperoxide isolated from the shrub *Artemisia annua* which had been used for centuries as a traditional chinese antimalarial medicine (named Qinghaosu). Using the base structure of artemisinin, many semi-synthetic compounds were made with the aim of optimizing the pharmacology of the base molecule. Now, artemisinin-based combination therapies are generally considered as the best current treatment for malaria [Clark, 1996].

Ephedrine was obtained as a pure substance from *Ephedra sinica* which had been known in traditional Chinese medicine for millennia as treatment for asthmatic and other bronchial conditions. It has been demonstrated that ephedrine can cause elevation of blood pressure, plus inotropic and chronotropic actions of the heart. Following regulatory approval, it became the first in a very long line of bronchodilator agents. Ephedrine significantly affected blood pressure due to its effects on cardiac output and on release of other sympathomimetic amines; one now has available related structures that are specific blockers of such activities on cardiac tissue and are excellent ‘reducers of hypertension’.

Morphine and **codeine** were isolated from the latex of the opium poppy (*Papaver somniferum*) for the conquest of pain. The crude extract of opium contains about a quarter of its weight as opium alkaloids with up to 20 more distinct alkaloids including thebaine, papaverine and noscapine. Some close relative substances are also prepared for use in cough syrups.

Cancer is the most dangerous disease to human beings, while plants have a long history of use in the treatment of cancer. Amongst the best known are vinca alkaloids, **vinblastine** and **vincristine**,

isolated from *Catharanthus roseus*, the Madagascan periwinkle. *C. roseus* was used by various cultures as a source of hypoglycemic agents [Pezzuto, 1997]. Vinblastine and vincristine (also known as leurocristine) are anti-mitotic drugs used to treat lung, breast, testicular cancer, and leukemia. Since the 1950's, vinblastine has increased the survival rate of childhood leukemia by 80%.

Podophyllotoxin was isolated as the anti-tumor agent from the rhizome of American mayapple, *Podophyllum peltatum*. This non-alkaloid toxin of the lignan family is also present in various other species of the genus *Podophyllum*. These plants were medicinal used by early American and Asian cultures to treat skin cancers and warts at length [Cragg *et al.*, 1994]. The two clinically-active agents, **etoposide** and **teniposide,** were subsequently synthesized from the naturally occurring epimer (epipodophyllotoxin) of podophyllotoxin. Etoposide phosphate is an inhibitor of the enzyme topoisomerase II and is used to treat malignancies, such as lung, testicular cancer, lymphoma and leukemia. Teniposide is mainly used in the treatment of childhood acute lymphocytic leukemia.

Camptothecin was isolated from the bark and stem of the Chinese native ornamental tree *Camptotheca acuminate*. It is a cytotoxic quinoline alkaloid inhibiting the DNA enzyme topoisomerase I specifically [Wall *et al.*, 1966]. Due to the adverse drug reaction, such as the severe bladder toxicity, two modified analogues, **topotecan** (Hycamptin®) and **irinotecan** (Camptosar®), have been approved and are used in cancer chemotherapy today. Topotecan is mainly used for the treatment of ovarian and lung cancer, while irinotecan is used to treat colon cancer.

Paclitaxel (Taxol®) as a complex diterpene was isolated from the bark of the pacific yew tree, *Taxus brevifolia*. In history, several native American tribes used the yew tree of *Taxus* species for some non-cancerous conditions [Newman *et al.*, 2000]. Today, paclitaxel is a mitotic inhibitor used to treat lung, ovarian, breast cancer. Together with its active analog, **docetaxal**, paclitaxel forms the drug category of the taxanes.

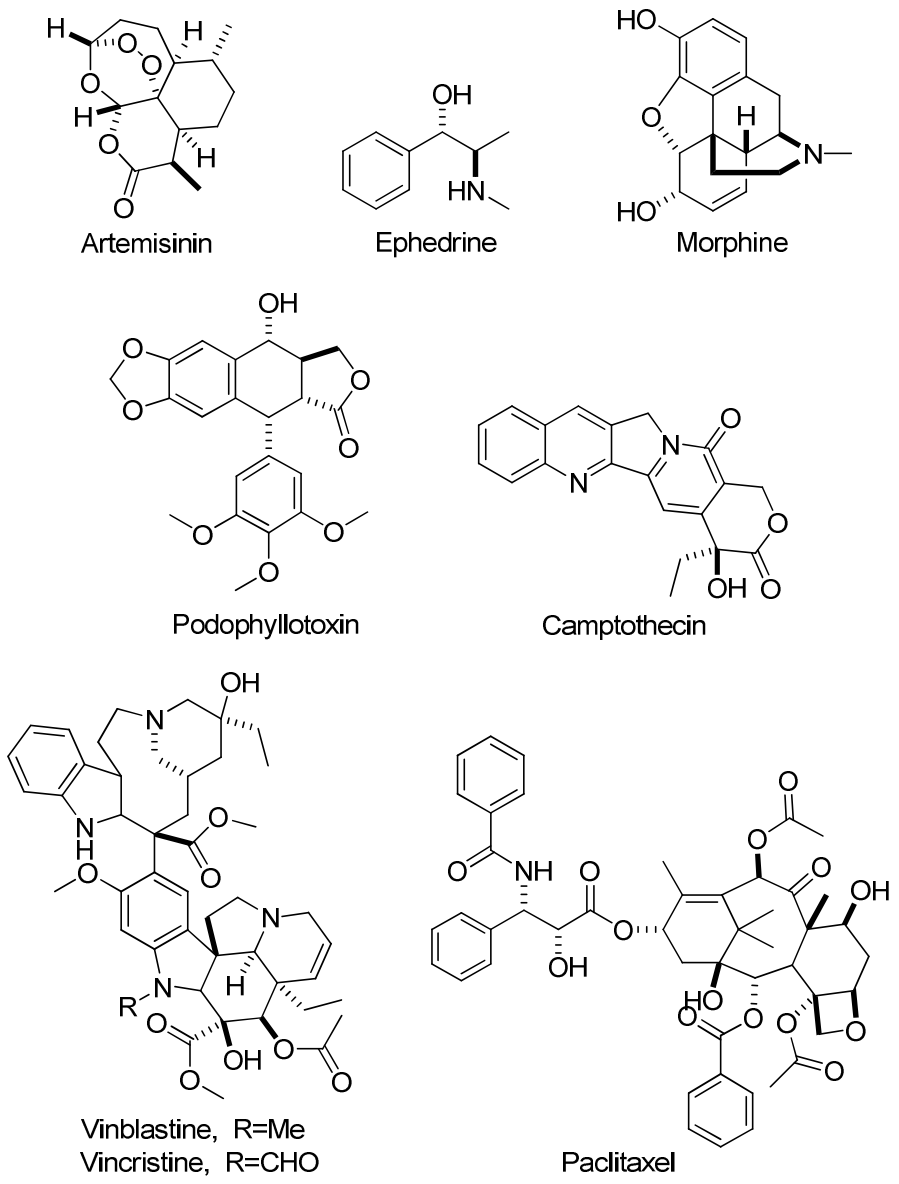

Figure 1.1 Plant natural products as drugs

1.2. Phenolic Compounds

Phenolic compounds of plant origin constitute one of the most numerous and ubiquitous groups of plant secondary metabolites. They have a wide variety of functions, including defense against herbivores, pathogens aggression, or other sources of injury; as structural components of cell walls; as protection from ultraviolet radiation; as pigments; and as signaling molecules [Bravo, 1998]. Phenolic compounds are attracting increasing attention due to their reputed beneficial effects on human health protection. They are reported to play a role in the prevention of cardiovascular disease, cancer, diabetes mellitus, and neurodegenerative disease [Scalbert *et al.*, 2005]. Particularly for the

diseases associated with oxidative stress, polyphenols inhibit oxidation of cholesterol and formation of low-density lipoprotein (LDL) particles that are involved in atherosclerosis [Marrugat *et al.*, 2004]. Phenolic compounds are also found in many medicinal plants, they modulate the activity of a wide range of enzymes and cell receptors [Manach *et al.*, 2004]. The main groups of polyphenols are: flavonoids, phenolic acids, stilbenes and lignans.

Flavonoids are the most abundant polyphenols and are divided into 6 subclasses according to the oxidation state of the central pyran ring. More than 7000 flavonoids have been identified in plants, and the list is constantly increasing [Harborne and Williams, 2000]. This is because of the occurrence of numerous substitution patterns in which primary substituents can themselves be substituented, sometimes yielding highly complex structures [D'Archivio *et al.*, 2007].

Flavonoids are most commonly known for their antioxidant activity. However, it is already established that thay make some contribution to disease resistance, such as against cancer and heart disease, and are the result of other mechanisms [Ververidis et al., 2007]. Flavonoids have been referred to as “nature’s biological response modifiers” because of strong experimental evidence of their inherent ability to modify the body's reaction to allergens, viruses, andcarcinogens [Yamamoto and Gaynor, 2001].

Phenolic acids can be classified into benzoic acid derivatives and cinnamic acid derivatives. Hydroxycinnamic acids are more common than hydroxybenzoic acid, and consist mainly of p-coumaric, caffeic, ferulic, and sinapic acids. These compounds are mostly found as glycosylated derivatives or esters of quinic acid, shikimic acid, and tartaric acid [Manach *et al.*, 2004].

Stilbenes are products from a cinnamoyl-CoA starter unit, which is a phytoalexin produced by plants when under attack by pathogens, such as bacteria or fungi, or to a variety of stress conditions [Delmas *et al.*, 2006]. The best known stilbene is resveratrol, which has assumed greater relevance in recent years with antioxidant, anti-inflammatory, cancer preventative, and beneficial cardiovascular properties [Roupe *et al.*, 2006]. Resveratrol has also been shown to extend the life span of several short-living species of animals [Baur and Sinclair, 2006].

Lignans are one of the major classes of phytoestrogens and also act as antioxidants, which are derived from phenylalanine. The interest in lignans and their synthetic derivatives is growing because of potential applications in cancer chemotherapy and various other pharmacological effects [Saleem *et al.*, 2005].

However, when incorporated at high doses, plant phenols may also be negative for human health or even toxic. It is important to study the potential risk of these compounds which involves a detailed analysis of their resorption, metabolism as well as structure activity studies. Based on such a detailed analysis a scientifically sound evaluation of the beneficial properties as well as of their risk potential will be possible.

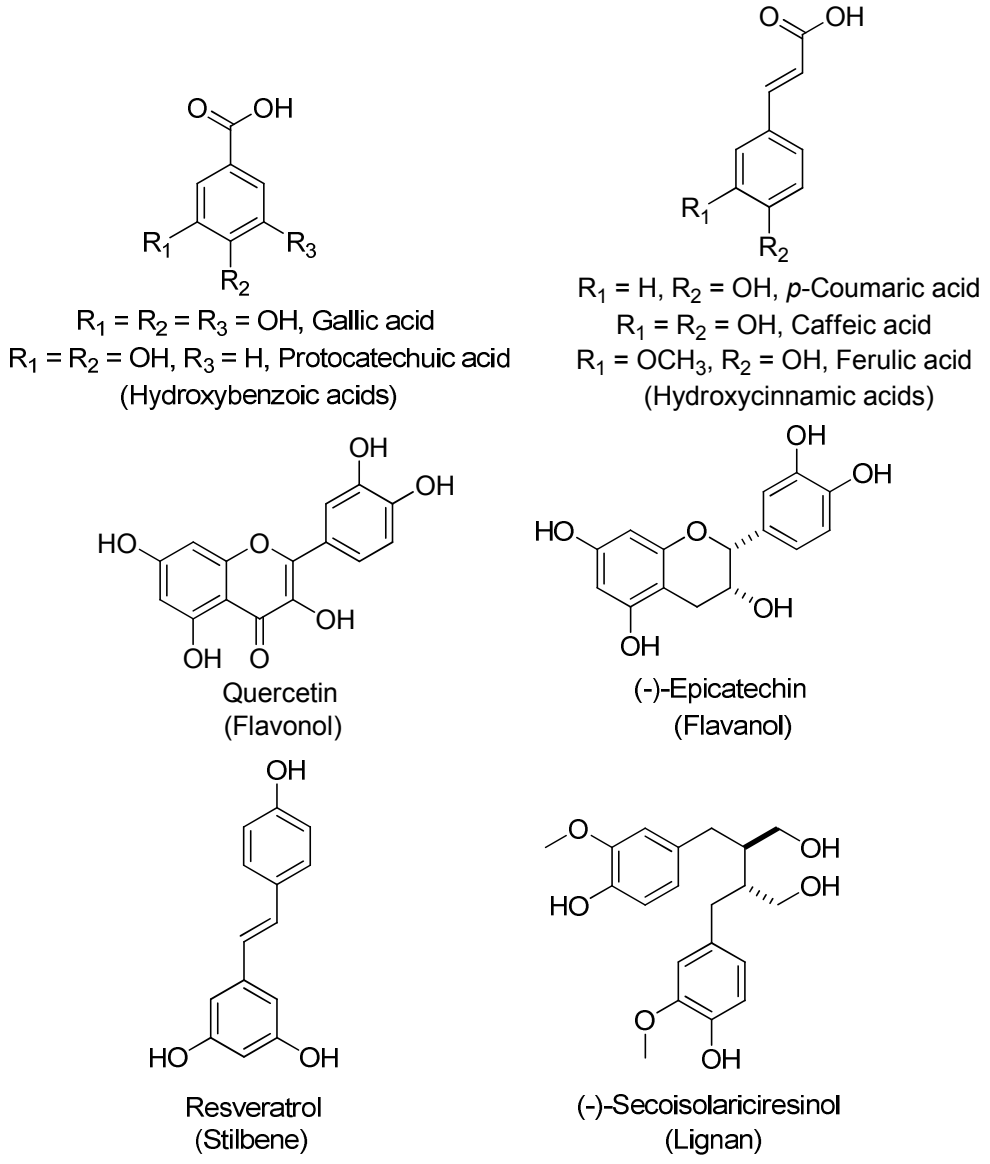

Figure 1.2 Phenolic compounds of plant origin

1.3. Herbs of traditional Mongolian medicine

Traditional Mongolian medicine was introduced by Tibetan Lamaists, and developed over many years among the Mongolian people. Herbs are the mainstay (about 72%) of Mongolian traditional medicine. Various medicinal plants and herbal prescriptions were used to prevent and cure human and animal diseases.

Mongolia mainly consists of steppes and has an extreme continental climate, which provide specific habitat for plants. There are 854 species of plants (about 32 % of total estimated Mongolian vascular plants) utilized as folk medicine in Mongolia, including 280 species containing alkaloids, 238 species containing flavanoids, 65 species containing cumarins, and 232 saponin-bearing plants [Gubanov, 1996].

However, only very few ancient literature about Mongolian plants remaines today, and modern investigations, such as phytochemical studies, for Mongolian plants were scarcely conducted. On the other hand, the worldwide information about Mongolian plants was scanty, due to most publications being in Mongolian or Russian [KLETTER *et al.*, 2008]. So far just three books with regard to Mongolian medicinal plants for traditional use have been published in English [Ligaa, 1994; Grubov, 2001; Boldsaikhan, 2004]. Consequently, there is a need to research on those fragile natural resources as a promising scientific task, and to prove the efficacy of the traditional medication which can be considered for a potential drug discovery.

1.4. Aim of the present study

The investigation on medicinal plants intends searching for new and bioactive natural products; studying the chemical diversity and chemical ecology; explaining the substances which play roles in medical use of plants; as well as their pharmacological targets. This study is focused on the isolation and characterization of biologically active secondary metabolites from Mongolian and Chinese medicine plant extracts. The isolated compounds were evaluated for their cytotoxic and antioxidant activities. Cytotoxicity was studied in vitro using mouse lymphoma (L5178Y), rat hepatoma

(H4IIE), human colon carcinoma (HCT116) and rat glioma (C6) cell lines and with 24 protein kinases. Some characteristic compounds were further investigated to understand the induced mechanism of cell death, such as apoptosis and necrosis, by Apo-ONE, LDH and SEAP assay. Antioxidant activity was determined by DPPH and TEAC assay. Different chromatographic techniques were used for the isolation of biologically active compounds like TLC, CC, or semi-preparative HPLC.

2. Material and Methods

2.1. Biological material

Aerial parts of Mongolian medicinal plants *Scorzonera radiata* and *Dianthus versicolor* were collected in July 2004 in Khandgait am forest, Ulaanbaatar region, Mongolia. The plants were identified by Prof. Sc. D. Sh. Darijmaa (Mongolian State University of Education). Voucher specimens have been deposited in the herbarium section of the Department of Organic and Food Chemistry, National University of Mongolia, Ulaanbaatar, Mongolia.

Figure 2.1 The map of mongolia

2.1.1. *Scorzonera radiata*

Taxomony

Phylum:	Magnoliophyta
Class:	Magnoliopsida
Order:	Asterales
Family:	Asteraceae
Genus:	*Scorzonera*
Species:	*Scorzonera radiata* Fisch.

2.1.2. *Dianthus versicolor*

Taxomony

Phylum:	Magnoliophyta
Class:	Magnoliopsida
Order:	Caryophyllales
Family:	Caryophyllaceae
Genus:	*Dianthus*
Species:	*Dianthus versicolor* Fisch.

2.1.3. *Psoralea corylifolia*

Taxomony

Phylum:	Magnoliophyta
Class:	Magnoliopsida
Order:	Fabales
Family:	Fabaceae
Subfamily:	Faboideae
Genus:	*Psoralea*
Species:	*Psoralea corylifolia* Linn.

Seeds of Chinese medicine plant *Psoralea corylifolia* were bought in September 2006 from Hangzhou Zhongmei Huadong Pharmaceutical Co., Ltd., Hangzhou, China. The plant material of *Psoralea corylifolia* was extracted in the working group of Prof. Yijia Lou (Institute of Parmacology and Toxicology, Zhejiang University, China) by Mr. Zhiqiang Wang.

2.2. Laboratory chemicals

2.2.1. General laboratory chemicals

Acetic acid	Merck
Anisaldehyde (4-methoxybenzaldehyde)	Merck
(-)-2-butanol	Merck
Hydrochloric acid	Merck
Potassium hydroxide	Merck
ortho-phosphoric acid 85% (p.a.)	Merck
Sulphuric acid, conc.	Merck
Trifloroacetic acid (TFA)	Merck

2.2.2. Solvents

2.2.2.1. General solvents:

Acetone
Acetonitrile
Dichloromethane
Ethanol
Ethyl acetate
Hexane
Methanol

The solvents were purchased from the Institute of Chemistry, University of Duesseldorf. They were distilled before using and special grade were used for spectroscopic measurements.

2.2.2.2. Solvents for HPLC:

Methanol was LiChroSolv HPLC (Merck), nano-pure water (distilled and heavy metals free water) was obtained by passing distilled water through nano- and ionexchange filter cells (Barnstead, France).

2.2.2.3. Solvents for optical rotation:

Chloroform spectral grade	Sigma
Methanol spectral grade	Sigma

2.2.2.4. Solvents for NMR:

Deuterated methanol, chloroform, dimethylsulfoxide, water (Uvasol, Merck) were used for NMR measurements.

2.2.3. Chromatography

Pre-coated TLC plates (Aluminium, Silica Gel 60 F_{254}, layer thickness 0.2mm)	Merck
Silica Gel 60, 40–63 μm mesh size	Merck
Pre-coated TLC plates (Aluminium, RP-18, F_{254} S, layer thickness 0.25mm)	Merck
RP-18, 40-63 μm mesh size	Merck
Amberlit XAD. Diaion PH 20, Dowex MCI Gel	Merck
Sephadex LH 20, 25–100 μm mesh size	Merck

2.3. Laboratory instruments

General instruments

Analytical balances MC-1	Sartorious
Half-micro and analytical balance MC-1	Sartorious
pH-meter inoLab, pH-Electrode Sen Tix 21	WTW
Desiccator	Glaswerk Werthein
Hot plate and magnetic stirrer: IKA-Combimag RCH	Janke & Kunkel KG
Glass ware	Schott Duran
Drying Oven ET6130	Heraeus
Ultra sonicator RK 510H	Bandelin
UV-Lamp (254 and 366 nm)	Camag
Rotary evaporator	Büchi Rotavapor R-200
Vacuum pump CVC 2000	Vacuubrand
Centrifuge Pico	Heraeus
Nitrogen generator UHPN 3001	Nitrox
Air generator ZA 20	WGA
Fraction collector Retriever II	ISCO
Lyvac GT2 (Freeze dryer)	Steris
Vacuum pump Trivag D10E (Freeze dryer)	Leybold
SPD 111V (Speedvac)	Savant
Cooling trap RVT 400 (Speedvac)	Savant
Vacuum pump VLP 80 (Speedvac)	Savant
Syringe	Hamilton 1701 RSN
Mill	Molinex 354
Magnetic stirrer	Variomag Multipoint HP
	Behrotest PH 10-Set

Semipreparative HPLC

Pump: L-7100	Merck/Hitachi
Detector: UV-L7400 (Photodiode array detector)	Merck/Hitachi
Printer: Chromato-Intergartor D-2000	Merck/Hitachi
Column: Eurospher 100-C18, [10 μm; 300 mm × 8 mm]	Knauer
Pre-column: Eurospher 100-C18, [10 μm; 30 mm × 8 mm]	Knauer

Analytical HPLC

Pump: P 580A LPG	Dionex
Autosampler: ASI-100T (injection volume = 20 μL)	Dionex
Detector: UVD 340S (Photodiode array detector)	Dionex
Column oven: STH 585	Dionex
Column: Eurospher 100-C18, [5 μm; 125 mm × 4 mm]	Knauer
Pre-column: Vertex column, Eurospher 100-5 C18 [5-4 mm]	Knauer
Software: Chromeleon (V. 6.30)	

HPLC-MS

Analytical HPLC: Agilent 1100 series (Photodiode array detector)	Agilent
MS: Finigan LCQ-DECA	Thermoquest
Ionizer: ESI and APCI	Thermoquest
Vacuum pump: Edwards 30	BOC
Column: Eurospher 100-C18, [5 μm; 227 mm × 2 mm]	Knauer
Pre-column: Vertex column, Eurospher 100-5 C18 [5–4 mm]	Knauer

NMR

DRX-500	Bruker
ARX-400	Bruker
DMX-600	Bruker

2.4. Chromatographic methods

The general features of the molecule that are helpful to ascertain the isolation process include solubility, acid-base properties, stability, and molecular size.

2.4.1. Thin layer chromatography (TLC)

Analytical TLC was applied in the detection and monitoring of compounds through a separation process, and was used to optimize solvent systems for column chromatography. It has use also in the biological evaluation of antioxidant metabolites. TLC was performed on pre-coated TLC plates with silica gel 60 F_{254} (layer thickness 0.2 mm, E. Merck, Darmstadt, Germany) with ethyl acetate : formic acid : water (85:10:5) as mobile phase. The band separation on the TLC describing the separation of compounds was detected under UV absorbance at 254 nm (fluorescence absorption) and 366 nm (fluorescence), followed by spraying the TLC plates with anisaldehyde-H_2SO_4 reagent and subsequent heating at 110 °C. TLC was conducted prior to further work to track the identity of each fraction and the qualitative purity of the isolated compounds.

Anisaldehyde-H_2SO_4 Spray Reagent (Per 100 mL)

Methanol: 85 mL
Glacial Acetic Acid (100%): 10 mL
Sulphuric acid, conc.: 5mL (added slowly)
Anisaldehyde: 0.5 mL
The reagent was stored in an amber-coloured bottle and kept refrigerated until use.

2.4.2. Column chromatography (CC)

Open column chromatography plays an important role in the separation of compounds from natural product extracts. The separation takes place through selective distribution of the components between a mobile phase and a stationary phase. Different choice of packing material and mobile phase can be applied depending on the class of compounds or fractions. Several types of separation processes involved in this study.

Silica Gel is regarded as a typical polar sorbent and has a weakly acidic surface. Polar compounds containing carboxylic or hydroxyl group are strongly absorbed on silica gel. It was only used for few lipophilic fractions.

Reversed phase C_{18} (RP-18, ODS) is chemically modified silica gel with octadecasilylchloride. It is retentive for nonpolar compounds, and is ideal for various types of hydrophilic natural product isolation. RP-18 has great reproducibility of packing material performance.

Diol is prepared by treating silica gel with the chloroalkoxysilane containing two hydroxyl function groups. It was utilized for the intermediate polarity natural product isolation. Diol also has better reproducibility comparing to standard normal-phase chromatography.

Sephadex® LH-20 is prepared by crosslinking water-soluble dextran with epichlorohydrin to be size-exclusion stationary phase. The separation is on the basis of molecular size and shape of the analyte molecules, accordingly molecules elute in order of decreasing size. It is particularly ideal for labile natural products and for removal of chlorophyll from plant extracts. Sephadex® LH-20 usually does not adsorb compounds irreversibly, and can be used for several experiments without the need for regeneration.

Diaion® HP-20 is a grade of polyaromatic adsorbent resin based on crosslinked polystyrenic matrix. The resin is a relatively large particle size bead (250–850 μm), which is a good alternative for the substances which give poor separation and recovery on silica-based materials. It especially is useful

for desalting.

2.4.3. Low-pressure liquid chromatography (LPLC)

Positive pressure was applied to the top of the column to accelerate the flow rate and achieve better resolution in LPLC. It uses particle size in the 40–60 μm range.

Flash chromatography is the liquid column chromatography (CC) under a pressure. The column was a silica gel 60 GF_{254} prepacked column (18 cm), and the pressure was supplied by an air pump.

Lobar®, ready-to-use glass column is filled with LiChroprep® RP18, 40–63 μm packing. A pump which can deliver a smooth and constant flow of solvent is involved for Lobar® column. The run time of LPLC is reduced considerably compared to that of open column chromatography.

2.4.4. Semi-preparative high-performance liquid chromatography (HPLC)

HPLC is a robust, versatile, and usually rapid technique to purify compounds from complex mixtures. The reversed-phase C_{18} chromatography was used as the exclusive stationary phase of HPLC in this study. All samples for semi-preparative HPLC must be analyzed thoroughly and pretreated to make the separation optimal and maintain the life-span of the HPLC system. The eluant used in semi-preparative HPLC comprises a mixture of nanopure water and methanol. The isocratic conditions were always the premier, even the only choice to achieve separations. 50 µL of approximately 40 mg/mL solution of the substance was injected for each time. The flow rate was stabilized at 5 mL/min, and the paper speed of the recorder was 5 mm/min. The eluted peaks were collected respectively by manual work based on the records of a UV-vis detector.

2.4.5. Analytical high-performance liquid chromatography (DAD-HPLC)

Analytical HPLC which is a HPLC coupled to a PDA (photodiode array) detector, is extremely useful for the analysis of natural products containing chromophores, such as phenolic compounds. It can help to analyze individual HPLC peaks, and to obtain complete UV spectrum of individual

components. The HPLC retention time and the UV spectrum for any component (HPLC peak) can be characteristic of certain compounds. The whole system was run by a sophisticated software (Chromeleon® Version 6.30) that allows building up of spectral libraries for reference compounds and automated compound search.

The conditions of analytical HPLC:

Flow rate: 1 mL/min
Injection volume: 20 μL
Sample concentration: ca. 0.1 mg/mL
Column temperature: 20 °C
UV detection wavelengths: 235, 254, 280, and 340 nm

For a standard method, the gradient eluant was composed by 0.15% phosphoric acid in nanopure water (pH 2.0) and methanol, which was showed in Table 2.1.

Table 2.1 Standard gradient for analytical HPLC

Time (min)	Acidic water (%)	Methanol (%)
0	90	10
5	90	10
35	0	100
45	0	100
50	0	10
60	0	10

2.5. Mass spectroscopy (MS)

Mass spectroscopy (MS) is an analytical technique for the determination of the elemental composition of a molecule and for elucidating the chemical structures of molecules. These include identifying unknown compounds, determining the isotopic composition of elements in a molecule, and determining the structure of a compound by observing its fragmentation The MS principle consists of ionizing chemical compounds to generate charged molecules or molecule fragments and measurement of their mass-to-charge ratio (*m/z*).

2.5.1. HPLC-MS

HPLC-MS refers to the coupling of an HPLC with a mass spectrometer (MS), which combines the chemical separating power of LC with the ability of a mass spectrometer to selectively detect and confirm molecular identity. It provides information on the molecular weight as well as on the fragmentation pattern of the analyte molecules. Consequently the separated sample emerging from the column can be identified on the basis of its mass spectral data. Electrospray (ESI) and atmospheric pressure chemical ionization (APCI) are the two interfaces used for LC-MS.

The conditions of HPLC-MS:

Flow rate: 0.4 mL/min
Injection volume: 10 μL
Sample concentration: ca. 0.1 mg/mL
Column temperature: room temperature
UV detection wavelengths: 235, 254, 280, and 340 nm

For a standard LC-ESI-MS-MS measurement, the gradient eluant was composed by 0.1% formic acid in nanopure water and acetonitrile, which was showed in Table 2.2. The samples were dissolved in water and methanol.

Table 2.2 Standard gradient for HPLC-MS

Time (min)	Acidic water (%)	Acetonitrile (%)
0	90	10
5	90	10
35	0	100
45	0	100
50	0	10
60	0	10

2.5.2. Electron spray ionization mass spectroscopy (ESIMS)

In ESI method, a solution of a substance is sprayed through a capillary into a chamber. Charged droplets are produced by an applied potential of a few kV, and in the following are driven by the electric field to move into the pre-analyser region. ESIMS is a powerful analytical method, because it allows one to analyse the molecular ions of polar and higher molecular compounds in aqueous

solution.

2.5.3. Electron impact mass spectroscopy (EIMS)

From the direct inlet, a fine and persistent beam of molecules streams into the ion source where it intersects perpendicularly with an electron beam. The interaction between the electrons and the neutral molecules generates positively charged molecular ions. EIMS was the alternative ionization procedure to LC-ESIMS for the natural products which have no chromophore, for instance triterpenes, and the compounds which did not yield a molecular ion or the intensity was too low under ESI conditions.

EI mass spectra were measured on a Finnigan MAT 8430 mass spectrometer in Institut für Anorganische Chemie und Strukturchemie, Heinrich-Heine Universität, Düsseldorf.

2.5.4. High resolution mass spectroscopy (HRMS)

High resolution is achieved by passing the ion beam through an electrostatic analyzer before it enters the magnetic sector. In such a double focusing mass spectrometer, ion masses can be measured with an accuracy of about 1 ppm. With measurement of this accuracy, the atomic composition of the molecular ions can be determined. HRESIMS spectra were determined on a ThermoFinnigan LTQ-Orbitrap FT-ESIMS. Measurements were processed by Dr. RuAngelie Edrada-Ebel at Strathclyde Institute of Pharmacy and Biomedical Sciences, University of Strathclyde, Glasgow, U.K..

2.6. Nuclear magnetic resonance spectroscopy (NMR)

The NMR phenomenon is based on the fact that nuclei of atoms have magnetic properties that can be utilized to yield chemical information. NMR spectroscopy is a preeminent technique for determining the structures of organic compounds. Of all the spectroscopic methods, it is the only one for which a complete analysis and interpretation of the entire spectrum is normally expected.

The NMR spectra were measured at Institut für Anorganische Chemie und Strukturchemie, Heinrich-Heine Universität, Düsseldorf with ARX-500 spectrometer (Bruker). For better analysis, some spectra were measured by Dr. Victor Wray with Bruker DPX 300, ARX 400, or DMX 600 NMR spectrometers at Helmholtz Centre for Infection Research, Braunschweig. All attached NMR spectra were processed using MestReNova V5.2.2.. Methanol-d_4, dimetyl sulfoxide-d_6 (DMSO-d_6), $CDCl_3$ and D_2O were used as solvents depending on the solubility of the samples and the effect of solvents. Residual solvent signals were used as internal standards (reference signal). The chemical shifts (δ) values were given in ppm and the coupling constants (J) in Hertz (Hz).

2.7. Optical activity

The rotation of plane-polarized light is known as optical activity. Rotation to the right is given a positive value, rotation to the left a negative one. Optical rotations were recorded on a Perkin-Elmer 241 MC polarimeter. The substance was stored in a 0.5 mL cuvette with 1 dm length. $[\alpha]^{20}_{D}$ is the specific optical rotation at the wavelength of the solium D-line, 589 nm, at a temperature of 20 °C.

2.8. Hydrolysis of the dihydrostilbene glucoside

An acid catalysed hydrolysis reaction was used to split the glucosides to aglycones and glucoses. A solution of dihydrostilbene derivative (2 mg) was hydrolysed with 2 mL 1% HCl under reflux for 1.5 hours

2.9. Procedure for isolation of secondary metabolites from medicinal plants

2.9.1. Isolation of secondary metabolites from *Scorzonera radiata*

The air-dried, powdered plant material of *S. radiata* (300 g) was extracted exhaustively by maceration with MeOH (3 × 400 mL) at room temperature. The total extract was concentrated to dryness under vacuum. The concentrated solids (32.0 g) were reconstituted with 100 mL of

MeOH/H_2O (3:7) and then partitioned successively with hexane (5 × 100 mL), EtOAc (5 × 100 mL), and *n*-BuOH (5 × 100 mL) to give the hexane, EtOAc, *n*-BuOH, and aqueous fractions.

Aliquot amounts of the EtOAc fractions of the MeOH extract derived from the aerial parts of *S. radiata* (1.98 g) were separated by HP-20 resin CC with gradient elution using H_2O and MeOH as solvents to afford 10 fractions. Compounds **1** (34.7 mg, 0.018% yield) and **2** (55.3 mg, 0.028% yield) were separated by Sephadex LH-20 CC using MeOH as mobile phase. Compounds **3** (14.1 mg, 0.007% yield), **4** (3.4 mg, 0.002% yield), and **5** (1.1 mg, 0.0006% yield) were purified by semipreparative HPLC utilizing RP-18 as stationary phase and mixtures of MeOH/H_2O as solvent.

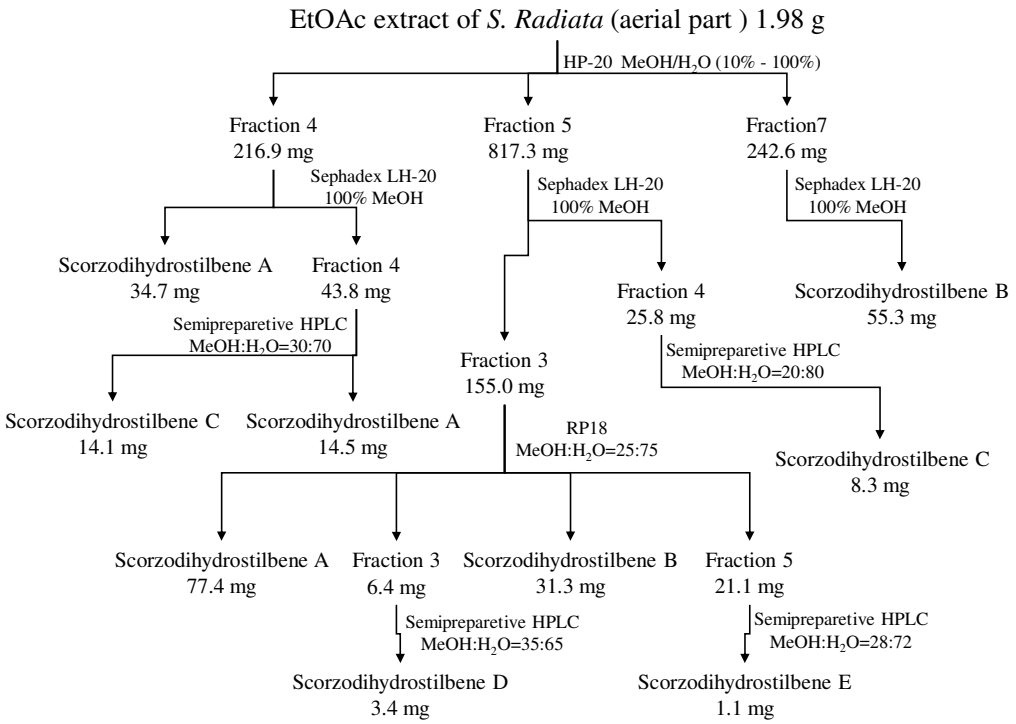

EtOAc extract of *S. Radiata* (aerial part) 1.98 g

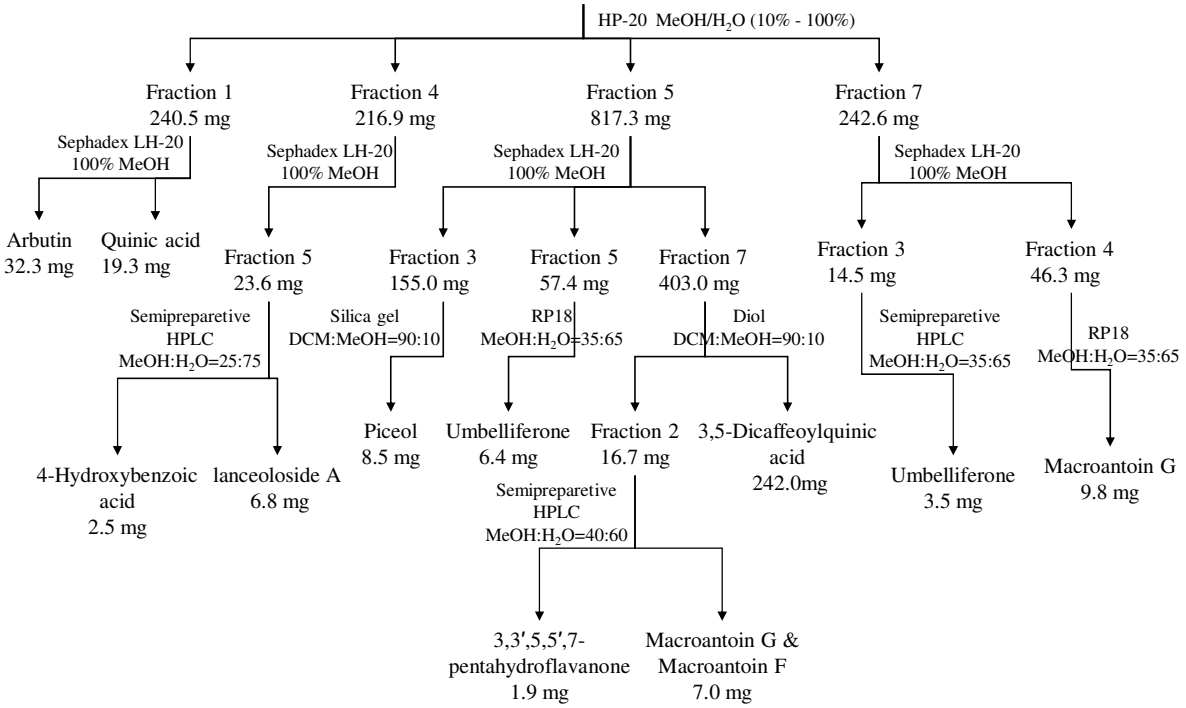

n-BuOH extract of *S. Radiata* (aerial part) 4.2 g

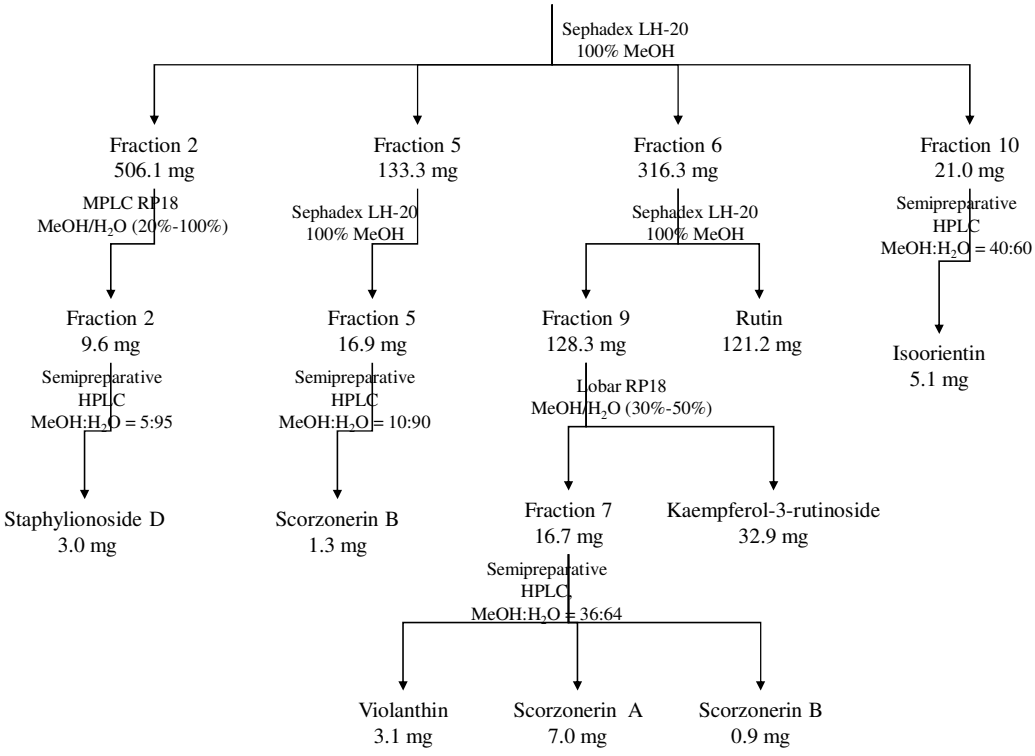

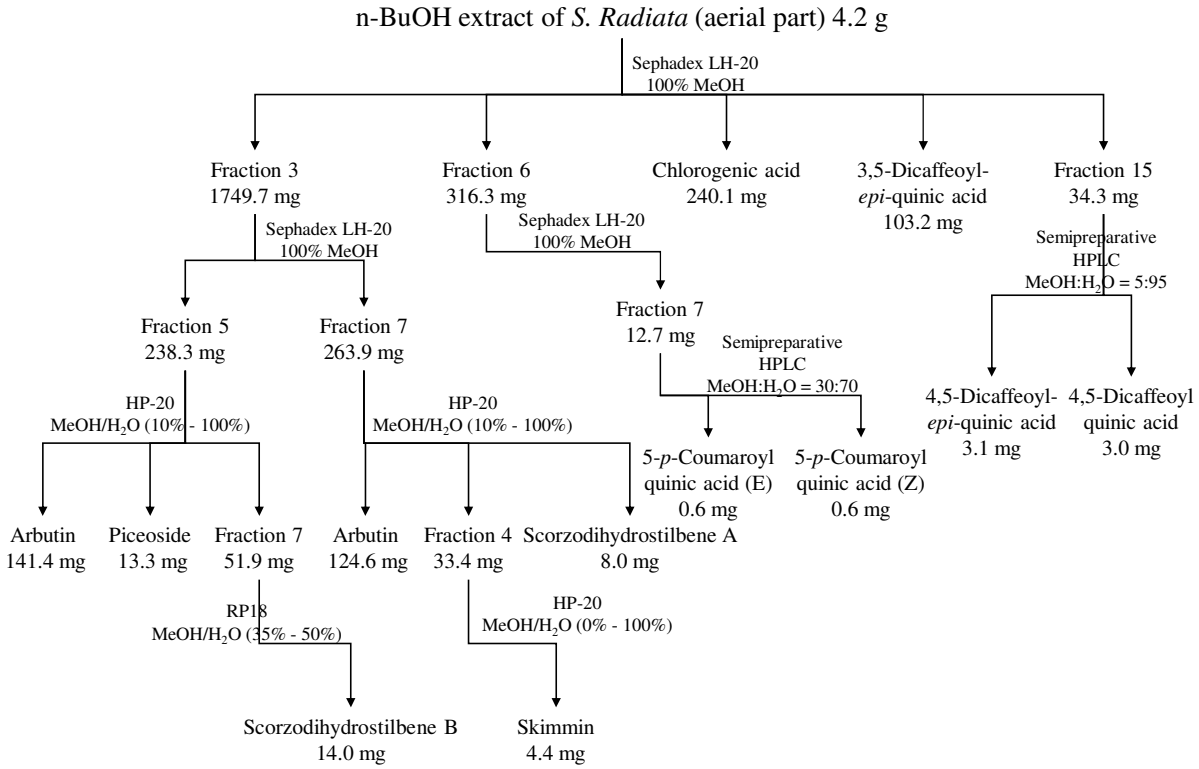

2.9.2. Isolation of secondary metabolites from *Dianthus versicolor*

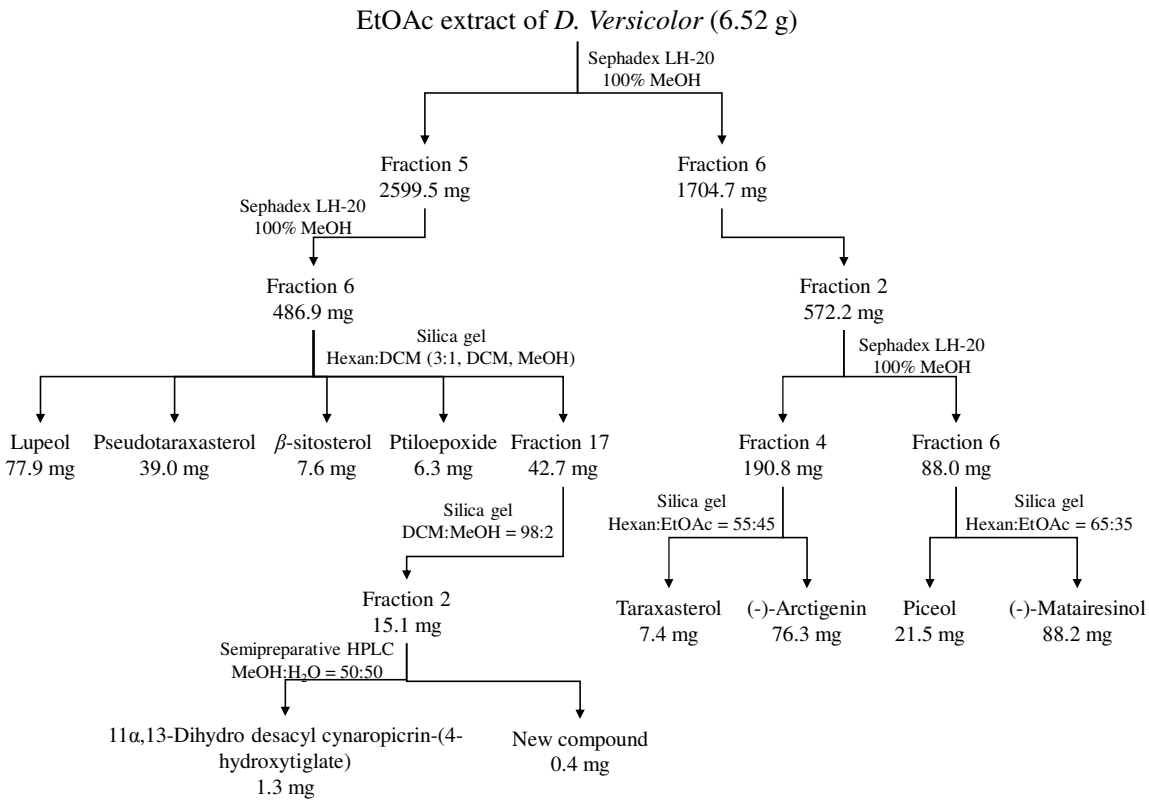

2.9.3. Isolation of secondary metabolites from *Psoralea corylifolia*

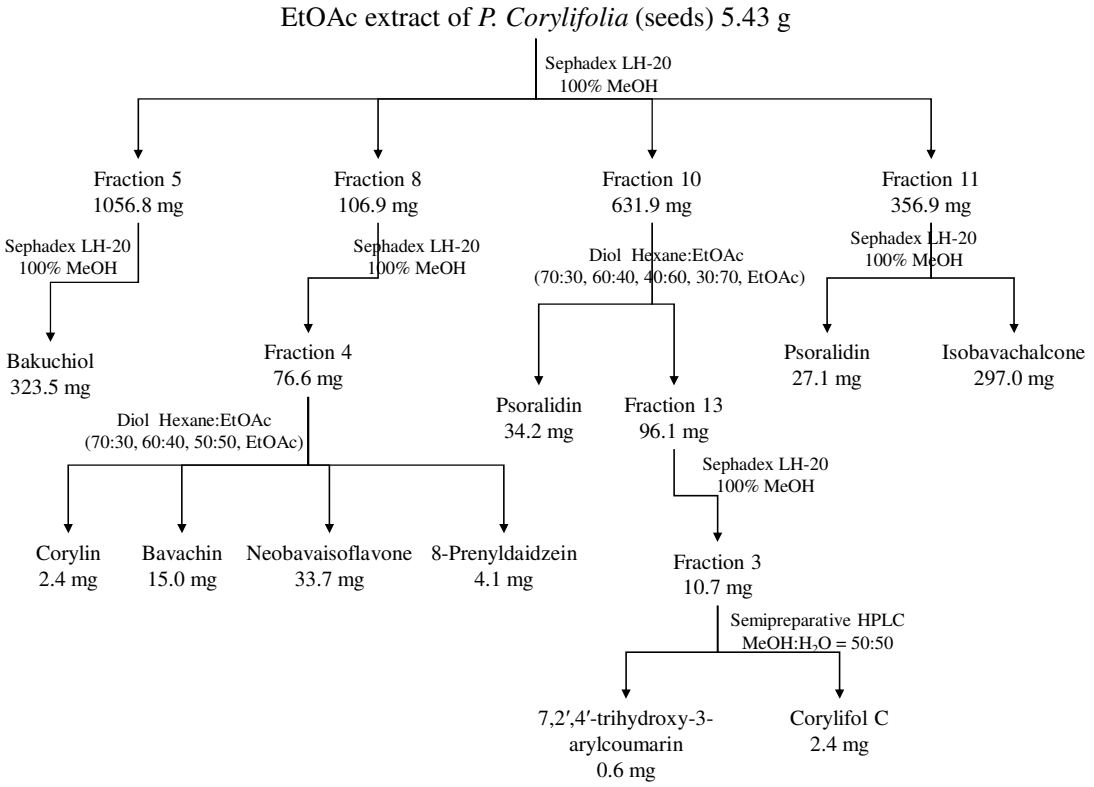

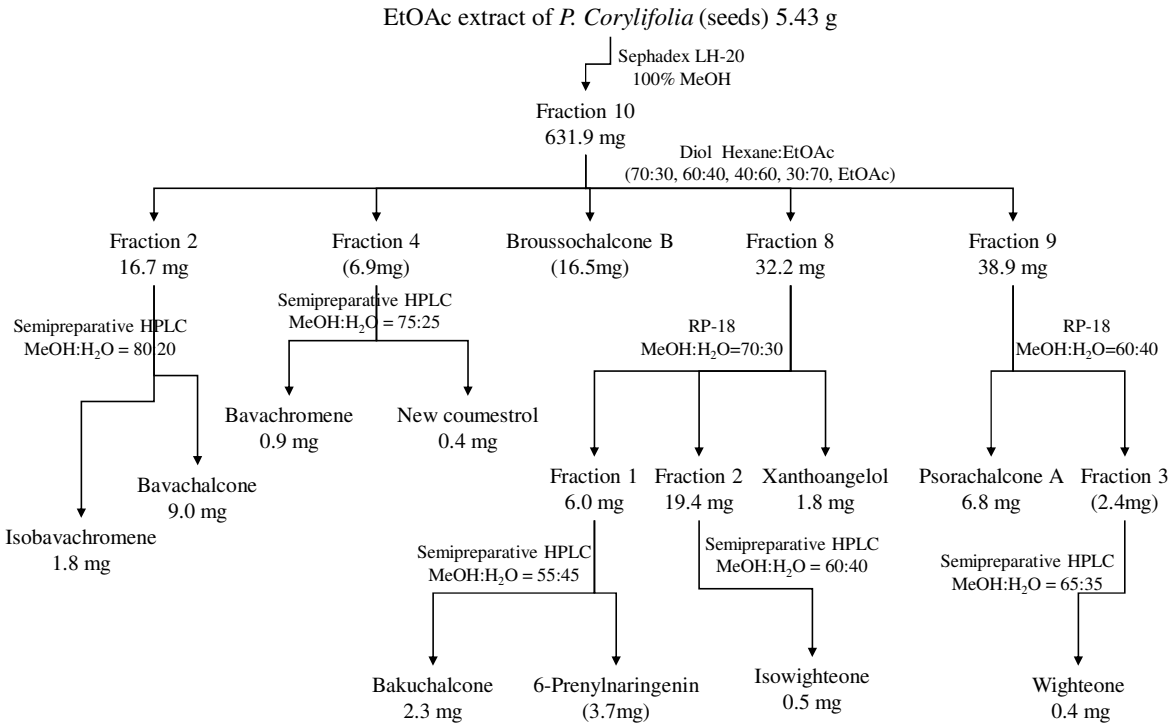

2.10.Biological assays

2.10.1. Antioxidant activity

2.10.1.1.Radical-scavenging activity by DPPH

Qualitative analysis of radical-scavenging activity of the extracts and fractions was carried out by spraying the TLC plates after development in an appropriate solvent system (EtOAc/HCO_2H/H_2O, 85:10:5) with 1% 2,2-diphenyl-1-picrylhydrazyl (DPPH) reagent. Active components were observed as yellow bands against a violet background.

To quantify the antioxidative capacity, absorption at 517 nm was determined after a test sample dissolved in 10 μL of MeOH had reacted with 490 μL DPPH solution (100 μM) at room temperature. Incubation time was 5 min. Prior to measurement, the difference in absorption between a DPPH blank solution and the positive control (propylgallate, 100 μM) was determined. This difference was then taken as 100% antioxidative activity. The percent antioxidative activity could be calculated from the difference in absorption between the test sample at 100 μM and the DPPH blank as follows: [Tsevegsuren *et al.*, 2007]

$$a_A\,(\%) = [(A_B - A_P)/(A_B - A_{Pos})] \times 100$$

where a_A = % antioxidative activity in comparison with the positive control, A_B = absorption of DPPH solution as blank, A_P = absorption of test sample, and A_{Pos} = absorption of positive control (propylgallate). Measurements were performed in triplicate, and IC_{50} values were calculated by linear regression.

2.10.1.2.TEAC-assay

TROLOX equivalent antioxidative capacity (TEAC) was measured spectro-photometrically analysing the decolourisation of a stable radical cation ABTS (2,2´-azino-bis(3-ethylbenz-thiazoline-6-sulfonic acid)) at 734 nm in comparison to the synthetic antioxidant TROLOX [Re *et al.*, 1999]. Absorption was measured after 4 min of mixing the isolated compound with the ABTS solution.

2.10.2. Inhibition of different protein kinases

The inhibitory profile of test compounds was determined using 24 protein kinases. The compounds were firstly tested at one concentration (1×10^{-6} g/mL) in singlicate. IC_{50} values were further measured by testing 10 concentrations of selected compounds in the range of 1×10^{-5} g/mL to 3×10^{-10} g/mL in singlicate.

A radiometric protein kinase assay (^{33}PanQinase® Activity Assay) was used for measuring the kinase activity of the 24 protein kinases. All kinase assays were performed in 96-well FlashPlates™ from Perkin Elmer/NEN (Boston, MA, USA) in a 50 μL reaction volume. The reaction cocktail was pipetted in 4 steps in the following order:

20 μL of assay buffer
5 μL of ATP solution (in H_2O)
5 μL of test compound (in 10 % DMSO)
10 μL of substrate / 10 μL of enzyme solution (premixed)

The assay for all enzymes contained 60 mM HEPES-NaOH, pH 7.5, 3 mM $MgCl_2$, 3 mM $MnCl_2$, 3 μM Na-orthovanadate, 1.2 mM DTT, 50 μg/mL PEG_{20000}, 1 μM [γ-^{33}P]-ATP (approx. 5×10^5 cpm per well).

All protein kinases were expressed in Sf9 insect cells as human recombinant GST-fusion proteins or His-tagged proteins by means of the baculovirus expression system. For the 24 kinases the following amounts of enzyme and substrate were used per well:

Kinase	Kinase Lot #	Kinase ng/50 µL	Substrate	Substrate ng/50 µL
AKT1	7	100	GSK3(14-27) (Lot 006)	1000
ARK5	2	100	RBER-CHKtide (Lot 14.1)	1000
Aurora-A	4	50	tetra (LRRWSLG)	500
Aurora-B	7	50	tetra (LRRWSLG)	250
AXL	3	100	Poly (Glu, Tyr)$_{4:1}$	125
B-RAF VE	1	20	MEK1 KM (Lot 021)	250
CDK2/CycA	5	100	RBER-CHKtide (Lot 14.1)	1000
CDK4/CycD1	6	50	RBER-CHKtide (Lot 14.1)	1000
CK2-alpha1	3	200	Casein	1000
COT	17	400	RBER-CHKtide (Lot 14.1)	1000
EGF-R	15	10	Poly (Glu, Tyr)$_{4:1}$	125
EPHB4	SP006	10	Poly (Glu, Tyr)$_{4:1}$	125
ERBB2	12	100	Poly (Glu, Tyr)$_{4:1}$	125
FAK	7	200	Poly (Glu, Tyr)$_{4:1}$	125
IGF1-R	12	20	Poly (Glu, Tyr)$_{4:1}$	125
INS-R	5	25	Poly (Ala, Glu, Lys, Tyr)$_{6:2:5:1}$	125
MET	SP011	100	Poly (Ala, Glu, Lys, Tyr)$_{6:2:5:1}$	125
PDGFR-beta	12	100	Poly (Ala, Glu, Lys, Tyr)$_{6:2:5:1}$	125
PLK1	11	50	RBER-CHKtide (Lot 14.1)	2000
PRK1	SP002	100	Histone H2B	1000
SAK	2	200	p38-alphaKRKR (Lot 003)	2000
SRC	SP004	10	Poly (Glu, Tyr)$_{4:1}$	125
TIE2	7	200	Poly (Glu, Tyr)$_{4:1}$	250
VEGF-R2	14	10	Poly (Glu, Tyr)$_{4:1}$	125

The reaction cocktails were incubated at 30 °C for 80 minutes. The reaction was stopped with 50 µL of 2 % (v/v) H_3PO_4, plates were aspirated and washed two times with 200 µL of 0.9 % (v/v) NaCl. Incorporation of $^{33}P_i$ was determined with a microplate scintillation counter (Microbeta Trilux, Wallac).

The median value of the counts in column 1 and 2 of each assay plate (n = 8) was defined as “low control” and “high control” respectively. This value reflects unspecific binding of radioactivity to the plate in the absence of a protein kinase but in the presence of the substrate. The difference between high and low control was taken as 100 % activity. The residual activity (in %) for each well of a particular plate was calculated by using the following formula:

Res. Activity (%) = 100 × [(cpm of compound – low control) / (high control – low control)]

The residual activities for each concentration and the compound IC_{50} values were calculated using Quattro Workflow V2.1.0.9.

2.10.3. Determination of cytotoxicity

2.10.3.1. L5178Y mouse lymphoma cells

The cytotoxicity tests aganst L5178Y mouse lymphoma cells were carried out using the MTT assay by Prof. W.E.G. Müller at Mainz University, Germany, and compared to that of untreated controls [Carmichael *et al.*, 1987]. From the test samples, stock solutions in ethanol 96% (v/v) were prepared. Exponentially growing cells were harvested, counted and diluted appropriately. Of the cell suspension, 50 μL containing 3750 cells were pipette into 96-well microtiter plates. Subsequently, 50 μL of a solution of the test samples containing the appropriate concentration was added to each well. The concentration range was 3 and 10 μg/mL. The small amount of ethanol present in the wells did not affect the experiments. The test plates were incubated at 37 °C with 5% CO_2 for 72 hrs. A solution of 3-(4,5-dimethylthiazol-2-yl)-2,5-diphenyltetrazolium bromide (MTT) was prepared at 5 mg/mL in phosphate buffered saline (PBS; 1.5 mM KH_2PO_4, 6.5 mM Na_2HPO_4, 137 mM NaCl, 2.7 mM KCl; pH 7.4) and from this solution, 20 μL was pipetted into each well. The yellow MTT penetrates the healthy living cells and in the presence of mitochondrial dehydrogenases, MTT is transformed to its blue formazan complex. After an incubation period of 3 hours and 45 minutes at 37 °C in a humidified incubator with 5% CO_2, the medium was centrifuged (15 min, 20 °C, 210 × g) with 200 μL DMSO, the cells were lysed to liberate the formed formazan products. After thorough mixing, the absorbance was measured at 520 nm using a scanning microtiter-well spectrophotometer. The colour intensity is correlated with the number of healthy living cells. Cell survival was calculated using the formula:

$$\text{Survival (\%)} = 100 \times \frac{(\text{absorbance of treated cells} - \text{absorbance of culture medium})}{(\text{absorbance of untreated cells} - \text{absorbance of culture medium})}$$

All experiments were carried out in triplicates and repeated three times. As controls, media with 0.1% EGMME/DMSO were included in the experiments.

PBS buffer, PH 7.4:
1.5 mM KH_2PO_2
6.5 mM Na_2HPO_4
137 mM NaCl
2.7 mM KCl

2.10.3.2. H4IIE rat hepatoma, Hct-116 human colon carcinoma and C6 rat glioma cells

The cytotoxicity tests aganst H4IIE rat hepatoma cells, Hct-116 human colon carcinoma cells and C6 rat glioma cells were carried out in the working group of Dr. Wim Wätjen (Institute of Toxicology, Heinrich-Heine Universität, Düsseldorf) by Dipl. Biol. Sven Ruhl and Mr. Christian Limper.

Tumor cell lines were grown in DMEM medium containing 4.5 g/L glucose and 2 mmol/L L-glutamine, supplemented with fetal bovine serum (FBS): metabolically active H4IIE rat hepatoma cells (10%) and rat C6 glioma cells (5%); Hct-116 human colon carcinoma cells were grown in RPMI medium containing 10% FCS. The cell culture medium contained 100 units/mL penicillin and 100 μg/mL streptomycin and was changed twice per week. The cells were maintained in a humidified atmosphere at 37 °C with 5% CO_2.

The effect of isolated compounds on cell viability was determined using the MTT assay according to a modified protocol of [Mosmann, 1983]. Cells were plated on 96-multiwell plates with 1×10^4–4×10^4 cells/well depending on the used cell line. The cells were allowed to attach for 24 h and then treated with different concentrations of the isolated compound for 24 h. After this treatment the medium was changed and the cells were incubated for 2 h under cell culture conditions with 20 μg/ml MTT. After this incubation time the cells were lysed with 50% ethanol/49% water/1% acetic acid. The concentration of reduced MTT as a marker for cell viability was measured photometrically (560 nm).

2.10.4. Determination of apoptotic cell death (Apo-ONE assay)

Caspase-3/7-activity was measured using the Apo-ONE® homogeneous caspase 3/7 assay (Promega) according to the manufacturer's protocol. Briefly, 50000 cells/well were plated on 96-multiwell plates, allowed to attach for 24 h and treated with tested compounds for 24 h. Then, 50 μL of

Apo-ONE Caspase-3/7-reagent was added and the increase in fluorescence was measured at 37 °C for 3 h (excitation: 485 nm, emission: 535 nm). Apoptotic cell death was further investigated by visualizing nuclear fragmentation using Hoechst 33342 staining essentially as described by [Michels *et al.*, 2006].

2.10.5. Determination of necrotic cell death (LDH assay)

The activity of the cellular enzyme lactate dehydrogenase (LDH) in the cell culture medium was taken as marker for necrotic cell death (membrane disruption). 10.000 cells/well were plated on 96 well plates and allowed to grow for 24 h. The compounds were added for 24 h, then LDH activity in the supernatant was detected using the LDH Cytotoxicity detection Assay® (Promega) according to the instruction of the manufacturer. To 50 µL of supernatant a defined concentration of LDH substrate (tetrazolium salt) was added. The formation of the reaction product (formazan) was monitored in a Wallac Victor 1420 multichannel reader (490 nm and 590 nm). Results are given as "% of maximal LDH activity" +/− SD. Maximal LDH activity (=100% necrotic cells) was reached by addition of 5 µL cell lysis reagent, minimal LDH activity (=0% necrotic cells) was defined as value of untreated cells. The viability of the corresponding cells was detected using the MTT assay.

2.10.6. Determination of NF-κB inhibiting activity

The NF-κB inhibiting assay was carried out by Dr. Yvonni Chovolou at Institut for Toxicology, Heinrich-Heine University, Düsseldorf.

Cell transfection: H4IIE were stably transfected with HiFect (Amaxa) transfection reagent according to manufacture's protocol. Briefly, H4IIE cells were seeded at a density of 1.5×10^5 per 35 mm petri dish and incubated overnight. Cells were transfected with 1.6 µg pNF-κB-secreted embryonic alkaline phosphatase (SEAP) and 0.4 µg pTKHyg by using 10 µL HiFect® (Amaxa) transfection reagent in 1 mL serum free DMEM medium. 48 h after transfection, cells were split 1:5 into 100 mm petri dishes and stably transfected cell clones (H4IIE-SEAP) were selected with 400 µg/mL hygromycin.

Reporter gene assay: H4IIE-SEAP cells were seeded at a density of 2×10^5 cells per 24-well plates and incubated for 48 h. Cells were preincubated with various concentrations of each tested compound for 3 h and then stimulated with 4 ng/mL tumor necrosis factor-alpha (TNF-α) for 24 h. Activity of the reporter enzyme (SEAP) in the medium was measured using a chemiluminescence-based detection method. In brief, 30 μL conditioned cell culture medium was mixed with 30 μL of 1 × dilution buffer (50 mM Tris, 150 mM NaCl, pH 7.4) and incubated for 30 min at 65 $^{\circ}$C to heat inactivate endogenous alkaline phosphatase activity. Samples were mixed with 30 μL assay buffer (2 M diethanolamine, 28 mM L-homoarginine) and 30 μL CSPD substrate (Tropix). After 15 min incubation at dark, SEAP activity was measured in a plate luminometer (Victor 1420, Wallac). In each experiment it was verified that inhibition of NFκB-dependent SEAP activity was not due to cytotoxic effects by MTT assay essentially as described in the section "Determination of cell viability".

3. Results

3.1. Compounds isolated from the Mongolian medicinal plant *Scorzonera radiata*

Scorzonera is a genus of the family Asteraceae that includes more than 150 species, which are distributed in the temperate zones of Eurasia [Tulin *et al.*, 1976; Malyschev and Peschkova, 1979; Mabberley, 1997]. Eleven species of *Scorzonera* are found on the Mongolian plateau, two of which are endemic [Grubov, 1982; Gubanov, 1996; Liu *et al.*, 2001]. Most of the Mongolian *Scorzonera* spp. are used in traditional medicine and as forage for livestock, especially in desert regions [Sancher *et al.*, 2003]. *Scorzonera radiata* Fisch. (Asteraceae) is a typical mesophyte and a perennial herbaceous rosette plant, which is widely distributed in Hangai, Douria, Kobodo, Mongolia-Altai, and East-Mongolia [Liu *et al.*, 2002]. It grows at an elevation between 900 and 1800 m above sea level, on rubble slopes, in underbrush, in forest fringe, in meadow, and in the gravel zone of floodplains. All parts of the plant are used in Mongolian folk medicine for the treatment of poisonous ulcers, for fever caused by bacterial and viral infections, and for its diuretic and galactagogue properties [Ligaa, 1996; He, 2004].

No phytochemical studies have been reported for *S. radiata*, although other species of this genus have been studied extensively, resulting in the isolation of sesquiterpenes, [Öksüz *et al.*, 1990; MacLeod and Ames, 1991; Bryanskii *et al.*, 1992; Zidorn *et al.*, 2000; Li *et al.*, 2004; Tsevegsuren *et al.*, 2007] lignans, [Bryanskii *et al.*, 1992; Tolstikhina *et al.*, 1999] neolignans, [Tolstikhina *et al.*, 1988; Tolstikhina and Semenov, 1998] phenolic acids, [Zidorn *et al.*, 2005; Tsevegsuren *et al.*, 2007] triterpene derivatives, [Tolstikhina *et al.*, 1988; Öksüz *et al.*, 1990; Menichini *et al.*, 1994] stilbene derivatives, [Zidorn *et al.*, 2000; Zidorn *et al.*, 2002; Zidorn *et al.*, 2003; Sari *et al.*, 2007] dihydroisocoumarins, [Paraschos *et al.*, 2001; Sari *et al.*, 2007] and flavonoids [Menichini *et al.*, 1994].

The study of the Mongolian medicinal plant *Scorzonera radiata* resulted in the isolation of five new dihydrostilbene derivatives (**1**–**5**), ten quinic acid derivatives (**6**–**15**), seven flavonoids (**16**–**22**), two coumarins (**23**,**24**), five phenolic compounds (**25**–**29**), and one norsesquiterpenoid glycoside (**30**).

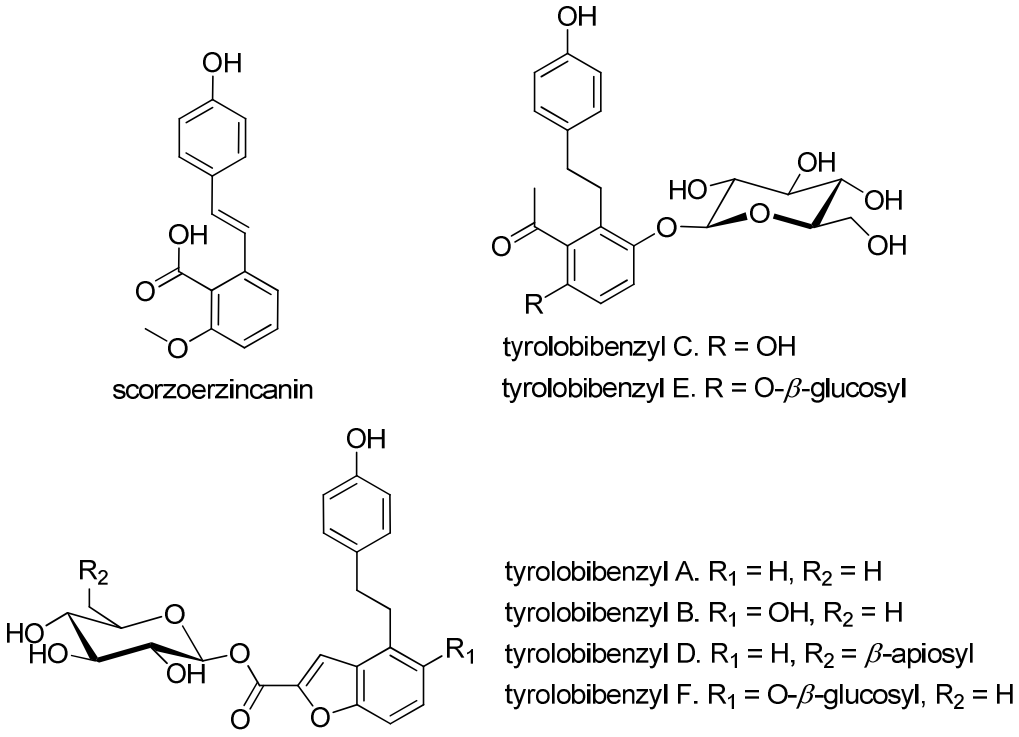

Figure 3.1 Reported stilbene derivatives isolated previously from the genus *Scorzonera*

3.1.1. Scorzodihydrostilbene A (1, new compound)

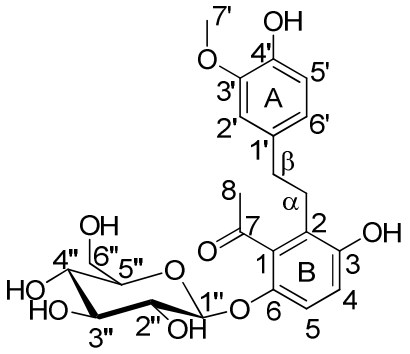

Molecular formula:	$C_{23}H_{28}O_{10}$
Molecular weight:	464.46
Amount:	34.7 mg

Compound **1**, obtained as a pale yellow solid, was shown to have the molecular formula $C_{23}H_{28}O_{10}$ as determined by HRESIMS (*m/z* 482.2021 $[M + NH_4]^+$). The ^1H NMR spectrum measured in CD_3OD (Figure 3.2) showed a pair of doublets with coupling constants of 8.8 Hz typical of *ortho*-coupled aromatic protons (H-4 and H-5). In the aromatic region, further resonances indicative for an ABX system [δ_H 6.64 (d, J = 1.6 Hz), 6.66 (d, J = 7.9 Hz), and 6.55 (dd, J = 7.9 and 1.6 Hz)] were observed, which were assigned to a 1,3,4-trisubstituted phenyl unit. Two methyl resonances (δ_H 3.77 and 2.31) indicated an aromatic *O*-methyl group and a methyl ketone function. From the ^1H NMR spectrum, along with analysis of the ^{13}C NMR data (Figure 3.5), two aromatic rings, two methylene groups (δ_H 2.70, m), and one sugar unit (δ_H 4.76–3.33, m) were inferred to be present. The assignments were supported by analysis of the ^1H-^1H COSY (Figure 3.6) and HMBC (Figure 3.8–3.10) spectra of **1**. Assignment of the *O*-methyl group at C-3' was determined from the HMBC cross-peak of the methyl singlet at δ_H 3.77 with δ_C 148.7, which further correlated with the *meta*-coupled proton at $\delta_{H\text{-}5'}$ 6.66 that was part of the ABX system. The methyl singlet at δ_H 2.31 gave a cross-peak with the carbonyl carbon at δ_C 208.7 and the aromatic carbon at $\delta_{C\text{-}1}$ 135.5, respectively. In the HMBC spectrum, carbons C-1' and C-2 correlated with methylene protons Hα and Hβ at δ_H 2.70, which in turn showed HMBC connectivities with C-1 (δ 135.5)/C-3 (δ 152.4) and C-2' (δ 113.3)/C-6' (δ 121.9), respectively. These HMBC correlations allowed the carbon and proton assignments of the dihydrostilbene framework in compound **1**.

The β-glucose moiety was evident from the ^{1}H NMR resonances of four oxymethine protons at δ_H 3.40, 3.36, 3.34, and 3.33, together with one pair of methylene protons at δ_H 3.85 and 3.66 for H_2-6" and an anomeric proton at δ_H 4.76. By inspection of the ^{13}C NMR spectrum, these resonances were in agreement with four oxymethine resonances at δ_C 78.2, 78.1, 74.9, and 71.4; one methylene cabon at δ_C 62.7; and an anomeric carbon at δ_C 103.7, all of which are characteristic of a β-glucopyranose unit. Butanolysis followed by capillary glc of the trimethylsilylated (–)-2-butyl derivatives established the sugar as β-D-glucose. The assignments for the glucose moiety were corroborated by analysis of the ^{1}H-^{1}H COSY and HMBC spectra of **1**. Attachment of the glucose at C-6 was deduced from the HMBC correlation between the anomeric proton H-1" and the oxygenated aromatic carbon (C-6) at δ_C 147.8, which in turn gave two cross-peaks with H-4 at δ_H 6.79 and H-5 at δ_H 6.97, respectively. Moreover, H-5 correlated with C-1, and H-4 correlated with C-2 as observed in the HMBC spectrum. The connectivity of the glucose to C-6 of ring B was also evident from the ^{13}C NMR chemical shift of the C-6-oxygenated carbon, which was shielded at δ_C 147.8 compared to tyrolobibenzyl C, which has a free OH group at C-6 (δ_C 150.4) [Zidorn *et al.*, 2000]. The chemical shift of C-3 (δ_C 152.4) bearing an OH group was deshielded compared to tyrolobibenzyl C (δ_C 150.5), which is substituted with a glucose moiety at this position.

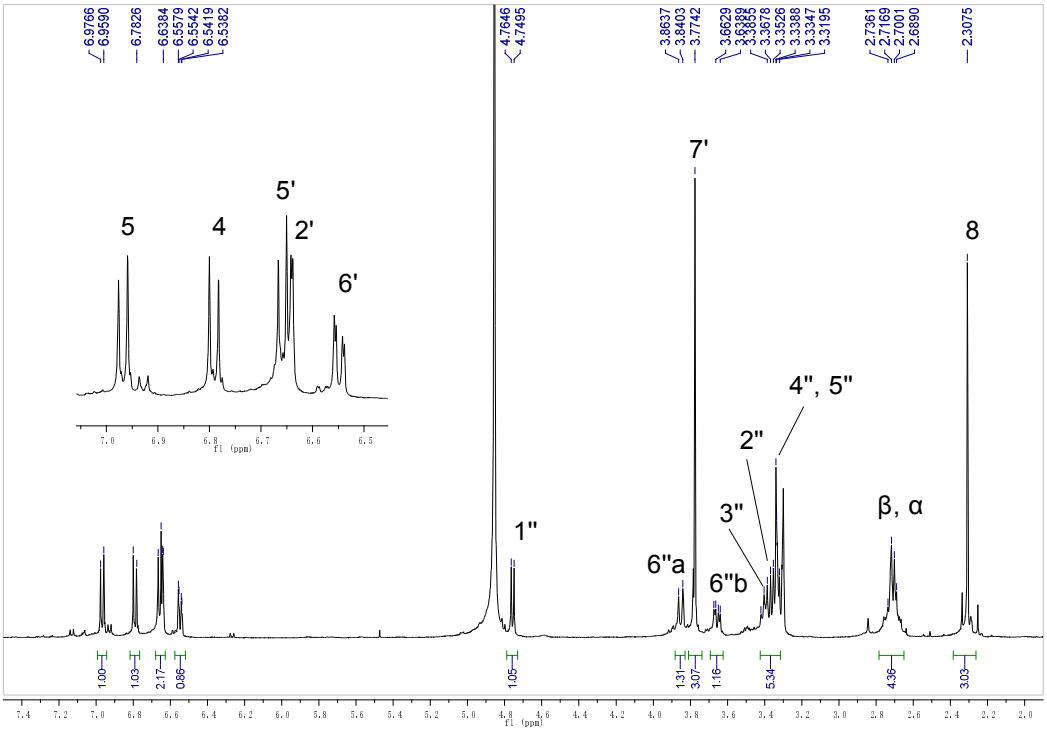

Figure 3.2 ^{1}H NMR spectrum of compound **1**

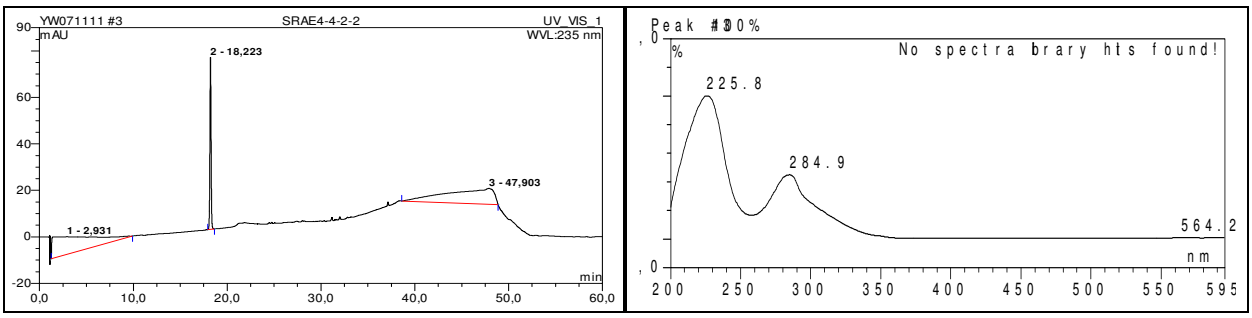

Figure 3.3 HPLC chromatogram and UV spectrum of compound **1**

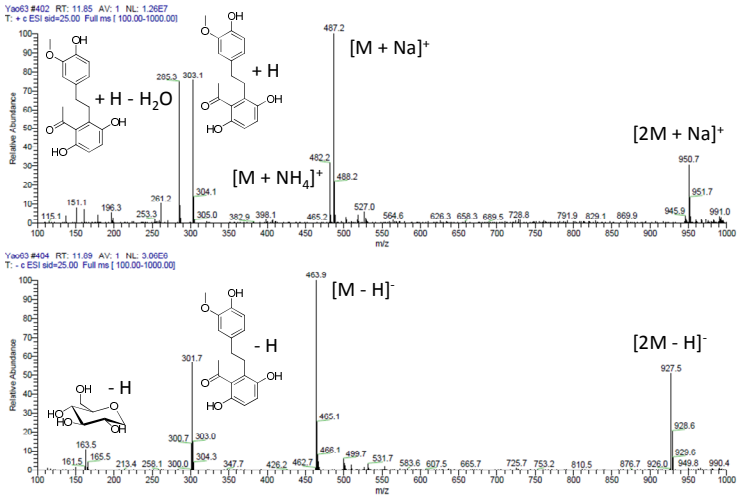

Figure 3.4 ESI-MS spectrum of compound **1**

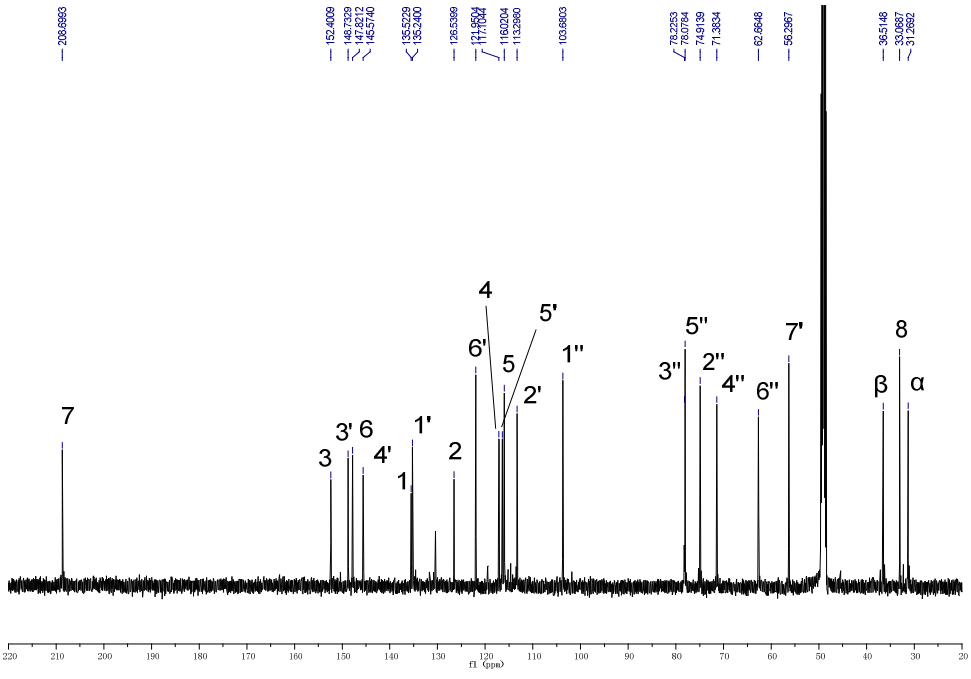

Figure 3.5 ^{13}C NMR spectrum of compound **1**

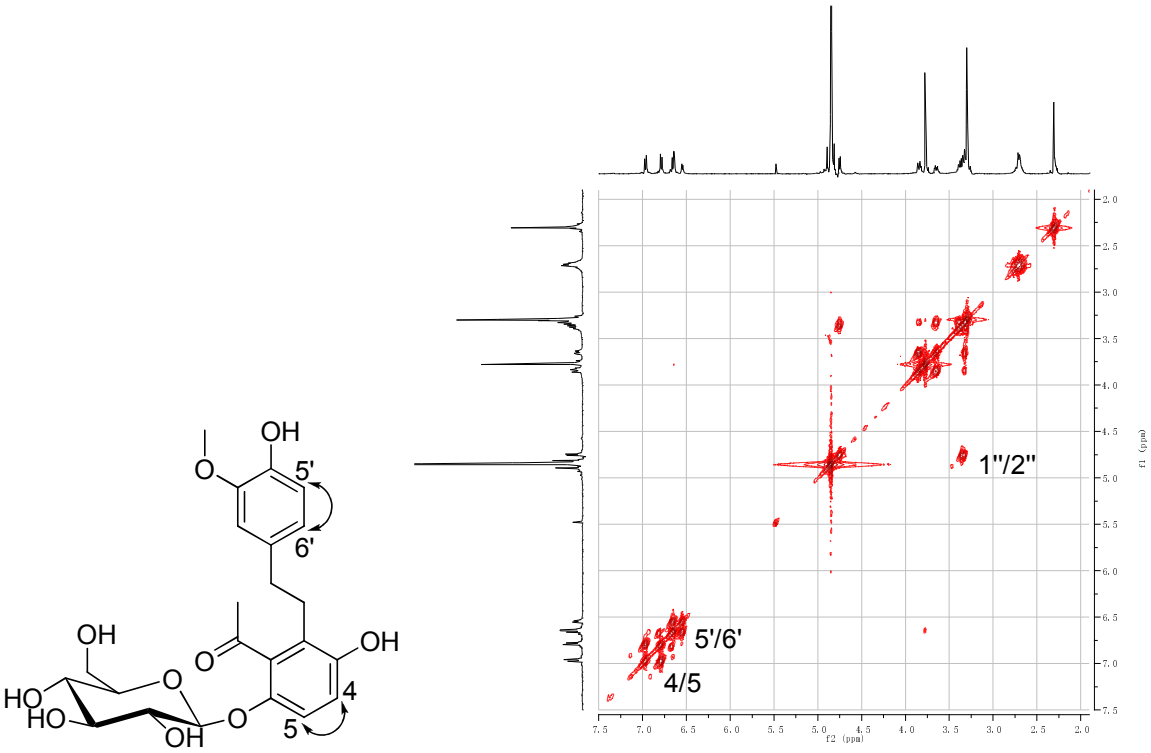

Figure 3.6 ^{1}H-^{1}H COSY spectrum of compound **1**

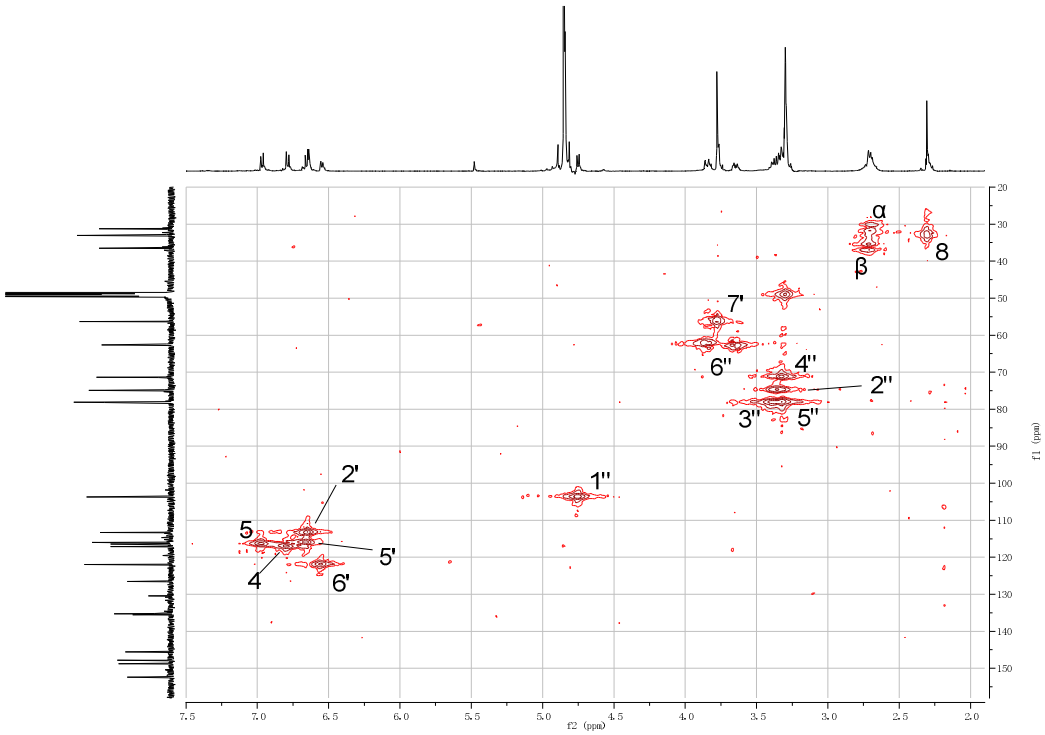

Figure 3.7 HMQC spectrum of compound **1**

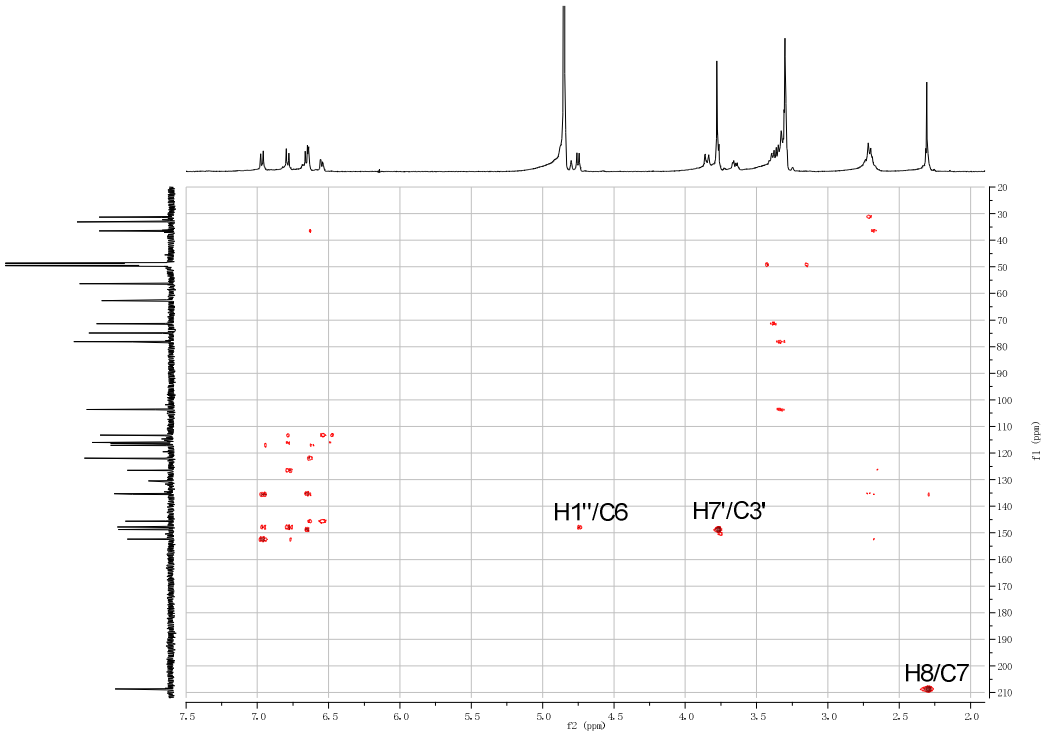

Figure 3.8 HMBC spectrum of compound **1**

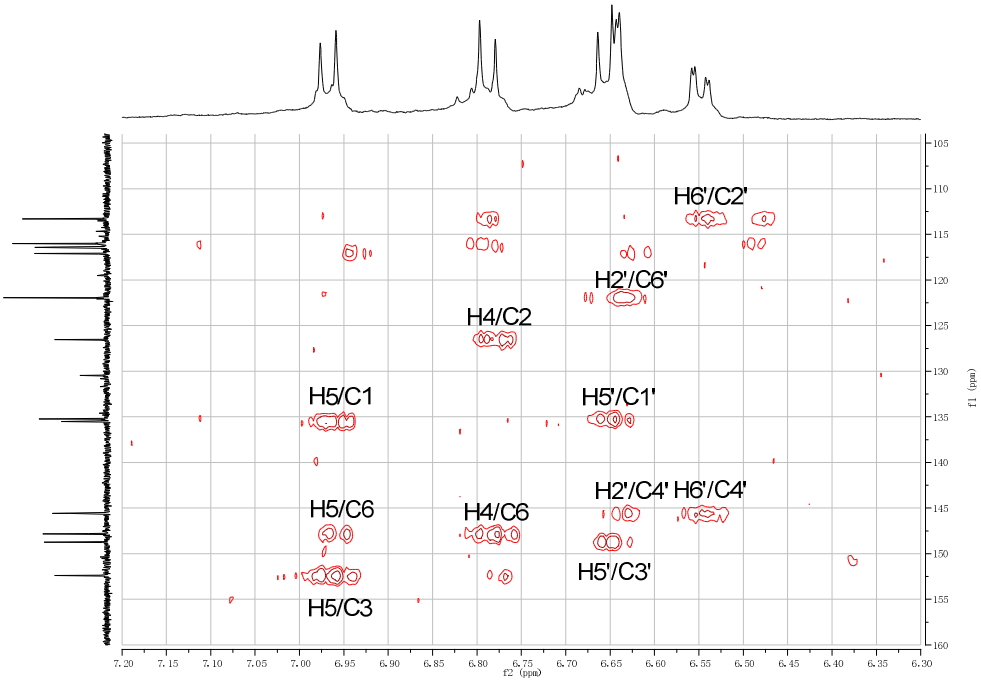

Figure 3.9 HMBC spectrum of the aromatic region of compound **1**

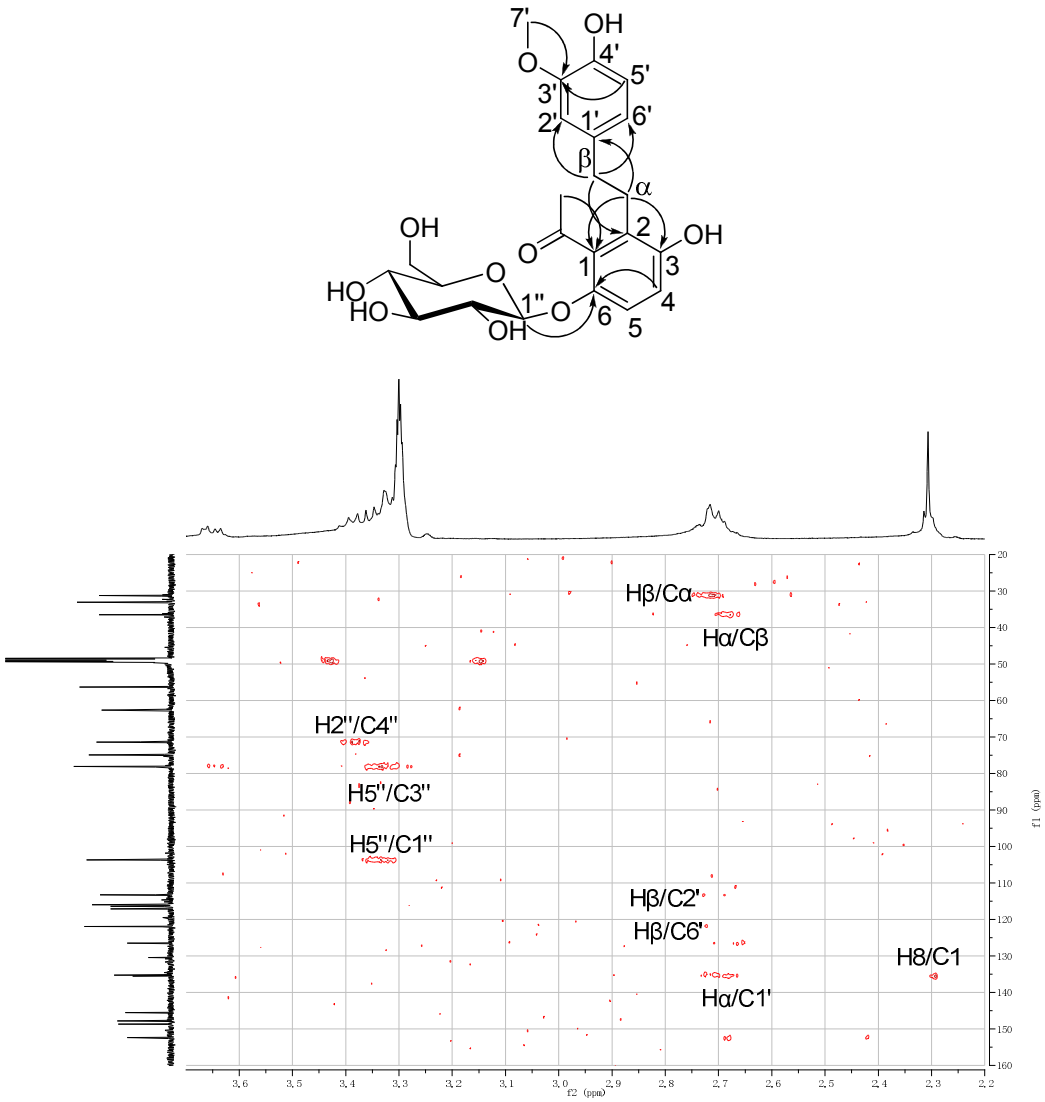

Figure 3.10 HMBC spectrum of the aliphatic region of compound **1**

Table 3.1 NMR spectroscopic data of compound **1** (CD_3OD, 500 MHz)

Position	δ_C	δ_H (mult., *J* in Hz)	COSY	HMBC
1	135.5, qC			
2	126.5, qC			
3	152.4, qC			
4	117.1, CH	6.79, d (8.8)	5	C2, C6
5	116.4, CH	6.97, d (8.8)	4	C1, C3, C6
6	147.8, qC			
7	208.7, qC			
8	33.1, CH_3	2.31, s		C1, C7
α	31.3, CH_2	2.70, m[a]	β	Cβ, C1′
β	36.5, CH_2	2.70, m[a]	α	Cα, C2′, C6′
1′	135.2, qC			
2′	113.3, CH	6.64, d (1.6)		C4′, C6′
3′	148.7, qC			
4′	145.6, qC			
5′	116.0, CH	6.66, d (7.9)	6′	C1′, C3′
6′	121.9, CH	6.55, dd (7.9, 1.6)	5′	C2′, C4′
7′	56.3, CH_3	3.77, s		C3′
1″	103.7, CH	4.76, d (7.6)	2″	C6
2″	74.9, CH	3.36, m[a]	1″	C4″
3″	78.2, CH	3.40, m[a]		
4″	71.4, CH	3.34, m[a]		
5″	78.1, CH	3.33, m[a]	6″a, 6″b	C1″, C3″
6″a	62.7, CH_2	3.85, dd (12.0, 1.3)	6″b, 5″	
6″b		3.66, dd (12.0, 5.4)	6″a, 5″	

[a] Overlapped signals assigned by ^1H-^1H COSY, HMBC, and HMQC spectra without designating multiplicity.

3.1.2. Scorzodihydrostilbene B (2, new compound)

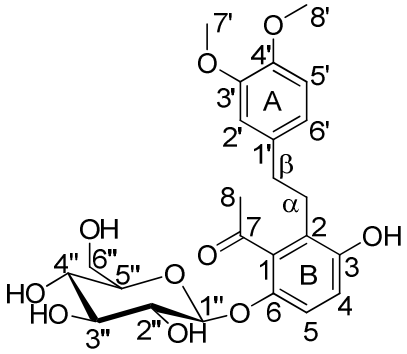

Molecular formula:	$C_{24}H_{30}O_{10}$
Molecular weight:	478.49
Amount:	55.3 mg

Compound **2** was isolated as a pale yellow solid with the molecular formula $C_{24}H_{30}O_{10}$, as determined by HRESIMS (*m/z* 496.2177 $[M + NH_4]^+$), indicating the presence of an additional CH_3 group compared to **1**. Compound **2** is a derivative of **1**, which was deduced from inspection of the ^1H and ^{13}C NMR spectra of **2** (Figure 3.13 and 3.14), which are almost superimposable to those of **1**. The only obvious difference in the NMR spectra between **1** and **2** was observed for the second *O*-methyl resonance at δ_H 3.75 in the ^1H NMR spectrum of **2**. This methoxy group was assigned at C-4' of ring A as suggested by the HMBC spectrum of **2**. This assignment was corroborated by the 3.1 ppm downfield shift of the C-4' resonance of **2** as compared to that of **1**. Moreover the resonances for H-5' were shifted downfield by 0.14 ppm compared to that of **1**, because of the inductive effect of the methoxy group at C-4'.

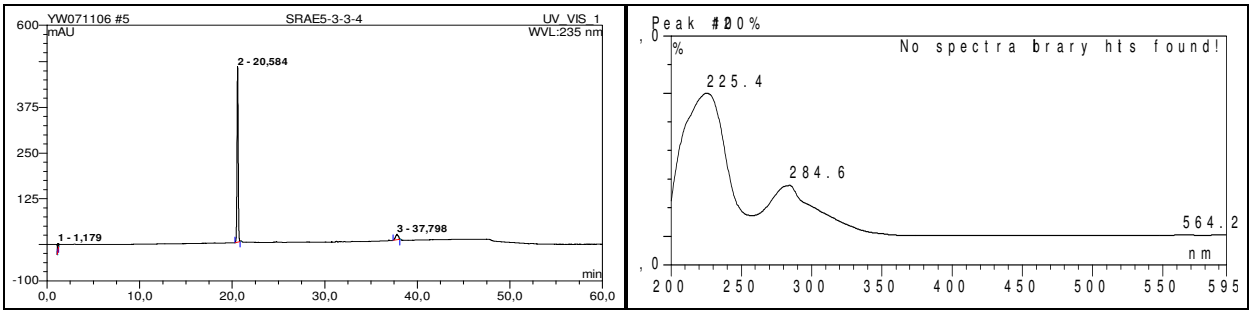

Figure 3.11 HPLC chromatogram and UV spectrum of compound **2**

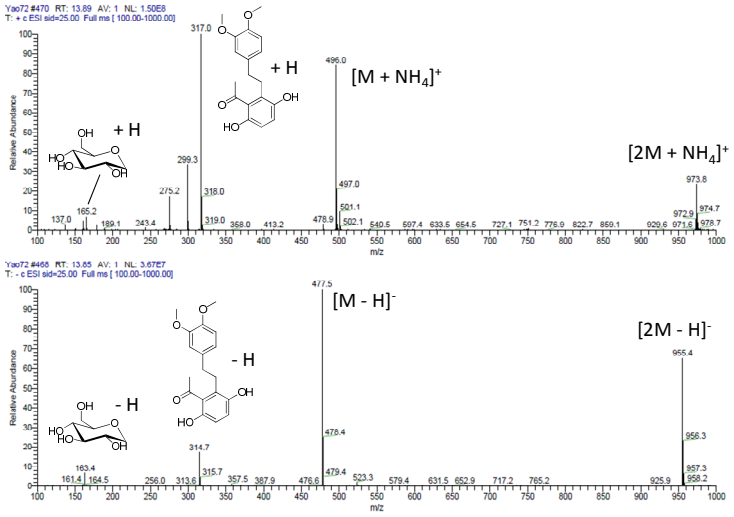

Figure 3.12 ESI-MS spectrum of compound **2**

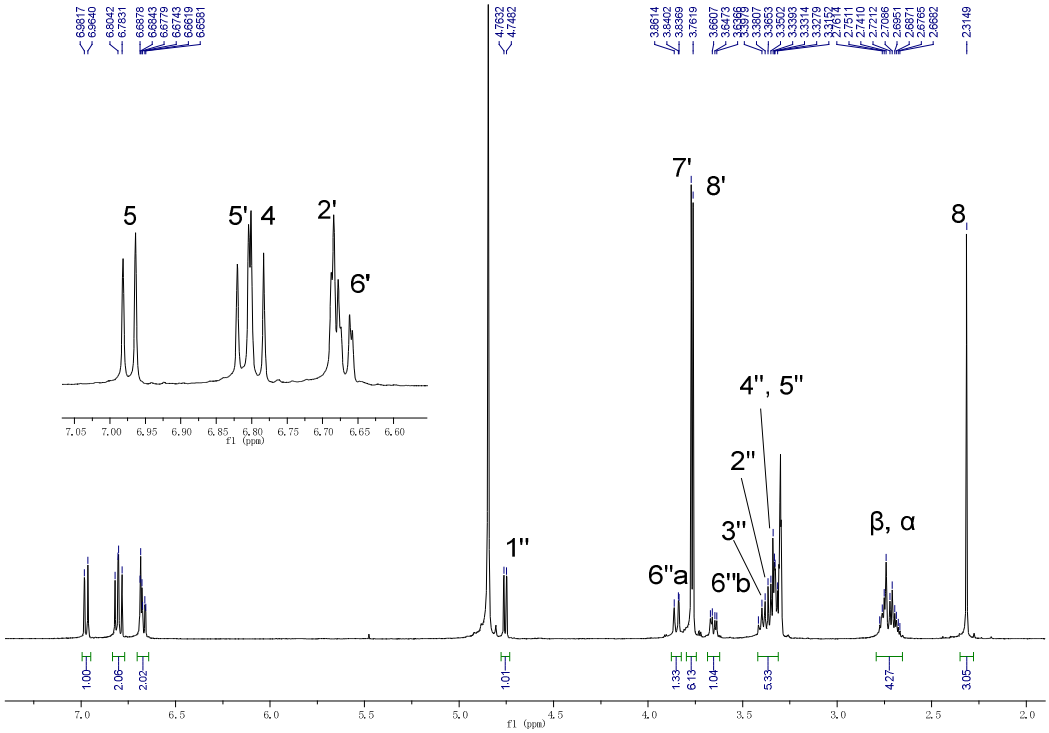

Figure 3.13 ^{1}H NMR spectrum of compound **2**

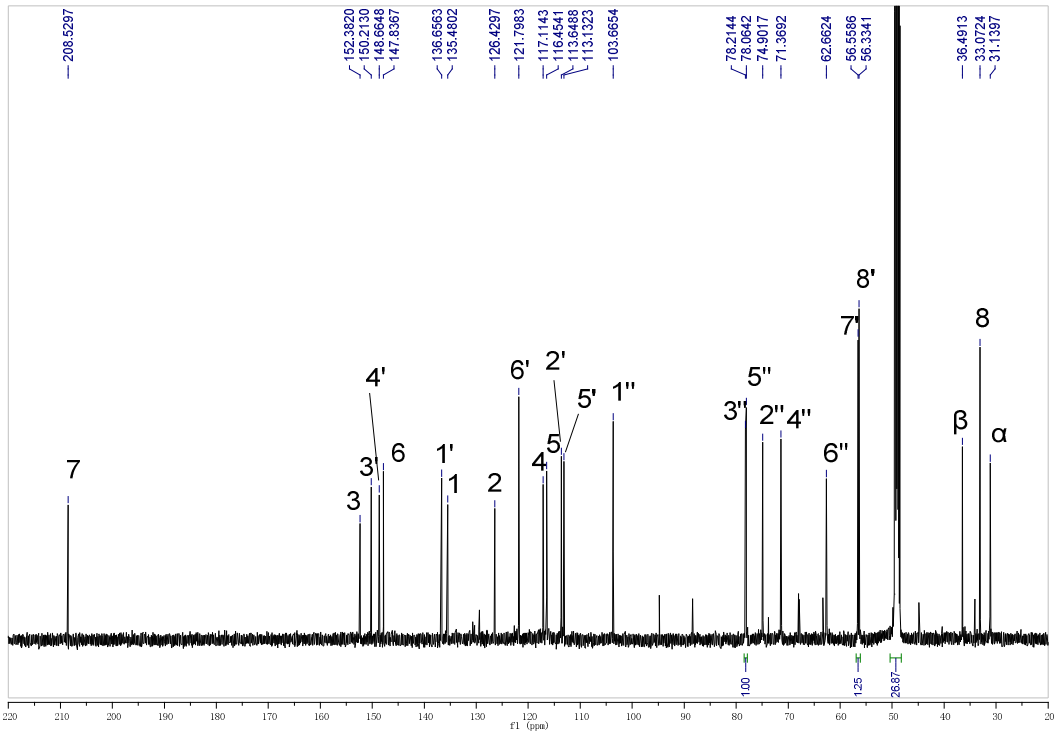

Figure 3.14 ^{13}C NMR spectrum of compound **2**

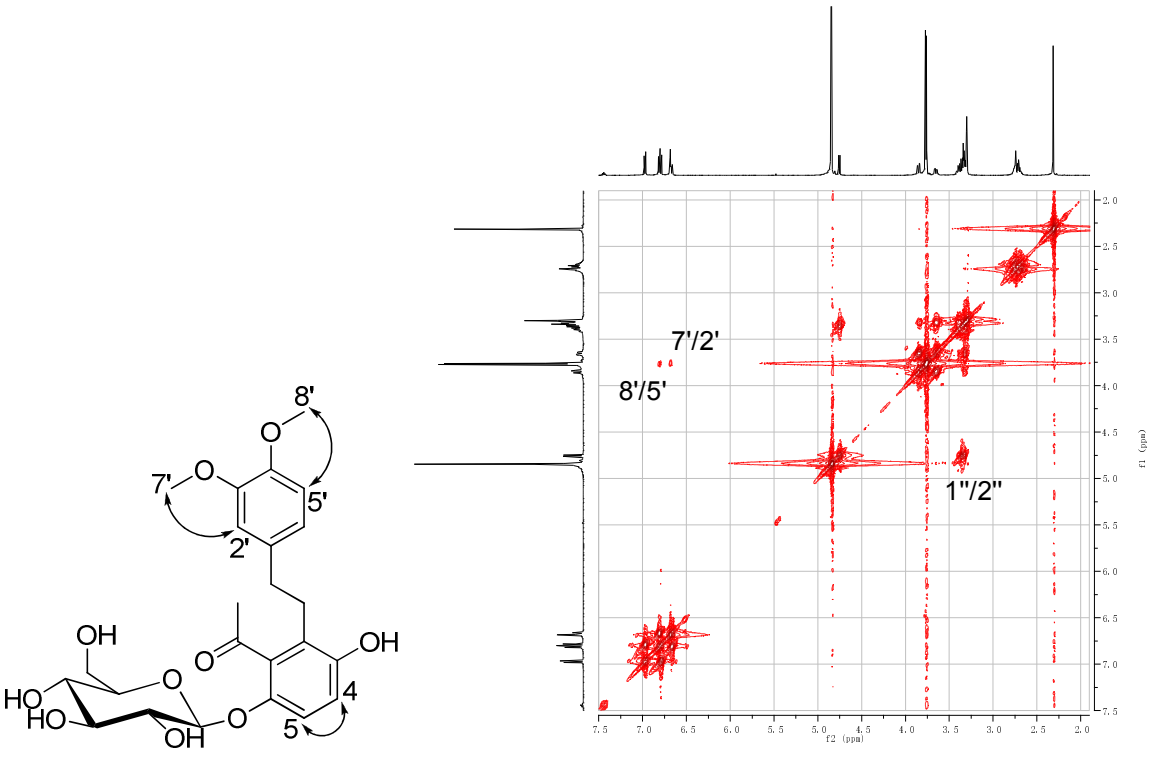

Figure 3.15 ^{1}H-^{1}H COSY spectrum of compound **2**

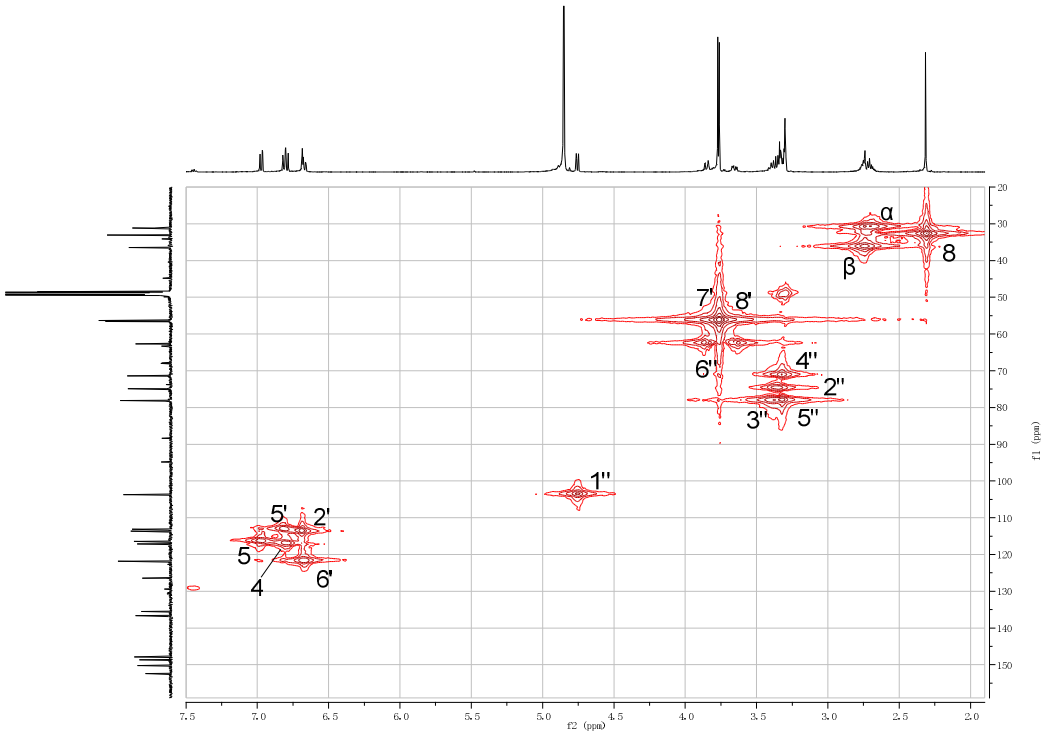

Figure 3.16 HMQC spectrum of compound **2**

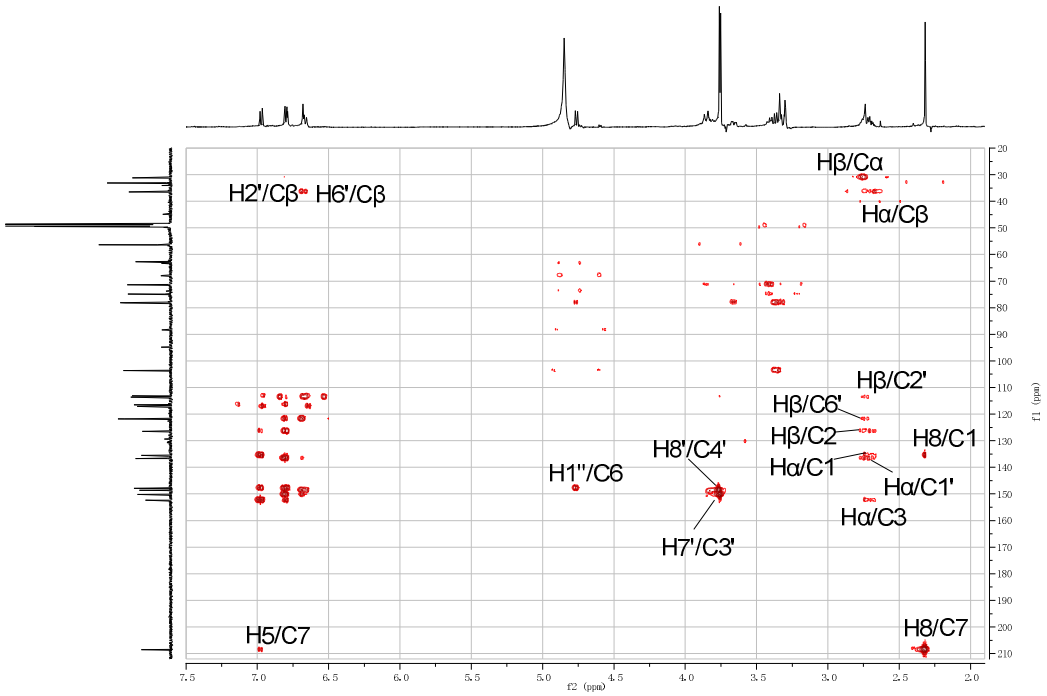

Figure 3.17 HMBC spectrum of compound **2**

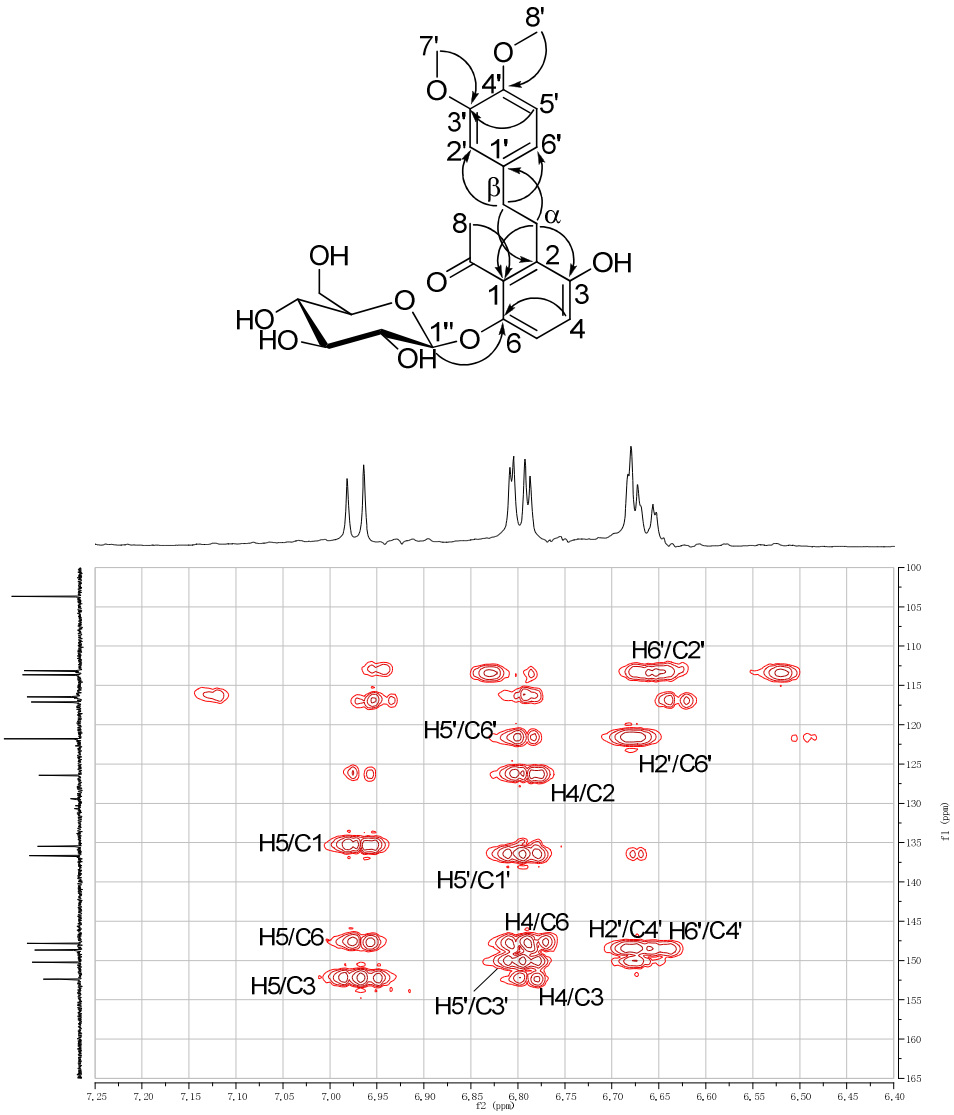

Figure 3.18 HMBC spectrum of the aromatic region of compound **2**

Table 3.2 NMR spectroscopic data of compound **2** (CD_3OD, 500 MHz)

Position	δ_C	δ_H (mult., *J* in Hz)	COSY	HMBC
1	135.5, qC			
2	126.4, qC			
3	152.4, qC			
4	117.1, CH	6.80, d (8.8)	5	C2, C3, C6
5	116.5, CH	6.97, d (8.8)	4	C1, C3, C6
6	147.8, qC			
7	208.5, qC			
8	33.1, CH_3	2.32, s		C1, C7
α	31.1, CH_2	2.71, m[a]	β	Cβ, C1, C1′, C3
β	36.5, CH_2	2.75, m[a]	α	Cα, C2, C2′, C6′
1′	136.7, qC			
2′	113.6, CH	6.68, d (1.9)		C4′, C6′
3′	150.2, qC			
4′	148.7, qC			
5′	113.1, CH	6.80, d (8.2)	6′	C1′, C3′, C6′
6′	121.8, CH	6.66, dd (8.2, 1.9)	5′	Cβ, C2′, C4′
7′	56.6, CH_3	3.76, s		C3′
8′	56.3, CH_3	3.75, s		C4′
1″	103.7, CH	4.76, d (7.6)	2″	C6, C5″
2″	74.9, CH	3.37, m[a]	1″	C1″, C3″
3″	78.2, CH	3.40, m[a]		C2″, C4″
4″	71.4, CH	3.34, m[a]		C3″
5″	78.1, CH	3.33, m[a]	6″a, 6″b	C1″, C3″
6″a	62.7, CH_2	3.85, dd (12.0, 0.6)	6″b, 5″	C4″
6″b		3.66, dd (12.0, 5.1)	6″a, 5″	C4″, C5″

[a] Overlapped signals assigned by ^1H-^1H COSY, HMBC, and HMQC spectra without designating multiplicity.

3.1.3. Scorzodihydrostilbene C (3, new compound)

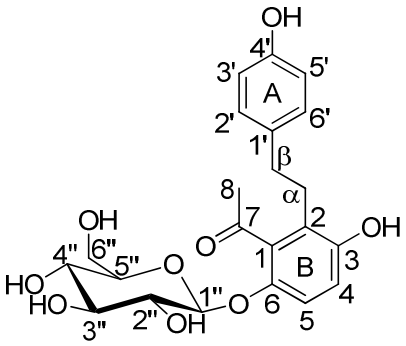

Molecular formula:	$C_{22}H_{26}O_9$
Molecular weight:	434.44
Amount:	14.1 mg

Congener **3** was obtained from the aerial parts of *S. radiata* as a pale yellow solid showing the molecular formula $C_{22}H_{26}O_9$, as determined from the positive HRESI mass spectrum (*m/z* 457.1469 $[M + Na]^+$). The main difference in the NMR spectra of **3** compared to those of **1** and **2** was observed with regard to the proton and carbon signals of the A-ring. The ^{1}H NMR spectrum of **3** (Figure 3.21) exhibited signals for the A-ring protons, which are typical of an AA'BB' system instead of an ABX system as present in compounds **1** and **2**. These differences in the ^{1}H NMR spectrum are mirrored by equally clear differences in the ^{13}C NMR spectrum of **3** (Figure 3.22) compared to those of **1** and **2**. Attachment of the *β*-glucose moiety to ring B at C-6 rather than at C-3 (as found for the known compound tyrolobibenzyl C) was confirmed on the basis of the HMBC cross-peak of the anomeric proton (H-1") at δ_H 4.76 with the aromatic carbon C-6 at δ 147.8. Compared with tyrolobibenzyl C, compound **3** differs from the latter only by the linkage of the *β*-glucose moiety in ring B [Zidorn *et al.*, 2000].

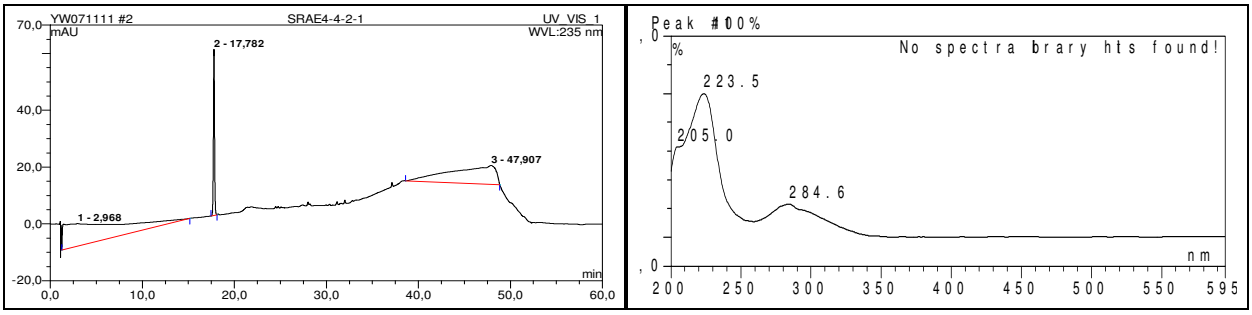

Figure 3.19 HPLC chromatogram and UV spectrum of compound **3**

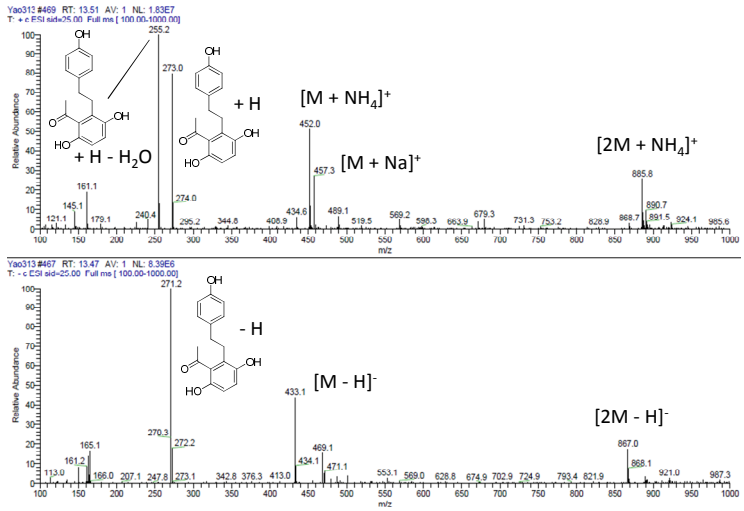

Figure 3.20 ESI-MS spectrum of compound **3**

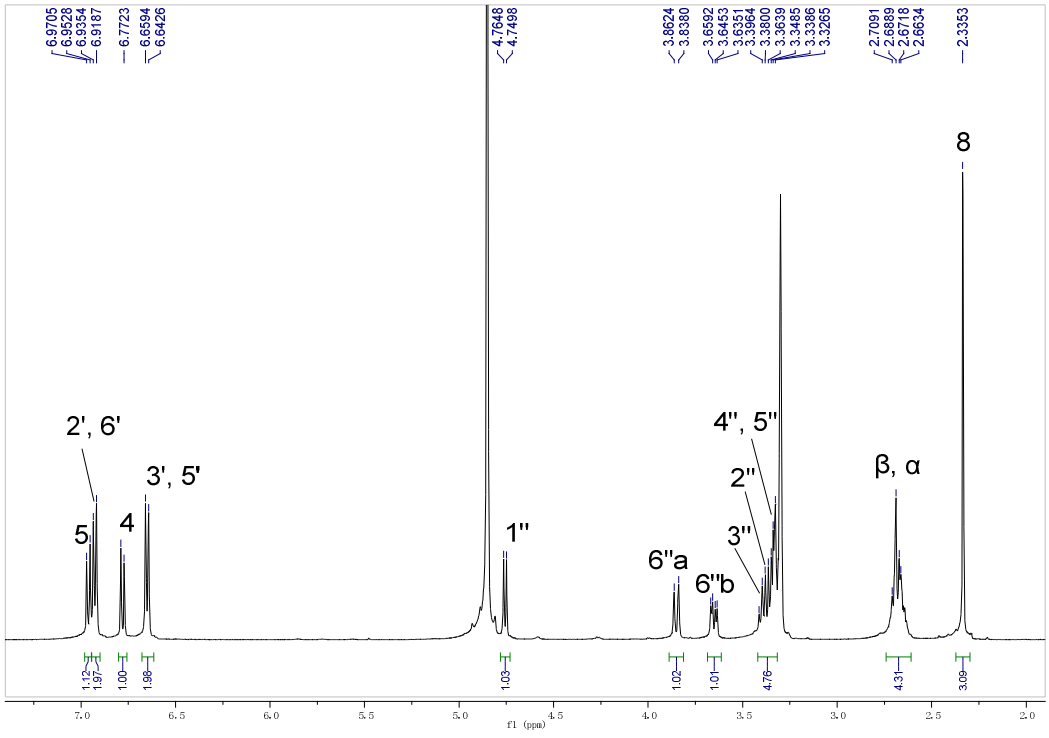

Figure 3.21 ^{1}H NMR spectrum of compound **3**

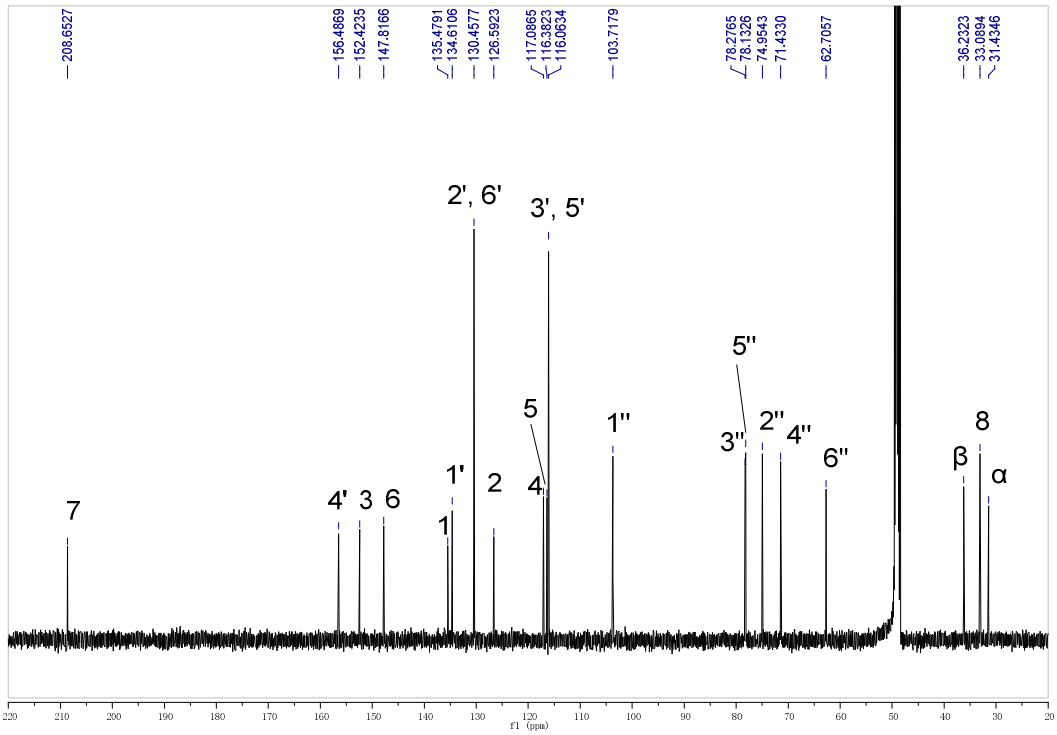

Figure 3.22 ^{13}C NMR spectrum of compound **3**

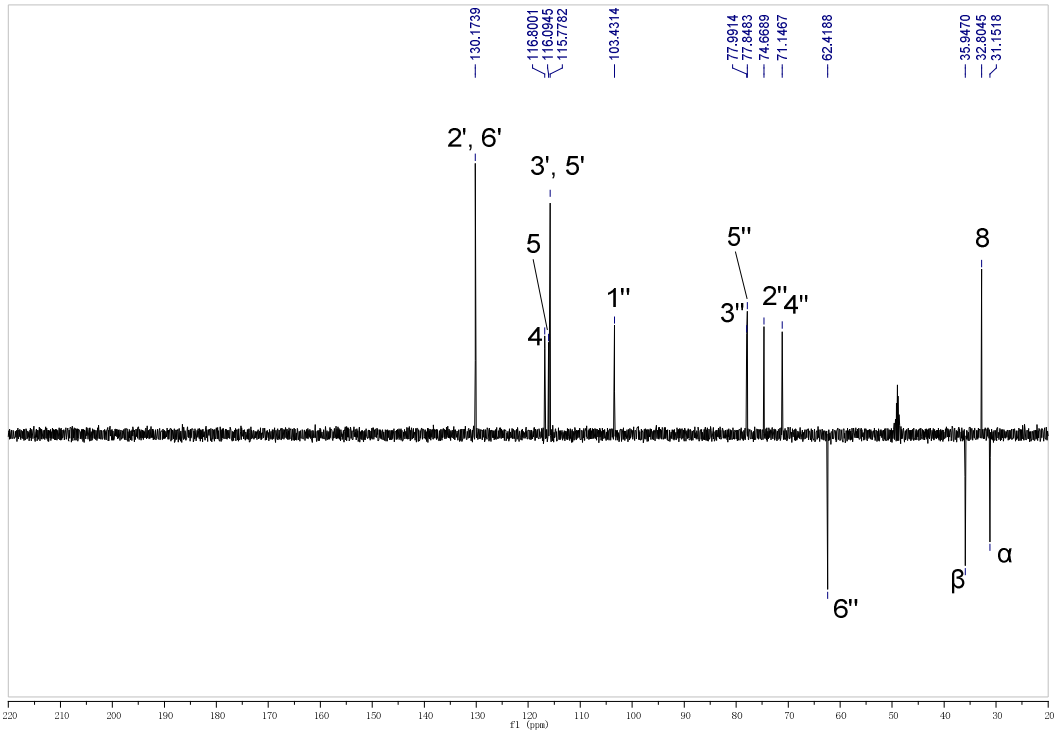

Figure 3.23 DEPT spectrum of compound **3**

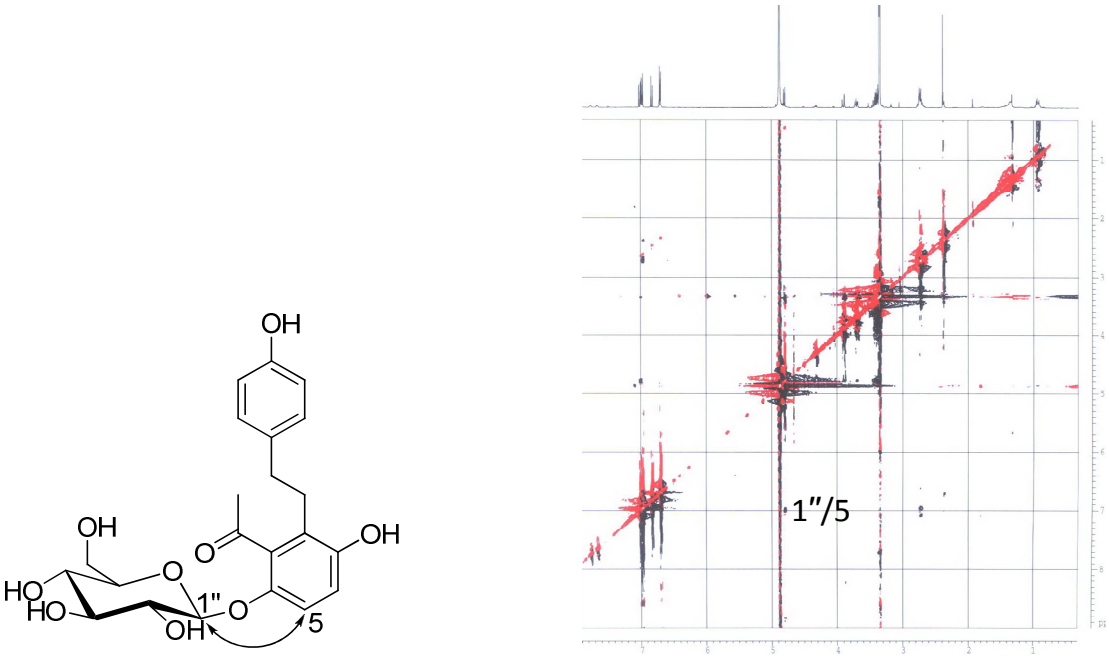

Figure 3.24 ROESY spectrum of compound **3**

Table 3.3 NMR spectroscopic data of compound **3** (CD_3OD, 500 MHz)

Position	δ_C	δ_H (mult., *J* in Hz)	ROESY
1	135.5, qC		
2	126.6, qC		
3	152.4, qC		
4	117.1, CH	6.78, d (8.8)	
5	116.4, CH	6.96, d (8.8)	1″
6	147.8, qC		
7	208.6, qC		
8	33.1, CH_3	2.33, s	3′, 5′
α	31.4, CH_2	2.66, m[a]	
β	36.2, CH_2	2.69, m[a]	2′, 6′
1′	134.6, qC		
2′	130.5, CH	6.93, d (8.5)	β
3′	116.1, CH	6.65, d (8.5)	8
4′	156.5, qC		
5′	116.1, CH	6.65, d (8.5)	8
6′	130.5, CH	6.93, d (8.5)	β
1″	103.7, CH	4.76, d (7.6)	5, 3″, 5″
2″	74.9, CH	3.37, m[a]	
3″	78.3, CH	3.40, m[a]	1″, 5″
4″	71.4, CH	3.34, m[a]	
5″	78.1, CH	3.33, m[a]	1″, 3″
6″a	62.7, CH_2	3.85, dd (12.0, 1.3)	
6″b		3.65, dd (12.0, 5.1)	

[a] Overlapped signals assigned by ^{1}H-^{1}H COSY, HMBC, and HMQC spectra without designating multiplicity.

3.1.4. Scorzodihydrostilbene D (4, new compound)

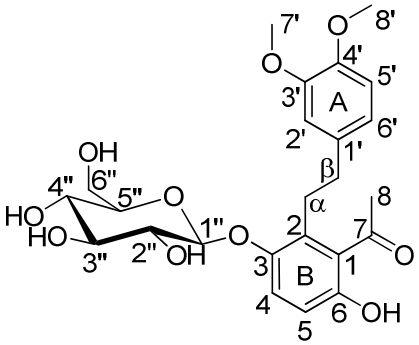

Molecular formula:	$C_{24}H_{30}O_{10}$
Molecular weight:	478.49
Amount:	3.4 mg

Congener **4** was obtained as a pale yellow solid with the molecular formula $C_{24}H_{30}O_{10}$, as indicated from the negative HRESI mass spectrum (*m/z* 523.1819 $[M - H + HCOOH]^-$), which was identical to the molecular formula of **2**. The compounds differed only with regard to the position of attachment of the glucose unit on ring B. An aromatic proton at δ_H 7.13 (H-4) showed a HMBC correlation with C-2 (δ_C 130.8), which implied the B-ring of **4** to be different from that of **2**. The attachment of the *β*-glucose moiety of compound **4** was inferred to be at C-3 rather than at C-6 as previously observed for **2**, which was confirmed from the ROESY correlation of the anomeric proton (H-1") at δ_H 4.80 with H-4 at δ_H 7.13 (Figure 3.27). The presence of the glucose substituent at C-3 was also indicated by the downfield shift of H-4 by −0.33 ppm and the upfield shift of H-5 by +0.32 ppm, compared to the respective signals in the ^{1}H NMR spectrum of compound **2**. Furthermore, when the ^{13}C NMR data of **4** were compared to those of **2**, the C-1, C-3, and C-5 signals of **4** were shifted upfield by +3.1, +1.7, and +1.7 ppm, while the C-2, C-4, and C-6 signals were shifted downfield by −4.4, −2.5, and −2.5 ppm, respectively, which implied that glycosylation had occurred at C-3 instead of at C-6.

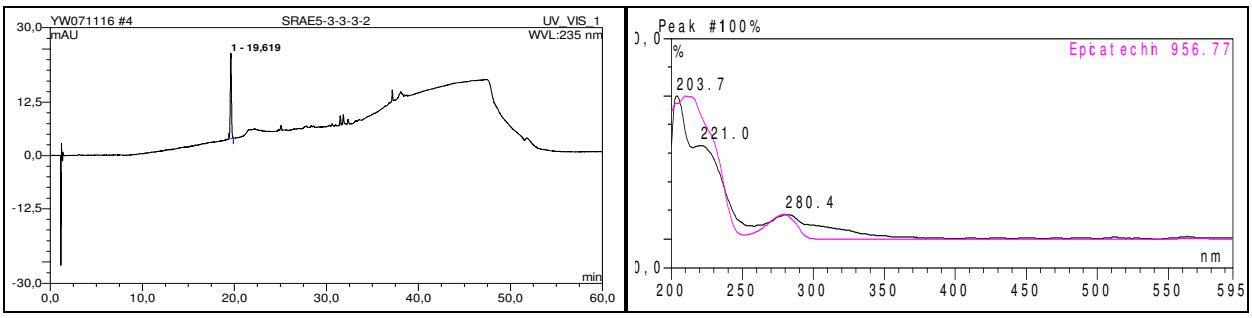

Figure 3.25 HPLC chromatogram and UV spectrum of compound **4**

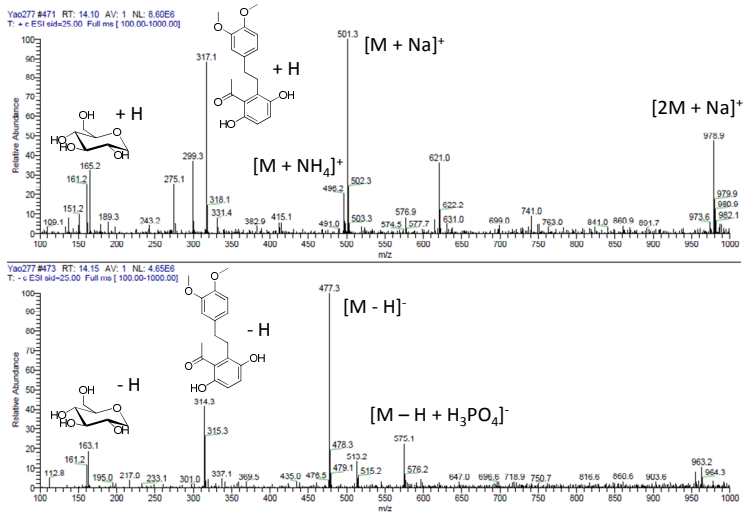

Figure 3.26 ESI-MS spectrum of compound **4**

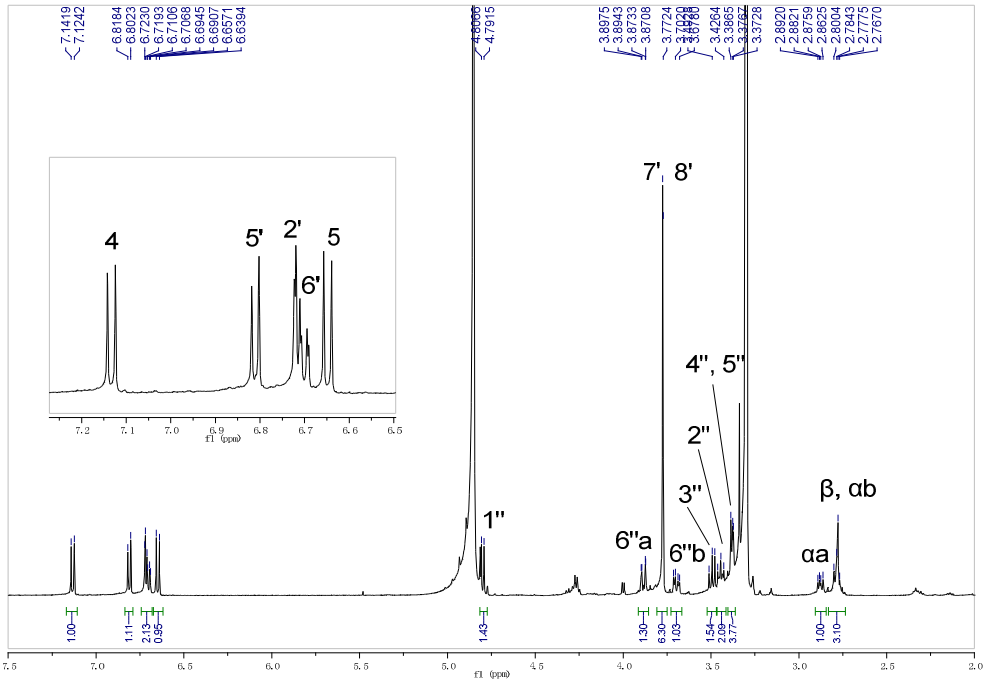

Figure 3.27 ^{1}H NMR spectrum of compound **4**

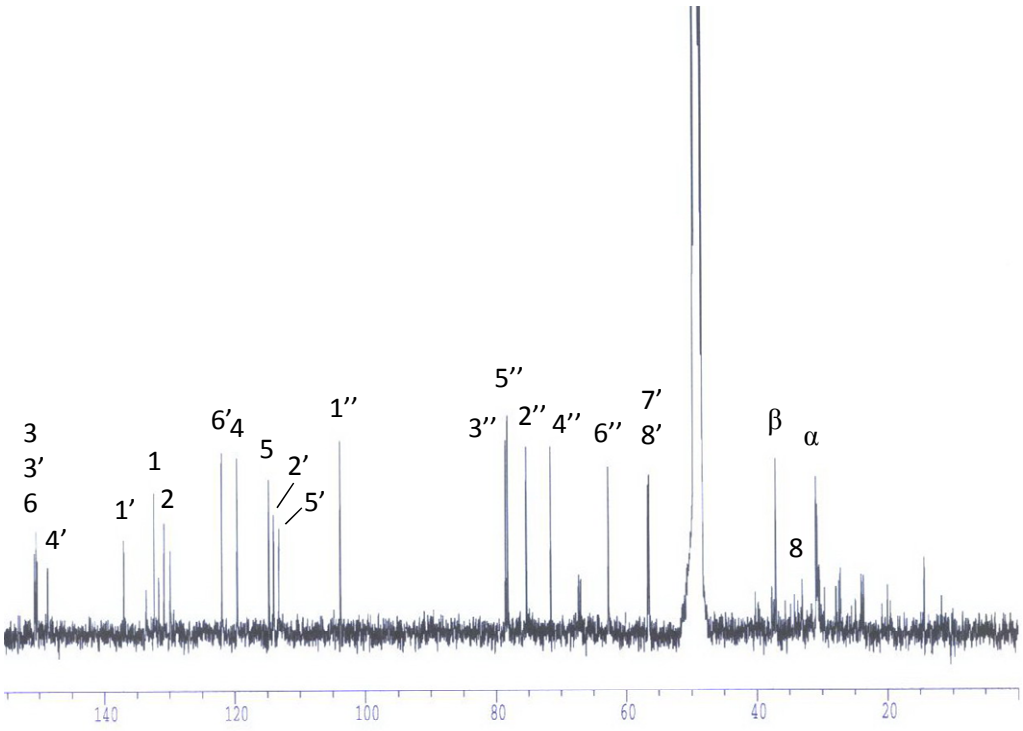

Figure 3.28 ^{13}C NMR spectrum of compound **4**

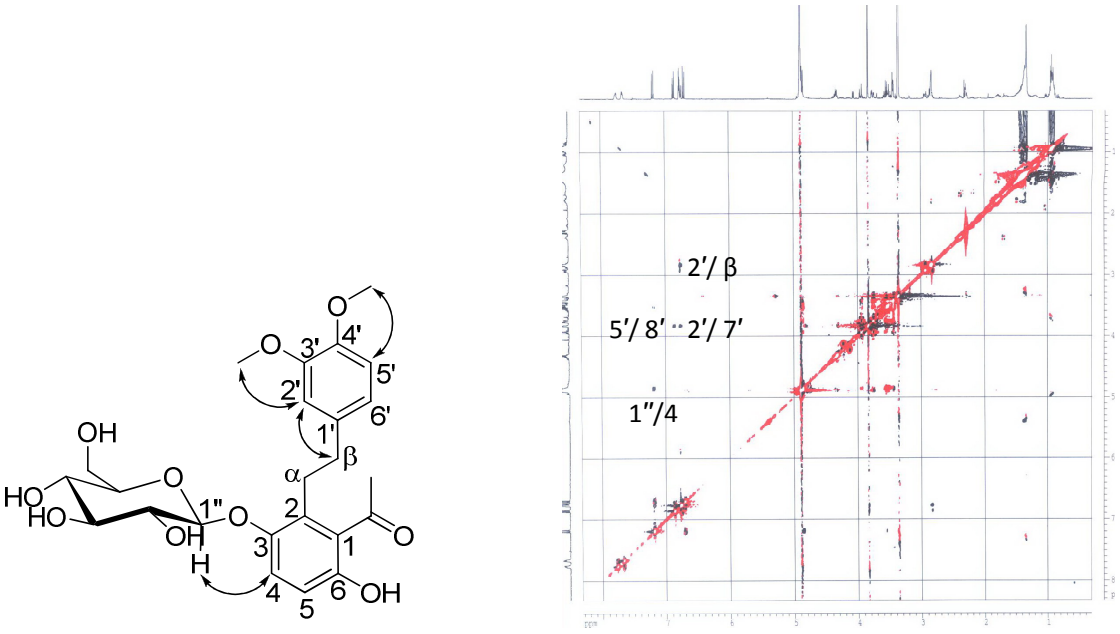

Figure 3.27 ROESY spectrum of compound **4**

Table 3.4 NMR spectroscopic data of compound **4** (CD_3OD, 500 MHz)

Position	δ_C	δ_H (mult., *J* in Hz)	ROESY
1	132.4, qC		
2	130.8, qC		
3	150.7, qC		
4	119.6, CH	7.13, d (8.8)	1″
5	114.8, CH	6.65, d (8.8)	
6	150.3, qC		
7	208.4, qC		
8	33.1, CH_3	2.29, s	
α	30.9, CH_2	2.88, m[a], 2.78, m[a]	
β	37.1, CH_2	2.78, m[a]	
1′	137.0, qC		
2′	114.0, CH	6.72, d (1.9)	7′, β
3′	150.4, qC		
4′	148.7, qC		
5′	113.2, CH	6.81, d (7.9)	8′
6′	122.0, CH	6.70, dd (7.9, 1.9)	
7′	56.6, CH_3	3.77, s	2′
8′	56.5, CH_3	3.77, s	5′
1″	103.8, CH	4.80, d (7.6)	4
2″	75.3, CH	3.44, dd (9.1, 8.5)	
3″	78.5, CH	3.49, dd (9.1, 7.3)	
4″	71.5, CH	3.38, m[a]	
5″	78.2, CH	3.38, m[a]	
6″a	62.7, CH_2	3.88, dd (12.0, 1.6)	
6″b		3.70, dd (12.0, 5.4)	

[a] Overlapped signals assigned by ^{1}H-^{1}H COSY, HMBC, and HMQC spectra without designating multiplicity.

3.1.5. Scorzodihydrostilbene E (5, new compound)

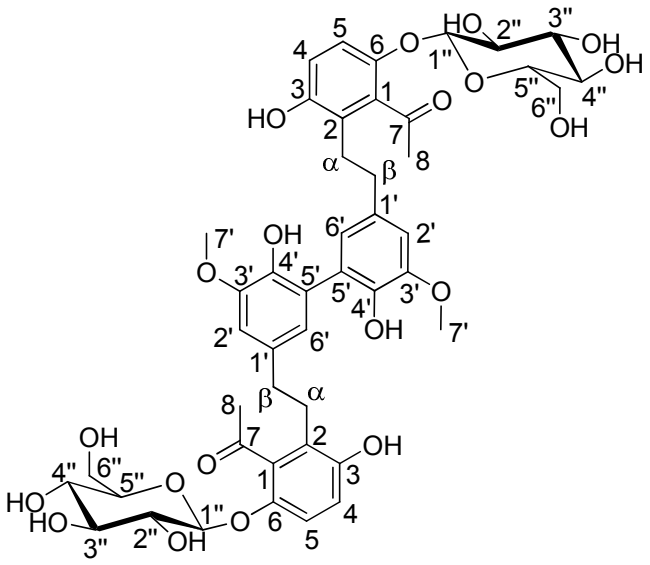

Molecular formula:	$C_{46}H_{54}O_{20}$
Molecular weight:	926.91
Amount:	1.1 mg

Compound **5** was isolated as a pale yellow solid. Its molecular formula was determined as $C_{46}H_{54}O_{20}$ by HRESIMS (*m/z* 949.3101 $[M + Na]^+$). Compound **5** was a dimer of **1**, which was inferred from inspection of the ^{1}H NMR (Figure 3.30) and mass spectra of **5**. Only one set of NMR resonances was displayed in the ^{1}H NMR spectrum of **5,** indicating that it was a symmetrical dimer. The only difference in the ^{1}H NMR spectrum of **5** compared to **1** was observed with regard to a pair of doublets [δ_H 6.54 (d, J = 1.9 Hz) and 6.53 (d, J = 1.9 Hz)] resonating close to each other instead of an ABX system in the aromatic region. The resonances of the two doublets were assigned to H-2' and H-6', which exhibited direct correlations to carbons at δ_C 111.6 (C-2') and 124.1 (C-6'), as shown in the HMQC spectrum of **5**. The nature and position of the linkage between the two monomers was determined from the HMBC spectrum (Figure 3) and ^{13}C chemical shifts. The strong cross peak observed between δ_C 130.5 (C-5') and δ_H 6.53 (H-6'), which further correlated with C-2' (δ_C 111.6) and C-4' (δ_C 148.4) of ring A, and the deshielding of the aromatic ring carbons C-5', C-4', C-6', and C-3' by −14.5, −2.8, −2.2, and −2.6 ppm, respectively, compared to the signals in the ^{13}C NMR spectrum of **1**, were indicative of a symmetrical dimer linked through C-5'.

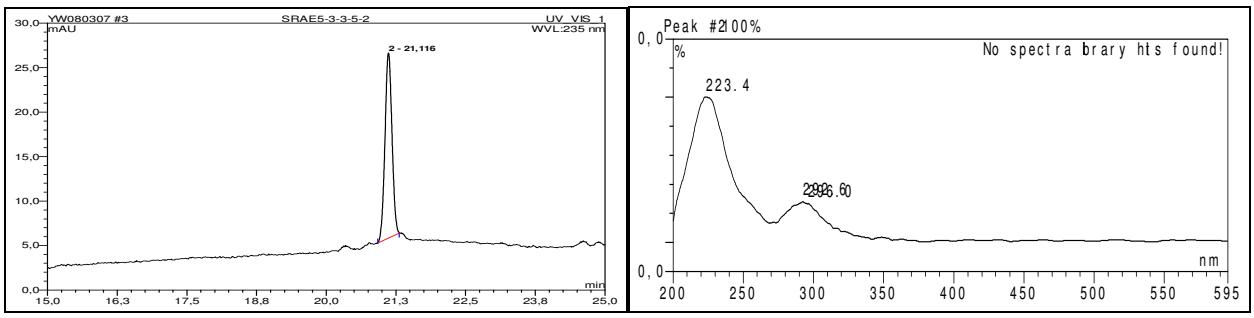

Figure 3.28 HPLC chromatogram and UV spectrum of compound **5**

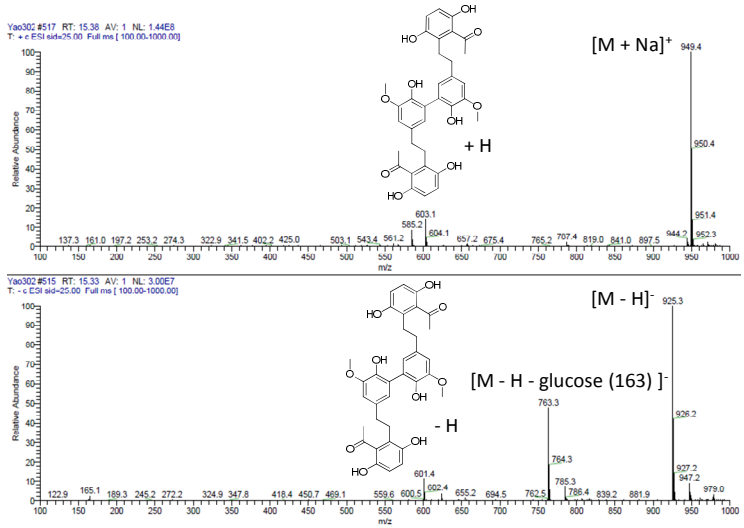

Figure 3.29 ESI-MS spectrum of compound **5**

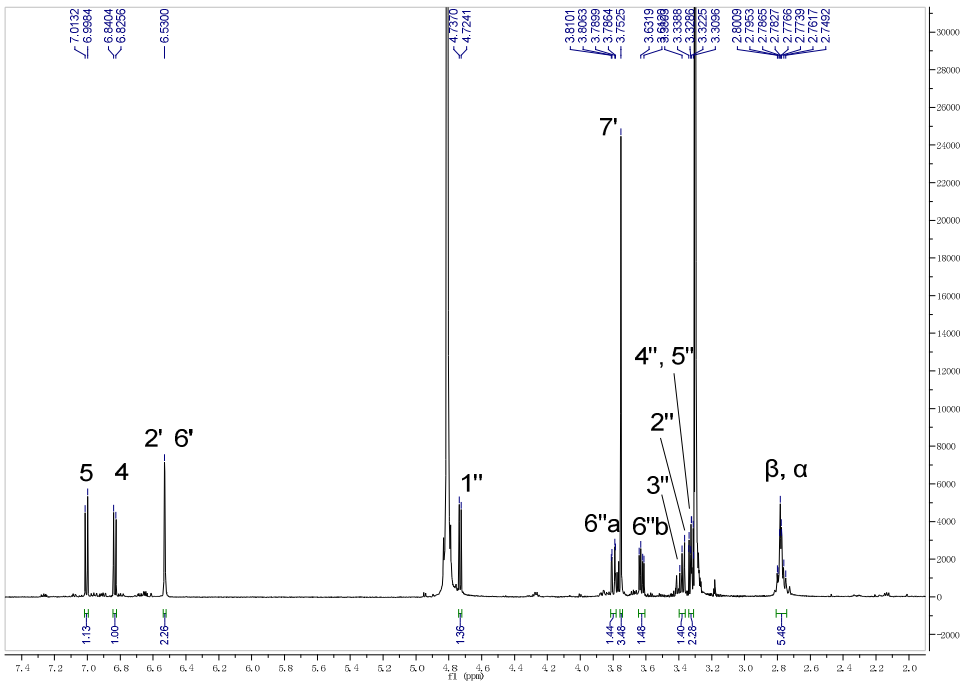

Figure 3.30 ^{1}H NMR spectrum of compound **5**

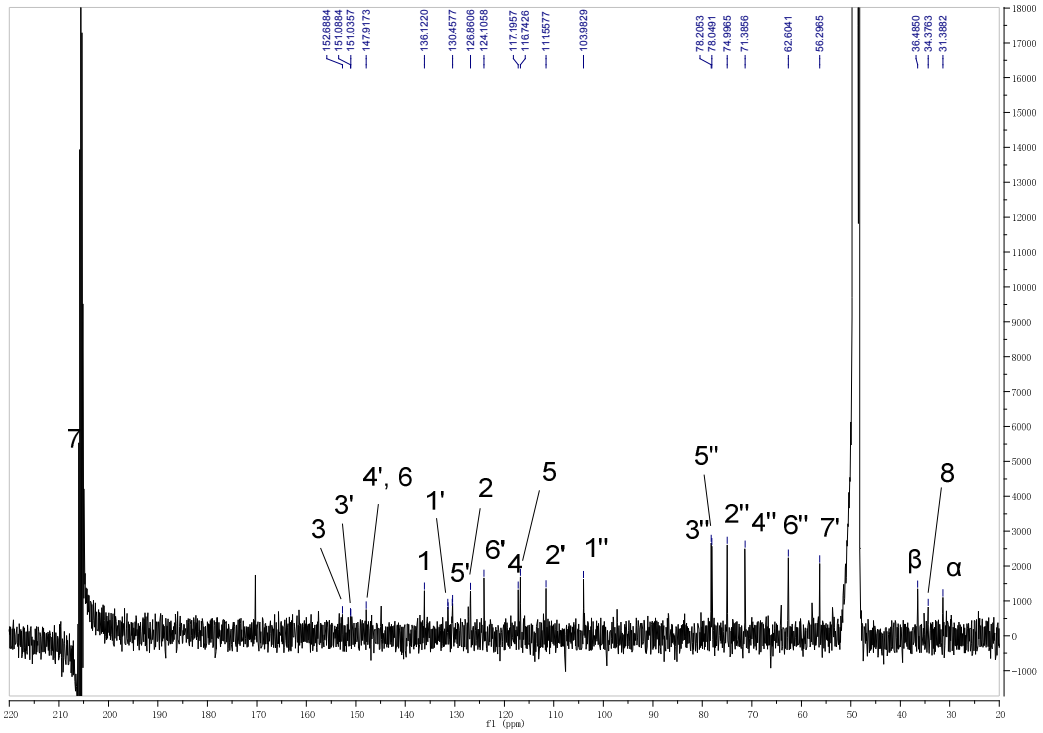

Figure 3.31 ^{13}C NMR spectrum of compound **5**

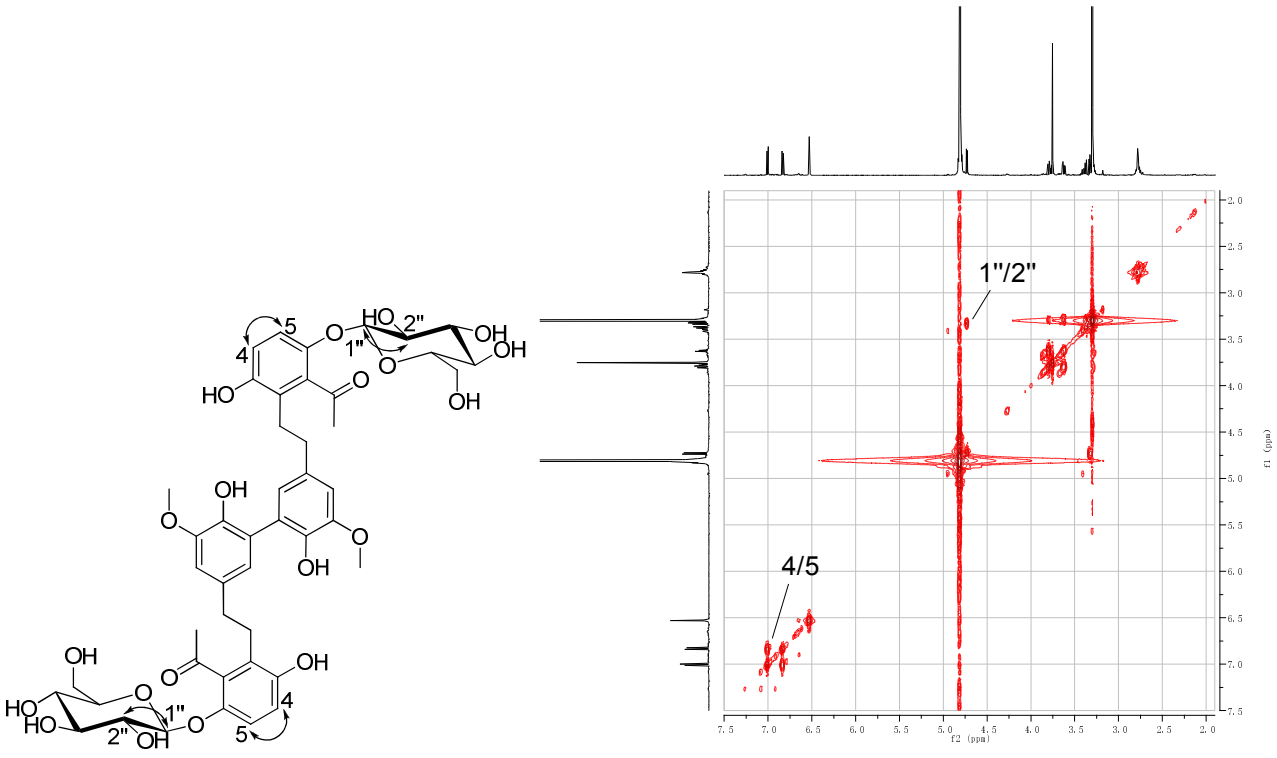

Figure 3.32 ^{1}H-^{1}H COSY spectrum of compound **5**

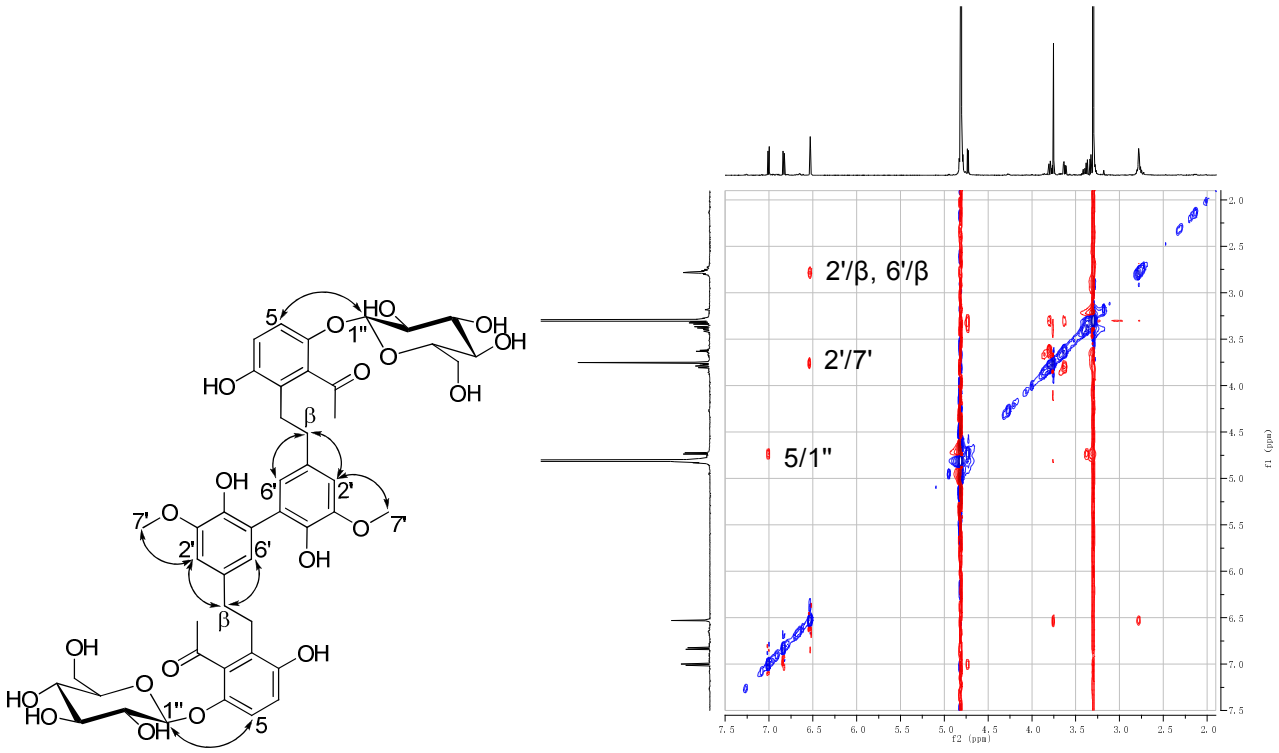

Figure 3.33 ROESY spectrum of compound **5**

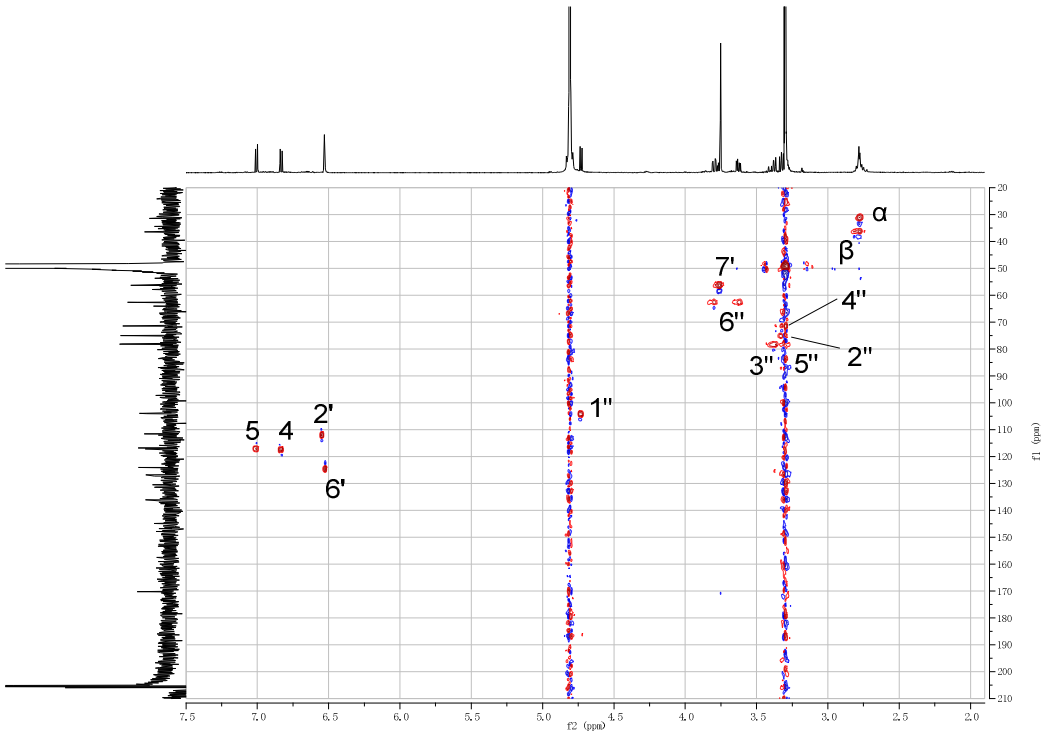

Figure 3.34 HMQC spectrum of compound **5**

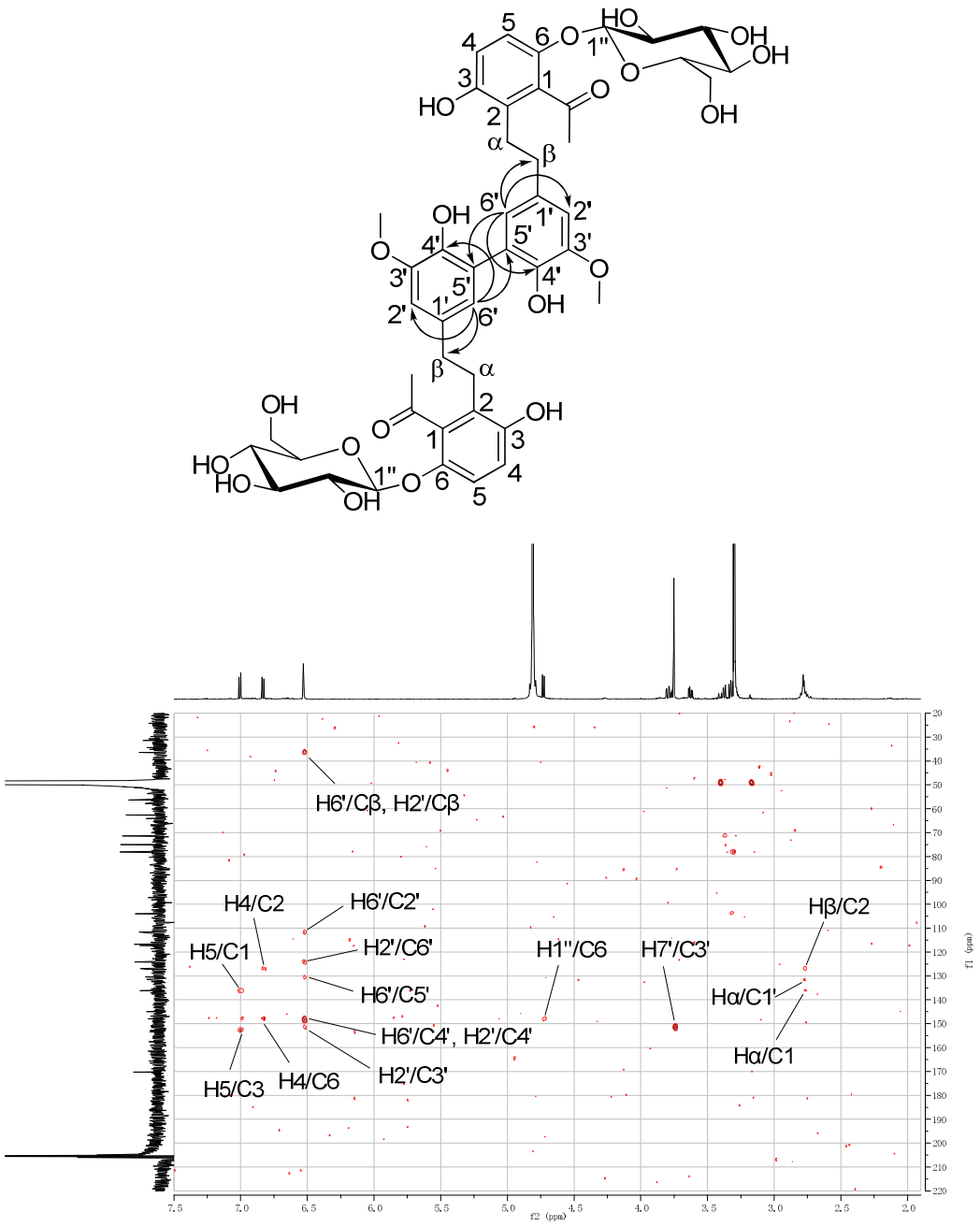

Figure 3.35 HMBC spectrum of compound **5**

Table 3.5 NMR spectroscopic data of compound **5** (CD_3OD, 500 MHz)

Position	δ_C	δ_H (mult., *J* in Hz)	COSY	ROESY	HMBC
1	136.1, qC				
2	126.9, qC				
3	152.7, qC				
4	117.2, CH	6.83, d (8.8)	5		C2, C6
5	116.7, CH	7.01, d (8.8)	4	1″	C1, C3
6	147.9, qC				
7	208.6, qC				
8	34.4, CH_3	2.21, s			
α	31.4, CH_2	2.78, m[a]			C1, C1′
β	36.5, CH_2	2.78, m[a]		2′, 6′	C2
1′	131.7, qC				
2′	111.6, CH	6.54, d (1.9)		7′, β	Cβ, C3′, C4′, C6′
3′	151.3, qC				
4′	148.4, qC				
5′	130.5, qC				
6′	124.1, CH	6.53, d (1.9)		β	Cβ, C2′, C4′, C5′
7′	56.3, CH_3	3.75, s		2′	C3′
1″	104.0, CH	4.73, d (7.8)	2″	5, 3″, 5″	C6
2″	75.0, CH	3.33, m[a]	1″		
3″	78.2, CH	3.38, m[a]		1″	C4″
4″	71.4, CH	3.31, m[a]			
5″	78.0, CH	3.30, m[a]		1″, 6″a, 6″b	C1″, C3″
6″a	62.6, CH_2	3.80, dd (12.0, 2.1)	6″b	5″	
6″b		3.63, dd (12.0, 5.3)	6″a	5″	

[a] Overlapped signals assigned by ^1H-^1H COSY, HMBC, and HMQC spectra without designating multiplicity.

3.1.6. Quinic acid (6, known compound)

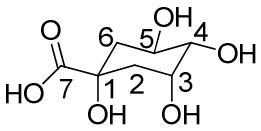

Molecular formula:	$C_7H_{12}O_6$
Molecular weight:	192.17
Amount:	19.3 mg

Compound **6** was isolated as colourless needles without any UV absorption. The ESI mass spectrum showed a negative pseudomolecular ion peak at *m/z* 191 (Figure 3.36). The ^{1}H NMR spectrum of **6** (Figure 3.37) displayed three oxymethine protons at δ_H 4.04, 3.91, and 3.45, together with two pairs of sp^3 methylene protons at δ_H 1.95/1.86 and 1.96/1.77 for H_2-2 and H_2-6, respectively. By inspection of the ^{13}C NMR spectrum (Figure 3.38), these resonances were in agreement with three oxymethine resonances at δ_C 67.4, 70.8, and 75.6; two sp^3 methylenes at δ_C 37.8 and 41.1; an oxygenated quaternary carbon at δ_C 77.5; and a carboxyl resonance at δ_C 181.8, all of which were characteristic of quinic acid. Comparing the data of (−)-**quinic acid** with that of compound **6**, both compounds were identical [Flores-Parra *et al.*, 1989].

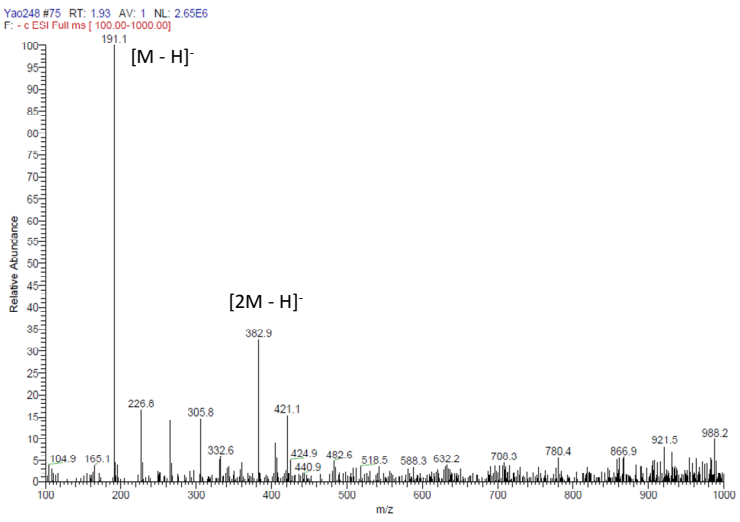

Figure 3.36 ESI-MS spectrum of compound **6**

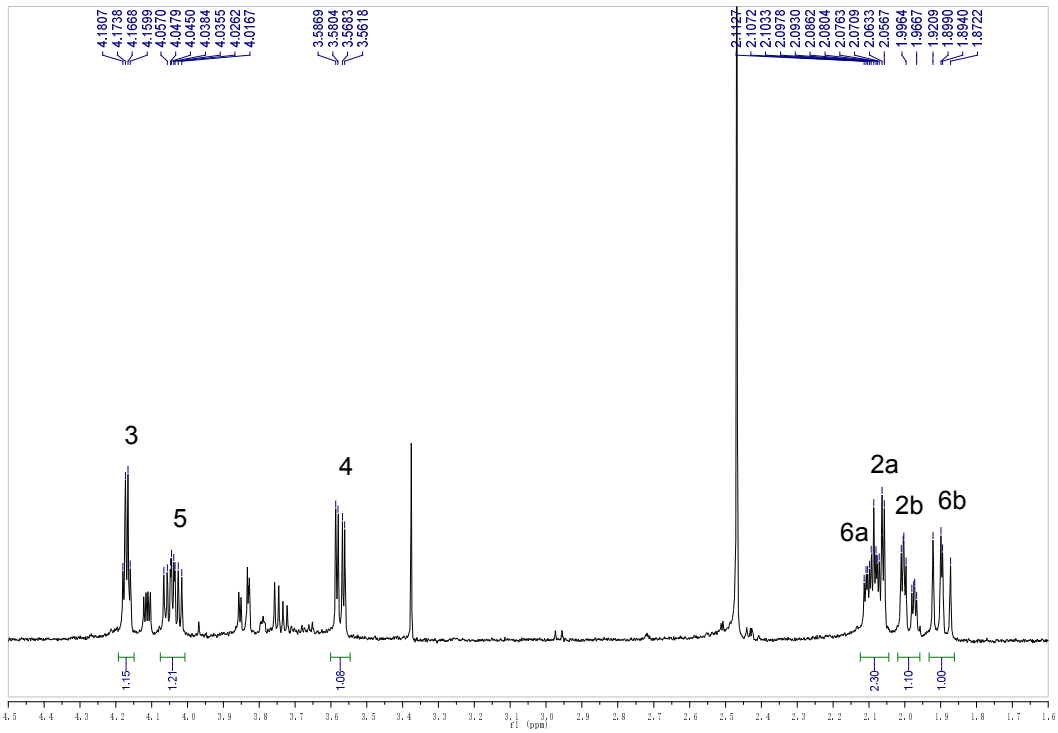

Figure 3.37 ^{1}H NMR spectrum of compound **6**

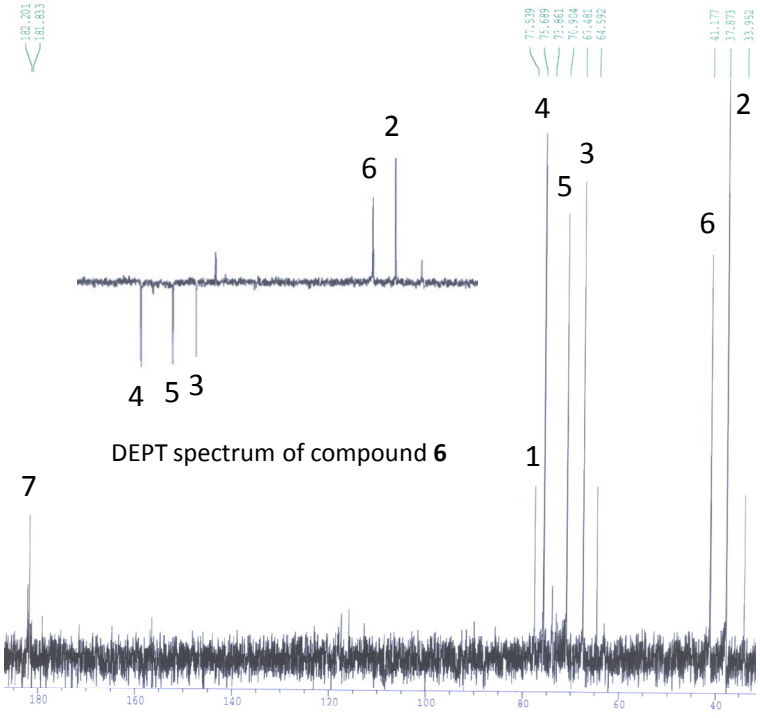

Figure 3.38 ^{13}C NMR spectrum of compound **6**

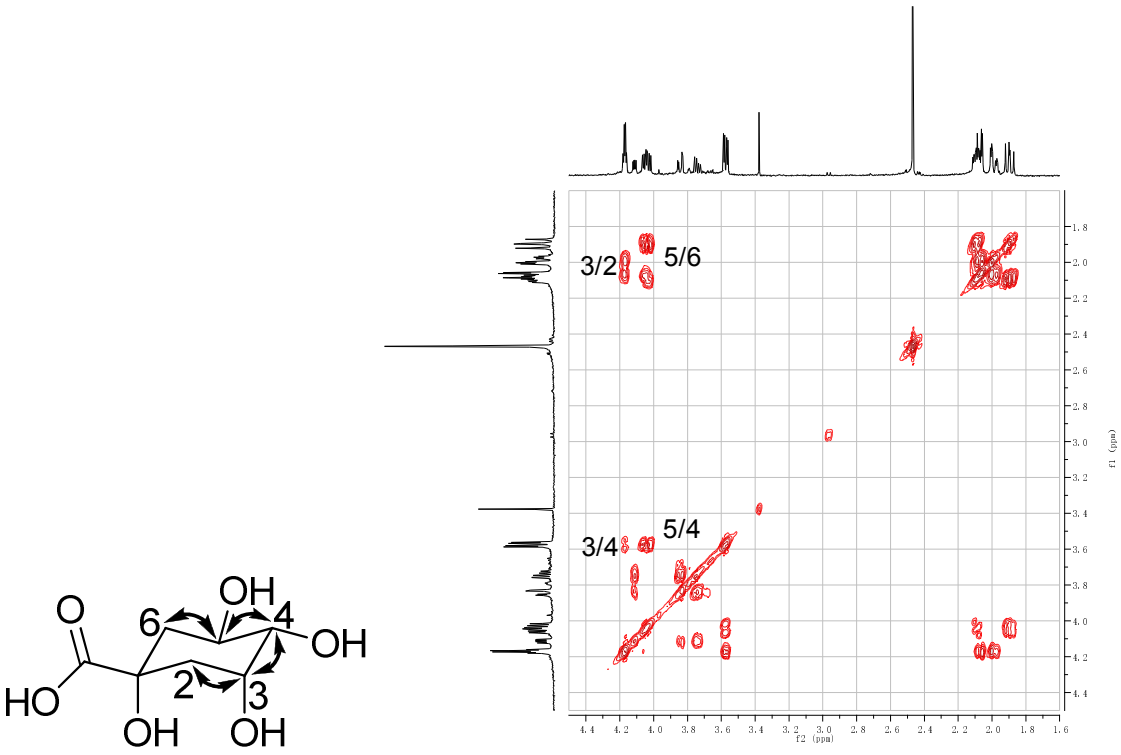

Figure 3.39 ^{1}H-^{1}H COSY spectrum of compound **6**

Table 3.6 NMR spectroscopic data of compound **6** (D_2O, 500 MHz)

	Quinic acid (DMSO) [Flores-Parra *et al.*, 1989]		Compound **6**	
Position	δ_C	δ_H (mult., *J* in Hz)	δ_C	δ_H (mult., *J* in Hz)
1	74.7, qC		77.5, qC	
2_{eq}	37.6, CH_2	1.7, dd (13, 3.3)	37.8, CH_2	2.10, dd (14.9, 3.4)
2_{ax}		1.6, dd (13, 3.3)		2.02, dd (14.8, 3.6)
3	69.3, CH	3.8, td (3.3, 2.2)	67.4, CH	4.20, ddd (3.5, 3.5, 3.4)
4	74.8, CH	3.2, dd (7.8, 2.2)	75.6, CH	3.60, dd (9.3, 3.3)
5	66.9, CH	3.7, td (7.8, 4)	70.8, CH	4.07, ddd (10.6, 9.4, 4.6)
6_{eq}	40.7, CH_2	1.8, dd (13, 4)	41.1, CH_2	2.12, dd (13.4, 4.7)
6_{ax}		1.7, dd (13, 7.8)		1.92, dd (13.4, 10.9)
7	175.8, qC		181.8, qC	

3.1.7. Chlorogenic acid (7, known compound)

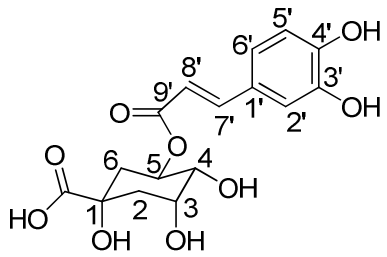

Molecular formula:	$C_{16}H_{18}O_9$
Molecular weight:	354.31
Amount:	240.1 mg

Compound **7** was isolated as an amorphous solid. It had UV absorption at λ_{max} 218, 242, and 326 nm (Figure 3.40), which were typical for caffeic acid derivatives. The molecular weight of **7** was determined as 354 by ion peaks found in ESIMS spectrum at *m/z* 355 $[M + H]^+$ and *m/z* 353 $[M - H]^-$ (Figure 3.41). The aliphatic region of the ^1H NMR spectrum was comparable to that of compound **6**, however in the aromatic region, resonances for an ABX system at δ_H 7.04 (d, J = 2.2 Hz), 6.76 (d, J = 8.2 Hz) and 6.94 (dd, J = 8.2, 2.2 Hz), as well as a pair of doublet with coupling constants of 15.8 Hz were observed. Along with the analysis of mass and UV spectrum, a caffeic acid unit was indicated to be present. Compound **7** was identified to be **chlorogenic acid** by comparing ^1H NMR and MS data with those of reference [Pauli *et al.*, 1998].

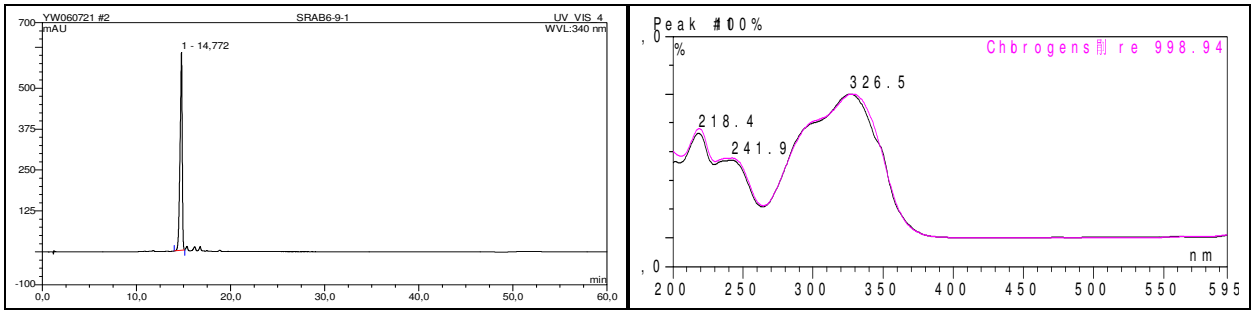

Figure 3.40 HPLC chromatogram and UV spectrum of compound **7**

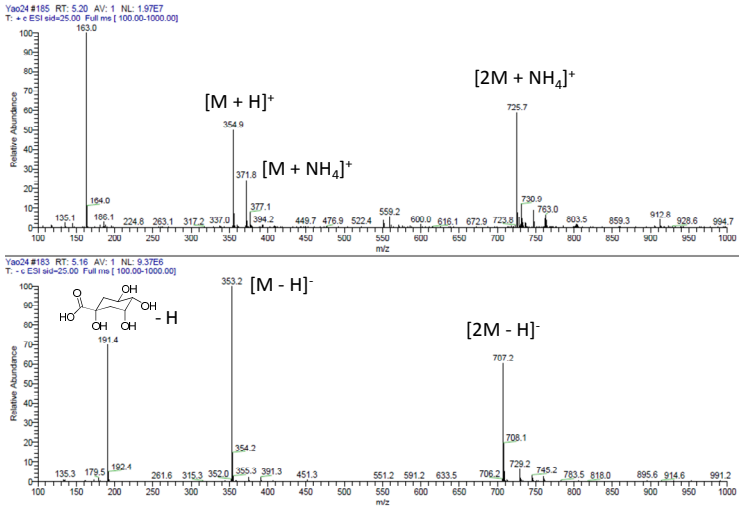

Figure 3.41 ESI-MS spectrum of compound **7**

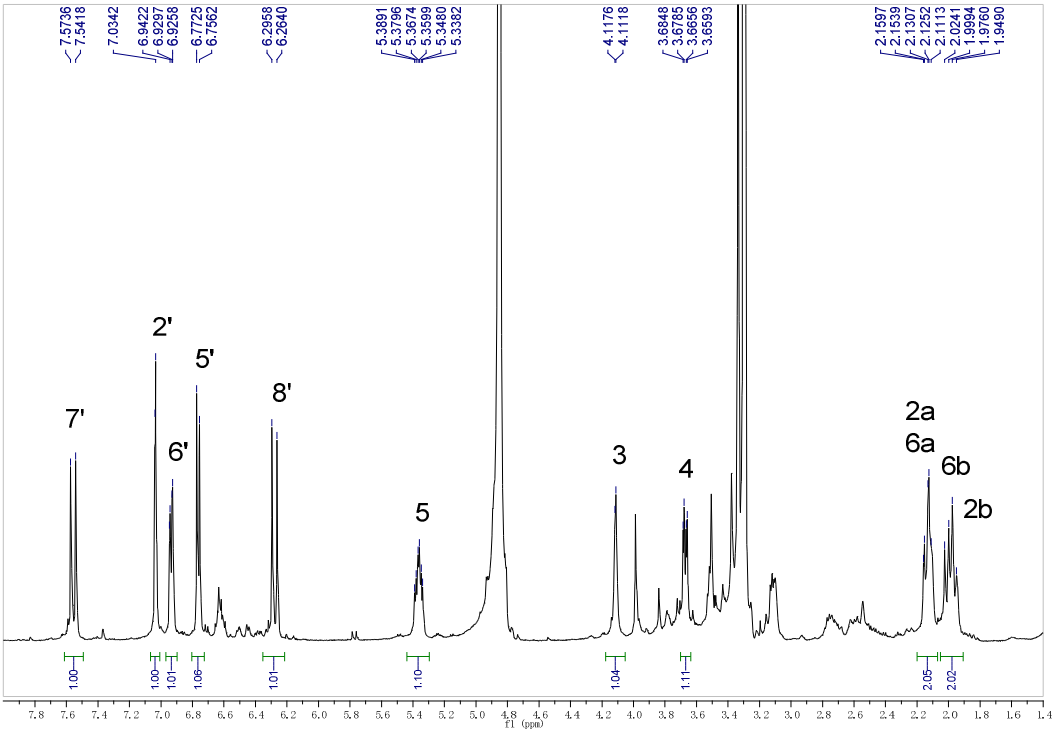

Figure 3.42 ^{1}H NMR spectrum of compound **7**

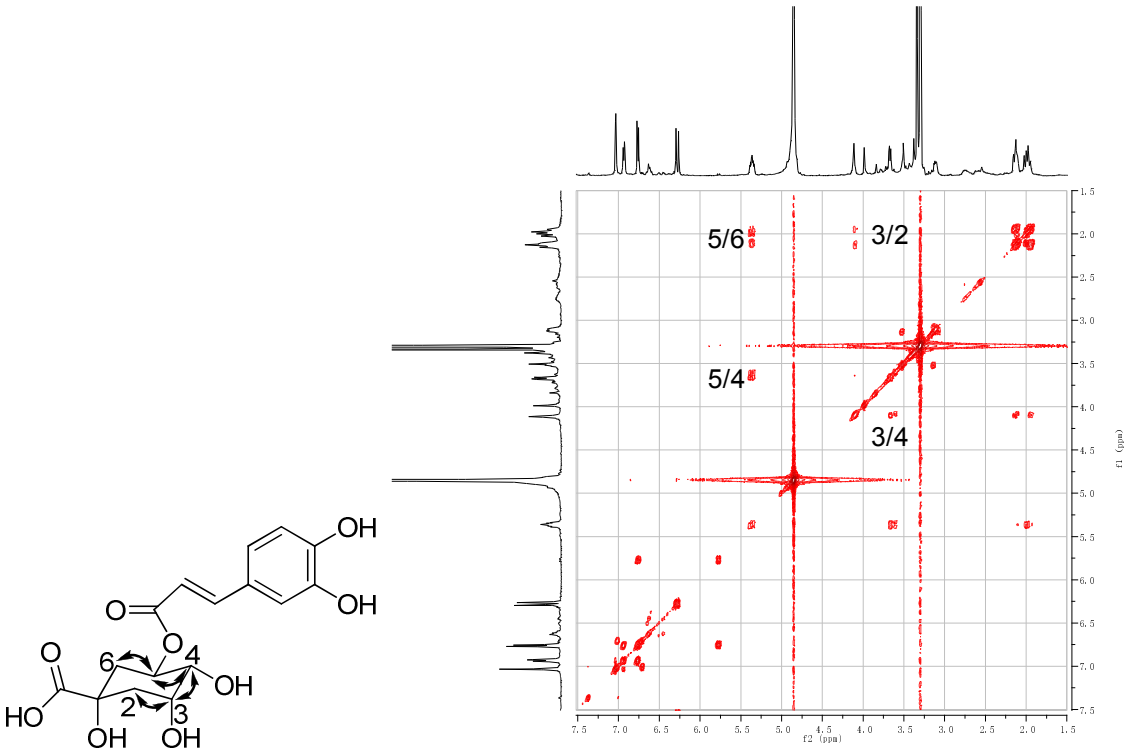

Figure 3.43 ^{1}H-^{1}H COSY spectrum of compound **7**

Table 3.7 NMR spectroscopic data of compound **7** (CD_3OD)

	Chlorogenic acid [Pauli *et al.*, 1998]	Compound **7**
Position	δ_H (mult., *J* in Hz)	δ_H (mult., *J* in Hz)
2_{ax}	2.166, dd (14.2, 5.1)	2.14, dd (14.5, 2.8)
2_{eq}	2.047, ddd (14.2, 3.3, 2.3)	1.96, br d (14.5)
3	4.165, dt (5.1, 3.3, 3.2)	4.11, br d (3.2)
4	3.721, dd (9.5, 3.6)	3.67, dd (9.5, 3.2)
5	5.336, ddd (11.2, 9.5, 4.5)	5.36, ddd (11.0, 10.1, 4.7)
6_{eq}	2.232, ddd (13.3, 4.5, 2.3)	2.12, m[a]
6_{ax}	2.063, dd (13.3, 9.7)	2.01, br d (12.6)
2′	7.040, d (2.1)	7.04, d (2.2)
5′	6.772, d (8.2)	6.76, d (8.2)
6′	6.938, dd (8.2, 2.1)	6.94, dd (8.2, 2.2)
7′	7.550, d (15.9)	7.56, d (15.8)
8′	6.251, d (15.9)	6.28, d (15.8)

[a] Overlapped signals assigned by ^{1}H-^{1}H COSY, HMBC, and HMQC spectra without designating multiplicity.

3.1.8. 3,5-Dicaffeoylquinic acid (8, known compound)

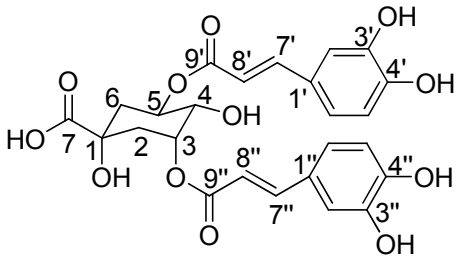

Molecular formula:	$C_{25}H_{24}O_{12}$
Molecular weight:	516.45
Amount:	242.0 mg

Compound **8** was obtained as a yellowish amorphous solid, and its molecular weight was determined to be 516 by ESIMS ion peaks at *m/z* 517 $[M + H]^+$ and *m/z* 515 $[M - H]^-$ (Figure 3.46). Its UV spectrum (Figure 3.45) displayed maximal absorption at 220, 243, and 328 nm indicating the presence of caffeic acid moiety. The ^1H (Figure 3.44) and ^{13}C NMR (Figure 3.47) spectra of **8** showed two methylenes, three oxygenated protons and a carbonyl carbon at δ 177.3, which were assigned for a qunic acid unit. In addition, the presence of two *trans*-caffeoyl groups was indicated by the observation of two ABX systems and two *trans*-olefinic protons. The above spectral data were consistent with those of 3,5-dicaffeoylquinic acid [Wald *et al.*, 1989; Pauli *et al.*, 1998]. Thus, compound **8** was concluded to be **3,5-dicaffeoylquinic acid**.

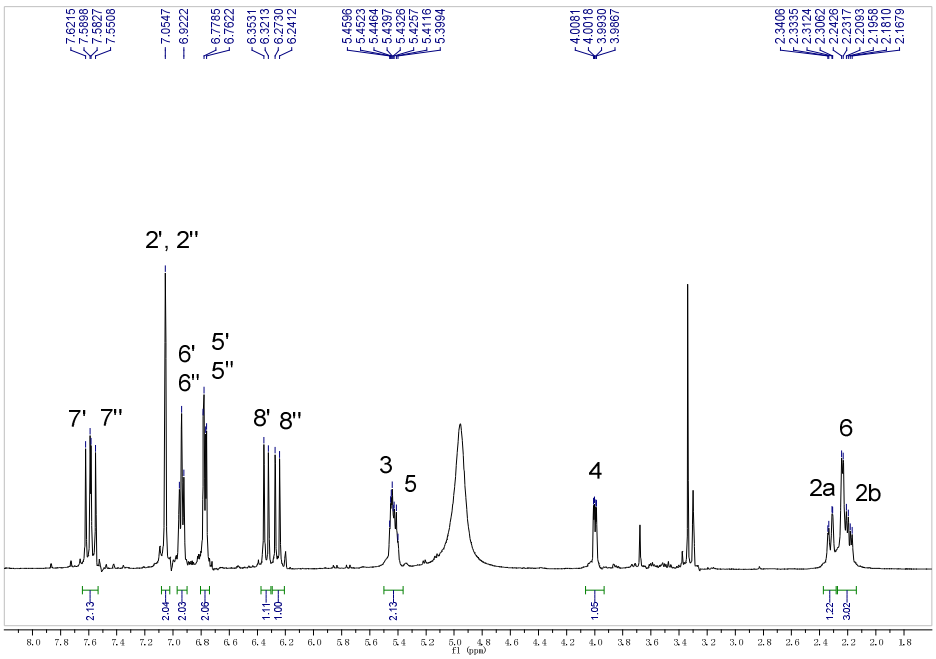

Figure 3.44 ^1H NMR spectrum of compound **8**

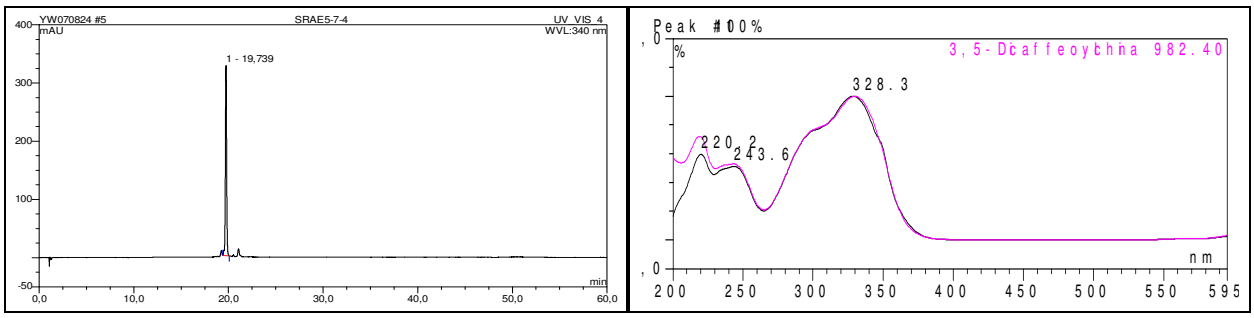

Figure 3.45 HPLC chromatogram and UV spectrum of compound **8**

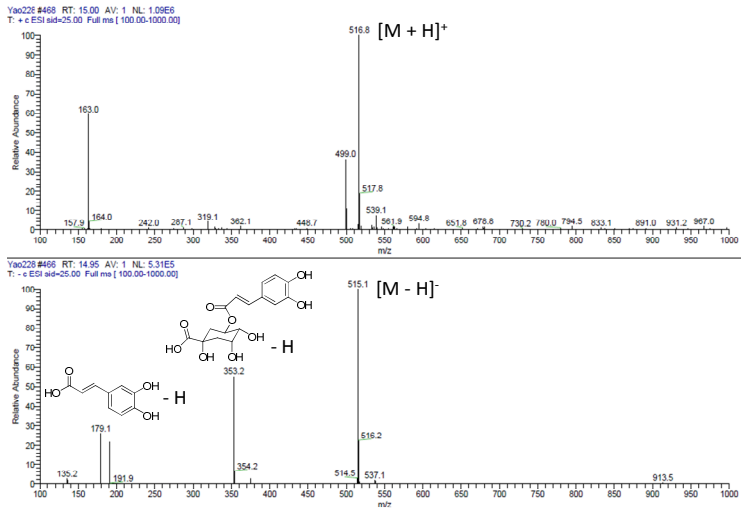

Figure 3.46 ESI-MS spectrum of compound **8**

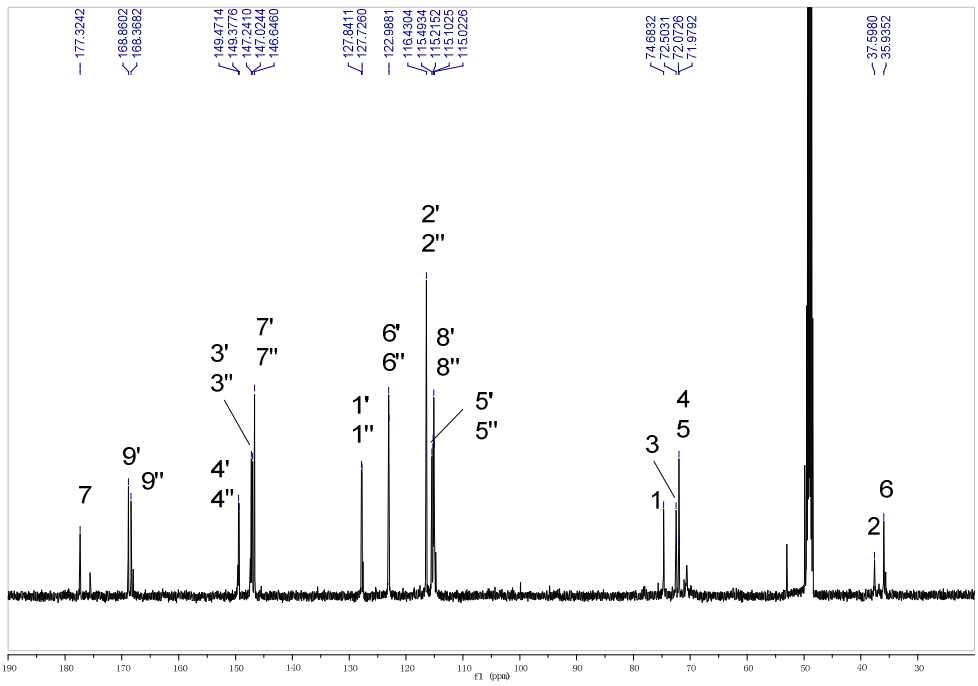

Figure 3.47 ^{13}C NMR spectrum of compound **8**

Table 3.8 NMR spectroscopic data of compound **8** (CD_3OD, 500 MHz)

	3,5-Dicaffeoylquinic acid [Wald *et al.*, 1989; Pauli *et al.*, 1998]		Compound **8**	
Position	δ_C	δ_H (mult., *J* in Hz)	δ_C	δ_H (mult., *J* in Hz)
1	74.79, qC		74.68, qC	
2_{ax}	37.79, CH_2	2.311, dd (13.8, 4.0)	37.60, CH_2	2.32, dd (13.6, 3.2)
2_{eq}		2.156, ddd (13.8, 7.0, 1.5)		2.19, dd (13.9, 6.3)
3	72.64, CH	5.421, dt (7.0, 4.0, 3.3)	72.50, CH	5.44, td (6.6, 3.5)
4	70.83, CH	3.963, dd (7.5, 3.3)	71.98, CH	4.00, dd (7.6, 3.2)
5	72.13, CH	5.378, ddd (7.5, 7.5, 4.2)	72.07, CH	5.41, t (6.7)
6_{eq}	36.08, CH_2	2.237, ddd (14.0, 4.2, 1.5)	35.93, CH_2	2.24, m[a]
6_{ax}		2.197, dd (14.0, 7.5)		2.22, m[a]
7	177.42, qC		177.32, qC	
1′	128.02, qC		127.83, qC	
2′	116.53, CH	7.059, d (2.1)	116.43, CH	7.06, br s
3′	147.22, qC		147.23, qC	
4′	149.51, qC		149.46, qC	
5′	116.53, CH	6.776, d (8.2)	115.49, CH	6.78, d (8.2)
6′	123.00, CH	6.966, dd (8.2, 2.1)	123.05, CH	6.94, td (7.9, 1.6)
7′	147.02, CH	7.610, d (15.9)	146.64, CH	7.61, d (15.8)
8′	115.37, CH	6.338, d (15.9)	115.10, CH	6.34, d (15.8)
9′	168.88, qC		168.86, qC	
1″	127.89, qC		127.73, qC	
2″	116.53, CH	7.054, d (2.1)	116.43, CH	7.06, br s
3″	147.22, qC		147.02, qC	
4″	149.42, qC		149.38, qC	
5″	115.69, CH	6.774, d (8.2)	115.21, CH	6.77, d (8.2)
6″	122.94, CH	6.956, dd (8.2, 2.1)	122.98, CH	6.94, td (7.9, 1.6)
7″	146.73, CH	7.568, d (15.9)	146.64, CH	7.57, d (15.8)
8″	115.27, CH	6.255, d (15.9)	115.02, CH	6.26, d (15.8)
9″	168.43, qC		168.37, qC	

[a] Overlapped signals assigned by ^1H-^1H COSY, HMBC, and HMQC spectra without designating multiplicity.

3.1.9. 3,5-Dicaffeoyl-*epi*-quinic acid (9, known compound)

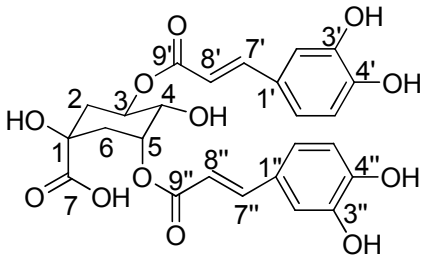

Molecular formula:	$C_{25}H_{24}O_{12}$
Molecular weight:	516.45
Amount:	103.2 mg

Compound **9** was obtained as a yellowish amorphous solid ($[\alpha]^{20}_{D}$: −113.0°) with a UV maximal absorption at 218, 243, and 329 nm. The molecular weight 516 was established by ESIMS (Figure 3.49). The ^{1}H and ^{13}C NMR spectra of **9** (Table 3.1) exhibited signals for two caffeic acids and a quinic acid moiety indicating a structure silimar to that of **8** except for the quinic acid moiety. In the ROESY spectrum (Figure 3.52), the proton at δ 3.89 (H-4) gave two cross-peaks with the protons at δ 5.53 (H-3) and δ 5.37 (H-5) respectively. This observation indicated proton H-4 is in the axial orientation. Comparing with the ^{1}H and ^{13}C NMR data of the reference compound, **9** was concluded to be **3,5-dicaffeoyl-*epi*-quinic acid** which is an epimer of **8** [Kim and Lee, 2005].

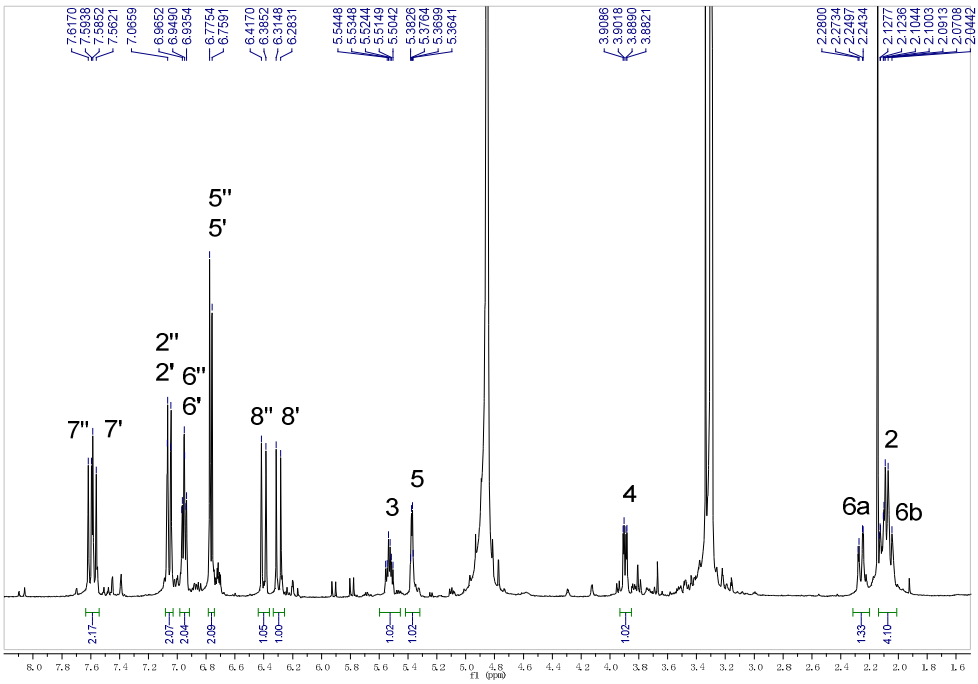

Figure 3.48 ^{1}H NMR spectrum of compound **9**

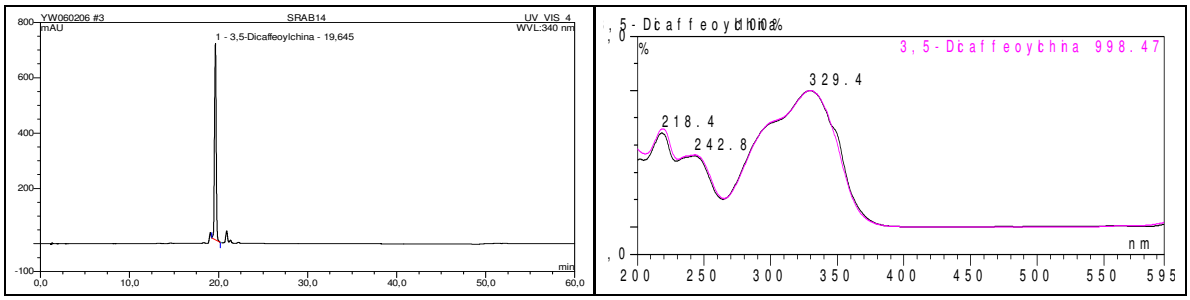

Figure 3.49 HPLC chromatogram and UV spectrum of compound **9**

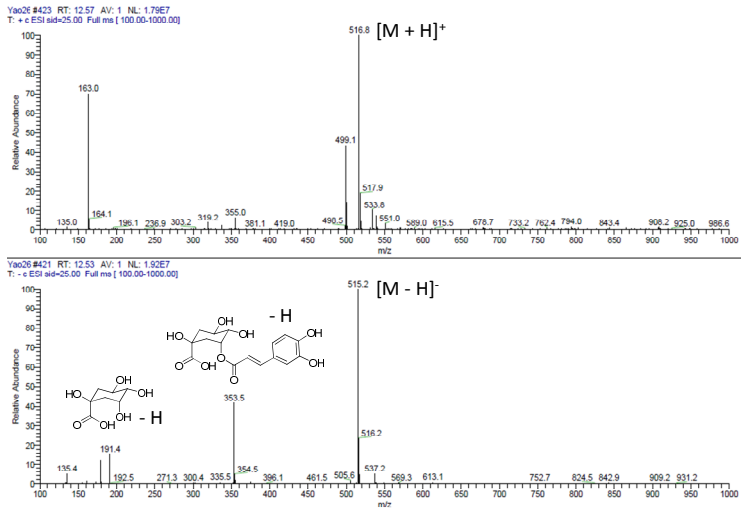

Figure 3.50 ESI-MS spectrum of compound **9**

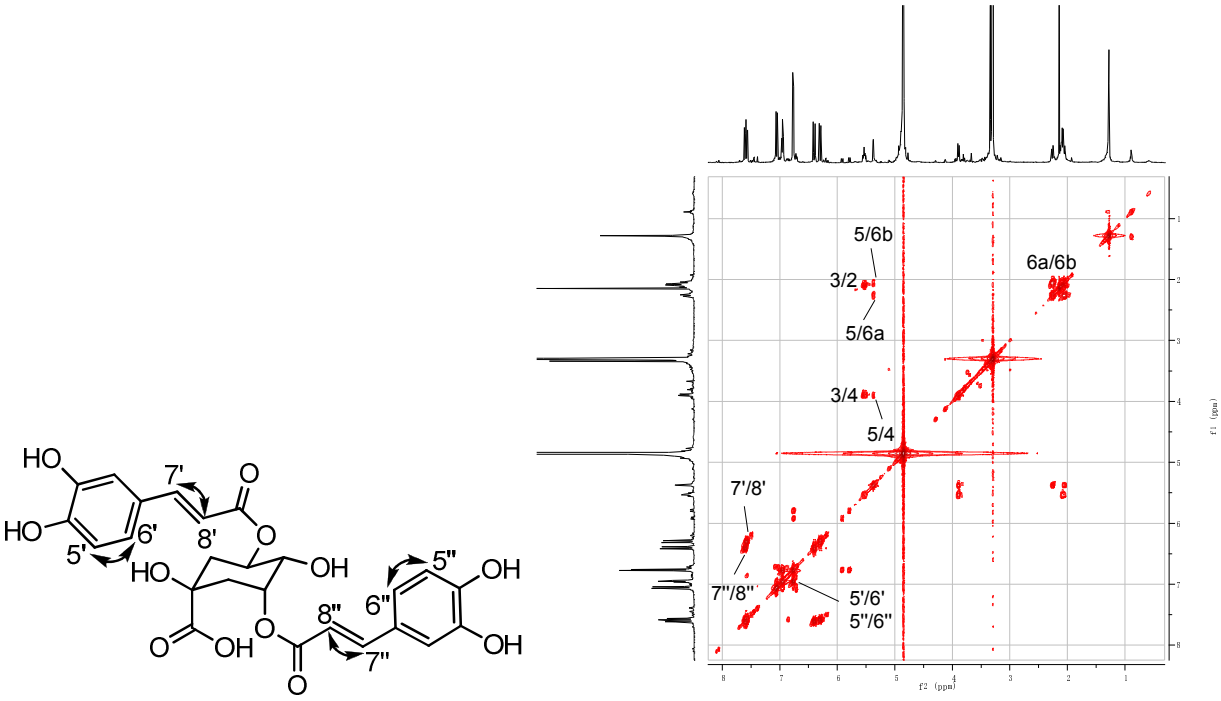

Figure 3.51 ^{1}H-^{1}H COSY spectrum of compound **9**

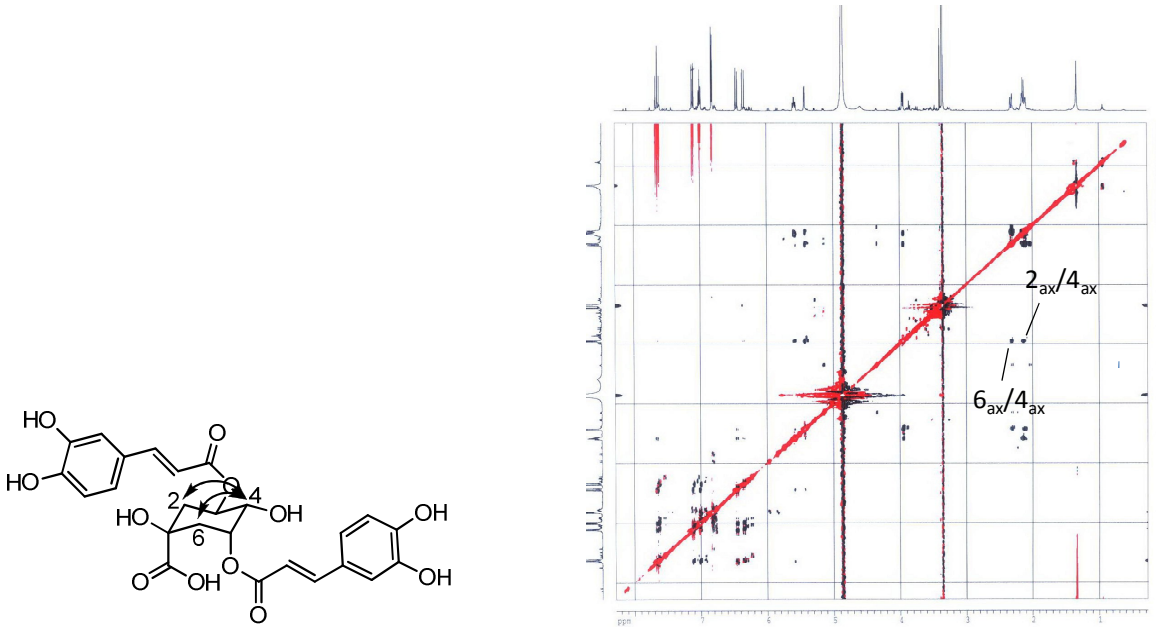

Figure 3.52 ROESY spectrum of compound **9**

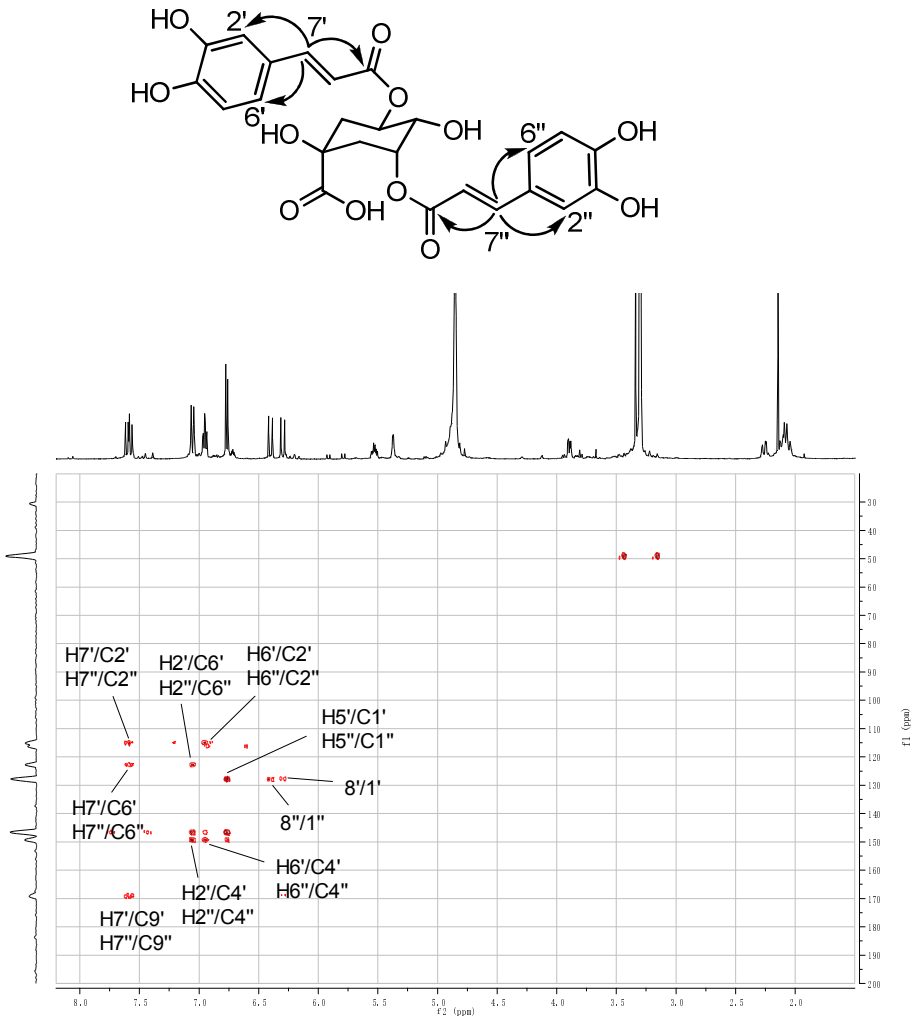

Figure 3.53 HMBC spectrum of compound **9**

Table 3.9 NMR spectroscopic data of compound **9** (CD_3OD, 500 MHz)

	3,5-Dicaffeoyl-*epi*-quinic acid [Kim and Lee, 2005]		Compound **9**	
Position	δ_C	δ_H (mult., *J* in Hz)	δ_C	δ_H (mult., *J* in Hz)
1	76.3, qC		76, qC	
2	40.6, CH_2	2.11, m	40.5, CH_2	2.10, m[a]
3_{ax}	72.4, CH	5.55, dt (10.0, 5.8)	72.5, CH	5.53, ddd (10.4, 9.8, 5.4)
4_{ax}	73.0, CH	3.91, dd (9.9, 3.4)	73, CH	3.89, dd (9.8, 3.5)
5_{eq}	74.4, CH	5.39, m	74, CH	5.37, dt (3.5, 3.2)
6_{eq}	37.5, CH_2	2.28, dd (15.2, 3.4)	37.5, CH_2	2.26, dd (15.1, 3.2)
6_{ax}		2.04, m		2.06, m[a]
7	181.3, qC		181.5, qC	
1′	127.8, qC		128.0, qC	
2′	115.2, CH	7.06, d (2.0)	115.0, CH	7.05, d (1.9)
3′	146.8, qC		146.4, qC	
4′	149.2, qC		149.5, qC	
5′	116.4, CH	6.78, d (8.2)	116.1, CH	6.77, d (8.2)
6′	122.9, CH	6.96, dd (8.2, 2.0)	122.7, CH	6.94, dd (8.2, 1.9)
7′	146.6, CH	7.59, d (15.8)	146.5, CH	7.58, d (15.8)
8′	115.4, CH	6.31, d (15.8)	115.3, CH	6.30, d (15.8)
9′	169.0, qC		169.0, qC	
1″	128.0, qC		128.0, qC	
2″	115.2, CH	7.08, d (2.0)	115.0, CH	7.07, d (1.9)
3″	146.9, qC		146.4, qC	
4″	149.4, qC		149.5, qC	
5″	116.4, CH	6.78, d (8.2)	116.1, CH	6.77, d (8.2)
6″	122.9, CH	6.97, dd (8.2, 2.0)	122.7, CH	6.96, dd (8.2, 1.9)
7″	146.6, CH	7.62, d (15.8)	146.5, CH	7.60, d (15.8)
8″	115.9, CH	6.43, d (15.8)	115.5, CH	6.40, d (15.8)
9″	169.4, qC		169.3, qC	

[a] Overlapped signals assigned by ^1H-^1H COSY, HMBC, and HMQC spectra without designating multiplicity.

3.1.10. Macroantoin G (10, known compound)

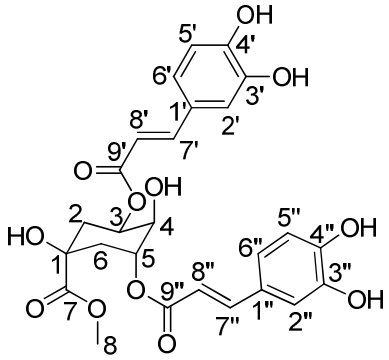

Molecular formula:	$C_{26}H_{26}O_{12}$
Molecular weight:	530.78
Amount:	13.3 mg

Compound **10** was isolated as a yellow amorphous powder ($[\alpha]^{20}_{D}$: −68°) with the molecular weight 530 deduced from ESIMS spectrum (Figure 3.54). The UV spectrum of **10** showed maximal absorption at 204, 219, and 330 nm. The ^{1}H NMR spectra of **10** (Figure 3.55) suggested the presence of one quinic acid and two caffeoyl moieties. Those resonances were remarkably similar to those of compound **8** but with an additional *O*-methyl group. Assignment of the *O*-methyl group at C-7 was determined from the HMBC cross-peak (Figure 3.56) of the methyl singlet at δ_H 3.74 with the carbonyl carbon at δ_C 175.4. This assignment was also testified by the 1.9 ppm upfield shift of the C-7 resonance of **10** as compared to that of **8**. Compound **10** was identical with the known compound **macroantoin G** [Zhang *et al.*, 2000].

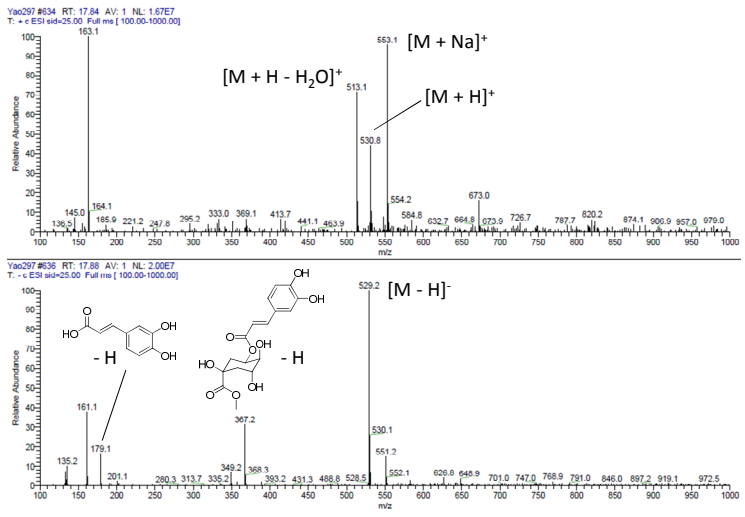

Figure 3.54 ESI-MS spectrum of compound **10**

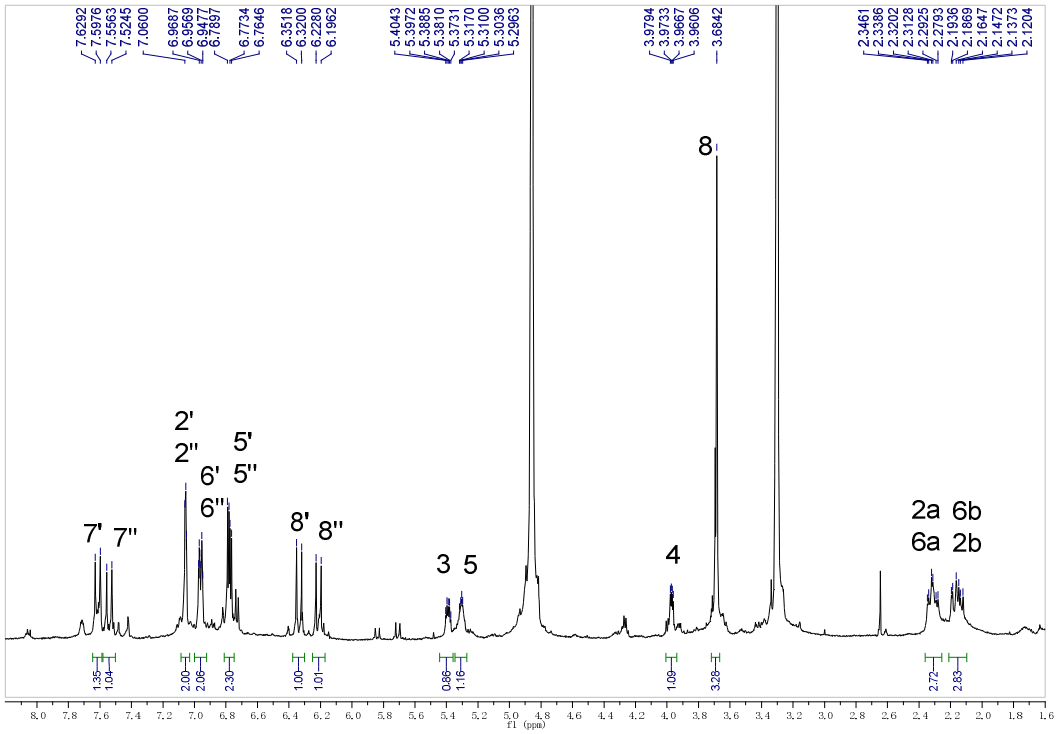

Figure 3.55 ^{1}H NMR spectrum of compound **10**

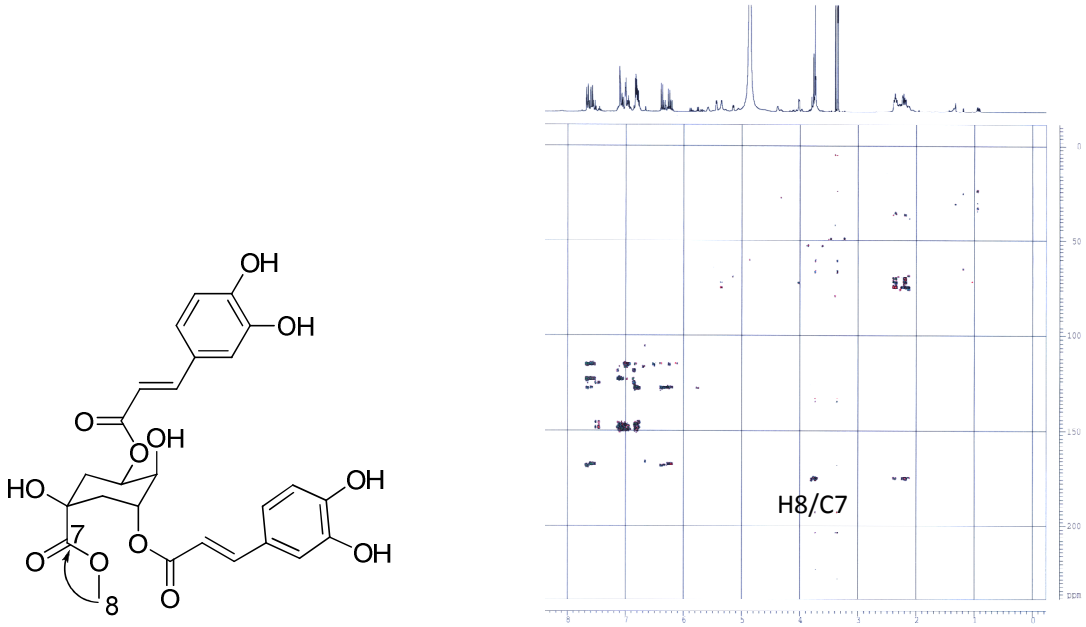

Figure 3.56 HMBC spectrum of compound **10**

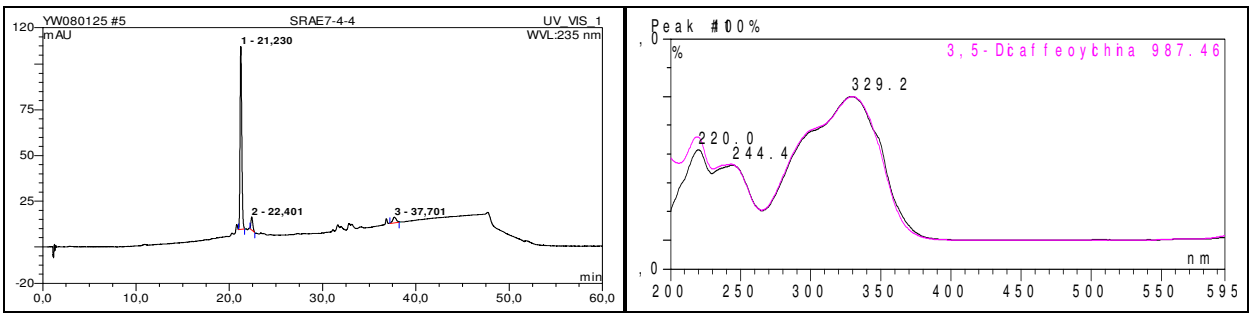

Figure 3.57 HPLC chromatogram and UV spectrum of compound **10**

Table 3.10 NMR spectroscopic data of compound **10** (CD_3OD, 600 MHz)

	Macroantoin G [Zhang *et al.*, 2000]		Compound **10**	
Position	δ_C	δ_H (mult., *J* in Hz)	δ_C	δ_H (mult., *J* in Hz)
1	74.64, qC		74.3, qC	
2_{eq}	36.78, CH_2	2.19, m	35.5, CH_2	2.38, dd (13.3, 4.1)
2_{ax}				2.20, dd (13.3, 8.5)
3_{ax}	72.08, CH	5.35, m	71.5, CH	5.44, dt (7.8, 4.2, 3.7)
4_{eq}	69.81, CH	3.98, dd (6.77, 3.17)	69.7, CH	4.02, dd (6.5, 3.1)
5_{eq}	71.98, CH	5.41, m	71.9, CH	5.35, ddd (8.1, 6.5, 3.9)
6_{eq}	35.63, CH_2	2.21, m	36.5, CH_2	2.35, dd (13.2, 7.1)
6_{ax}				2.23, dd (13.8, 3.6)
7	175.59, qC		175.4, qC	
8	53.03, CH_3		52.9	3.74, s
1′	127.56, qC		127.8, qC	
2′	115.14, CH	7.06, d (2.0)	114.9, CH	7.11, d (2.4)
3′	146.65, qC		146.7, qC	
4′	149.56, qC		149.4, qC	
5′	116.46, CH	6.79, d (8.17)	116.4, CH	6.83, d (8.2)
6′	123.05, CH	6.96, dd (8.17, 2.0)	122.9, CH	7.01, dd (8.2, 2.4)
7′	147.37, CH	7.54, d (15.92)	147.7, CH	7.66, d (15.9)
8′	114.81, CH	6.21, d (15.92)	115.3, CH	6.38, d (15.9)
9′	167.98, qC		168.7, qC	
1″	127.81, qC		127.4, qC	
2″	115.14, CH	7.06, d (2.0)	114.9, CH	7.10, d (2.4)
3″	146.65, qC		146.7, qC	
4″	149.40, qC		149.4, qC	
5″	116.45, CH	6.76, d (8.12)	116.4, CH	6.82, d (8.2)
6″	122.99, CH	6.93, dd (8.12, 2.0)	122.9, CH	7.01, dd (8.2, 2.4)
7″	147.09, CH	7.62, d (15.89)	147.3, CH	7.59, d (15.9)
8″	115.38, CH	6.33, d (15.89)	114.8, CH	6.26, d (15.9)
9″	168.73, qC		167.9, qC	

[a] Overlapped signals assigned by ^1H-^1H COSY, HMBC, and HMQC spectra without designating multiplicity.

3.1.11. 4,5-Dicaffeoylquinic acid (11, known compound)

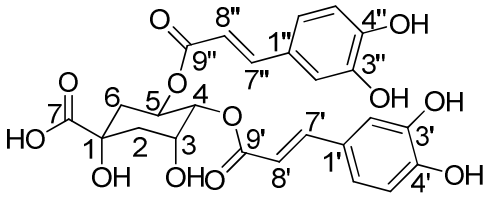

Molecular formula:	$C_{25}H_{24}O_{12}$
Molecular weight:	516.45
Amount:	3.0 mg

Compound **11** was isolated as a yellowish amorphous solid ($[\alpha]^{20}_{D}$: −74°) with UV absorbances at λ_{max} 219, 244, and 329 nm (Figure 3.58). Its molecular weight 516 was deduced from the ESIMS spectrum (Figure 3.59). The ^{1}H NMR spectrum (Figure 3.60) of **11** exhibited one quinic acid and two caffeoyl moieties. The assignments and the configuration of the quinic acid moiety were determined by analysis of the ^{1}H-^{1}H COSY (Figure 3.61) and ROESY (Figure 3.62) spectra of **11**. The proton resonances at δ_H 5.09 and 5.69 were assigned to H-4 and H-5 respectively. When comparing the ^{1}H NMR data of **11** to those of quinic acid, downfield shift for H-4 by −1.49 ppm and for H-5 by −1.62 ppm were observed, respectively, which implied that the attachments of the two caffeoyl units were at carbon 4 and 5. From above results, compound **11** was identified as **4,5-dicaffeoylquinic acid** [Pauli *et al.*, 1998].

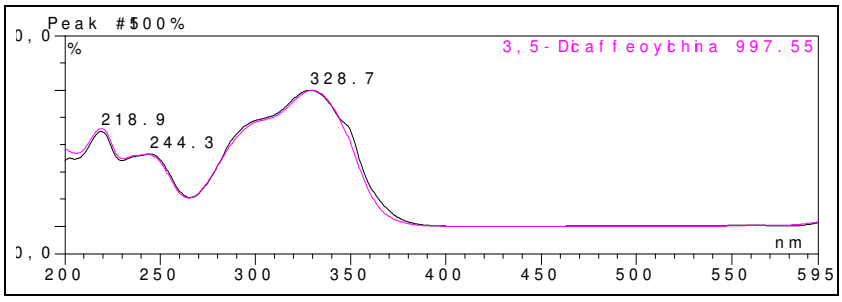

Figure 3.58 UV spectrum of compound **11**

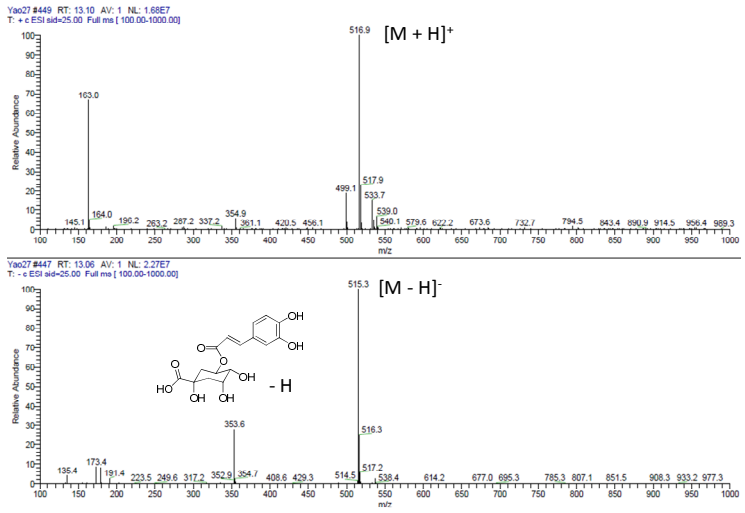

Figure 3.59 ESI-MS spectrum of compound **11**

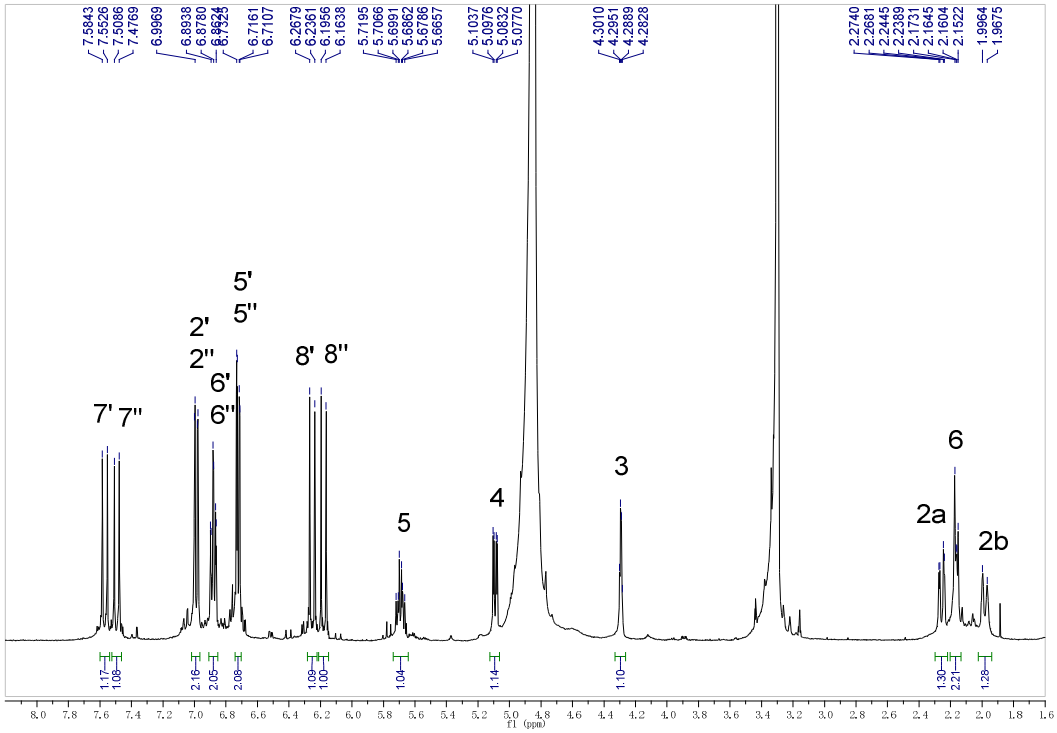

Figure 3.60 ^{1}H NMR spectrum of compound **11**

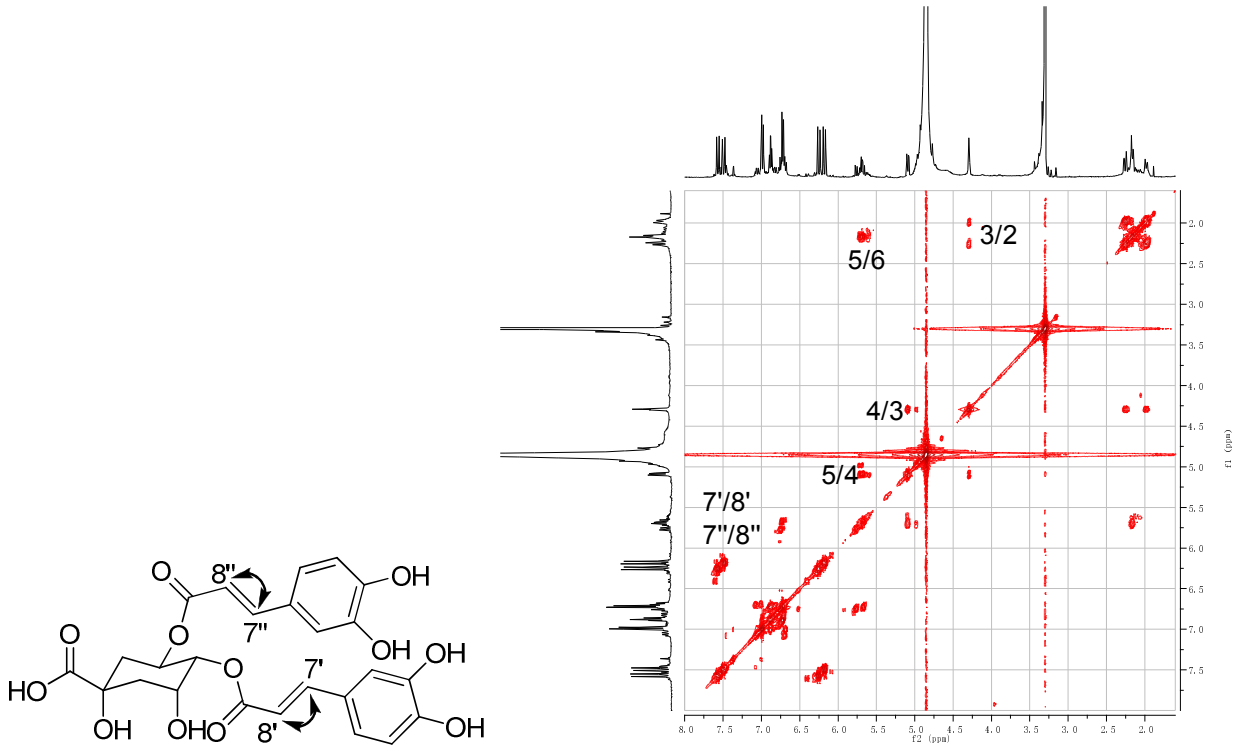

Figure 3.61 ^{1}H-^{1}H COSY spectrum of compound **11**

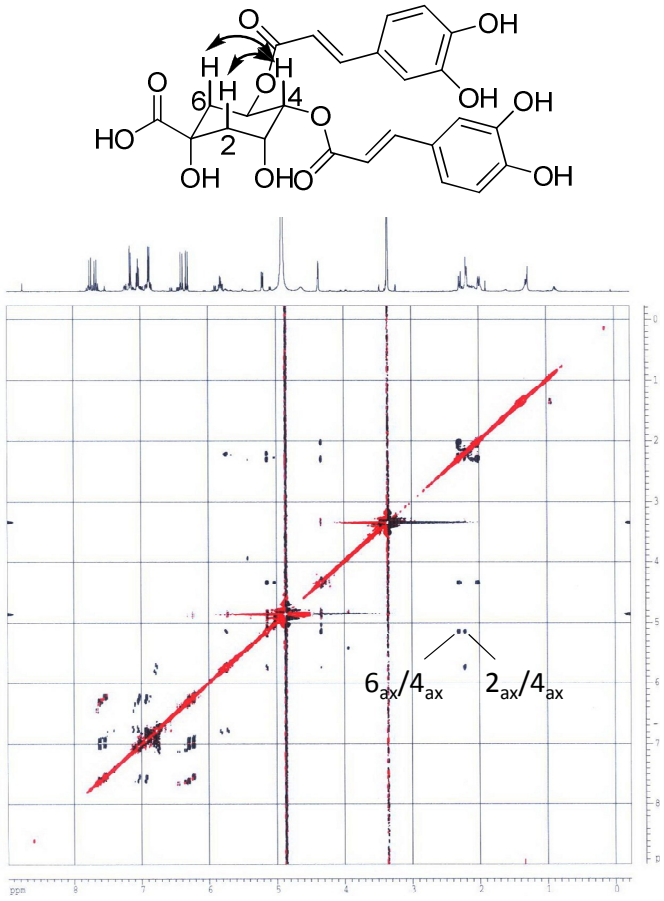

Figure 3.62 ROESY spectrum of compound **11**

Table 3.11 NMR spectroscopic data of compound **11** (CD_3OD, 500 MHz)

	4,5-Dicaffeoylquinic acid [Pauli *et al.*, 1998]	Compound **11**
Position	δ_H (mult., *J* in Hz)	δ_H (mult., *J* in Hz)
2_{ax}	2.287, dd (14.2, 3.3)	2.26, dd (14.5, 2.8)
2_{eq}	2.100, ddd (14.2, 5.1, 2.0)	1.98, dt (14.5, 2.2)
3_{eq}	4.359, dt (3.3, 3.1)	4.29, dt (3.2, 2.8)
4_{ax}	5.103, dd (9.1, 3.1)	5.09, dd (10.4, 3.2)
5_{ax}	5.620, ddd (13.3, 4.8, 2.0)	5.69, dt (6.6, 10.4)
6_{eq}	2.272, ddd (13.3, 4.8, 2.0)	2.16, m[a]
6_{ax}	2.214, dd (13.3, 9.6)	2.16, m[a]
2′	7.013, d (2.1)	7.00, d (2.1)
5′	6.740, d (8.3)	6.72, d (8.2)
6′	6.913, dd (8.3, 2.1)	6.89, dd (8.2, 2.1)
7′	7.587, d (15.9)	7.57, d (15.9)
8′	6.271, d (15.9)	6.25, d (15.9)
2″	6.993, d (2.1)	6.98, d (2.1)
5″	6.726, d (8.3)	6.72, d (8.1)
6″	6.890, dd (8.3, 2.1)	6.87, dd (8.1, 2.1)
7″	7.507, d (15.9)	7.49, d (15.8)
8″	6.179, d (15.9)	6.18, d (15.8)

[a] Overlapped signals assigned by ^1H-^1H COSY, HMBC, and HMQC spectra without designating multiplicity.

3.1.12. 4,5-Dicaffeoyl-*epi*-quinic acid (12, new compound)

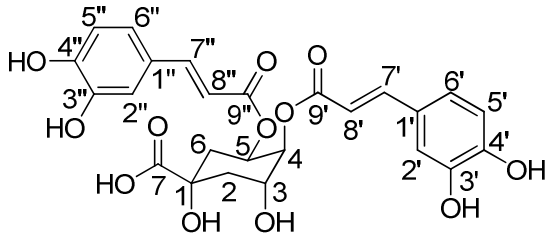

Molecular formula:	$C_{25}H_{24}O_{12}$
Molecular weight:	516.45
Amount:	3.1 mg

Compound **12** was obtained as an amorphous solid. The molecular formula was determined as $C_{25}H_{24}O_{12}$ from the HRESIMS data (*m/z* 517.1341 $[M + H]^+$). The UV spectrum of **12** showed absorption maxima at 325, 243 and 218 nm typical of a caffeic acid derivative. The ^{1}H NMR data were very similar to those of **11** for the caffeic acid moieties, but differed from known compounds with regard to the signals of the quinic acid moiety [Pauli *et al.*, 1998; Lin *et al.*, 1999]. The ^{1}H NMR spectrum of **12** (Figure 3.65) showed two pairs of doublets with coupling constants of 15.9 Hz indicative of *trans* olefinic protons found in hydroxy cinnamic acids. In the aromatic region, resonances for two ABX systems [δ_H 7.05 (d, J = 2.1 Hz), 6.78 (d, J = 8.1 Hz) and 6.92 (dd, J = 8.1, 2.1 Hz); and δ_H 7.09 (d, J = 2.2 Hz), 6.80 (d, J = 8.2 Hz) and 6.97 (dd, J = 8.2, 2.2 Hz)] were observed, which were assigned to two 1,3,4-trisubstituted phenyl units. From these observations, along with the analysis of the ^{13}C NMR data, two caffeic acid moieties were inferred to be present. The assignments were further supported by analysis of the ROESY spectrum of **12** (Figure 3.67). The protons at δ 7.05 (H-2′) and 7.09 (H-2″) gave ROESY cross-peaks with the olefinic protons at δ_H 7.55 (H-7′) and 7.62 (H-7″). The presence of the quinic acid moiety was indicated by ^{1}H NMR resonances of three oxymethine protons at δ_H 5.67 (ddd, J = 8.6, 4.1, 3.3 Hz), 5.24 (dd, J = 6.1, 3.0 Hz) and 4.16 (ddd, J = 5.6, 5.4, 5.3 Hz), together with two pairs of sp^3 methylene protons at δ_H 2.22/2.10 and 2.11/2.08 for H_2-6 and H_2-2, respectively. All of the latter are characteristic of a quinic acid unit, with regard to their multiplicity and coupling patterns. The assignments of the protons of the quinic acid nucleus were corroborated by analysis of the ^{1}H-^{1}H COSY (Figure 3.66) and ROESY spectra of **12**. The attachments of the two caffeoyl moieties at C-4 and C-5 of quinic acid part were deduced from the HMBC correlation of H-4 and H-5, respectively, with their ester carbonyl carbons

(C-9′ and C-9″) at δ_C 168.3. The deshielded resonances of two oxymethine protons in the quinic acid nucleus at δ_H 5.67 (H-5) and 5.24 (H-4) implied acylation of the hydroxyl group at these positions as earlier reported for other naturally occurring quinic acid derivatives [Pauli *et al.*, 1998; Lin *et al.*, 1999]. From these observations, the structure of **12** was initially thought to be the known compound **11**. However, the ^{1}H NMR spectrum of **12** showed slightly but distinctly different peak patterns of the quinic acid unit compared to the known **11** [$\delta_{H\text{-}3}$ 4.29, (dt, J = 3.2, 2.8 Hz), $\delta_{H\text{-}4}$ 5.09, (dd, J = 10.4, 3.2 Hz) and $\delta_{H\text{-}5}$ 5.69, (dt, J = 6.6, 10.4 Hz)], which was also isolated from this plant. The structure of the known **11** had been ascertained by a detailed comparison of the physical and spectral data with those of the literature [Pauli *et al.*, 1998].

Thus, we assumed that compound **12** is a conformational isomer of **11**. To elucidate the conformation of **12**, comprehensive NMR studies were undertaken. Firstly, a ROESY experiment was recorded and the data, together with the magnitude of the coupling constants and data from the COSY spectrum, compared to the known **11**. No clear ROESY cross-peaks from the oxymethine proton H-4 (δ 5.24) to any of the sp^3 methylene protons H-2 (δ 2.11 and 2.08) or H-6 (δ 2.22 and 2.10) were evident compared to those found for **11**, which suggested that H-4 is equatorial compared to its axial position in the known compound. Moreover, the physical properties (solubility, optical rotation) of **12** were different from those of the known **11**. Like other *epi*-quinic acid derivatives [Kim and Lee, 2005], **12** is of limited solubility in methanol, while the known derivative is freely soluble in the same solvent. Conformational isomers of quinic acid have been investigated thoroughly, and three principal structures have been confirmed, namely (–)-quinic acid, (–)-epiquinic acid and (+)-quinic acid [Kim and Lee, 2005]. The negative optical rotation of **12** of $[\alpha]^{20}_D$: –32° eliminates the probability of a (+)-quinic acid derivative and the magnitude differs from that of the known **11** ($[\alpha]^{20}_D$: –74°). Taken together these data indicate **12** contains the *epi*-isomer of quinic acid and is 4,5-dicaffeoyl-*epi*-quinic acid.

However the coupling constants in the ^{1}H NMR spectrum of **12** measured at 600 MHz were not in agreement with a single chair-like conformation as shown. A detailed study [Flores-Parra *et al.*, 1989; Eliel and Ramirez, 1997] disclosed that quinic acid moiety exists as two conformers in rapid equilibrium. Therefore the ^{1}H NMR of **12** was measured at low temperature (300 °K, 273 °K and

253 °K). Although the spectra recorded for **12** were not absolutely unambiguous, it did appear that lowering the temperature from 300 °K to 253 °K caused a broaching of the signals of H-4 and H-3 of the major isomer. This implied the molecule exists as an equilibrium mixture of various (approximately 3) conformations at room temperature. This would rationalize the "unusual" couplings observed for H-3 (ddd, J = 5.6, 5.4, 5.3 Hz).

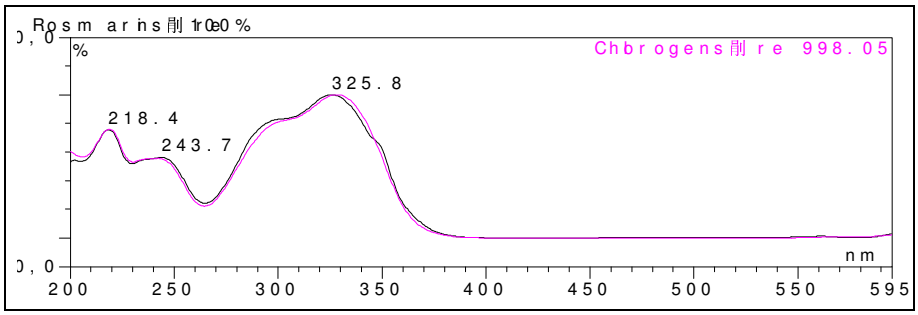

Figure 3.63 UV spectrum of compound **12**

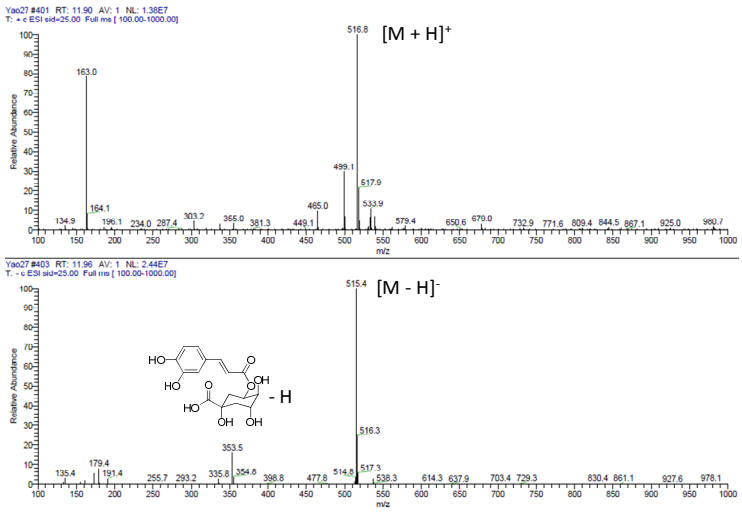

Figure 3.64 ESI-MS spectrum of compound **12**

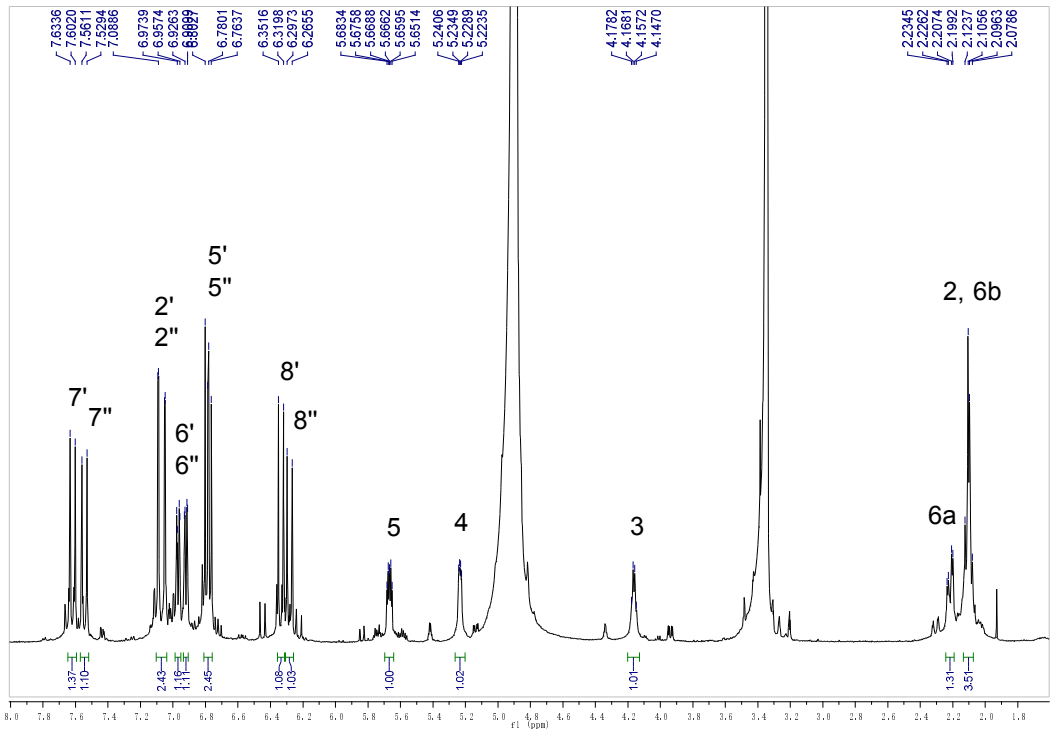

Figure 3.65 ^{1}H NMR spectrum of compound **12**

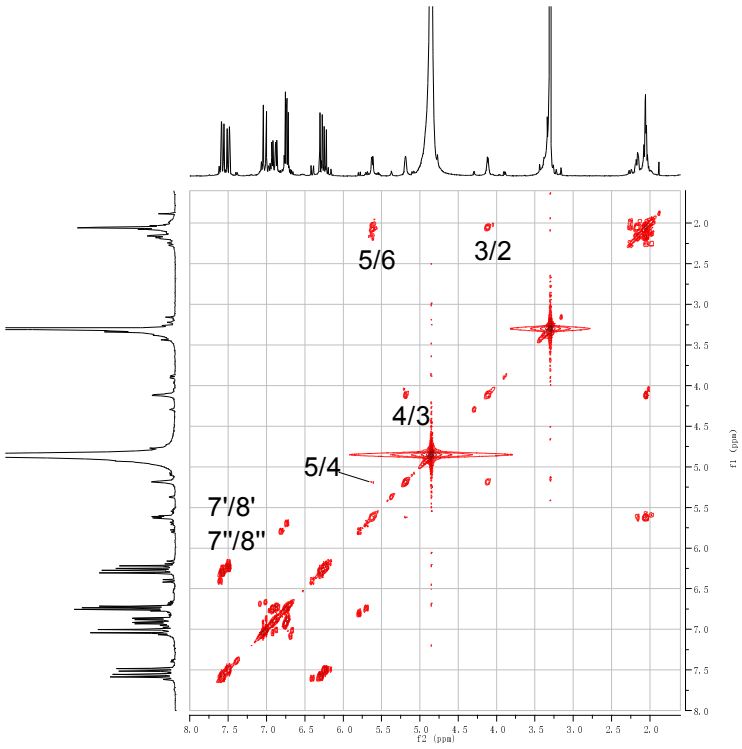

Figure 3.66 ^{1}H-^{1}H COSY spectrum of compound **12**

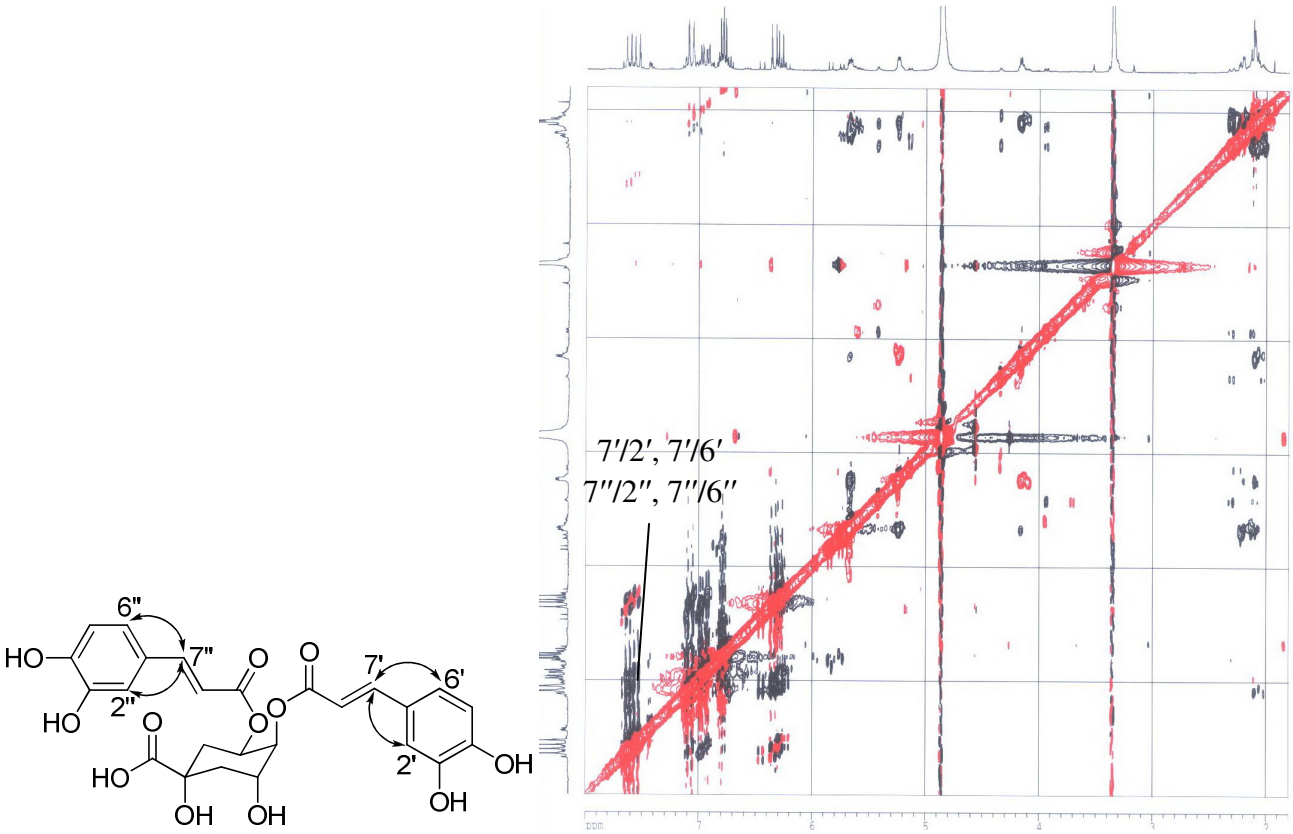

Figure 3.67 ROESY spectrum of compound **12**

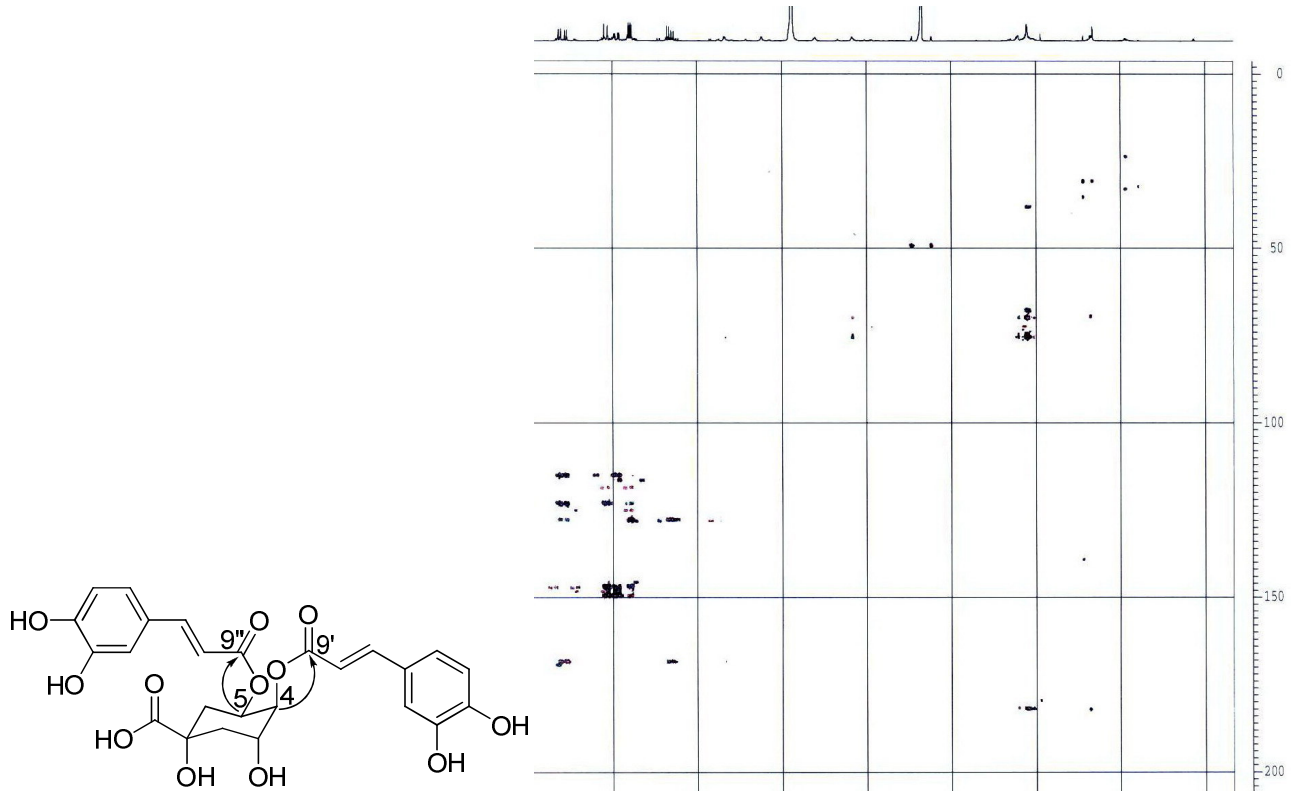

Figure 3.68 HMBC spectrum of compound **12**

Figure 3.69 NMR spectroscopic data of compound **12** (CD_3OD, 600 MHz)

Position	δ_C	δ_H (mult., *J* in Hz)	COSY	ROESY	HMBC
1	75.5, qC				
2_{eq}	38.0, CH_2	2.11, m[a]	3		
2_{ax}		2.08, dd (13.1, 5.3)	3	6_{ax}	
3_{ax}	67.9, CH	4.16, ddd (5.6, 5.4, 5.3)	2_{eq}, 2_{ax}, 4		C1, C5
4_{eq}	72.8, CH	5.24, dd (6.1, 3.0)	3, 5		C3, C9′
5_{eq}	70.0, CH	5.67, ddd (8.6, 4.1, 3.3)	4, 6_{eq}, 6_{ax}		C1, C6, C9″
6_{eq}	39.7, CH_2	2.22, dd (13.2, 4.1)	5		
6_{ax}		2.10, m[a]	5	2_{ax}	
7	182.0, qC				
1′	127.8, qC				
2′	115.0, CH	7.09, d (2.2)	6′		C4′, C6′, C7′
3′	146.7, qC				
4′	149.6, qC				
5′	116.5, CH	6.80, d (8.2)	6′		C1′, C3′, C4′
6′	123.1, CH	6.97, dd (8.2, 2.2)	2′, 5′		C2′, C4′, C7′
7′	147.1, CH	7.62, d (15.9)	8′	2′, 6′	C2′, C6′, C9′
8′	115.1, CH	6.34, d (15.9)	7′		C1′, C9′
9′	168.3, qC				
1″	127.8, qC				
2″	115.0, CH	7.05, d (2.1)	6″		C4″, C6″, C7″
3″	146.7, qC				
4″	149.6, qC				
5″	116.5, CH	6.78, d (8.1)	6″		C1″, C3″, C4″
6″	123.1, CH	6.92, dd (8.1, 2.1)	2″, 5″		C2″, C4″, C7″
7″	147.1, CH	7.55, d (15.9)	8″	2″, 6″	C2″, C6″, C9″
8″	115.1, CH	6.28, d (15.9)	7″		C1″, C9″
9″	168.3, qC				

[a] Overlapped signals assigned by ^1H-^1H COSY, HMBC, and HMQC spectra without designating multiplicity.

3.1.13. 5-*p*-Coumaroylquinic acid (*trans*) (13, known compound)

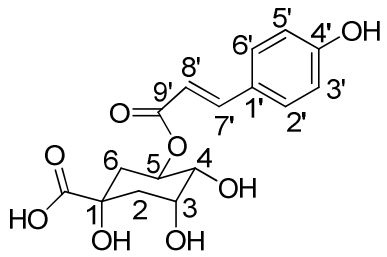

Molecular formula:	$C_{16}H_{18}O_8$
Molecular weight:	338.31
Amount:	0.6 mg

Compound **13** was isolated as an amorphous solid and had a molecular weight of 338 as deduced from the ESIMS spectrum (Figure 3.71). It had UV absorbances at λ_{max} 205, 210, and 308 nm (Figure 3.70) indicative of the presence of *p*-coumaric acid moiety as the sole chromophore. In the ^{1}H NMR spectrum of **13** (Figure 3.72), the olefinic protons showed a *J* value of 16.0 Hz indicating the *p*-coumaric acid moiety had a *trans*-configuration. Corroborating ^{1}H NMR resonances with ^{1}H-^{1}H COSY spectrum (Figure 3.73) of **13**, the observation in the high field suggested the presence of a quinic acid aliphatic ring system. The ^{1}H NMR data of **13** agreed well with that of reference compound, thus **13** was assigned to be **5-*p*-coumaroylquinic acid (*trans*)** [Lu *et al.*, 2000].

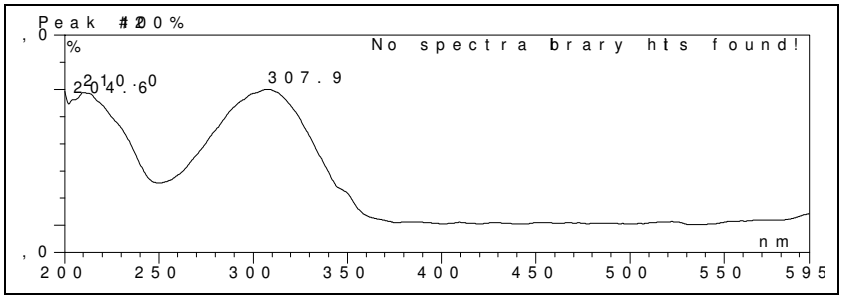

Figure 3.70 UV spectrum of compound **13**

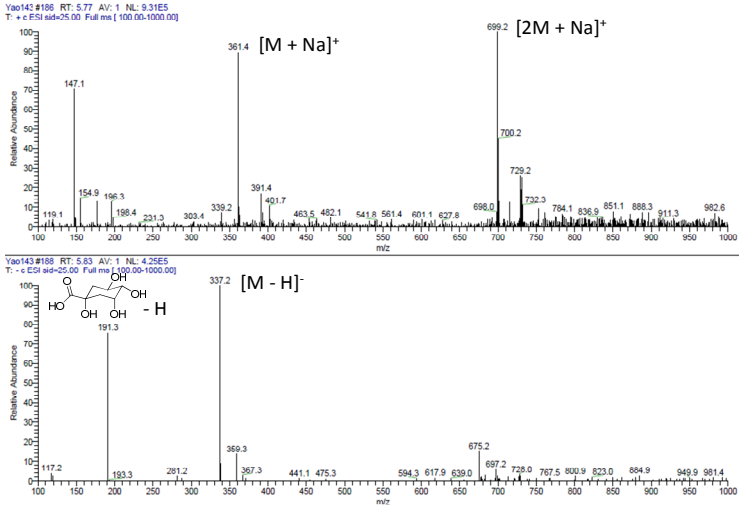

Figure 3.71 ESI-MS spectrum of compound **13**

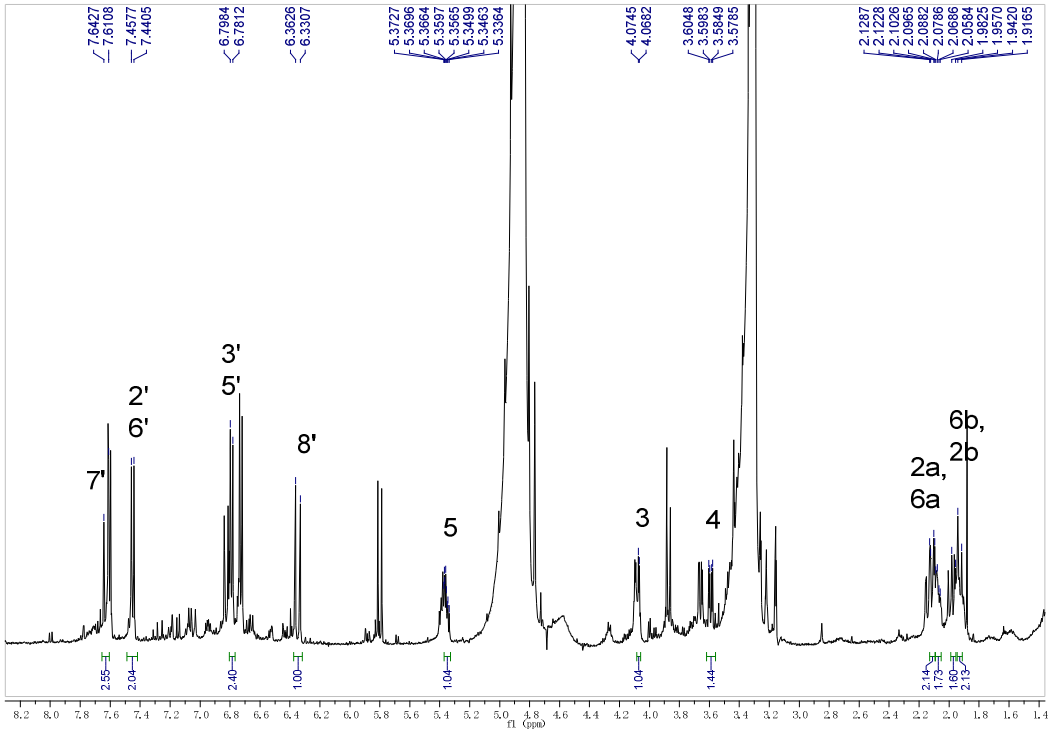

Figure 3.72 ^{1}H NMR spectrum of compound **13**

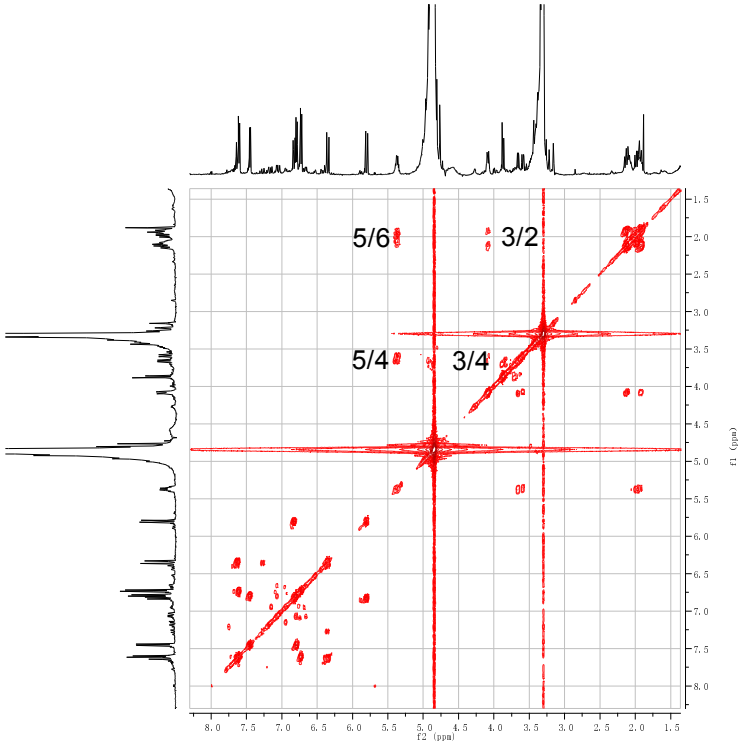

Figure 3.73 ^{1}H-^{1}H COSY spectrum of compound **13**

Table 3.12 NMR spectroscopic data of compound **13** (CD_3OD, 500 MHz)

	5-*p*-coumaroylquinic acid (*trans*) [Lu *et al.*, 2000]	Compound **13**
Position	δ_H (mult., *J* in Hz)	δ_H (mult., *J* in Hz)
2	2.29-2.01, m	2.11, dd (13.3, 3.2)
		1.93, d (12.6)
3	3.90, d (3.1)	4.07, d (3.2)
4	3.77, dd (8.6, 3.0)	3.59, dd (9.8, 3.2)
5	5.33, m	5.36, m[a]
6	2.29-2.01, m	2.08, m[a]; 1.97, m[a]
2’	7.48, d (8.6)	7.45, d (8.5)
3’	6.84, d (8.6)	6.79, d (8.5)
5’	6.84, d (8.6)	6.79, d (8.5)
6’	7.48, d (8.6)	7.45, d (8.5)
7’	7.65, d (16.0)	7.63, d (16.1)
8’’	6.34, d (16.0)	6.35, d (16.1)

[a] Overlapped signals assigned by ^{1}H-^{1}H COSY, HMBC, and HMQC spectra without designating multiplicity.

3.1.14. 5-*p*-Coumaroylquinic acid (*cis*) (14, known compound)

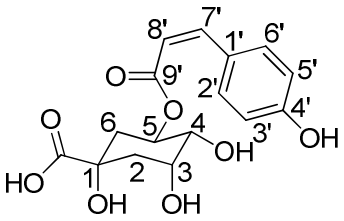

Molecular formula:	$C_{16}H_{18}O_8$
Molecular weight:	338.31
Amount:	0.6 mg

Compound **14** was obtained as an amorphous solid. It had the same molecular weight and UV absorbances as compound **13** (Figure 3.76 and Figure 3.75). Compound **14** was further established as 5-*p*-coumaroylquinic acid (*cis*) by ^{1}H NMR of **14** (Figure 3.74) which showed that the olefinic protons had a smaller *J* value of 12.6 Hz compared with the *J* value (16.0 Hz) in **13**. It was relatively unstable and readily converted to the *trans* isomer **13**. From the above observations and through comparison with the literature it was confirmed that compound **14** was **5-*p*-coumaroylquinic acid (*cis*)** [Lu *et al.*, 2000].

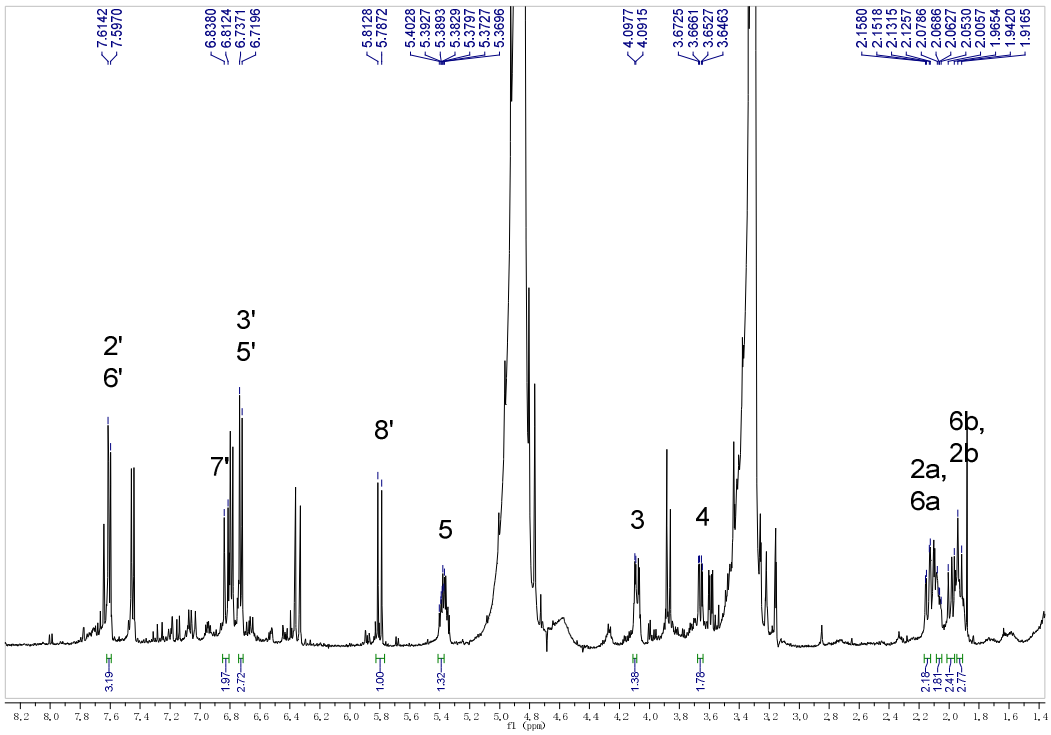

Figure 3.74 ^{1}H NMR spectrum of compound **14**

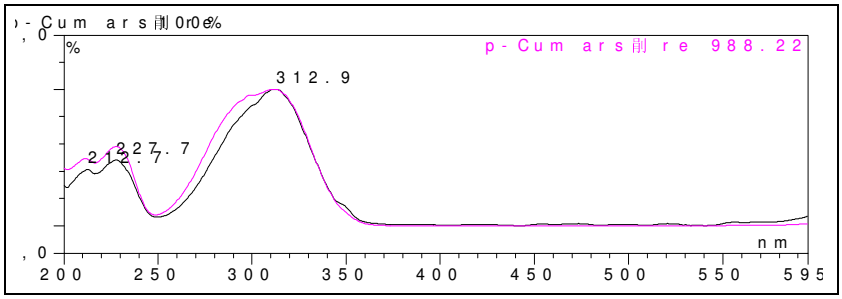

Figure 3.75 UV spectrum of compound **14**

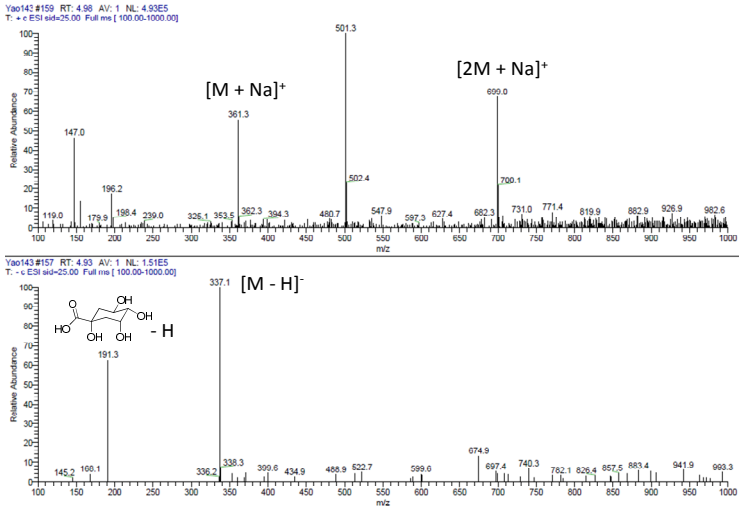

Figure 3.76 ESI-MS spectrum of compound **14**

Table 3.13 NMR spectroscopic data of compound **14** (CD_3OD, 500 MHz)

	5-*p*-coumaroylquinic acid (*cis*) [Lu *et al.*, 2000]	Compound **14**
Position	δ_H (mult., *J* in Hz)	δ_H (mult., *J* in Hz)
2	2.33-1.99, m	2.14, dd (13.3, 3.2)
		1.93, d (12.6)
3	4.27, d (3.1)	4.09, d (3.2)
4	3.71, m	3.66, dd (9.8, 3.2)
5	5.37, br s	5.38, m[a]
6	2.33-1.99, m	2.06, m[a]; 1.99, m[a]
2’	7.63, d (8.2)	7.61, d (8.5)
3’	6.76, d (8.2)	6.73, d (8.5)
5’	6.76, d (8.2)	6.73, d (8.5)
6’	7.63, d (8.2)	7.61, d (8.5)
7’	6.83, d (12.7)	6.83, d (12.6)
8’’	5.79, d (12.7)	5.80, d (12.6)

[a] Overlapped signals assigned by ^1H-^1H COSY, HMBC, and HMQC spectra without designating multiplicity.

3.1.15. Isoorientin (15, known compound)

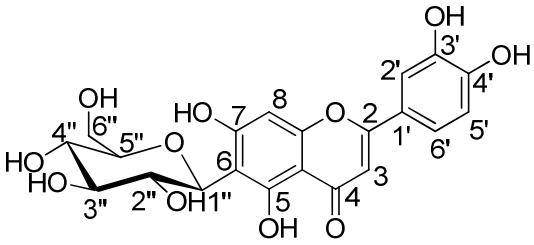

Molecular formula:	$C_{21}H_{20}O_{11}$
Molecular weight:	448.38
Amount:	5.1 mg

Compound **15** was isolated as a yellow amorphous solid. The UV spectrum of **15** (Figure 3.77) exhibited absorption maxima at 211, 270, and 349 nm which were the same as those of isoorientin. Its ESI mass spectrum showed pseudomolecular ion peak $[M + H]^+$ at *m/z* 449 and $[M - H]^-$ at *m/z* 447 (Figure 3.78). The ^{1}H NMR spectrum of **15** showed an ABX system at δ_H 7.35 (br s), 6.88 (d, 8.4 Hz) and 7.36 (d, J = 8.4 Hz), respectively, and two singlet signals (δ_H 6.52 and 6.47) in the aromatic region. The assignments were further supported by analysis of the ^{1}H-^{1}H COSY (Figure 3.80), HMBC (Figure 3.81) and HMQC (Figure 3.82) spectra of **15**. The attachment of the glucose at C-6 was deduced from the HMBC correlation between C-6 (δ 108.8) and the anomeric proton H-1″, which in turn gave two cross-peaks with C-5 at δ 161.7 and C-7 at δ 164.9, respectively. Thus compound **15** was doubtless assigned to be **isoorientin** [Kumazawa *et al.*, 2000].

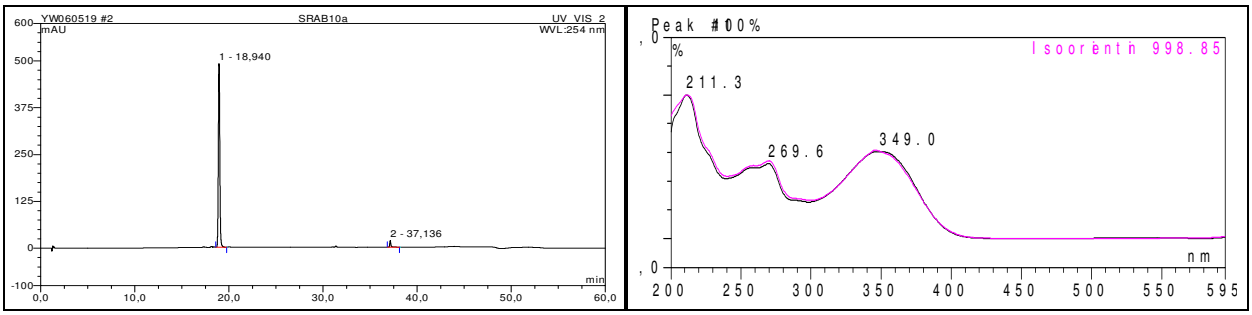

Figure 3.77 HPLC chromatogram and UV spectrum of compound **15**

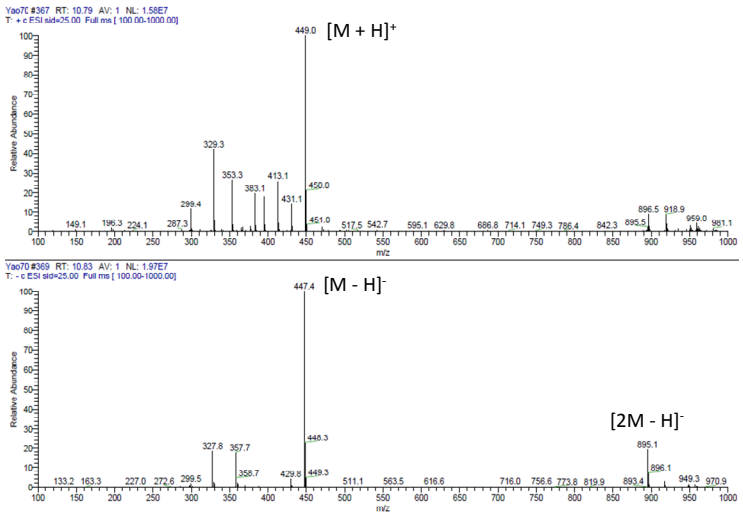

Figure 3.78 ESI-MS spectrum of compound **15**

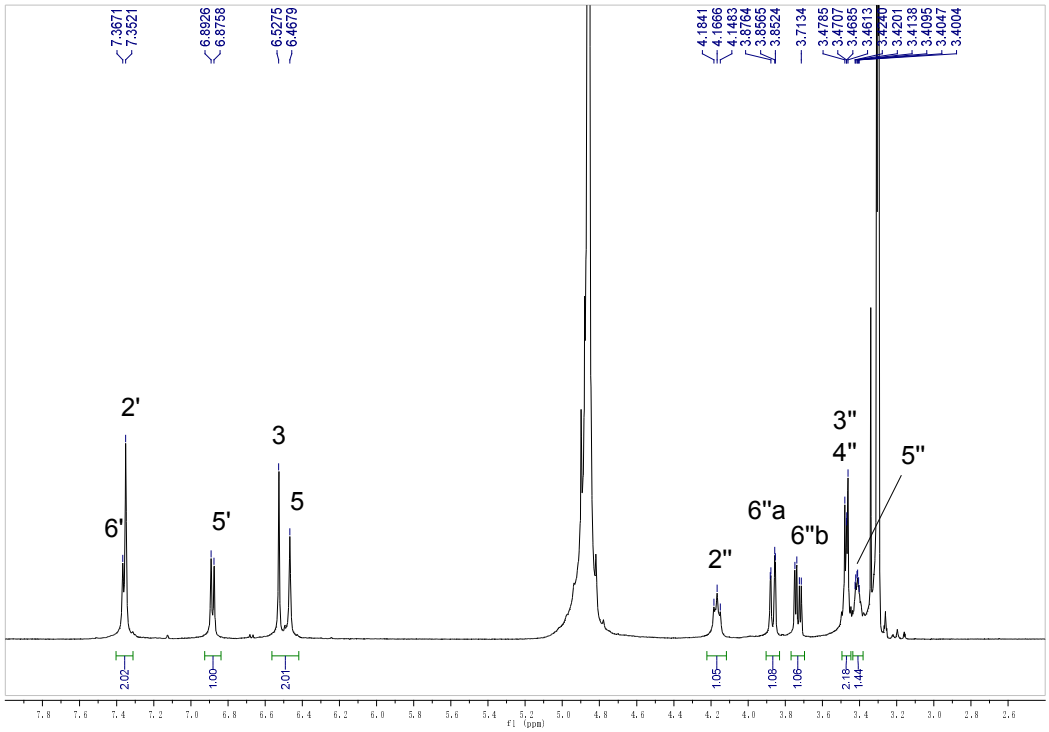

Figure 3.79 ^{1}H NMR spectrum of compound **15**

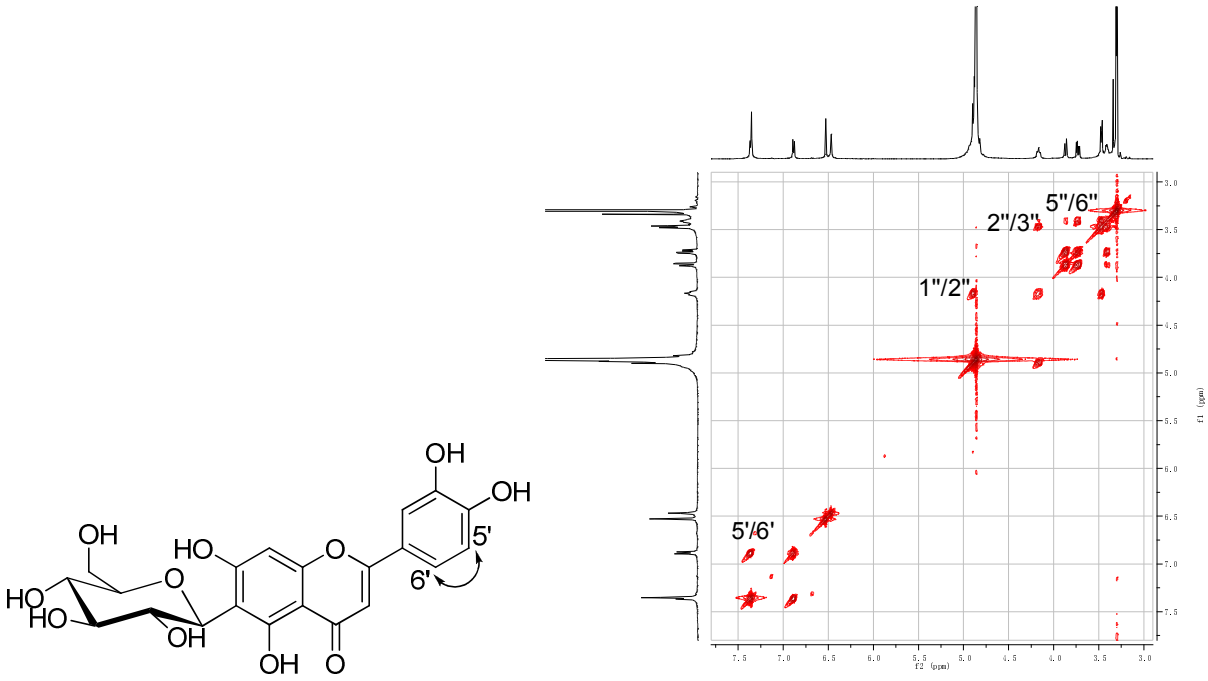

Figure 3.80 ^{1}H-^{1}H COSY spectrum of compound **15**

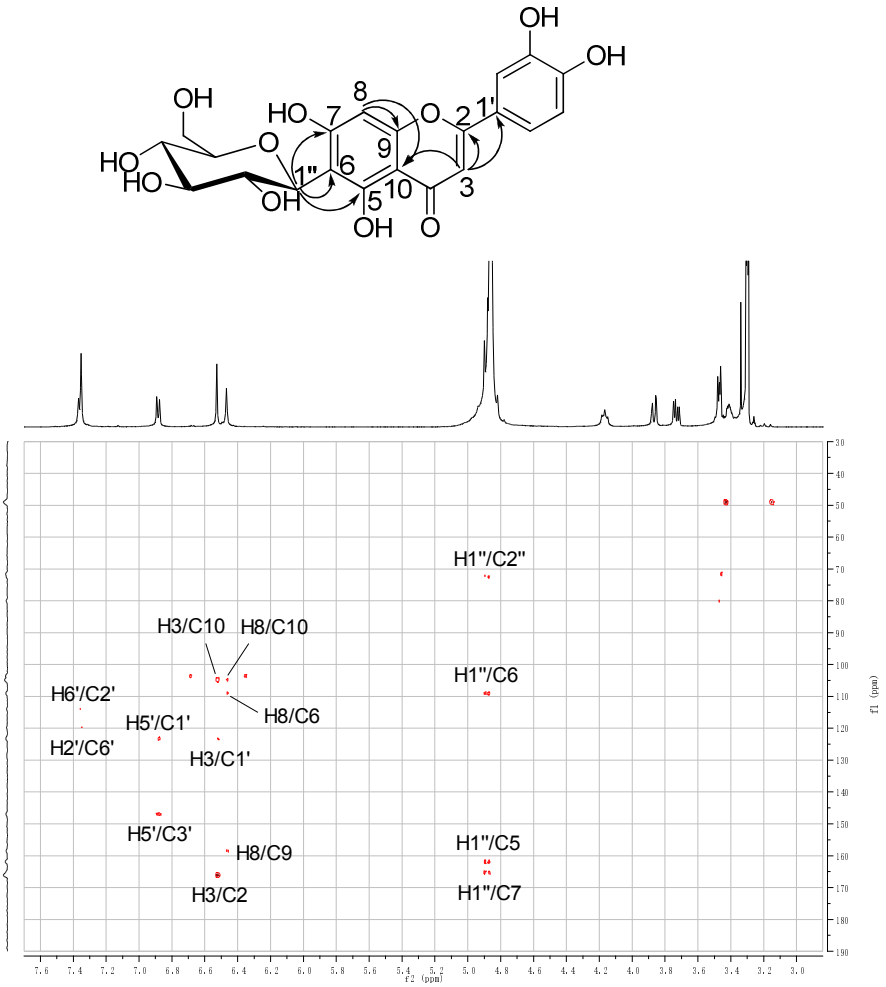

Figure 3.81 HMBC spectrum of compound **15**

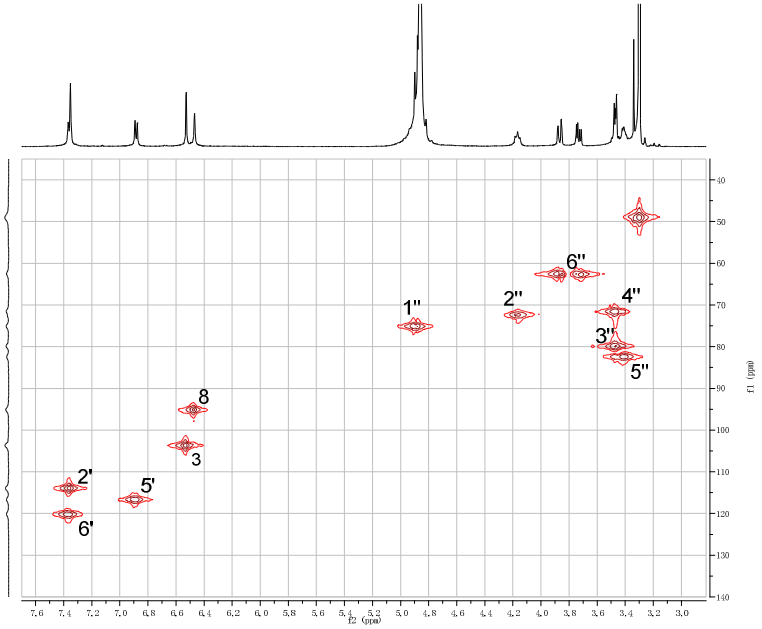

Figure 3.82 HMQC spectrum of compound **15**

Table 3.14 NMR spectroscopic data of compound **15** (CD_3OD, 500 MHz)

	Isoorientin (DMSO) [Kumazawa *et al.*, 2000]		Compound **15**	
Position	δ_C	δ_H (mult., *J* in Hz)	δ_C	δ_H (mult., *J* in Hz)
2	163.6, qC		165.8, qC	
3	102.7, CH	6.67, s	103.4, CH	6.53, s
4	181.7, qC		183.7, qC	
5	160.6, qC		161.7, qC	
6	108.8, qC		108.8, qC	
7	163.2, qC		164.9, qC	
8	93.4, CH	6.48, s	94.7, CH	6.47, s
9	156.1, qC		158.3, qC	
10	103.3, qC		104.7, qC	
1′	121.4, qC		123.1, qC	
2′	113.2, CH	7.40, d (2.3)	113.7, CH	7.35, br s
3′	145.7, qC		146.6, qC	
4′	149.6, qC		150.6, qC	
5′	116.0, CH	6.89, d (8.2)	116.5, CH	6.88, d (8.4)
6′	118.8, CH	7.42, dd (8.2, 2.3)	119.9, CH	7.36, br d (8.4)
1″	73.0, CH	4.58, d (9.8)	75.1, CH	4.89, d (9.9)
2″	70.5, CH	4.07, dd (10.2, 9.8)	72.2, CH	4.17, dd (9.1, 8.9)
3″	78.9, CH	3.19, dd (10.2, 8.5)	79.6, CH	3.47, m
4″	70.2, CH	3.12, dd (8.5, 8.9)	71.4, CH	3.47, m
5″	81.4, CH	3.17, ddd (8.9, 6.1, 1.8)	82.1, CH	3.41, m
6″	61.4, CH_2	3.68, dd, (11.3, 1.8)	62.5, CH_2	3.87, dd (12.1, 2.2)
		3.40, dd (11.3, 6.1)		3.73, dd, (12.1, 5.4)

3.1.16. Scorzonerin A (16, new compound)

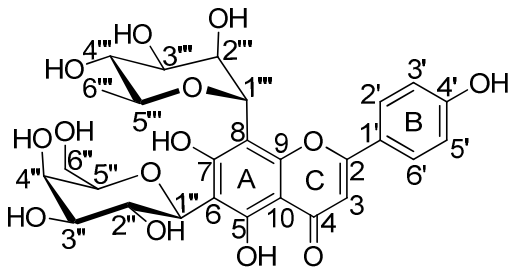

Molecular formula:	$C_{27}H_{30}O_{14}$
Molecular weight:	578.52
Amount:	7.0 mg

Compound **16** was isolated as a yellow amorphous solid. Its molecular formula was determined as $C_{27}H_{30}O_{14}$ by HRESIMS (*m/z* 579.1708 $[M + H]^+$). The UV spectrum of **16** showed absorption maxima at 335, 272 and 215nm, and closely resembled that of isovitexin. The ^1H (Figure 3.85) and ^{13}C (Figure 3.86) NMR spectra of **16** confirmed the presence of a flavone glycoside characterized by an AA′BB′ system with signals at δ_H 6.97 (d, J = 8.0 Hz, H-3′ and H-5′)/δ_C 117.2 (C-3′ and C-5′) and δ_H 7.88 (d, J = 8.0 Hz, H-2′ and H-6′)/δ_C 129.5 (C-2′ and C-6′), and a further aromatic proton signal at δ_H 6.62 (s, H-3)/δ_C 103.6. The identity of the two sugar units followed from the magnitude of the vicinal coupling constants determined from the 1D ^1H and connectivities from the 2D COSY and TOCSY (Figure 3.87) spectra. In the ^1H-^1H COSY spectrum, a cross-peak was observed between the anomeric proton at δ_H 4.90 (d, J = 9.8 Hz) and the broad triplet at δ 4.57, corresponding to H-2″, which was further coupled to the double doublet of H-3″ at 3.60 ppm. Hence all three protons are in axial positions of a β-galactopyranose ring system that is evident from the small vicinal couplings to H-4″ that clearly distinguish it from a β-glucopyranose system found in violanthin [Carnat *et al.*, 1998]. Similarly the magnitude of the vicinal coupling constants and chemical shifts of the second sugar unit, with the anomeric proton at 5.33 ppm, indicated this was a rhamnopyranose system. Currently we assume that the rhamnose has an α anomeric configuration and the absolute configuration of the galactose and rhamnose units are D and L, respectively. The linkage of the sugar moieties to the flavone aglycone were established from HMBC data (Figure 3.88). The anomeric proton at δ_H 4.90 of the galactose moiety showed a HMBC correlation with C-6 (δ_C 109.9) in ring A of the flavone and two hydroxylated carbons C-5 at δ_C 161.5 and C-7 at δ_C 166.8, respectively, thus establishing the C-glycosidic linkage at C-6 of the flavone nucleus. The second anomeric proton at

δ_H 5.33 belonging to the rhamnose moiety gave a HMBC cross-peak with the hydroxylated carbon at δ_C 166.8 (C-7), the oxygen-bearing carbon C-9 (δ_C 155.9) and C-8 (δ_C 104.4) respectively, indicating that the rhamnose moiety was bound to C-8 via a C-glycosidic linkage, similar to violanthin [Carnat *et al.*, 1998]. Thus compound **16** is considered to be apigenin-6-C-*β*-D-galactopyranosyl-8-C-*α*-L-6-rhamnopyranoside and given the trivial name scorzonerin A.

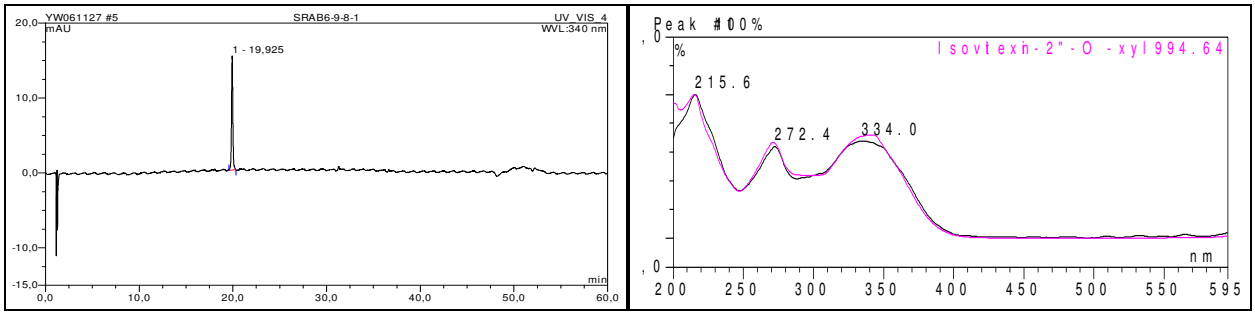

Figure 3.83 HPLC chromatogram and UV spectrum of compound **16**

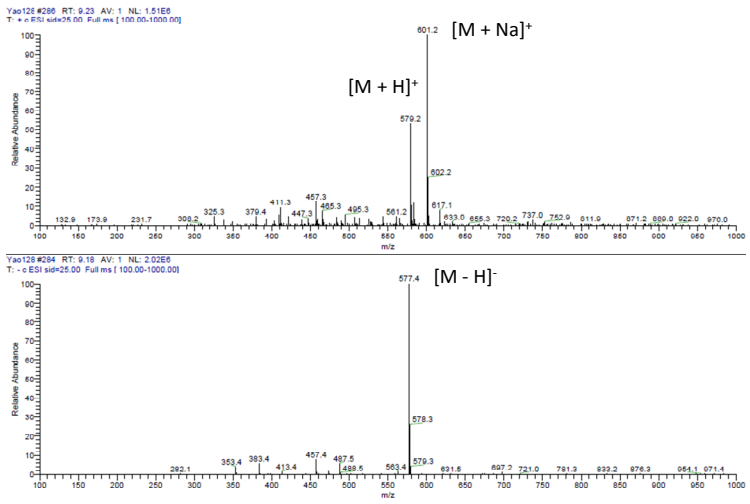

Figure 3.84 ESI-MS spectrum of compound **16**

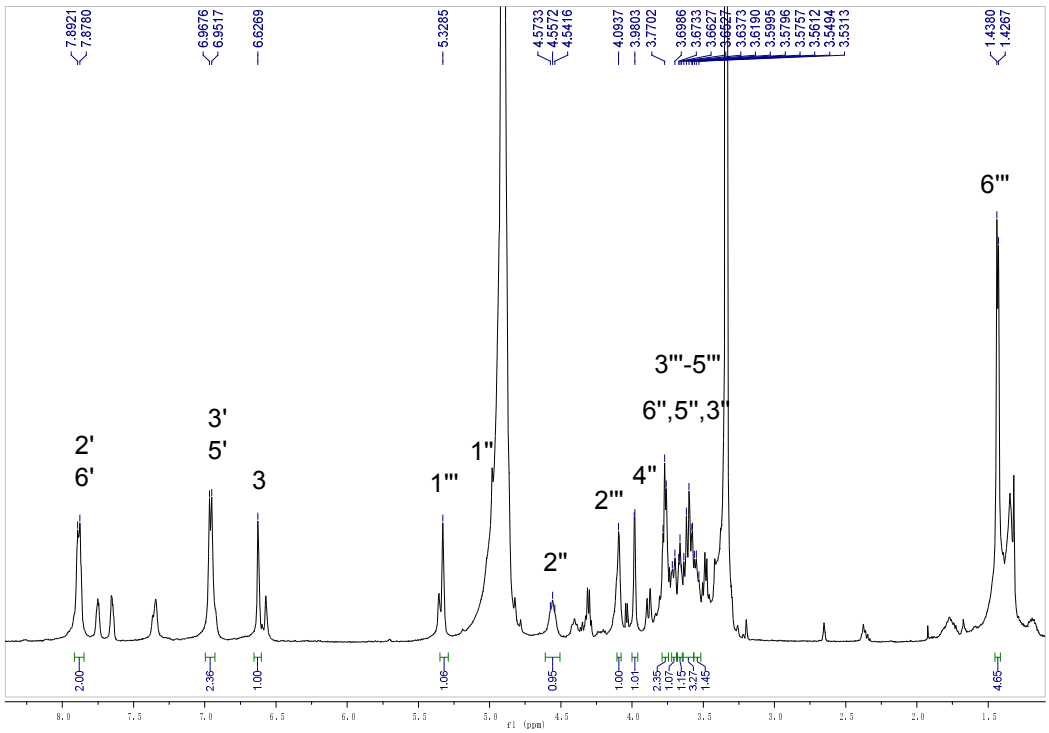

Figure 3.85 ^{1}H NMR spectrum of compound **16**

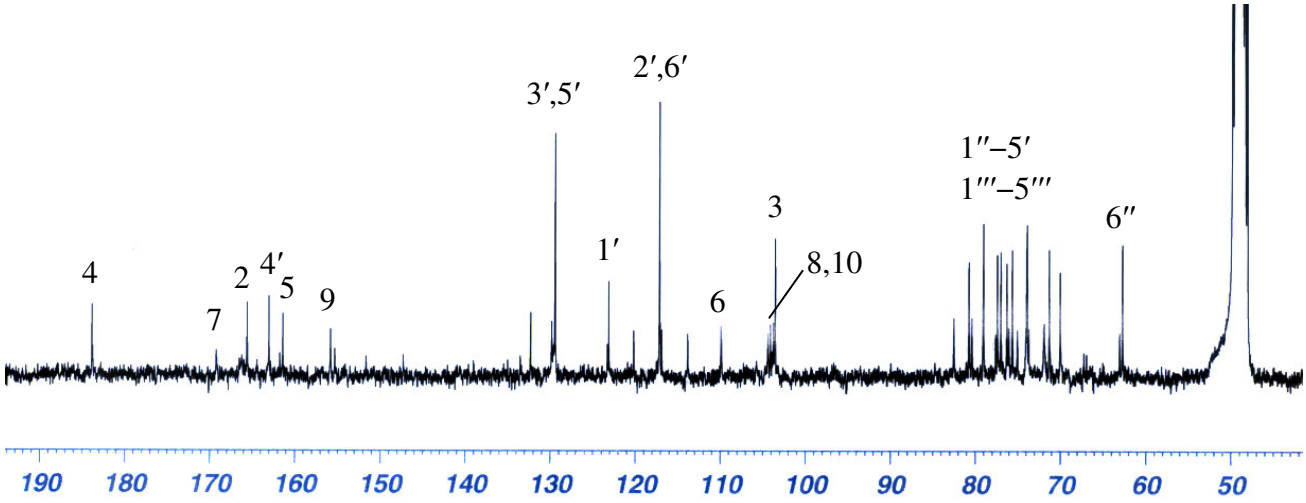

Figure 3.86 ^{13}C NMR spectrum of compound **16**

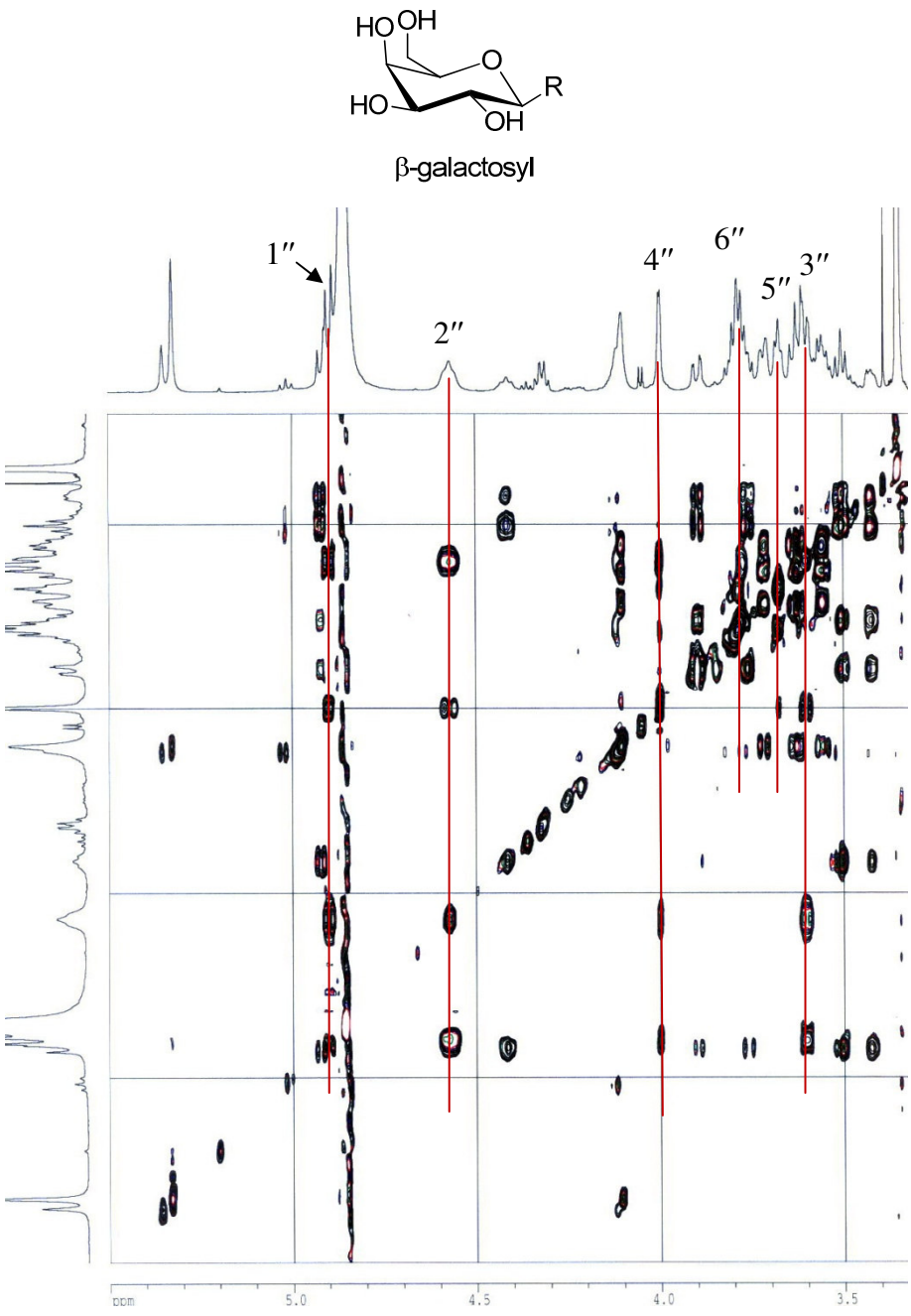

Figure 3.87 TOCSY spectrum of compound **16**

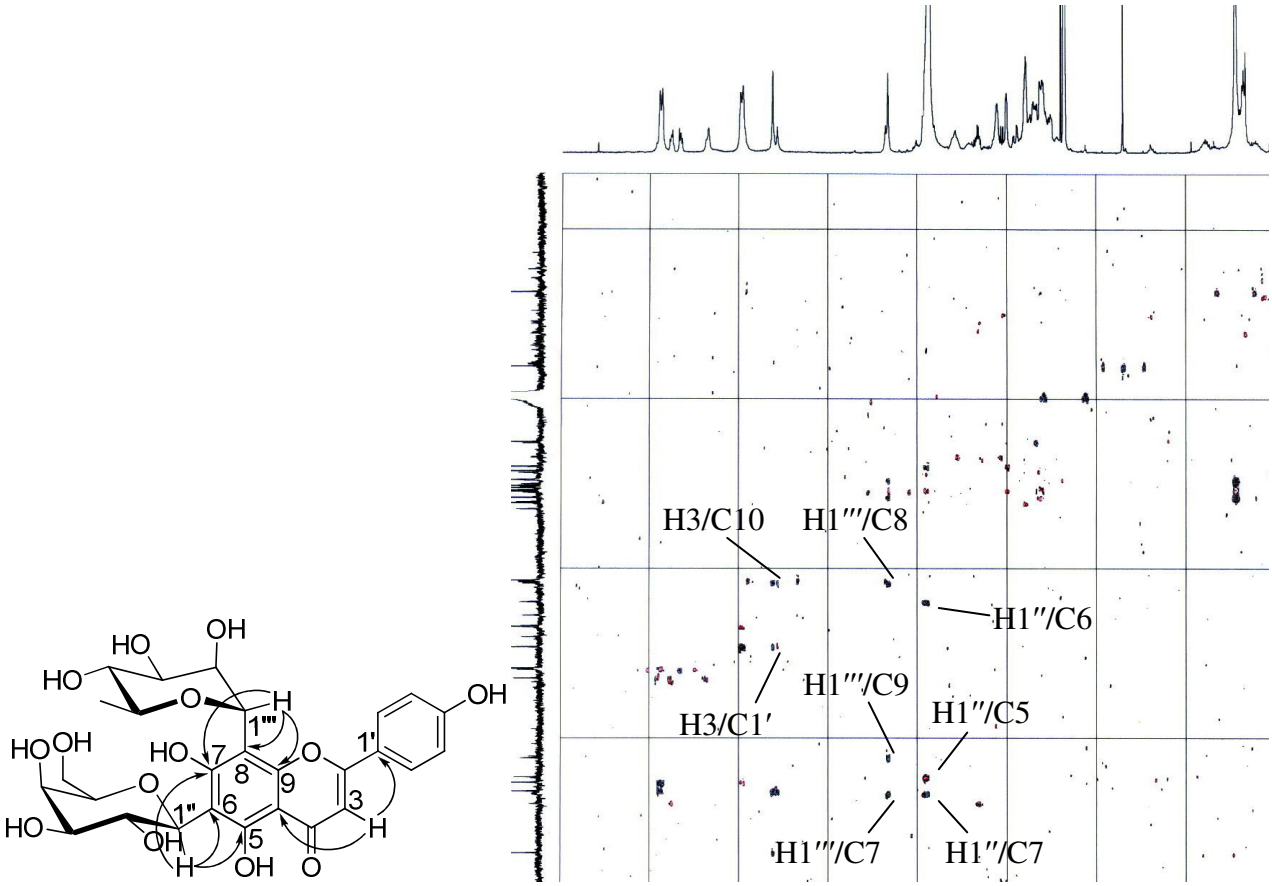

Figure 3.88 HMBC spectrum of compound **16**

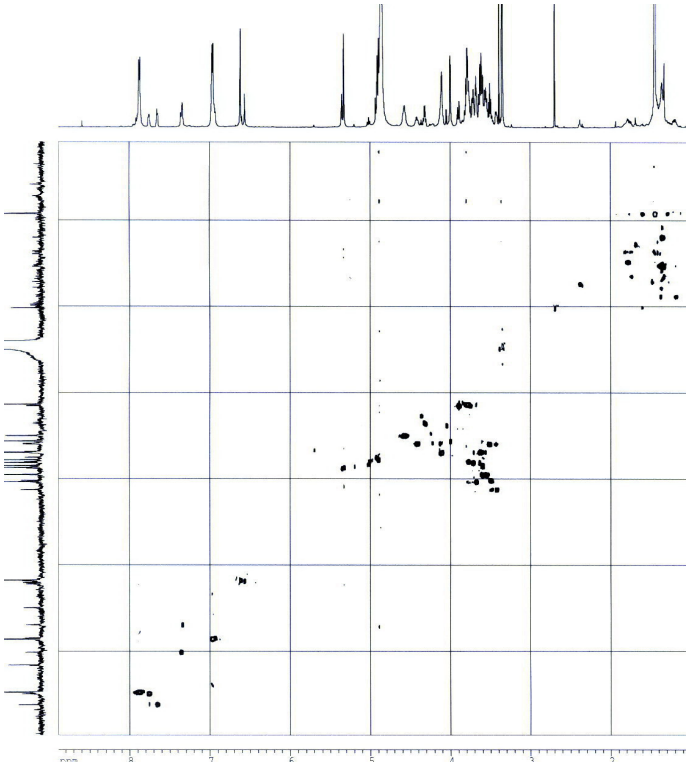

Figure 3.89 HMQC spectrum of compound **16**

Table 3.15 NMR spectroscopic data of compound **16** (CD_3OD, 500 MHz)

Position	δ_C	δ_H (mult., *J* in Hz)	TOCSY	HMBC
2	165.7, qC			
3	103.6, CH	6.62, s		C1′, C10
4	183.9, qC			
5	161.5, qC			
6	109.9, qC			
7	166.8, qC			
8	104.4, qC			
9	155.9, qC			
10	104.1, qC			
1′	123.2, qC			
2′	117.2, CH	7.88, d (8.2)		
3′	129.5, CH	6.97, d (8.2)		
4′	163.1, qC			
5′	129.5, CH	6.97, d (8.2)		
6′	117.2, CH	7.88, d (8.2)		
1″ Galactosyl	75.6, CH	4.90, d (9.8)	2″, 3″, 4″	C5, C6, C7
2″ Galactosyl	70.0, CH	4.57, br t	1″, 3″, 4″	
3″ Galactosyl	77.0, CH	3.60, dd (9.1, 2.1)	1″, 2″, 4″	
4″ Galactosyl	71.3, CH	4.00, d (2.4)	1″, 2″, 3″, 5″, 6″	
5″ Galactosyl	80.8, CH	3.67, t (5.5)	4″, 6″	
6″ Galactosyl	62.8, CH_2	3.78, m[a]; 3.76, m[a]	5″	
1‴ Rhamnosyl	77.4, CH	5.33, s		C7, C8, C9
2‴ Rhamnosyl	74.0, CH	4.10, br s		
3‴ Rhamnosyl	76.3, CH	3.72, br d (9.0)		
4‴ Rhamnosyl	73.9, CH	3.63, t (9.0)		
5‴ Rhamnosyl	79.1, CH	3.56, dq (8.8, 5.8)		
6‴ Rhamnosyl	18.5, CH_3	1.44, d (5.8)		

[a] Overlapping signals assigned by ^1H-^1H COSY and HMBC spectra without designating multiplicity.

3.1.17. Scorzonerin B (17, new compound)

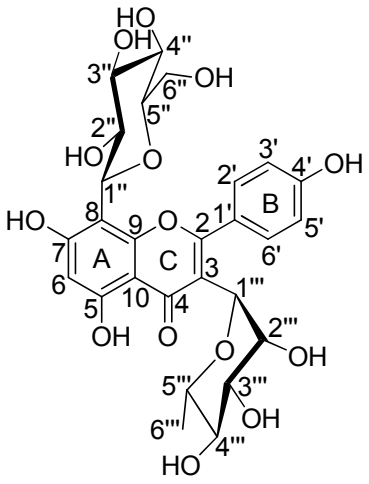

Molecular formula:	$C_{27}H_{30}O_{14}$
Molecular weight:	578.52
Amount:	0.9 mg

Compound **17** was isolated as a yellow amorphous solid with a molecular formular of $C_{27}H_{30}O_{14}$ from the HRESIMS (*m/z* 579.1708 $[M + H]^+$). The UV spectrum of **17** showed absorption maxima at 335, 272 and 215 nm similar to compound **16**. In the aromatic region of the ^1H NMR spectrum of **17** (Figure 3.92), an AA′BB′ system at δ_H 7.83 (d, J = 8.8 Hz, H-2′ and H-6′) and 6.94 (d, J = 8.8 Hz, H-3′ and H-5′) and one singlet signal at δ_H 6.53 (H-6) were observed, characteristic of an apigenine moiety. In the upfield region, two anomeric protons were presented at δ_H 4.92 (d, J = 9.9 Hz) and 5.29 (br s), which differed from the chemical shifts of anomeric protons of O-glycosides that are usually observed at δ_H 5–6 ppm [Hesse *et al.*, 1997]. Along with the molecular weight and the residual resonances of the ^1H and ^{13}C NMR spectrum, two carbon bound sugar units were inferred to be present. The connections between the flavone aglycone and the sugar moieties were determined by ROESY (Figure 3.93) and HMBC (Figure 3.94) spectra. The aromatic proton at δ_H 7.83 (H2′ and H6′) gave a ROESY cross-peak with the anomeric proton of the rhamnose moiety at δ_H 5.29, which further correlated with the oxygen-bearing carbon C-2 at δ_C 156.9 and C-3 at δ_C 105.8 in the HMBC spectrum, thus establishing the linkage of the rhamnose moiety at C-3 of the flavone core. Attachment of the glucose moiety was determined from the HMBC cross-peaks of the anomeric proton at δ_H 4.92 (d, J = 9.9 Hz) with the oxygen-bearing carbon C-9 at δ_C 162.0 and C-8 at δ_C 110.8 in ring A, respectively, which indicated that the glucose unit was attached to C-8 via a C-glycosidic

bond. This was corroborated from the chemical shifts of the ^{13}C NMR spectrum of **17** and comparison with the ^{13}C NMR data of the reference compound vitexin [Tomczyk *et al.*, 2002]. From these data, we tentative conclude that **17** is apigenin-3-C-*α*-L-6-rhamnopyranosyl-8-C-*β*-D-glucopyranoside, to which we assigned the trivial name scorzonerin B.

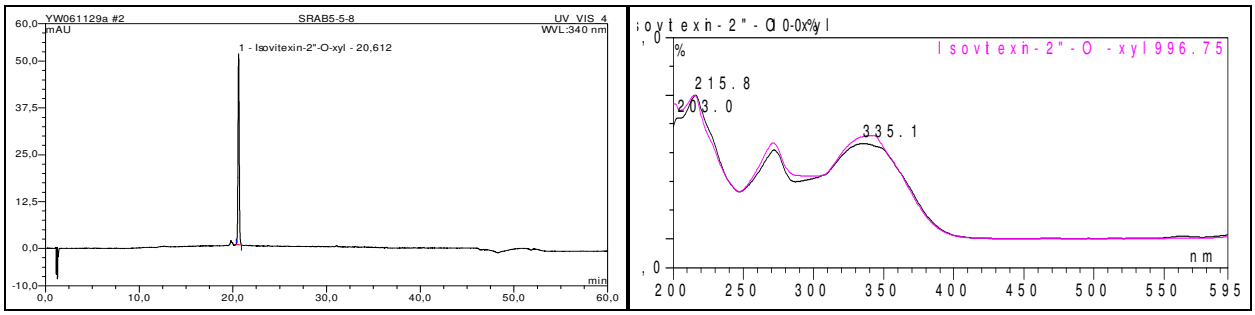

Figure 3.90 HPLC chromatogram and UV spectrum of compound **17**

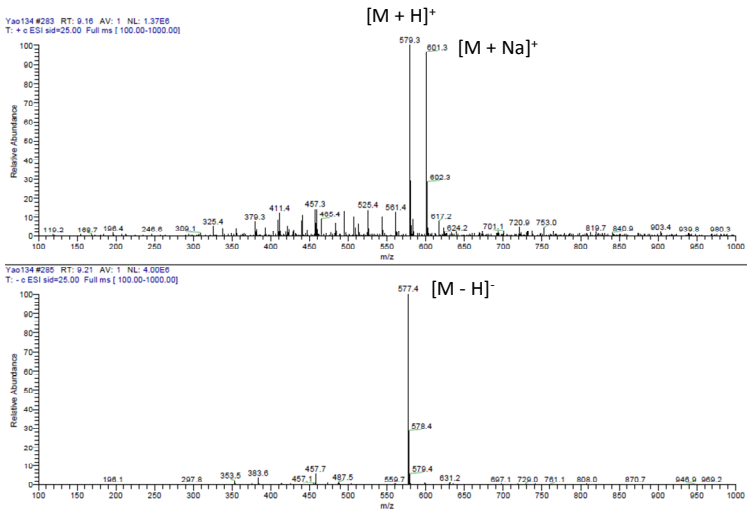

Figure 3.91 ESI-MS spectrum of compound **17**

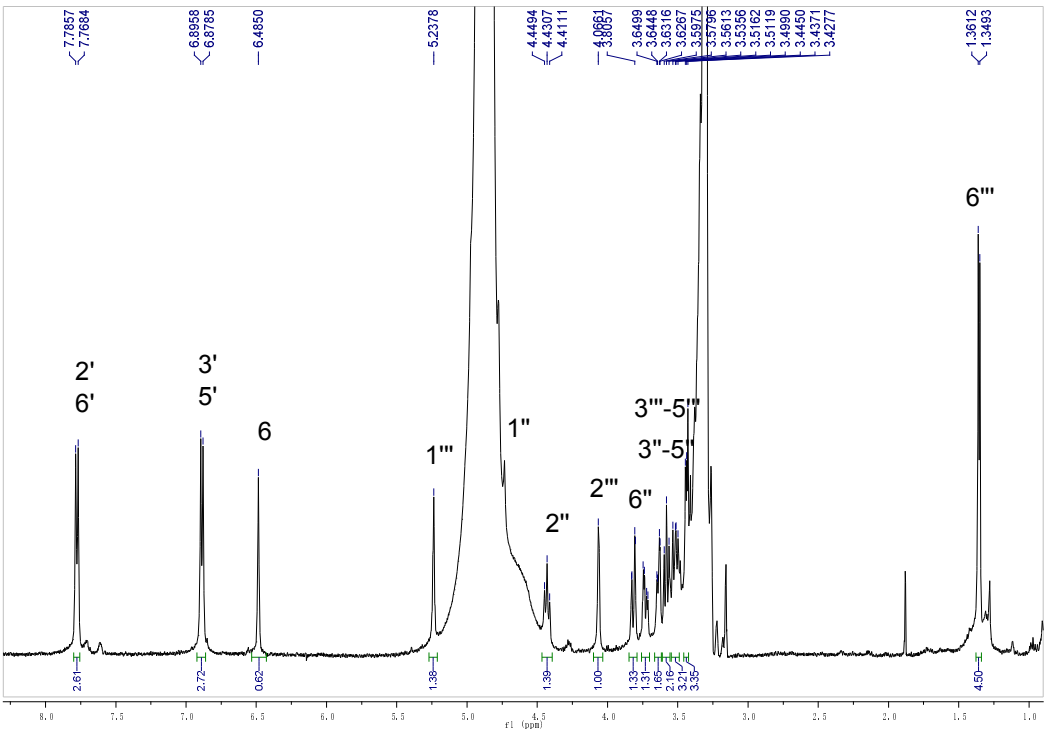

Figure 3.92 ^{1}H NMR spectrum of compound **17**

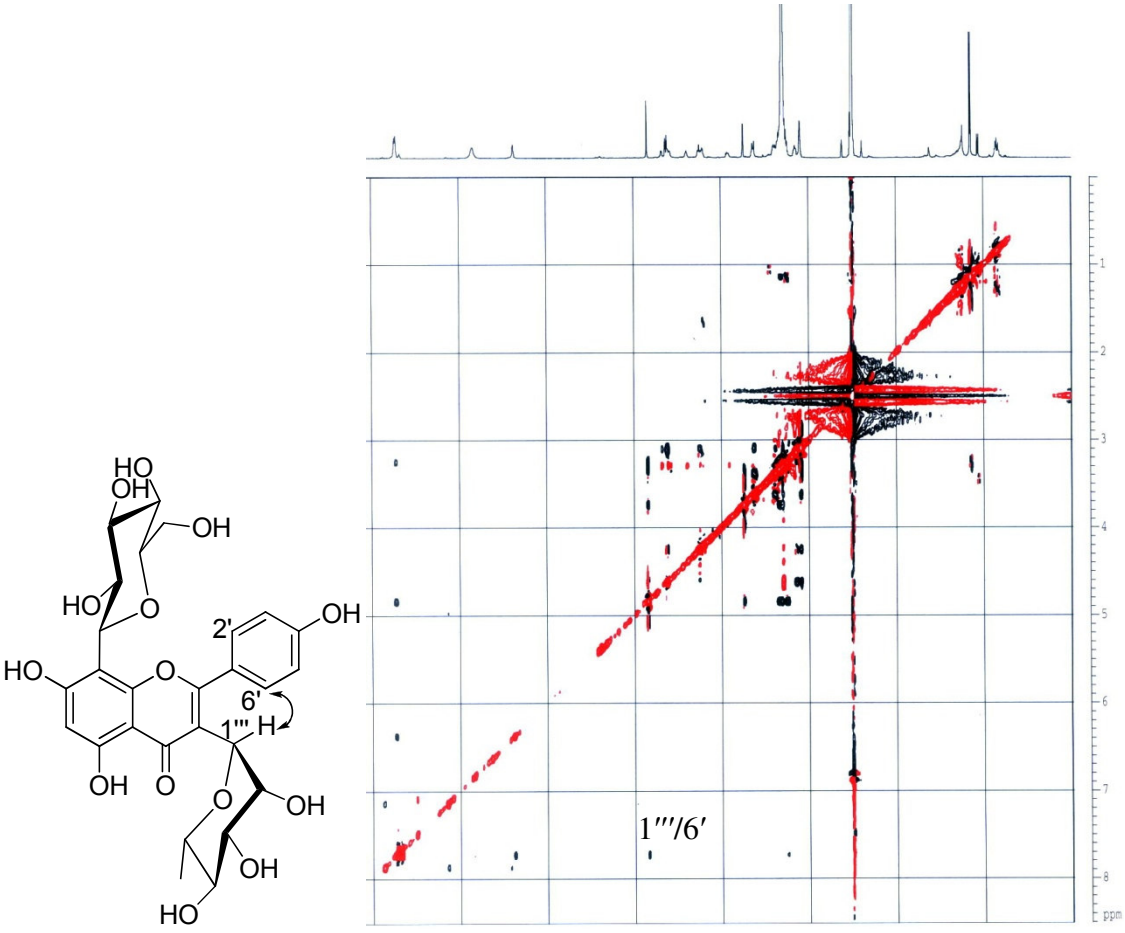

Figure 3.93 ROESY spectrum of compound **17**

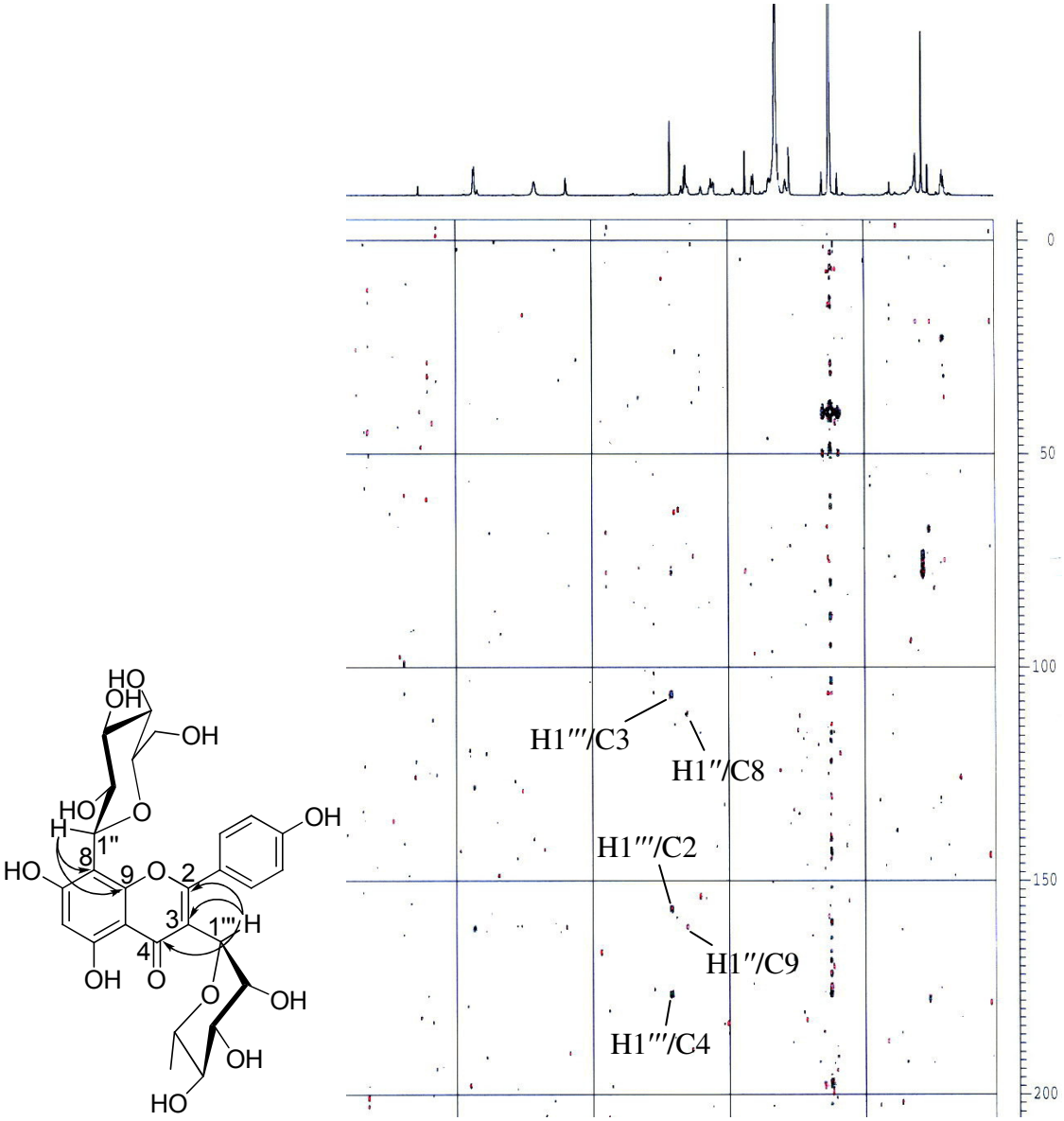

Figure 3.94 HMBC spectrum of compound **17**

Table 3.16 NMR spectroscopic data of compound **17** (CD_3OD, 500 MHz)

Position	δ_C	δ_H (mult., *J* in Hz)	ROESY	HMBC
2	156.9 qC			
3	105.8 qC			
4	qC [a]			
5	165.1 qC			
6	103.0 CH	6.53 s		
7	165.5 qC			
8	110.8 qC			
9	162.0 qC			
10	102.3 qC			
1′	123.0 qC		6‴	
2′	129.2 CH	7.83 d (8.8)		
3′	117.6 CH	6.94 d (8.8)		
4′	163.9 qC			
5′	117.6 CH	6.94 d (8.8)		
6′	129.2 CH	7.83 d (8.8)		
1″ Glucosyl	75.5 CH	4.92 d (9.9)		C8, C9
2″ Glucosyl	71.8 CH	4.48 dd (9.9, 9.2)		
3″ Glucosyl	80.7 CH	3.48 dd (9.2, 9.1)		
4″ Glucosyl	71.6 CH	3.59 dd (9.7, 9.1)		
5″ Glucosyl	82.3 CH	3.40 ddd (9.7, 4.7, 2.2)		
6″ Glucosyl	62.8 CH_2	3.86 dd (12.1, 2.2)		
		3.78 dd (12.1, 4.7)		
1‴ Rhamnosyl	76.9 CH	5.29 br s		C2, C3, C4
2‴ Rhamnosyl	74.2 CH	4.12 d (3.0)		
3‴ Rhamnosyl	77.1 CH	3.69 dd (9.1, 3.0)		
4‴ Rhamnosyl	74.1 CH	3.63 t (9.1)		
5‴ Rhamnosyl	79.0 CH	3.55 dq (9.1, 6.1)		
6‴ Rhamnosyl	18.4 CH_3	1.40 d (6.1)	1′	

[a] Due to the low amount of compound, no ^{13}C NMR signal could be obtained

3.1.18. Kaempferol-3-rutinoside (18, known compound)

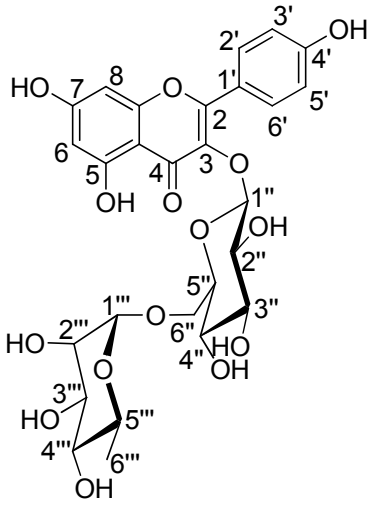

Molecular formula:	$C_{27}H_{30}O_{15}$
Molecular weight:	594.52
Amount:	32.9 mg

Compound **18** was isolated as yellow powder. The UV spectrum of **18** exhibited absorption maxima at 266 and 348 nm in accordance with a flavonol derivative. A pseudomolecular ion $[M + H]^+$ at *m/z* 595 and fragment ions $[F + H]^+$ at *m/z* 449 and 287 were obtained in the positive ion ESI mass spectrum of **18** (Figure 3.96) corresponding to kaempferol-hexose-deoxyhexose. The aromatic region of the ^{1}H NMR spectrum of **18** (Figure 3.97) showed an AA′BB′ system at δ 8.05 (dd, J = 8.8, 1.9 Hz) and 6.88 (dd, J = 8.8, 1.9 Hz), and a 2H AX system at δ 6.39 (d, J = 2.2 Hz) and δ 6.19 (d, J = 2.2 Hz) in accordance to kaempferol aglycone. Assignments of the ^{13}C resonances belonging to the aglycone, as well as the inter-residual connections, were determined by the HMBC (Figure 3.100) and HMQC (Figure 3.99) experiment. The HMBC crosspeak at δ 5.11/135.2 (H-1″/C-3) confirmed the linkage between the glucopyranose unit and the aglycone at the 3-hydroxyl. The interglycosidic linkage between the α-rhamnopyranosyl and the glucopyranose was determined to be at the 6″-hydroxyl by the crosspeak at δ 4.50/68.3 (H-1‴/C-6″) observed in the HMBC spectrum. Compound **18** was identical with the known compound **kaempferol-3-rutinoside** [Slimestad *et al.*, 2008].

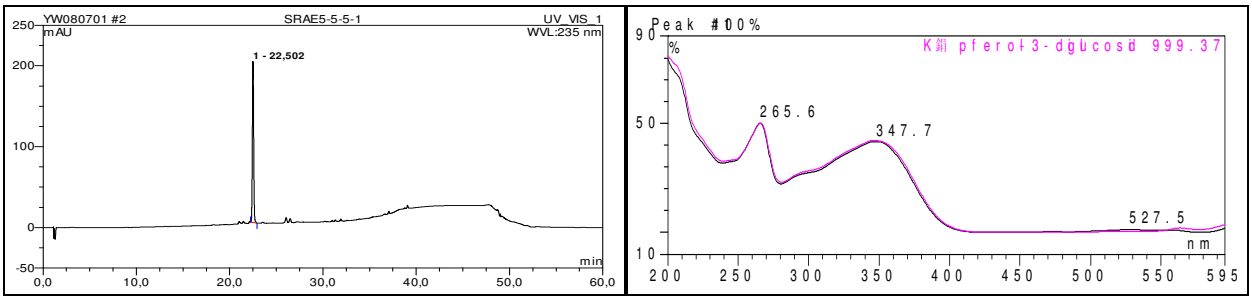

Figure 3.95 HPLC chromatogram and UV spectrum of compound **18**

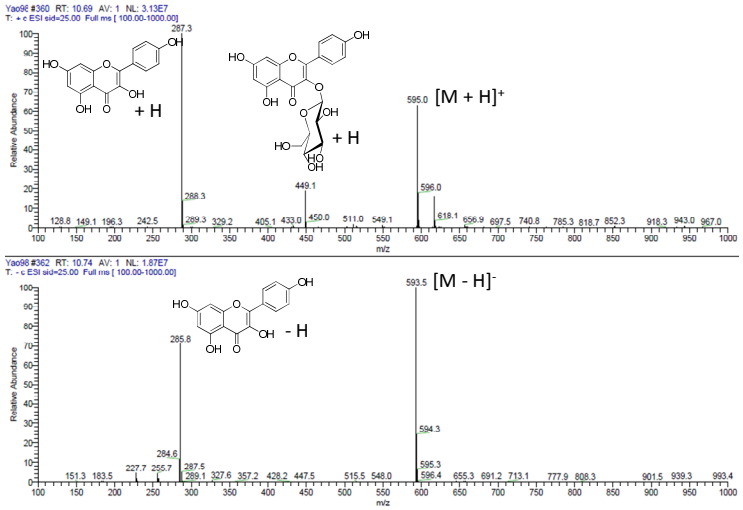

Figure 3.96 ESI-MS spectrum of compound **18**

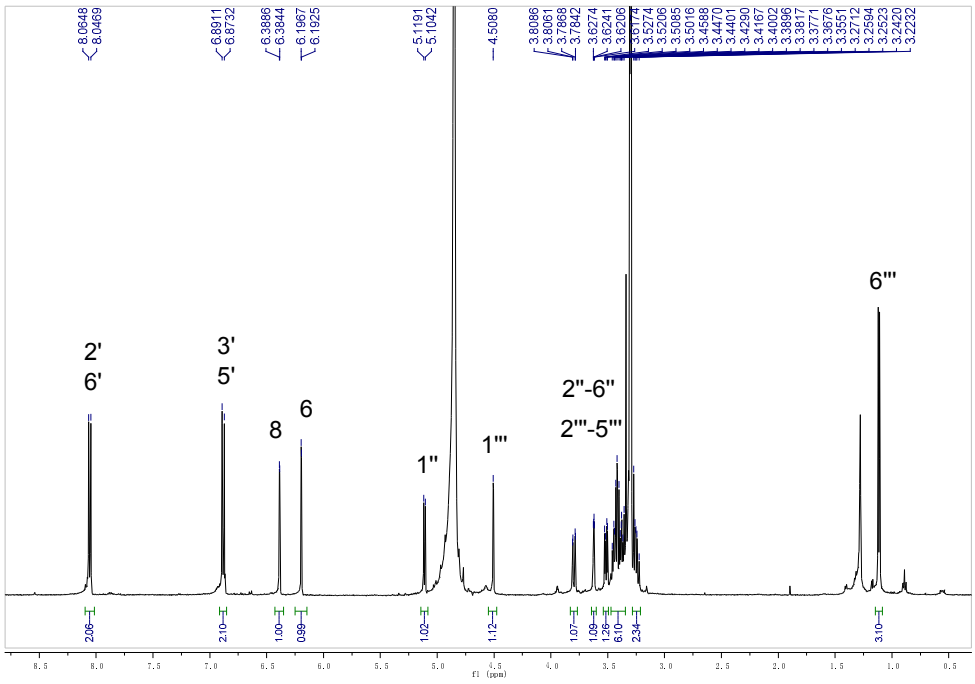

Figure 3.97 ^{1}H NMR spectrum of compound **18**

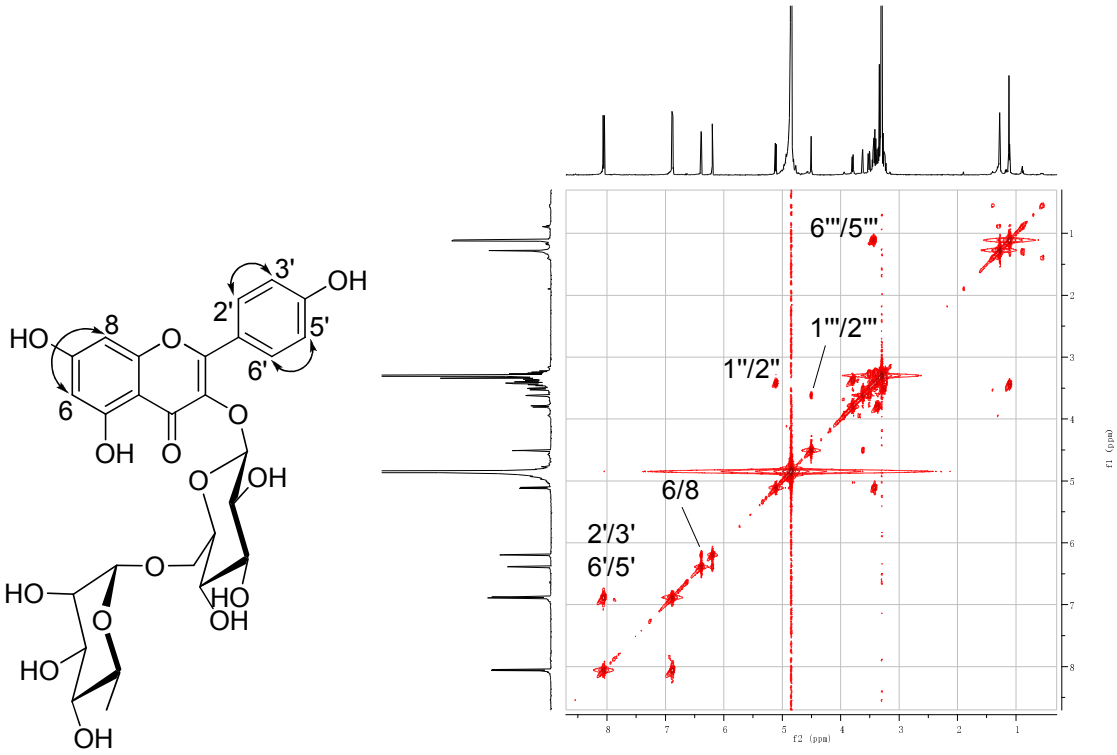

Figure 3.98 ^{1}H-^{1}H COSY spectrum of compound **18**

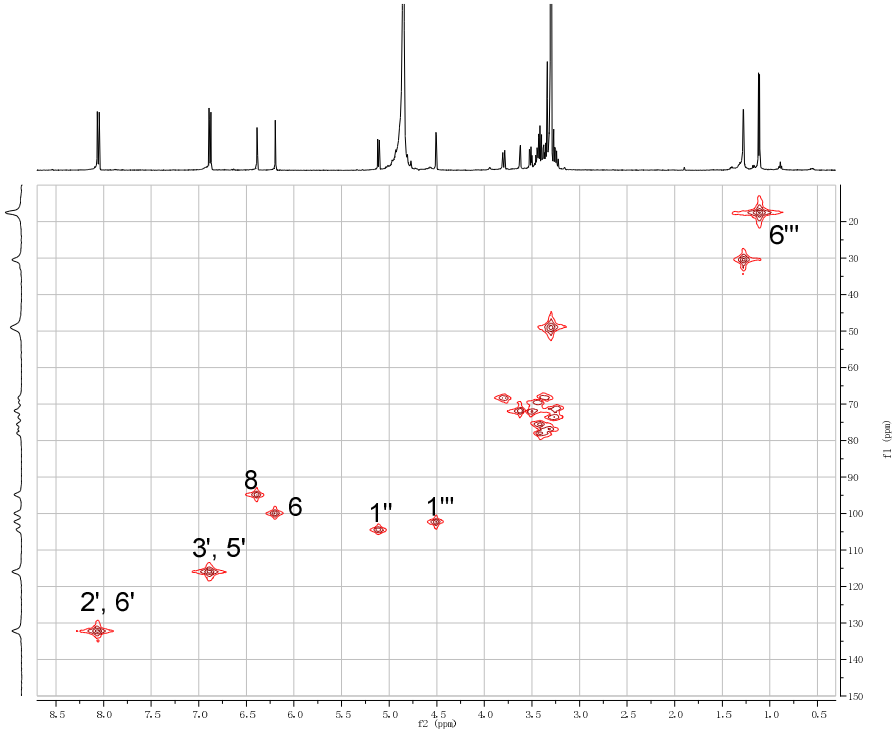

Figure 3.99 HMQC spectrum of compound **18**

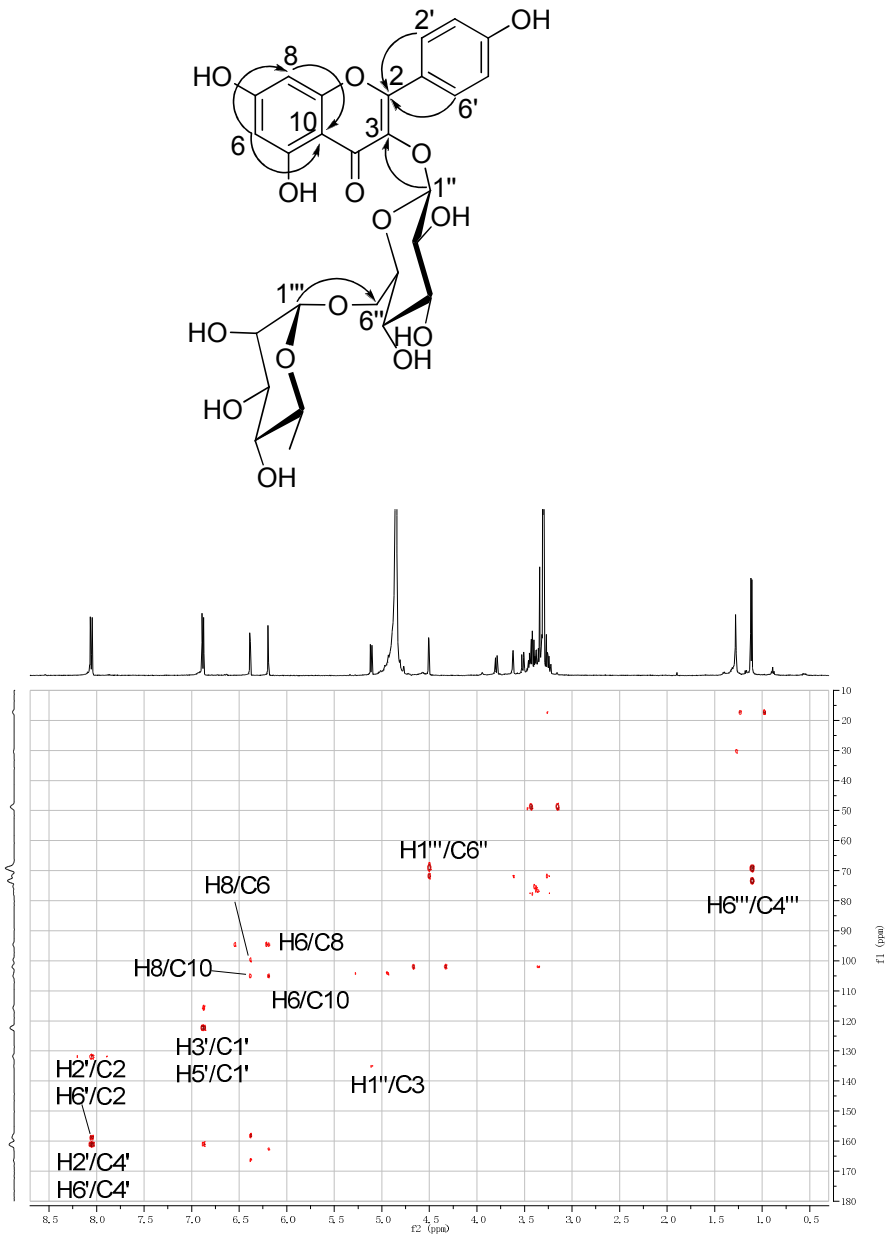

Figure 3.100 HMBC spectrum of compound **18**

Table 3.17 NMR spectroscopic data of compound **18** (CD_3OD, 500 MHz)

	Kaempferol (DMSO) [Slimestad *et al.*, 2008]		Compound **18**	
Position	δ_C	δ_H (mult., *J* in Hz)	δ_C	δ_H (mult., *J* in Hz)
2	156.93, qC		159.1, qC	
3	133.29, qC		135.2, qC	
4	177.47, qC			
5	161.27, qC		162.7, qC	
6	98.80, CH	6.19, d (2.1)	99.8, CH	6.19, d (2.2)
7	164.20, qC		166.4, qC	
8	93.82, CH	6.40, d (2.1)	94.7, CH	6.39, d (2.2)
9	156.56, qC		158.3, qC	
10	104.07, qC		105.2, qC	
1′	120.96, qC		122.4, qC	
2′	130.96, CH	7.97, d (8.9)	132.0, CH	8.05, dd (8.8, 1.9)
3′	115.17, CH	6.87, d (8.9)	115.8, CH	6.88, dd (8.8, 1.9)
4′	159.99, qC		161.2, qC	
5′	115.17, CH	6.87, d (8.9)	115.8, CH	6.88, dd (8.8, 1.9)
6′	130.96, CH	7.97, d (8.9)	132.0, CH	8.05, dd (8.8, 1.9)
1″ Glucosyl	101.40, CH	5.30, d (7.6)	104.2, CH	5.11, d (7.6)
2″ Glucosyl	74.25, CH	3.20, m	75.5, CH	3.41, m[a]
3″ Glucosyl	75.82, CH	3.31, m	78.0, CH	3.42, m[a]
4″ Glucosyl	70.00, CH	3.04, m	71.2, CH	3.24, m[a]
5″ Glucosyl	76.44, CH	3.21, m	77.1, CH	3.37, m[a]
6″ Glucosyl	66.96, CH_2	3.67, dd (11.4, 1.8)	68.3, CH_2	3.80, d (11.2)
		3.26, m		
1‴ Rhamnosyl	101.84, CH	4.36, d (1.8)	102.0, CH	4.50, s
2‴ Rhamnosyl	70.37, CH	3.37, m	71.9, CH	3.62, dd (1.6, 1.6)
3‴ Rhamnosyl	70.67, CH	3.33, m	72.0, CH	3.51, dd (9.5, 3.2)
4‴ Rhamnosyl	71.91, CH	3.07, t (9.4)	73.5, CH	3.27, m[a]
5‴ Rhamnosyl	68.34, CH	3.25, m	69.3, CH	3.45, m[a]
6‴ Rhamnosyl	17.81, CH_3	0.97, d (6.3)	17.5, CH_3	1.11, d (6.3)

[a] Overlapped signals assigned by ^1H-^1H COSY, HMBC, and HMQC spectra without designating multiplicity.

3.1.19. Rutin (19, known compound)

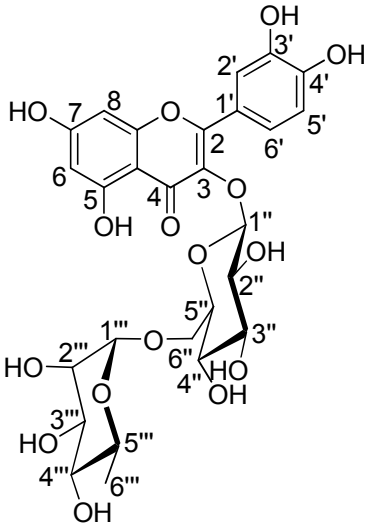

Molecular formula:	$C_{27}H_{30}O_{16}$
Molecular weight:	610.52
Amount:	121.2 mg

Compound **19** was isolated as yellow powders. It has UV absorbance of typical flavonol derivatives at λ_{max} 206, 256 and 357 nm. Compound **19** showed a positive pseudomolecular ion peak $[M + H]^+$ at *m/z* 611 and a negative pseudomolecular ion peak $[M - H]^-$ at *m/z* 609 (Figure 3.102) suggesting the molecular weight *m/z* 610. The ^{1}H NMR spectrum of **19** (Figure 3.103) exhibited different signals for the B-ring protons compared to those of **18**, which are an ABX spin system [δ_H 7.66 (d, J = 1.9 Hz), 6.86 (d, J = 8.5 Hz) and 7.62 (dd, J = 8.5, 1.9 Hz)] instead of an AA′BB′ system as present in **18**. Comparison of the ^{1}H NMR spectrum and the MS fragmentations of compound **19** with that of **rutin** confirmed that both compounds were identical [Khalifa *et al.*, 1983].

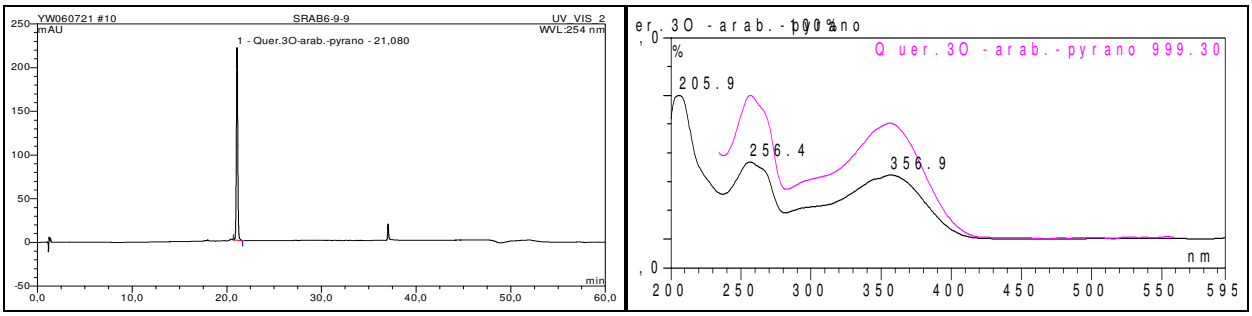

Figure 3.101 HPLC chromatogram and UV spectrum of compound **19**

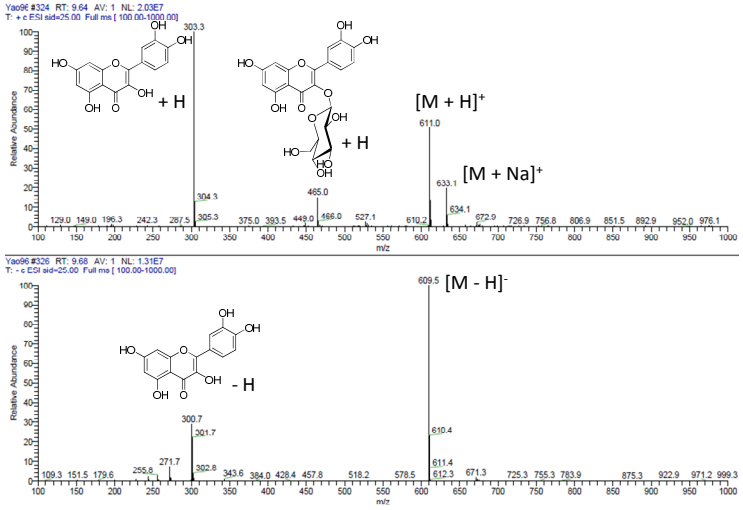

Figure 3.102 ESI-MS spectrum of compound **19**

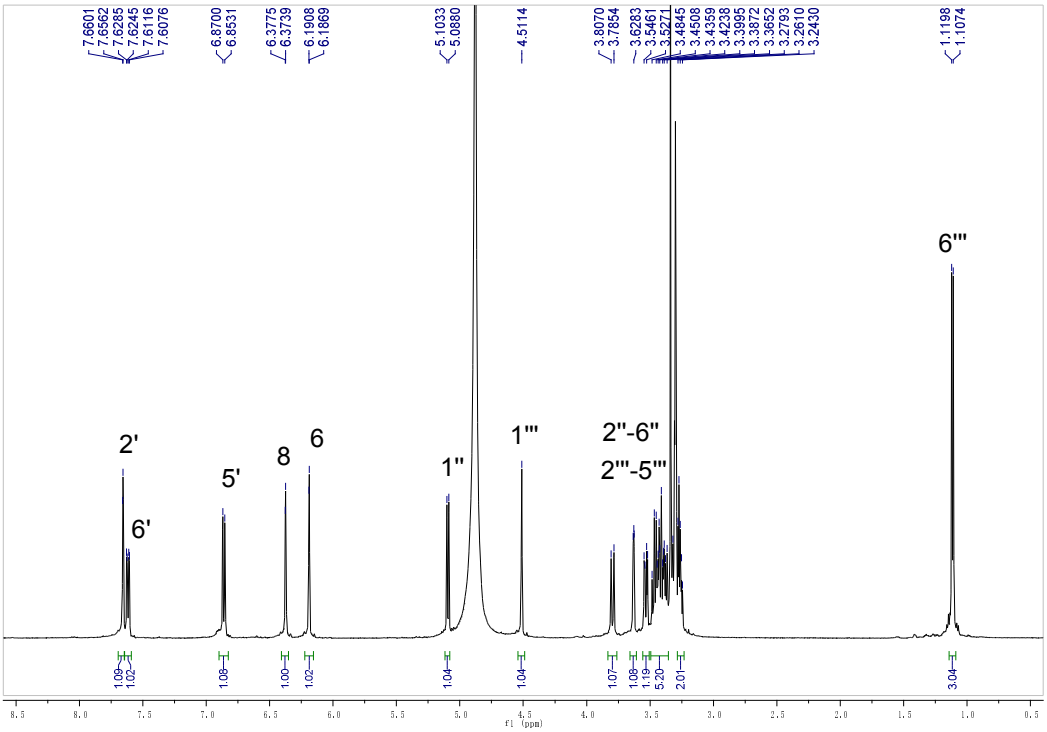

Figure 3.103 ^{1}H NMR spectrum of compound **19**

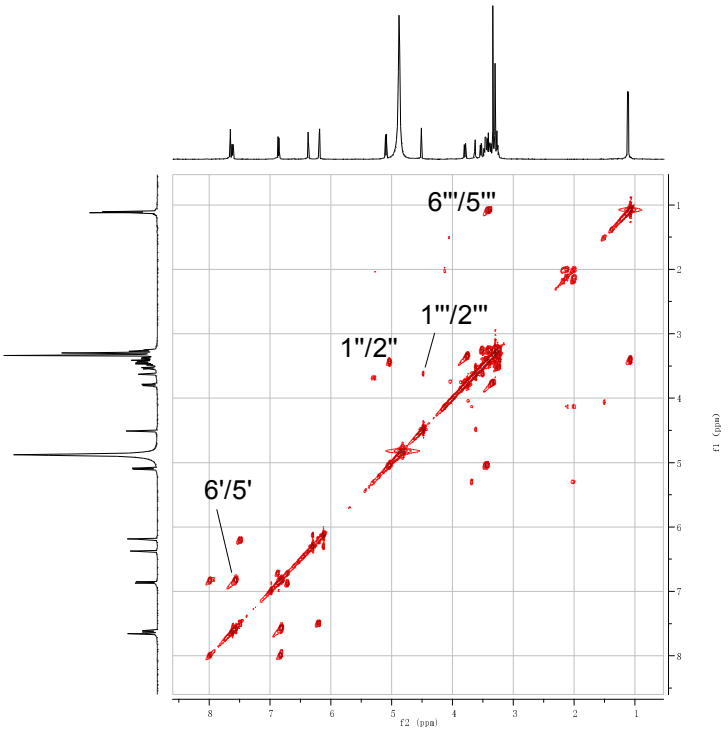

Figure 3.104 ^{1}H-^{1}H COSY spectrum of compound **19**

Table 3.18 NMR spectroscopic data of compound **19** (DMSO-d_6, 500 MHz)

	Rutin [Khalifa *et al.*, 1983]	Compound **19**
Position	δ_H (mult., *J* in Hz)	δ_H (mult., *J* in Hz)
6, CH	6.17, s	6.14, s
8, CH	6.36, s	6.34, s
2′, CH	7.50, s	7.51, br s
5′, CH	6.80, s	6.82, d (8.5)
6′, CH	7.50, br s	7.53, br d (8.5)
1″ Glucosyl, CH	5.30, br s	5.31, d (6.9)
2″ Glucosyl, CH		3.04–3.37, m[a]
3″ Glucosyl, CH		3.04–3.37, m[a]
4″ Glucosyl, CH		3.04–3.37, m[a]
5″ Glucosyl, CH		3.04–3.37, m[a]
6″ Glucosyl, CH_2		3.68, br d (10.8)
1‴ Rhamnosyl, CH	4.40, s	4.37, br s
2‴ Rhamnosyl, CH		3.04–3.37, m[a]
3‴ Rhamnosyl, CH		3.04–3.37, m[a]
4‴ Rhamnosyl, CH		3.04–3.37, m[a]
5‴ Rhamnosyl, CH		3.04–3.37, m[a]
6‴ Rhamnosyl, CH_3	1.03, s	0.98, d (6.0)

[a] Overlapped signals assigned by ^{1}H-^{1}H COSY, HMBC, and HMQC spectra without designating multiplicity.

3.1.20. 3,3',5,5',7-Pentahydroxyflavanone (20, known compound)

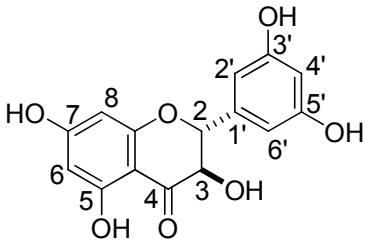

Molecular formula:	$C_{15}H_{12}O_7$
Molecular weight:	304.25
Amount:	1.9 mg

Compound **20** was isolated as pale yellow needles. The UV spectrum of **20** (Figure 3.106) showed absorption maxima at 204, 216 and 289 nm. ESI mass spectrum (Figure 3.107) displayed the ion peak at *m/z* 304. The ^{1}H NMR spectrum of **20** (Figure 3.105) indicated two doublets with coupling constants of 1.6 Hz indicating a pair of *meta*-coupling aromatic protons. Other pair of doublet [δ_H 4.96 (d, J = 11.0 Hz) and 4.47 (d, J = 11.0 Hz)] were observed in the upper field which are the typical signals for the *trans* H-2 and H-3 of dihydroflavonol. The singlet signal for two protons was indicated for an AA′ system (H-2′ and H-6′). Comparison of the ^{1}H NMR data with those reported for **3,3',5,5',7-pentahydroxyflavanone** proved both compounds to be identical [Ding *et al.*, 1997].

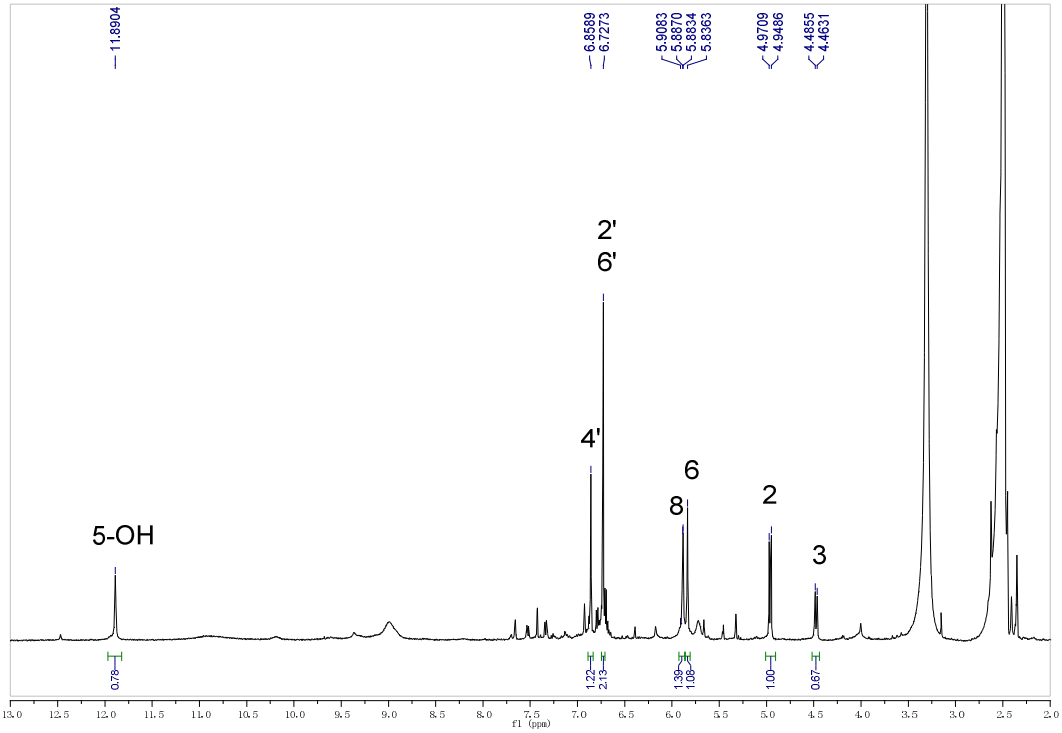

Figure 3.105 ^{1}H NMR spectrum of compound **20**

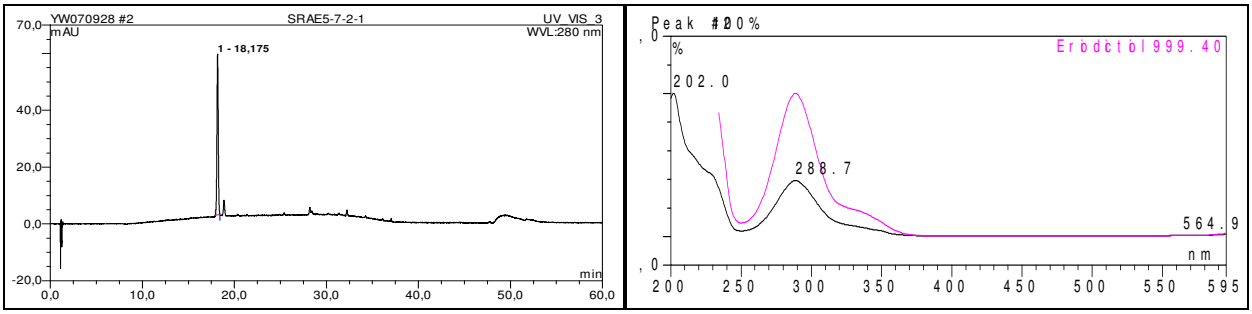

Figure 3.106 HPLC chromatogram and UV spectrum of compound **20**

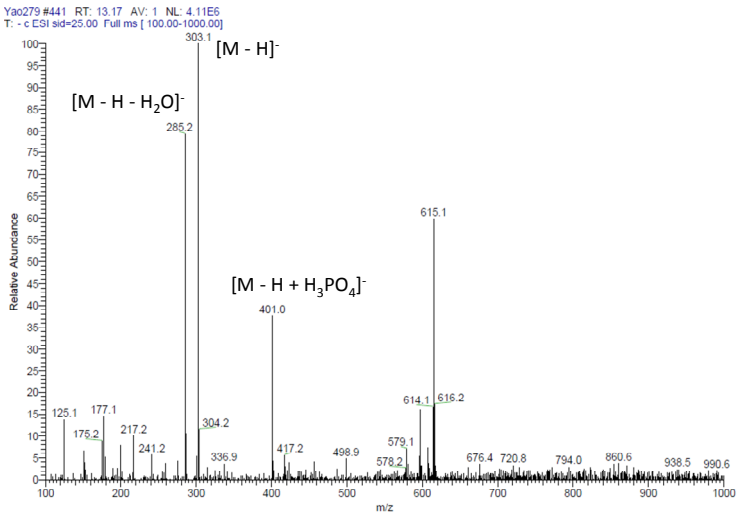

Figure 3.107 ESI-MS spectrum of compound **20**

Table 3.19 NMR spectroscopic data of compound **20** (DMSO, 500 MHz)

	3,3′,5,5′,7-pentahydroxyflavanone [Ding *et al.*, 1997]	Compound **20**
Position	δ_H (mult., *J* in Hz)	δ_H (mult., *J* in Hz)
2, CH	4.98, d (11.1)	4.96, d (11.0)
3, CH	4.50, dd (11.1, 6.0)	4.47, d (11.0)
6, CH	5.86, d (2.0)	5.84, d (1.6)
8, CH	5.91, d (2.0)	5.89, d (1.6)
2′, CH	6.74, s	6.73, s
4′, CH	6.87, s	6.86, s
6′, CH	6.74, s	6.73, s
5-OH	11.90, s	11.89, s

3.1.21. Umbelliferone (21, known compound)

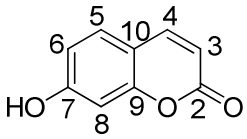

Molecular formula:	$C_9H_6O_3$
Molecular weight:	162.14
Amount:	9.9 mg

Compound **21** was isolated as an amorphous solid. The coumarin nature of **21** was deduced from UV maximal absorption at 217 and 324 nm (Figure 3.109). Compound **21** had a molecular weight of 162, as derived from the ESIMS measurement which showed the ion peak at *m/z* 161 $[M - H]^-$. (Figure 3.110) The ^{1}H NMR spectrum of **21** (Figure 3.108) revealed a pair of doublet with coupling constants of 9.5 Hz, characteristic of an α,β-unsaturated ketone of a coumarin ring. The residual resonances indicative for an ABX system [δ_H 6.69 (d, J = 2.2 Hz), 6.78 (dd, J = 8.5 and 2.2 Hz) and 7.44 (d, J = 8.5 Hz)] were observed indicating the presence of a trisubstituted aromatic ring. Along with its molecular weight, compound **21** was identical to those of **umbelliferone** [Jeong *et al.*, 2006].

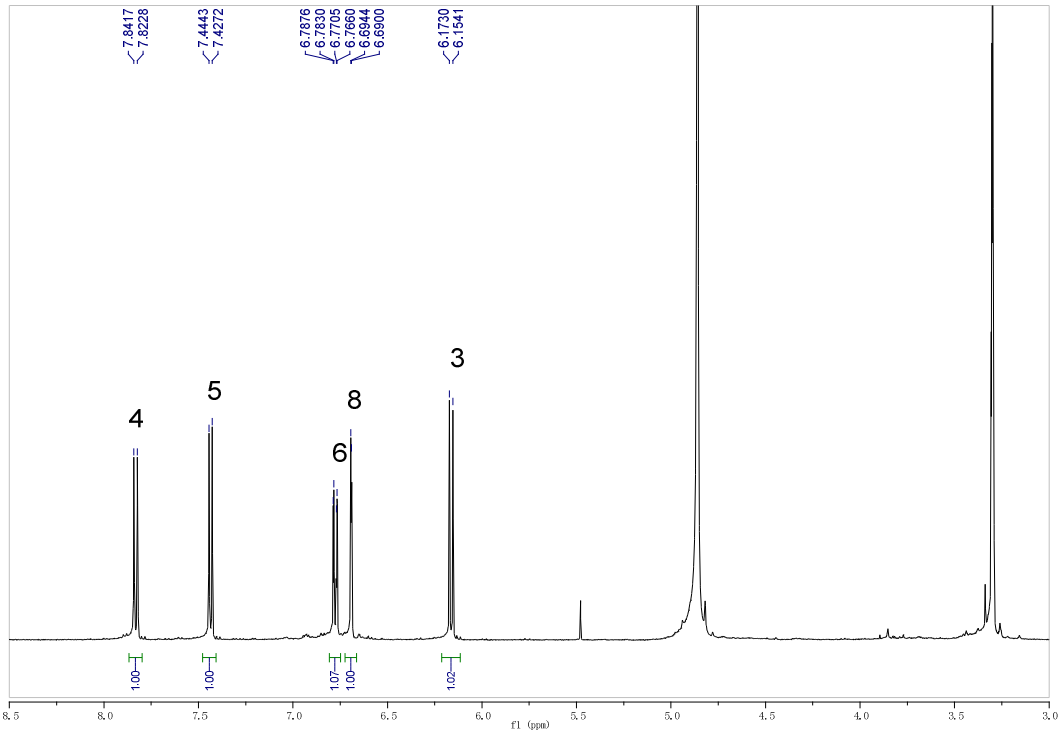

Figure 3.108 ^{1}H NMR spectrum of compound **21**

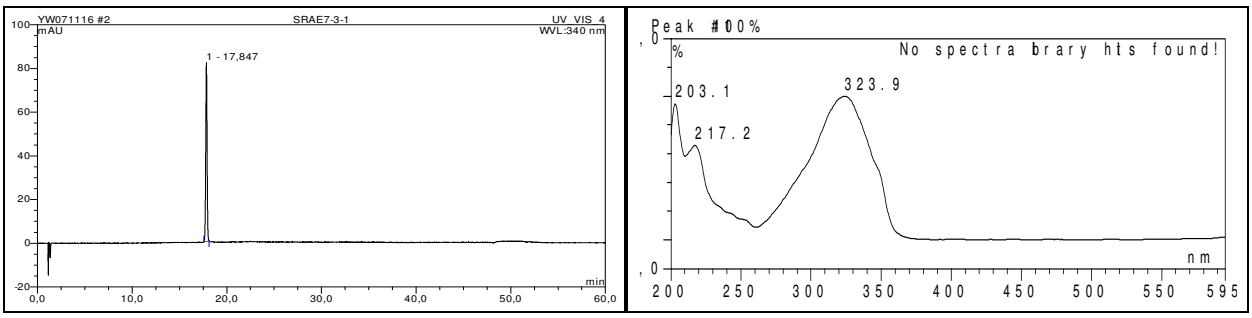

Figure 3.109 HPLC chromatogram and UV spectrum of compound **21**

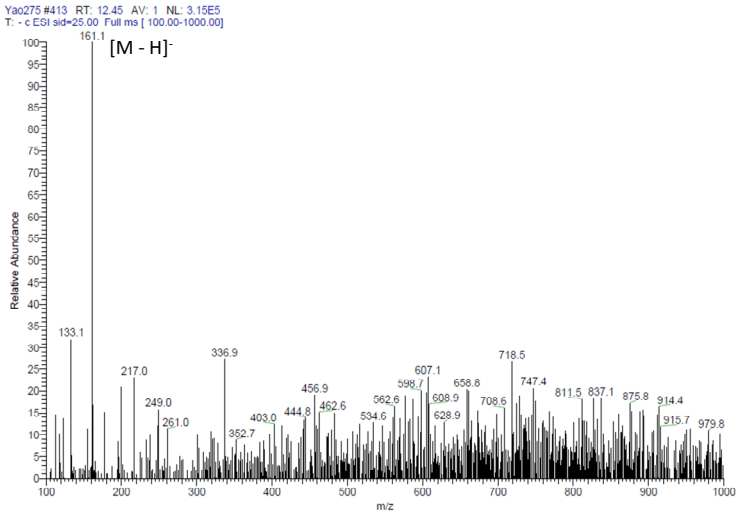

Figure 3.110 ESI-MS spectrum of compound **21**

Table 3.20 NMR spectroscopic data of compound **21** (CD_3OD, 500 MHz)

	Umbelliferone [Jeong *et al.*, 2006]	Compound **21**
Position	δ_H (mult., *J* in Hz)	δ_H (mult., *J* in Hz)
3, CH	6.15, d (9.5)	6.16, d (9.5)
4, CH	7.85, d (9.5)	7.83, d (9.5)
5, CH	7.50, d (8.4)	7.44, d (8.5)
6, CH	6.84, dd (8.4, 2.2)	6.78, dd (8.5, 2.2)
8, CH	6.74, d (2.2)	6.69, d (2.2)

3.1.22. Skimmin (22, known compound)

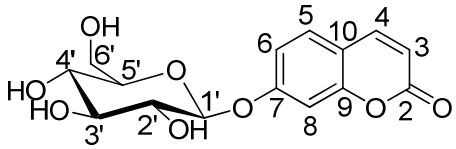

Molecular formula:	$C_{15}H_{16}O_8$
Molecular weight:	324.28
Amount:	4.4 mg

Compound **22** was obtained as an amorphous solid. The UV spectrum exhibited a maximal absorption at 317 nm. (Figure 3.112) The ESIMS spectrum of **22** (Figure 3.113) showed molecular ion peak at *m/z* 324. The ^{1}H NMR data of **22** (Figure 3.111) were very similar to those of **21** in the aromatic region. However the presence of an additional sugar moiety was indicated by an anomeric proton signal at δ_H 5.03 and the proton signals from δ_H 3.90 to 3.39 comparing to **21**. The HMBC spectrum (Figure 3.115) confirmed the sugar linkage by a cross peak between C-7 (δ 161.9) and the anomeric proton of glucose. Compound **22** was identified as **skimmin** through comparison of its spectral data with the previously published ones [Khalil *et al.*, 2003].

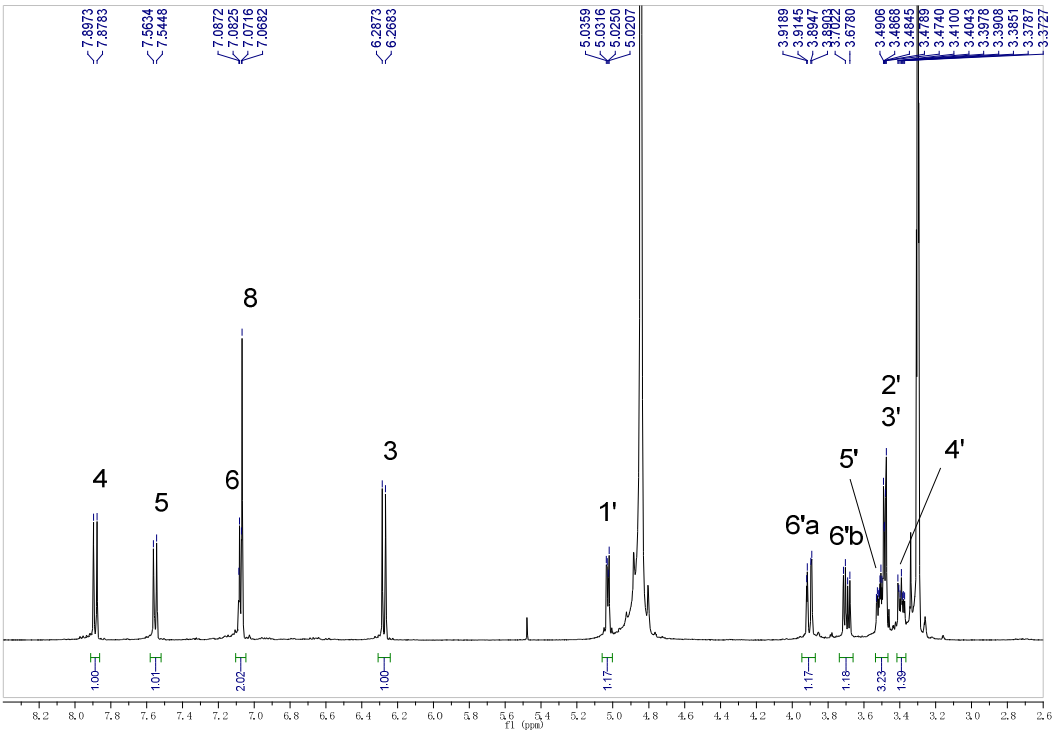

Figure 3.111 ^{1}H NMR spectrum of compound **22**

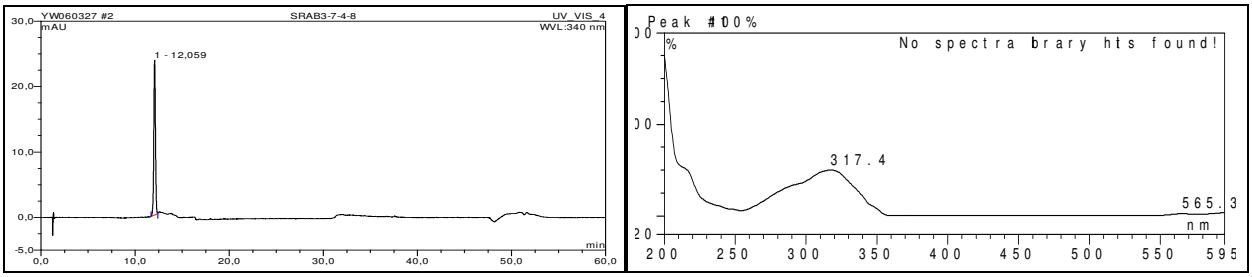

Figure 3.112 HPLC chromatogram and UV spectrum of compound **22**

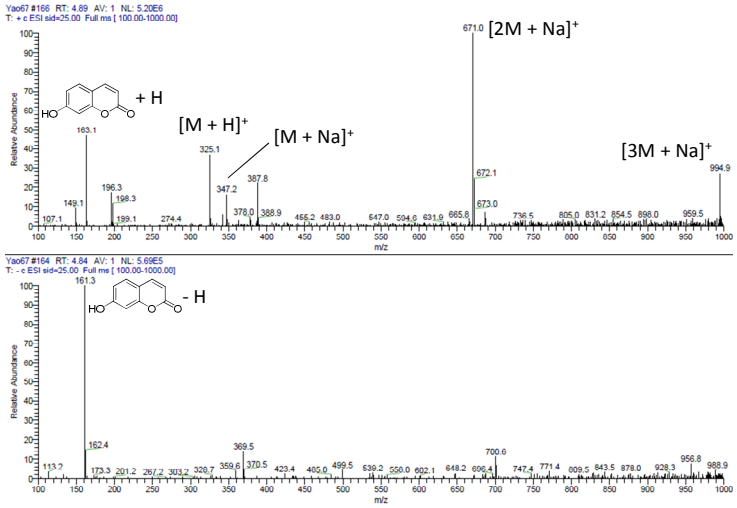

Figure 3.113 ESI-MS spectrum of compound **22**

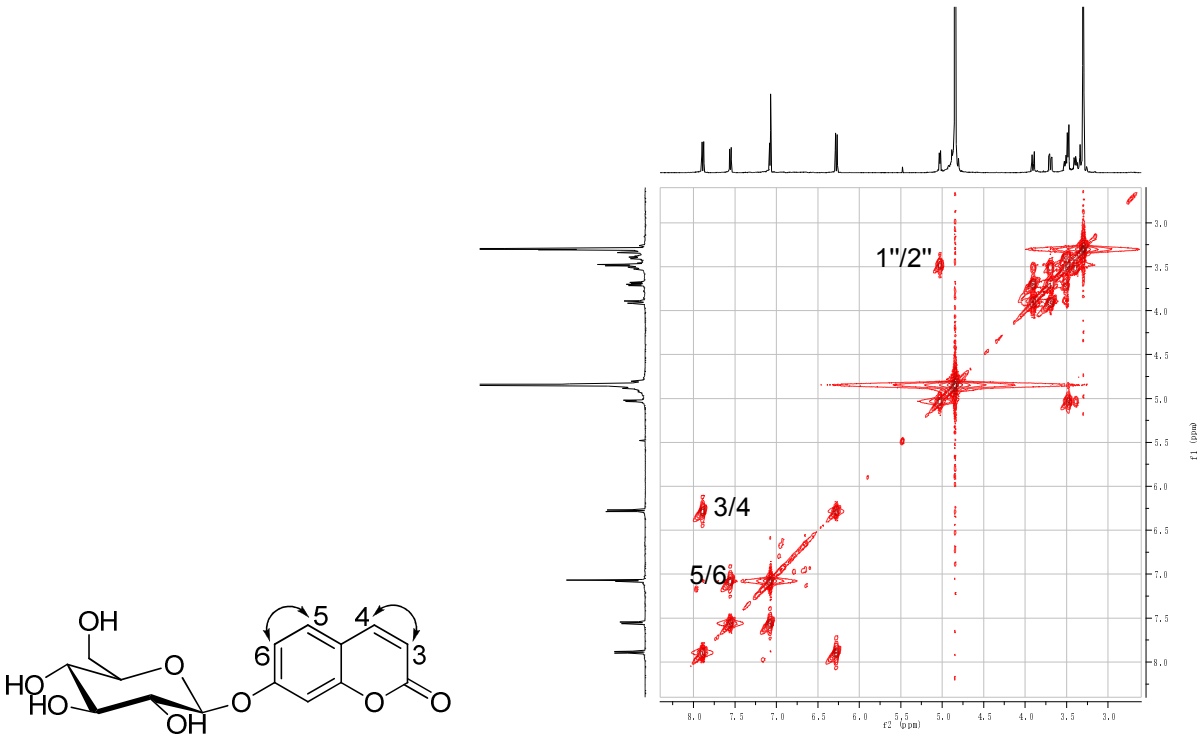

Figure 3.114 ^{1}H-^{1}H COSY spectrum of compound **22**

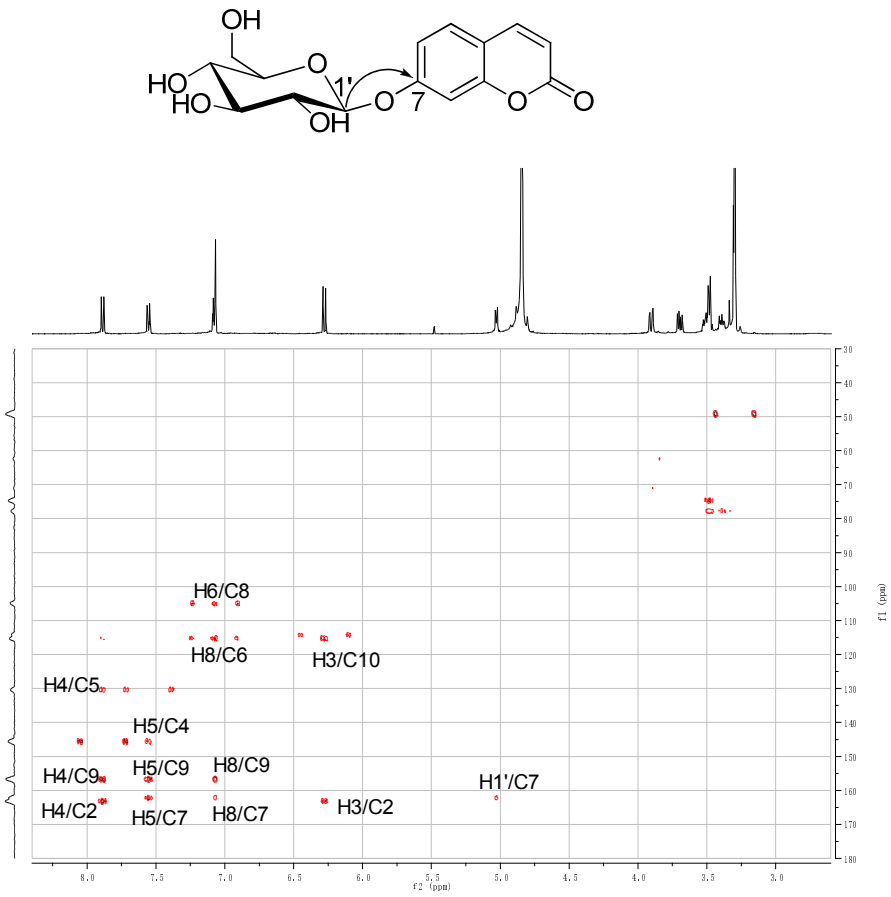

Figure 3.115 HMBC spectrum of compound **22**

Table 3.21 NMR spectroscopic data of compound **22** (CD_3OD, 500 MHz)

	skimmin (Pyridine-d_5) [Khalil *et al.*, 2003]		Compound **22**	
Position	δ_C	δ_H (mult., *J* in Hz)	δ_C	δ_H (mult., *J* in Hz)
2	162.6, qC		162.9, qC	
3	112.8, CH	6.30, d (9.6)	114.0, CH	6.28, d (9.5)
4	144.5, CH	7.62, d (9.6)	145.2, CH	7.89, d (9.8)
5	129.3, CH	7.37, d (8.8)	130.1, CH	7.55, dd (7.6, 1.9)
6	113.7, CH	7.17, dd (8.4, 2.4)	115.0, CH	7.08, dd (7.5, 2.1)
7	161.4, qC		161.9, qC	
8	103.0, CH	7.23, d (2.4)	104.7, CH	7.07, d (1.9)
9	155.9, qC		156.5, qC	
10	111.9, qC		115.1, qC	
1′	99.6, CH	5.69, d (7.6)	101.6, CH	5.03, dd (5.6, 2.1)
2′	73.5, CH		74.5, CH	3.48, dd (6.2, 2.1)
3′	77.4, CH		77.5, CH	3.48, dd (6.2, 2.1)
4′	69.6, CH		71.0, CH	3.39, m
5′	76.7, CH		78.1, CH	3.51, m
6′	60.8, CH_2		62.1, CH_2	3.90, dd (12.0, 2.2)
				3.70, dd (12.3, 5.7)

3.1.23. Piceol (23, known compound)

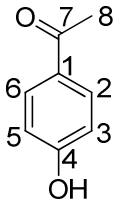

Molecular formula:	$C_8H_8O_2$
Molecular weight:	136.15
Amount:	8.5 mg

Compound **23** was isolated as an amorphous solid with UV absorbances at λ_{max} 221 and 277 nm. (Figure 3.116) The ESIMS spectrum (Figure 3.117) showed a pseudomolecular ion peak at *m/z* 135 $[M - H]^-$ (negative). The ^1H (Figure 3.118), ^{13}C (Figure 3.119) and DEPT NMR (Figure 3.120) spectra of **23** exhibited an AA′BB′ system [δ_H 7.88 (d, J = 8.5 Hz); δ_C 132.1 and 6.83 (d, J = 8.5 Hz); δ_C 116.2] and a methyl ketone function [δ_H 2.51, δ_C 26.3]. According to these data and through comparison with the literature [Pouchert, 1992], compound **23** was concluded to be **piceol**.

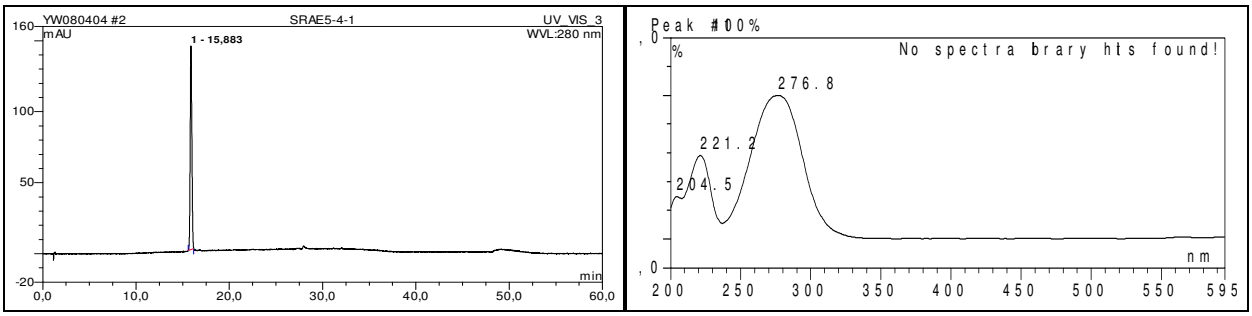

Figure 3.116 HPLC chromatogram and UV spectrum of compound **23**

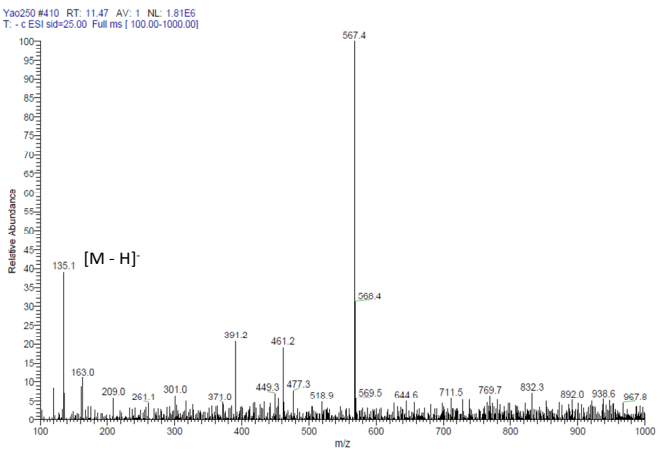

Figure 3.117 ESI-MS spectrum of compound **23**

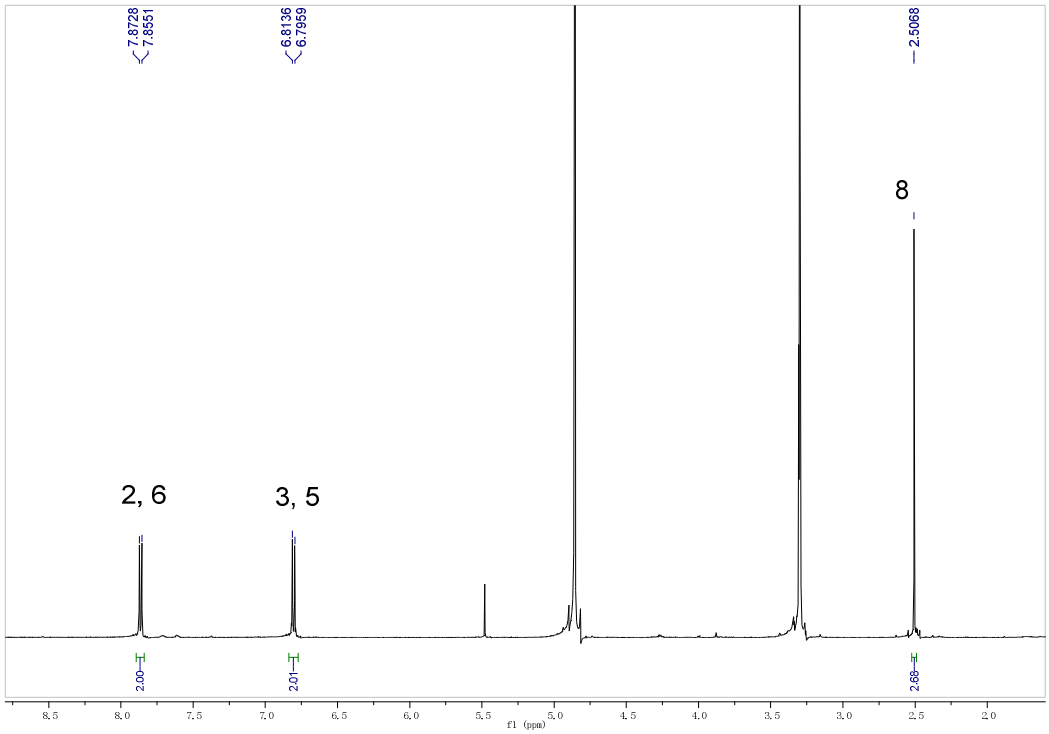

Figure 3.118 ^{1}H NMR spectrum of compound **23**

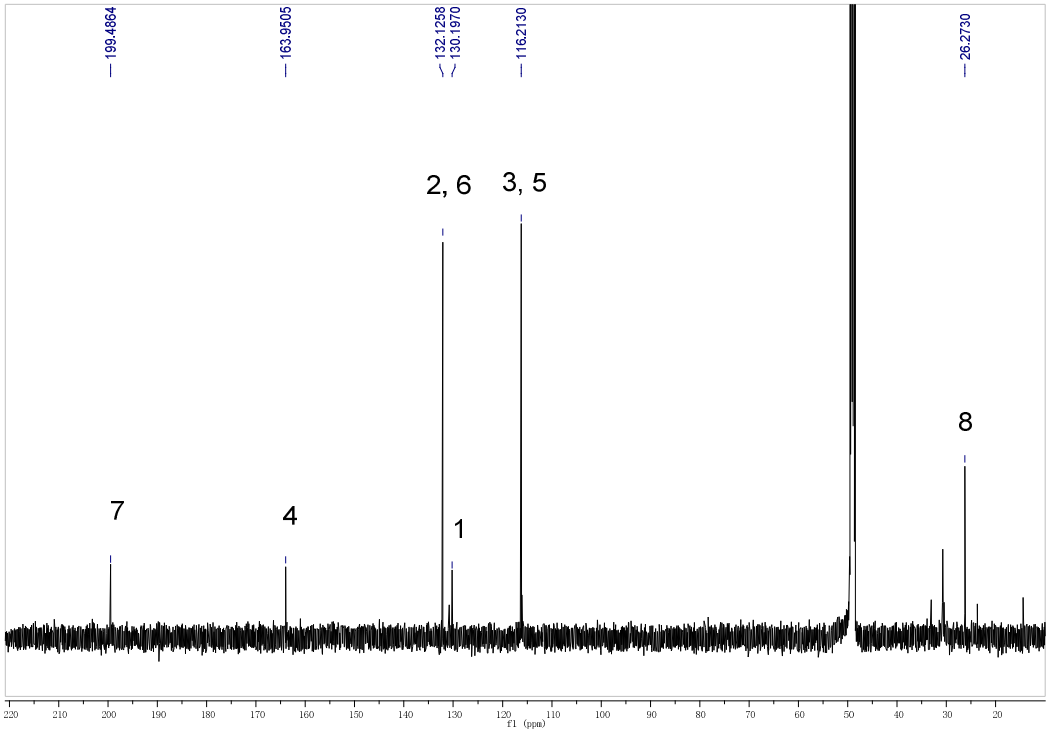

Figure 3.119 ^{13}C NMR spectrum of compound **23**

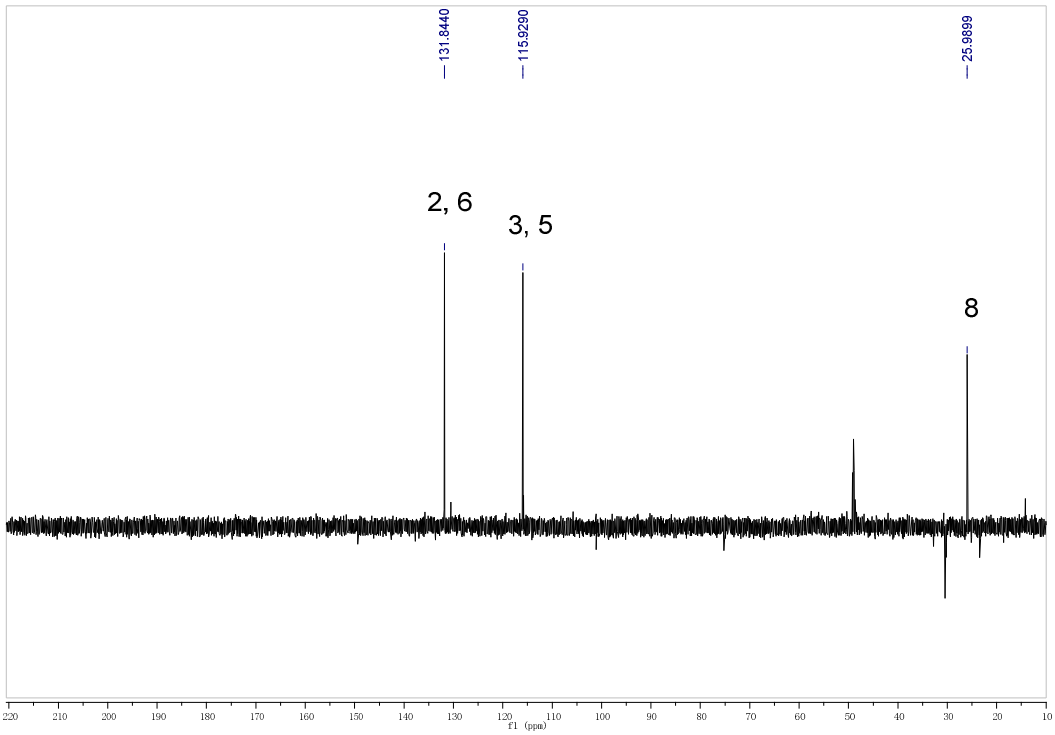

Figure 3.120 DEPT spectrum of compound **23**

Table 3.22 NMR spectroscopic data of compound **23** (CD_3OD, 500 MHz)

	Piceol (acetone-d_6) [Kametani *et al.*, 2007]		Compound **23**	
Position	δ_C	δ_H (mult., *J* in Hz)	δ_C	δ_H (mult., *J* in Hz)
1	130.5, qC		130.2, qC	
2	131.5, CH	7.89, d (8.8)	132.1, CH	7.88, d (8.5)
3	115.9, CH	6.92, d (8.8)	116.2, CH	6.83, d (8.5)
4	162.6, qC		164.0, qC	
5	115.9, CH	6.92, d (8.8)	116.2, CH	6.83, d (8.5)
6	131.5, CH	7.89, d (8.8)	132.1, CH	7.88, d (8.5)
7	196.2, qC		199.5, qC	
8	26.3, CH_3	2.49, s	26.3, CH_3	2.51, s

3.1.24. Piceoside (24, known compound)

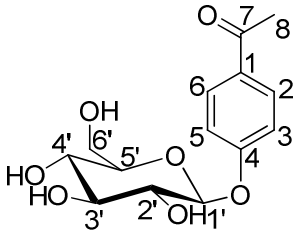

Molecular formula:	$C_{14}H_{18}O_7$
Molecular weight:	298.29
Amount:	13.3 mg

Compound **24** was obtained as an amorphous solid and has UV absorptions at λ_{max} 214 and 265 nm. (Figure 3.122) The molecular weight of compound **24** was determined from the ESI mass spectrum as 298. (Figure 3.124) The ^{1}H NMR spectral data of **24** (Figure 3.121) were very similar to those of **23** with an additional sugar unit. The assignment of the glucose moiety at C-4 was determined from the HMBC cross-peak (Figure 3.123) of the anomeric proton at δ_H 5.02 (d, J = 7.6 Hz) with δ_C 163.0. The methyl singlet at δ_H 2.55 gave a cross-peak with the carbonyl carbon at $\delta_{C\text{-}7}$ 199.4 and the aromatic carbon at $\delta_{C\text{-}1}$ 132.5, respectively. Compound **24** was identified as **piceoside** [Karikas *et al.*, 1987].

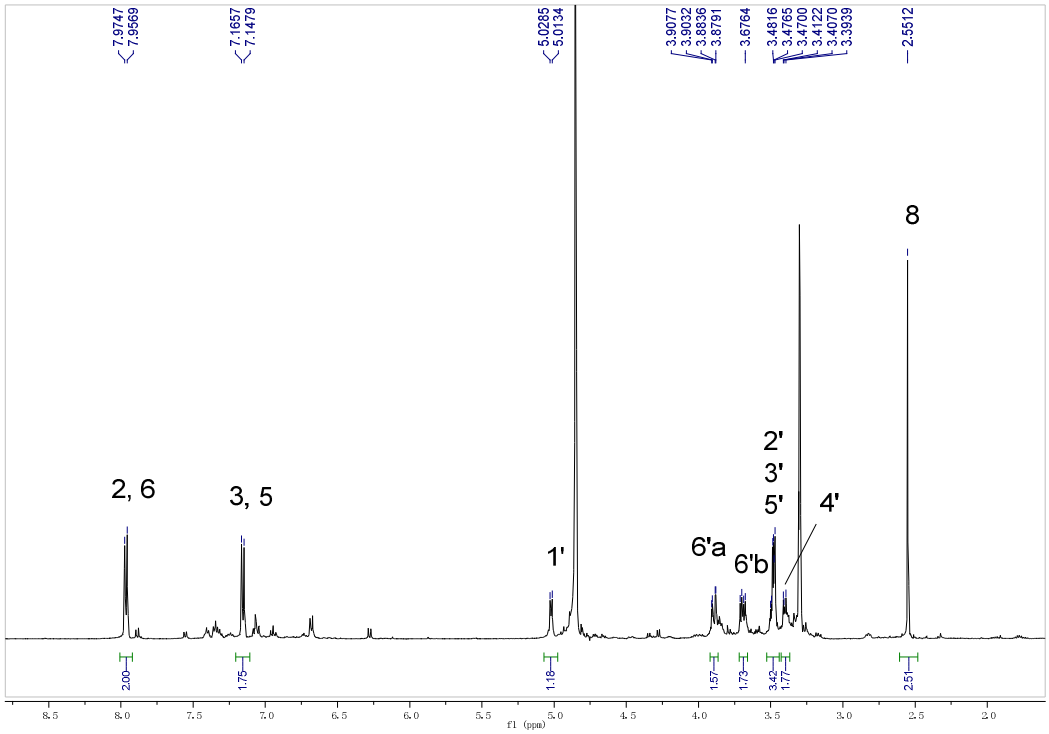

Figure 3.121 ^{1}H NMR spectrum of compound **24**

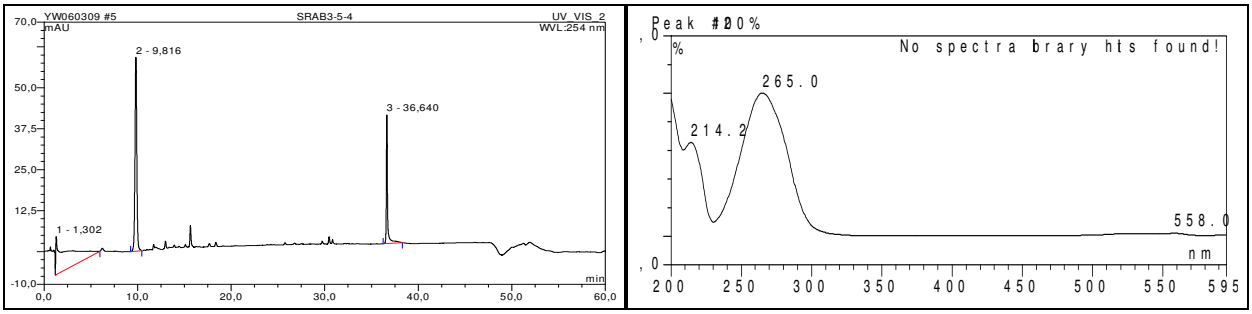

Figure 3.122 HPLC chromatogram and UV spectrum of compound **24**

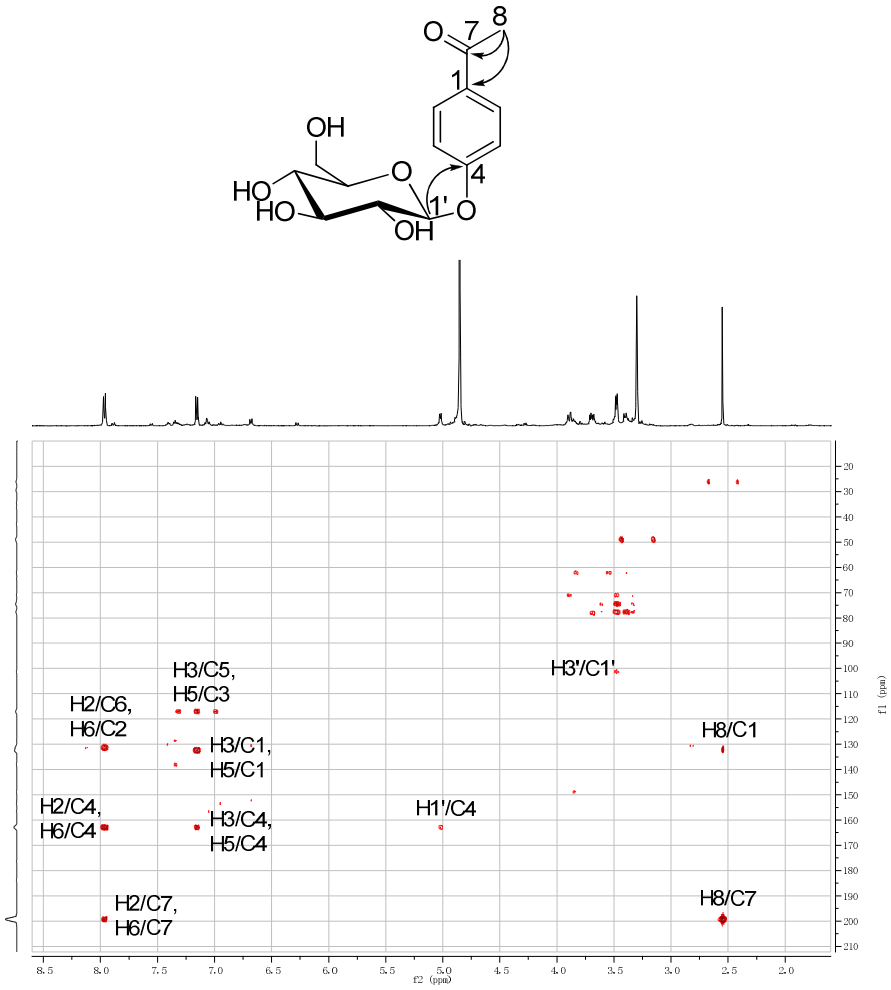

Figure 3.123 HMBC spectrum of compound **24**

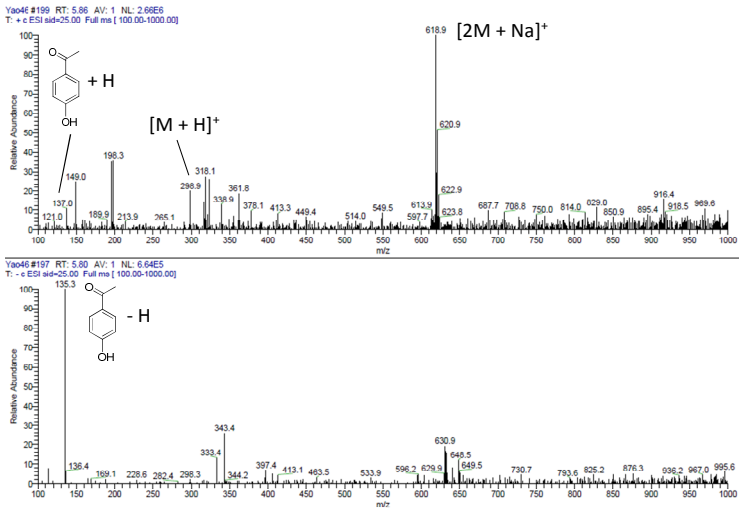

Figure 3.124 ESI-MS spectrum of compound **24**

Table 3.23 NMR spectroscopic data of compound **24** (CD_3OD, 500 MHz)

	Piceoside (D_2O) [Karikas *et al.*, 1987]		Compound **24**	
Position	δ_C	δ_H (mult., *J* in Hz)	δ_C	δ_H (mult., *J* in Hz)
1	qC		132.5, qC	
2	131.0, CH	7.8-7.9, d (8.2)	131.6, CH	7.96, d (9.1)
3	116.1, CH	7.0-7.1, d (8.2)	117.1, CH	7.15, d (8.8)
4	157.4, qC		163.0, qC	
5	116.1, CH	7.0-7.1, d (8.2)	117.1, CH	7.15, d (8.8)
6	131.0, CH	7.8-7.9, d (8.2)	131.6, CH	7.96, d (9.1)
7	qC		199.4, qC	
8	26.0, CH_3	2.47, s	26.2, CH_3	2.55, s
1′	99.5, CH	5.0, d	101.5, CH	5.02, d (7.6)
2′	72.9, CH	3.3-4.8, m	74.5, CH	3.48, m[a]
3′	76.2, CH	3.3-4.8, m	77.7, CH	3.48, m[a]
4′	69.4, CH	3.3-4.8, m	71.2, CH	3.40, m[a]
5′	75.5, CH	3.3-4.8, m	78.2, CH	3.48, m[a]
6′	60.6, CH_2	3.3-4.8, m	62.2, CH_2	3.89, d (12.0, 2.2)
				3.69, d (12.3, 5.7)

[a] Overlapped signals assigned by ^1H-^1H COSY, HMBC, and HMQC spectra without designating multiplicity.

3.1.25. 4-Hydroxybenzoic acid (25, known compound)

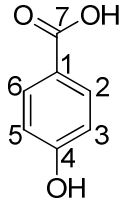

Molecular formula:	$C_7H_6O_3$
Molecular weight:	138.12
Amount:	2.5 mg

Compound **25** was isolated as an amorphous solid. It has UV absorbances at λ_{max} 210 and 255 nm. (Figure 3.126) The EIMS spectrum showed a pseudomolecular ion peak at *m*/*z* 138 $[M]^+$. (Figure 3.127) Fragment ions were observed at *m*/*z* 121, 83, 57 and 43, respectively, representing a *p*-hydroxybenzoic acid skeleton. The ^{1}H NMR spectrum (Figure 3.125) exhibited a *para*-substituted phenyl ring containing two pairs of *ortho*-coupled proton at δ_H 7.85 (d, J = 8.5 Hz) and 6.77 (d, J = 8.5 Hz). From the above data and through comparison with the literature, compound **25** was confirmed to be **4-hydroxybenzoic acid** [Scott, 1970].

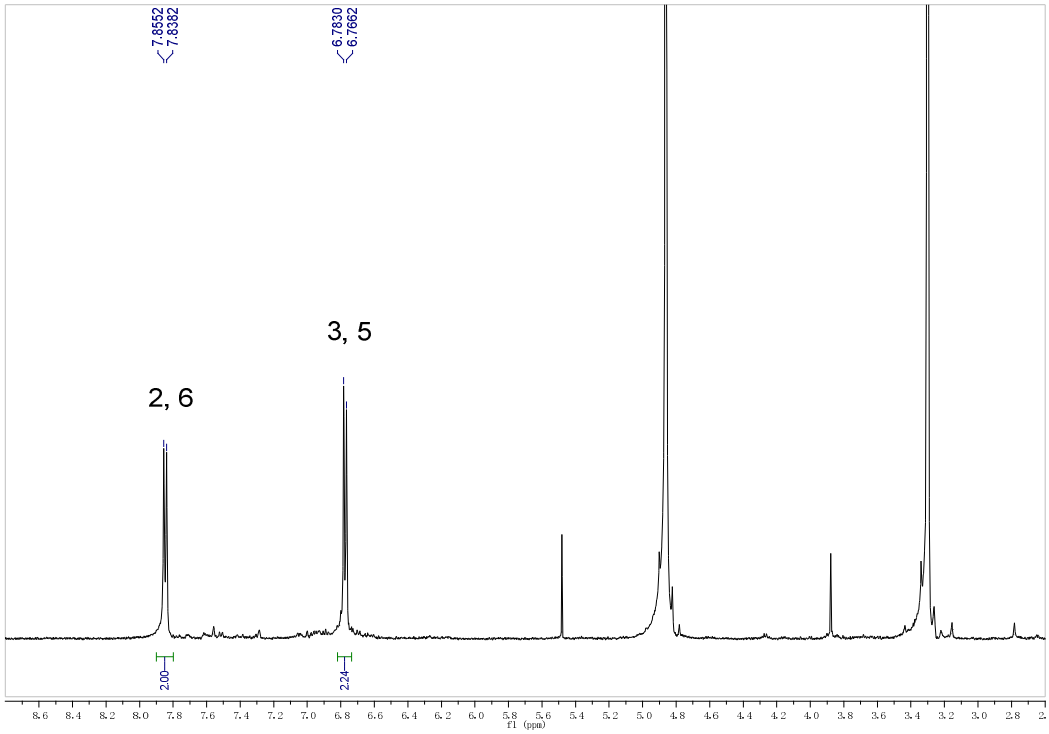

Figure 3.125 ^{1}H NMR spectrum of compound **25**

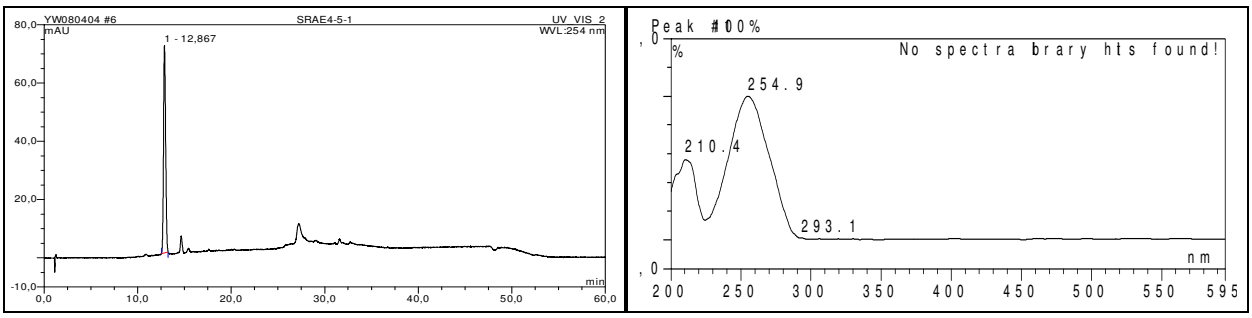

Figure 3.126 HPLC chromatogram and UV spectrum of compound **25**

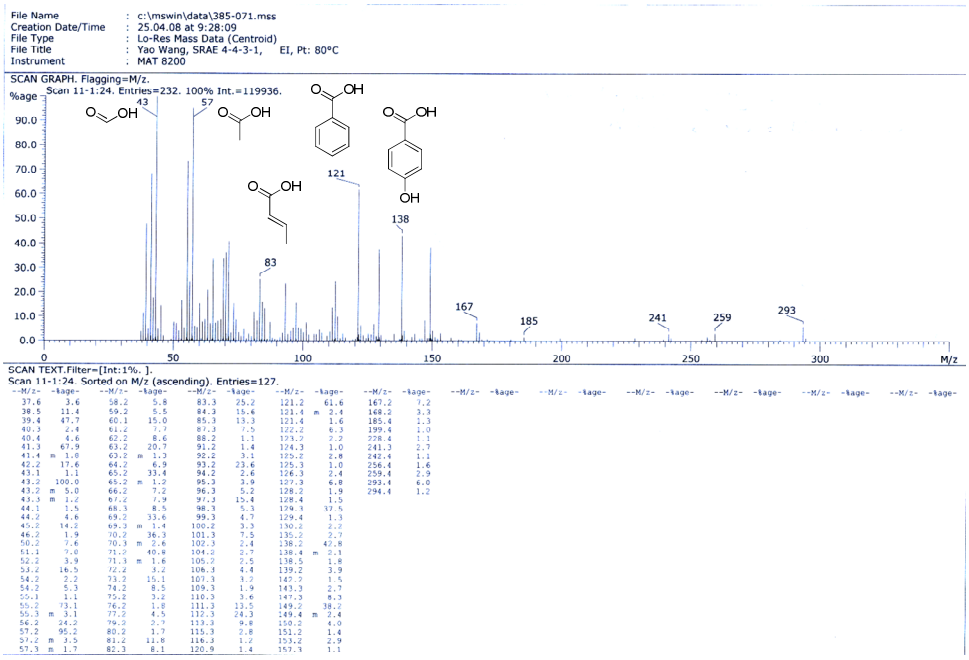

Figure 3.127 EI-MS spectrum of compound **25**

Table 3.24 NMR spectroscopic data of compound **25** (CD_3OD, 500 MHz)

	4-Hydroxybenzoic acid (DMSO-d_6) [Scott, 1970]	Compound **25**
Position	δ_H (mult., J in Hz)	δ_H (mult., J in Hz)
2, CH	7.98, dd (8.7, 2.4)	7.85, d (8.5)
3, CH	6.96, dd (8.7, 2.4)	6.77, d (8.5)
5, CH	6.96, dd (8.7, 2.4)	6.77, d (8.5)
6, CH	7.98, dd (8.7, 2.4)	7.85, d (8.5)

3.1.26. Arbutin (26, known compound)

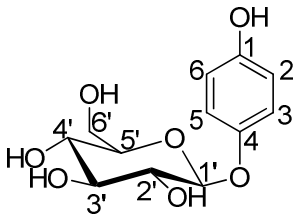

Molecular formula:	$C_{12}H_{16}O_7$
Molecular weight:	272.25
Amount:	173.7 mg

Compound **26** was obtained as a colourless crystal showing the molecular weight of 272 in ESI mass spectrum. (Figure 3.130) The ^{1}H (Figure 3.128) and ^{13}C NMR (Figure 3.131) spectra of **26** exhibited an AA′BB′ system [δ_H 6.90 (d, J = 9.0 Hz) and δ_C 119.1; δ_H 6.72 (d, J = 9.0 Hz) and δ_C 121.3] and a sugar moiety. From the HMBC spectrum of **26** (Figure 3.132), a correlation was noticed between the anomeric proton at δ 4.82 (H-1′) and the carbon (δ 154.1) of the *para*-hydroxyphenol residue, establishing that the glucosidic bond is between C-4 and C-1′. The ^{1}H and ^{13}C NMR spectra were identical to those of **arbutin** [Perry *et al.*, 1996].

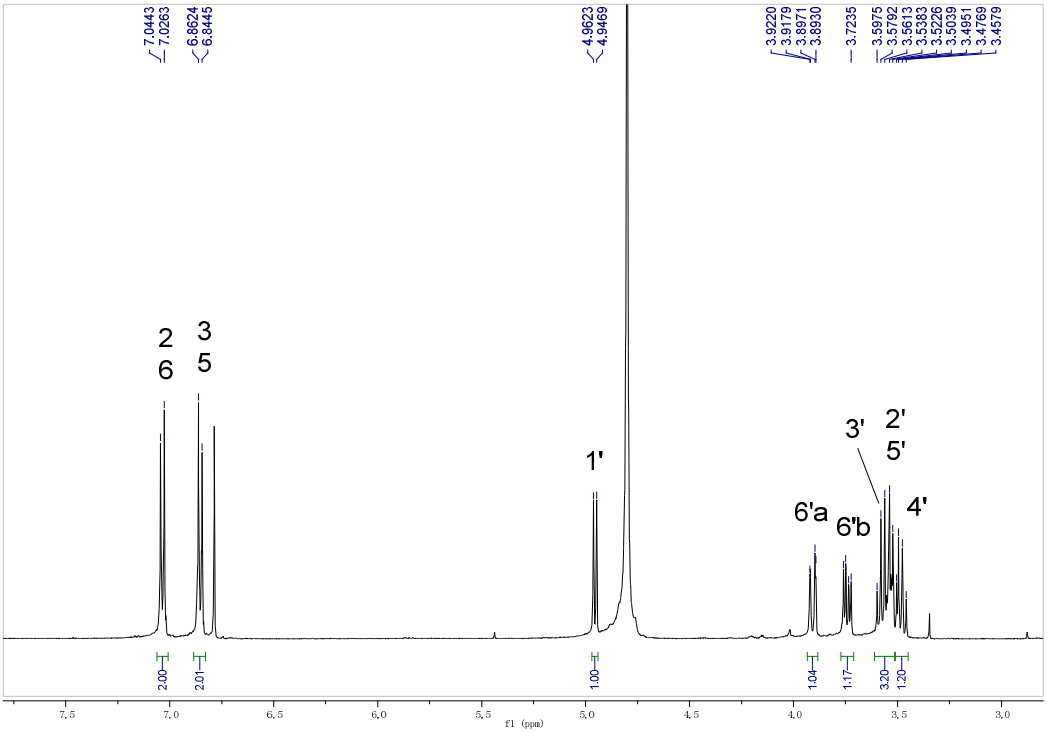

Figure 3.128 ^{1}H NMR spectrum of compound **26**

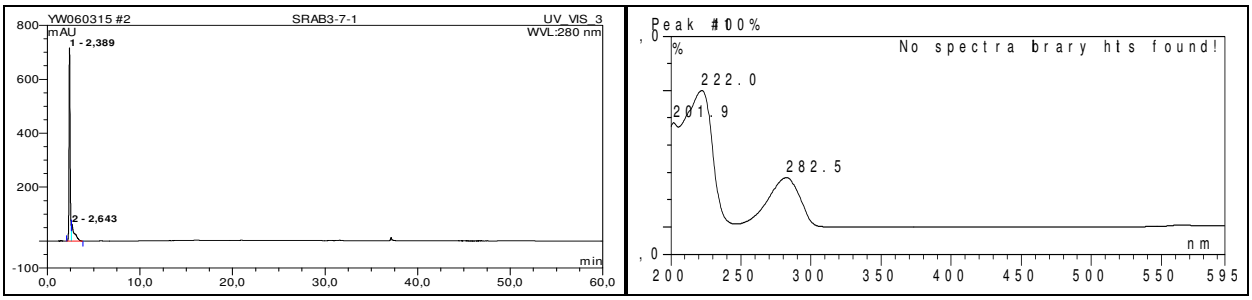

Figure 3.129 HPLC chromatogram and UV spectrum of compound **26**

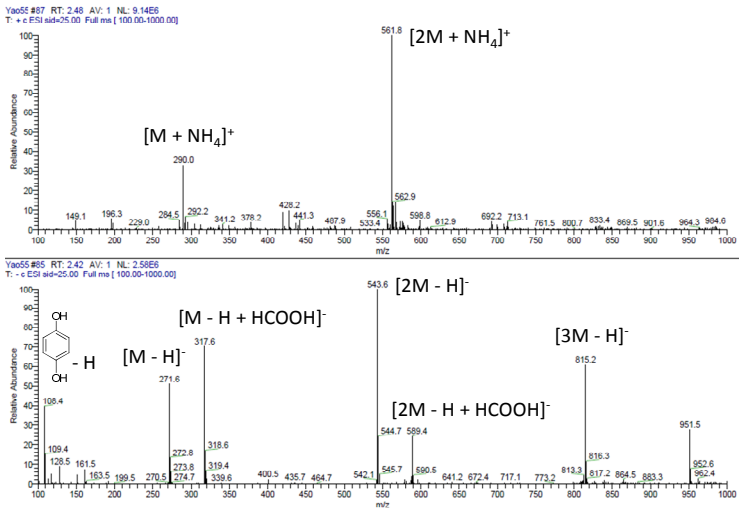

Figure 3.130 ESI-MS spectrum of compound **26**

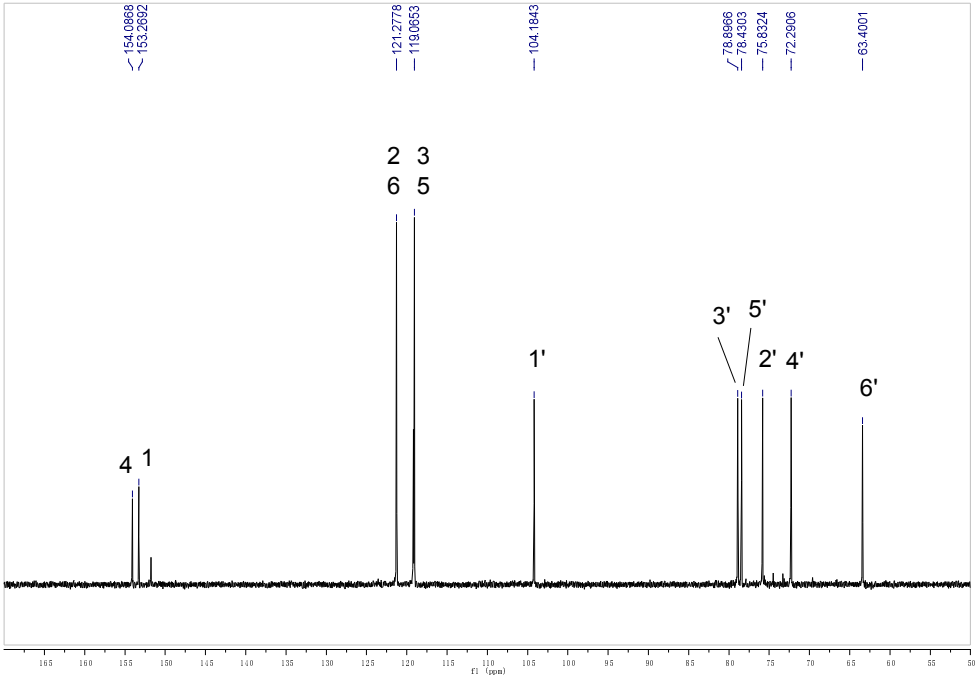

Figure 3.131 ^{13}C NMR spectrum of compound **26**

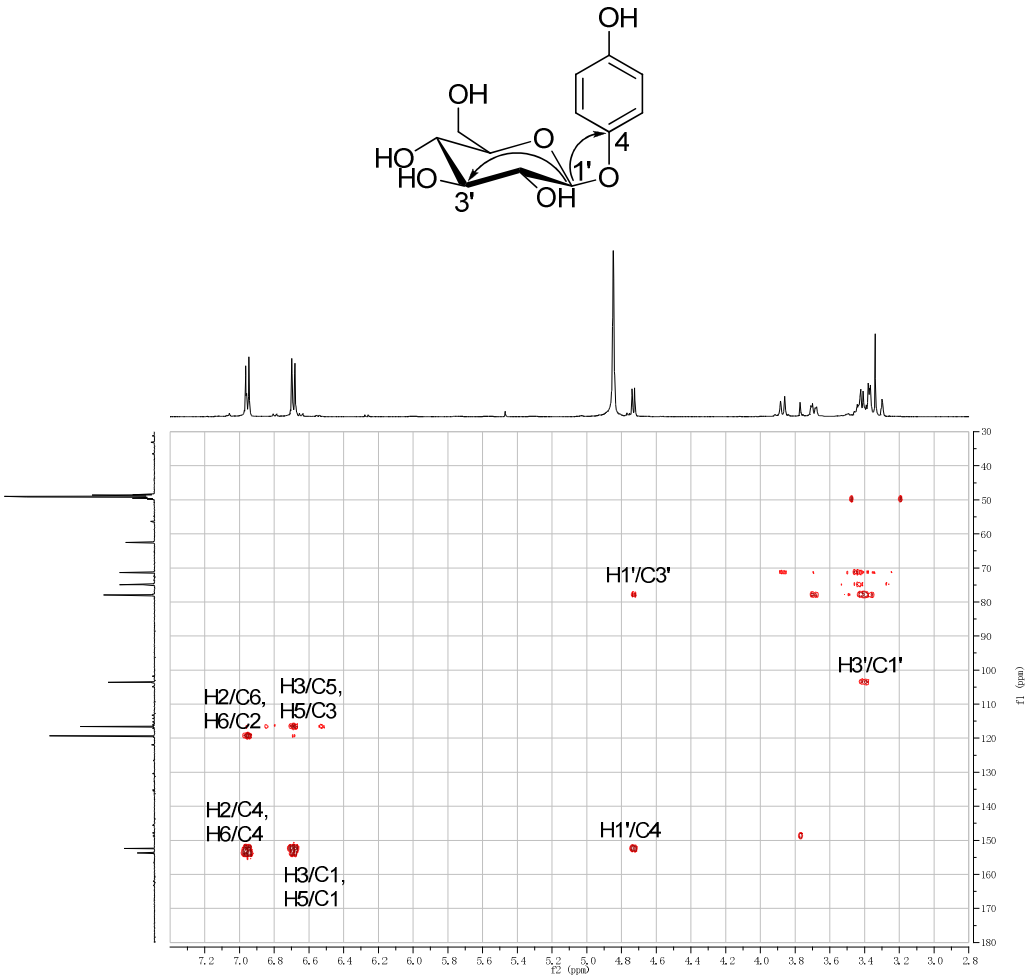

Figure 3.132 HMBC spectrum of compound **26**

Table 3.25 NMR spectroscopic data of compound **26** (D_2O, 500 MHz)

	Arbutin [Perry *et al.*, 1996]		Compound **26**	
Position	δ_C	δ_H (mult., *J* in Hz)	δ_C	δ_H (mult., *J* in Hz)
1	153.2, qC		153.3, qC	
2	121.3, CH	7.06, d (9)	121.3, CH	7.04, d (9.0)
3	119.1, CH	6.88, d (9)	119.1, CH	6.85, d (9.0)
4	154.1, qC		154.1, qC	
5	119.1, CH	6.88, d (9)	119.1, CH	6.85, d (9.0)
6	121.3, CH	7.06, d (9)	121.3, CH	7.04, d (9.0)
1′	104.2, CH	4.97, d (7)	104.2, CH	4.95, d (7.6)
2′	75.8, CH		75.8, CH	3.54, m[a]
3′	78.9, CH		78.9, CH	3.58, m[a]
4′	72.3, CH		72.3, CH	3.48, m[a]
5′	78.4, CH		78.4, CH	3.54, m[a]
6′	63.4, CH_2	3.93, dd (12, 2)	63.4, CH_2	3.91, dd (12.3, 1.9)
		3.77, dd (12, 5)		3.74, dd (12.3, 5.4)

[a] Overlapped signals assigned by ^1H-^1H COSY, HMBC, and HMQC spectra without designating multiplicity.

3.1.27. Lanceoloside A (27, known compound)

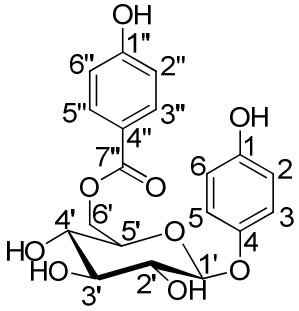

Molecular formula:	$C_{19}H_{20}O_9$
Molecular weight:	392.36
Amount:	6.8 mg

Compound **27** was isolated as an amorphous solid with the molecular weight of 392 determined by ESIMS analysis (Figure 3.134). The UV spectrum (Figure 3.133) showed an absorption maximum at 215 and 258 nm. From ^{1}H NMR spectrum of **27** (Figure 3.135), a *p*-hydroxybenzoyl group [7.74 (2H, *ortho*); 6.75 (2H, *meta*)] and a *p*-hydroxyphenoxy group [6.59 (2H, *ortho*); 6.85 (2H, *meta*)] were observed. The ^{13}C and DEPT NMR spectra of **27** (Figure 3.136) had signals for 19 carbon atoms among which were one ketone carbonyl, eight aromatic methines, four quaternary sp^2 carbons (three bearing an oxygen), and six sp^3 methines (each carrying an oxygen substituent). Compound **27** was identified as **lanceoloside A** [Pegnyemb *et al.*, 1998].

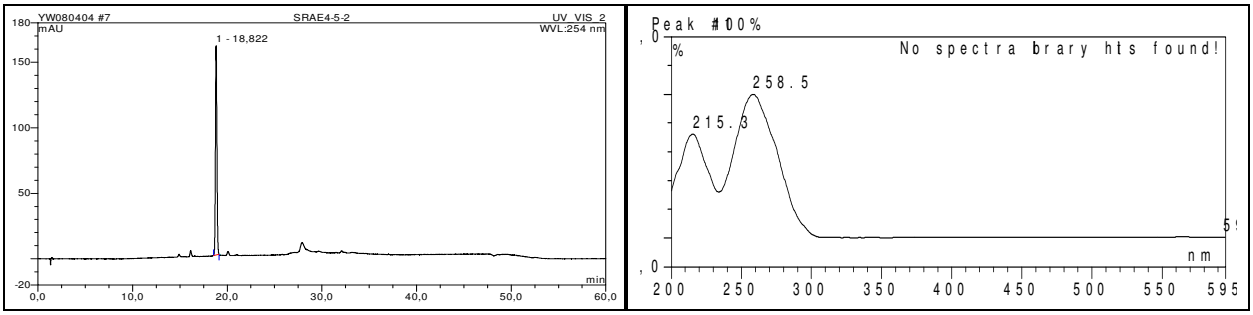

Figure 3.133 HPLC chromatogram and UV spectrum of compound **27**

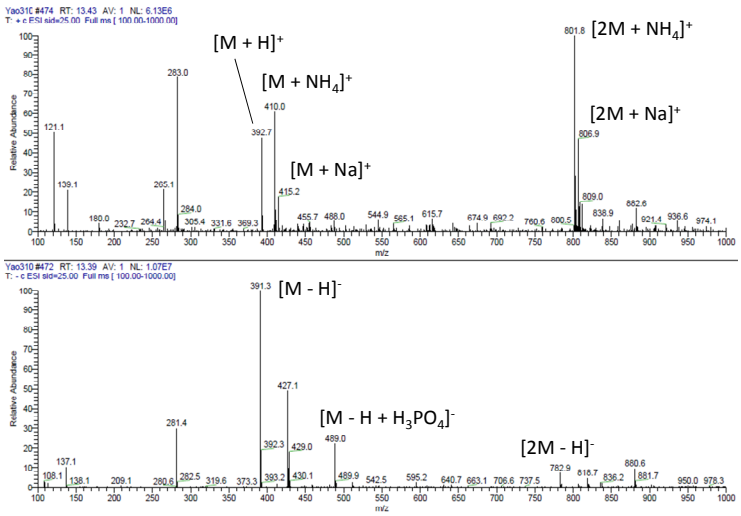

Figure 3.134 ESI-MS spectrum of compound **27**

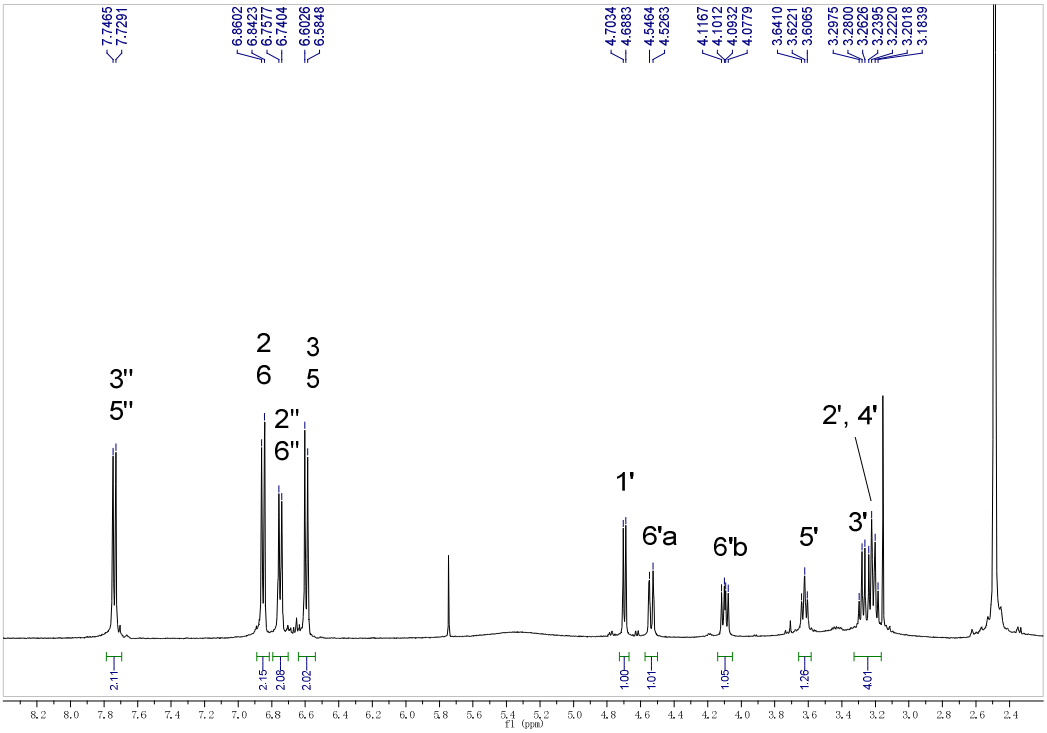

Figure 3.135 ^{1}H NMR spectrum of compound **27**

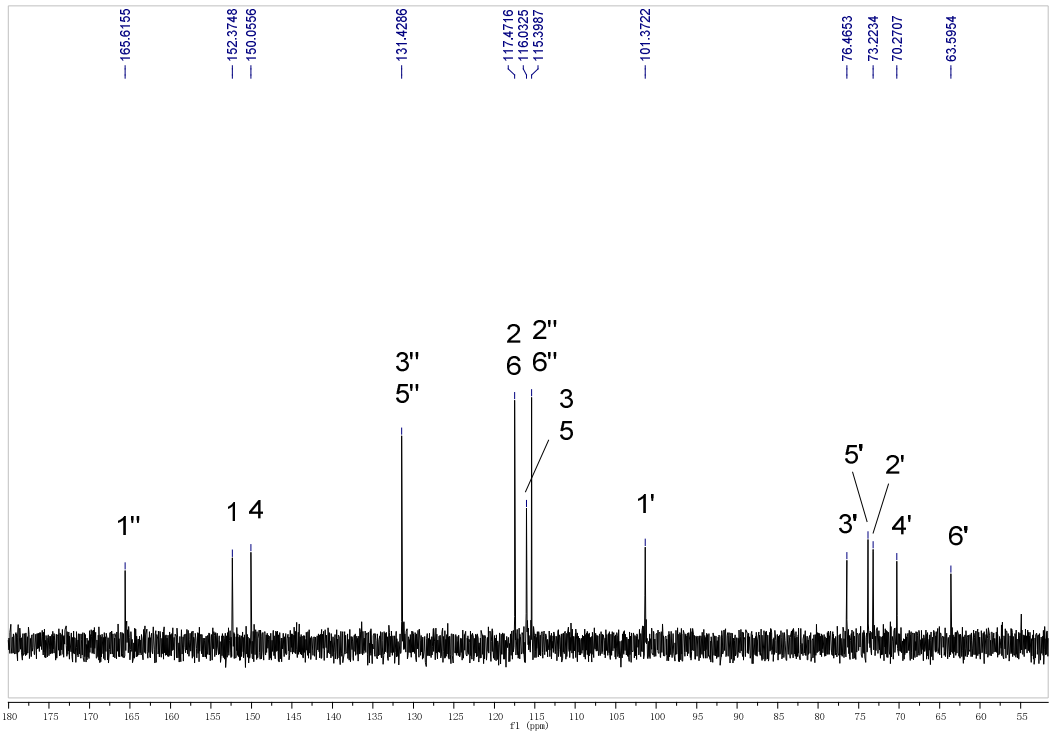

Figure 3.136 ^{13}C NMR spectrum of compound **27**

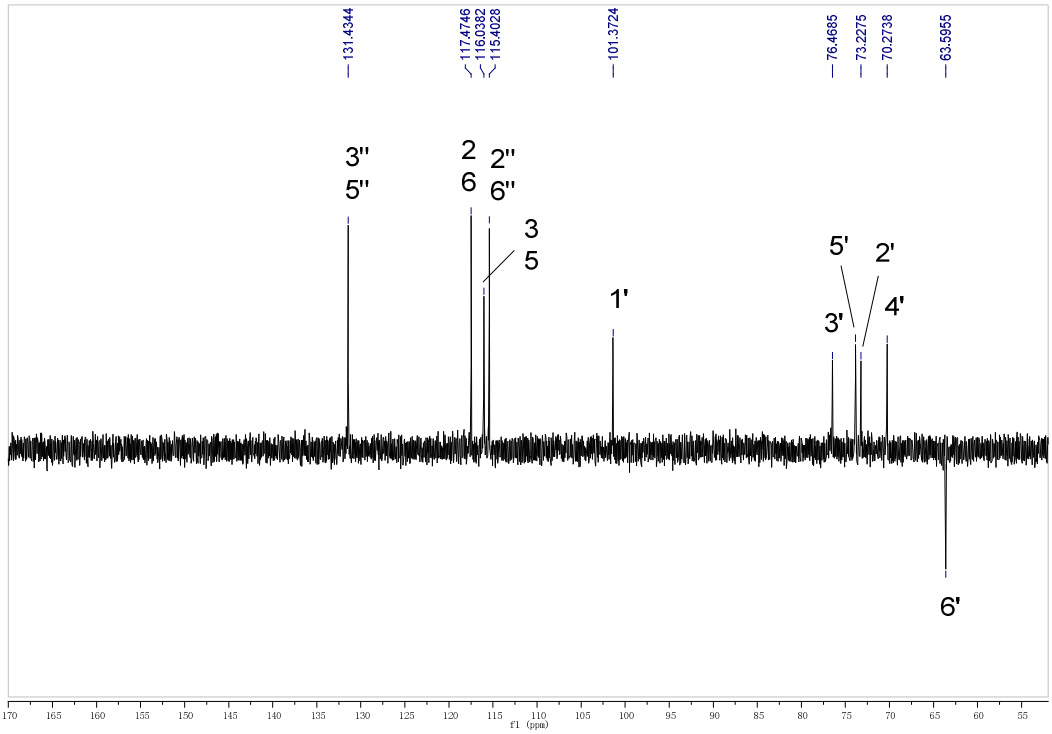

Figure 3.137 DEPT spectrum of compound **27**

Table 3.26 NMR spectroscopic data of compound **27** (CD_3OD, 500 MHz)

	Lanceoloside A (Me_2CO-d_6) [Pegnyemb *et al.*, 1998]		Compound **27**	
Position	δ_C	δ_H (mult., *J* in Hz)	δ_C	δ_H (mult., *J* in Hz)
1	153.5, qC		152.4, qC	
2	118.9, CH	6.95, m	117.5, CH	6.85, d (8.8)
3	116.3, CH	6.66, m	116.0, CH	6.59, d (8.8)
4	151.9, qC		150.0, qC	
5	116.3, CH	6.66, m	116.0, CH	6.59, d (8.8)
6	118.9, CH	6.95, m	117.5, CH	6.85, d (8.8)
1′	103.1, CH	4.80, d (7.3)	101.4, CH	4.70, d (7.6)
2′	74.6, CH	3.56, m	73.2, CH	3.22, t (8.8)
3′	77.8, CH	3.60, m	76.5, CH	3.28, t (8.8)
4′	71.5, CH	3.58, m	70.3, CH	3.20, t (8.8)
5′	75.0, CH	3.80, m	73.8, CH	3.62, dt (8.5, 1.6)
6′	64.7, CH_2	4.70, dd (9.5, 2.3)	63.6, CH_2	4.54, dd (11.7, 1.6)
		4.34, dd (9.5, 2.3)		4.10, dd (11.7, 7.6)
1″	162.8, qC		165.6, qC	
2″	116.0, CH	6.94, m	115.4, CH	6.75, d (8.8)
3″	132.5, CH	7.92, m	131.4, CH	7.74, d (8.8)
4″	116.8, qC		117.5, qC	
5″	132.5, CH	7.92, m	131.4, CH	7.74, d (8.8)
6″	116.0, CH	6.94, m	115.4, CH	6.75, d (8.8)
7″	196.4, qC		165.6, qC	

3.1.28. Staphylionoside D (28, known compound)

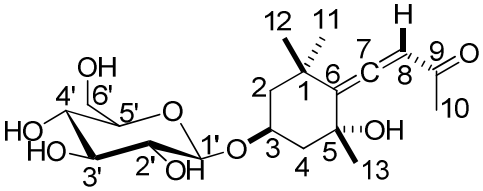

Molecular formula:	$C_{19}H_{30}O_8$
Molecular weight:	386.44
Amount:	3.0 mg

Compound **28** was isolated as an amorphous solid. The UV spectrum (Figure 3.138) exhibited a maximal absorption as 235 nm. The ^{1}H (Figure 3.139) and ^{13}C NMR (Figure 3.140) spectra of **28** showed signals indicating four methyl, two methylene, two methine and three sp^3 quaternary carbons, suggesting that **28** had a skeleton same as that of staphylionoside D. In the HMBC (Figure 3.143), the ^{1}H-^{13}C long-range correlations between the anomeric proton at δ = 4.43 (H-1′) and the oxymethine carbon at δ = 72.6 (C-3) suggested that the glucosyl unit was linked with C-3 via oxygen. The presence of the allenic moiety was confirmed further by HMBC correlations from the proton at δ = 5.82 (H-8) to carbon at δ = 120.1 (C-6). The relative stereochemistry of **28** was determined by ROESY experiments as shown in Figure 3.142. Compound **28** was identical with the known compound **staphylionoside D** [Wang *et al.*, 2005; Yu *et al.*, 2005].

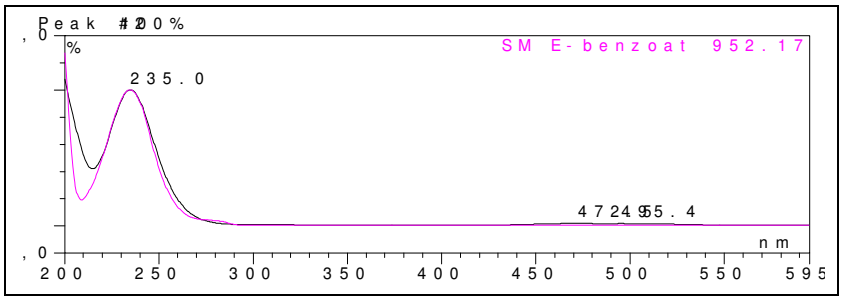

Figure 3.138 UV spectrum of compound **28**

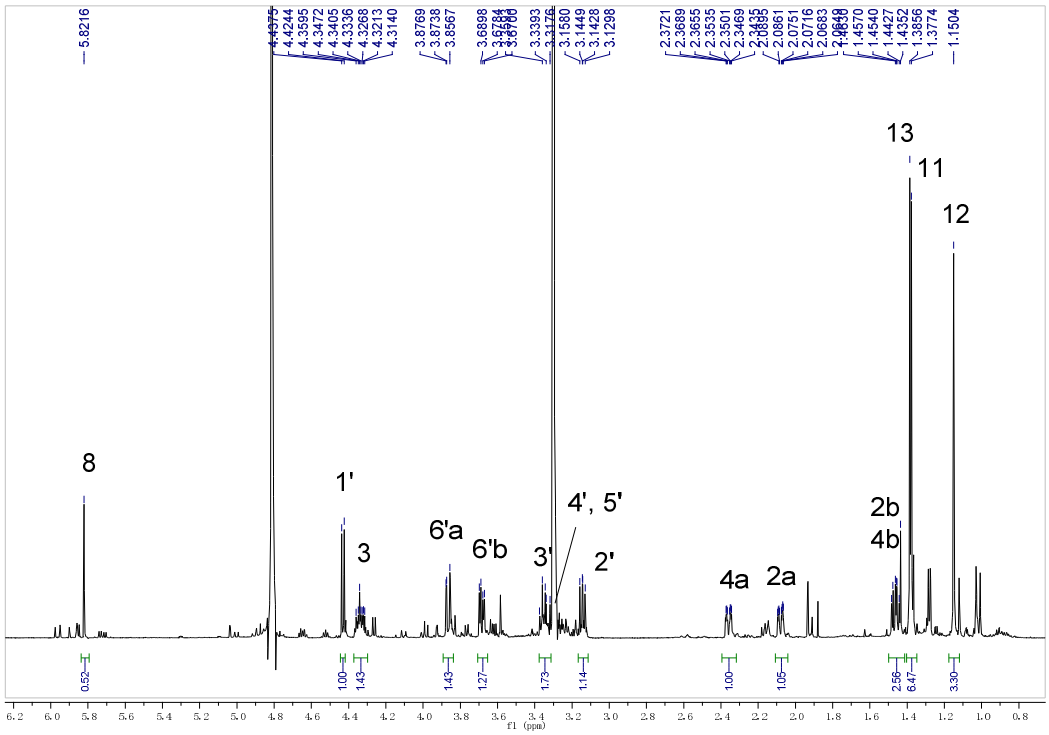

Figure 3.139 ^{1}H NMR spectrum of compound **28**

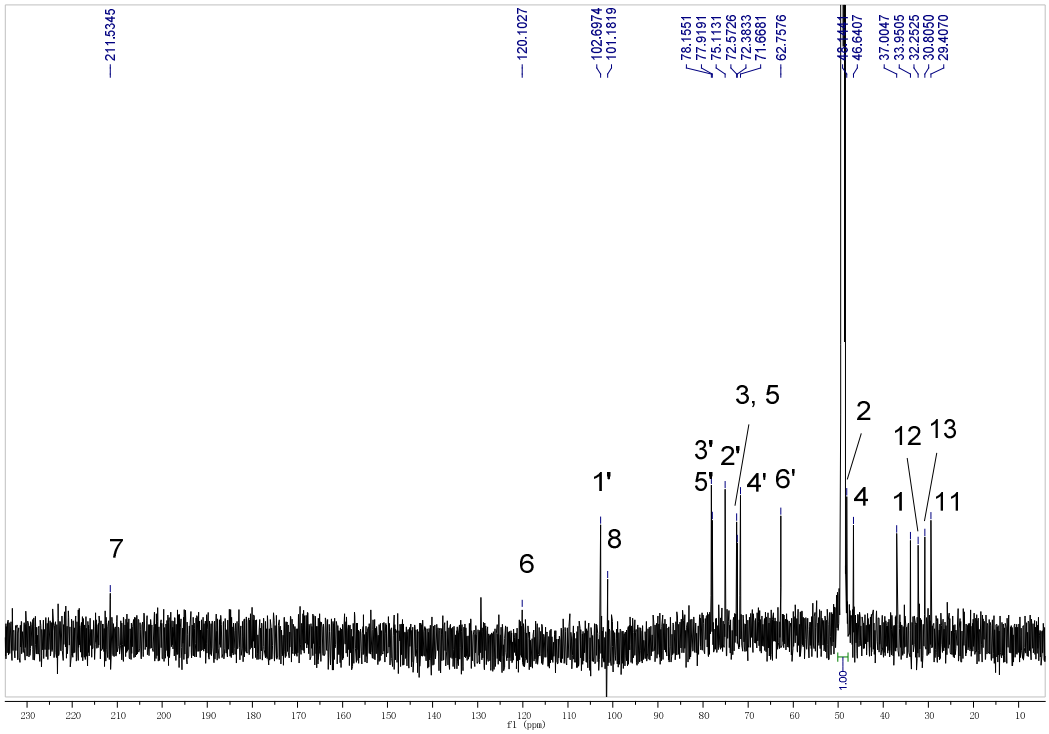

Figure 3.140 ^{13}C NMR spectrum of compound **28**

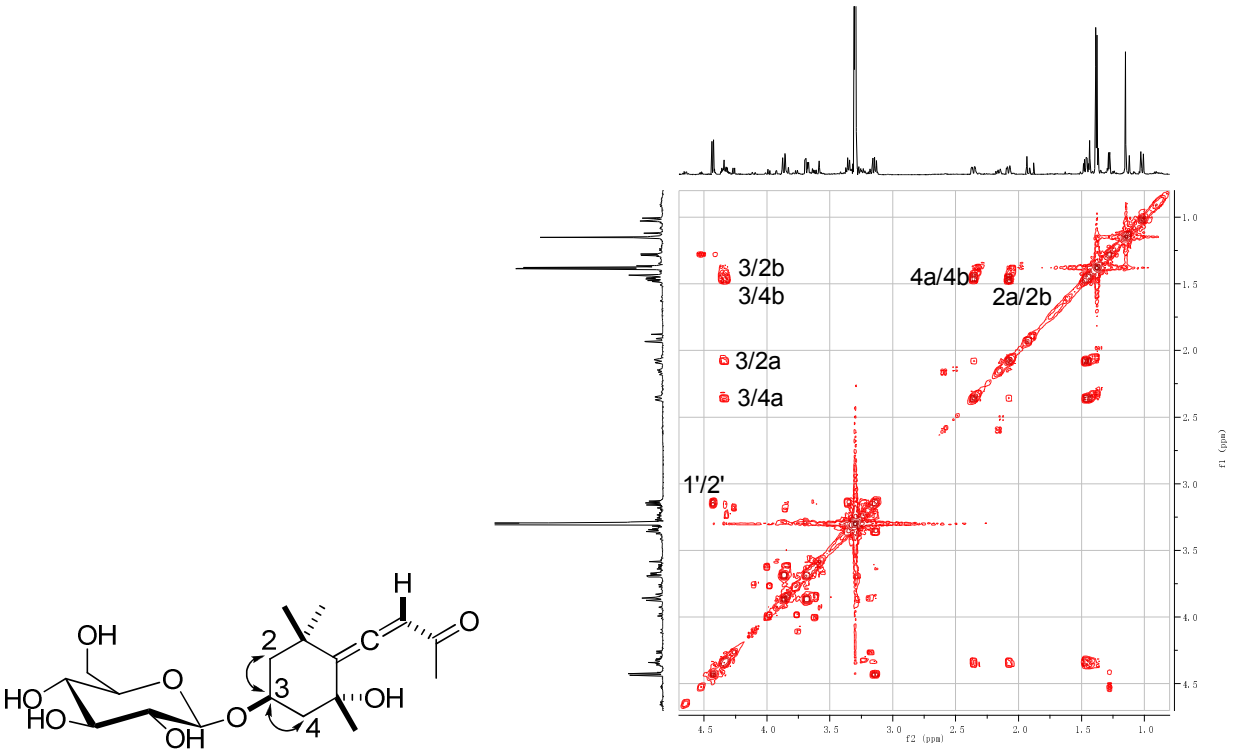

Figure 3.141 ^{1}H-^{1}H COSY spectrum of compound **28**

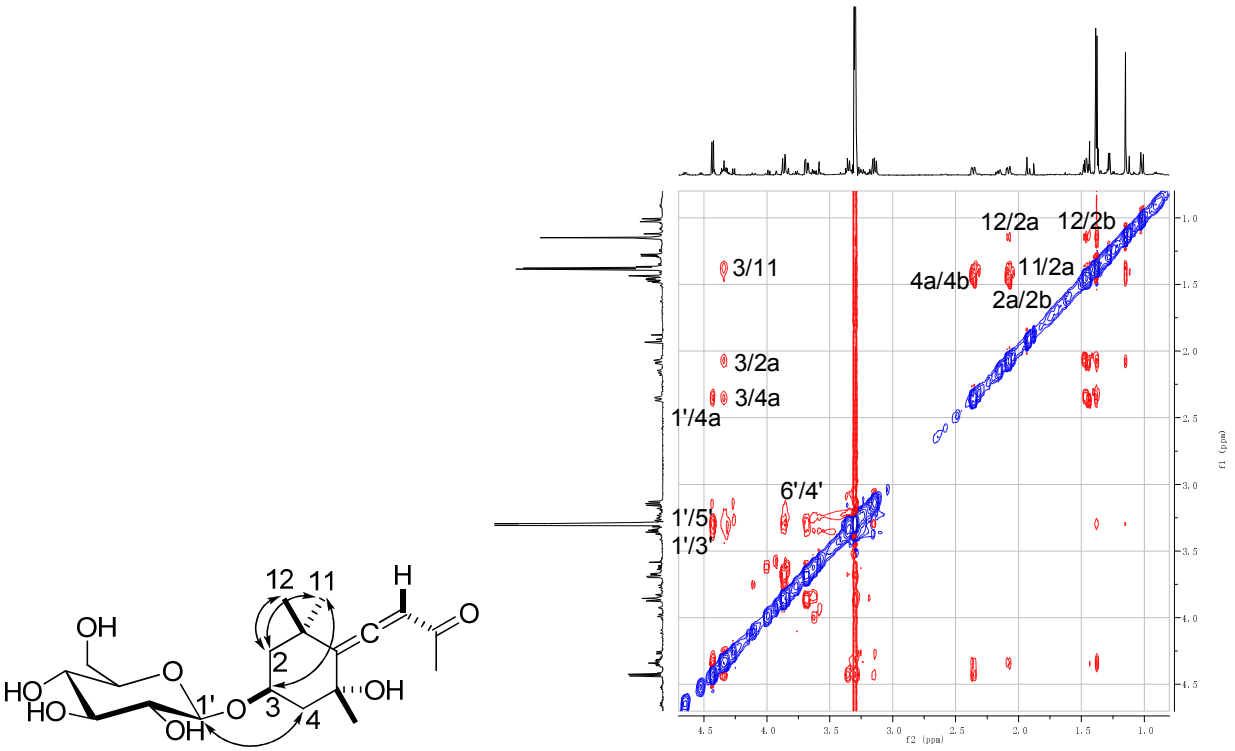

Figure 3.142 ROESY spectrum of compound **28**

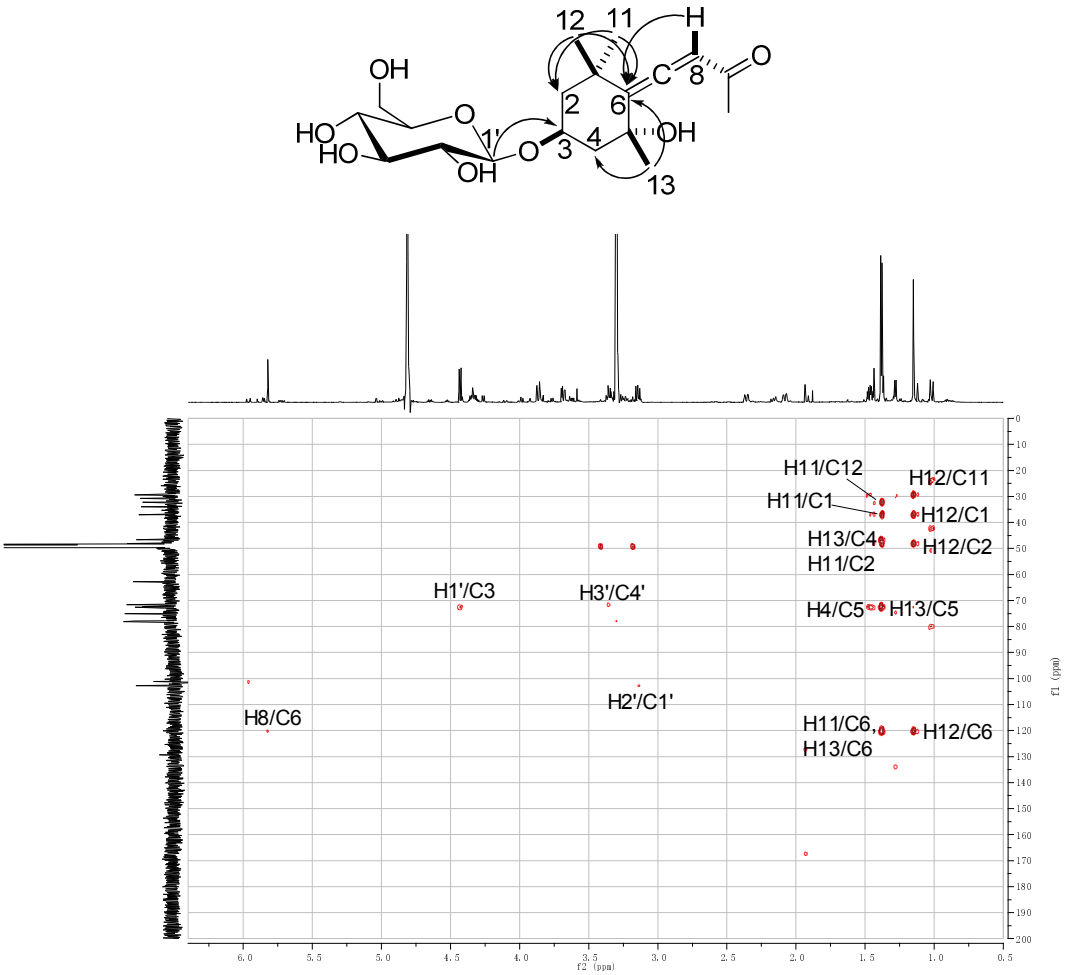

Figure 3.143 HMBC spectrum of compound **28**

Table 3.27 NMR spectroscopic data of compound **28** (CD_3OD, 500 MHz)

	Staphylionoside D [Yu *et al.*, 2005]		Compound **28**	
Position	δ_C	δ_H (mult., *J* in Hz)	δ_C	δ_H (mult., *J* in Hz)
1	37.0, qC		37.0, qC	
2	46.7, CH_2	2.10, ddd (13, 4, 2), 1.47, dd (13, 13)	48.1, CH_2	2.08, ddd (12.7, 4.1, 2.0), 1.46, dd (12.2, 12.2)
3	72.7, CH	4.35, dddd(13, 13, 4, 4)	72.6, CH	4.34, m[a]
4	48.2, CH_2	2.38, ddd (13, 4, 2), 1.46, dd (13, 13)	46.6, CH_2	2.36, ddd (13.2, 4.0, 2.1), 1.46, dd (13.1, 11.3)
5	72.4, qC		72.4, qC	
6	120.2, qC		120.1, qC	
7	200.9, qC		211.5, qC	
8	101.2, CH	5.83, s	101.2, CH	5.82, s
9	211.5, qC		201.0, qC	
10[b]	26.6, CH_3	2.19, s	26.3, CH_3	2.18, s
11	29.5, CH_3	1.38, s	29.4, CH_3	1.38, s
12	32.3, CH_3	1.16, s	32.3, CH_3	1.15, s
13	30.9, CH_3	1.39, s	30.8, CH_3	1.39, s
1′	102.8, CH	4.46, d (8)	102.7, CH	4.43, d (7.8)
2′	75.2, CH	3.16, dd (9, 8)	75.1, CH	3.14, dd (9.1, 7.8)
3′	78.2, CH		78.2, CH	3.36, m[a]
4′	71.7, CH		71.7, CH	3.31, m[a]
5′	77.9, CH		77.9, CH	3.30, m[a]
6′	62.8, CH	3.88, dd (12, 2), 3.69, dd (12, 5)	62.8, CH	3.87, dd (12.2, 1.9), 3.68, dd (12.0, 5.1)

[a] Overlapped signals assigned by ^1H-^1H COSY, HMBC, and HMQC spectra without designating multiplicity. [b] A time-dependent H/D exchange was observed for this signal in CD_3OD. The original singlet decreased in intensity, while all other signals remained unchanged.

3.1.29. Bioactivity test results for the compounds isolated from *Scorzonera radiata*

Radical-scavenging activity of the five new dihydrostilbene derivatives (**1–5**) and the isolated quinic acid derivatives (**7–13**) was assessed using the DPPH assay. As a reference compound, the well known naturally occurring antioxidative stilbene resveratrol was included. IC_{50} values were determined for each of these compounds and are presented in Table 3.28. Compounds **1** and **5** were more active than resveratrol or compounds **2–4**.

The five new dihydrostilbene derivatives (**1–5**) and their aglycones were measured for inhibiting cell viability by MTT or neutral red assay (Figure 3.144) in H4IIE rat hepatoma cells to determine their cytotoxicity. Then those compounds were principally evaluated the TNF dependent NF-κB activation by SEAP-Assay in H4IIE cells (Figure 3.145–Figure 3.147). The aglycone of **1**, the only active compound, was further tested for caspase 3/7 stimulating activity (Figure 3.148).

Scorzodihydrostilbene A and B (**1** and **2**) were also tested for cytotoxicity toward the mouse lymphoma cell line (L5178Y), and showed 102.8% and 96.1% growth inhibition respectively. Neither of them was active when assayed at a concentration of 10 μg/mL.

Three dihydrostilbene derivatives (**1–3**), three quinic acid derivatives (**7–9**) and **25** were further evaluated for their protein kinase inhibitory profiles. The results are presented as residual activity in percent related to the 100% controls and shown in Table 3.29. Compound **2**, **8**, **9** and **25** were selected for IC_{50} determination since they showed an inhibition of $\geq$ 40 % at a concentration of 1 μg/mL with at least one of the 24 kinases. The IC_{50} values in molar concentrations are exhibited in Table 3.30.

Table 3.28 IC_{50} values of dihydrostilbene derivatives, quinic acid derivatives and resveratrol in DPPH assay

compound	**IC_{50} (μM)**
scorzodihydrostilbene A (**1**)	105.51
scorzodihydrostilbene B (**2**)	663.13
scorzodihydrostilbene C (**3**)	486.38
scorzodihydrostilbene D (**4**)	730.99
scorzodihydrostilbene E (**5**)	102.90
resveratrol	149.52
chlorogenic acid (**7**)	48.69
3,5-dicaffeoylquinic acid (**8**)	41.46
3,5-dicaffeoyl-*epi*-quinic acid (**9**)	40.40
macroantoin G (**10**)	41.27
4,5-dicaffeoylquinic acid (**11**)	42.23
4,5-dicaffeoyl-*epi*-quinic acid (**12**)	40.55
5-*p*-coumaroylquinic acid (*trans*) (**13**)	378.21

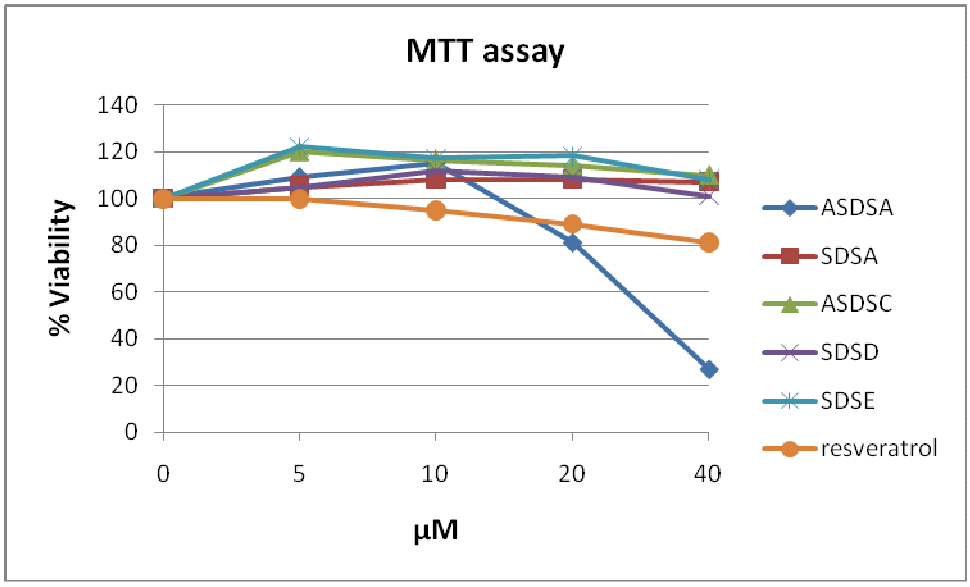

Figure 3.144 Cell viability of scorzodihydrostilbene derivatives in H4IIE

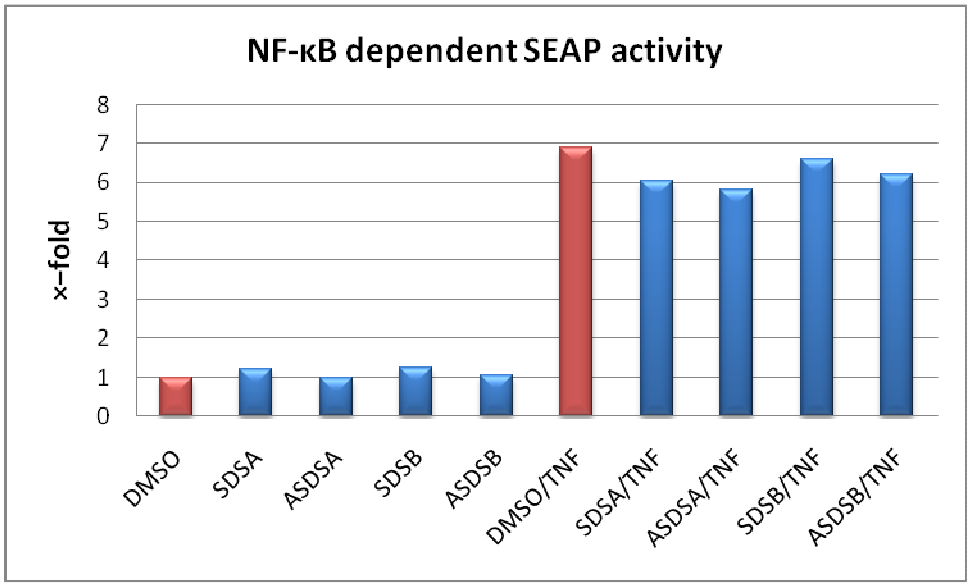

Figure 3.145 Inhibition of TNF-α induced activation of NF-κB by 40 μM dihydrostilbene derivatives

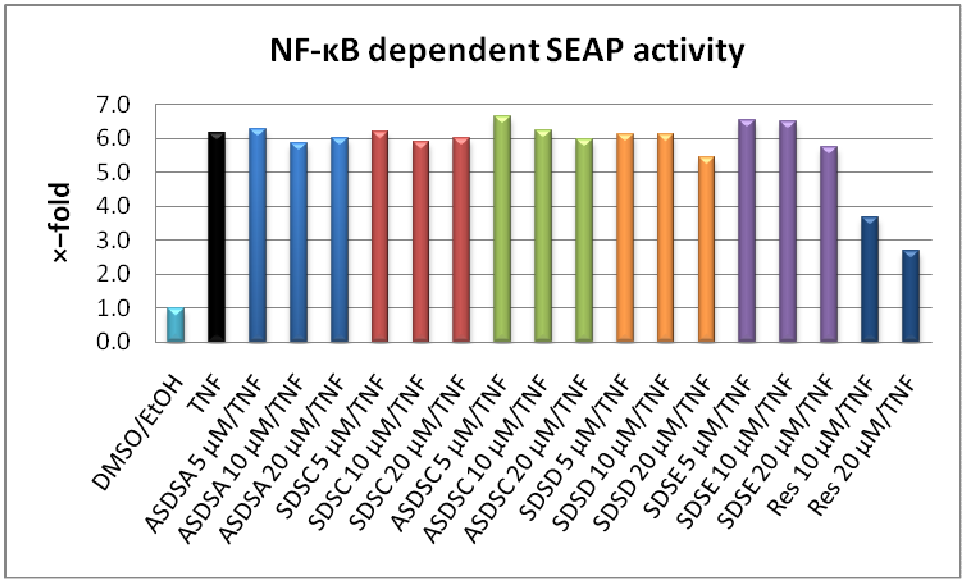

Figure 3.146 Inhibition of TNF-α induced activation of NF-κB by dihydrostilbene derivatives

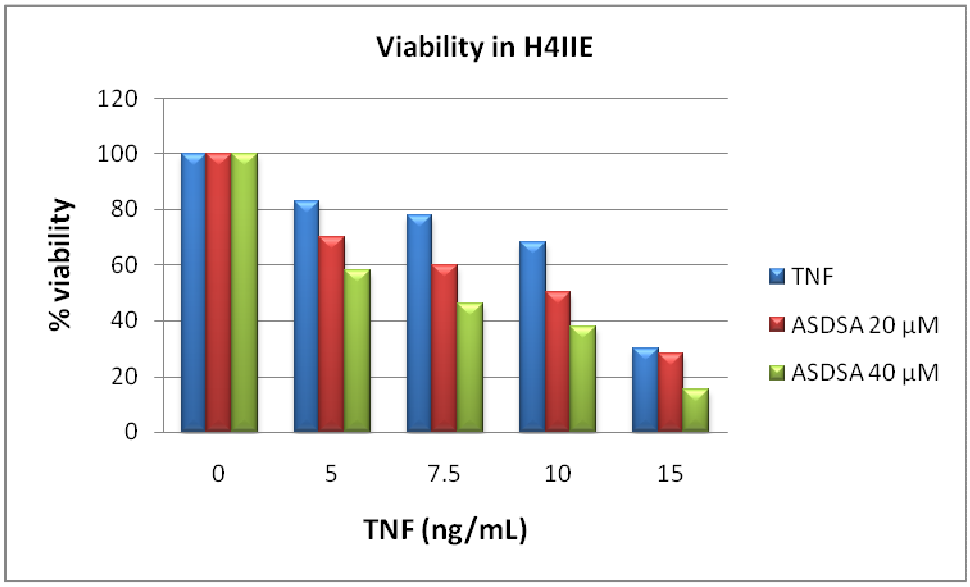

Figure 3.147 Cell viability of the aglycone of scorzodihydrostilbene A stimulated with TNF in H4IIE

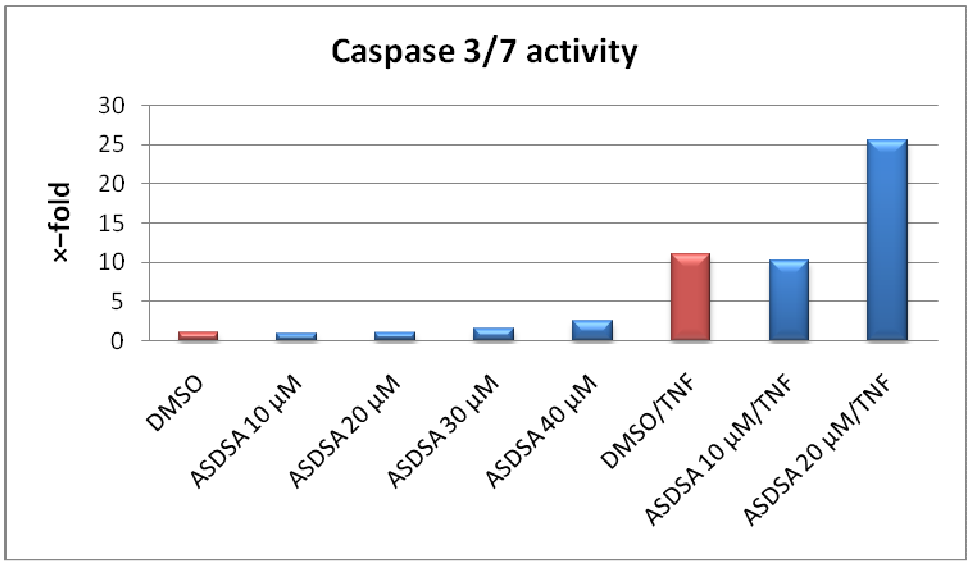

Figure 3.148 Caspase 3/7 activation by the aglycone of scorzodihydrostilbene A and stimulated with 5 ng/mL TNF

Table 3.29 Selectivity profiling of seven compounds isolated from *Scorzonera radiata* using 24 protein kinases

		Residual activities (% of control activity)						
	Compound	**1**	**2***	**3**	**7**	**8***	**9***	**25***
Protein kinase	AKT1	97	96	72	95	51	88	96
	ARK5	94	95	101	96	89	90	94
	Aurora-A	97	95	89	86	66	49	93
	Aurora-B	86	59	82	74	28	29	93
	AXL	99	96	103	83	43	76	99
	B-RAF-VE	104	121	111	99	75	102	99
	CDK2/CycA	98	96	103	115	80	96	110
	CDK4/CycD1	116	75	92	100	42	74	113
	CK2-alpha1	104	95	100	97	75	80	104
	COT	99	95	86	99	74	95	94
	EGF-R	94	92	98	103	27	55	72
	EPHB4	95	88	100	89	28	63	74
	ERBB2	99	87	91	99	61	90	78
	FAK	99	94	96	88	80	87	90
	IGF1-R	94	90	100	92	10	40	61
	INS-R	99	99	97	103	34	41	101
	MET	94	91	94	110	69	78	96
	PDGFR-beta	92	95	97	97	68	74	98
	PLK1	96	89	103	97	75	83	99
	PRK1	99	90	88	80	62	69	86
	SAK	110	115	122	82	8	14	109
	SRC	99	83	102	85	23	60	45
	TIE2	99	99	94	102	13	50	72
	VEGF-R2	90	84	90	84	13	48	64
	IC_{50}	86	59	72	74	8	14	45

*showing at least 40 % inhibition at 1 μg/mL with at least one of 24 kinases

Table 3.30 IC_{50} profiling of four selected compounds using 24 protein kinases (variable highest molar concentration)

		IC_{50} values (M)			
		scorzodihydro-stilbene B (**2**)	3,5-dicaffeoyl-quinic acid (**8**)	3,5-dicaffeoyl-*epi*-quinic acid (**9**)	piceol (**25**)
Protein kinase	AKT1	A	7.2E-06	1.1E-05	A
	ARK5	A	4.8E-06	7.4E-06	A
	Aurora-A	A	3.0E-06	2.4E-06	A
	Aurora-B	A	9.4E-07	2.0E-06	A
	AXL	A	1.4E-06	3.6E-06	A
	B-RAF-VE	A	3.7E-06	1.7E-05	A
	CDK2/CycA	A	6.5E-06	1.3E-05	A
	CDK4/CycD1	A	2.3E-06	4.9E-06	A
	CK2-alpha1	A	5.5E-06	8.0E-06	A
	COT	A	8.5E-06	7.8E-06	A
	TIE2	A	1.2E-06	1.6E-06	A
	EGF-R	A	7.1E-07	3.1E-06	1.9E-05
	EPHB4	A	1.2E-06	3.9E-06	A
	ERBB2	A	2.6E-06	9.1E-06	A
	FAK	A	5.0E-06	1.2E-05	A
	IGF1-R	A	3.8E-07	1.9E-06	1.6E-05
	INS-R	A	1.1E-06	1.7E-06	A
	MET	A	2.0E-06	3.3E-06	A
	PDGFR-beta	A	2.4E-06	3.4E-06	A
	PLK1	A	4.9E-06	6.6E-06	A
	PRK1	A	2.9E-06	5.3E-06	A
	SAK	A	3.5E-07	5.4E-07	A
	SRC	A	7.4E-07	4.0E-06	1.1E-05
	VEGF-R2	A	4.5E-07	2.4E-06	2.5E-05

A above maximal molar assay concentration of compound
moderately active
active

3.2. Compounds isolated from the Mongolian medicinal plant *Dianthus versicolor*

Dianthus versicolor Fisch. ex Link (Caryophyllaceae) is also a Mongolian folk medicinal plant. This plant is used as a diuretic, as an anti-inflammatory agent, and in the treatment of urinary infections, carbuncles, and carcinomas [Ma *et al.*, 2009]. In the previous phytochemical studies of *Dianthus* spp, saponins, flavonoids, and glycosides have been reported as the main constituents of this genus. Especially many bioactive saponins have been investigated which are shown in Figure 3.149 [Hikino *et al.*, 1984; Li *et al.*, 1993; Li *et al.*, 1994]. So far only few studies have been done for the species *Dianthus versicolor* [Boguslavskaya *et al.*, 1983; Ma *et al.*, 2009]. In our research for biologically active metabolites from the Mongolia medicinal plant *D. versicolor*, two lignans (**29**, **30**) and several triterpenoids (**31**–**34**) were isolated.

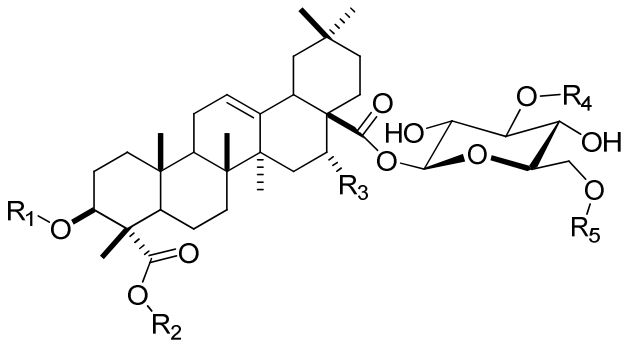

compound	R_1	R_2	R_3	R_4	R_5
dianosides H	H	H	H	H	H
dianosides G	H	H	H	Glc	Glc
dianosides A	Glc	H	H	H	H
azukisaponin lV	Glc	H	H	H	Glc
dianosides B	Glc	H	H	Glc	Glc
hainanenside	H	H	OH	H	H
dianchinenoside D	H	H	OH	H	Glc
dianchinenoside C	H	Glc	OH	H	H
dianchinenoside A	Ara	H	OH	H	H
dianchinenoside B	Xyl	H	OH	H	H

Figure 3.149 Some saponins isolated from the genus *Dianthus*

3.2.1. (–)-Matairesinol (29, known compound)

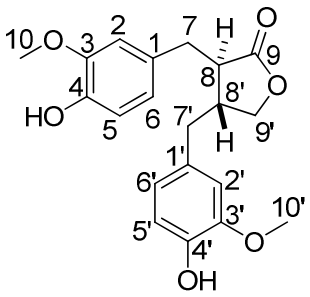

Molecular formula:	$C_{20}H_{22}O_6$
Molecular weight:	358.39
Amount:	88.2 mg

Compound **29** was obtained as an amorphous solid, and shown to have the molecular weight 358 as determined by ESI mass spectrum (Figure 3.151). The UV spectrum of **29** (Figure 3.150) exhibited absorption maxima at 211, 228, and 281 nm. The ^{1}H (Figure 3.152) and ^{13}C NMR (Figure 3.153) spectra of **29** showed resonances for two ABX systems [δ_H 6.81 (d, J = 7.9 Hz), 6.60 (d, J = 1.9 Hz) and 6.59 (dd, J = 7.9, 1.9 Hz); and δ_H 6.79 (d, J = 8.0), 6.50 (dd, J = 8.0, 1.9 Hz) and 6.40 (d, J = 1.9 Hz)] in the aromatic region, which were assigned to two 1,3,4-trisubstituted phenyl units. Two methyl resonances at δ_H 3.80 and 3.79 indicated two *O*-methyl functions. From the observations in the aliphatic region, along with the analysis of the DEPT (Figure 3.154) and ^{1}H-^{1}H COSY spectra of **29** (Figure 3.155), three methylene groups and two methane groups were presented. The attachment of two *O*-methyl groups at C-3 and C-3′ were shown from the HMBC cross-peaks (Figure 3.157) of the methyl singlet at δ_H 3.80 and 3.79 with δ_C 146.67 and 146.55, respectively. The NMR data and $[\alpha]^{20}_{D}$ [–92 (*c* 0.10, MeOH)] value of compound **29** were in good agreement with those of **(–)-matairesinol** [Youssef and Frahm, 1995], which is one of the well known lignans.

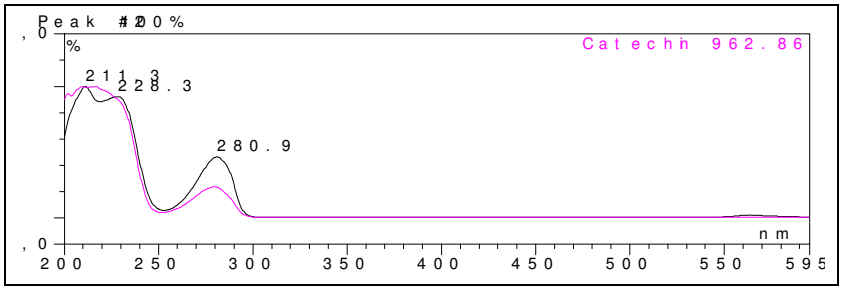

Figure 3.150 UV spectrum of compound **29**

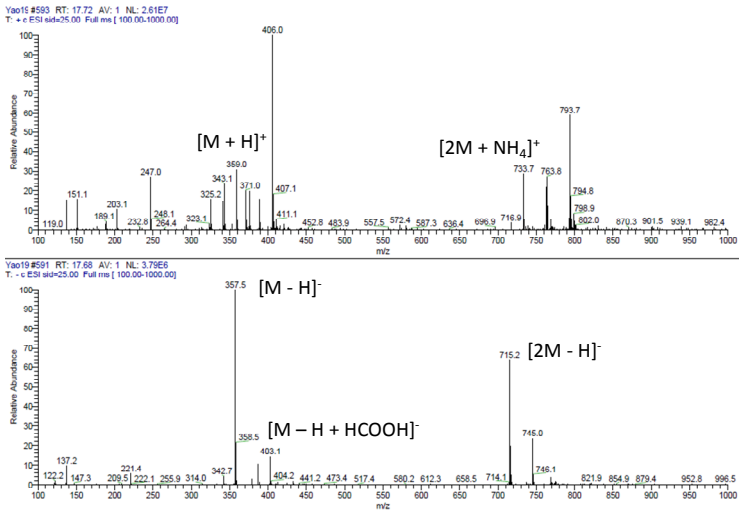

Figure 3.151 ESI-MS spectrum of compound **29**

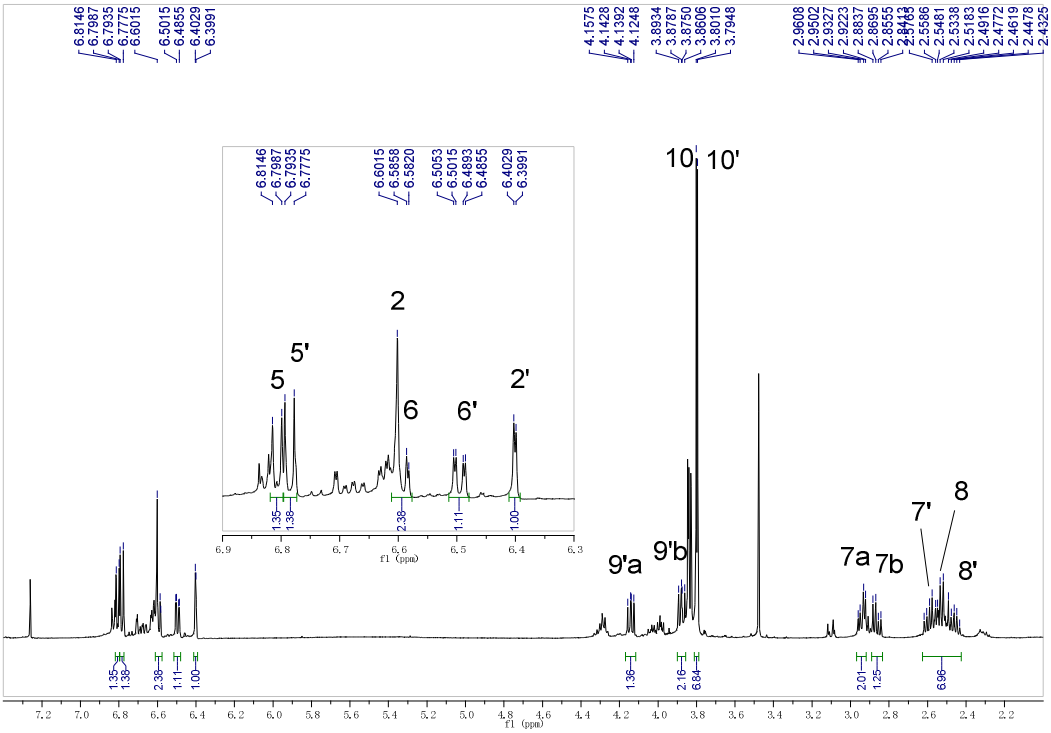

Figure 3.152 ^{1}H NMR spectrum of compound **29**

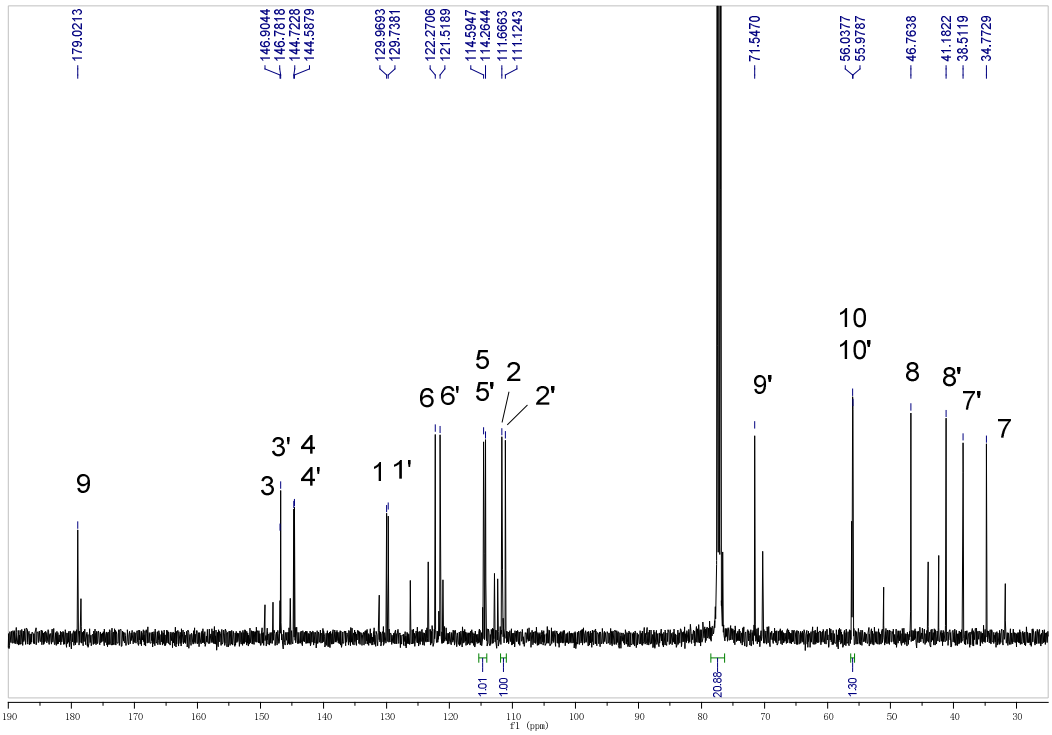

Figure 3.153 ^{13}C NMR spectrum of compound **29**

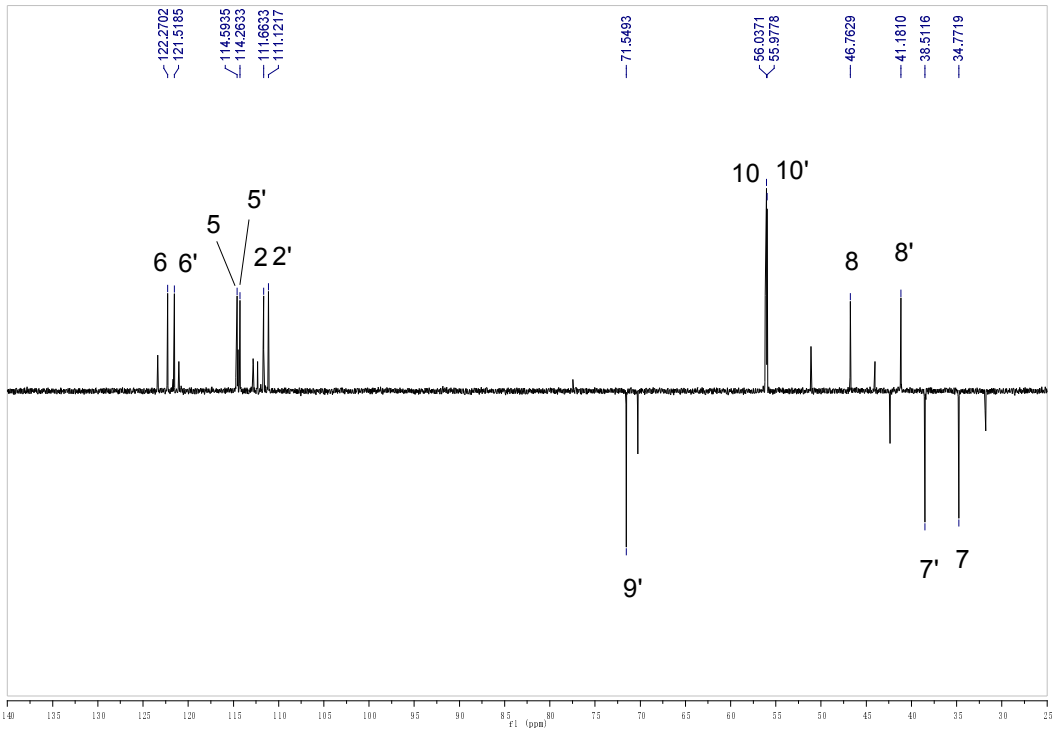

Figure 3.154 DEPT spectrum of compound **29**

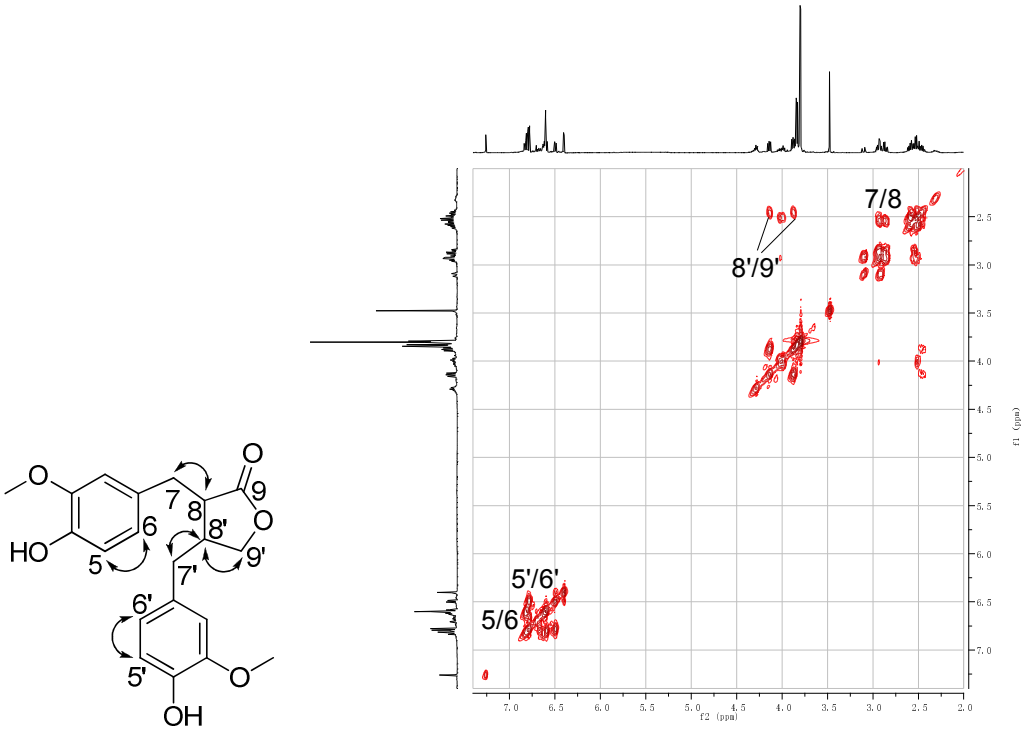

Figure 3.155 ^{1}H-^{1}H COSY spectrum of compound **29**

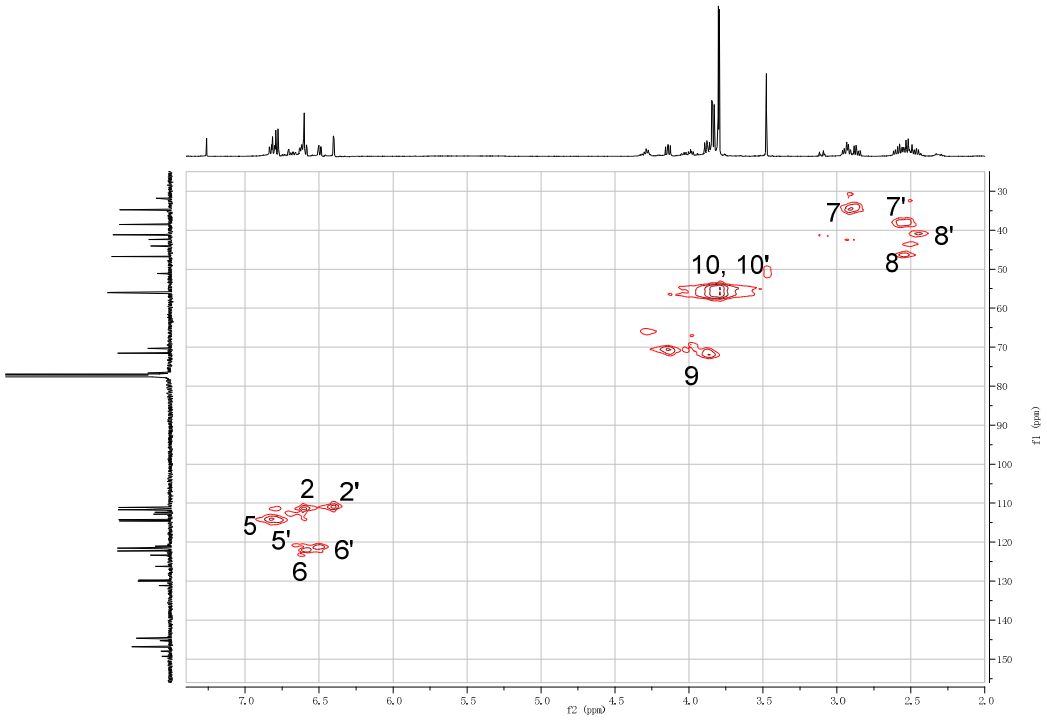

Figure 3.156 HMQC spectrum of compound **29**

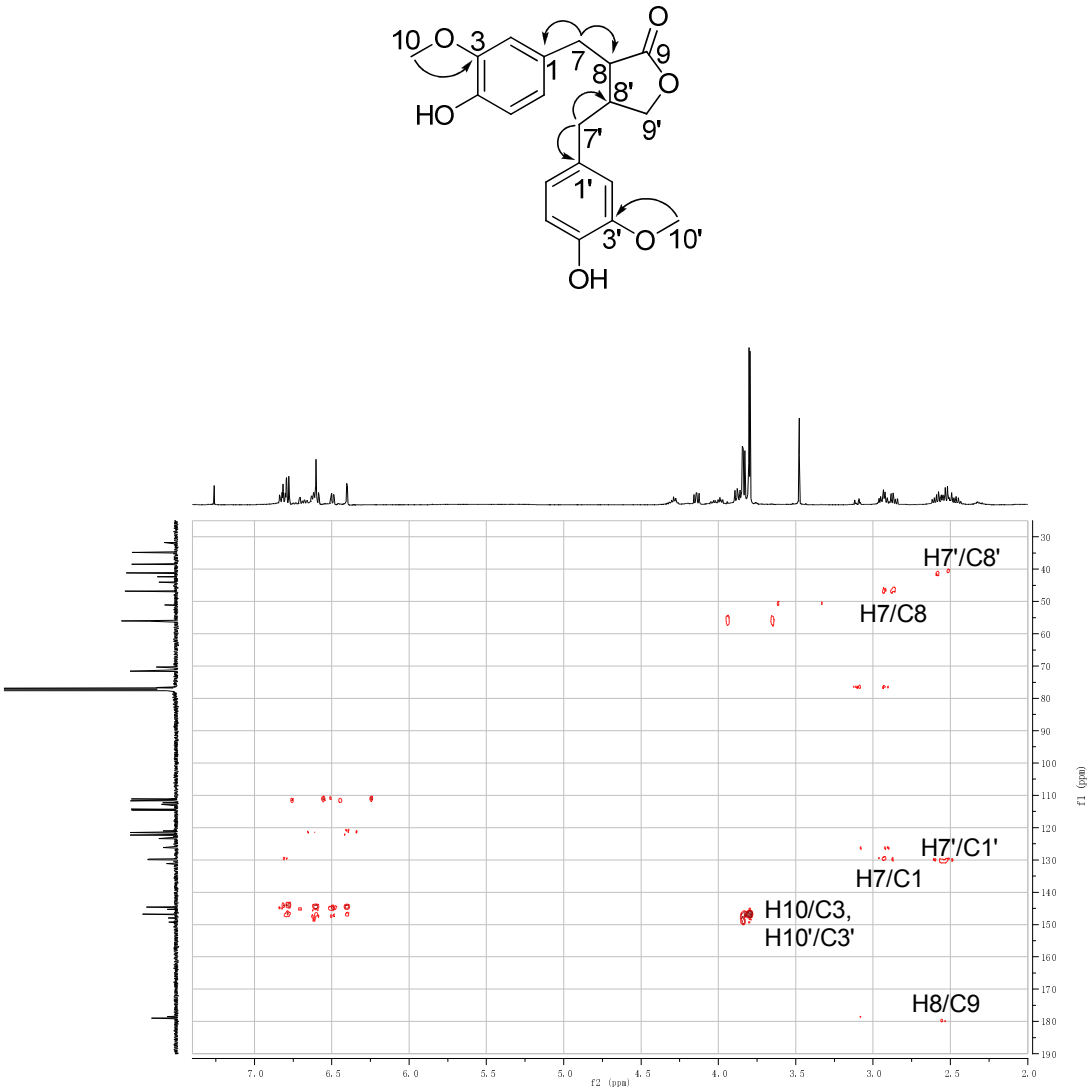

Figure 3.157 HMBC spectrum of compound **29**

Table 3.31 NMR spectroscopic data of compound **29** ($CDCl_3$, 500 MHz)

	(−)-Matairesinol [Youssef and Frahm, 1995]		Compound **29**	
Position	δ_C	δ_H (mult., *J* in Hz)	δ_C	δ_H (mult., *J* in Hz)
1	129.73, qC		129.74, qC	
2	111.51, CH	6.58, d	111.43, CH	6.60, d (1.9)
3	146.70, qC		146.67, qC	
4	144.52, qC		144.49, qC	
5	114.40, CH	6.78, d	114.36, CH	6.81, d (7.9)
6	122.03, CH	6.57, dd	122.04, CH	6.59, dd (7.9, 1.9)
7	34.55, CH_2	2.92, m	34.54, CH_2	2.94, dd (14.0, 5.3)
		2.84, m		2.86, dd (14.0, 7.1)
8	46.53, CH	2.50, m	46.53, CH	2.53, m[a]
9	178.77, qC		178.79, qC	
10	55.81, CH_3	3.79, s	55.80, CH_3	3.80, s
1′	129.50, qC		129.51, qC	
2′	110.97, CH	6.38, d	110.89, CH	6.40, d (1.9)
3′	146.59, qC		146.55, qC	
4′	144.39, qC		144.36, qC	
5′	114.08, CH	6.76, d	114.03, CH	6.79, d (8.0)
6′	121.28, CH	6.48, dd	121.29, CH	6.50, dd (8.0, 1.9)
7′	38.27, CH_2	2.57, m	38.28, CH_2	2.56, m[a]
8′	40.97, CH	2.42, m	40.95, CH	2.46, m[a]
9′	71.30, qC	4.12, dd	71.32, qC	4.14, dd (9.1, 7.3)
		3.85, dd		3.88, dd (9.1, 7.3)
10′	55.76, CH_3	3.78, s	55.74, CH_3	3.79, s

[a] Overlapped signals assigned by ^1H-^1H COSY, HMBC, and HMQC spectra without designating multiplicity.

3.2.2. (–)-Arctigenin (30, known compound)

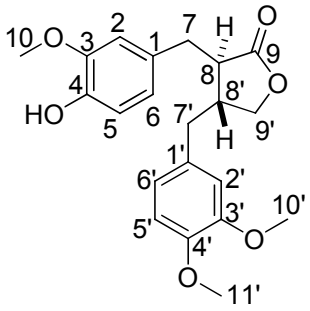

Molecular formula:	$C_{21}H_{24}O_6$
Molecular weight:	372.41
Amount:	76.3 mg

Compound **30** was isolated as an amorphous solid with UV absorbances at λ_{max} 218 and 283 nm. The ESI mass spectrum (Figure 3.161) showed the molecular weight was 372, indicating the presence of an additional CH_3 group compared to **29**. The ^1H (Figure 3.159) and ^{13}C NMR spectra of **30** were almost superimposable to those of **29**. The obvious difference in the NMR spectra between **30** and **29** was observed for the third *O*-methyl resonance at δ_H 3.83 (H-11′) in the ^1H NMR spectrum of **30**. The attachment of the methoxy group at C-4′ was deduced from the HMBC correlation (Figure 3.160) of H_3-11′ with C-4′ at δ_C 147.9. The optical rotation of **30** was determined to be $[\alpha]^{20}_D$ –26 (*c* 0.10, MeOH). From the above data and through comparison with those of the literature [Xie *et al.*, 2003] it was confirmed that compound **30** was **(–)-arctigenin**.

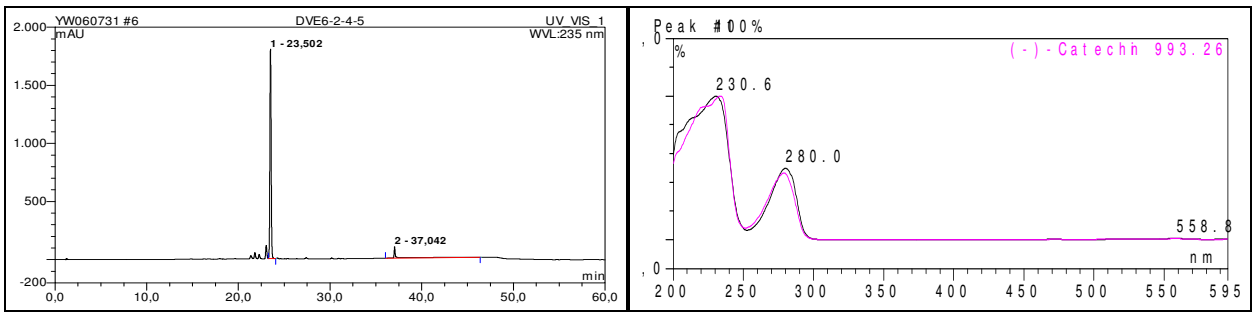

Figure 3.158 HPLC chromatogram and UV spectrum of compound **30**

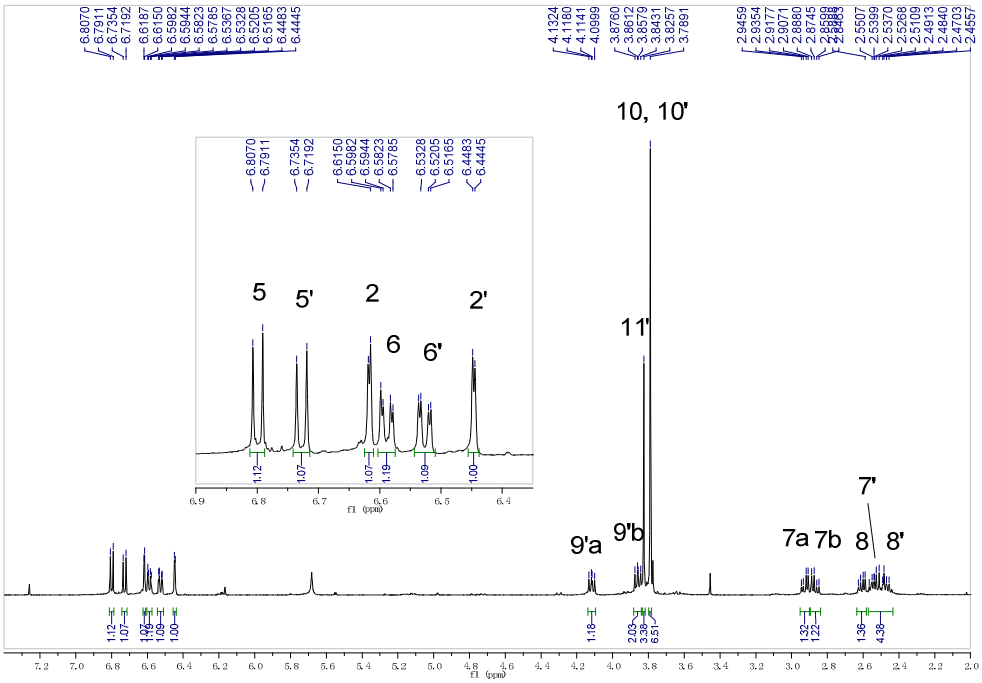

Figure 3.159 ^{1}H NMR spectrum of compound **30**

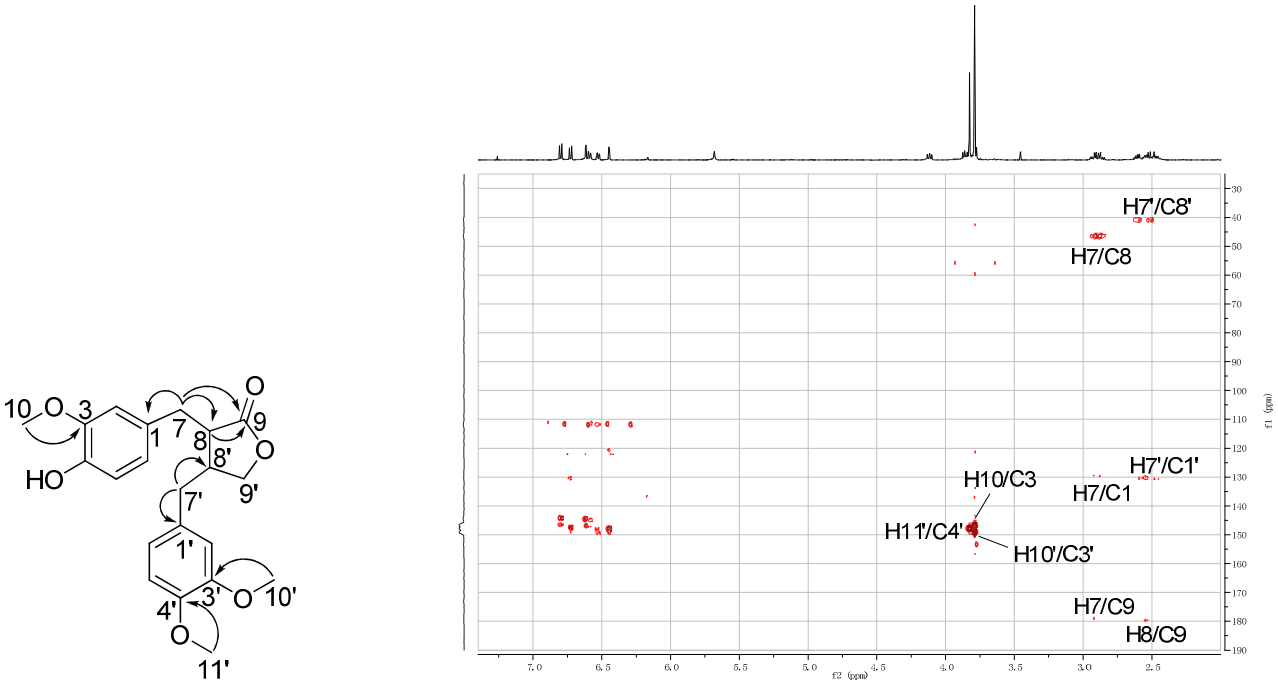

Figure 3.160 HMBC spectrum of compound **30**

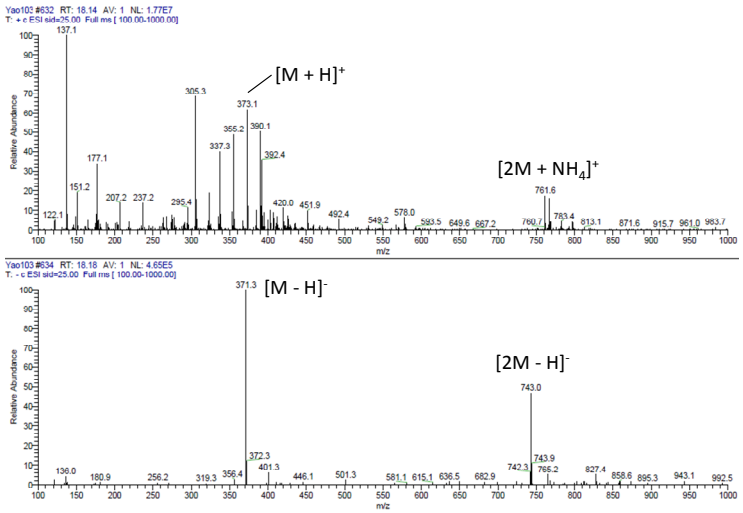

Figure 3.161 ESI-MS spectrum of compound **30**

Table 3.32 NMR spectroscopic data of compound **30** ($CDCl_3$, 500 MHz)

	(−)-Arctigenin [Xie *et al.*, 2003]		Compound **30**	
Position	δ_C	δ_H (mult., *J* in Hz)	δ_C	δ_H (mult., *J* in Hz)
1	129.5, qC		129.6, qC	
2	111.6, CH	6.64, d (1.94)	111.8, CH	6.62, d (1.9)
3	146.7, qC		147.0, qC	
4	144.6, qC		144.8, qC	
5	114.1, CH	6.83, d (7.99)	114.1, CH	6.80, d (7.9)
6	122.1, CH	6.61, dd (7.99, 1.94)	122.1, CH	6.59, dd (7.9, 1.9)
7	34.5, CH_2	2.92, m	34.6, CH_2	2.93, dd (14.2, 5.4)
				2,87, dd (14.2, 6.6)
8	46.6, CH	2.66, m	46.7, CH	2.61, m[a]
9	178.7, qC		179.0, qC	
10	55.8, CH_3	3.81, s	55.5, CH_3	3.79, s
1′	130.5, qC		130.5, qC	
2′	111.9, CH	6.46, d (1.94)	111.9, CH	6.45, d (1.9)
3′	149.1, qC		149.2, qC	
4′	147.9, qC		147.9, qC	
5′	111.4, CH	6.75, d (8.19)	111.3, CH	6.73, d (7.9)
6′	120.6, CH	6.55, dd (8.19, 1.94)	120.6, CH	6.53, dd (7.9, 1.9)
7′	38.2, CH_2	2.55, m	38.4, CH_2	2.55, m[a]
8′	41.0, CH	2.45, m	41.0, CH	2.49, m[a]
9′	71.3, qC	4.13, dd (9.18, 7.24)	71.4, qC	4.12, dd (9.2, 7.3)
		3.88, dd (9.18, 7.28)		3.86, dd (9.2, 7.3)
10′	55.8, CH_3	3.82, s	55.5, CH_3	3.79, s
11′	55.9, CH_3	3.85, s	56.4, CH_3	3.83, s

[a] Overlapped signals assigned by ^{1}H-^{1}H COSY, HMBC, and HMQC spectra without designating multiplicity.

3.2.3. Lupeol (31, known compound)

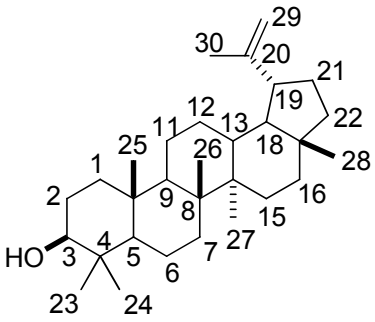

Molecular formula:	$C_{30}H_{50}O$
Molecular weight:	426.72
Amount:	77.9 mg

Compound **31** was obtained as white crystal needles. The EI mass spectrum (Figure 3.162) showed the molecular ion peak at *m/z* 426 $[M]^+$ indicating the molecular weight as 426. The ^{13}C NMR (Figure 3.164) and DEPT spectra (Figure 3.166) revealed 30 carbons including seven methyls, eleven methylenes, six methines and six quaternary carbons. The ^1H NMR spectrum exhibited one oxymethine proton at δ_H 3.20, which was assigned to be H-3. A pair of germinal coupled olefinic protons was observed at δ_H 4.69 and 4.56 indicating the presence of a carbon-carbon double bond. In comparison with the ^1H and ^{13}C NMR data of the literature [Aratanechemuge *et al.*, 2004], compound **31** was identified as **lupeol**.

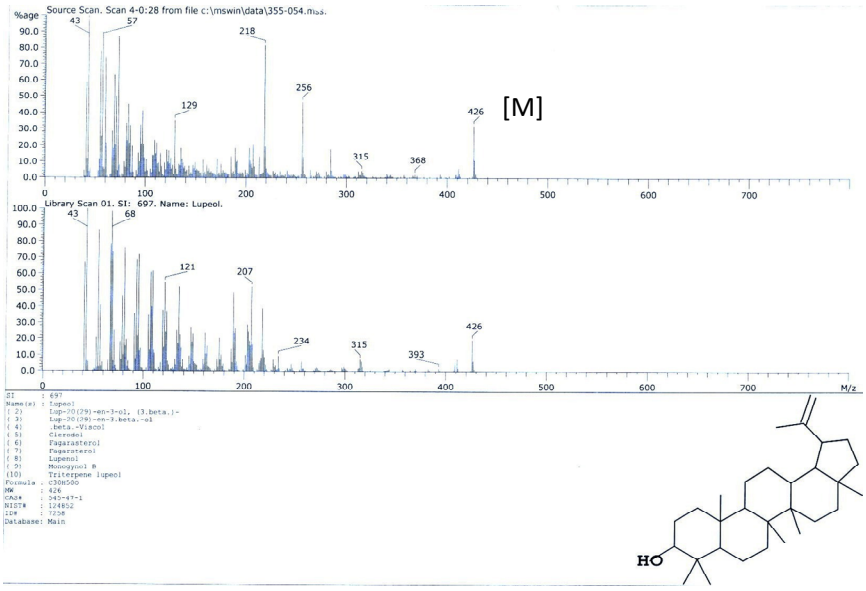

Figure 3.162 EI-MS spectrum of compound **31**

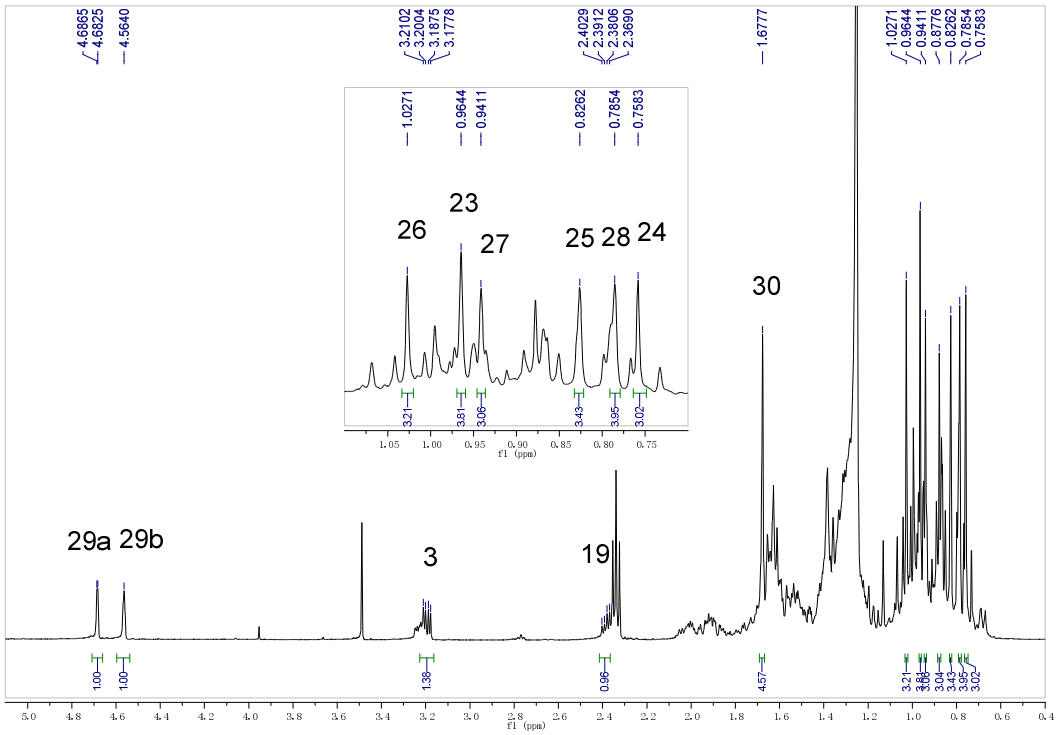

Figure 3.163 ^{1}H NMR spectrum of compound **31**

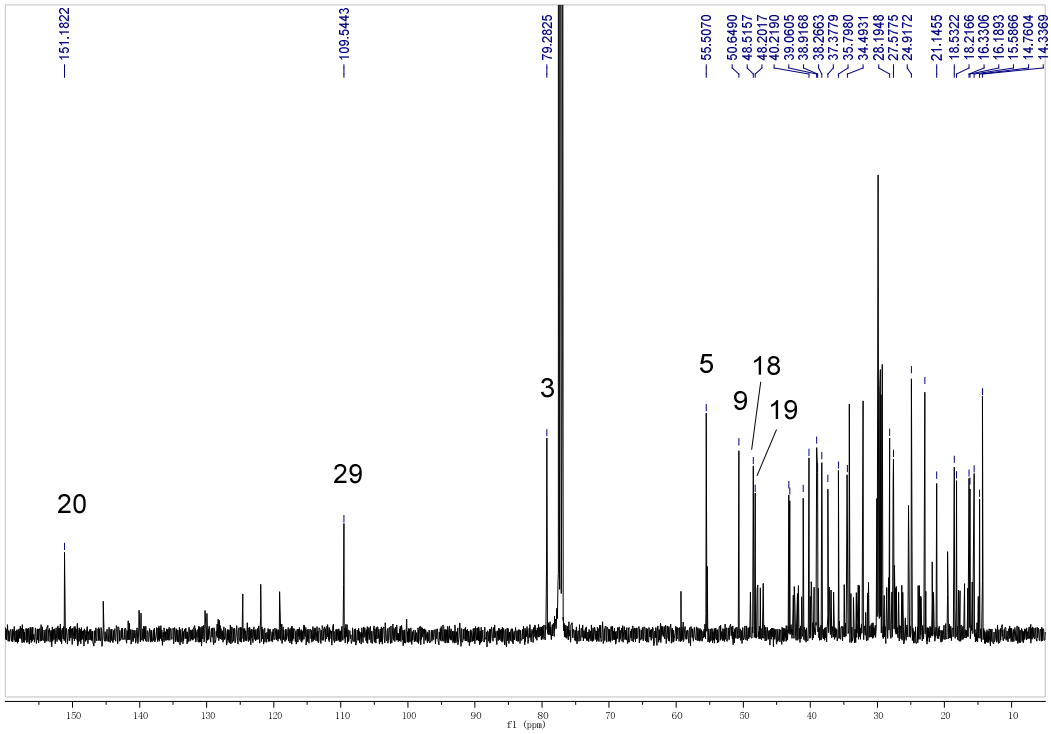

Figure 3.164 ^{13}C NMR spectrum of compound **31**

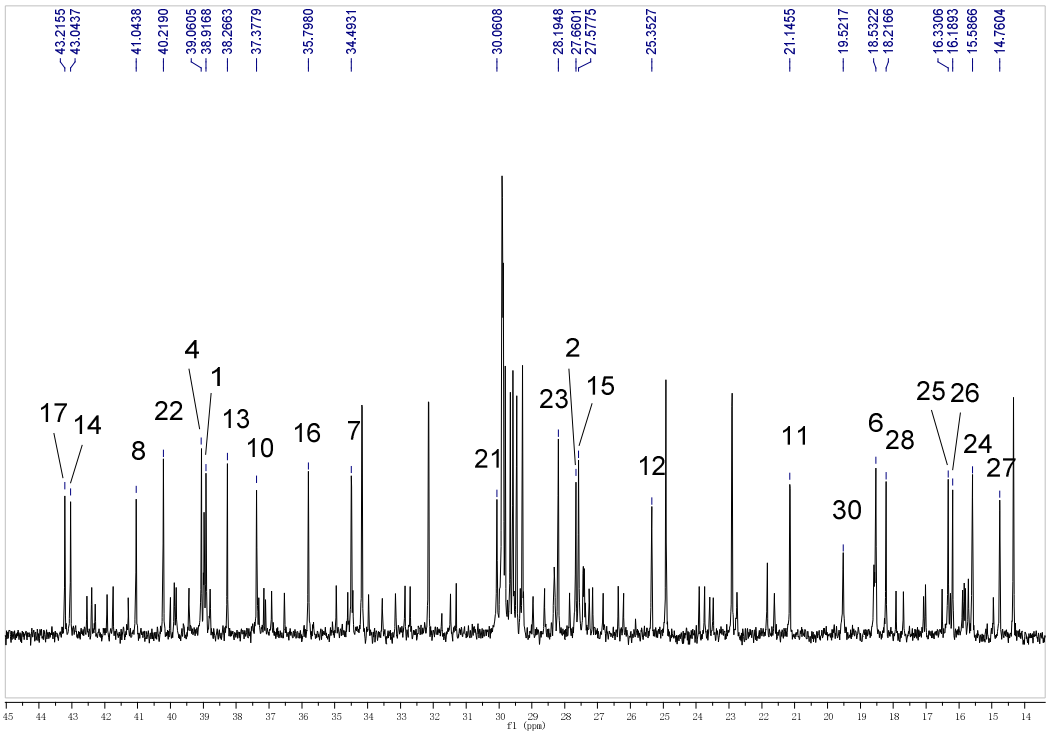

Figure 3.165 ^{13}C NMR spectrum of compound **31**

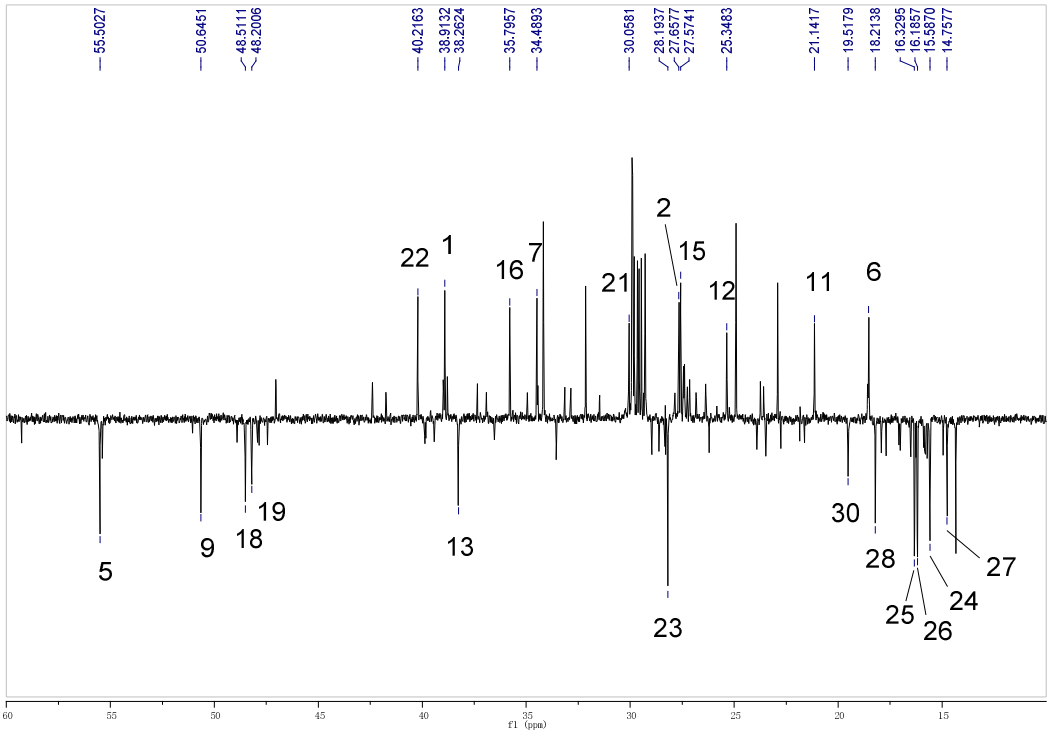

Figure 3.166 DEPT spectrum of compound **31**

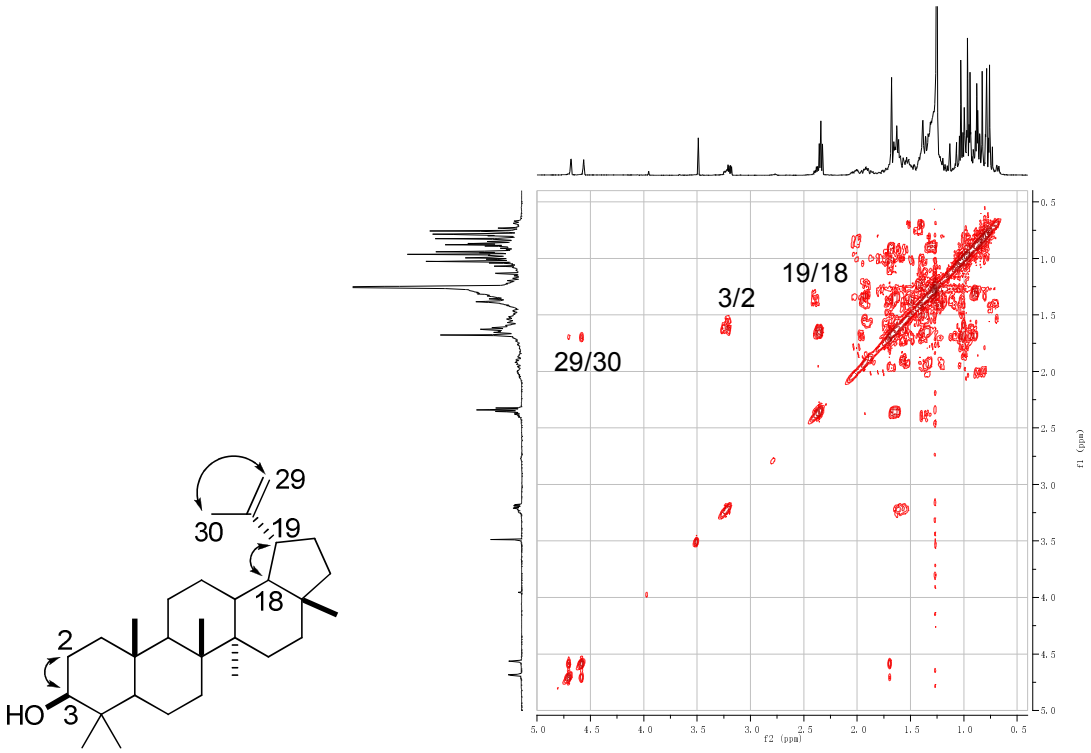

Figure 3.167 ^{1}H-^{1}H COSY spectrum of compound **31**

Table 3.33 NMR spectroscopic data of compound **31** ($CDCl_3$, 500 MHz)

	Lupeol (CD_3OD) [Aratanechemuge *et al.*, 2004]		Compound **31**	
Position	δ_C	δ_H (mult., *J* in Hz)	δ_C	δ_H (mult., *J* in Hz)
1	38.7, CH_2	1.65, m; 0.90, m	38.7, CH_2	0.90–1.92, m[a]
2	27.4, CH_2	1.67, m; 1.59, m	27.4, CH_2	0.90–1.92, m[a]
3	79.0, CH	3.20, dd (11.5, 5.03)	79.0, CH	3.19, dd (11.4, 5.0)
4	38.8, qC		38.8, qC	
5	55.3, CH	0.68, m	55.3, CH	0.68, m[a]
6	18.3, CH_2	1.50, m; 1.40, m	18.3, CH_2	0.90–1.92, m[a]
7	34.3, CH_2	1.42, m; 1.32, m	34.3, CH_2	0.90–1.92, m[a]
8	40.8, qC		40.8, qC	
9	50.4, CH	1.29, m	50.4, CH	0.90–1.92, m[a]
10	37.1, qC		37.2, qC	
11	20.9, CH_2	1.40, m; 1.20, m	20.9, CH_2	0.90–1.92, m[a]
12	25.1, CH_2	1.68, m; 1.07, m	25.1, CH_2	0.90–1.92, m[a]
13	38.1, CH	1.68, m	38.0, CH	0.90–1.92, m[a]
14	42.8, qC		42.8, qC	
15	27.4, CH_2	1.68, m; 1.00, m	27.4, CH_2	0.90–1.92, m[a]
16	35.6, CH_2	1.48, m; 1.37, m	35.6, CH_2	0.90–1.92, m[a]
17	42.9, qC		43.0, qC	
18	48.3, CH	1.37, m	48.3, CH	0.90–1.92, m[a]
19	47.9, CH	2.38, ddd (11.0, 11.0, 5.6)	48.0, CH	2.38, ddd (11.0, 11.0, 6.0)
20	150.9, qC		151.0, qC	
21	29.8, CH_2	1.92, m; 1.37, m	29.8, CH_2	0.90–1.92, m[a]
22	39.9, CH_2	1.37, m; 1.19, m	40.0, CH_2	0.90–1.92, m[a]
23	27.9, CH_3	0.97, s	28.0, CH_3	0.97, s
24	15.4, CH_3	0.76, s	15.4, CH_3	0.76, s
25	16.1, CH_3	0.83, s	16.1, CH_3	0.83, s
26	15.9, CH_3	1.03, s	16.0, CH_3	1.03, s
27	14.5, CH_3	0.94, s	14.5, CH_3	0.94, s
28	17.9, CH_3	0.79, s	18.0, CH_3	0.79, s
29	109.3, CH_2	4.67, br s; 4.54, br s	109.3, CH_2	4.69, d (2.2); 4.56, br s
30	19.3, CH_3	1.68, s	19.3, CH_3	1.68, s

[a] Overlapped signals assigned by ^1H-^1H COSY, HMBC, and HMQC spectra without designating multiplicity.

3.2.4. Taraxasterol (32, known compound)

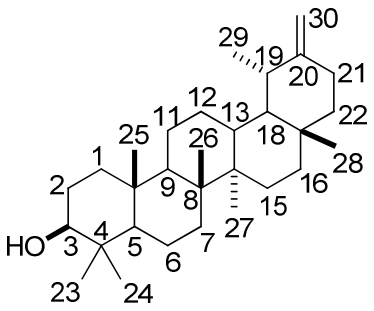

Molecular formula:	$C_{30}H_{50}O$
Molecular weight:	426.72
Amount:	7.4 mg

Compound **32** was obtained as white crystal needles. The EI-MS mass spectrum (Figure 3.168) showed a molecular ion peak at *m/z* 426 $[M]^+$. The ^{1}H NMR spectrum (Figure 3.169) of compound **32** exhibited the signal of seven tertiary methyls between 0.76 and 1.02 ppm. An oxymethine at δ_H 3.20 (dd, J = 11.7, 5.0 Hz) was observed, which was assigned to be H-3. As in **31**, a pair of geminal coupled olefinic protons [δ_H 4.62 (t, J = 2.2 Hz) and 4.60 (t, J = 2.2 Hz)] was also present in **32**. Comparison of the ^{1}H NMR data and molecular weight of compound **32** with those of **taraxasterol** [Reynolds *et al.*, 1986] indicated that both compounds were identical.

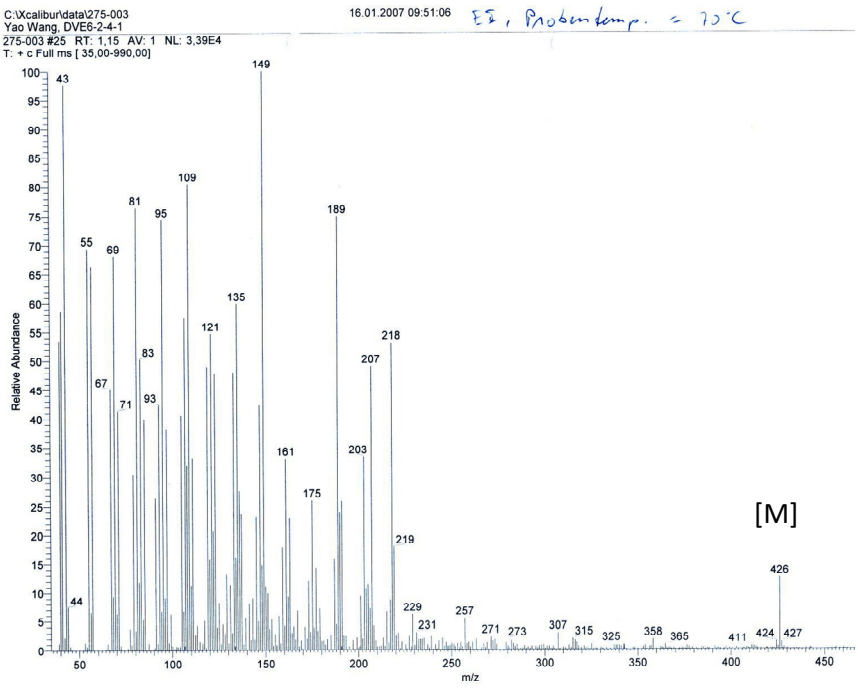

Figure 3.168 EI-MS spectrum of compound **32**

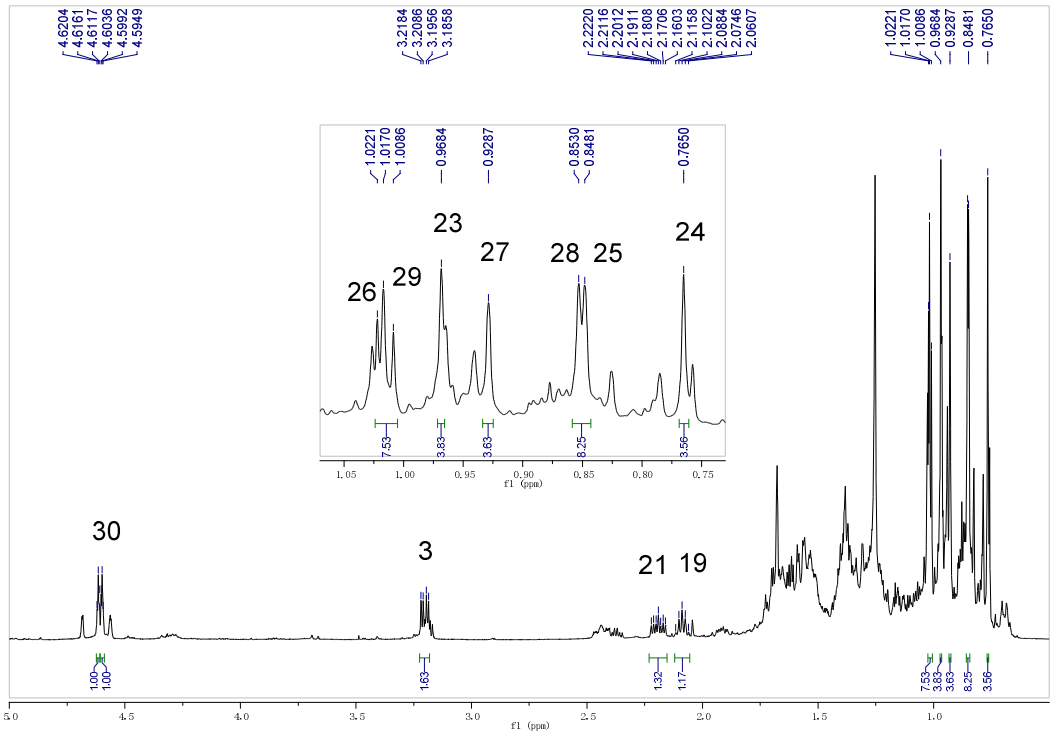

Figure 3.169 ^{1}H NMR spectrum of compound **32**

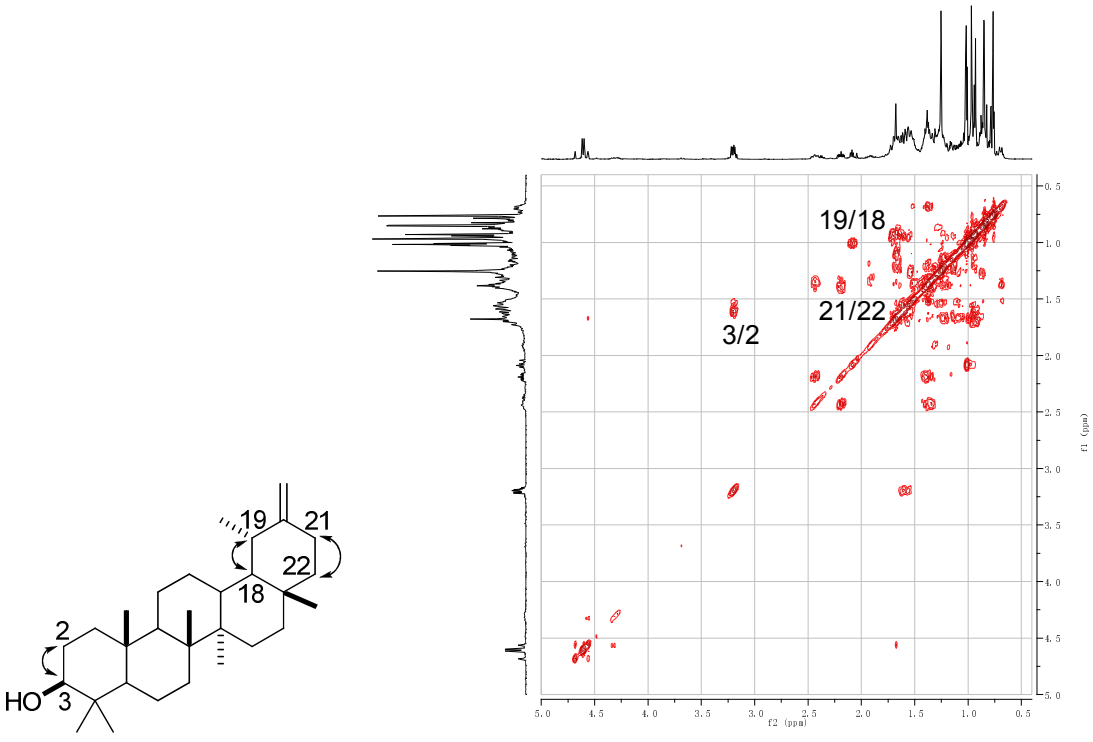

Figure 3.170 ^{1}H-^{1}H COSY spectrum of compound **32**

Table 3.34 NMR spectroscopic data of compound **32** ($CDCl_3$, 500 MHz)

	Taraxasterol [Reynolds *et al.*, 1986]	Compound **32**
Position	δ_H (mult., *J* in Hz)	δ_H (mult., *J* in Hz)
1	1.73, d; 0.95, t	0.95–1.73, m[a]
2	1.63, d; 1.59, q	0.95–1.73, m[a]
3	3.20, dd	3.20, dd (11.7, 5.0)
5	0.70	0.69, m[a]
6	1.52, d; 1.38, q	0.95–1.73, m[a]
7	1.39, m; 1.35, m	0.95–1.73, m[a]
9	1.33	0.95–1.73, m[a]
11	1.54, d; 1.28, q	0.95–1.73, m[a]
12	1.69, d; 1.10, q	0.95–1.73, m[a]
13	1.60, t	0.95–1.73, m[a]
15	1.68, t; 0.96, d	0.95–1.73, m[a]
16	1.25, d; 1.16, t	0.95–1.73, m[a]
18	0.97, t	0.95–1.73, m[a]
19	2.11, m	2.09, m[a]
21	2.45, m; 2.20, m	2.44, m[a]; 2.19, m[a]
22	1.41, m; 1.37, m	0.95–1.73, m[a]
23	0.97, s	0.97, s
24	0.76, s	0.76, s
25	0.85, s	0.85, s
26	1.02, s	1.02, s
27	0.94, s	0.93, s
28	0.86, s	0.85, s
29	1.02, d	1.01, d (4.4)
30	4.61, m	4.62, t (2.2), 4.60, t (2.2)

[a] Overlapped signals assigned by ^1H-^1H COSY, HMBC, and HMQC spectra without designating multiplicity.

3.2.5. Pseudotaraxasterol (33, known compound)

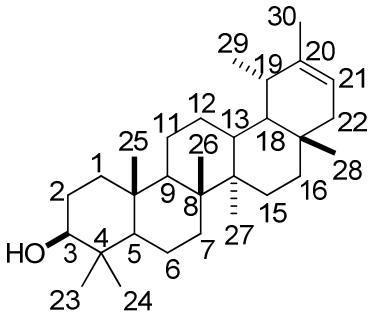

Molecular formula:	$C_{30}H_{50}O$
Molecular weight:	426.72
Amount:	39.0 mg

Compound **33** was isolated as white crystals. The GC-MS mass spectrum (Figure 3.171) showed the molecular ion peak at *m/z* 426 $[M]^+$, which was the same as compound **31** and **32**. The ^1H NMR spectrum (Figure 3.172) of compound **33** exhibited the signals of eight tertiary methyls between 0.74 and 1.63 ppm and an oxymethine at δ_H 3.20 in the aliphatic region. In the ^{13}C NMR spectrum (Figure 3.173) of **33**, 30 carbons resonances were observed including two olefinic carbons at δ_C 139.8 and 118.9. Along with the analysis of the DEPT NMR spectrum (Figure 3.175), nine methylenes, seven methines and six quaternary carbons were indicated. According to these data and through comparison with the literature [Reynolds *et al.*, 1986], compound **33** was concluded to be **pseudotaraxasterol**, which was a derivative of compound **32**.

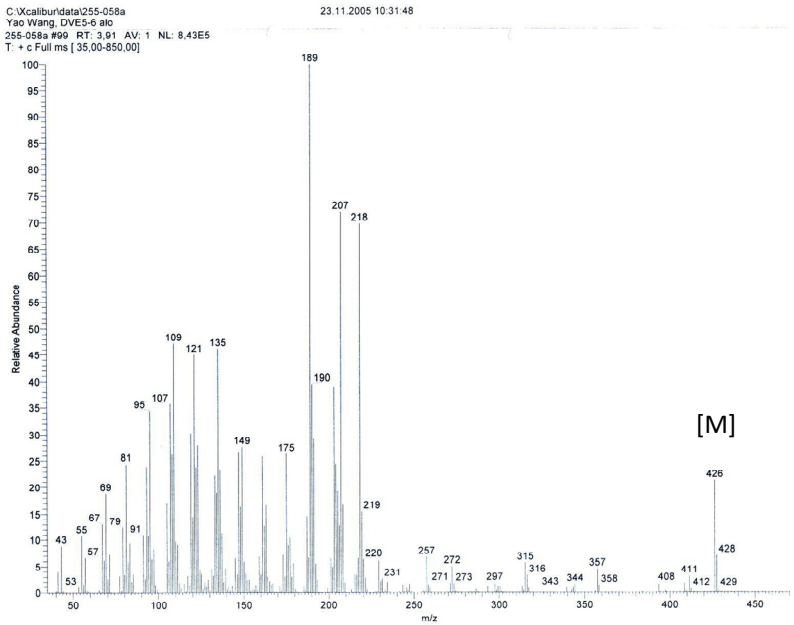

Figure 3.171 GC-MS spectrum of compound **33**

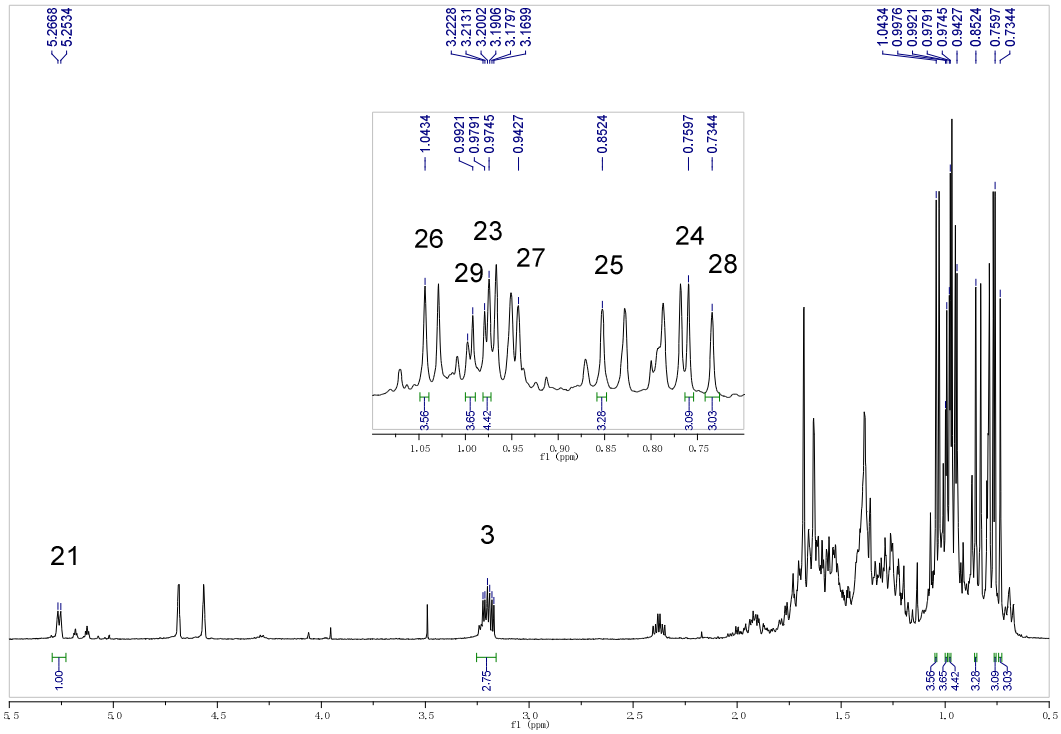

Figure 3.172 ^{1}H NMR spectrum of compound **33**

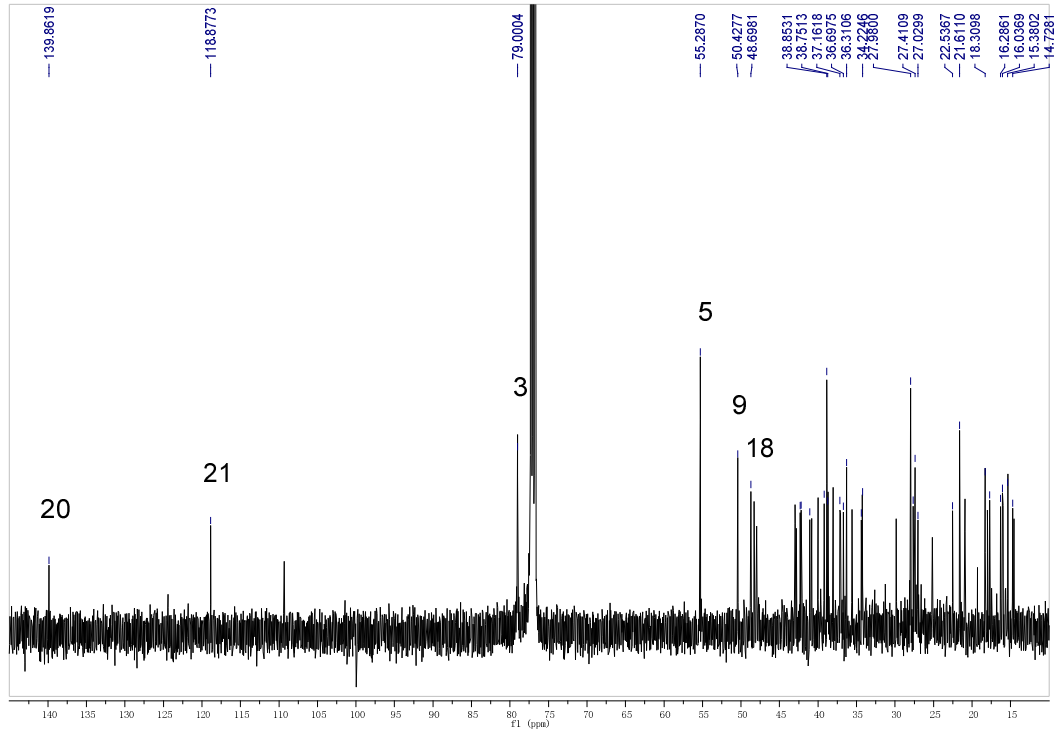

Figure 3.173 ^{13}C NMR spectrum of compound **33**

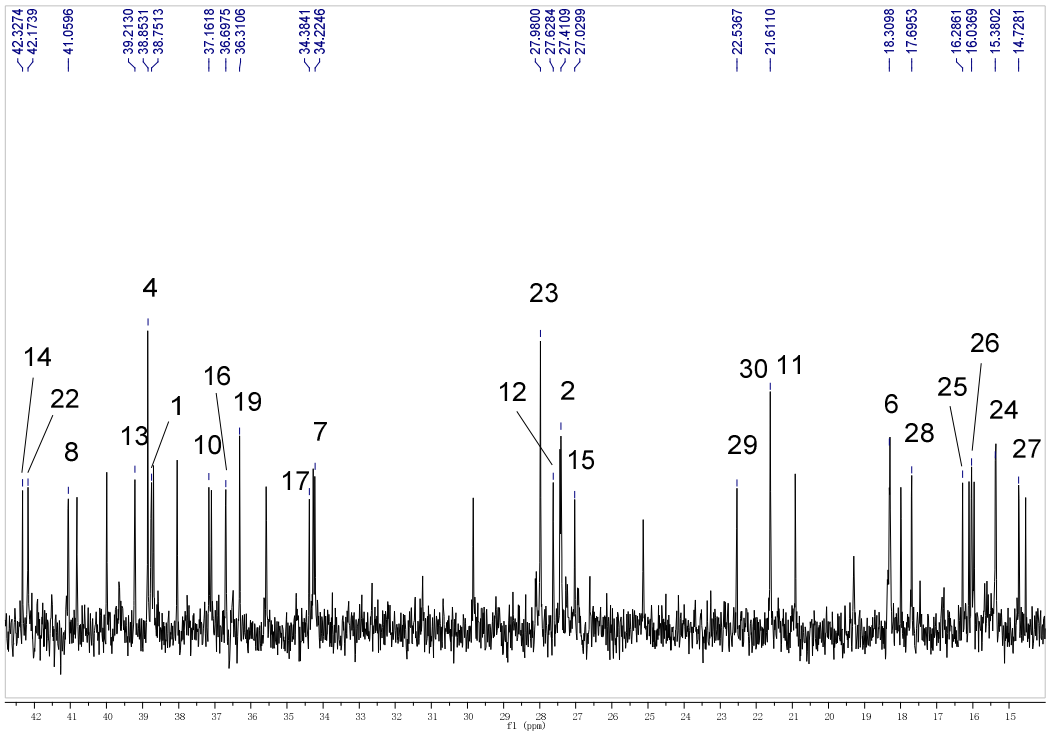

Figure 3.174 ^{13}C NMR spectrum of compound **33**

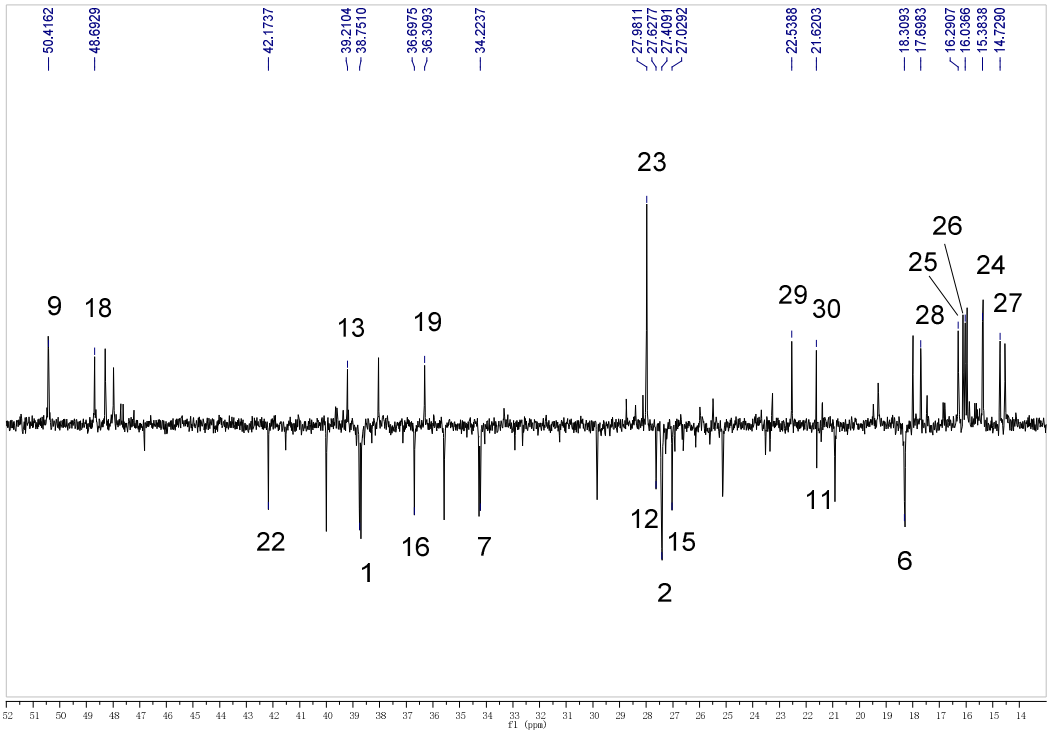

Figure 3.175 DEPT spectrum of compound **33**

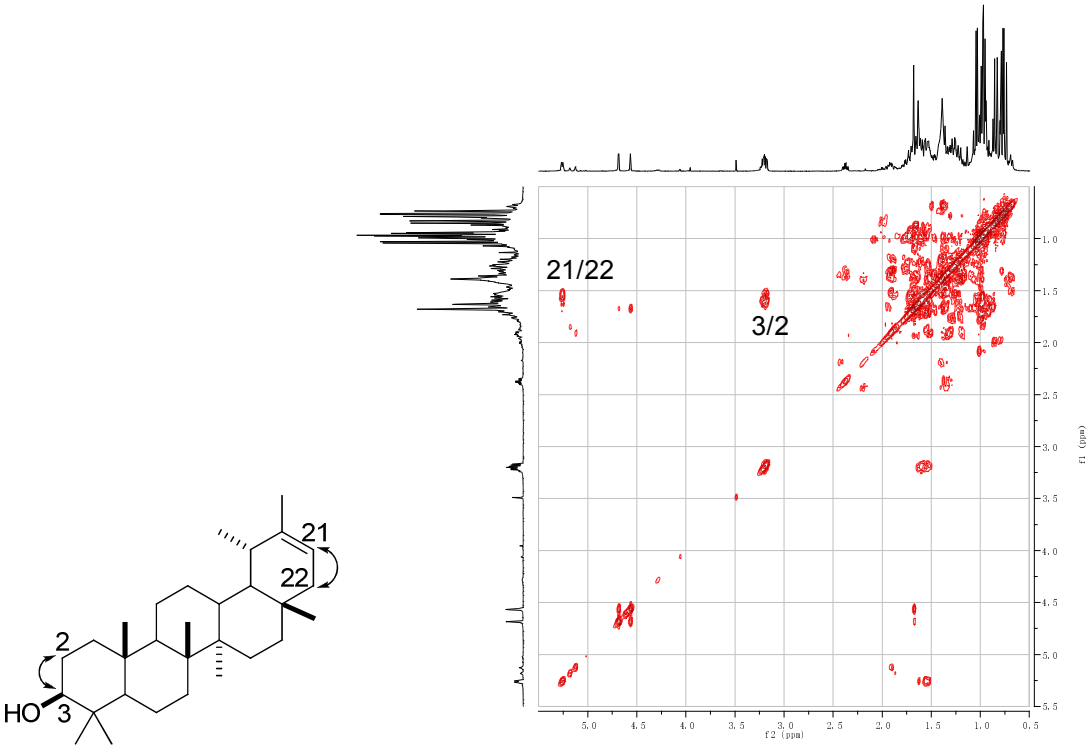

Figure 3.176 ^{1}H-^{1}H COSY spectrum of compound **33**

Table 3.35 NMR spectroscopic data of compound **33** ($CDCl_3$, 500 MHz)

	Pseudotaraxasterol [Reynolds *et al.*, 1986]		Compound **33**	
Position	δ_C	δ_H (mult., *J* in Hz)	δ_C	δ_H (mult., *J* in Hz)
1	38.8, CH_2	1.73, d; 0.95, t	38.7, CH_2	0.95–1.78, m[a]
2	27.4, CH_2	1.64, d; 1.58, q	27.4, CH_2	0.95–1.78, m[a]
3	79.0, CH	3.19, dd	79.0, CH	3.20, m[a]
4	38.9, qC		38.9, qC	
5	55.3, CH	0.70	55.3, CH	0.69, m[a]
6	18.3, CH_2	1.52, d; 1.38, q	18.3, CH_2	0.95–1.78, m[a]
7	34.3, CH_2	1.41, m; 1.37, m	34.2, CH_2	0.95–1.78, m[a]
8	41.1, qC		41.1, qC	
9	50.4, CH	1.30, d	50.4, CH	0.95–1.78, m[a]
10	37.1, qC		37.2, qC	
11	21.6, CH_2	1.58, d; 1.26, q	21.6, CH_2	0.95–1.78, m[a]
12	27.6, CH_2	1.62, d; 1.23, q	27.6, CH_2	0.95–1.78, m[a]
13	39.2, CH	1.61, t	39.2, CH	0.95–1.78, m[a]
14	42.3, qC		42.3, qC	
15	27.0, CH_2	1.78, t; 1.01, d	27.0, CH_2	0.95–1.78, m[a]
16	36.7, CH_2	1.31, d; 1.21, t	36.7, CH_2	0.95–1.78, m[a]
17	34.4, qC		34.4, qC	
18	48.7, CH	1.04, t	48.7, CH	0.95–1.78, m[a]
19	36.3, CH	1.57, m	36.3, CH	0.95–1.78, m[a]
20	139.8, qC		139.9, qC	
21	118.9, CH	5.25, d	118.9, CH	5.26, d (6.9)
22	42.2, CH_2	1.72, d; 1.56, d	42.2, CH_2	0.95–1.78, m[a]
23	28.0, CH_3	0.98, s	28.0, CH_3	0.98, d (2.2)
24	15.4, CH_3	0.78, s	15.4, CH_3	0.76, s
25	16.3, CH_3	0.86, s	16.3, CH_3	0.85, s
26	16.1, CH_3	1.04, s	16.0, CH_3	1.04, s
27	14.8, CH_3	0.95, s	14.7, CH_3	0.94, s
28	17.7, CH_3	0.73, s	17.7, CH_3	0.74, s
29	22.5, CH_3	0.99, d	22.5, CH_3	1.00, d (2.5)
30	21.7, CH_3	1.64, m	21.6, CH_3	1.63, s

[a] Overlapped signals assigned by ^1H-^1H COSY, HMBC, and HMQC spectra without designating multiplicity.

3.2.6. Ptiloepoxide (34, known compound)

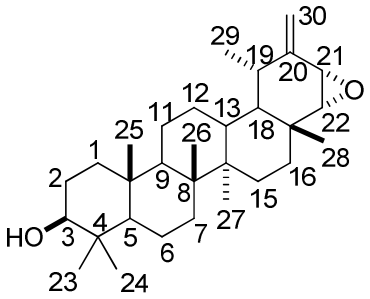

Molecular formula:	$C_{30}H_{48}O_2$
Molecular weight:	440.70
Amount:	6.3 mg

Compound **34** was isolated as a white solid. The GC-MS mass spectrum (Figure 3.177) exhibited the molecular ion peak at *m/z* 440 $[M]^+$. The ^{1}H NMR data (Figure 3.178) of compound **33** were comparable to those of compound **34** with the exception of the presence of two oxymethine protons [δ_H 3.47 (d, J = 4.4 Hz) and 2.91 (d, J = 4.4 Hz)]. The ^{13}C NMR spectrum (Figure 3.179) showed 30 carbons including seven tertiary methyls, nine methylenes, eight methines and six quaternary carbons. From the presence of two oxygenated carbons at δ_C 151.2 and 112.0, along with the molecular weight, an epoxide ring was inferred to be present. In the ^{1}H-^{1}H COSY spectrum of **34** (Figure 3.181), the proton at $\delta_{H\text{-}21}$ 3.47 gave a cross-peak with the proton at $\delta_{H\text{-}22}$ 2.91, and this correlation also comfirmed the oxygen linkage between C-21 and C-22 of the epoxy ring. In comparison with the literature data [Menichini *et al.*, 1996], compound **34** was identified as **ptiloepoxide** which was an epoxide derivative of **32**.

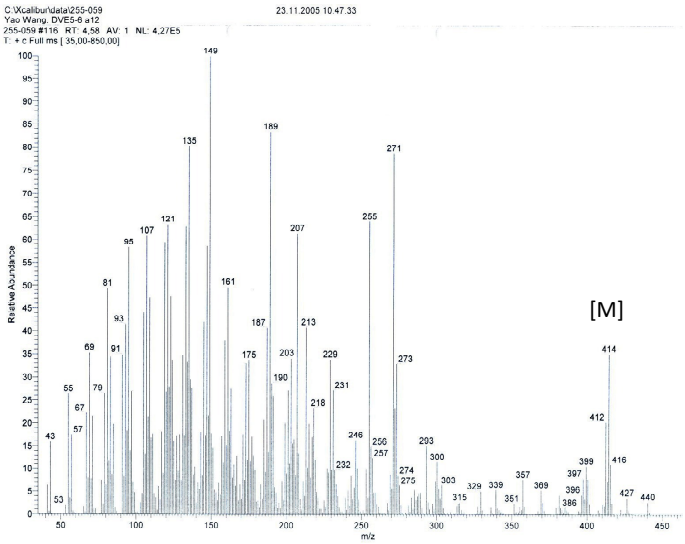

Figure 3.177 GC-MS spectrum of compound **34**

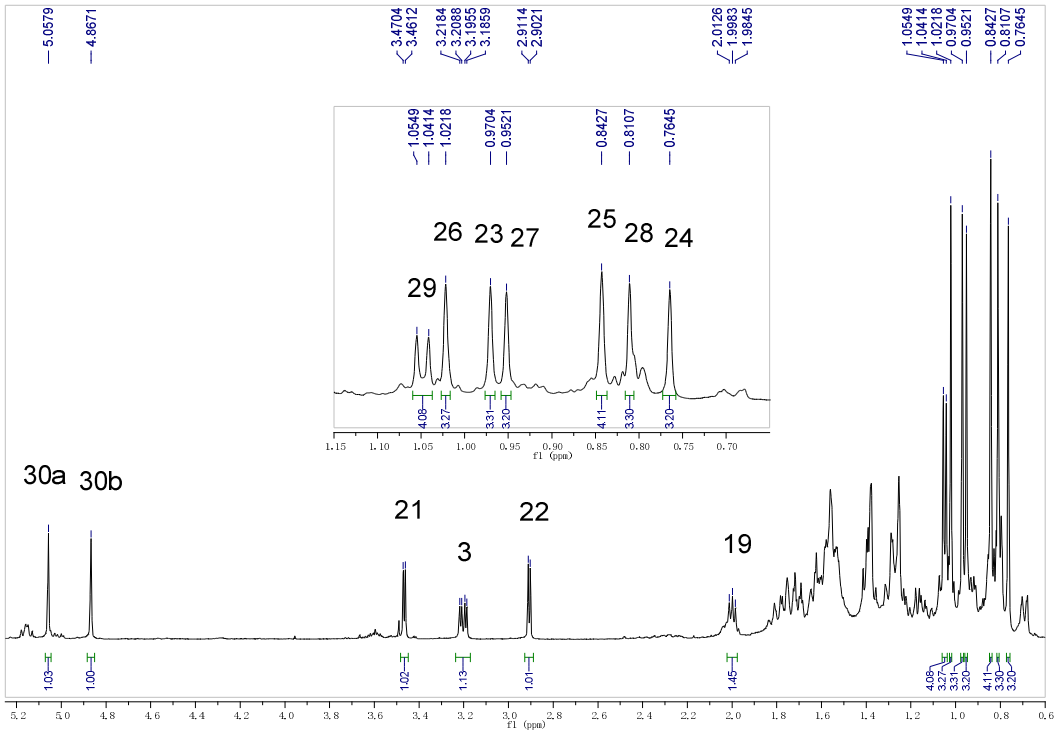

Figure 3.178 ^{1}H NMR spectrum of compound **34**

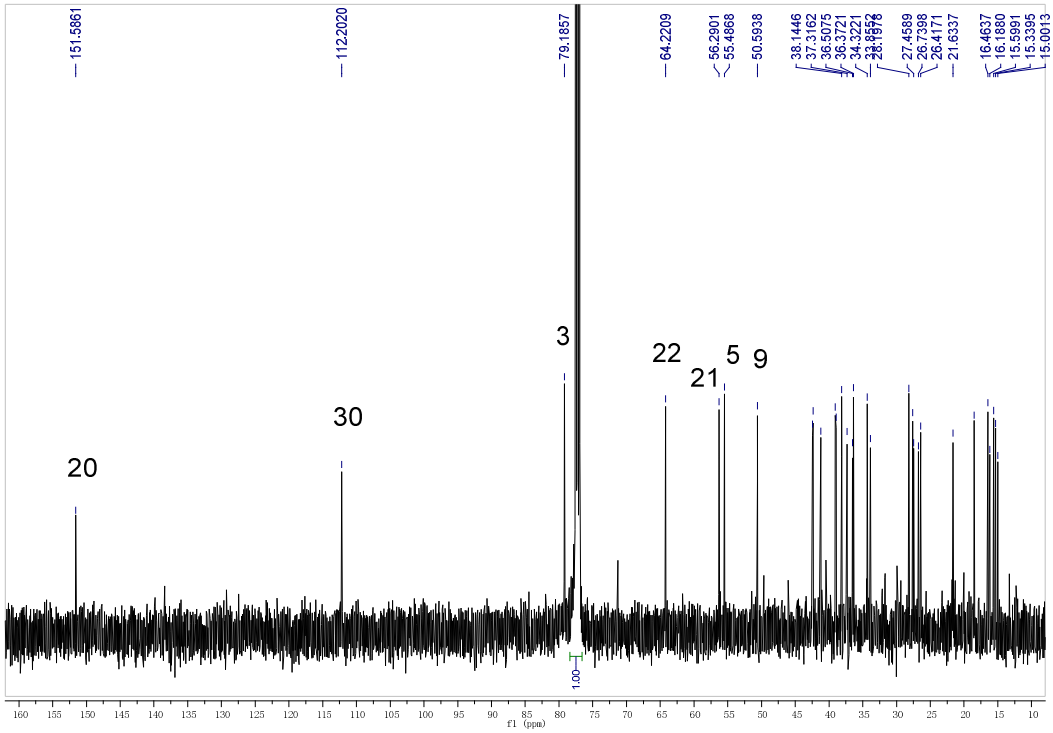

Figure 3.179 ^{13}C NMR spectrum of compound **34**

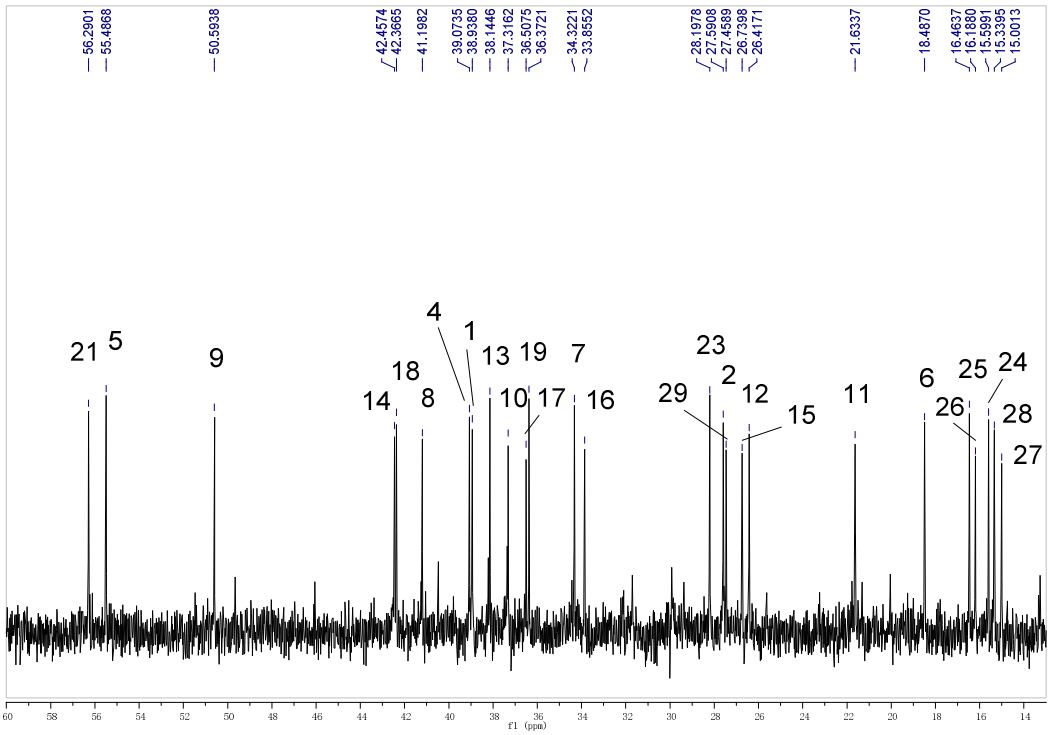

Figure 3.180 ^{13}C NMR spectrum of compound **34**

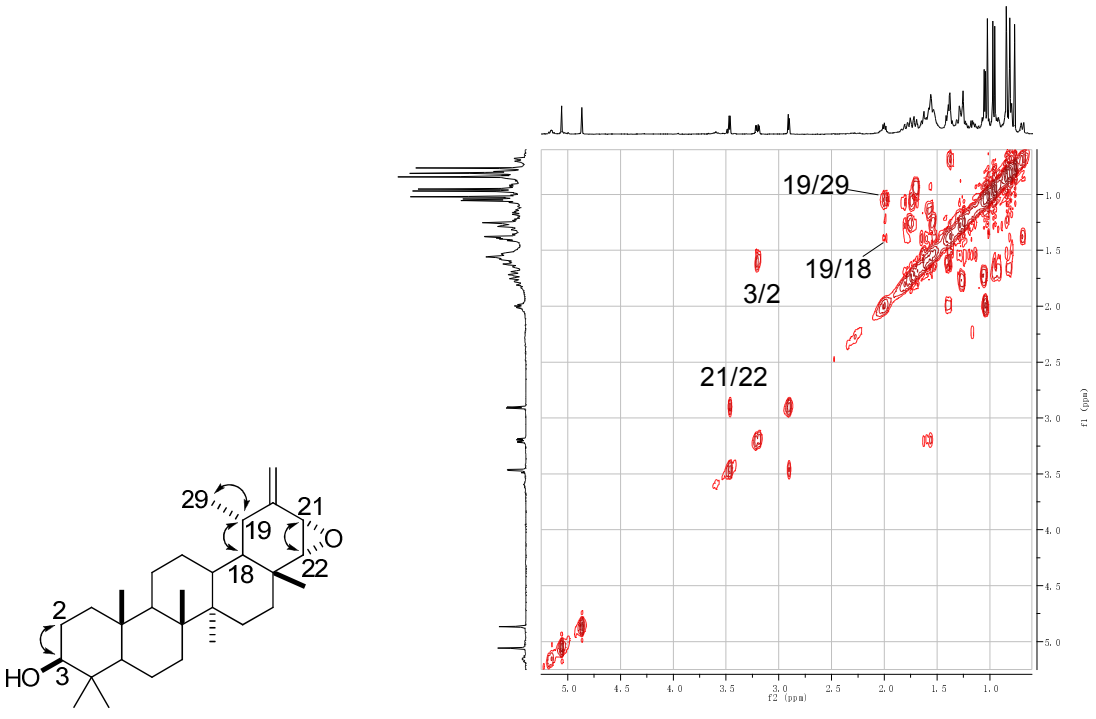

Figure 3.181 ^{1}H-^{1}H COSY spectrum of compound **34**

Table 3.36 NMR spectroscopic data of compound **34** ($CDCl_3$, 500 MHz)

	Ptiloepoxide [Menichini *et al.*, 1996]		Compound **34**	
Position	δ_C	δ_H (mult., *J* in Hz)	δ_C	δ_H (mult., *J* in Hz)
1	38.7, CH_2	1.73, 0.90	38.7, CH_2	0.90–1.75, m[a]
2	27.4, CH_2	1.65	27.4, CH_2	0.90–1.75, m[a]
3	78.9, CH	3.20, dd (10.7, 5.4)	79.0, CH	3.20, dd (11.4, 4.7)
4	38.9, qC		38.8, qC	
5	55.3, CH	0.71	55.3, CH	0.69, m[a]
6	18.3, CH_2	1.45	18.3, CH_2	0.90–1.75, m[a]
7	34.1, CH_2	1.37	34.1, CH_2	0.90–1.75, m[a]
8	41.0, qC		41.0, qC	
9	50.4, CH	1.30	50.4, CH	0.90–1.75, m[a]
10	37.1, qC		37.1, qC	
11	21.4, CH_2	1.58	21.4, CH_2	0.90–1.75, m[a]
12	26.2, CH_2	1.55	26.2, CH_2	0.90–1.75, m[a]
13	37.9, CH	1.63	37.9, CH	0.90–1.75, m[a]
14	42.2, qC		42.2, qC	
15	26.5, CH_2	1.75, 1.05	26.5, CH_2	0.90–1.75, m[a]
16	33.6, CH_2	1.72, 1.20	33.6, CH_2	0.90–1.75, m[a]
17	36.3, qC		36.3, qC	
18	42.1, CH	1.40	42.1, CH	0.90–1.75, m[a]
19	36.2, CH	2.00, q (7.9, 6.7)	36.1, CH	2.00, br t (6.9)
20	151.2, qC		151.4, qC	
21	56.1, CH	3.47, d (4.6)	56.1, CH	3.47, d (4.4)
22	64.0, CH	2.90, d (4.6)	64.0, CH	2.91, d (4.4)
23	28.0, CH_3	0.97, s	28.0, CH_3	0.97, s
24	15.4, CH_3	0.77, s	15.4, CH_3	0.76, s
25	16.2, CH_3	0.84, s	16.2, CH_3	0.84, s
26	16.0, CH_3	1.02, s	16.0, CH_3	1.02, s
27	14.8, CH_3	0.95, s	14.8, CH_3	0.95, s
28	15.1, CH_3	0.81, s	15.1, CH_3	0.81, s
29	27.2, CH_3	1.05, d (6.7)	27.2, CH_3	1.05, d (6.6)
30	112.0, CH_2	5.06, br s; 4.87, br s	112.0, CH_2	5.06, br s; 4.87, br s

[a] Overlapped signals assigned by ^1H-^1H COSY, HMBC, and HMQC spectra without designating multiplicity.

3.2.7. *β*-Sitosterol (35, known compound)

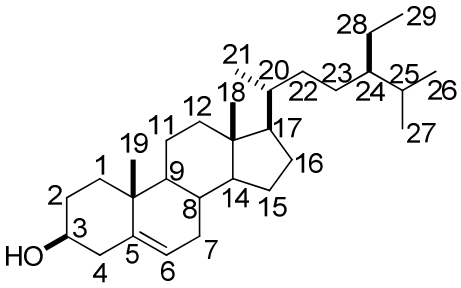

Molecular formula:	$C_{29}H_{50}O$
Molecular weight:	414.71
Amount:	7.6 mg

Compound **35** was isolated as white crystal needles. The EIMS mass spectrum (Figure 3.182) showed a molecular ion peak at *m/z* 414 $[M]^+$. The ^1H NMR spectrum (Figure 3.183) of compound **35** exhibited the signal of six methyls between δ_H 0.68 and 1.01 and an oxymethine at δ_H 3.52. Most of those methyl groups coupled with their neighbouring protons characterizing a steroide skeleton. From NMR data and EIMS compound **35** was assigned as ***β*-sitosterol** [Kojima *et al.*, 1990] which was presented in many plants.

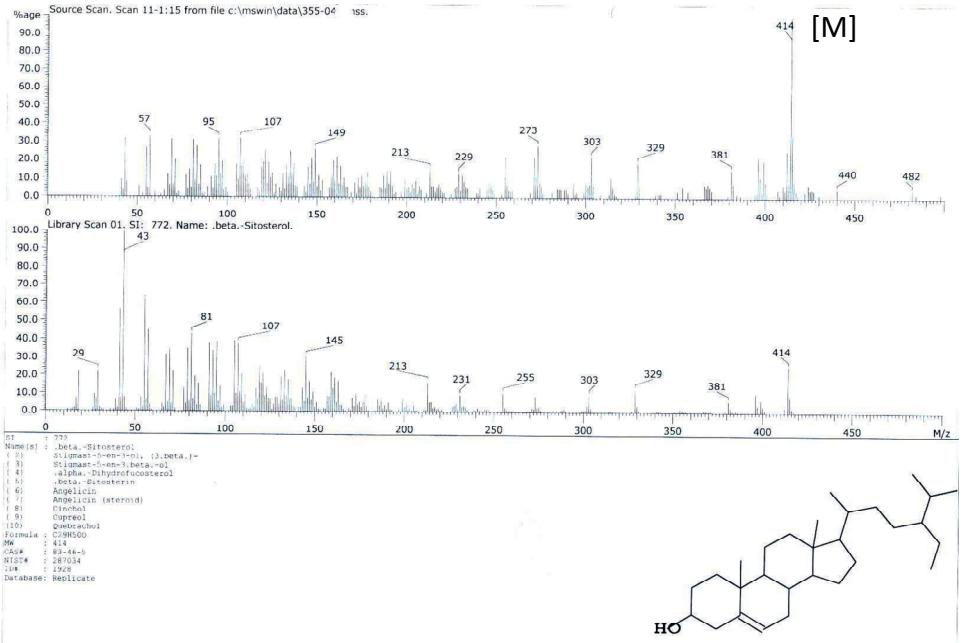

Figure 3.182 EI-MS spectrum of compound **35**

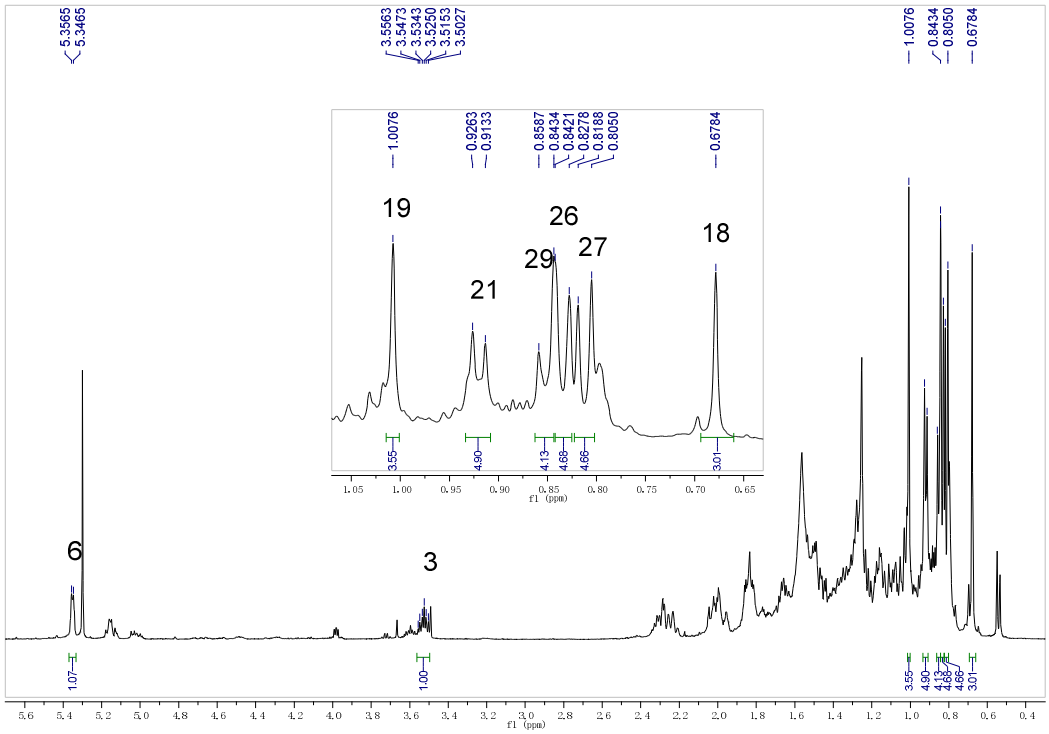

Figure 3.183 ^{1}H NMR spectrum of compound **35**

Table 3.37 NMR spectroscopic data of compound **35** ($CDCl_3$, 500 MHz)

	β-Sitosterol [Kojima *et al.*, 1990]	Compound **35**
Position	δ_H (mult., *J* in Hz)	δ_H (mult., *J* in Hz)
3	3.52, m	3.52, m[a]
6	5.35, m	5.35, d-like (5.0)
18	0.68, s	0.68, s
19	1.01, s	1.01, s
21	0.92, d (6.5)	0.92, d (6.5)
26	0.83, d (6.5)	0.83, d (7.1)
27	0.81, d (6.5)	0.81, d (6.9)
29	0.84, t (7.5)	0.85, d (7.6)

[a] Overlapped signals assigned by ^{1}H-^{1}H COSY, HMBC, and HMQC spectra without designating multiplicity.

3.2.8. Bioactivity test results for compounds isolated from *Dianthus versicolor*

Lupeol (**31**), (−)-matairesinol (**29**) and (−)-arctigenin (**30**) were evaluated for their protein kinase inhibitory profiles, which are shown in Table 3.38. Lupeol was also subjected to bioassays aimed to determine its cytotoxicity. The results are shown in Table 3.39.

Table 3.38 Selectivity profiling of three compounds isolated from *Dianthus versicolor* using 24 protein kinases

		Residual activities (% of control activity)			**IC_{50} values (g/mL)**
	Compound	(−)-matairesinol (**29**)	(−)-arctigenin (**30**)	Lupeol (**31**)	Lupeol (**31**)
Protein kinase	AKT1	100	107	96	>1E-05
	ARK5	103	101	99	>1E-05
	Aurora-A	120	104	84	>1E-05
	Aurora-B	96	97	84	>1E-05
	AXL	91	104		
	B-RAF-VE	111	105	93	>1E-05
	CDK2/CycA	100	96	81	>1E-05
	CDK4/CycD1	86	118	89	>1E-05
	CK2-alpha1	109	95	82	>1E-05
	COT	109	107	84	4.0E-06
	EGF-R	97	91	61	1.5E-06
	EPHB4	94	86	82	>1E-05
	ERBB2	108	92	94	>1E-05
	FAK	103	107	91	8.8E-06
	IGF1-R	101	89	65	1.1E-06
	INS-R	108	105	94	>1E-05
	MET	98	102	92	>1E-05
	PDGFR-beta	101	101	96	>1E-05
	PLK1	117	115	105	>1E-05
	PRK1	102	98		
	SAK	114	102	103	>1E-05
	SRC	95	77	54	1.4E-06
	TIE2	101	88	110	5.9E-06
	VEGF-R2	93	84	87	2.8E-06
	VEGF-R3			90	6.5E-06
	FLT3			89	>1E-05
	IC_{50}	86	77		

Table 3.39 Cytotoxicity results of lupeol against L5178Y

compound	**% growth inhibition**	
	3 μg/mL	**10 μg/mL**
lupeol (**31**)	86.8	84.1

3.3. Compounds isolated from the medicinal plant *Psoralea corylifolia*

3.3.1. Isobavachalcone (36, known compound)

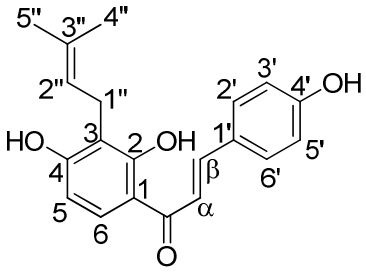

Molecular formula:	$C_{20}H_{20}O_4$
Molecular weight:	324.37
Amount:	297.0 mg

Compound **36** was isolated as yellow crystal needles. The UV spectrum (Figure 3.184) resembled that of a chalcone (λ_{max} 209 and 372 nm). The ESI mass spectrum (Figure 3.185) gave signals corresponding to a compound with the molecular weight 324. The ^{1}H NMR spectrum (Figure 3.186) of **36** showed an AA′BB′ system at δ 7.56 (dd, J = 8.5, 1.9 Hz) and 6.88 (dd, J = 8.5, 1.9 Hz), a pair of *trans*-olefinic protons at δ 7.84 (d, J = 15.4 Hz) and 7.46 (d, J = 15.4 Hz), and two *ortho*-coupled aromatic protons in the aromatic region. The presence of a prenyl group was deduced from the proton signals in the up-field region and from ^{1}H-^{1}H COSY spectrum (Figure 3.189). From these observation, along with the ^{13}C NMR (Figure 3.187) and DEPT data (Figure 3.188), compound **36** was found to be identical to **isobavachalcone** [Pistelli *et al.*, 1996].

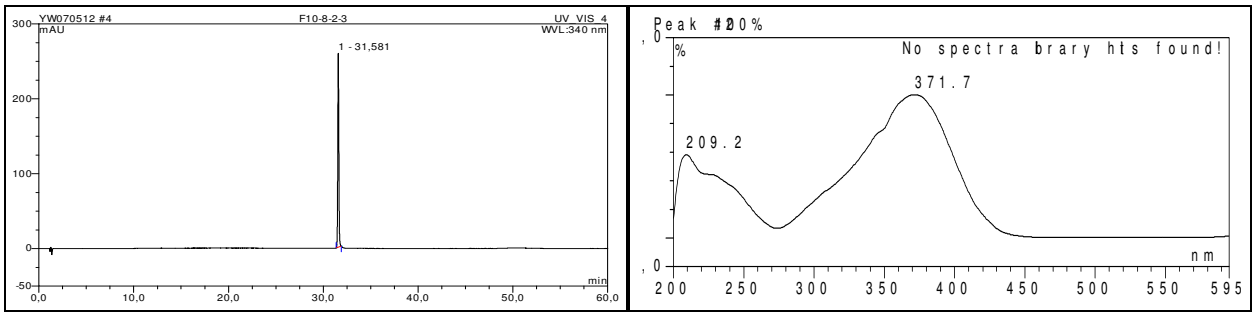

Figure 3.184 HPLC chromatogram and UV spectrum of compound **36**

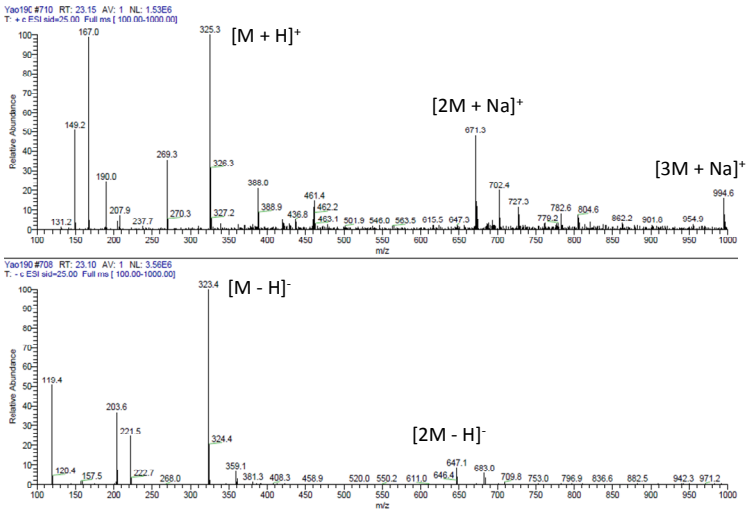

Figure 3.185 ESI-MS spectrum of compound **36**

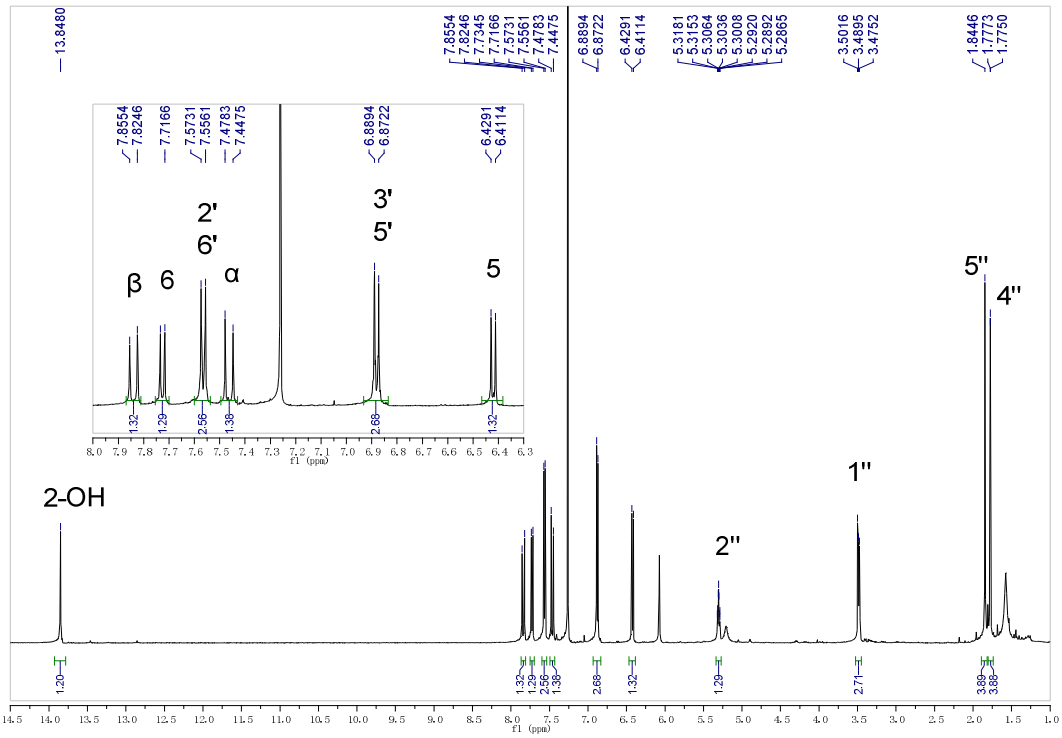

Figure 3.186 ^{1}H NMR spectrum of compound **36**

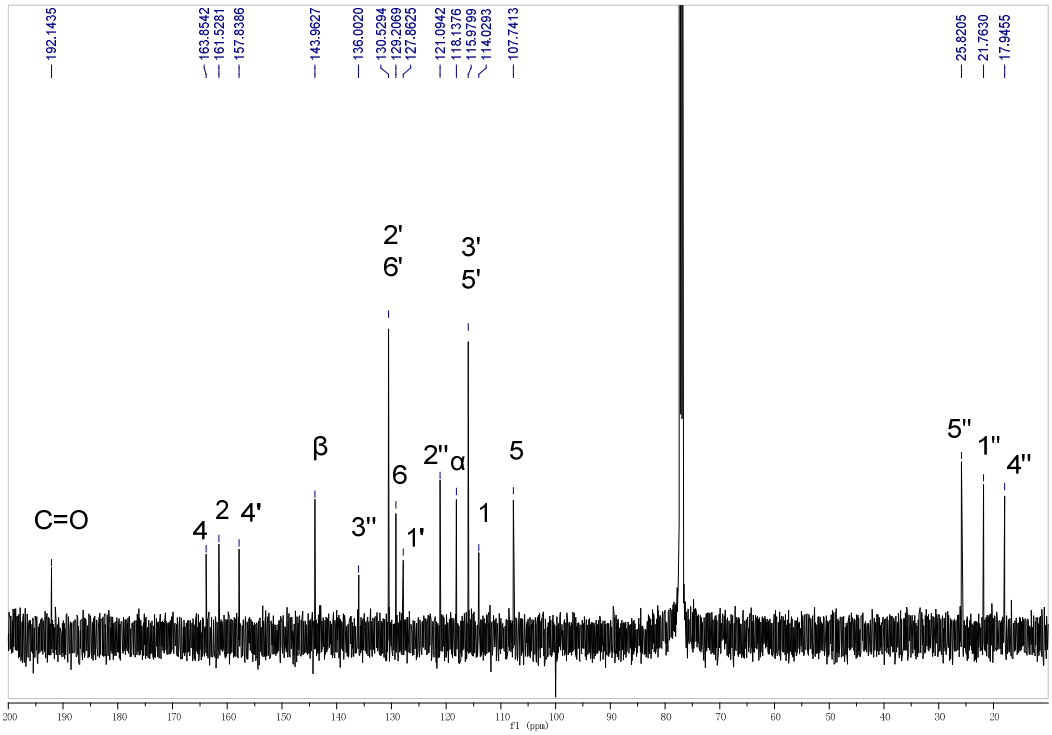

Figure 3.187 ^{13}C NMR spectrum of compound **36**

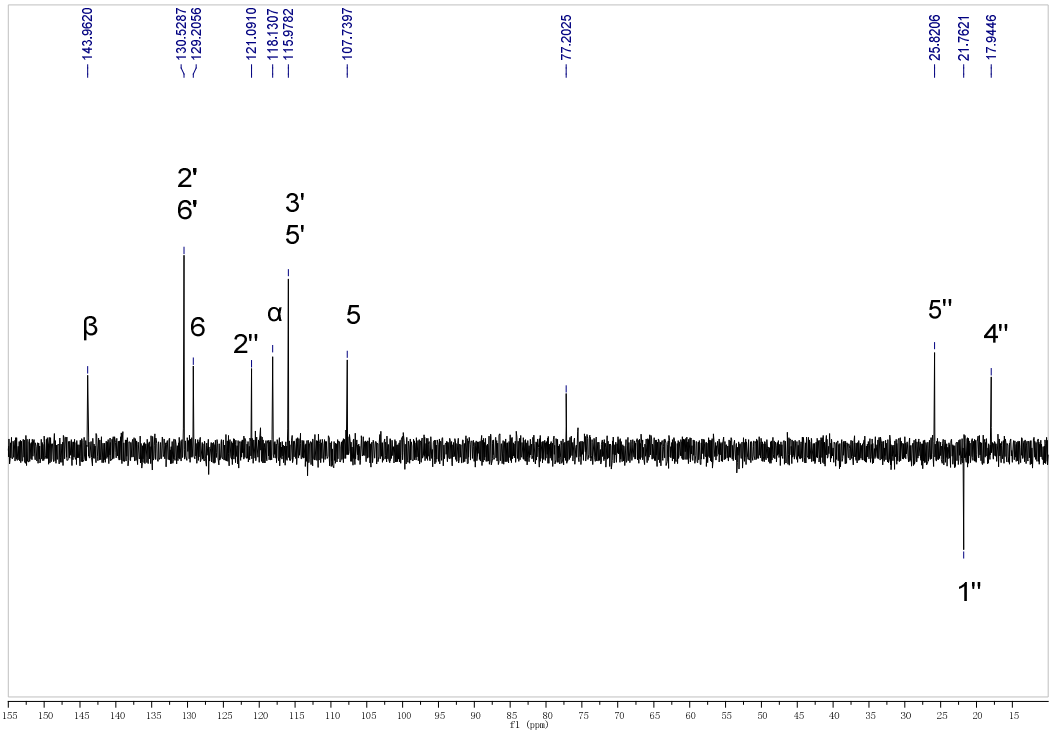

Figure 3.188 DEPT spectrum of compound **36**

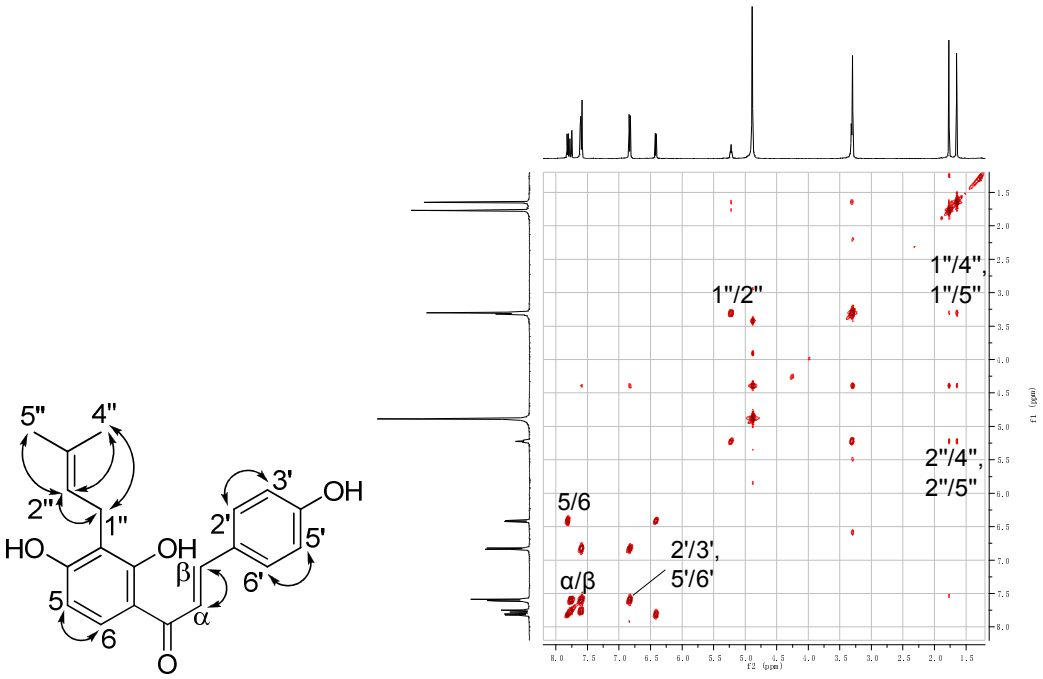

Figure 3.189 ^{1}H-^{1}H COSY spectrum of compound **36**

Table 3.40 NMR spectroscopic data of compound **36** ($CDCl_3$, 500 MHz)

	Isobavachalcone (CD_3OD) [Pistelli *et al.*, 1996]		Compound **36**	
Position	δ_C	δ_H (mult., *J* in Hz)	δ_C	δ_H (mult., *J* in Hz)
1	114.5, qC		114.0, qC	
2	163.7, qC		161.5, qC	
3	116.6, qC		114.1, qC	
4	165.0, qC		163.9, qC	
5	108.3, CH	6.43, d (8.9)	107.7, CH	6.42, d (9.1)
6	130.4, CH	7.83, d (8.9)	129.2, CH	7.72, d (9.1)
α	118.6, CH	7.61, d (15.2)	118.1, CH	7.46, d (15.4)
β	145.3, CH	7.78, d (15.4)	144.0, CH	7.84, d (15.4)
1′	127.9, qC		127.9, qC	
2′	131.7, CH	7.60, d (8.6)	130.5, CH	7.56, d (8.5)
3′	117.0, CH	6.84, d (8.6)	116.0, CH	6.88, d (8.5)
4′	161.4, qC		157.8, qC	
5′	117.0, CH	6.84, d (8.6)	116.0, CH	6.88, d (8.5)
6′	131.7, CH	7.60, d (8.6)	130.5, CH	7.56, d (8.5)
1″	22.5, CH_2	3.35, m	21.8, CH_2	3.49, d (7.3)
2″	123.6, CH	5.23, t-like m	121.1, CH	5.30, tqq (7.3, 1.6, 1.3)
3″	131.9, qC		136.0, qC	
4″	17.9, CH_3	1.66, br s	18.0, CH_3	1.78, d (1.3)
5″	25.9, CH_3	1.78, br s	25.8, CH_3	1.84, br s
C=O	193.7		192.1	
C2-OH				13.85, s

3.3.2. Isobavachromene (37, known compound)

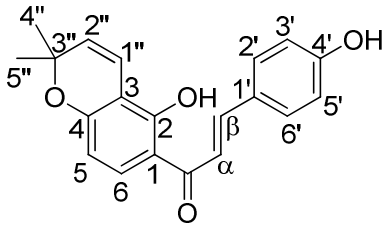

Molecular formula:	$C_{20}H_{18}O_4$
Molecular weight:	322.35
Amount:	1.8 mg

Compound **37** was isolated as a yellow solid with UV absorption maxima at λ_{max} 206, 231 and 374 nm. (Figure 3.191) The ESI mass spectrum (Figure 3.192) of **37** suggested the molecular weight as 322. The ^{1}H NMR spectrum (Figure 3.190) of **37** was closely related to that of **36**, except for the presence of *gem*-dimethylpyran ring instead of the prenyl group in **36**. This was indicated by the signals of *cis*-ethylenic protons at δ 6.76 (d, J = 10 Hz) and 5.59 (d, J = 10 Hz), and two methyl protons at δ 1.47 (s). On the basis of above evidences and comparison of the reported spectral data [Lee et al., 2005], compound **37** was identified as **isobavachromene**.

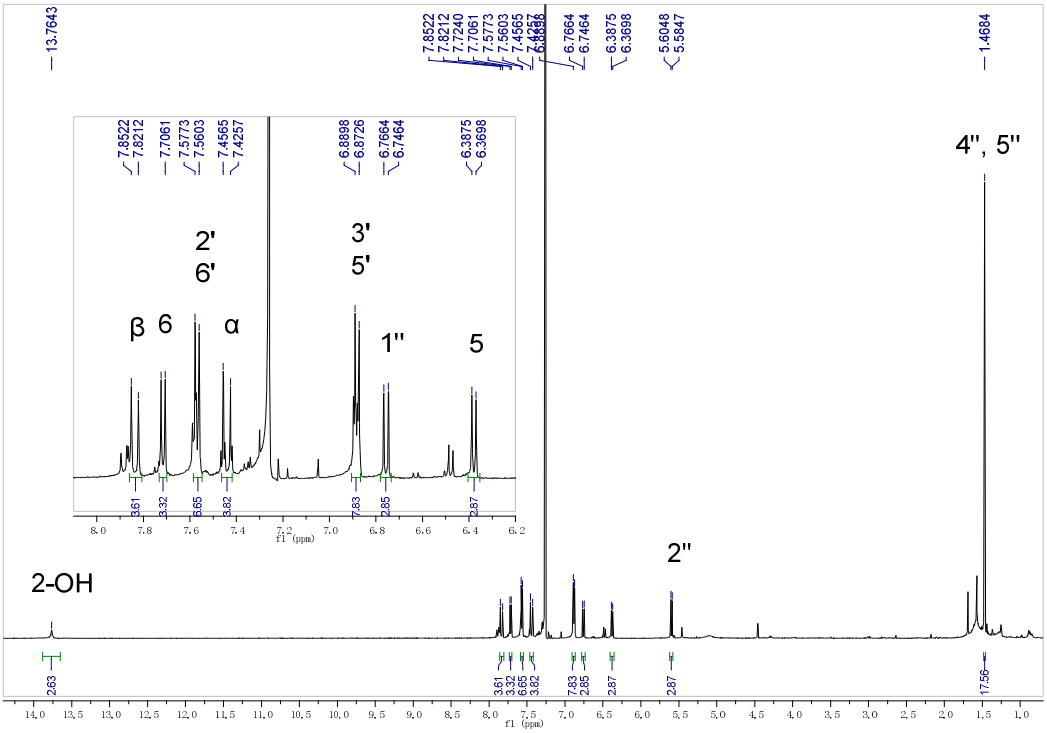

Figure 3.190 ^{1}H NMR spectrum of compound **37**

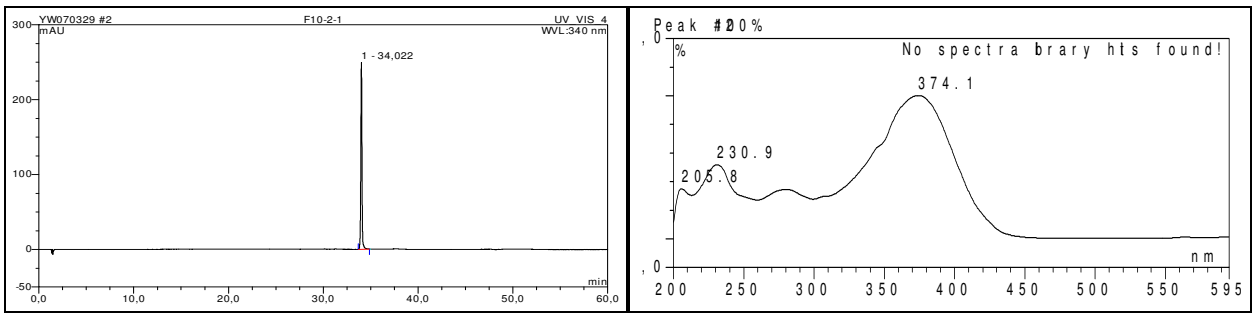

Figure 3.191 HPLC chromatogram and UV spectrum of compound **37**

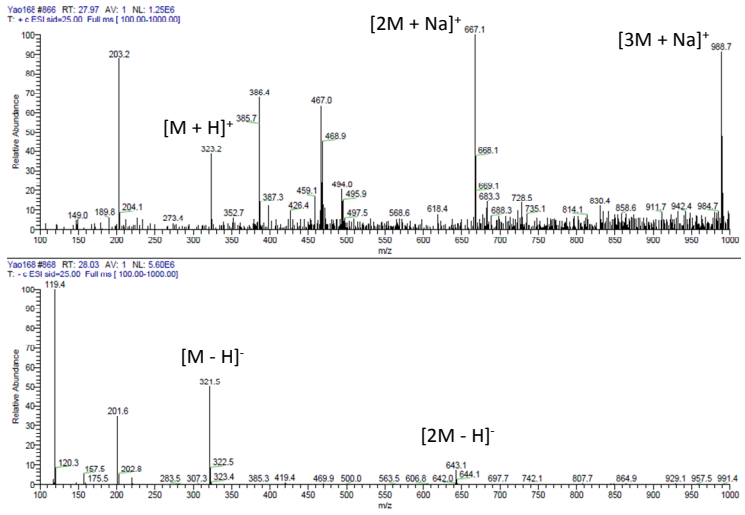

Figure 3.192 ESI-MS spectrum of compound **37**

Table 3.41 NMR spectroscopic data of compound **37** ($CDCl_3$, 500 MHz)

	Isobavachromene [Lee *et al.*, 2005]	Compound **37**
Position	δ_H (mult., *J* in Hz)	δ_H (mult., *J* in Hz)
5	6.38, d (8.8)	6.38, d (8.8)
6	7.71, d (8.8)	7.71, d (8.8)
α	7.43, d (15.2)	7.44, d (15.5)
β	7.83, d (15.2)	7.84, d (15.5)
2′	7.56, d (8.4)	7.57, d (8.5)
3′	6.88, d (8.4)	6.88, d (8.5)
5′	6.88, d (8.4)	6.88, d (8.5)
6′	7.56, d (8.4)	7.57, d (8.5)
1″	6.75, d (10.4)	6.76, d (10.1)
2″	5.59, d (10.4)	5.59, d (10.1)
4″	1.47, s	1.47, s
5″	1.47, s	1.47, s
C2′-OH		13.76, s

3.3.3. Psorachalcone A (38, known compound)

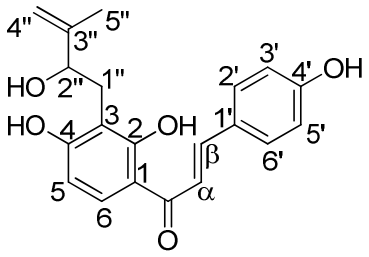

Molecular formula:	$C_{20}H_{20}O_5$
Molecular weight:	340.37
Amount:	6.8 mg

Compound **38** was obtained as a yellow amorphous solid. The ESI-MS spectrum (Figure 3.194) of **38** exhibited a negative pseudomolecular ion peak at *m/z* 339 $[M - H]^-$. It had UV absorption at λ_{max} 207, 228 and 372 nm. (Figure 3.193) The ^1H NMR spectrum (Figure 3.195) of **37** showed a chalcone skeleton as **36** and a 2-hydroxy-3-methyl-3-butenyl group. This five carbon side chain was determined by the following ^1H NMR data: one proton triplet at δ 4.38 assigned to the methine proton at 2″, three protons singlet at δ 1.82 (CH_3-5″) and two singlets at δ 4.79 and 4.70 as-signed to the exomethylene (CH_2-4″). The above NMR data together with the ESIMS data confirmed compound **38** to be **psorachalcone A** [ElSohly et al., 2001].

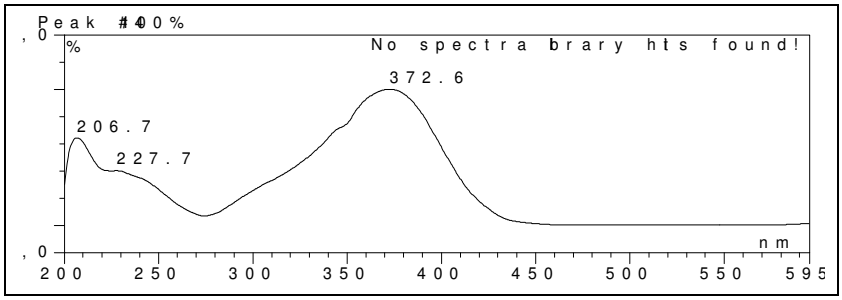

Figure 3.193 UV spectrum of compound **38**

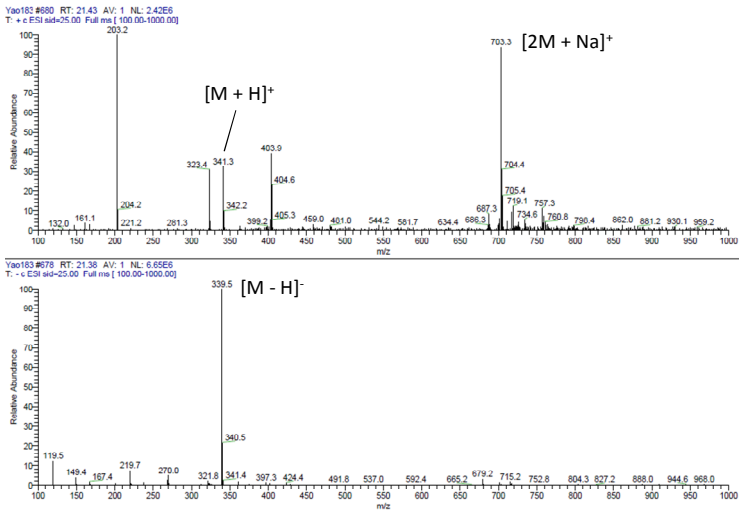

Figure 3.194 ESI-MS spectrum of compound **38**

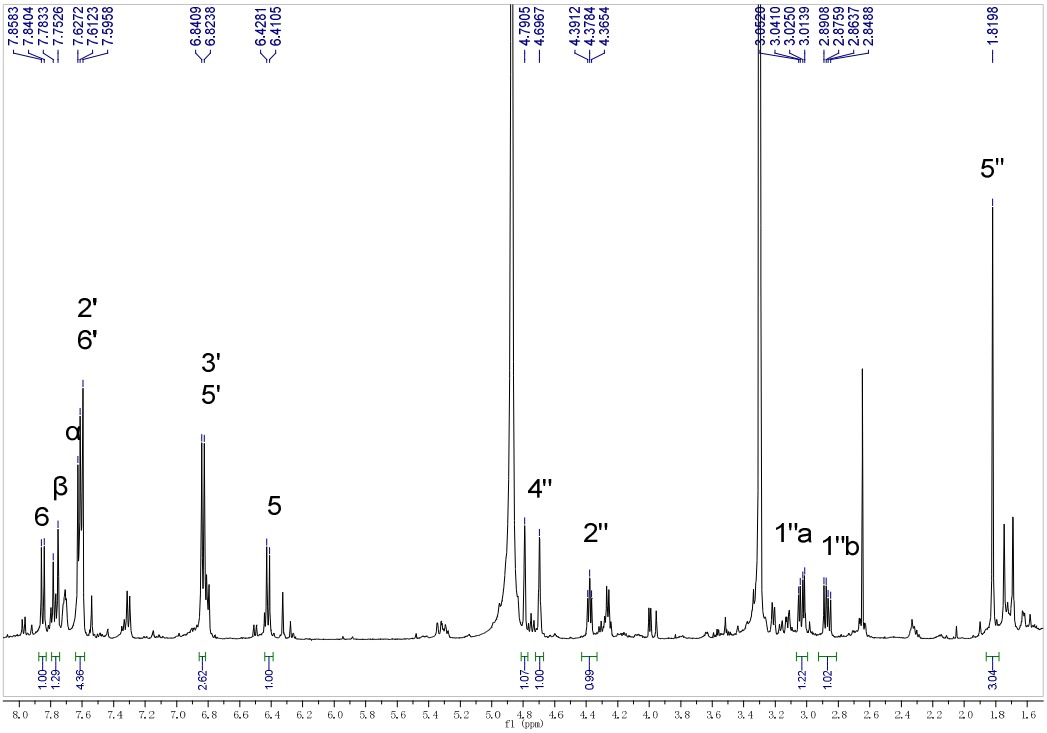

Figure 3.195 ^{1}H NMR spectrum of compound **38**

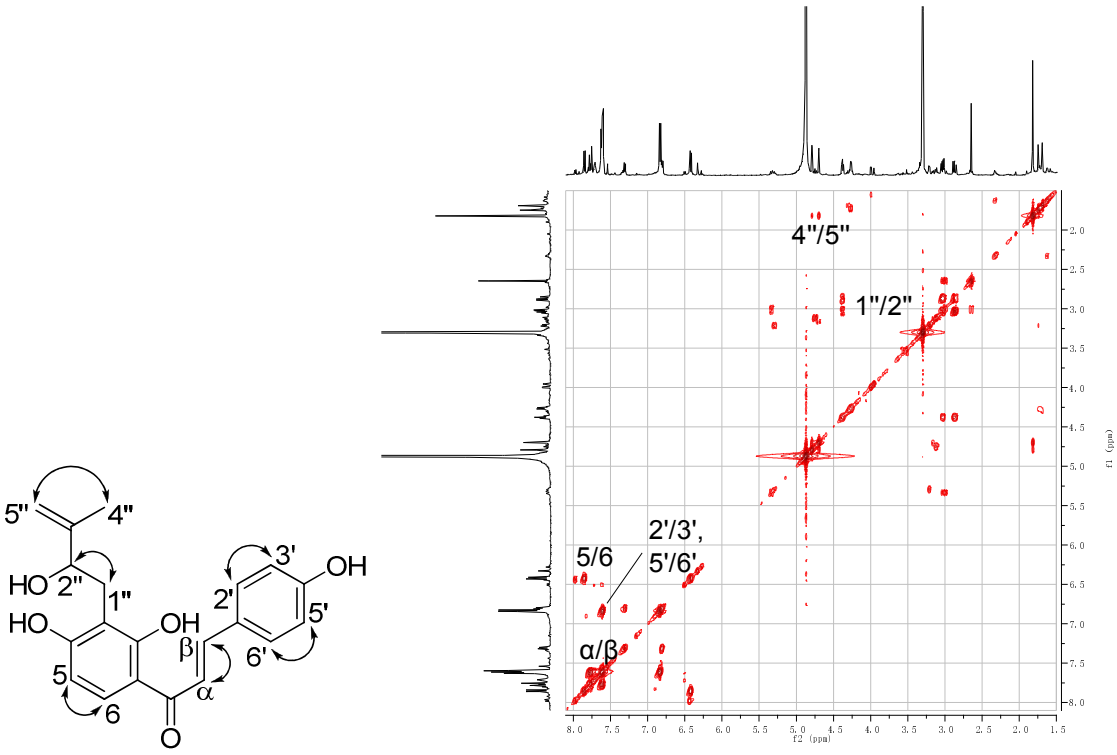

Figure 3.196 ^{1}H-^{1}H COSY spectrum of compound **38**

Table 3.42 NMR spectroscopic data of compound **38** (CD_3OD, 500 MHz)

	Psorachalcone A (DMSO-d_6) [ElSohly *et al.*, 2001]	Compound **38**
Position	δ_H (mult., *J* in Hz)	δ_H (mult., *J* in Hz)
5	6.42, d (8.9)	6.42, d (8.8)
6	8.02, d (8.9)	7.85, d (8.8)
α	7.78-7.72, m	7.61, d (15.1)
β	7.78-7.72, m	7.77, d (15.1)
2′	7.78-7.72, m	7.60, d (8.5)
3′	6.83, d (8.5)	6.83, d (8.5)
5′	6.83, d (8.5)	6.83, d (8.5)
6′	7.78-7.72, m	7.60, d (8.5)
1″	2.82, dd (13, 6.7); 2.72, dd (13, 6.9)	3.05, dd (13.6, 5.7); 2.87, dd (13.6, 7.6)
2″	4.27, t (6.9)	4.38, br t (6.6)
4″	4.62, br s; 4.58, br s	4.79, br s; 4.70, br s
5″	1.73, s	1.82, s
C2′-OH	14.06, s	

3.3.4. Bakuchalcone (39, known compound)

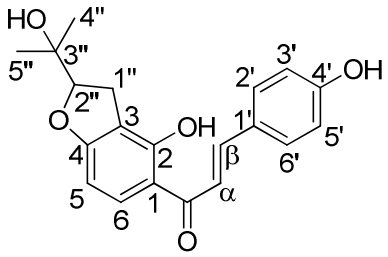

Molecular formula:	$C_{20}H_{20}O_5$
Molecular weight:	340.37
Amount:	2.3 mg

Compound **39** was obtained as pale yellow needles. In the ESI-MS spectrum (Figure 3.198), the molecular ion at 341 $[M + H]^+$ gave its molecular weight as 340. Its chalcone structure was indicated by the UV bands at 373 and 208 nm. (Figure 3.197) The ^{1}H NMR spectrum (Figure 3.199) of **39** showed two singlets at δ 1.27 and 1.23 for gem dimethyl protons. The signal at δ 3.14 showed the presence of two benzylic protons. Along with a methane proton appearing at δ 4.80, those observations were characteristic of a dihydrobenzofuran ring. The residual ^{1}H NMR resonances were closely related to those of compound **37**. Based on the above data and the comparison of the reference [Gupta et al., 1982], compound **39** was concluded to be **bakuchalcone**.

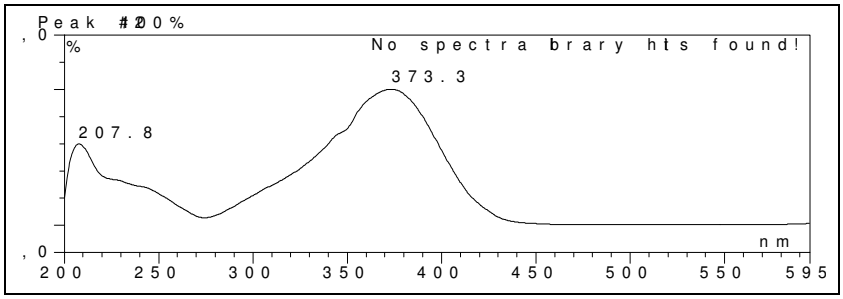

Figure 3.197 UV spectrum of compound **39**

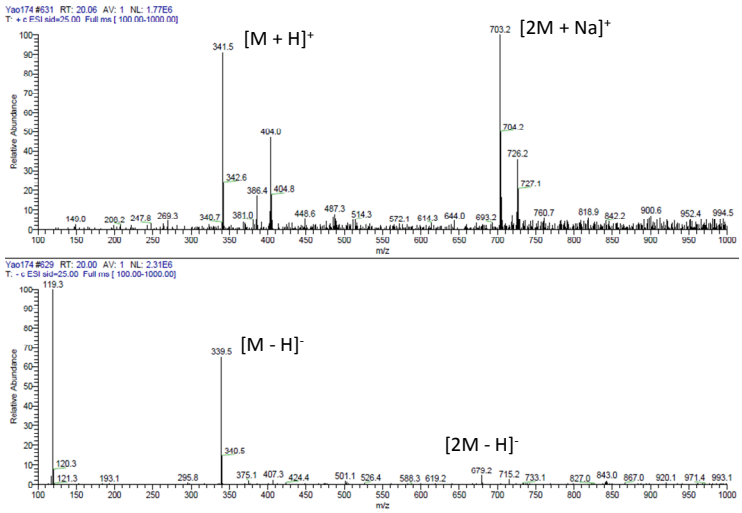

Figure 3.198 ESI-MS spectrum of compound **39**

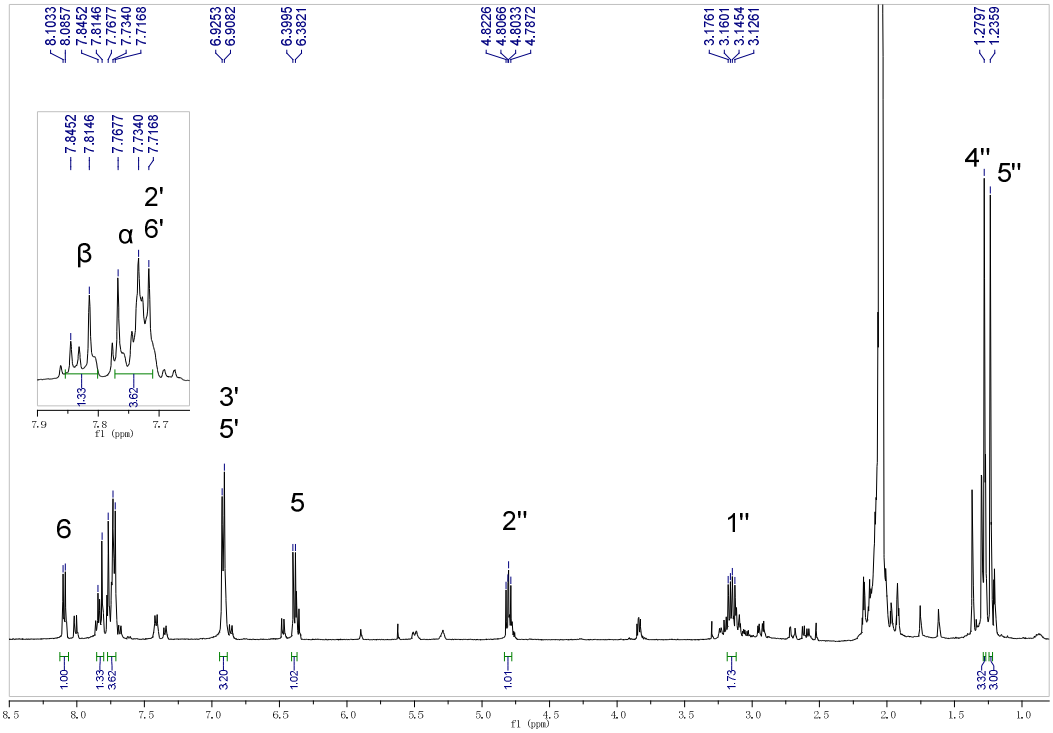

Figure 3.199 ^{1}H NMR spectrum of compound **39**

Table 3.43 NMR spectroscopic data of compound **39** (Me_2CO-d_6, 500 MHz)

	Bakuchalcone [Gupta *et al.*, 1982]	Compound **39**	
Position	δ_H (mult., *J* in Hz)	δ_C	δ_H (mult., *J* in Hz)
1		118.3, qC	
2		162.0, qC	
3		115.0, qC	
4		168.1, qC	
5	6.33, d (8)	102.3, CH	6.38, d (8.8)
6	7.98, d (8)	133.1, CH	8.08, d (8.8)
α	7.73, s	128.9, CH	7.74, d (15.4)
β	7.73, s	145.2, CH	7.82, d (15.4)
1′		127.3, qC	
2′	7.65, d (7.5)	131.8, CH	7.72, d (8.5)
3′	6.89, d (7.5)	116.8, CH	6.91, d (8.5)
4′		161.4, qC	
5′	6.89, d (7.5)	116.8, CH	6.91, d (8.5)
6′	7.65, d (7.5)	131.8, CH	7.72, d (8.5)
1″	3.1, d	27.8, CH_2	3.14, dd (17.0, 9.5)
2″	4.75, t	71.3, CH	4.80, dd (9.8, 8.2)
3″		92.5, qC	
4″	1.25, s	25.9, CH_3	1.27, s
5″	1.25, s	25.4, CH_3	1.23, s
C=O		193.0	

3.3.5. Xanthoangelol (40, known compound)

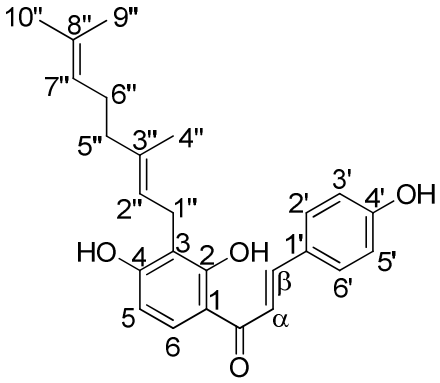

Molecular formula:	$C_{25}H_{28}O_4$
Molecular weight:	392.49
Amount:	1.8 mg

Compound **40** was isolated as yellow needles with UV absorption at λ_{max} 371 and 207 nm. (Figure 3.200) The ESI-MS spectrum (Figure 3.201) of **40** exhibited a negative pseudomolecular ion peak at *m/z* 391 $[M - H]^-$. In the ^1H NMR spectrum (Figure 3.202) of **40**, the coupling patterns and the chemical shift of the most protons were quite similar to those of **36**, except for the presence of a typical geranyl moiety 3″,8″-dimethy-octa-2″,7″-dienyl. Since compound **40** exhibited identical spectral data (UV, MS and ^1H NMR) to the literature values [Baba et al., 1990], **40** was identified as **xanthoangelol**.

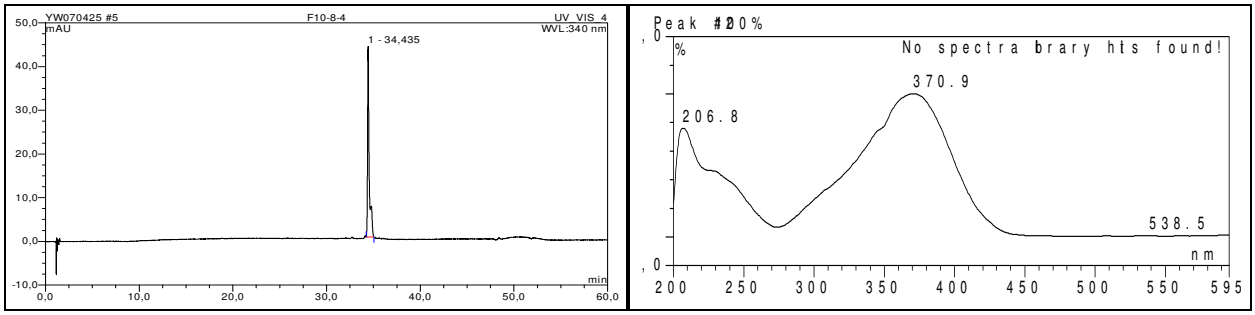

Figure 3.200 HPLC chromatogram and UV spectrum of compound **40**

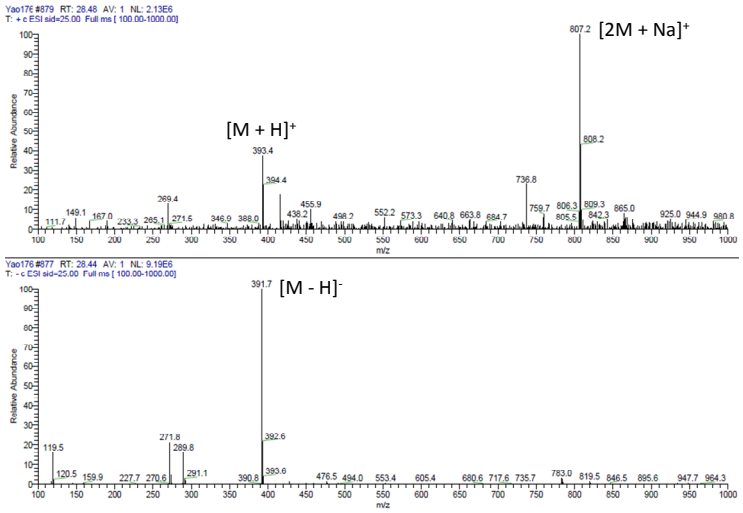

Figure 3.201 ESI-MS spectrum of compound **40**

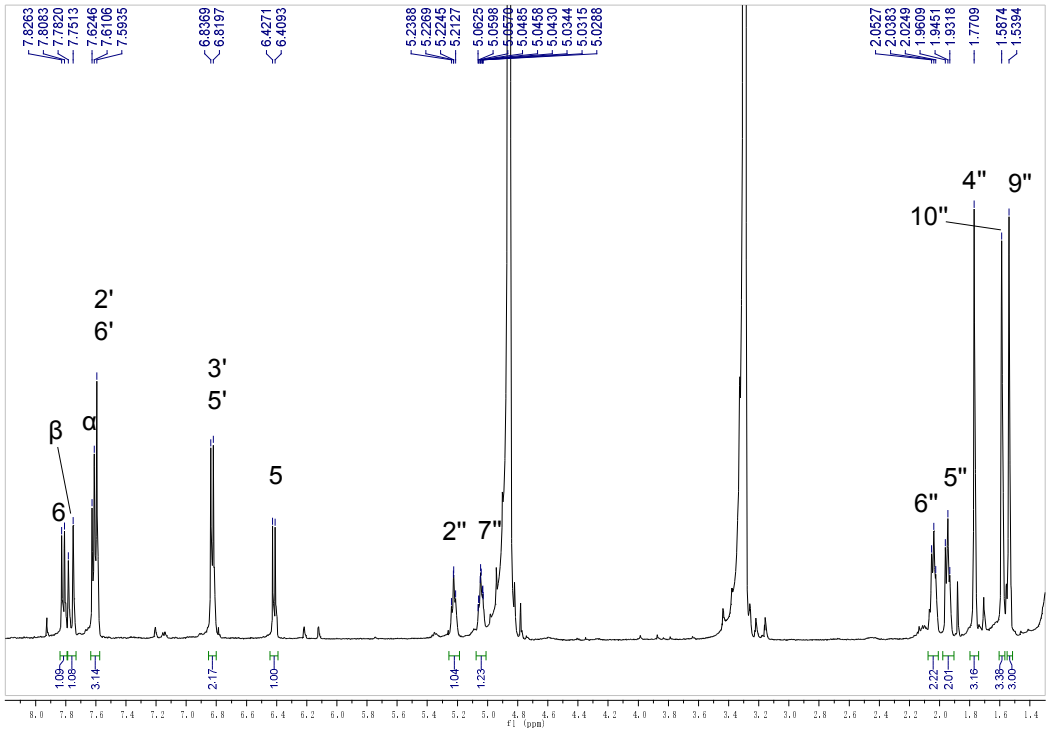

Figure 3.202 ^{1}H NMR spectrum of compound **40**

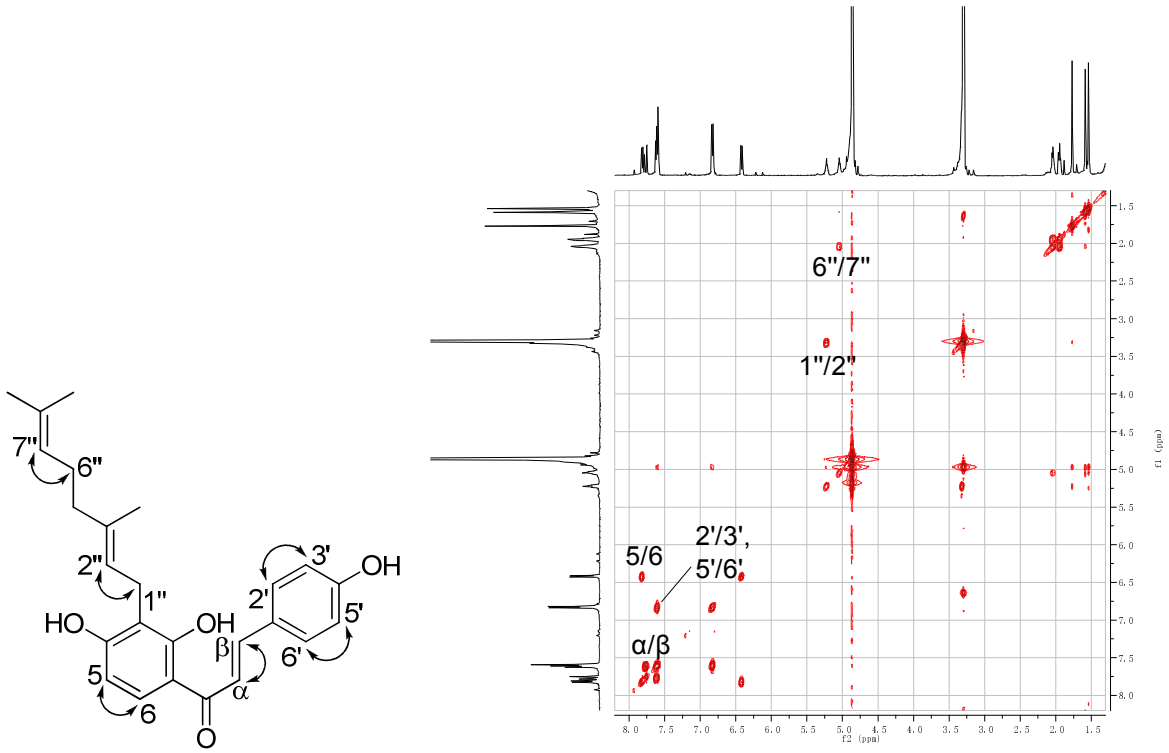

Figure 3.203 ^{1}H-^{1}H COSY spectrum of compound **40**

Table 3.44 NMR spectroscopic data of compound **40** (CD_3OD, 500 MHz)

	Xanthoangelol ($CDCl_3$) [Baba *et al.*, 1990]	Compound **40**
Position	δ_H (mult., *J* in Hz)	δ_H (mult., *J* in Hz)
5	6.47, d (8.8)	6.42, d (8.8)
6	7.66, d (8.8)	7.82, d (8.8)
α	7.43, d (15.4)	7.61, d (15.4)
β	7.81, d (15.4)	7.78, d (15.4)
2′	7.52, d (8.6)	7.60, d (8.6)
3′	6.89, d (8.6)	6.83, d (8.6)
5′	6.89, d (8.6)	6.83, d (8.6)
6′	7.52, d (8.6)	7.60, d (8.6)
1″	3.41, d (7.0)	3.32, m[a]
2″	5.30, t (7.0)	5.23, t (6.9)
4″	1.81, s	1.77, s
5″	2.01, m	1.95, t (6.9)
6″	2.05, m	2.04, dt (7.3, 6.6)
7″	5.07, m	5.05, tq (7.3, 1.3)
9″	1.57, s	1.54, s
10″	1.65, s	1.59, s

[a] Overlapped signals assigned by ^{1}H-^{1}H COSY, HMBC, and HMQC spectra without designating multiplicity.

3.3.6. Corylifol C (41, known compound)

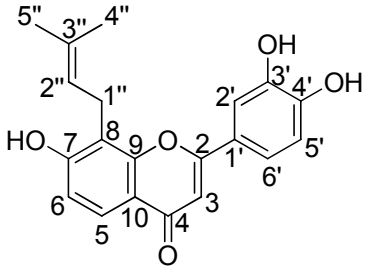

Molecular formula:	$C_{20}H_{18}O_5$
Molecular weight:	338.35
Amount:	2.4 mg

Compound **41** was obtained as a yellow amorphous powder. The molecular weight of **41** was determined as 338 by ESI-MS spectrum (Figure 3.206). It had UV absorption at λ_{max} 204, 258 and 402 nm. The ^{1}H NMR spectrum of **41** (Figure 3.204) showed an ABX system at δ_H 7.59 (d, J = 1.9 Hz), 6.94 (d, J = 8.2 Hz) and 7.40 (dd, J = 8.2, 1.9 Hz). The presence of a singlet proton signal at δ 6.61 instead of the two *trans*-olefinic proton signals of **36** was observed indicating that **41** was a flavone. Comparison of the ^{1}H NMR data with those reported for **corylifol C** [Yin et al., 2004] proved both compounds were identical.

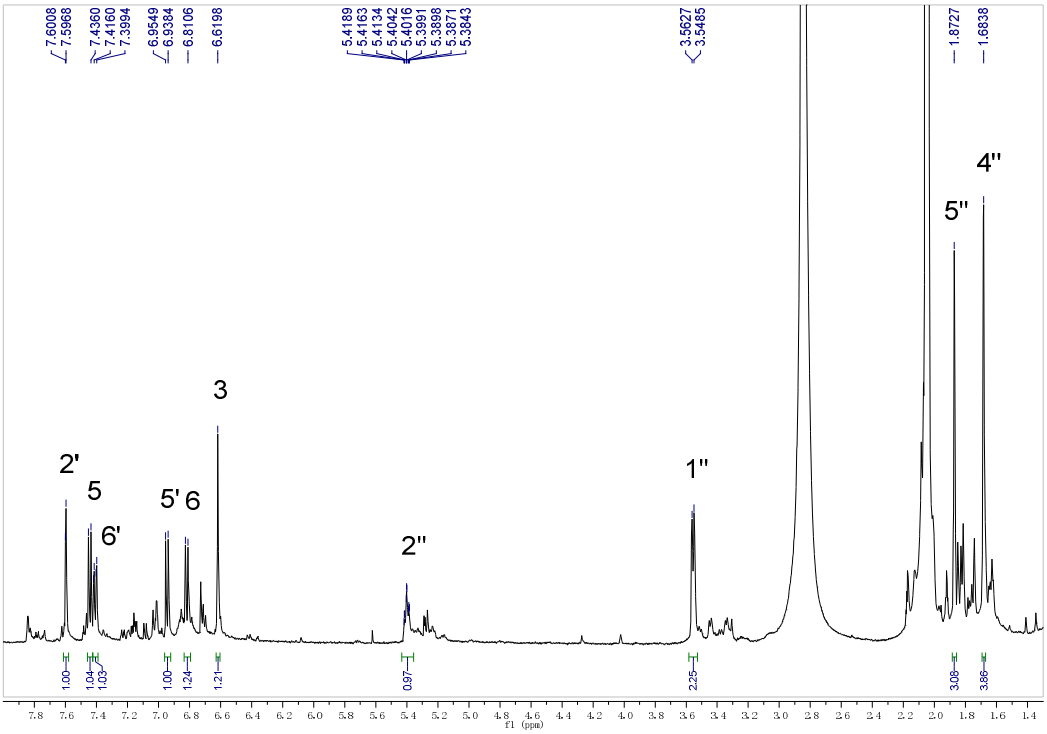

Figure 3.204 ^{1}H NMR spectrum of compound **41**

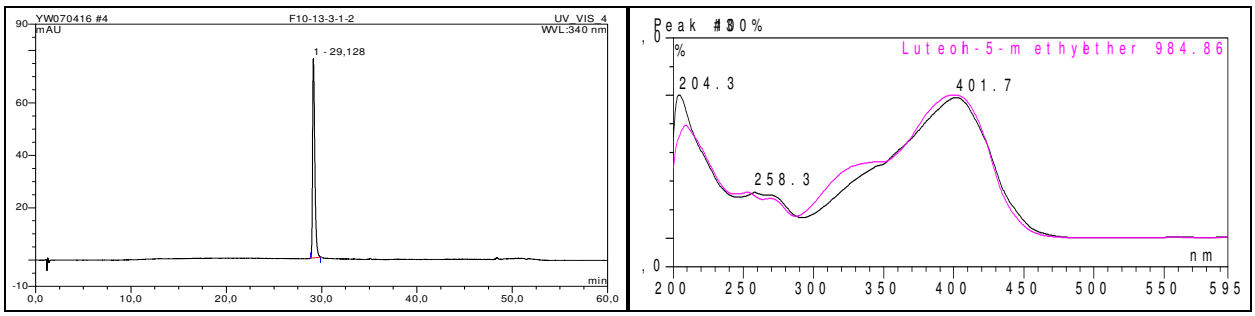

Figure 3.205 HPLC chromatogram and UV spectrum of compound **41**

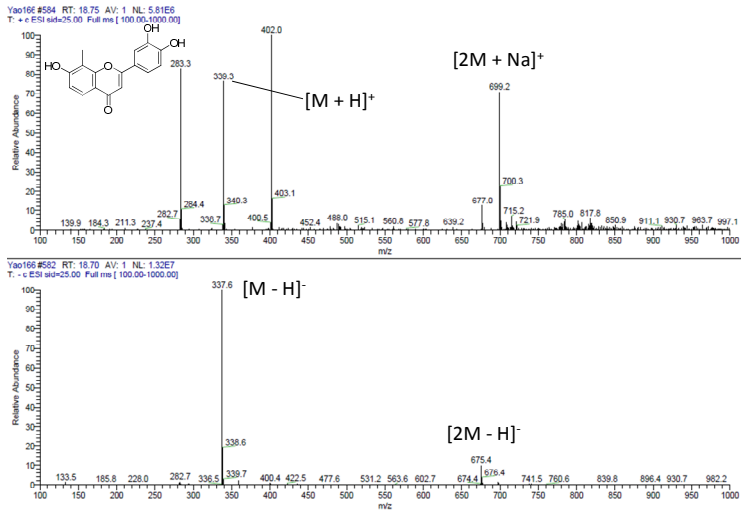

Figure 3.206 ESI-MS spectrum of compound **41**

Table 3.45 NMR spectroscopic data of compound **41** (CD_3COCD_3, 500 MHz)

	Corylifol C [Yin *et al.*, 2004]	Compound **41**
Position	δ_H (mult., *J* in Hz)	δ_H (mult., *J* in Hz)
3	6.64, s	6.61, s
5	7.46, d (8.4)	7.43, d (8.2)
6	6.82, d (8.4)	6.81, d (8.2)
2′	7.60, d (2.0)	7.59, d (1.9)
5′	6.95, d (8.3)	6.94, d (8.2)
6′	7.42, dd (8.3, 2.0)	7.40, dd (8.2, 1.9)
1″	3.56, d (7.4)	3.55, br d (6.9)
2″	5.41, t-like (7.4)	5.39, tq (7.3, 1.3)
4″	1.88, s	1.86, s
5″	1.68, s	1.67, s

3.3.7. Broussochalcone B (42, known compound)

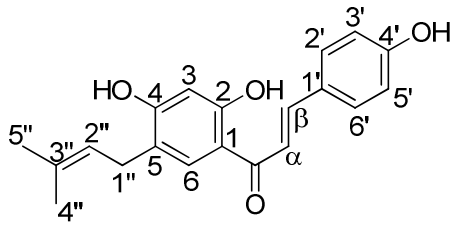

Molecular formula:	$C_{20}H_{20}O_4$
Molecular weight:	324.37
Amount:	16.5 mg

Compound **42** was isolated as a yellow amorphous powder. Its molecular weight was determined as 324 from the ESI-MS spectrum (Figure 3.208). The UV absorptions at 211, 231 and 377 nm were suggestive of a chalcone skeleton. The ^{1}H NMR spectrum of **42** (Figure 3.209) displayed signals for four aromatic protons which form an AA′BB′ system at δ 7.59 (d, J = 8.5 Hz) and 6.84 (d, J = 8.5 Hz). In its ^{1}H NMR, two doublet at δ 7.75 and 7.54 (each, d, J = 15.5 Hz) were assigned to the AB system of a chalcone, and the presence of a prenyl group was observed in the up-field region. The remaining two aromatic proton singlets at δ 7.72 and 6.29 were located in ring A. From these observation, along with the analysis of the ^{13}C (Figure 3.210) and DEPT (Figure 3.211) NMR data, compound **42** appeared to be identical with **broussochalcone B** [Yin et al., 2004].

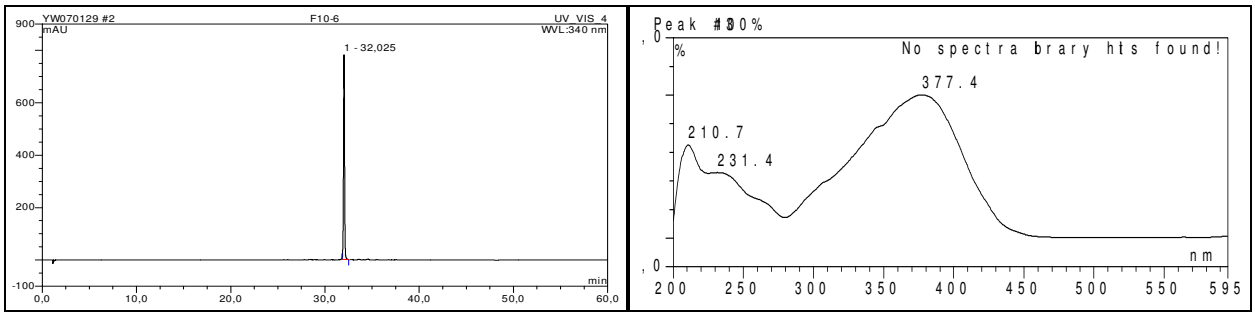

Figure 3.207 HPLC chromatogram and UV spectrum of compound **42**

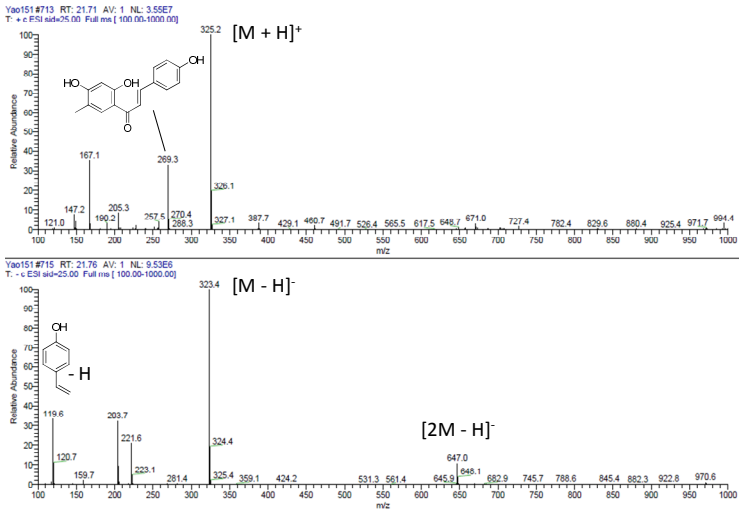

Figure 3.208 ESI-MS spectrum of compound **42**

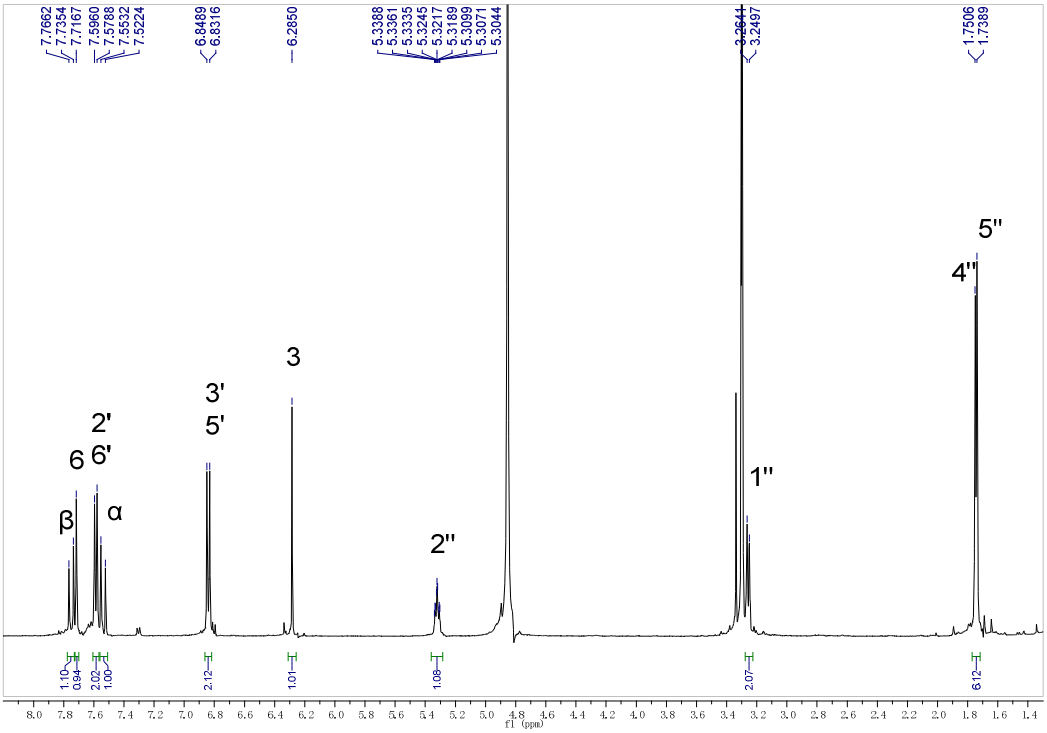

Figure 3.209 ^{1}H NMR spectrum of compound **42**

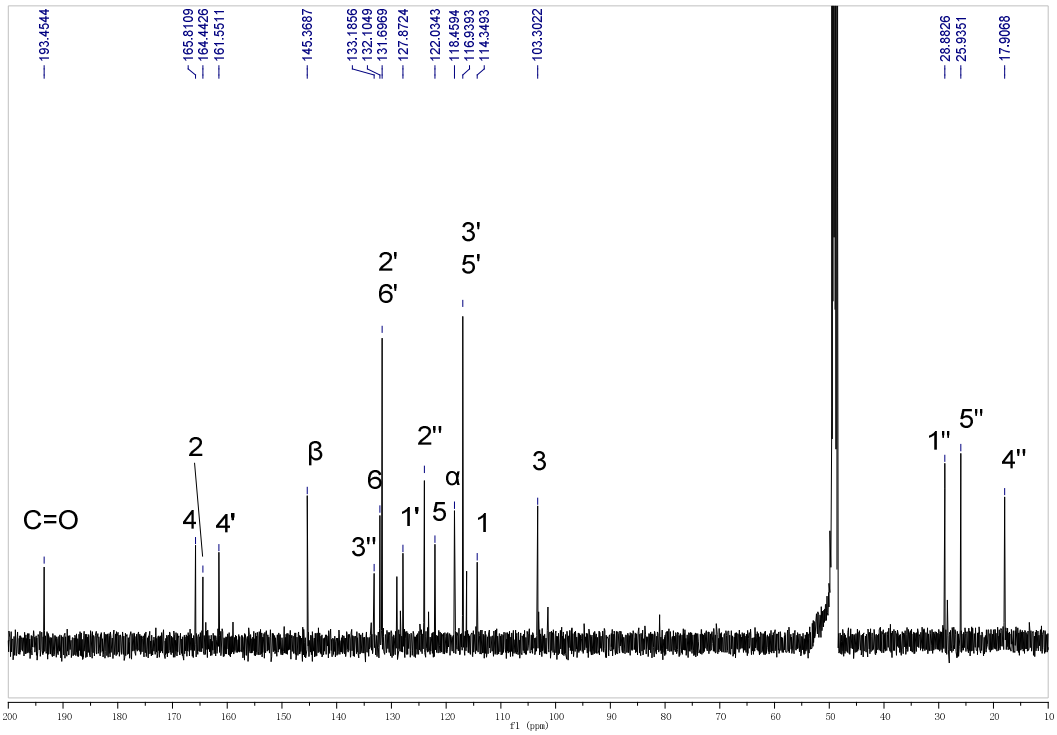

Figure 3.210 ^{13}C NMR spectrum of compound **42**

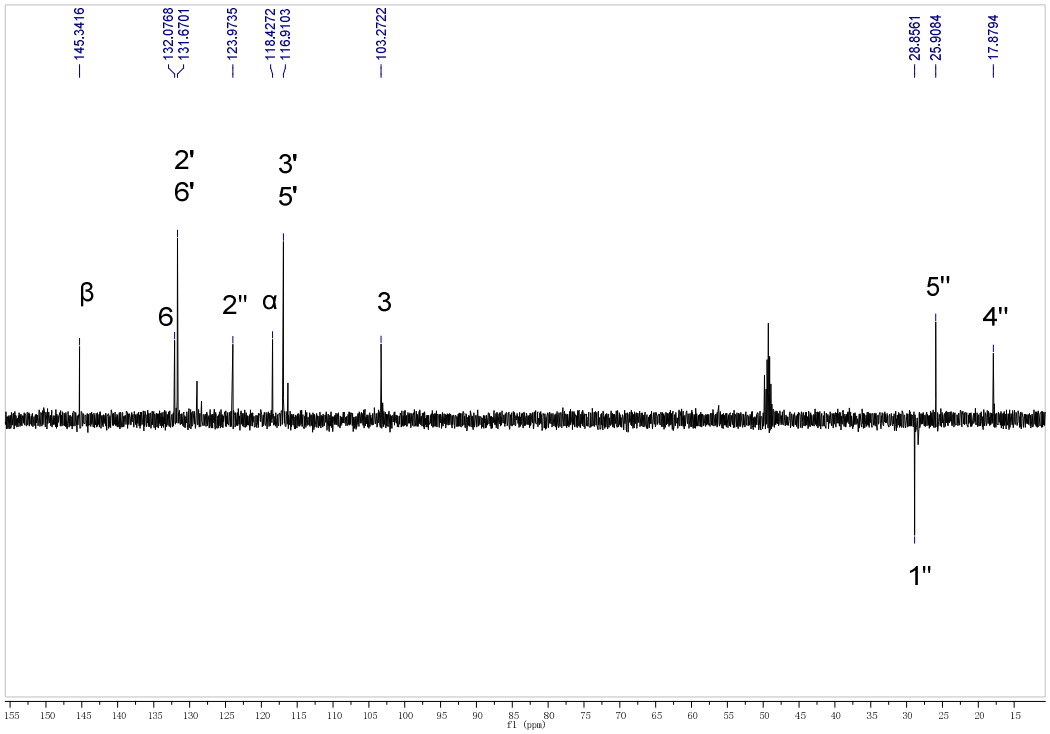

Figure 3.211 DEPT spectrum of compound **42**

Table 3.46 NMR spectroscopic data of compound **42** (CD_3OD, 500 MHz)

	Bavachalcone ($CDCl_3$) [Yin *et al.*, 2004]		Compound **42**	
Position	δ_C	δ_H (mult., *J* in Hz)	δ_C	δ_H (mult., *J* in Hz)
1	113.2, qC		114.3, qC	
2	163.9, qC		164.4, qC	
3	99.2, qC	6.44, s	103.3, CH	6.29, s
4	164.9, qC		165.8, qC	
5	121.6, CH		122.0, qC	
6	129.6, CH	7.59, s	132.1, CH	7.72, s
α	117.6, CH	7.43, d (15.4)	118.5, CH	7.54, d (15.5)
β	144.0, CH	7.83, d (15.4)	145.4, CH	7.75, d (15.5)
1′	127.2, qC		127.9, qC	
2′	130.4, CH	7.55, d (8.5)	131.7, CH	7.59, d (8.5)
3′	116.0, CH	6.90, d (8.5)	116.9, CH	6.84, d (8.5)
4′	158.4, qC		161.5, qC	
5′	116.0, CH	6.90, d (8.5)	116.9, CH	6.84, d (8.5)
6′	130.4, CH	7.55, d (8.5)	131.7, CH	7.59, d (8.5)
1″	28.2, CH_2	3.26, d (7.0)	28.9, CH_2	3.26, br d (7.3)
2″	122.0, CH	5.28, br t (7.1)	124.0, CH	5.32, tqq (7.3, 1.6, 1.3)
3″	132.8, qC		133.2, qC	
4″	18.0, CH_3	1.78, s	17.9, CH_3	1.75, br s
5″	25.9, CH_3	1.74, s	25.9, CH_3	1.74, br s
C=O	191.7, qC		193.5	
4-OCH_3	55.8, CH_3			

3.3.8. Bavachromene (43, known compound)

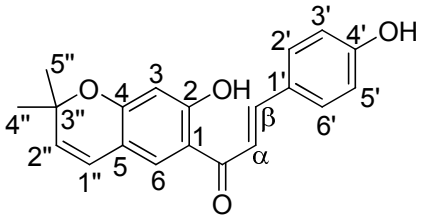

Molecular formula:	$C_{20}H_{18}O_4$
Molecular weight:	322.35
Amount:	0.9 mg

Compound **43** was isolated as a yellow powder. It had UV absorbances at λ_{max} 224, 240 and 387 nm. (Figure 3.212) The ESIMS spectrum of **43** (Figure 3.213) exhibited the molecular ion peak at *m/z* 321 $[M - H]^-$. The ^1H NMR spectrum of **43** (Figure 3.214) was closely related to that of **42**, except for the presence of a 2,2-dimethylpyran ring. This was deduced from the 6H singlet at δ 1.43 due to the *gem*-dimethyl group and from the two *ortho*-coupled aromatic protons at δ 6.45 (d, J = 9.8 Hz) and 5.66 (d, J = 9.8 Hz) assignable to H-1‴ and H-2‴, respectively. The assignments were further supported by analysis of the HMBC (Figure 3.216) and HMQC (Figure 3.215) spectra of **43**. From those above observations and comparison with the reference compound [Lee et al., 2005], compound **43** was concluded to be **bavachromene**.

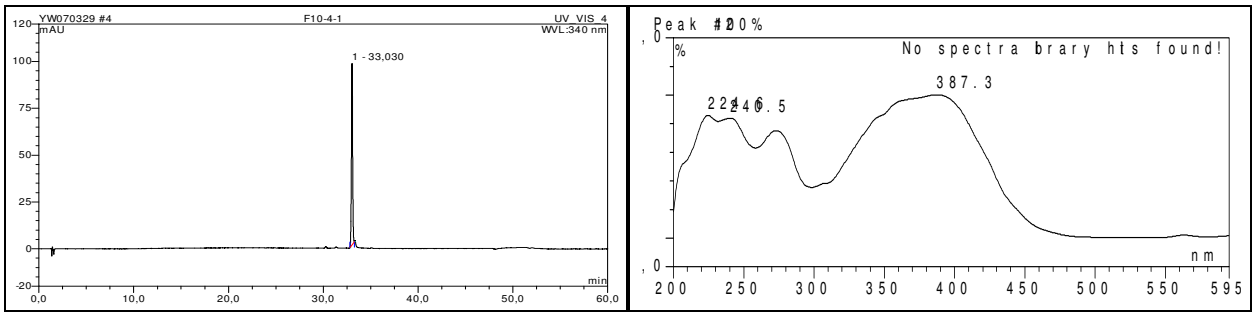

Figure 3.212 HPLC chromatogram and UV spectrum of compound **43**

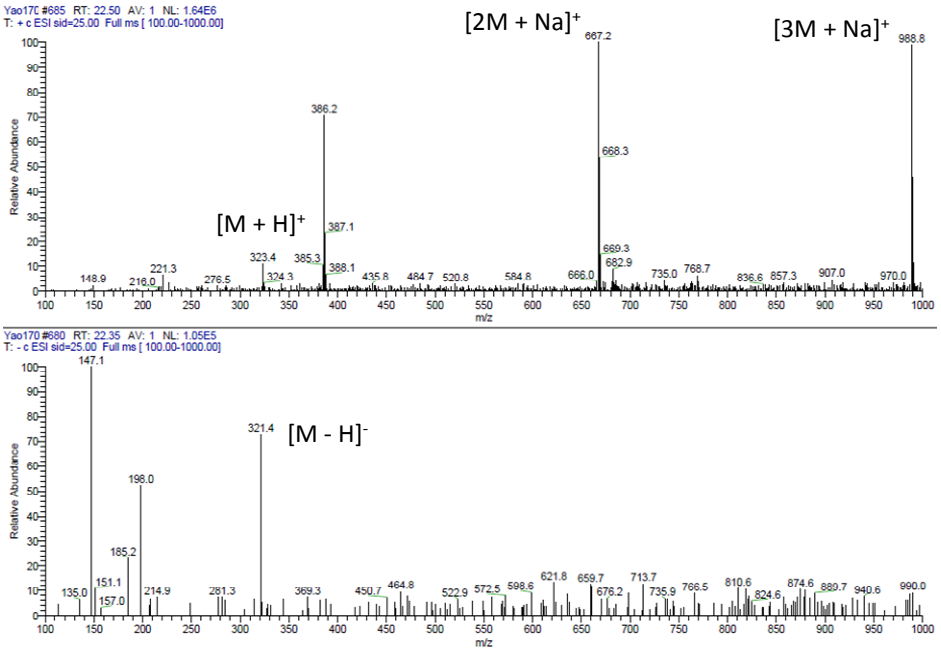

Figure 3.213 ESI-MS spectrum of compound **43**

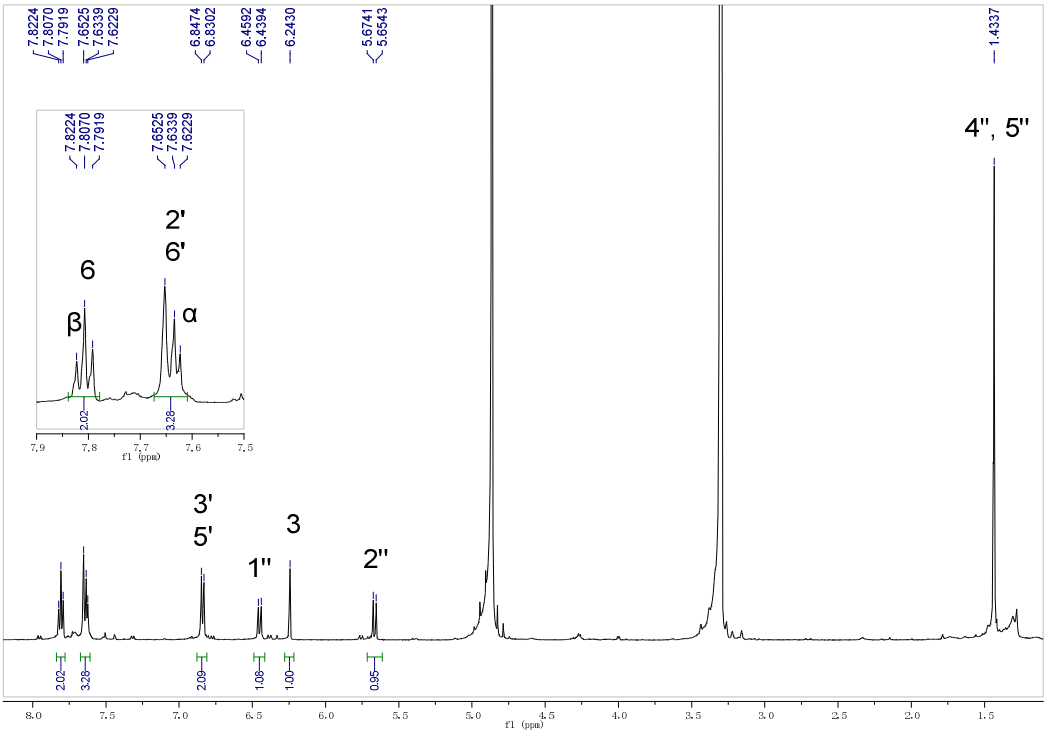

Figure 3.214 ^{1}H NMR spectrum of compound **43**

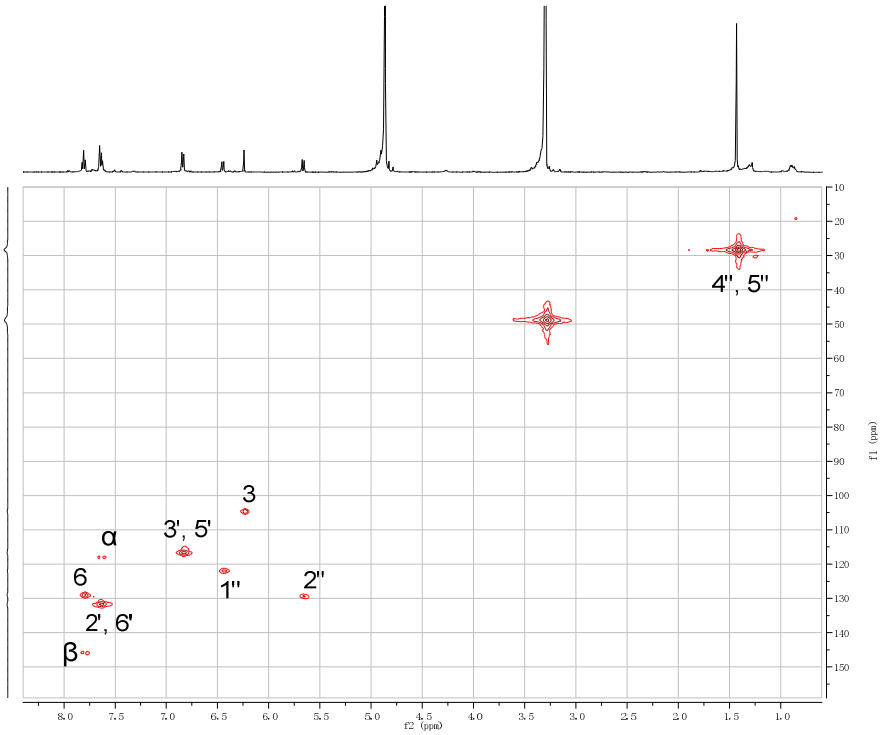

Figure 3.215 HMQC spectrum of compound **43**

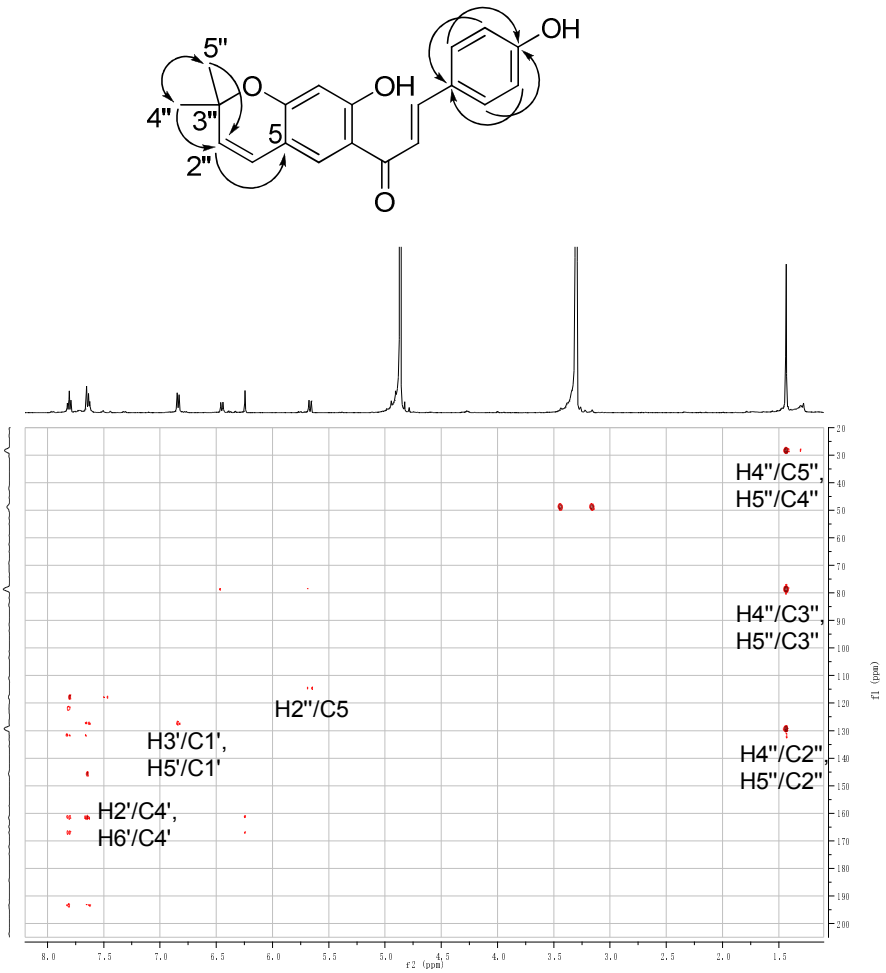

Figure 3.216 HMBC spectrum of compound **43**

Table 3.47 NMR spectroscopic data of compound **43** (CD_3OD, 500 MHz)

	Isobavachromene[a] ($CDCl_3$) [Lee *et al.*, 2005]		Compound **43**	
Position	δ_C	δ_H (mult., *J* in Hz)	δ_C	δ_H (mult., *J* in Hz)
1	109.4, qC		131.7, qC	
2	159.7, qC		166.9, qC	
3	114.1, CH		104.8, CH	6.24, s
4	160.9, qC		161.4, qC	
5	108.3, CH	6.38, d (8.8)	114.6, qC	
6	130.6, CH	7.71, d (8.8)	129.1, CH	7.81, s
α	117.9, CH	7.43, d (15.2)	117.9, CH	7.64, d (15.5)
β	144.1, CH	7.83, d (15.2)	145.8, CH	7.81, d (15.5)
1′	127.8, qC		127.4, qC	
2′	130.6, CH	7.56, d (8.4)	131.7, CH	7.64, d (8.5)
3′	116.0, CH	6.88, d (8.4)	116.8, CH	6.84, d (8.5)
4′	158.0, qC		161.6, qC	
5′	116.0, CH	6.88, d (8.4)	116.8, CH	6.84, d (8.5)
6′	130.6, CH	7.56, d (8.4)	131.7, CH	7.64, d (8.5)
1″	115.9, CH_2	6.75, d (10.4)	121.9, CH	6.45, d (9.8)
2″	128.1, CH	5.59, d (10.4)	129.4, CH	5.66, d (9.8)
3″	77.8, qC		78.8, qC	
4″	28.4, CH_3	1.47, s	28.5, CH_3	1.43, s
5″	28.4, CH_3	1.47, s	28.5, CH_3	1.43, s
C=O	192.1		193.3, qC	

[a] No available NMR data of bavachromene were obtained, so a closely related compound was used to compare.

3.3.9. Bavachalcone (44, known compound)

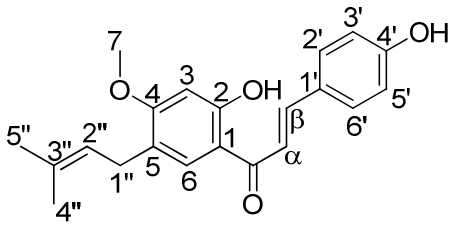

Molecular formula:	$C_{21}H_{22}O_4$
Molecular weight:	338.40
Amount:	9.0 mg

Compound **44** was obtained as a yellow amorphous powder with UV maximal absorption at 211, 237 and 377 nm. (Figure 3.217) The molecular weight of **44** was 338 by ESIMS (Figure 3.218) at *m/z* 339 $[M + H]^+$ indicating the presence of an additional CH_3 group compared to **42**. The ^1H NMR spectrum (Figure 3.219) of **44** was almost superimposable to those of **42**. The additional *O*-methyl resonance was deduced from the singlet proton signal at δ 3.86 in the ^1H NMR spectrum, and was assigned at C-4 as suggested by the HMBC spectrum of **44**. (Figure 3.221) Compound **44** was identified as **bavachalcone** through comparison of its spectral data with the previously published one [Yin et al., 2004].

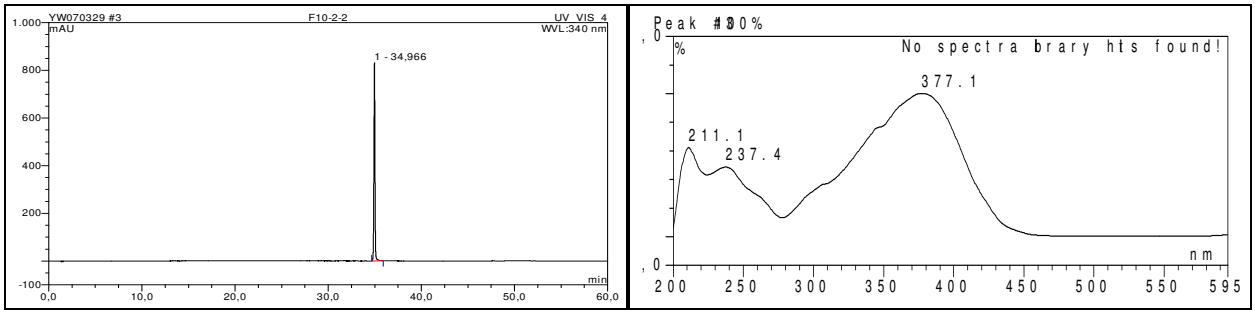

Figure 3.217 HPLC chromatogram and UV spectrum of compound **44**

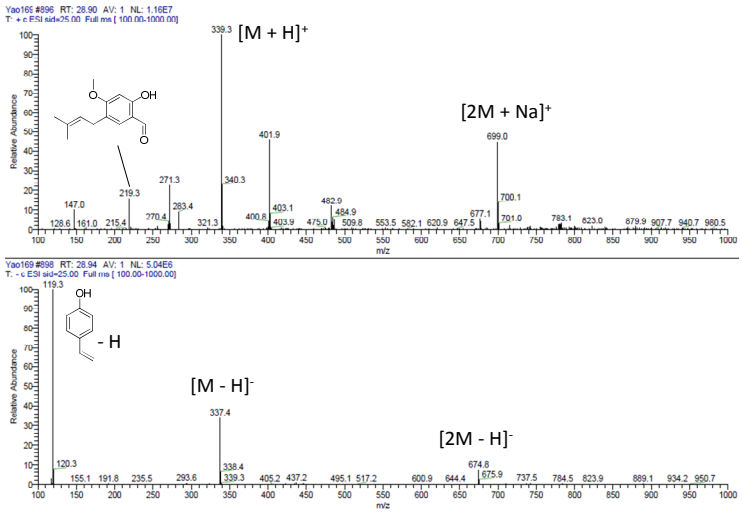

Figure 3.218 ESI-MS spectrum of compound **44**

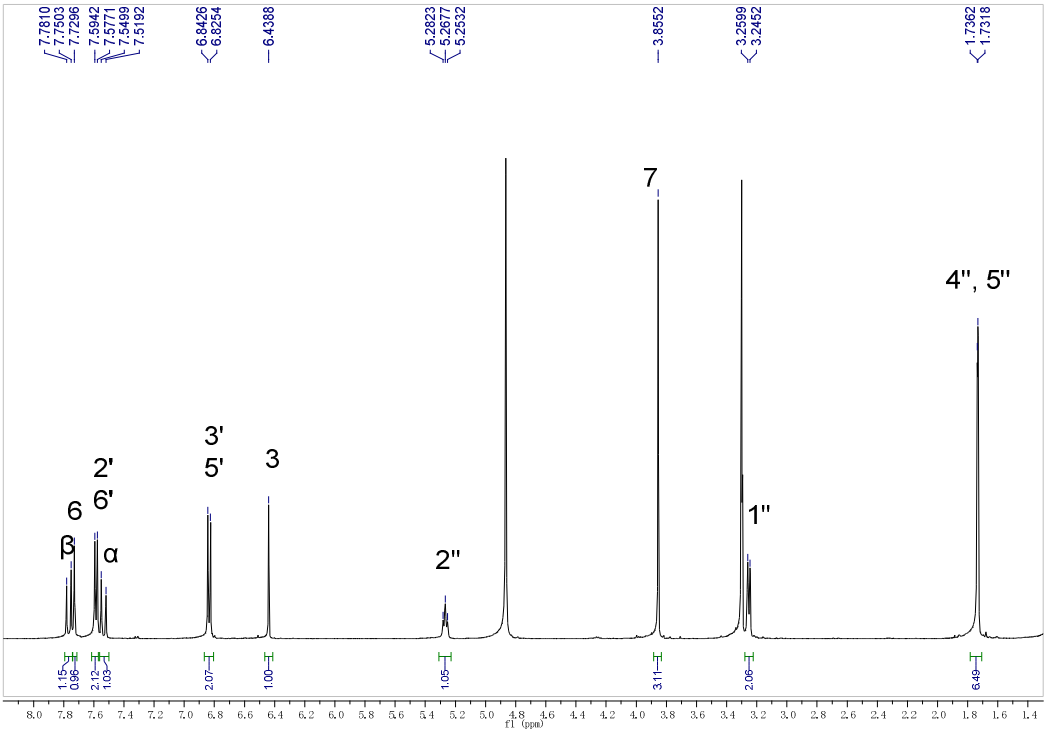

Figure 3.219 ^{1}H NMR spectrum of compound **44**

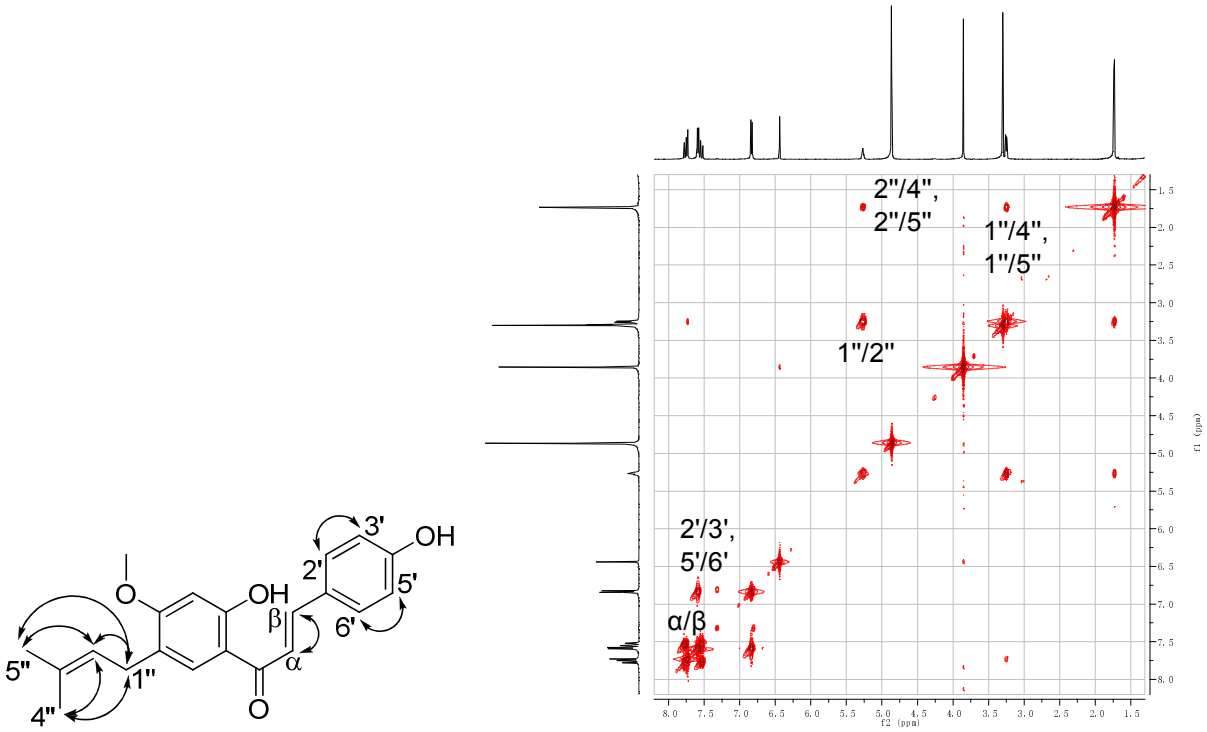

Figure 3.220 ^{1}H-^{1}H COSY spectrum of compound **44**

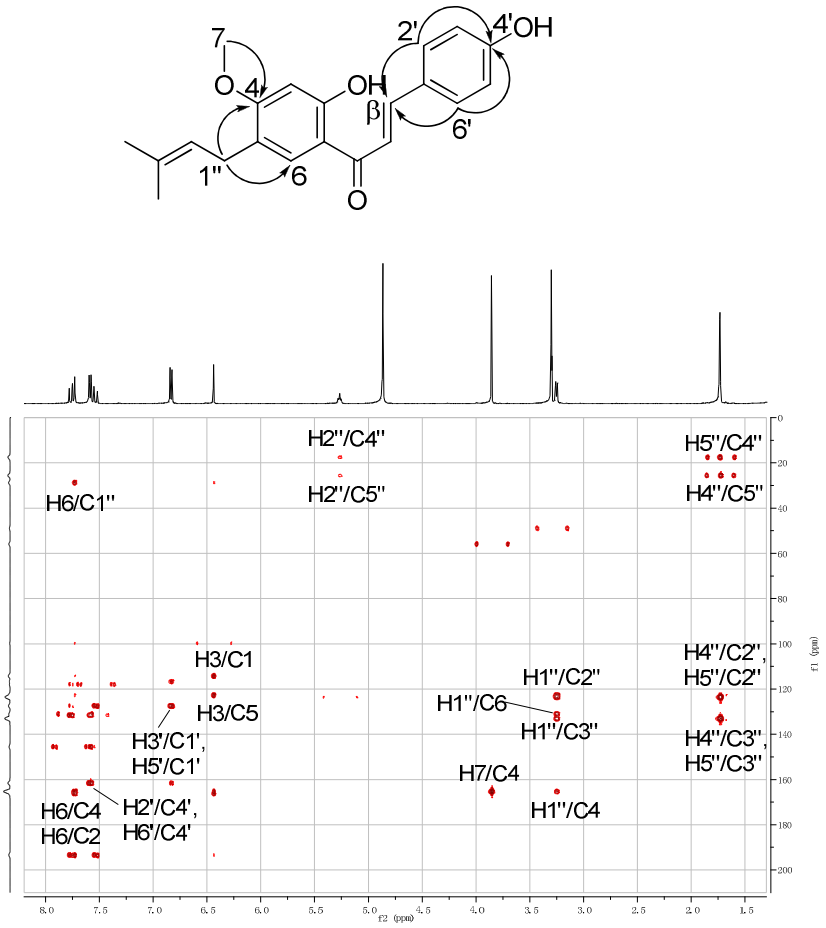

Figure 3.221 HMBC spectrum of compound **44**

Table 3.48 NMR spectroscopic data of compound **44** (CD_3OD, 500 MHz)

	Bavachalcone ($CDCl_3$) [Yin *et al.*, 2004]		Compound **44**	
Position	δ_C	δ_H (mult., *J* in Hz)	δ_C	δ_H (mult., *J* in Hz)
1	113.2, qC		114.4, qC	
2	163.9, qC		165.9,qC	
3	99.2, CH	6.44, s	99.8, CH	6.44, s
4	164.9, qC		165.2, qC	
5	121.6, qC		122.8, CH	
6	129.6, CH	7.59, s	131.0, CH	7.73, s
7	55.8, CH_3		56.0, CH_3	3.86, s
α	117.6, CH	7.43, d (15.4)	118.0, CH	7.54, d (15.5)
β	144.0, CH	7.83, d (15.4)	145.5, CH	7.77, d (15.5)
1′	127.2, qC		127.5, qC	
2′	130.4, CH	7.55, d (8.5)	131.6, CH	7.59, d (8.5)
3′	116.0, CH	6.90, d (8.5)	116.7, CH	6.83, d (8.5)
4′	158.4, qC		161.5, qC	
5′	116.0, CH	6.90, d (8.5)	116.7, CH	6.83, d (8.5)
6′	130.4, CH	7.55, d (8.5)	131.6, CH	7.59, d (8.5)
1″	28.2, CH_2	3.26, d (7.0)	28.9, CH_2	3.25, br d (7.3)
2″	122.0, CH	5.28, br t (7.0)	123.6, CH	5.27, tq (7.3, 1.3)
3″	132.8, qC		133.1, qC	
4″	18.0, CH_3	1.78, s	17.6, CH_3	1.74, br s
5″	25.9, CH_3	1.74, s	25.7, CH_3	1.73, br s
C=O	191.7		193.4	

3.3.10. Bavachin (45, known compound)

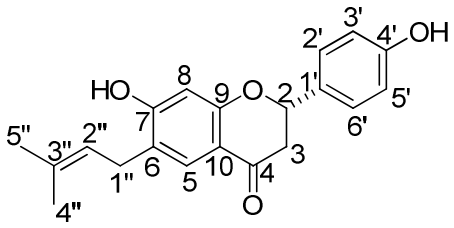

Molecular formula:	$C_{20}H_{20}O_4$
Molecular weight:	324.37
Amount:	15.0 mg

Compound **45** was isolated as a yellow amorphous powder. It had UV absorbances at λ_{max} 222, 237 and 279 nm (Figure 3.222) indicating a typical flavanone. The ESI mass spectrum (Figure 3.223) of **45** showed the pseudomolecular ion peak at *m/z* 325 $[M + H]^+$. The ^1H NMR spectrum (Figure 3.224) of **45** exhibited a pair of geminal coupled protons at δ 3.20 (dd, J = 17.0, 13.2 Hz) and 2.65 (dd, J = 17.0, 2.8 Hz) and an oxygenated proton at δ 5.37 (dd, J = 13.2, 2.8 Hz) assigned to be H_2-3 and H-2 of flavanone. Moreover, one oxymethine (C-2), one methylene (C-3) and one carbonyl (C-4) carbon were found in the ^{13}C NMR (Figure 3.225) and DEPT (Figure 3.226) spectra of **45**. Those above observations confirmed the flavanone skeleton of compound **45**. Through comparison with the literature [Lee *et al.*, 2005] it was concluded that compound **45** was **bavachin**.

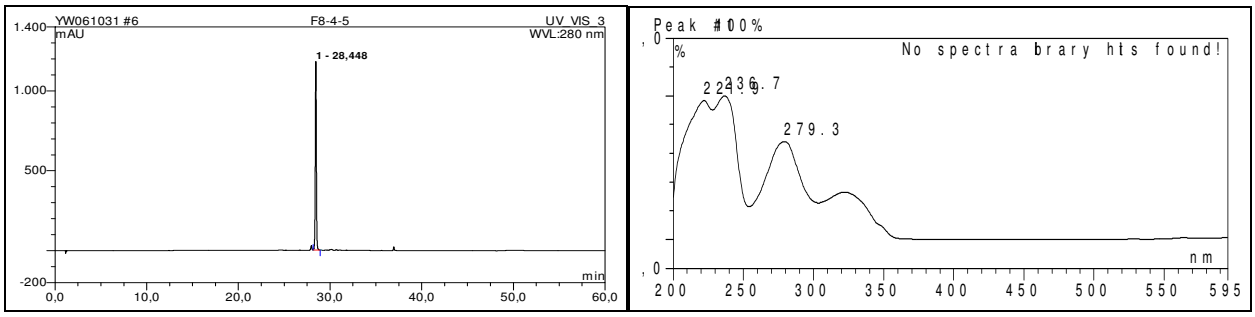

Figure 3.222 HPLC chromatogram and UV spectrum of compound **45**

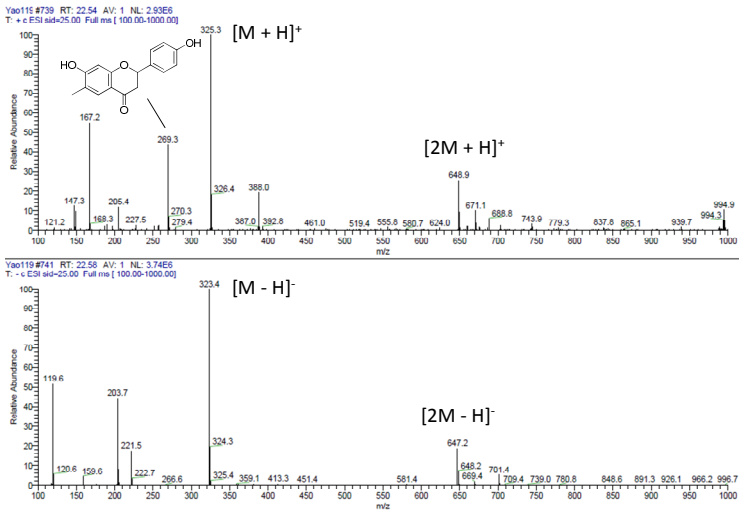

Figure 3.223 ESI-MS spectrum of compound **45**

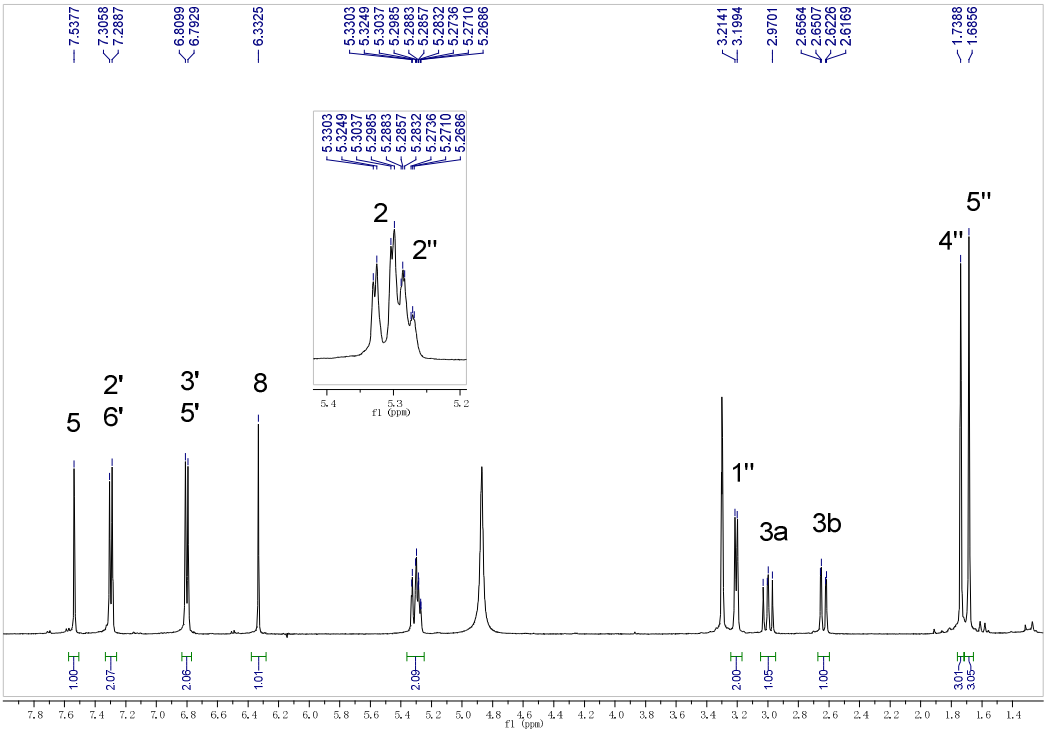

Figure 3.224 ^{1}H NMR spectrum of compound **45**

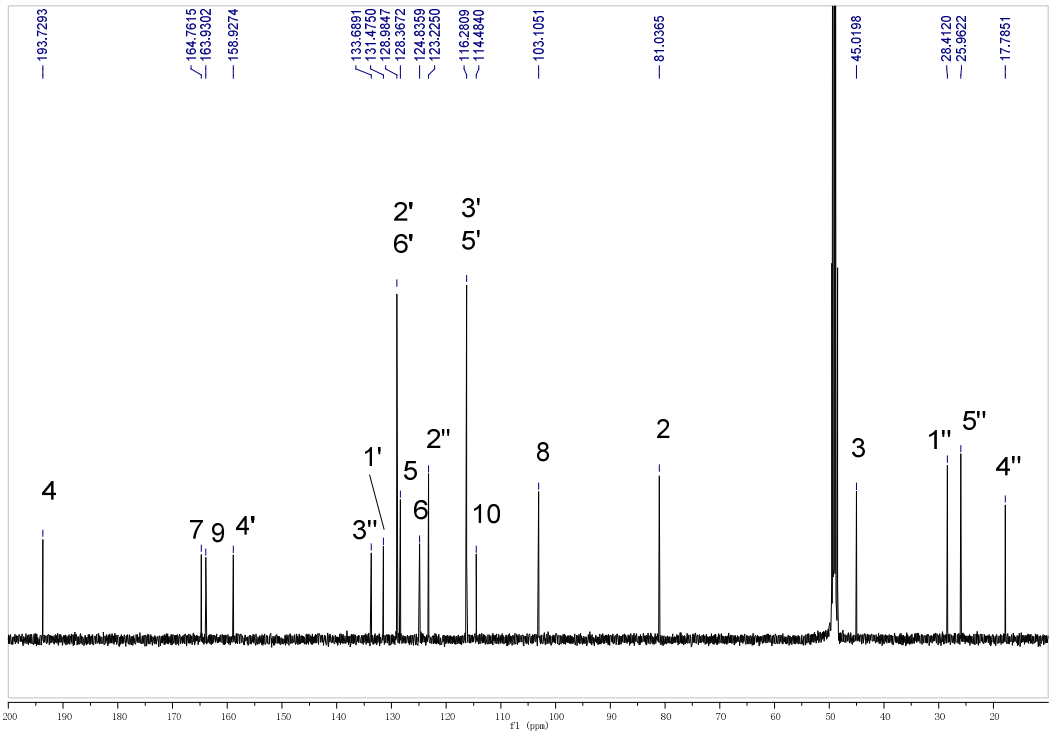

Figure 3.225 ^{13}C NMR spectrum of compound **45**

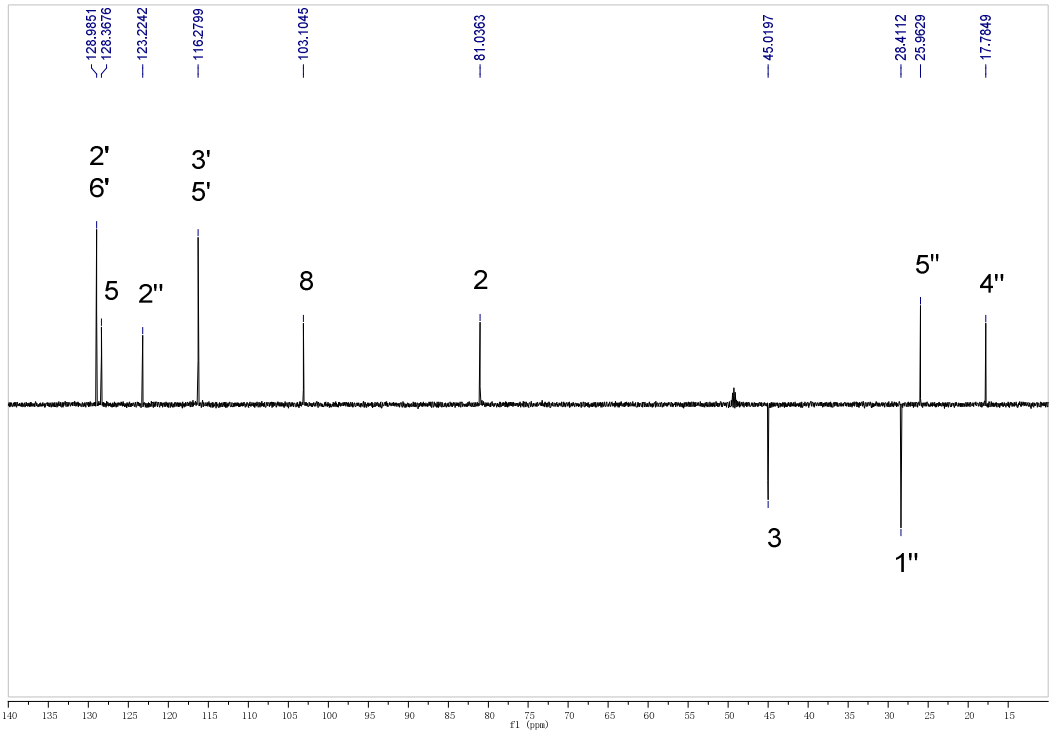

Figure 3.226 DEPT spectrum of compound **45**

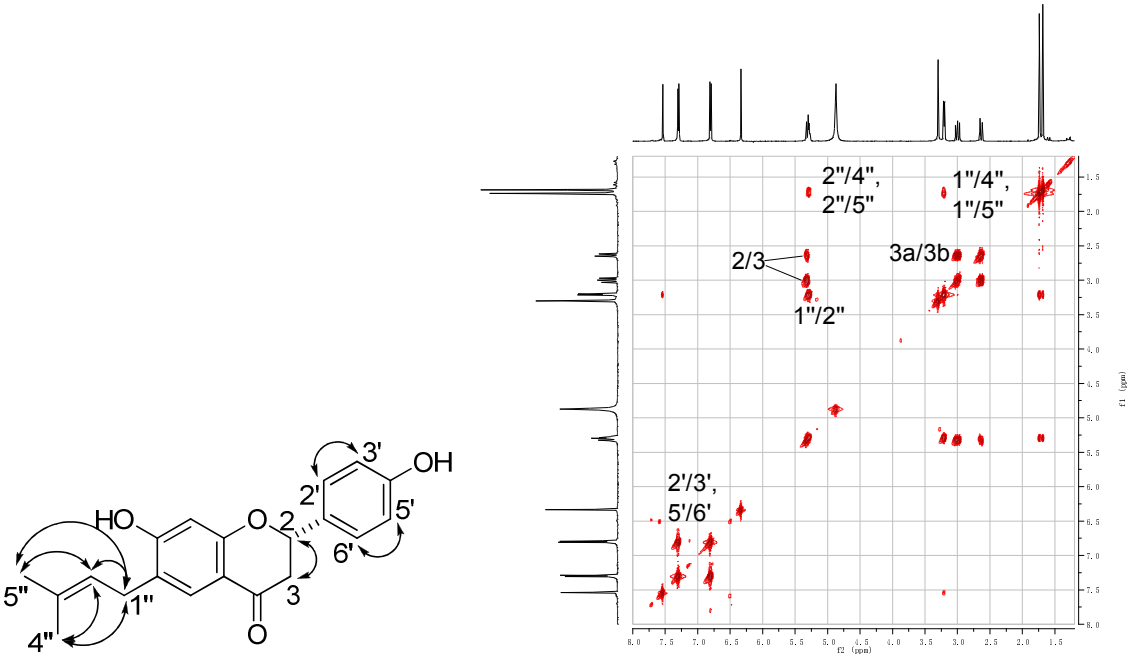

Figure 3.227 ^{1}H-^{1}H COSY spectrum of compound **45**

Table 3.49 NMR spectroscopic data of compound **45** (CD_3OD, 500 MHz)

	Bavachinin[a] ($CDCl_3$) [Lee *et al.*, 2005]		Compound **45**	
Position	δ_C	δ_H (mult., *J* in Hz)	δ_C	δ_H (mult., *J* in Hz)
2	79.8, CH	5.38, dd (13.2, 2.8)	81.0, CH	5.31, dd (13.2, 2.8)
3	44.0, CH_2	3.04, dd (16.8, 13.2); 2.78, dd (16.8, 2.8)	45.0, CH_2	3.00, dd (17.0, 13.2); 2.64, dd (17.0, 2.8)
4	191.5, qC		193.7, qC	
5	127.1, CH	7.68, s	128.4, CH	7.54, s
6	124.9, qC		124.8, qC	
7	164.3, qC		164.8, qC	
8	98.8, CH	6.44, s	103.1, CH	6.33, s
9	162.4, qC		163.9, qC	
10	113.8, qC		114.5, qC	
1′	130.8, qC		131.5, qC	
2′	127.9, CH	7.34, d (8.4)	129.0, CH	7.30, d (8.5)
3′	115.7, CH	6.90, d (8.4)	116.3, CH	6.80, d (8.5)
4′	156.3, qC		158.9, qC	
5′	115.7, CH	6.90, d (8.4)	116.3, CH	6.80, d (8.5)
6′	127.9, CH	7.34, d (8.4)	129.0, CH	7.30, d (8.5)
1″	27.8, CH_2	3.24, d (7.2)	28.4, CH_2	3.21, br d (7.3)
2″	121.7, CH	5.27, t (7.2)	123.2, CH	5.28, dt (7.3, 1.3)
3″	133.1, qC		133.7, qC	
4″	25.8, CH_3	1.74, s	17.8, CH_3	1.74, s
5″	17.7, CH_3	1.69, s	26.0, CH_3	1.69, s

[a] No available NMR data of bavachin were obtained, so a closely related compound was used to compare.

3.3.11. 6-Prenylnaringenin (46, known compound)

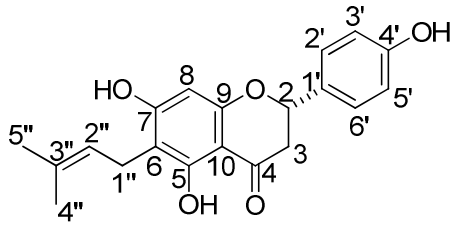

Molecular formula:	$C_{20}H_{20}O_5$
Molecular weight:	340.37
Amount:	3.7 mg

Compound **46** was isolated as a yellow amorphous powder. It yielded a UV spectrum (Figure 3.228) with maximum absorbances at 220, 224 and 295 nm which was similar to that of **45**. The molecular weight of **46** was determined as 340 by ESI mass spectrum (Figure 3.231), indicating the presence of an additional OH group compared to **45**. The ^{1}H (Figure 3.229) and ^{13}C NMR spectra of **46** were closely related to those of **45** except for the third hydroxyl group. A singlet proton at δ 12.42 was observed in the ^{1}H NMR spectrum assigned to the OH group at C-5. The chemical shift of this signal was shifted downfield by approximately 2 ppm compared to the common region of hydroxyl group because of the forming of the hydrogen bonding with the carbonyl group at C-4. The attachment of the OH group was also confirmed by the HMBC spectrum (Figure 3.230) of **46**. Comparison of compound **46** with **6-prenylnaringenin** [Stevens *et al.*, 1997], proved both compounds to be identical.

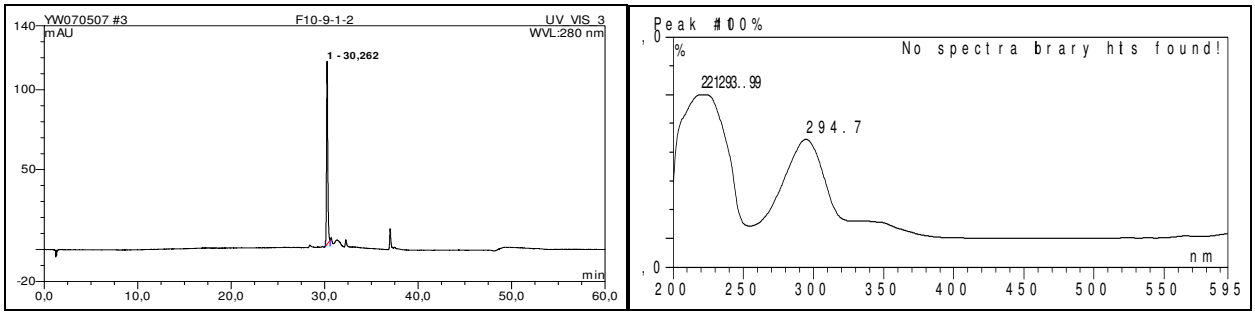

Figure 3.228 HPLC chromatogram and UV spectrum of compound **46**

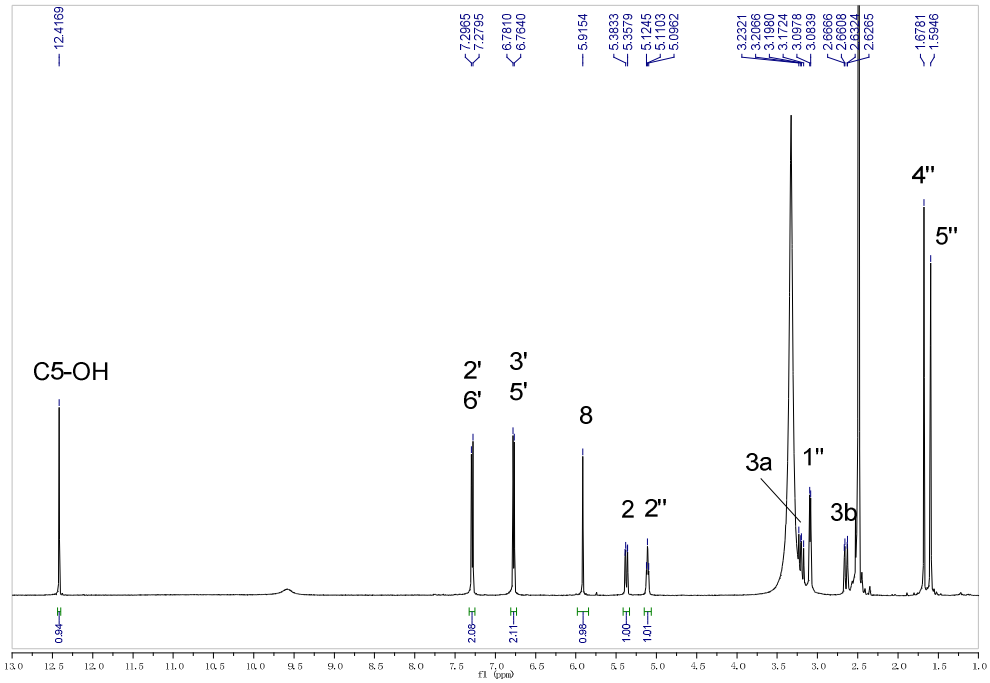

Figure 3.229 ^{1}H NMR spectrum of compound **46**

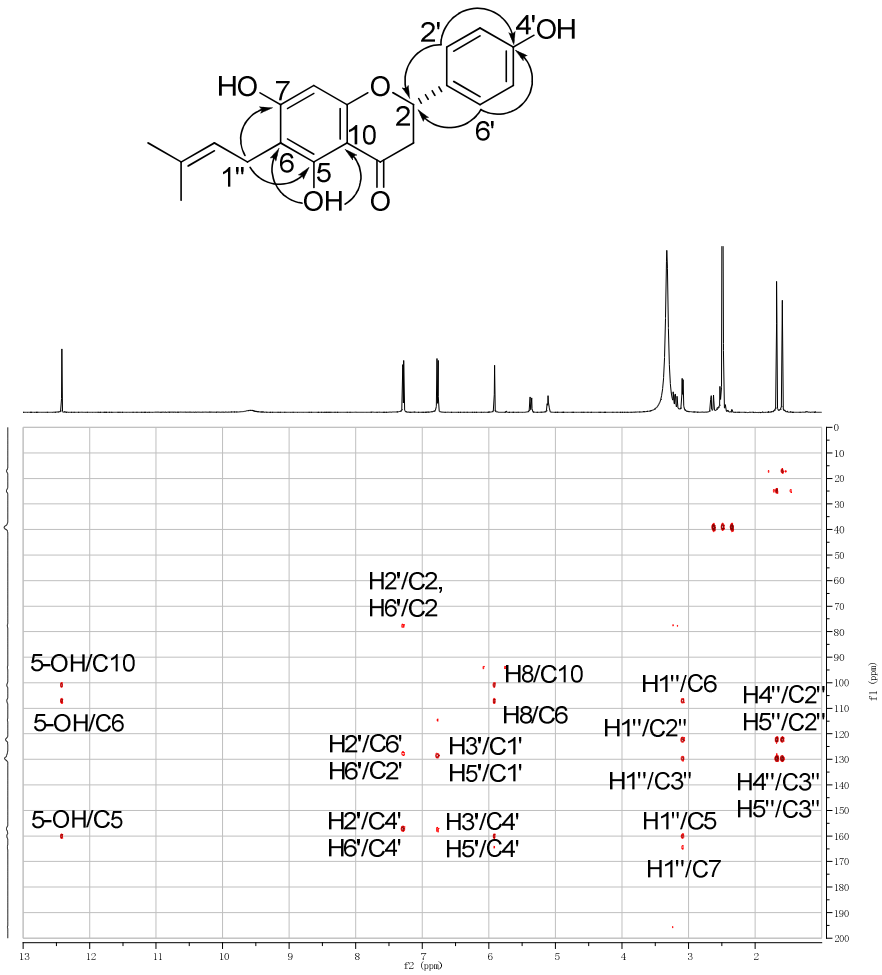

Figure 3.230 HMBC spectrum of compound **46**

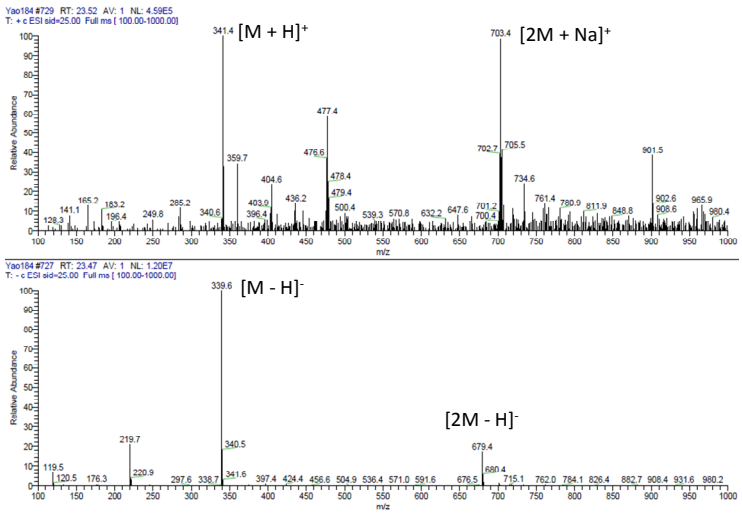

Figure 3.231 ESI-MS spectrum of compound **46**

Table 3.50 NMR spectroscopic data of compound **46** (DMSO-d_6, 500 MHz)

	6-Prenylnaringenin [Stevens *et al.*, 1997]		Compound **46**	
Position	δ_C	δ_H (mult., *J* in Hz)	δ_C	δ_H (mult., *J* in Hz)
2_{ax}	78.3, CH	5.39, dd (12.7, 2.9)	78.2, CH	5.37, dd (12.6, 2.8)
3_{ax}	42.0, CH_2	3.22, dd (17.1, 12.7)	CH_2[a]	3.20, dd (17.1, 12.9)
3_{eq}		2.78, dd (17.1, 3.0)		2.65, dd (17.1, 2.8)
4	196.4, qC		196.0, qC	
5	160.53, qC		160.6, qC	
6	107.5, qC		107.5, qC	
7	164.2, qC		164.6, qC	
8	94.3, CH	5.97, s	94.4, CH	5.92, s
9	160.49, qC		qC[a]	
10	101.6, qC		101.3, qC	
1′	129.0, qC		129.0, qC	
2′	128.2, CH	7.30, d (8.5)	128.2, CH	7.29, d (8.5)
3′	115.1, CH	6.79, d (8.4)	115.0, CH	6.78, d (8.5)
4′	157.7, qC		157.6, qC	
5′	115.1, CH	6.79, d (8.4)	115.0, CH	6.78, d (8.5)
6′	128.2, CH	7.30, d (8.5)	128.2, CH	7.29, d (8.5)
1″	20.6, CH_2	3.11, d (7.1)	CH_2[a]	3.09, br d (6.9)
2″	122.6, CH	5.13, t (7.1)	122.6, CH	5.11, br t (6.9)
3″	130.2, qC		130.2, qC	
4″	17.6, CH_3	1.69, s	17.6, CH_3	1.68, s
5″	25.4, CH_3	1.61, s	25.3, CH_3	1.59, s
C5-OH		12.41, s		12.42, s

[a] Due to the low amount of compound, no ^{13}C NMR signal could be obtained

3.3.12. Neobavaisoflavone (47, known compound)

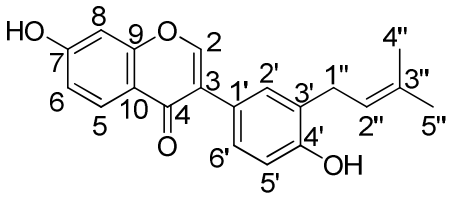

Molecular formula:	$C_{20}H_{18}O_4$
Molecular weight:	322.35
Amount:	33.7 mg

Compound **47** was obtained as a yellow amorphous powder. It had the molecular weight as 322 determined by ESIMS (Figure 3.234). It showed UV maximal absorbances at 209 and 249 nm (Figure 3.233). The ^{1}H NMR spectrum (Figure 3.232) of **47** indicated the signals of two 1,3,4-trisubstituted benzene rings and a typical proton signal at δ 8.09 (s) assignable for the H-2 of isoflavonoid. Along with the analysis of the ^{13}C NMR (Figure 3.235) and DEPT data (Figure 3.236), it was inferred that compound **47** had characteristic 3′-alkyl-4′,7-dihydroxyisoflavone features. In the HMBC spectrum (Figure 3.237) of **47**, the strong correlations between H_2-1″ and the carbon signals at δ 128.4 (C-3′) and 155.7 (C-4′), respectively, suggested the prenyl moiety was attached to C-3′. On the basis of above evidences and comparison with the literature [Saxena and Bhadoria, 1990; Nkengfack *et al.*, 1994], compound **47** was identified to be **neobavaisoflavone**.

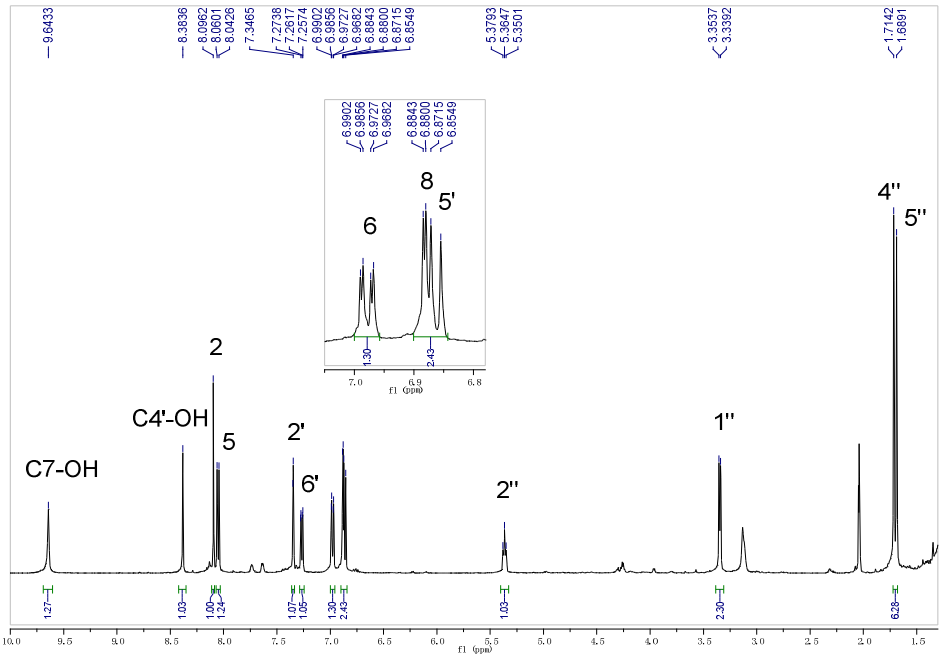

Figure 3.232 ^{1}H NMR spectrum of compound **47**

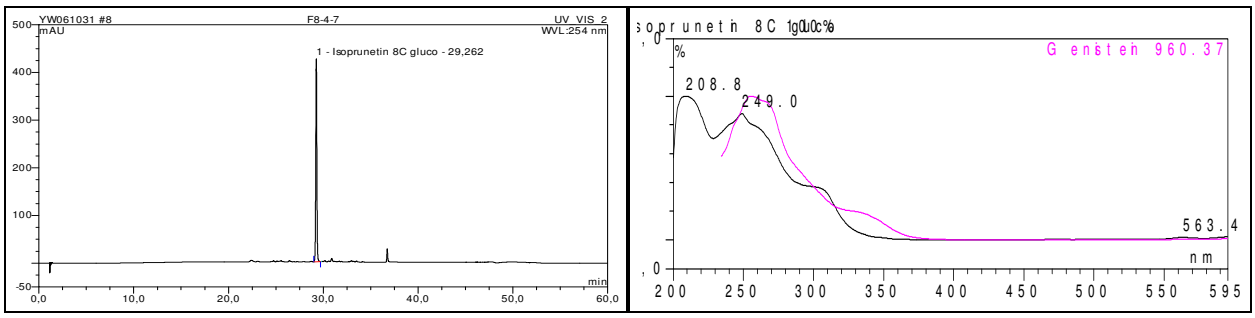

Figure 3.233 HPLC chromatogram and UV spectrum of compound **47**

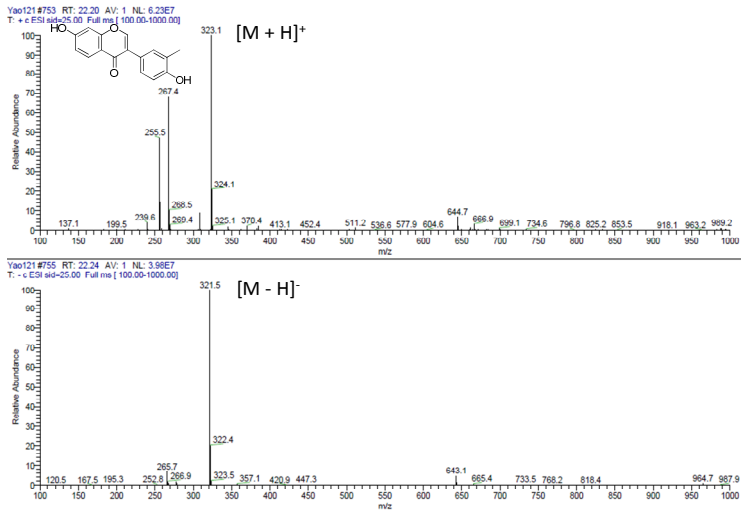

Figure 3.234 ESI-MS spectrum of compound **47**

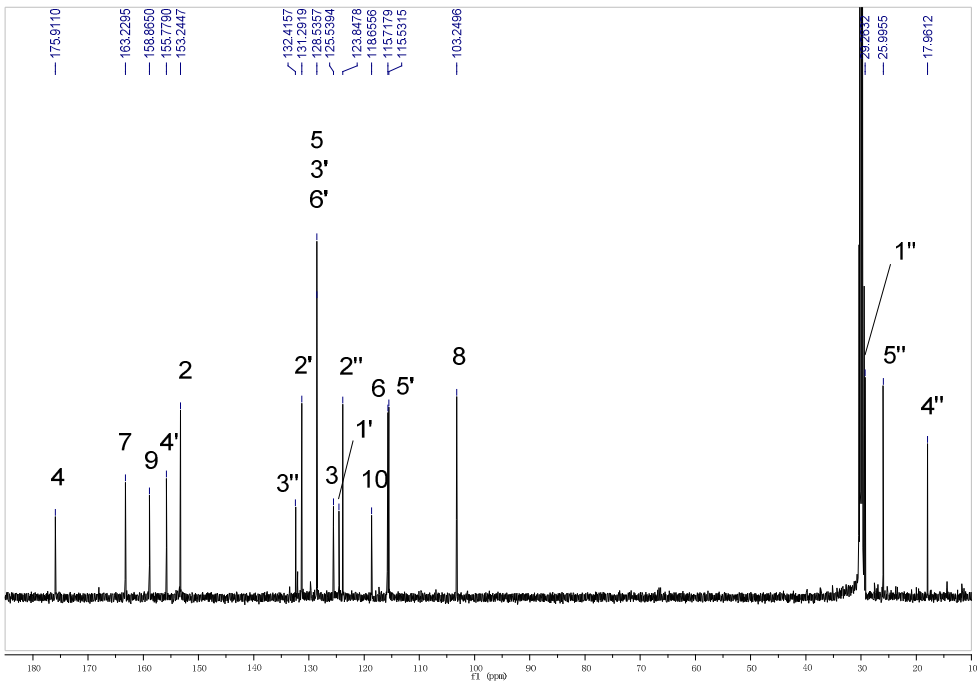

Figure 3.235 ^{13}C NMR spectrum of compound **47**

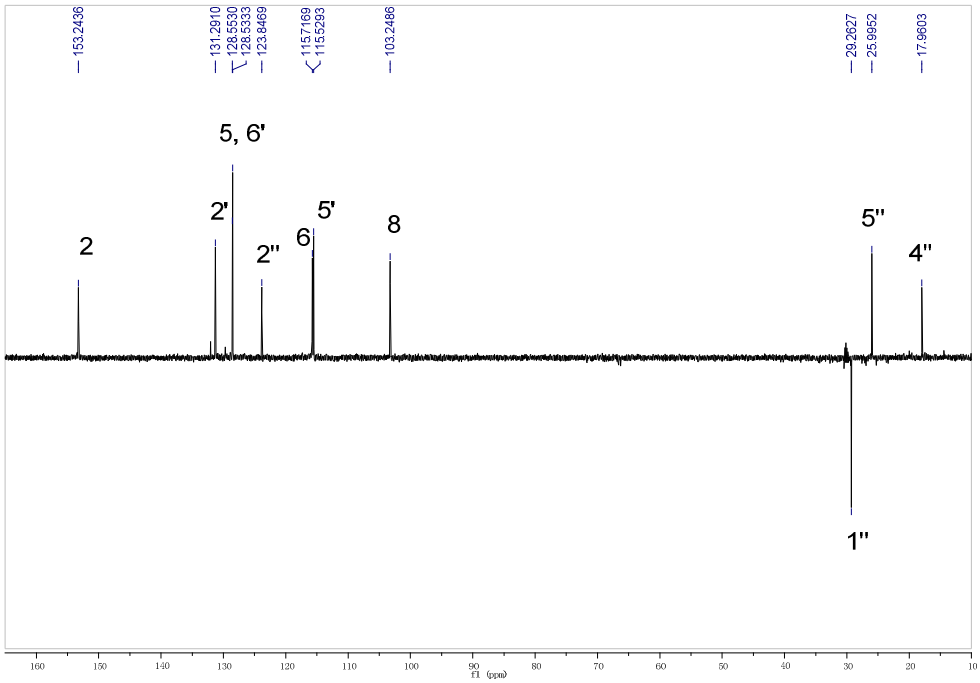

Figure 3.236 DEPT spectrum of compound **47**

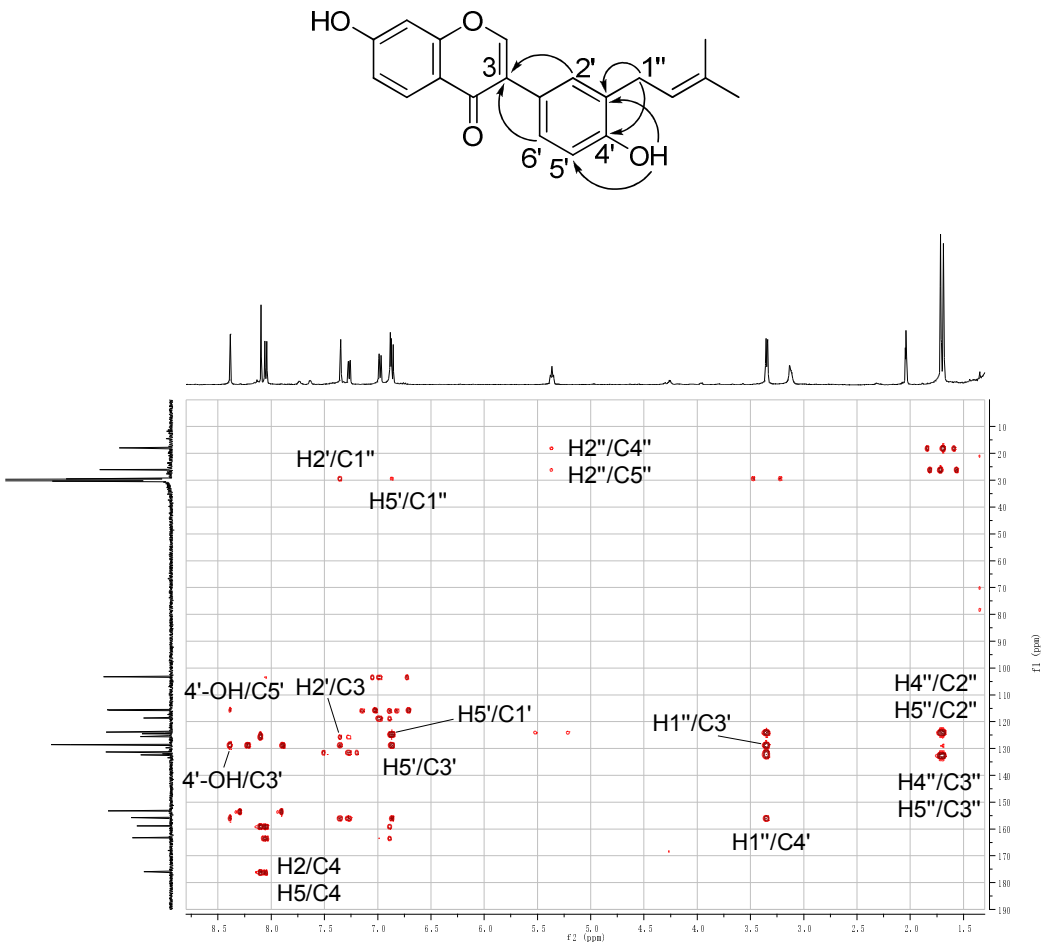

Figure 3.237 HMBC spectrum of compound **47**

Table 3.51 NMR spectroscopic data of compound **47** (DMSO-d_6, 500 MHz)

	Neobavaisoflavone [Saxena and Bhadoria, 1990] [Nkengfack *et al.*, 1994]		Compound **47**	
Position	δ_C	δ_H (mult., *J* in Hz)	δ_C	δ_H (mult., *J* in Hz)
2	155.7, CH	8.06, s	153.1, CH	8.09, s
3	125.5, qC		125.4, qC	
4	175.8, qC		175.8, qC	
5	128.4, CH	8.34, dd (10)	128.4, CH	8.05, d (8.8)
6	115.4, CH	7.0, dd (10)	115.6, CH	6.98, dd (8.8, 2.2)
7	163.2, qC		163.1, qC	
8	103.1, CH	7.45, m	103.1, CH	6.88, d (2.2)
9	158.8, qC		158.7, qC	
10	118.6, qC		118.5, qC	
1′	124.5, qC		124.4, qC	
2′	128.4, CH	7, m	131.2, CH	7.34, d (2.1)
3′	125.0, qC		128.4, qC	
4′	153.0, qC		155.7, qC	
5′	115.6, CH	7, m	115.4, CH	6.87, d (8.2)
6′	131.2, CH	7.12, m	128.4, CH	7.27, dd (8.2, 2.1)
1″	25.0, CH_2	3.34, d (7)	29.1, CH_2	3.35, d (7.3)
2″	123.8, CH	5.24, t	123.7, CH	5.37, br t (7.3)
3″	132.2, qC		132.3, qC	
4″	17.9, CH_3	1.72, s	17.8, CH_3	1.71, s
5″	29.0, CH_3	1.72, s	25.9, CH_3	1.69, s
C7-OH				9.65, s
C4′-OH				8.39, s

3.3.13. Corylin (48, known compound)

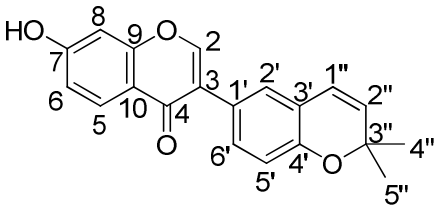

Molecular formula:	$C_{20}H_{16}O_4$
Molecular weight:	320.34
Amount:	2.4 mg

Compound **48** was obtained as a yellow amorphous powder. Its molecular weight was deduced as 320 from the ESI mass data (Figure 3.240). The UV spectrum (Figure 3.239) of **48** showed absorbances at λ_{max} 249 and 303 nm implying an isoflavone skeleton. This skeleton was further supported by the ^{1}H (Figure 3.238) and ^{13}C (Figure 3.241) NMR spectra of **48**, which were similar to those of **47**. The 6H singlet at δ_H 1.42/δ_C 28.2 and an *ortho*-coupled doublet at δ_H 6.40/δ_C 122.2 and δ_H 5.71/δ_C 131.7, respectively, indicated the presence of a 2,2-dimethylpyran moiety. From the above spectroscopic data of compound **48** and comparison with those of **corylin** [Nkengfack *et al.*, 1994], both compounds were found to be identical.

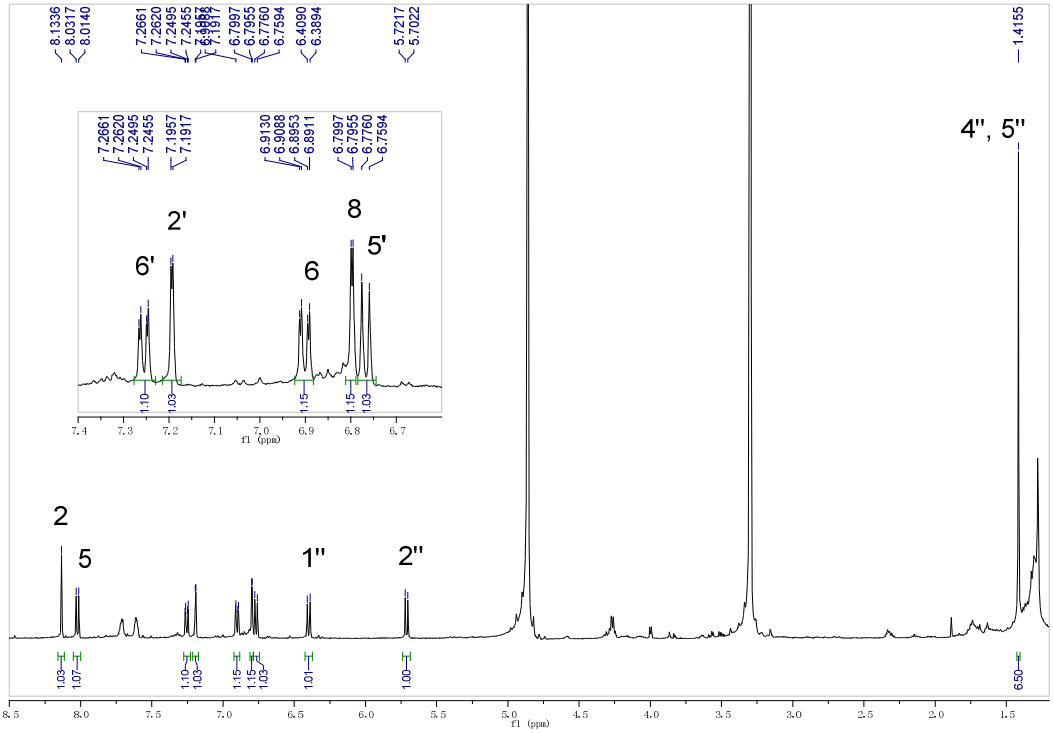

Figure 3.238 ^{1}H NMR spectrum of compound **48**

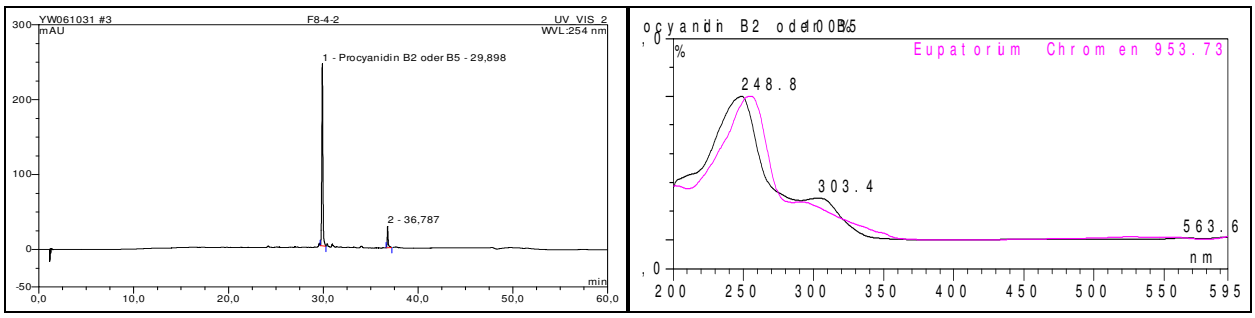

Figure 3.239 HPLC chromatogram and UV spectrum of compound **48**

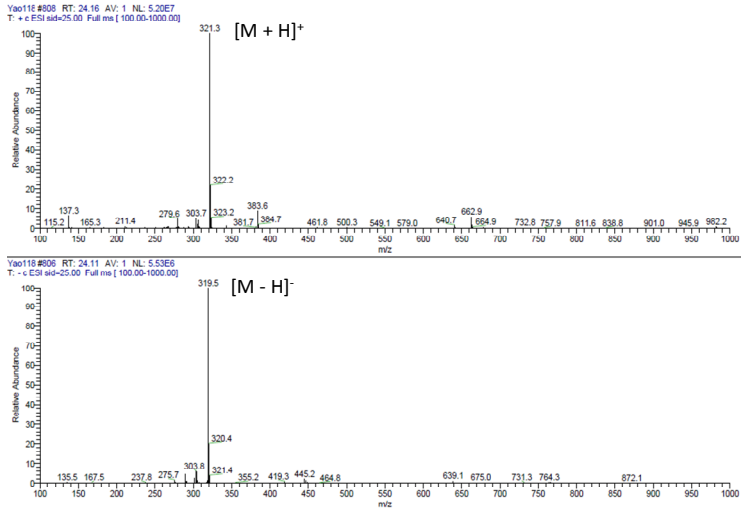

Figure 3.240 ESI-MS spectrum of compound **48**

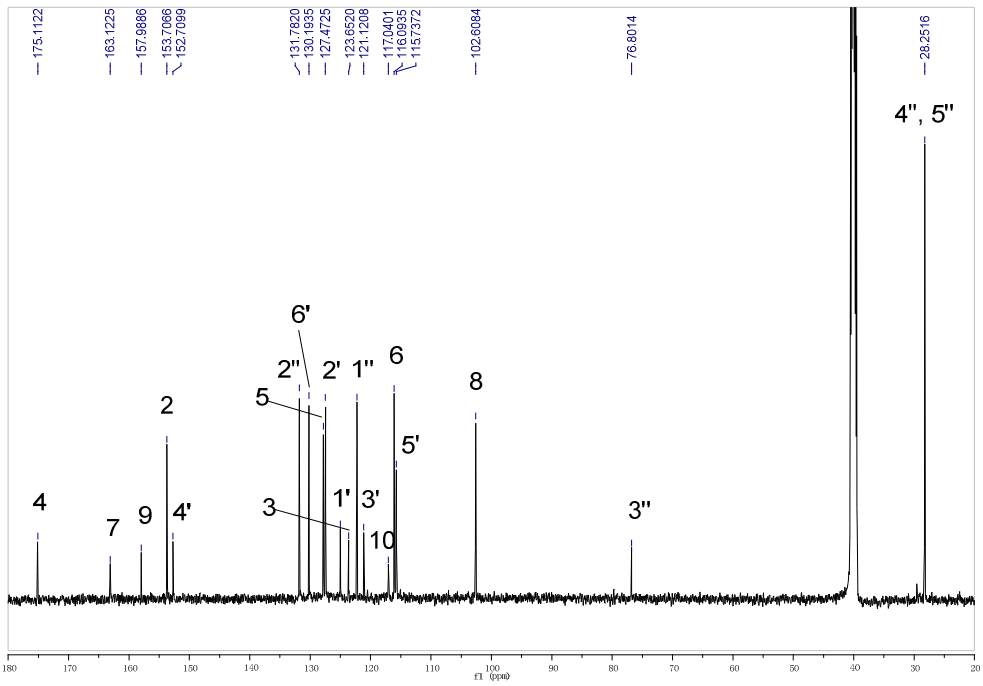

Figure 3.241 ^{13}C NMR spectrum of compound **48**

Table 3.52 NMR spectroscopic data of compound **48** (500 MHz)

Position	Corylin (CD_3COCD_3) [Nkengfack *et al.*, 1994]		Compound **48**	
	δ_C	δ_H (mult., *J* in Hz)	δ_C (DMSO-d_6)	δ_H (mult., *J* in Hz) (CD_3OD)
2	153.4, CH	8.18, s	153.5, CH	8.13, s
3	122.0, qC		123.5, qC	
4	175.6, qC		175.0, qC	
5	128.5, CH	8.10, d (8.7)	127.6, CH	8.02, d (8.8)
6	115.7, CH	7.0, dd (8.7, 2.2)	116.1, CH	6.90, dd (8.8, 2.2)
7	158.8, qC		164.5, qC[a]	
8	103.0, CH	6.89, d (2.2)	102.5, CH	6.80, d (2.2)
9	163.2, qC		158.1, qC[a]	
10	115.7, qC		117.0, qC	
1′	122.9, qC		125.0, qC	
2′	128.9, CH	7.31, d (2.3)	127.4, CH	7.19, d (1.9)
3′	121.9, qC		121.0, qC	
4′	153.4, qC		152.6, qC	
5′	122.9, CH	6.78, d (8.2)	116.0, CH	6.77, d (8.2)
6′	131.8, CH	7.36, dd (8.2, 2.2)	130.1, CH	7.26, dd (8.2, 2.2)
1″	116.6, CH_2	6.44, d (10)	122.2, CH_2	6.40, d (9.8)
2″	130.5, CH	5.73, d (10)	131.7, CH	5.71, d (9.8)
3″	77.0, qC		76.7, qC	
4″	28.2, CH_3	1.41, s	28.2, CH_3	1.42, s
5″	28.2, CH_3	1.41, s	28.2, CH_3	1.42, s

[a] The ^{13}C NMR assignment was corrected and confirmed by 2D NMR.

3.3.14. 8-Prenyldaidzein (49, known compound)

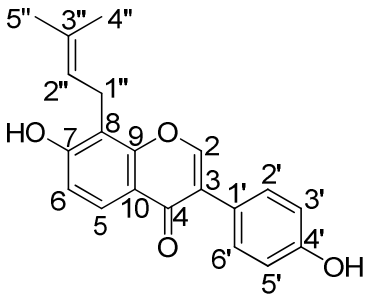

Molecular formula:	$C_{20}H_{18}O_4$
Molecular weight:	322.35
Amount:	4.1 mg

Compound **49** was isolated as a yellow amorphous powder. The ESI-MS spectrum (Figure 3.244) of **49** showed a negative pseudomolecular ion peak at *m/z* 321 $[M - H]^-$. The UV spectrum (Figure 3.242) of **49** exhibited intense maximum at 203, 252 and 306 nm, which was characteristic of an isoflavone. In the ^{1}H NMR spectrum (Figure 3.243), H-2 appeared as a singlet at δ_H 8.24. Signals at δ 1.83 (s), 1.65 (s), 3.57 (br d, J = 7.3 Hz), and 5.28 (tqq, J = 7.3, 1.6, 1.3 Hz) indicated the presence of a 3,3-dimethylally group. The attachment of the prenyl moiety at C-8 was confirmed by the HMBC spectrum (Figure 3.245) of **49** and the two *ortho*-coupled aromatic protons (δ 7.92 and 7.02) of A-ring. Comparing to the NMR data of the reference compound [Hakamatsuka *et al.*, 1991], compound **49** was confirmed to be **8-prenyldaidzein**.

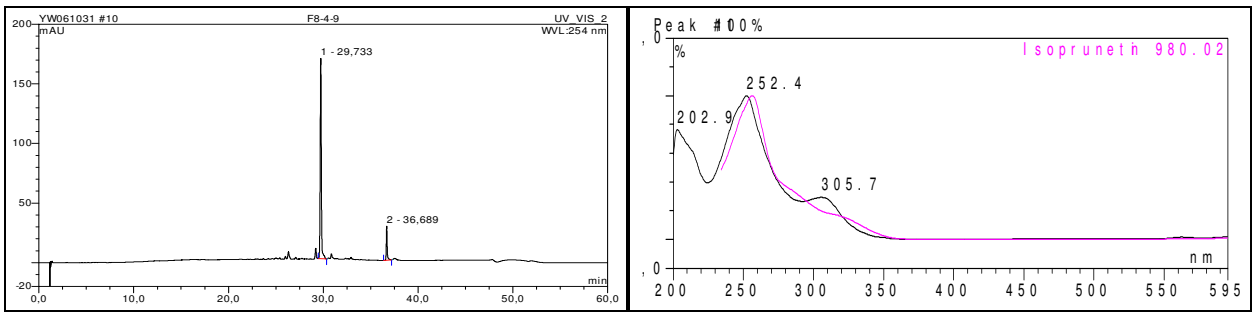

Figure 3.242 HPLC chromatogram and UV spectrum of compound **49**

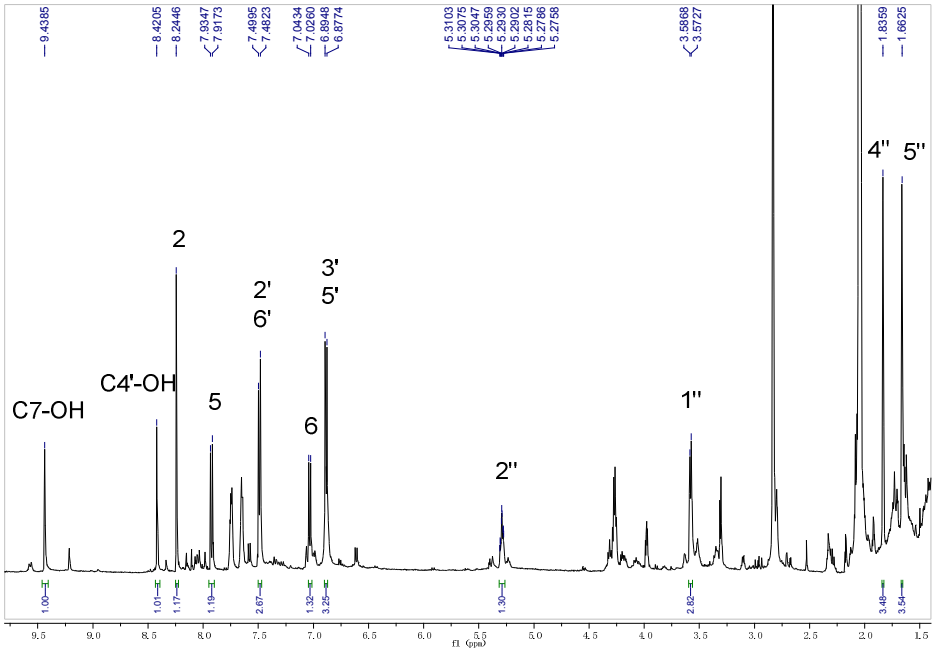

Figure 3.243 ^{1}H NMR spectrum of compound **49**

Table 3.53 NMR spectroscopic data of compound **49** (CD_3COCD_3, 500 MHz)

	8-Prenyldaidzein [Hakamatsuka *et al.*, 1991]	Compound **49**	
Position	δ_H (mult., *J* in Hz)	δ_C	δ_H (mult., *J* in Hz)
2	8.29, s	153.2, CH	8.24, s
3		130.8, qC	
4		176.1, qC	
5	7.97, d (8.6)	125.3, CH	7.92, d (8.8)
6	7.08, d (8.6)	116.4, CH	7.02, d (8.8)
7		159.9, qC	
8		116.4, qC	
9		156.6, qC	
10		118.8, qC	
1′		124.7, qC	
2′	7.54, d (8.5)	132.0, CH	7.48, dd (8.5)
3′	6.94, d (8.5)	115.8, CH	6.88, dd (8.5)
4′		158.0, qC	
5′	6.94, d (8.5)	115.8, CH	6.88, dd (8.5)
6′	7.54, d (8.5)	132.0, CH	7.48, dd (8.5)
1″	3.63, d (7.3)	, CH_2	3.57, br d (7.3)
2″	5.34, br t (7.3)	122.4, CH	5.28, tqq (7.3, 1.6, 1.3)
3″		132.6, qC	
4″	1.88, s	17.8, CH_3	1.83, s
5″	1.71, s	25.8, CH_3	1.65, s
C7-OH			9.43, s
C4′-OH			8.41, s

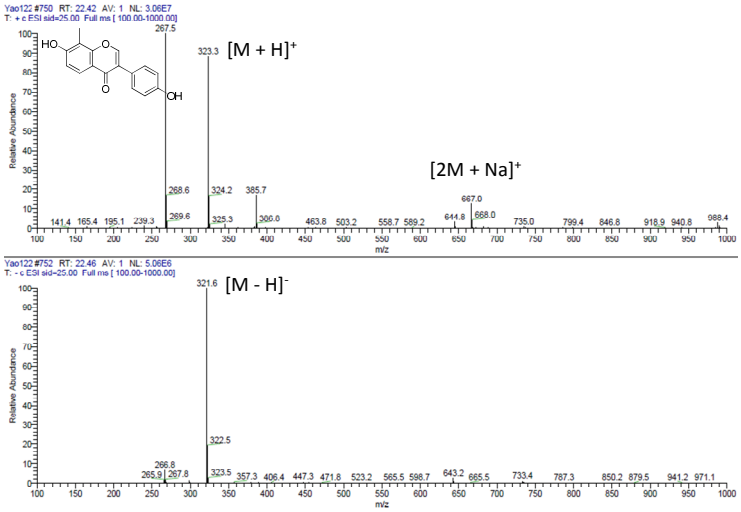

Figure 3.244 ESI-MS spectrum of compound **49**

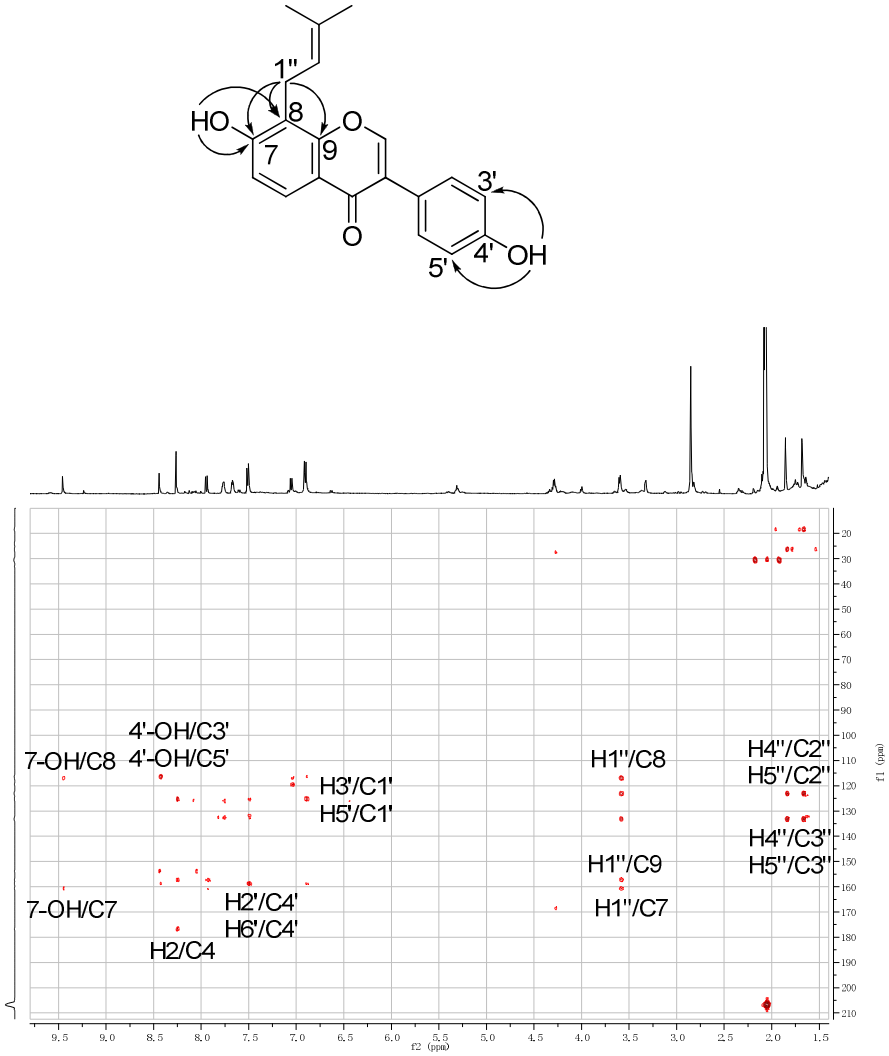

Figure 3.245 HMBC spectrum of compound **49**

3.3.15. Wighteone (50, known compound)

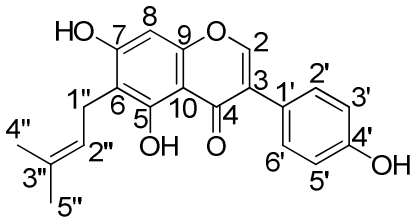

Molecular formula:	$C_{20}H_{18}O_5$
Molecular weight:	338.35
Amount:	0.4 mg

Compound **50** was obtained as pale yellow needles. The ESI-MS spectrum (Figure 3.248) revealed a pseudomolecular ion peak at *m*/*z* 337 $[M - H]^-$. The UV spectrum (Figure 3.247) of **50** showed absorption maximum at 202, 204 and 267 nm suggesting a typical isoflavone. The ^{1}H NMR spectrum (Figure 3.246) of **50** exhibited the presence of 4″,5″-dimethylallyl group, AA′BB′ aromatic protons assignable to the B-ring and a characteristic proton signal at δ 8.08 (H-2). The prenyl group was found to be located at C-6 by comparison of ^{1}H NMR chemical shifts of H-8 with those of related prenyl isoflavones. From above analysis, compound **50** was identified to be **wighteone** [Kinoshita *et al.*, 1990].

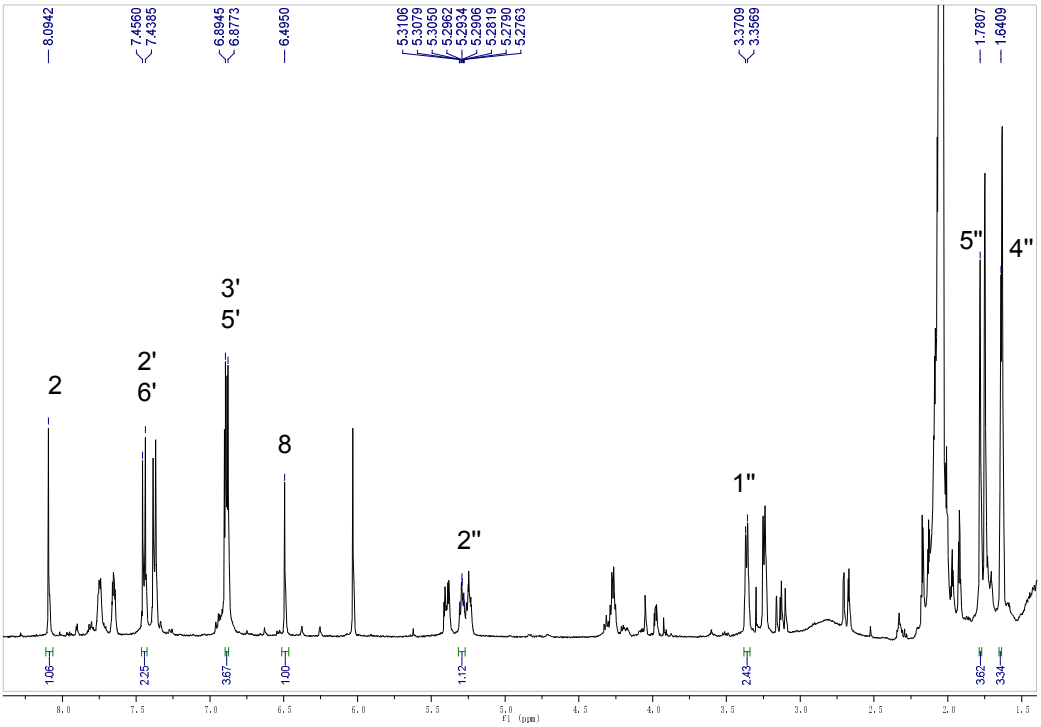

Figure 3.246 ^{1}H NMR spectrum of compound **50**

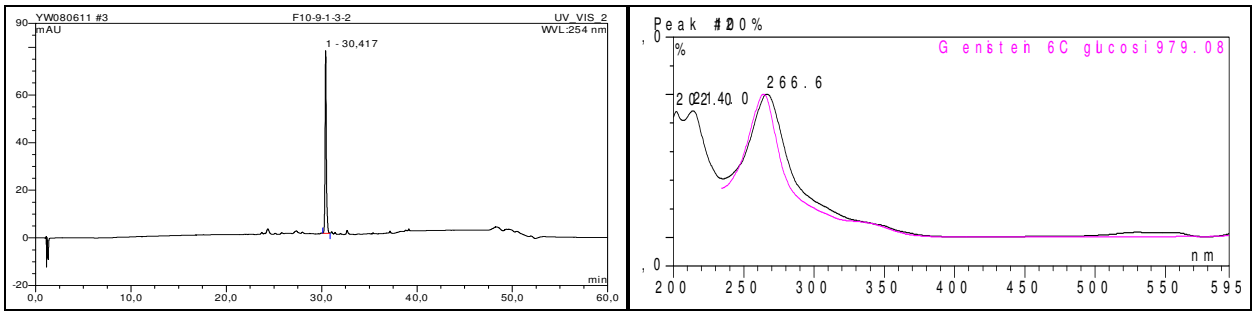

Figure 3.247 HPLC chromatogram and UV spectrum of compound **50**

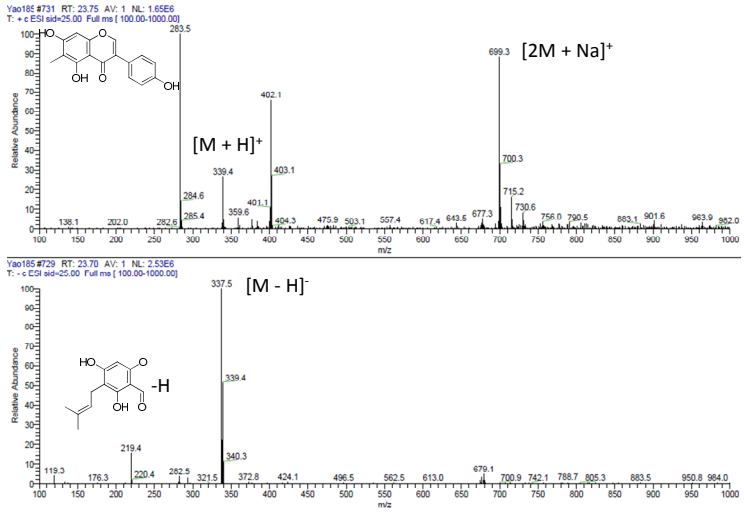

Figure 3.248 ESI-MS spectrum of compound **50**

Table 3.54 NMR spectroscopic data of compound **50** (CD_3COCD_3, 500 MHz)

	Wighteone (DMSO-d_6) [Kinoshita *et al.*, 1990]	Compound **50**
Position	δ_H (mult., *J* in Hz)	δ_H (mult., *J* in Hz)
2	8.10, s	8.08, s
8	6.49, s	6.49, s
2′	7.44, d (8.5)	7.44, d (8.5)
3′	6.89, d (8.5)	6.88, d (8.5)
5′	6.89, d (8.5)	6.88, d (8.5)
6′	7.44, d (8.5)	7.44, d (8.5)
1″	3.35, br d (8)	3.35, br d (7.1)
2″	5.27, br t (8)	5.28, tq (7.1, 1.6)
4″	1.66, s	1.63, s
5″	1.78, s	1.77, s

3.3.16. Isowighteone (51, known compound)

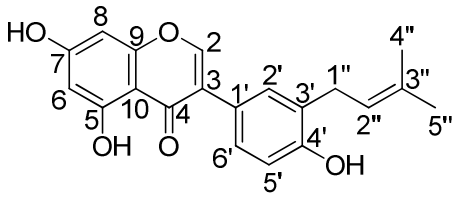

Molecular formula:	$C_{20}H_{18}O_5$
Molecular weight:	338.35
Amount:	0.4 mg

Compound **51** was obtained as a yellow powder and exhibited UV absorption maximum at 211 and 261 nm (Figure 3.250), which were similar to those of **50**. The molecular weight of **51** determined from the ESI-MS data (Figure 3.251) was the same as **50** deducing compound **51** was an isomer of **50**. In the ^{1}H NMR spectrum (Figure 3.249) of **51**, an ABX spin system [δ 7.32 (d, J = 2.2 Hz), 6.87 (d, J = 8.2 Hz) and 7.25 (dd, J = 8.2, 2.2 Hz)] was observed instead of an AA′BB′ system in **50**. Furthermore, a pair of *meta*-coupled aromatic protons [δ 6.33 (d, J = 2.1 Hz) and 6.22 (d, J = 2.1 Hz)] was found for A-ring. Comparing the NMR data of compound **51** with those of **isowighteone** [Tanaka *et al.*, 1997], it was revealed that two compounds were identical.

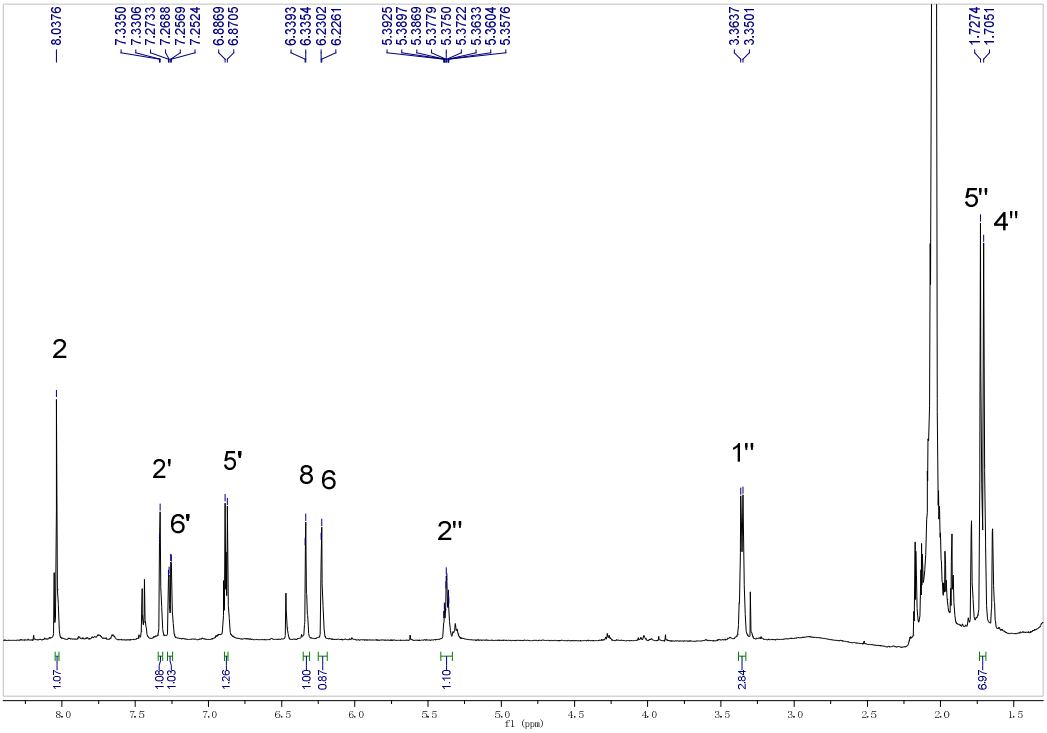

Figure 3.249 ^{1}H NMR spectrum of compound **51**

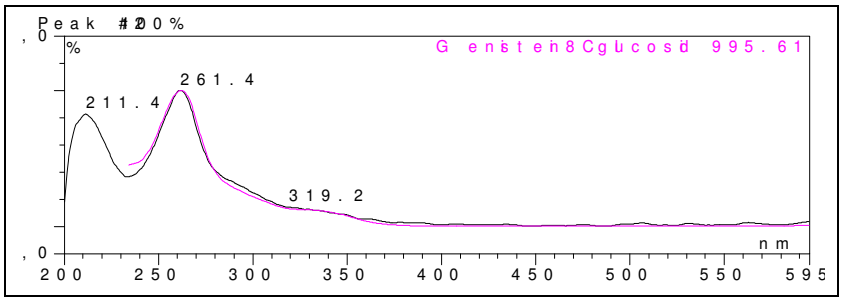

Figure 3.250 UV spectrum of compound **51**

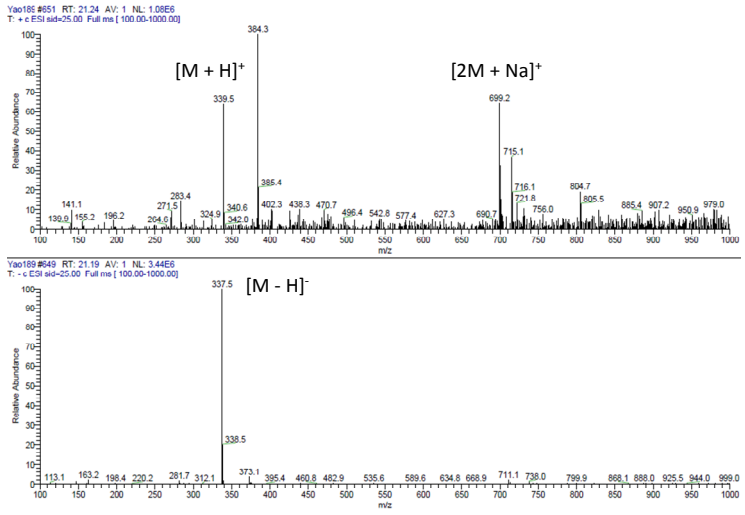

Figure 3.251 ESI-MS spectrum of compound **51**

Table 3.55 NMR spectroscopic data of compound **51** (CD_3COCD_3, 500 MHz)

	Isowighteone [Tanaka *et al.*, 1997]	Compound **51**
Position	δ_H (mult., *J* in Hz)	δ_H (mult., *J* in Hz)
2	8.12, s	8.03, s
6	6.28, d (2)	6.22, d (2.1)
8	6.41, d (2)	6.33, d (2.1)
2′	7.36, d (2)	7.32, d (2.2)
5′	6.89, d (8)	6.87, d (8.2)
6′	7.27, dd (8.2)	7.25, dd (8.2, 2.2)
1″	3.36, d (7)	3.35, br d (7.1)
2″	5.38, t-like m	5.36, tq (7.1, 1.3)
4″	1.72, br s	1.70, s
5″	1.73, br s	1.72, s

3.3.17. 7,2′,4′-Trihydroxy-3-arylcoumarin (52, new compound)

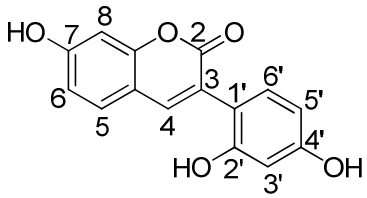

Molecular formula:	$C_{15}H_{10}O_5$
Molecular weight:	270.24
Amount:	0.6 mg

Compound **52** was isolated as an amorphous powder, and was shown to have the molecular formula $C_{15}H_{10}O_5$ as determined by HRESIMS data (*m/z* 271.0609 $[M + H]^+$). The UV spectrum of **52** (Figure 3.252) showed absorption maxima at 204, 218 and 248 nm, typical of a coumarin nucleus. The ^{1}H NMR spectrum of **52** (Figure 3.253) exhibited two ABX system [δ 7.89 (d, J = 8.8 Hz), 6.85 (dd, J = 8.8, 2.2 Hz) and 6.72 (d, J = 2.2 Hz); δ 6.99 (d, J = 1.9 Hz), 6.83 (dd, J = 8.8, 1.9 Hz) and 6.80 (d, J = 8.8 Hz)], which were further supported by analysis of the ^{1}H-^{1}H COSY spectrum of **52** (Figure 3.254). Moreover in the aromatic region, resonance for a proton singlet at δ_H 8.05 was observed. Comparing the ^{1}H NMR and mass spectra of **52** with those of the known compound 7,2′-dihydroxy-4′-methoxy-3-arylcoumarin indicated the subtraction of a CH_3 group for **52**. This difference was corroborated by the upfield shift of the H-3′ and H-5′ resonances of **52**, because of the disappearance of the inductive effect of the methoxy group at C-4′. From these results, the structure of compound **52** was concluded to be **7,2′,4′-trihydroxy-3-arylcoumarin**.

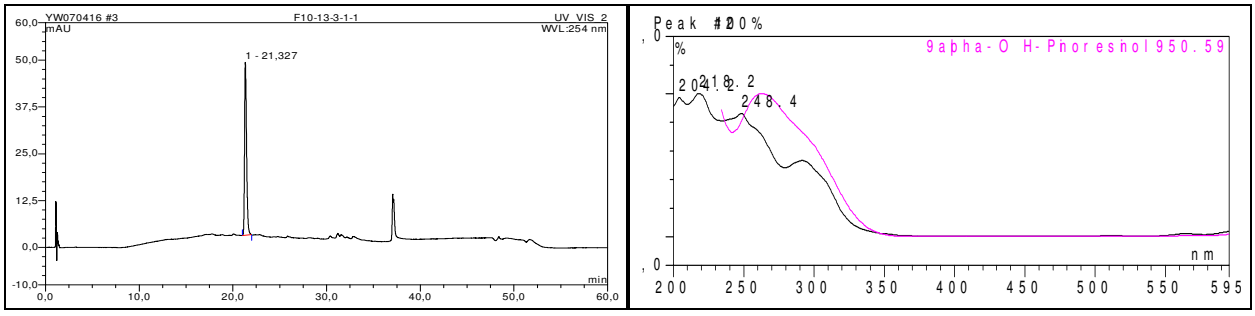

Figure 3.252 HPLC chromatogram and UV spectrum of compound **52**

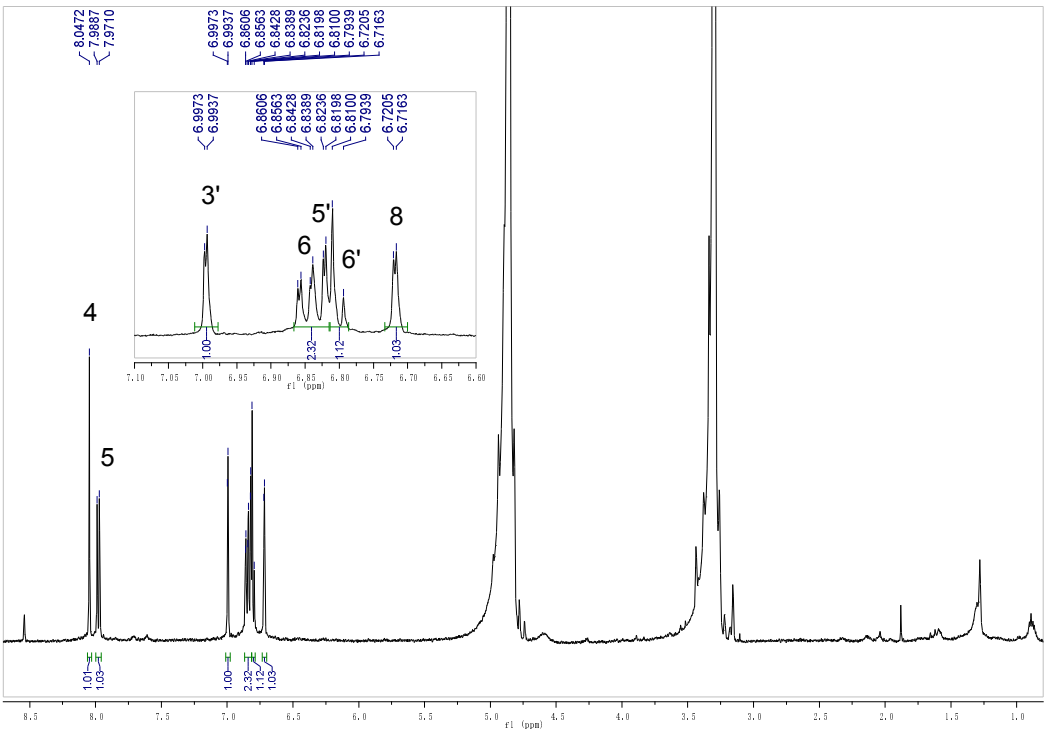

Figure 3.253 ^{1}H NMR spectrum of compound **52**

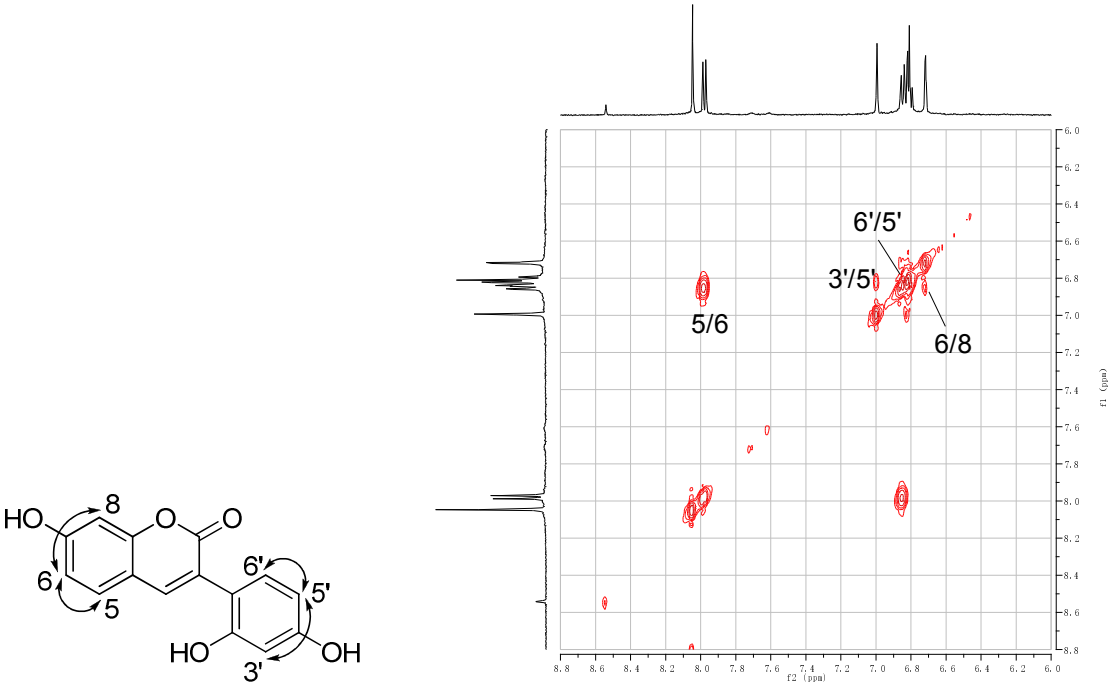

Figure 3.254 ^{1}H-^{1}H COSY spectrum of compound **52**

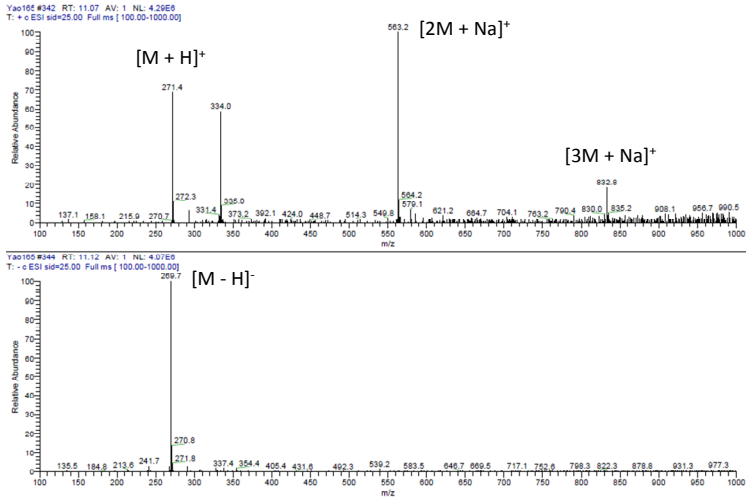

Figure 3.255 ESI-MS spectrum of compound **52**

Table 3.56 NMR spectroscopic data of compound **52** (CD_3OD, 500 MHz)

	Compound **52**	COSY
Position	δ_H (mult., *J* in Hz)	
4	8.05, s	
5	7.98, d (8.8)	6
6	6.85, dd (8.8, 2.2)	5, 8
8	6.72, d (2.2)	6
3′	6.99, d (1.9)	5′
5′	6.83, dd (8.8, 1.9)	3′, 6′
6′	6.80, d (8.8)	5′

3.3.18. Psoralidin (53, known compound)

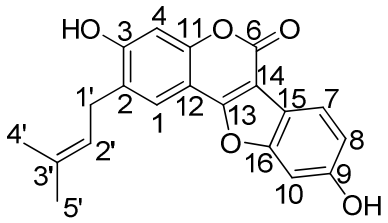

Molecular formula:	$C_{20}H_{16}O_5$
Molecular weight:	336.34
Amount:	61.3 mg

Compound **53** was isolated as a white amorphous powder. Its molecular weight was deduced from the ESI mass spectrum (Figure 3.259). The UV spectrum (Figure 3.256) of **53** exhibited absorption bands at λ_{max} 208, 244 and 347 nm consistent with the coumestan chromophore. The ^{1}H NMR spectrum (Figure 3.257) of **53** displayed an ABX system [δ 7.66 (d, J = 8.2 Hz), 6.92 (dd, J = 8.2, 1.9 Hz) and 7.16 (d, J = 1.9 Hz)], two aromatic singlets (δ 7.60 and 6.91) and one prenyl moiety. The ^{13}C NMR spectrum (Figure 3.258) of **53** revealed 20 carbon signals which were sorted into five aromatic methines, nine aromatic quaternary carbons, one carbonyl group, two olefinic carbons, two methyls and one methylene. The attachment of the prenyl group at C-2 was indicated from the HMBC correlations (Figure 3.260) of H-1′ with C-1 and C-2 respectivly. According to these data and through comparison with the literature [Yang *et al.*, 1996], compound **53** was concluded to be **psoralidin**.

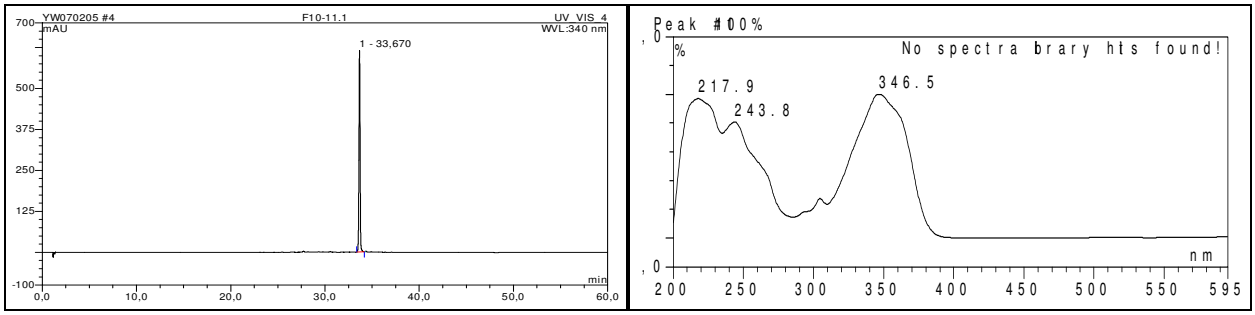

Figure 3.256 HPLC chromatogram and UV spectrum of compound **53**

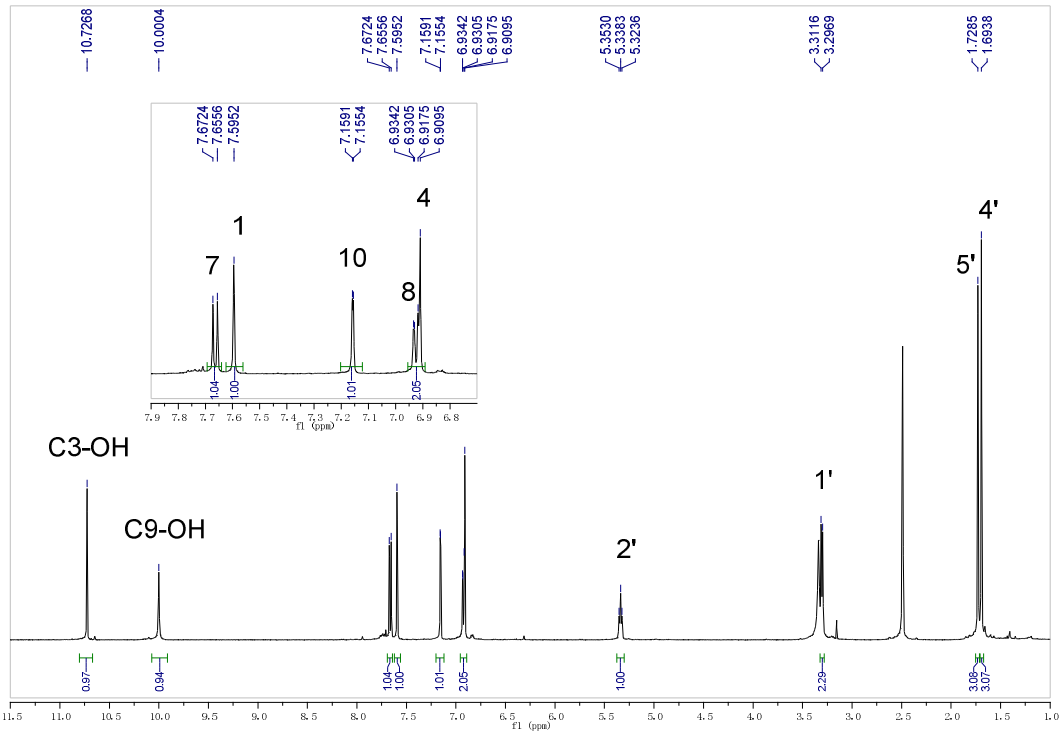

Figure 3.257 ^{1}H NMR spectrum of compound **53**

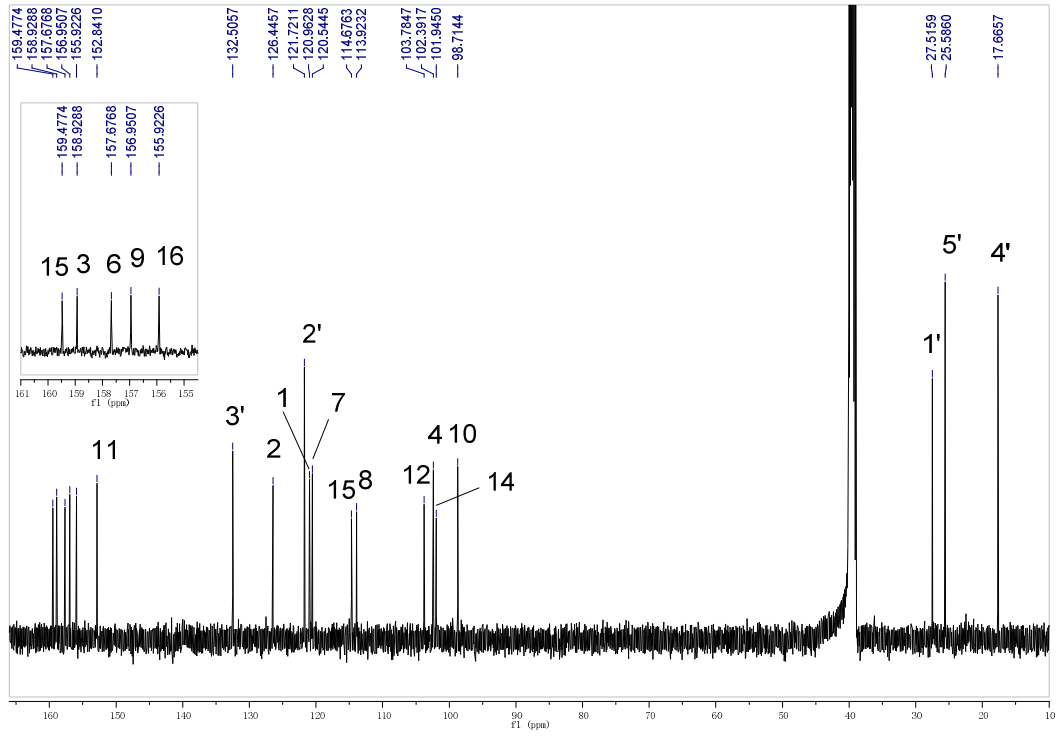

Figure 3.258 ^{13}C NMR spectrum of compound **53**

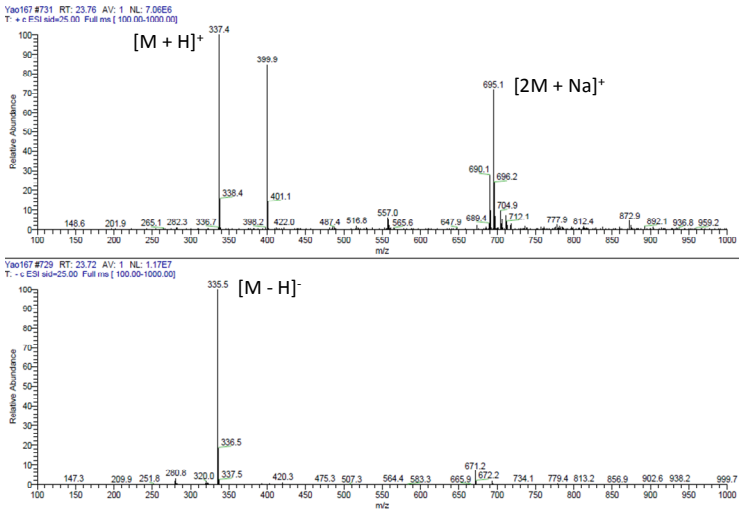

Figure 3.259 ESI-MS spectrum of compound **53**

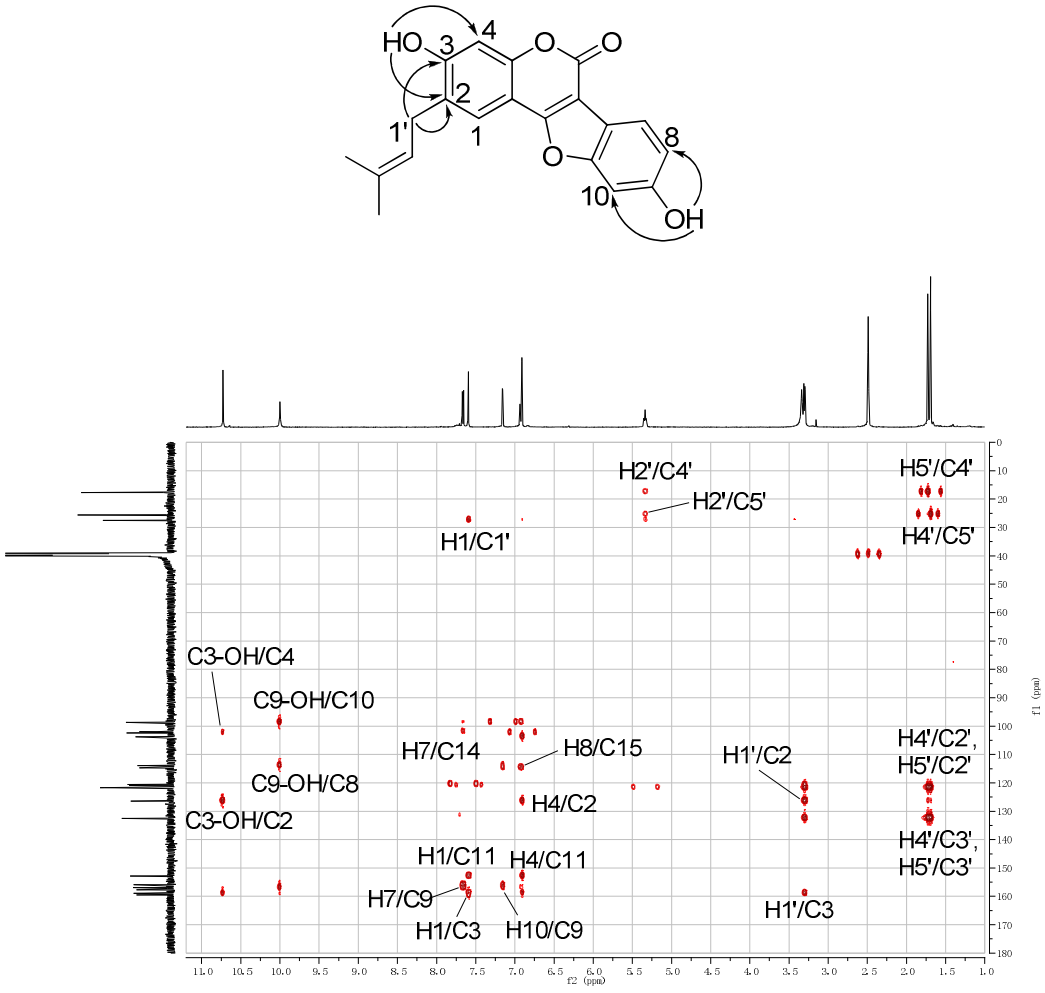

Figure 3.260 HMBC spectrum of compound **53**

Table 3.57 NMR spectroscopic data of compound **53** (DMSO-d_6, 500 MHz)

	Psoralidin [Yang *et al.*, 1996]		Compound **53**	
Position	δ_C	δ_H (mult., *J* in Hz)	δ_C	δ_H (mult., *J* in Hz)
1	121.3, CH	7.62, s	121.0, CH	7.60, s
2	126.4, qC		126.4, qC	
3	158.9, qC		158.9, qC	
4	102.7, CH	6.92, s	102.4, CH	6.91, s
6	157.6, qC		157.7, qC	
7	120.8, CH	7.68, d (8.4)	120.5, CH	7.66, d (8.2)
8	114.2, CH	6.93, dd (8.4, 1.9)	113.9, CH	6.92, dd (8.2, 1.9)
9	156.9, qC		156.9, qC	
10	99.0, CH	7.17, d (1.9)	98.7, CH	7.16, d (1.9)
11	152.8, qC		152.8, qC	
12	103.8, qC		103.8, qC	
13	159.4, qC		159.5, qC	
14	101.9, qC		101.9, qC	
15	113.9, qC		114.7, qC	
16	155.9, qC		155.9, qC	
1′	27.8, CH_2	3.32, br t (7.1)	27.5, CH_2	3.30, d (7.6)
2′	122.0, CH	5.35, m	121.7, CH	5.34, t (7.6)
3′	132.4, qC		132.5, qC	
4′	17.6, CH_3	1.70, s	17.7, CH_3	1.69, s
5′	25.8, CH_3	1.74, s	25.6, CH_3	1.73, s
C3-OH				10.73, s
C9-OH				10.00, s

3.3.19. Psoracoumestan (54, new compound)

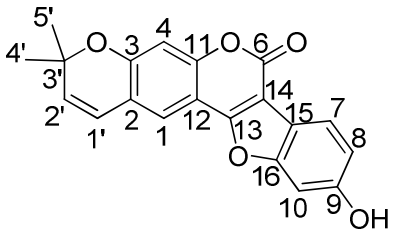

Molecular formula:	$C_{20}H_{14}O_5$
Molecular weight:	334.32
Amount:	0.4 mg

Compound **54** was obtained as colorless needles with the molecular formula $C_{20}H_{14}O_5$, as determined by HRESIMS (*m/z* 335.0909 $[M + H]^+$). The UV spectrum (Figure 3.261) indicated a coumestan structure, with absorption maxima at 207, 250 and 368 nm. The ^{1}H NMR spectrum of **54** showed one 2,2-dimethylchromene ring indicated by the signals at δ 1.44 (s, $CH_3 \times 2$), 6.62 (d, J = 9.9 Hz) and 5.92 (d, J = 9.9 Hz). In addition, resonances for an ABX system [δ 7.70 (d, J = 8.2 Hz), 6.95 (br d, J = 8.6 Hz) and 7.16 (br s)] and two singlet protons at δ 7.78 and 6.96 were observed, which implied the 2,2-dimethylchromene ring of **54** must be located at either C-2 or C-8. The substitution pattern of these functional groups was determined by comparison of the ^{1}H NMR data of **54** with other coumestan derivatives, such as psoralidin (**53**) [Yang *et al.*, 1996] and sophoracoumestan A (Figure 3.264) [Komatsu *et al.*, 1981]. If the 2,2-dimethylchromene ring is located at C-8, the proton signals of the ABX spin system of **54** would be similar to those of H-1, H-2 and H-4 in sophoracoumestan A. However, such signals of **54** were almost identical to those of H-7, H-8 and H-10 in psoralidin. Therefore, 2,2-dimethylchromene was located at C-2, which was corroborated by the 0.18 ppm downfield shift of the H-1 resonance of **54** as compared to that of psoralidin. Moreover, psoralidin (**53**) was also isolated from the same extract, and is considered to be the precursor of **54** in the biosynthetic pathway, which supported the structure of **54**. From above spectral data and biosynthetic considerations, the structure of compound **54** was concluded to be **psoracoumestan**.

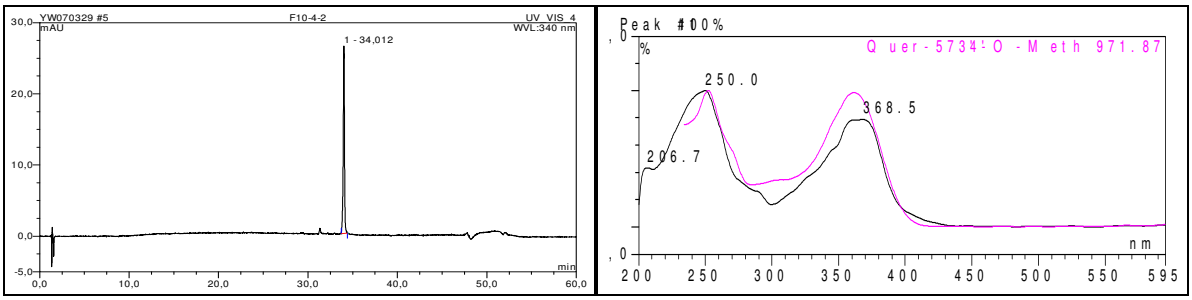

Figure 3.261 HPLC chromatogram and UV spectrum of compound **54**

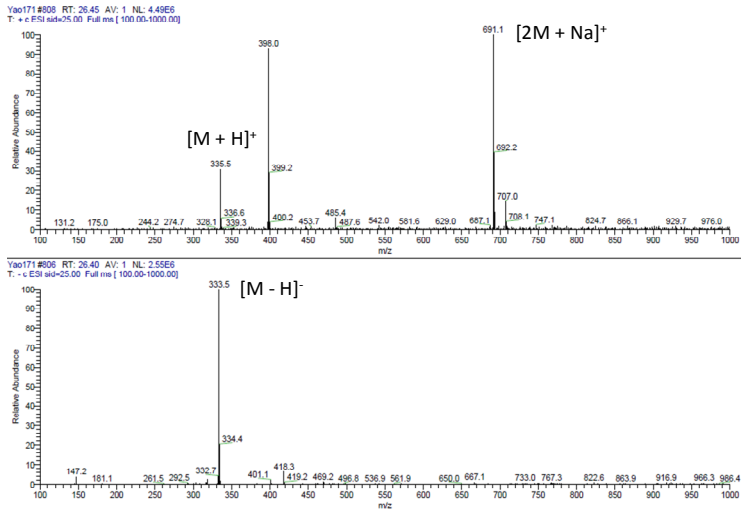

Figure 3.262 ESI-MS spectrum of compound **54**

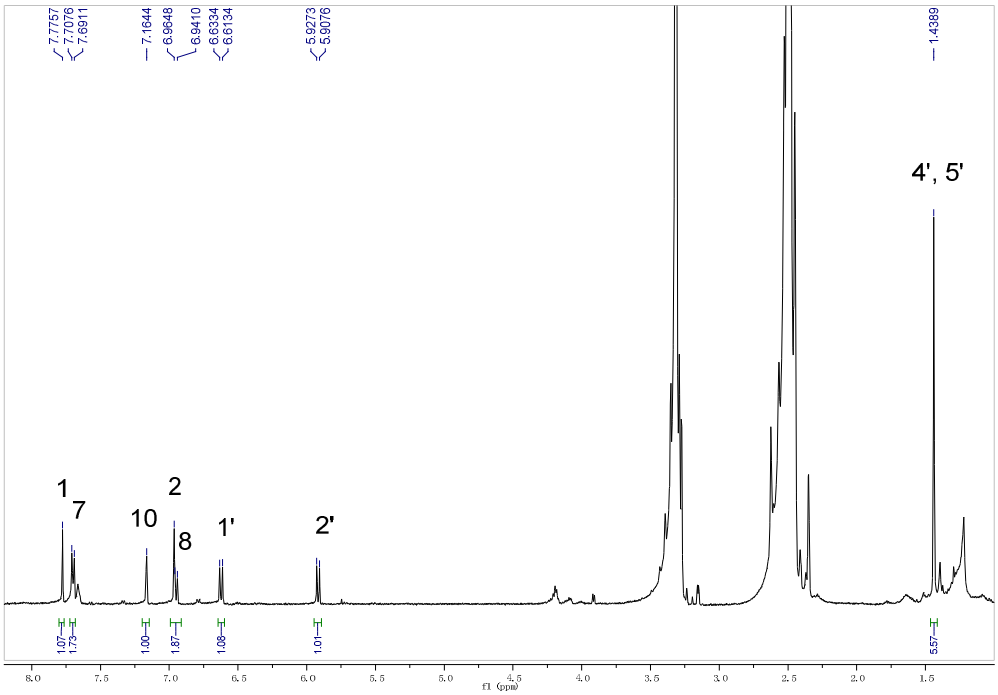

Figure 3.263 ^{1}H NMR spectrum of compound **54**

Table 3.58 NMR spectroscopic data of compound **54** (DMSO-d_6, 500 MHz)

	Compound **54**
Position	δ_H (mult., *J* in Hz)
1	7.78, s
4	6.96, s
7	7.70, d (8.2)
8	6.95, br d (8.6)
10	7.16, br s
1′	6.62, d (9.9)
2′	5.92, d (9.9)
4′	1.44, s
5′	1.44, s

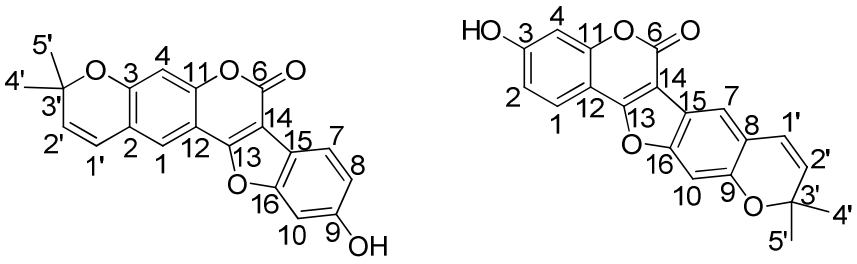

54 sophoracoumestan A

Figure 3.264 The structure of compound **54** and sophoracoumestan A

3.3.20. Bakuchiol (55, known compound)

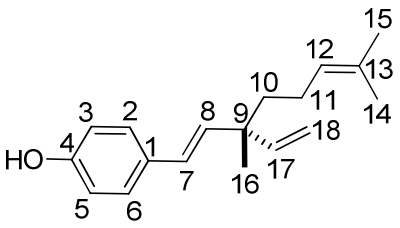

Molecular formula:	$C_{18}H_{24}O$
Molecular weight:	256.38
Amount:	323.5 mg

Compound **55** was obtained as oil with UV absorption maximum at 209 and 261 nm (Figure 3.265). The ^{1}H NMR spectrum (Figure 3.266) of **55** showed the presence of a set of *trans* double bond and an AA′BB′ spin system in the down-field. Along with ^{13}C NMR (Figure 3.267) and DEPT (Figure 3.268) spectra, six olefinic carbons, three methyls, two methylenes and one quaternary carbon were deduced. The assignments were further supported by analysis of the ^{1}H-^{1}H COSY (Figure 3.270) and HMBC spectra (Figure 3.269) of **55**. A pair of geminal coupled olefinic proton at δ 5.04 and 5.01 gave COSY cross-peaks with the olefinic methine at δ 5.88 (dd, J = 17.3, 10.7 Hz) indicating a terminal double bond. The attachment of this group at C-9 was shown from the HMBC cross-peaks of the signal at δ_H 5.88 (H-17) with the methylene at δ_C 41.3 (C-10) and the olefinic methine at δ_C 135.8 (C-7), respectively. Comparison of the ^{1}H and ^{13}C NMR resonances of **bakuchiol** [Labbe *et al.*, 1996] with those of compound **55** indicated that both compounds were identical.

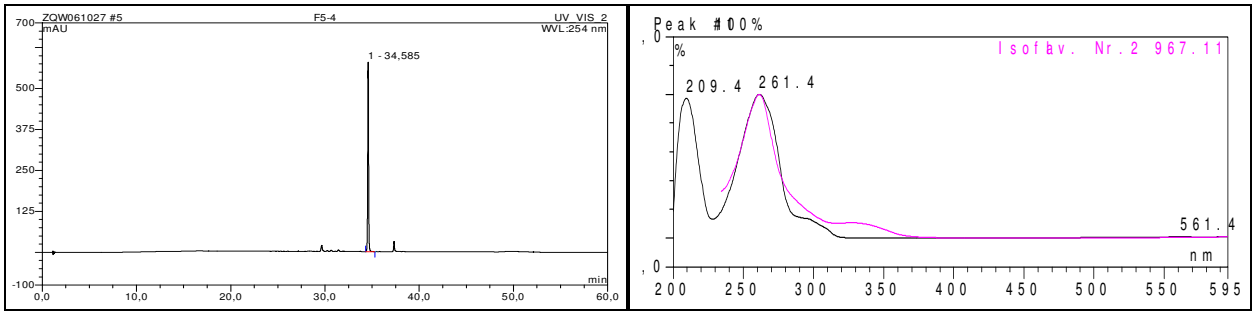

Figure 3.265 HPLC chromatogram and UV spectrum of compound **55**

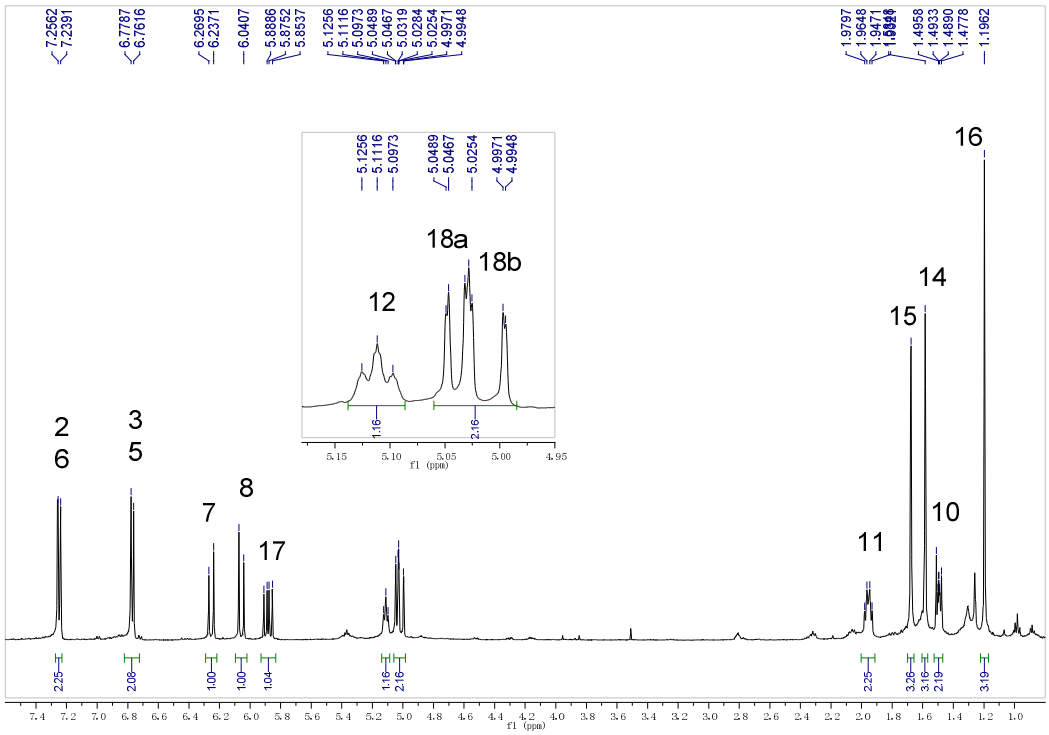

Figure 3.266 ^{1}H NMR spectrum of compound **55**

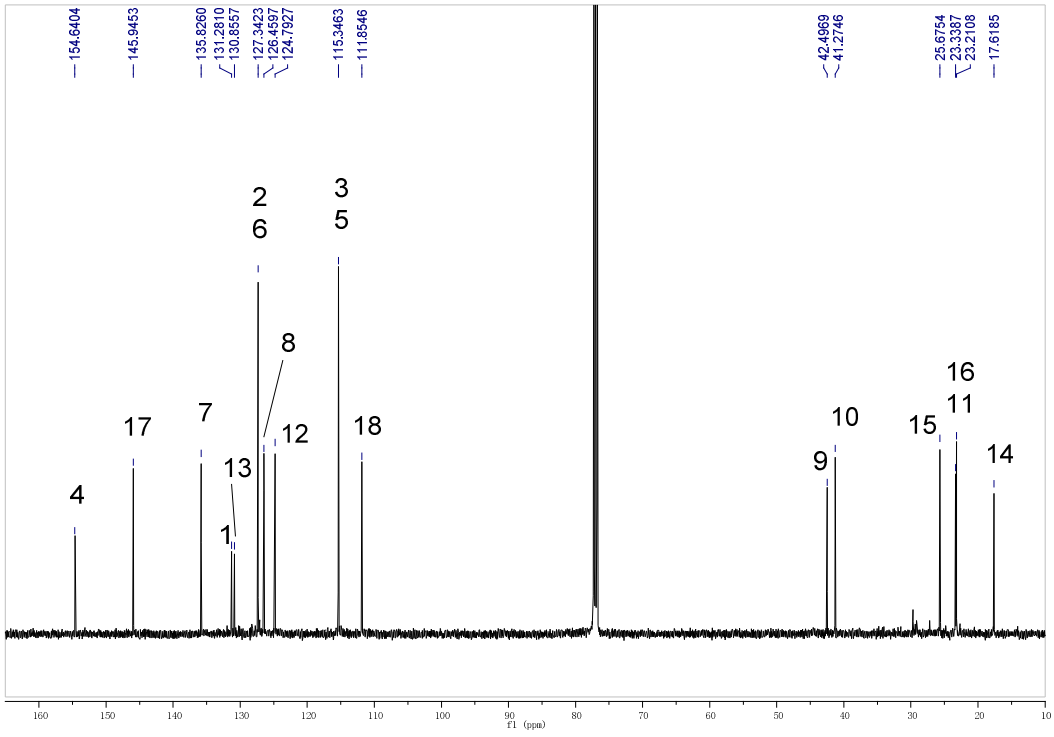

Figure 3.267 ^{13}C NMR spectrum of compound **55**

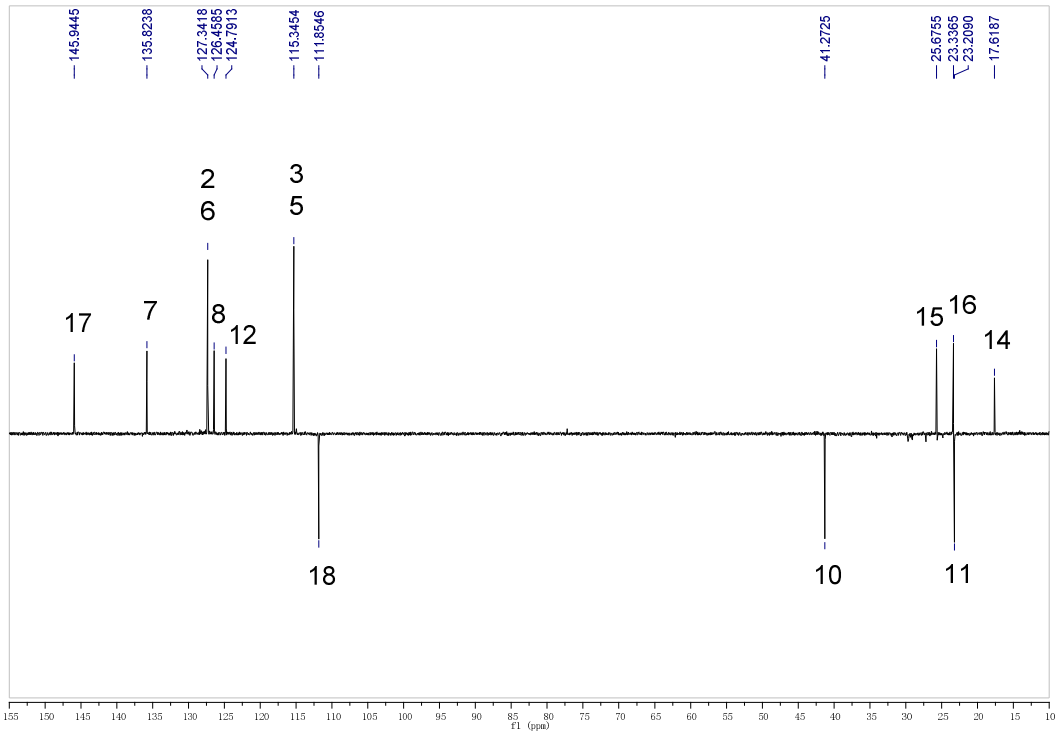

Figure 3.268 DEPT spectrum of compound **55**

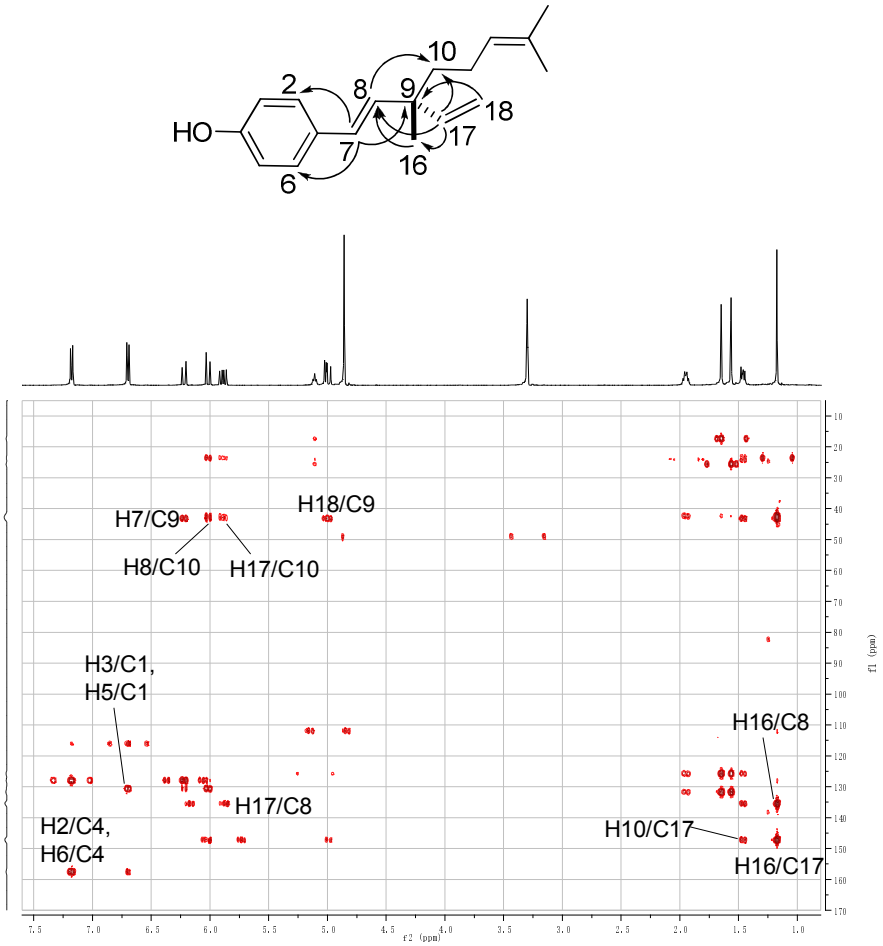

Figure 3.269 HMBC spectrum of compound **55**

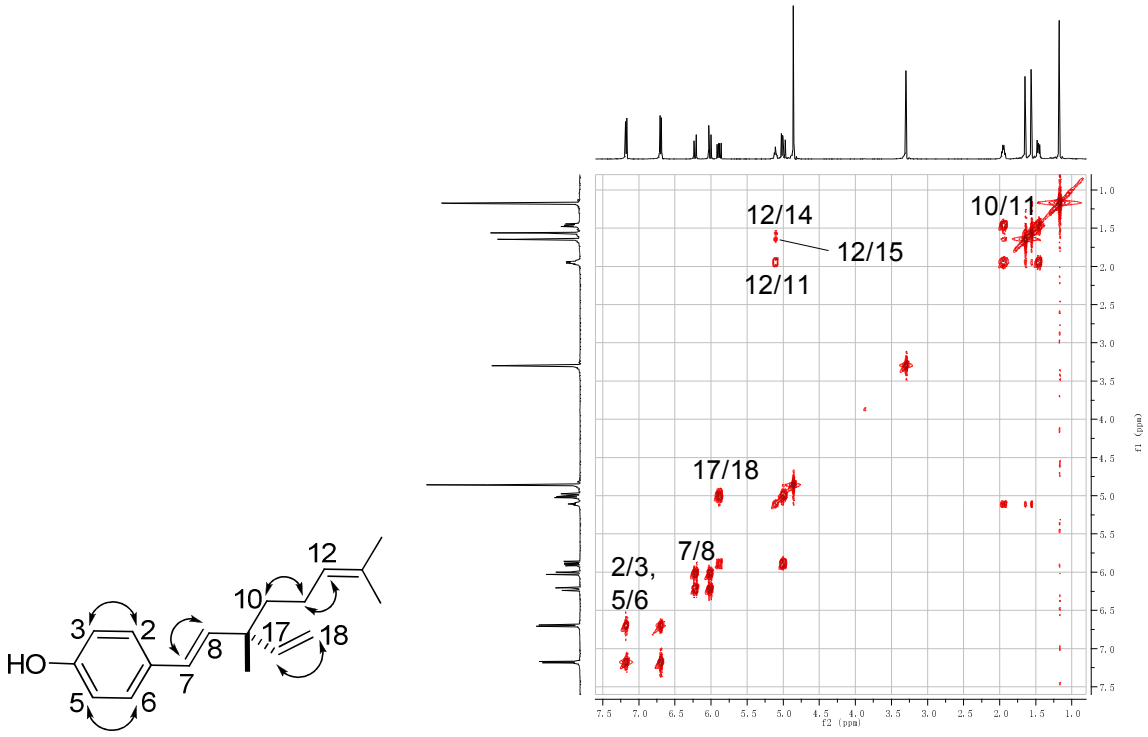

Figure 3.270 ^{1}H-^{1}H COSY spectrum of compound **55**

Table 3.59 NMR spectroscopic data of compound **55** ($CDCl_3$, 500 MHz)

	Bakuchiol [Labbe *et al.*, 1996]		Compound **55**	
Position	δ_C	δ_H (mult., *J* in Hz)	δ_C	δ_H (mult., *J* in Hz)
1	131.7, qC		131.3, qC	
2	127.4, CH	7.22, d (7.2)	127.3, CH	7.25, d (8.5)
3	115.4, CH	6.74, d (7.2)	115.3, CH	6.77, d (8.5)
4	154.5, qC		154.6, qC	
5	115.4, CH	6.74, d (7.2)	115.3, CH	6.77, d (8.5)
6	127.4, CH	7.22, d (7.2)	127.3, CH	7.25, d (8.5)
7	135.9, CH	6.23, d (16.2)	126.5, CH[a]	6.25, d (16.3)
8	126.5, CH	6.03, d (16.2)	135.8, CH[a]	6.06, d (16.3)
9	42.5, qC		42.5, qC	
10	41.3, CH_2	1.93, m	41.3, CH_2	1.49, m
11	23.3, CH_2	1.47, m	23.2, CH_2	1.96, dd (16.4, 7.3)
12	124.8, CH	5.09, bt	124.8, CH	5.11, tq (7.3, 1.6)
13	131.4, qC		130.9, qC	
14	17.7, CH_3	1.65, s	17.6, CH_3	1.58, br s
15	25.7, CH_3	1.56, s	25.7, CH_3	1.68, br s
16	23.4, CH_3	1.17, s	23.3, CH_3	1.20, s
17	146.0, CH	5.86, dd (17.3, 10.9)	145.9, CH	5.88, dd (17.3, 10.7)
18	111.9, CH_2	4.98, m	111.9, CH_2	5.04, dd (10.7, 1.3); 5.01, dd (17.3, 1.3)

[a] The ^{13}C NMR assignment was corrected and confirmed by 2D NMR.

3.3.21. Bioactivity test results for compounds isolated from *Psoralea corylifolia*

All isolated compounds from *Psoralea corylifolia* (**26–45**) were tested for their cytotoxic activities by MTT-assay on H4IIE, Hct-116, and C6 cell lines**.** The EC_{50} values are exhibited in Table 3.60. Some of them were further determined for their apoptotic potentials and necrotic potentials by ApoONE assay (caspase 3/7 assay) and LDH-assay respectively (Figure 3.271 and Figure 3.272). Moreover, some compounds were also measured in TEAC-assay for monitoring the antioxidant capacity which is exhibited in Figure 3.273.

Twelve isolated compounds were also evaluated for their protein kinase inhibitory profiles. The results are presented as residual activity in Table 3.61. Seven compounds which showed an inhibition of ≥ 40 % with at least one kinase were selected for IC_{50} determination. The data are shown in Table 3.62.

Table 3.60 EC_{50} (μM) in MTT-assay (H4IIE) for the isolated compounds from *Psoralea corylifolia*

compound	EC_{50} (μM)			
	H4IIE (24 h)	**H4IIE (48 h)**	**Hct 116**	**C6**
isobavachalcon (**36**)	50	18		
isobavachromene (**37**)	22	22		
psorachalcone A (**38**)	> 50		> 50	> 50
bakuchalcone (**39**)	> 50		> 50	> 50
xanthoangelol (**40**)	40		27	35
corylifol C (**41**)	> 50		> 50	> 50
broussochalcone B (**42**)	12	9		
bavachromene (**43**)	35		17	50
bavachalcone (**44**)	10	10		
bavachin (**45**)	35	35		
6-prenylnaringenin (**46**)	23		25	36
neobavaisoflavone (**47**)	170	125		
corylin (**48**)	38		37.5	> 50
8-prenyldaidzein (**49**)	n.d.	n.d.		
wighteone (**50**)	48		41	> 50
isowighteone (**51**)	22		17	30
7,2′,4′-trihydroxy-3-arylcoumarin (**52**)	48		48	> 50
psoralidin (**53**)	30	10		
psoracoumestan (**54**)	> 50		> 50	> 50
bakuchiol (**55**)	12	8		

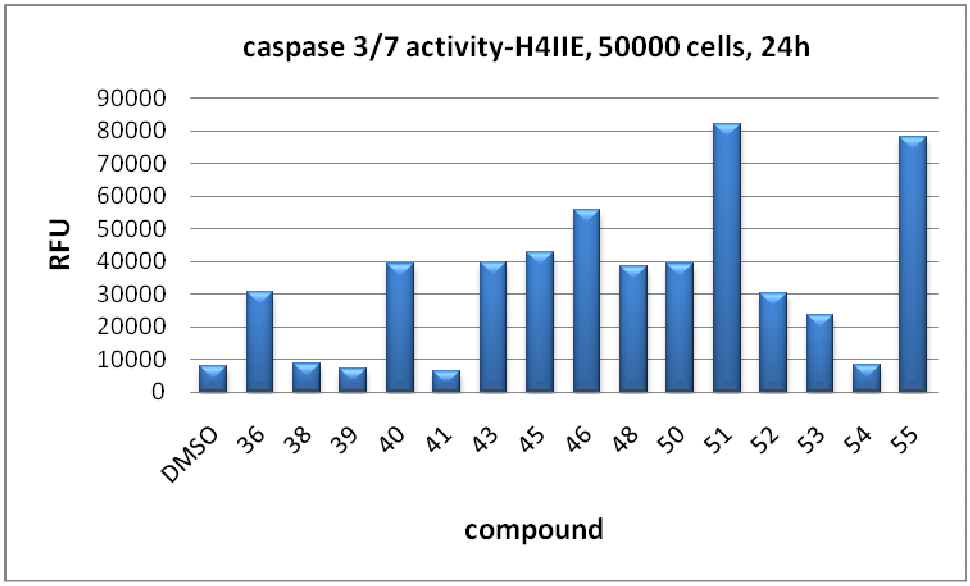

Figure 3.271 Apoptosis result (ApoONE caspase 3/7 assay) in 25 μM for 24 h of some isolated compounds from *Psoralea corylifolia*

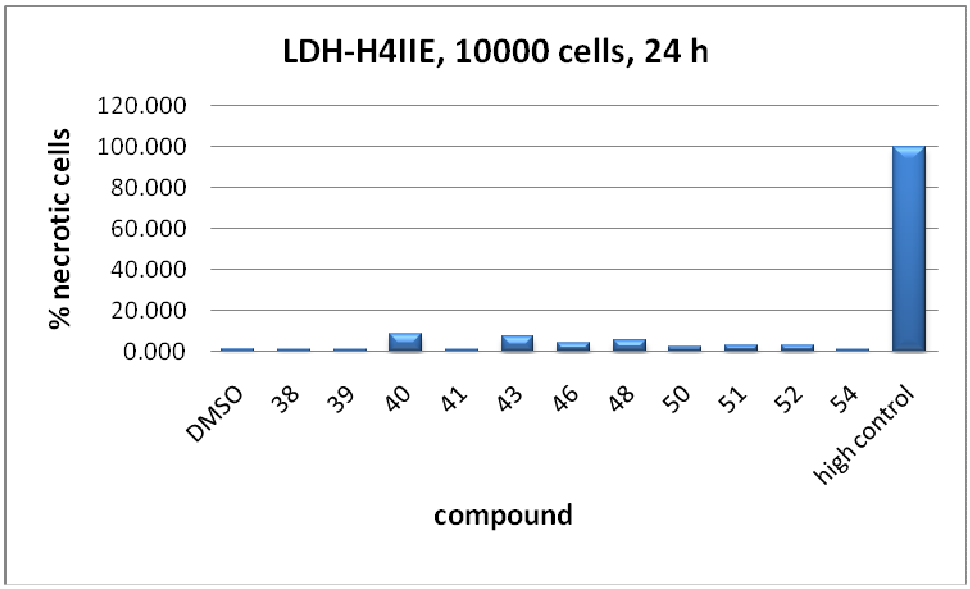

Figure 3.272 Necrosis results (LDH assay) in 25 μM for 24 h of some isolated compounds from *Psoralea corylifolia*

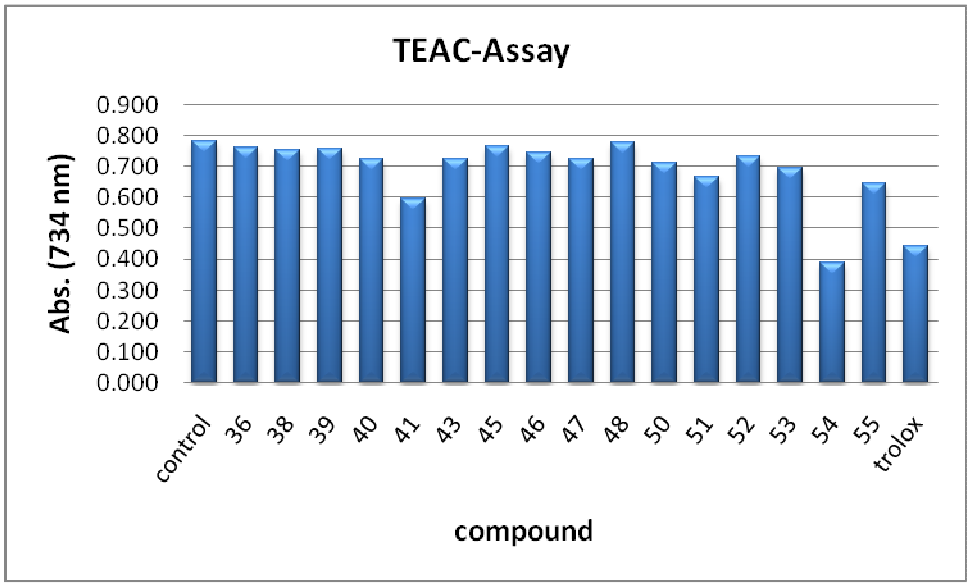

Figure 3.273 Results of TEAC-Assay for the isolated compounds from *Psoralea corylifolia*

Table 3.61 Selectivity profiling of compounds isolated from *Psoralea corylifolia* using 24 protein kinases

		Residual activities (% of control activity)											
	Compound	**36***	**38**	**40***	**41***	**42**	**44***	**45**	**46**	**47**	**49***	**53***	**55***
Protein kinase	AKT1	97	98	98	90	69	74	105	99	107	75	108	107
	ARK5	66	99	95	75	99	104	110	96	93	97	95	108
	Aurora-A	40	80	64	47	76	77	81	73	75	107	87	59
	Aurora-B	68	73	49	33	69	70	87	71	84	73	62	75
	AXL		92	98	76	93	85		101		96	89	
	B-RAF-VE	156	103	109	84	96	106	120	102	134	107	107	142
	CDK2/CycA	101	101	111	82	99	116	95	98	105	98	95	98
	CDK4/CycD1	88	104	66	68	96	53	96	94	98	74	115	84
	CK2-alpha1	104	98	104	88	90	92	101	93	106	103	95	107
	COT	111	102	106	87	100	94	99	101	106	100	99	85
	EGF-R	72	77	82	27	69	79	91	84	95	56	72	87
	EPHB4	115	83	87	71	85	83	106	87	92	75	74	105
	ERBB2	104	83	78	66	89	82	96	88	60	84	99	103
	FAK	121	83	109	81	101	92	109	108	117	92	97	102
	IGF1-R	116	88	106	58	95	104	103	110	93	65	79	96
	INS-R	83	97	91	55	93	88	100	89	98	93	89	113
	MET	88	98	79	75	82	91	95	88	101	101	89	80
	PDGFR-beta	85	90	86	60	76	72	92	94	92	94	87	93
	PLK1	97	112	100	96	104	116	109	101	90	92	80	82
	PRK1		99	106	69	98	103		100		101	81	
	SAK	109	101	109	42	91	118	106	101	111	93	74	103
	SRC	130	84	81	34	84	81	101	99	92	53	57	107
	TIE2	97	81	81	37	89	93	106	97	107	62	57	114
	VEGF-R2	100	81	79	52	64	67	91	89	101	67	67	92
	VEGF-R3	113						108		115			109
	FLT3	68						90		93			53
	IC_{50}		73	49	27	64	53		71		53	57	

*showing at least 40 % inhibition at 1 μg/mL with at least one of 24 kinases

Table 3.62 IC_{50} profiling of four selected compounds using 24 protein kinases (variable highest molar concentration)

		IC_{50} values (M)						
		36	**40**	**41**	**44**	**49**	**53**	**55**
Protein kinase	AKT1	A	A	2.3E-05	A	A	A	A
	ARK5	A	A	8.7E-06	A	A	A	A
	Aurora-A	1.9E-06	4.3E-06	3.0E-06	8.4E-06	2.2E-05	A	3.5E-06
	Aurora-B	1.6E-06	4.1E-06	2.1E-06	1.1E-05	2.0E-05	A	3.8E-06
	AXL		2.0E-05	6.4E-06	1.6E-05	A	A	
	B-RAF-VE	A	A	4.5E-06	A	A	A	A
	CDK2/CycA	A	A	1.2E-05	A	A	A	A
	CDK4/CycD1	7.8E-06	A	6.2E-06	2.3E-05	A	A	A
	CK2-alpha1	A	A	2.4E-05	A	A	A	A
	COT	6.2E-06	A	1.3E-05	A	A	A	A
	TIE2	7.8E-06	A	2.3E-06	1.6E-05	2.7E-05	A	A
	EGF-R	5.1E-06	4.4E-06	1.2E-06	4.4E-06	5.9E-06	2.7E-05	4.2E-06
	EPHB4	A	A	5.1E-06	2.1E-05	2.6E-05	A	A
	ERBB2	A	1.1E-05	4.2E-06	1.3E-05	2.3E-05	A	A
	FAK	A	A	1.1E-05	A	A	A	A
	IGF1-R	A	2.2E-05	3.6E-06	A	7.0E-06	A	8.7E-06
	INS-R	A	A	3.1E-06	2.2E-05	A	A	A
	MET	A	A	6.0E-06	2.5E-05	A	A	A
	PDGFR-beta	A	A	4.5E-06	8.3E-06	A	A	A
	PLK1	A	A	9.5E-06	A	A	A	A
	PRK1		2.3E-05	4.7E-06	1.8E-05	A	A	
	SAK	5.5E-06	2.0E-05	1.6E-06	2.0E-05	5.4E-06	A	8.7E-06
	SRC	A	2.3E-05	1.8E-06	2.1E-05	7.8E-06	A	A
	VEGF-R2	5.8E-06	1.6E-05	3.0E-06	1.3E-05	1.2E-05	A	A
	VEGF-R3	7.8E-06						A
	FLT3	3.4E-06						9.4E-06

A above maximal molar assay concentration of compound

moderately active

active

4. Discussion

4.1. Metabolites isolated from the Mongolian medicinal plant *Scorzonera radiata*

4.1.1. Biosynthesis of dihydrostilbene derivatices

So far only seven stilbene derivatives were reported from *Scorzonera* spp. [Wang *et al.*, 2009]. Among those, six were isolated from *S. humilis* as dihydrostilbene glycosides [Zidorn *et al.*, 2003], and the residual one is a stilbene from *S. tomentosa* [Sari *et al.*, 2007]. The dihydrostilbene derivatives from *S. humilis* are closely related to scorzodihydrostilbenes A–E (**1**–**5**).

Stilbenes are natural products in which a cinnamoyl-CoA C_6C_3 precursor from the shikimate pathway has acted as a starter unit. 4-Hydroxycinnamoyl-CoA is chain extended with three molecules of malonyl-CoA. This initially gives a polyketide chain, which is folded according to the nature of the enzyme responsible. Then it allows aldol reaction catalysed by stilbene synthase to occur thus generating an aromatic ring. The carbonyl carbon of the cinnamoyl group is incorporated into the aromatic ring [Dewick, 2001]. Alike compounds **1**–**5**, all the reported stilbene derivatives from *Scorzonera* spp. have a carbonyl function in B-ring introduced by malonyl-CoA. However, in general a decarboxylation reaction takes place during which the terminal carboxyl of stilbenes is lost, like in resveratrol [Dewick, 2001]. Thus it is suggested that the acetyl group substituting the B-ring is introduced afterwards. Based on above hypothesis, the supposed biosynthetic pathway of the new dihydrostilbene derivatives of *S. radiata* is suggested in Figure 4.1. Moreover, the biosynthetic relationships of scorzodihydrostilbenes A–E are shown in Figure 4.2.

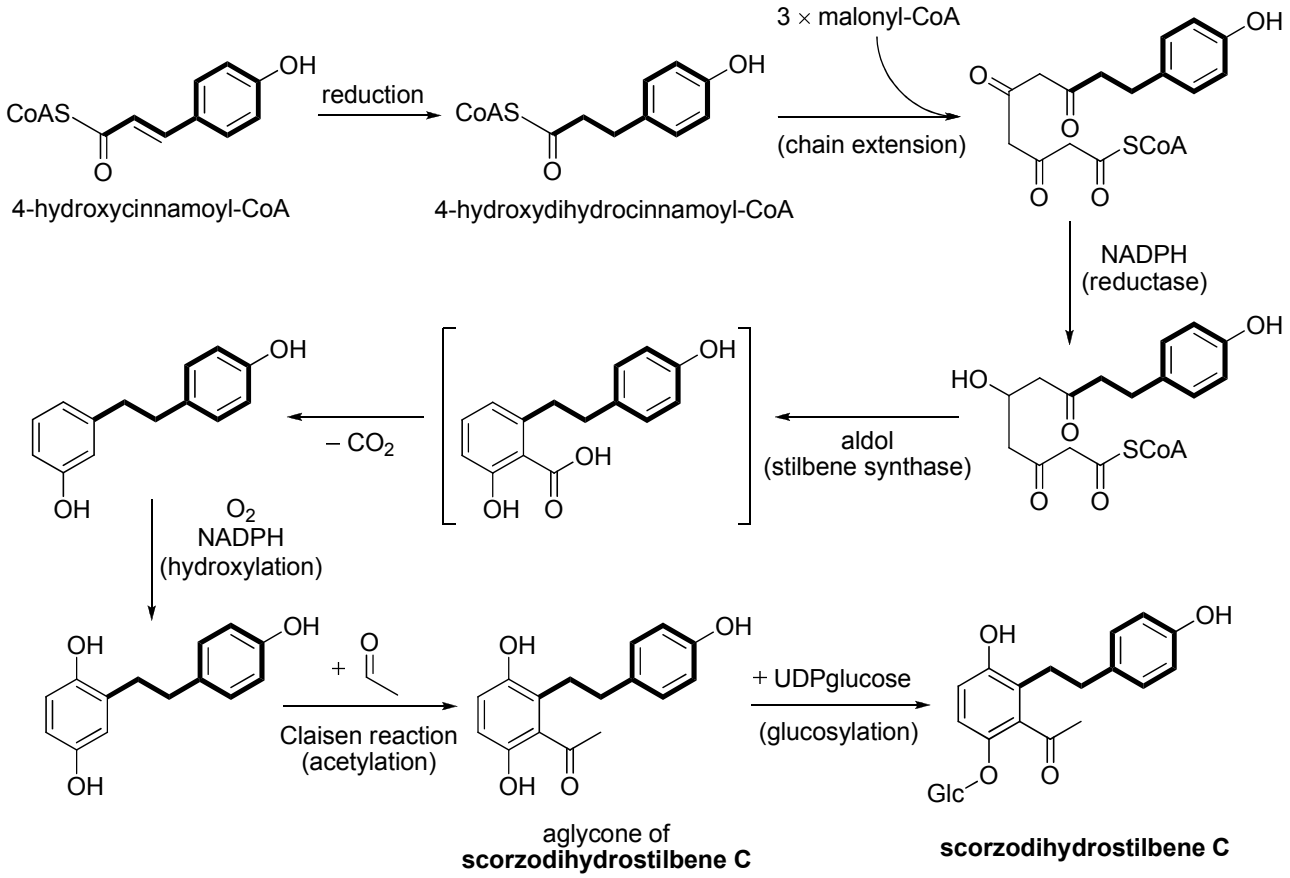

Figure 4.1 Suggested biosynthetic pathway of scorzodihydrostilbene C (**3**)

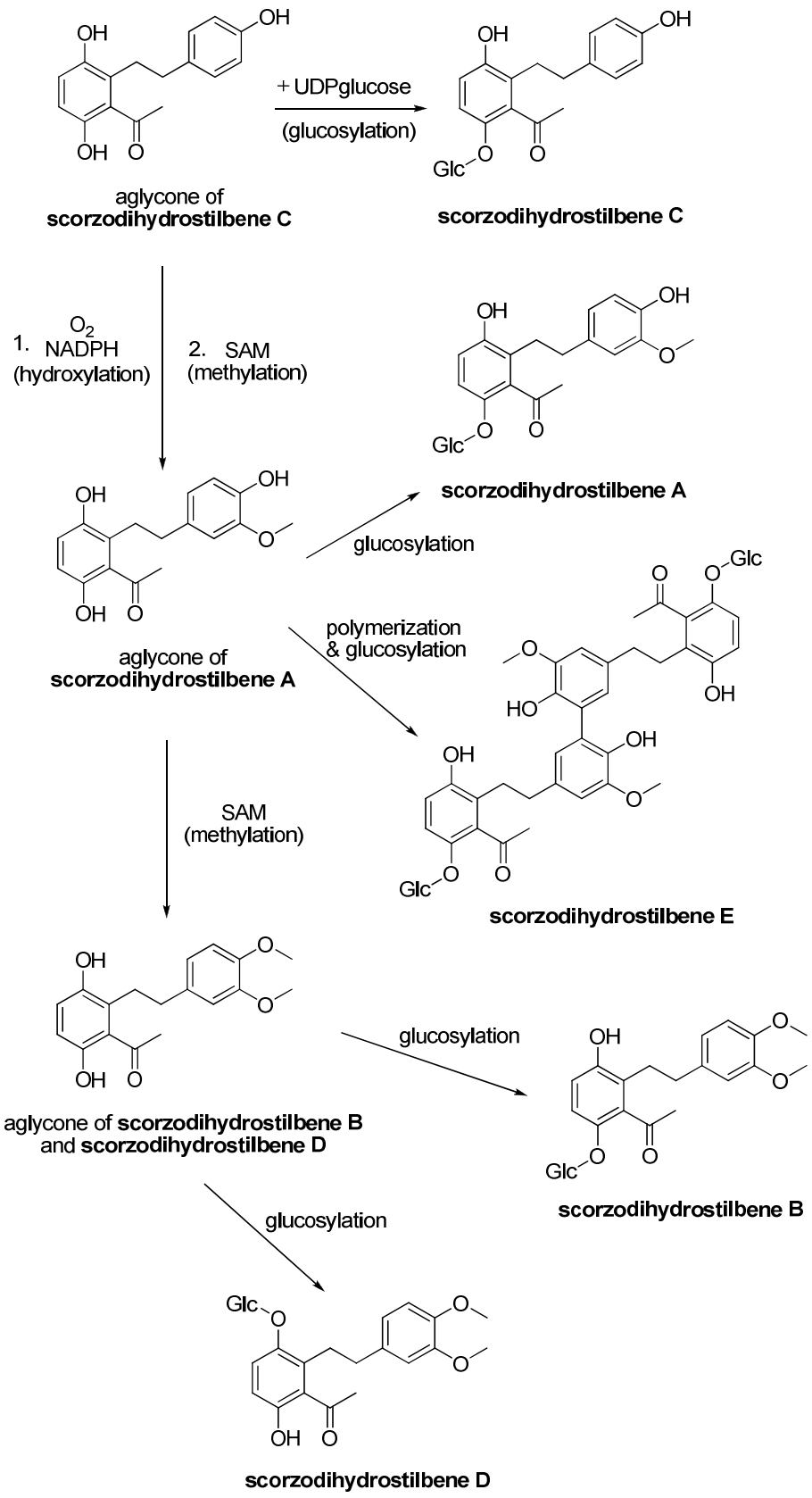

Figure 4.2 Suggested biosynthetic relationship of scorzodihydrostilbenes A–E (**1**–**5**)

Based on the supposed biosynthetic pathway of the dihydrostilbenes and the obtained compounds, several unknown dihydrostilbenes are suggested to exist as secondary metabolites of *S. radiata* which are shown in Figure 4.3. If the phytochemical study for *S. radiata* can be continued and there is enough amount of plant material, those conjectural dihydrostilbenes are expected to be found in the extract. This is in respect that the undiscovered compounds follow the same biosynthetic pathway as the found ones or that they are precursors of the found ones.

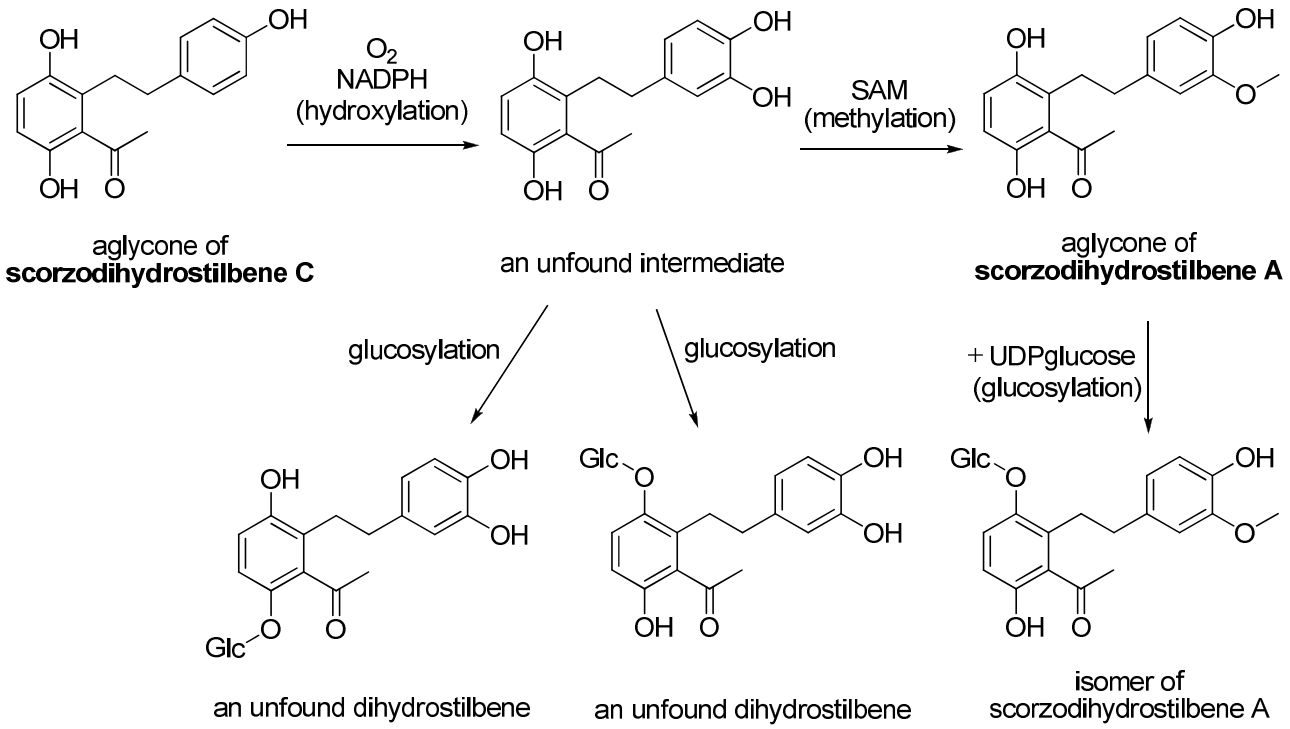

Figure 4.3 So far undiscovered dihydrostilbene derivatives

4.1.2. Biosynthesis of quinic acid derivatices

Quinic acid is a fairly common natural product found in the free form or as esters. It is biosynthesized by the shikimate pathway. This pathway begins with a coupling of phosphoenolpyruvate (PEP) and D-erythrose 4-phosphate to give the seven-carbon 3-deoxy-D-arabino-heptulosonic acid 7-phosphate (DAHP). Elimination of phosphoric acid from DAHP followed by an intramolecular aldol reaction generates the first carboxylic intermediate 3-dehydroquinic acid. Reduction of 3-dehydroquinic acid leads to quinic acid [Dewick, 2001]. This process is shown in Figure 4.4.

In this study, two unusual epiquinic acid derivatives were obtained including a new one. Due to the fact that epimers of quinic acid derivatives are studied rarely, the biosynthetic pathway has never been published. Here we suggest the possible reactions for forming epiquinic acid. There are two possibilities. The first one is that an epimer of 3-dehydroquinic acid is generated as a bi-product when aldol reaction occurs to produce 3-dehydroquinic acid, and then this is reduced to form epiquinic acid. The second is that the starting compound, D-erythrose, is replaced by D-threose. The latter reactions are exactly the same one as the regular one. These two pathways are also presented in Figure 4.4. However, it has not been confirmed, and more studies are necessary in order to understand the biosynthesis pathway.

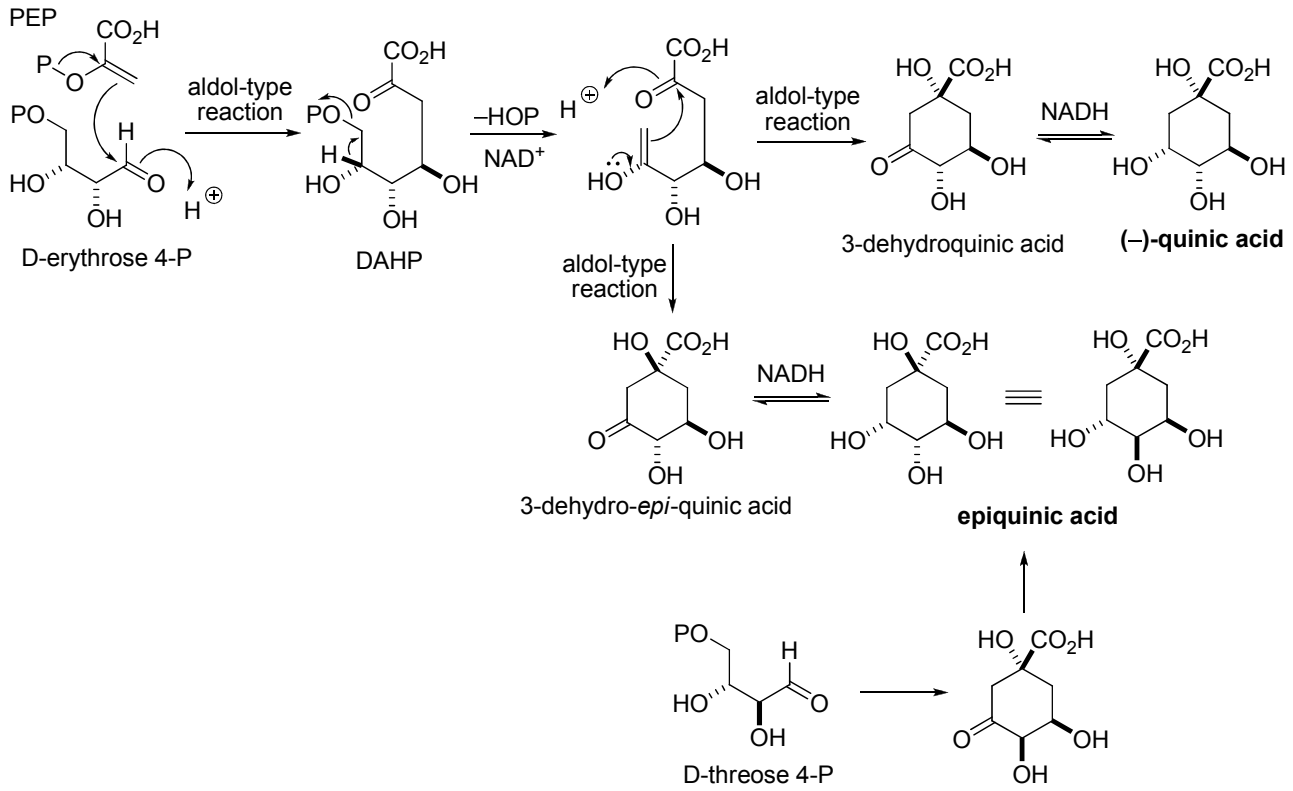

Figure 4.4 Suggested biosynthetic pathway of epiquinic acid

The biosynthetic relationship of all isolated quinic acid derivatives from *S. radiata* is shown in Figure 4.5. On the basis of obtained quinic acids and the biosynthetic pathway, several epiquinic acid derivatives are suspected to be present as metabolites of *S. radiata*, which have not been found so far. It is considered that the epiquinic acid derivatives must occur in *S. radiata* as very minor components, because those epimers are not distributed as widely as the normal ones. This is the reason for the fact

that so far only few epiquinic acid derivatives were isolated as natural products.

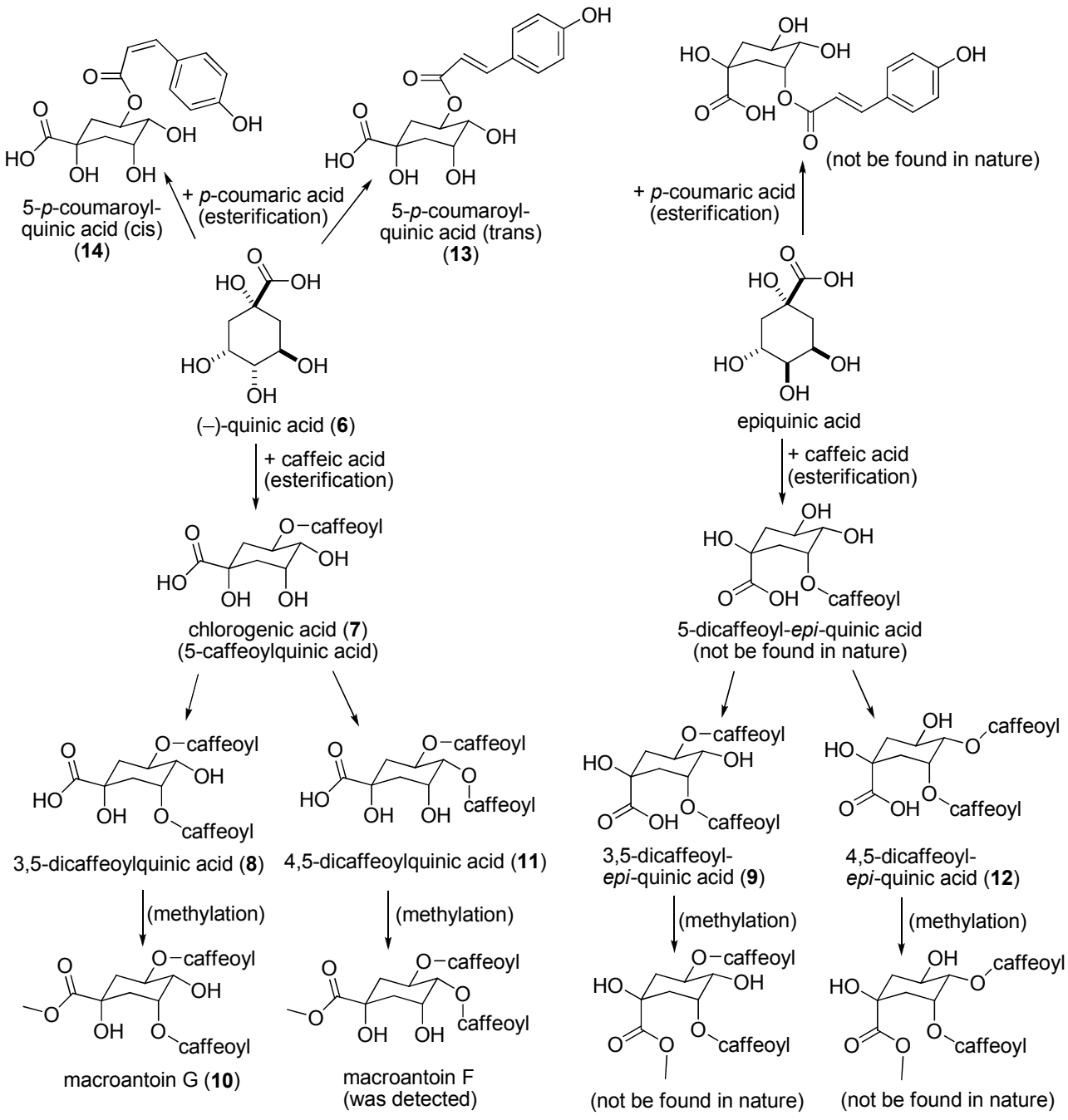

Figure 4.5 Biosynthetic relationship of isolated quinic acid derivatives

4.1.3. Relationship between secondary metabolites from Mongolian *S. radiata* and the nature and climate of Mongolia

Mongolian medicinal plants *S. radiata* were collected in the Ulaanbaatar region of Mongolia, which has an extreme continental climate with long, cold winters and short summers. The country averages 257 cloudless days a year, and it is usually at the center of a region of high atmospheric pressure. Ulaanbaatar lies at 1351 meters above sea level in the valley of the river Tuul Gol. Located in the relatively well-watered north, it receives an annual average of 31 centimeters of precipitation, almost all of which falls in July and in August. Ulaanbaatar has an average annual temperature of –2.9 °C and a frost-free period extending on the average from mid-June to late August [Worden *et al.*, 1991].

Mongolia's weather is characterized by extreme variability and short-term unpredictability in the summer, and the multiyear averages conceal wide variations in precipitation, dates of frosts, and occurrences of spring dust storms. Such weather poses severe challenges to animal and plant survival. Plant yields fluctuate widely and unpredictably as a result of the amount and the timing of rain and the dates of killing frosts [Worden *et al.*, 1991].

As a result of the high, cold, and dry climate conditions, the plants growing in that area may have inimitable biosynthetic pathways and enzymatic reaction systems making the plants to adapt to the ecotypic environment. Consequently the Mongolian plants sometimes can metabolize the natural products with distinct configuration and prominent biological activities.

In the phytochemical study for *S. radiata*, five dihydrostilbenes, ten quinic acid derivatives, six flavonoids, two coumarins, five simple benzoic acids, and one monoterpene were obtained. Most of those compounds are present in their glycosidic form. From the amount of the isolated compounds, along with analysis by DAD-HPLC of the crude extract of *S. radiata* (Figure 4.6–4.9), quinic acid derivatives were concluded to be the principal components of the secondary metabolites, particularly chlorogenic acid (approx. 33% of the crude extract) and 3,5-dicaffeoylquinic acid (approx. 22%). Additionally, dihydrostilbenes (approx. 10%) and flavonoids (approx. 14%) were also found to be the essential metabolites of *S. radiata.* Except minor terpenes, approximately 90% metabolites were

phenolic compounds which were likewise produced by the shikimate pathway.

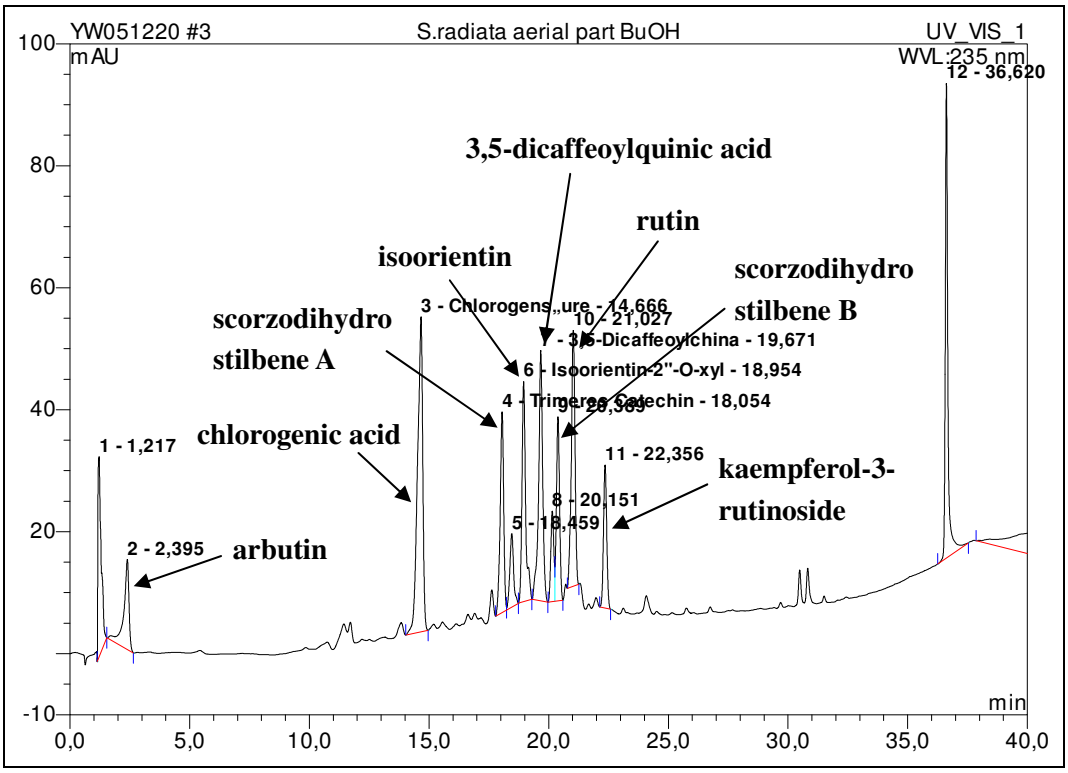

Figure 4.6 DAD-HPLC chromatogram of n-BuOH fraction of *S. radiata* aerial parts

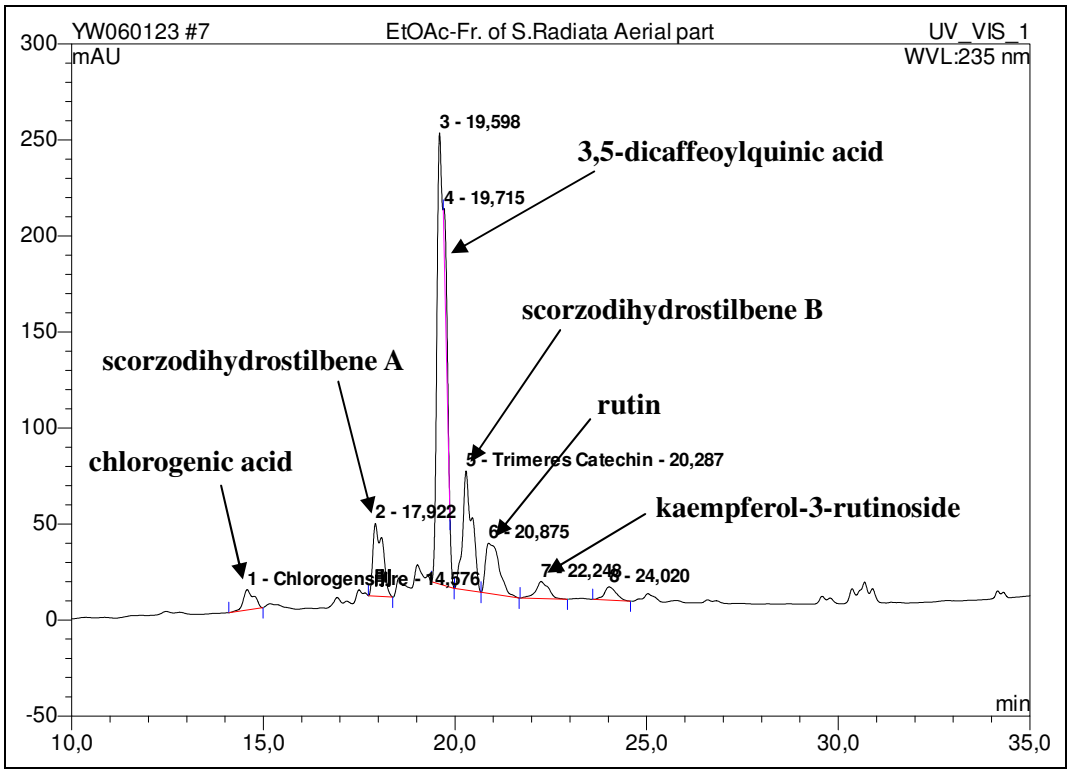

Figure 4.7 DAD-HPLC chromatogram of EtOAc fraction of *S. radiata* aerial parts

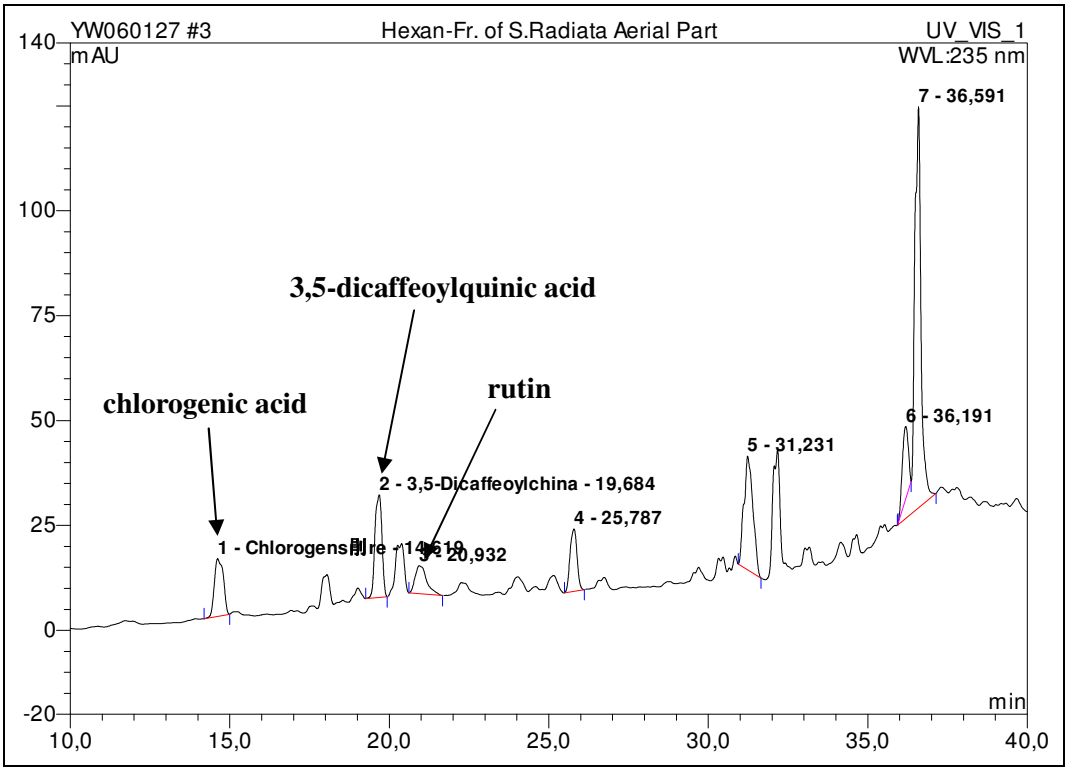

Figure 4.8 DAD-HPLC chromatogram of n-hexan fraction of *S. radiata* aerial parts

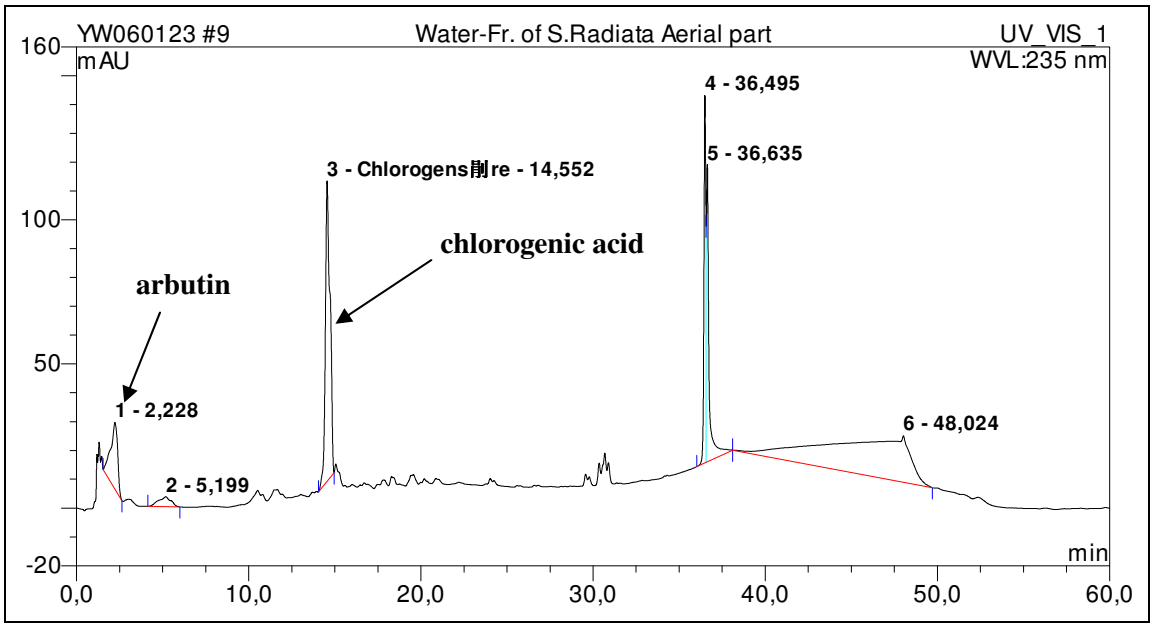

Figure 4.9 DAD-HPLC chromatogram of water fraction of *S. radiata* aerial parts

4.1.3.1. Quinic acid derivatives

The great proportion of caffeoylquinic acids in *Scorzonera* spp. was proven by a chemotaxonomic investigation indicated that *Scorzonera* provides about 180 mg/kg caffeoylquinic acids with little or none of other conjugates [Clifford, 1999]. Furthermore the accumulation of quinic acid derivatives is probably on account of the stress of Mongolian rigorous environment. It was reported that apple tree adaptation to cold climate was found to be associated with a high level of chlorogenic acid [Solecka, 1997]. Hereby cold stress might increase the production of caffeoylquinic acids. In addition, chlorogenic acid may be induced in response to wounding or to feeding by herbivores, and then act directly as defence compounds or may serve as precursor for the wound-induced polyphenolic barriers [Dixon and Paiva, 1995]. In Mongolia, the strong storms and the activity of herbivores are common stress factors for plants.

4.1.3.2. Dihydrostilbenes

Since the related dihydrostilbene derivatives were only found from *S. humilis* previously, these congeners were inferred to be the characteristic secondary metabolites of some species of *Scorzonera*. From the chemotaxonomic point of view, this also implied that *S. radiata* has a closer taxonomic relationship with *S. humilis* compared to the other *Scorzonera* spp..

Many phenylpropanoids exhibit a broad range of antimicrobial activities and are therefore believed to help the plant fight microbial diseases. Such compounds can be classified as phytoalexins [Dixon *et al.*, 2002]. Plants naturally resistant to pathogens may have inherented higher phenolic contents resulting from higher activity of the enzymes responsible for phenolic synthesis [Solecka, 1997]. Stilbene biosynthetic genes and metabolites are also induced by wounding and fungal infection, and by the protective plant activator, laminarin [Sandermann Jr, 2004]. It is considered that the dihydrostilbenes (**1–5**) play a similar rule as the well-known stilbene phytoalexin resveratrol provided by a grapevine SS gene [Dixon, 2001], resulting in plants with increased resistance to the fungal pathogen.

4.1.3.3. Flavonoids

Flavones can increase in concentration in response to high light irradiation, and help attenuate the amount of light reaching the photosynthetic cells. It was reported that UV irradiation induces the synthesis of flavonoids particularly kaempferol derivatives. These UV-absorbing compounds are thought to provide a means of protection against UV-B damage and subsequent cell death by protecting DNA from dimerization and breakage [Dixon and Paiva, 1995]. *S. radiata* was collected from a high latitude and high elevation area with a chiefly sunny sky, which provides exceeding UV irradiation. This might be the reason that a high percentage of flavones especially kaempferol derivatives was found in the extract of *S. radiata.*

4.1.3.4. Multiple phytoalexins and stereoisomers

3,5-dicaffeoyl-*epi*-quinic acid (**9**) and 4,5-dicaffeoyl-*epi*-quinic acid (**12**) were isolated as the stereoisomers of 3,5-dicaffeoylquinic acid (**8**) and 4,5-dicaffeoylquinic acid (**11**) respectively. The epimers of quinic acid derivatives are not commonly occurring in nature. As phytoalexins it is interesting to understand the reason that the plants synthesize a pair of isomers. So far it is still unclear whether the accumulation of different but structurally related phytoalexins in a plant is important for resistance or is insurance for survival. It has been reported that stereoisomers of a phytoalexin can markedly differ in antifungal activity. It was suggested that the conjugates of some phytoalexins may be very important for the rapid release of free phytoalexin after infection, and that they may not be synthesized or hydrolyzed as quickly in the presence of stereoisomers unnatural to the host. This is an exciting area of investigation that requires a thorough understanding of phytoalexin biosynthesis, factors influencing accumulation, and mode of action [Kuć, 1995].

4.1.4. Acid catalysis of the acetyl group in deuterated methanol

During ^{1}H NMR measurements of the new dihydrostilbene derivatives, it was observed that the signal of the acetyl protons disappeared when the compound was kept in deuteromethanol for one day. Obviously, an exchange of the α-carbonyl protons occurred through the formation of the enol, which might have been mediated by traces of acid or base. The fact that the H/D exchange was not observed in deuterated DMSO indicates that the acidity of deuteromethanol is crucial to enolization

and redeuteration [Clayden *et al.*, 2001]. The potential reaction is shown in Figure 4.10. The noncommittal catalyzer could also be involved by the uncleaned and residual acid when cleaning the used NMR tubes.

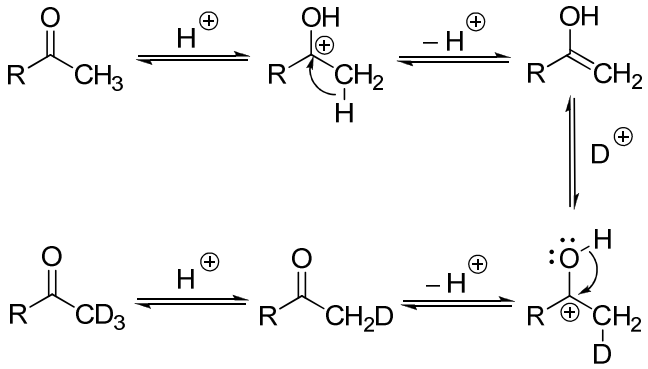

Figure 4.10 Acid catalysis of the acetyl group in deuterated methanol

When the stilbenes were exposed to deuteromethanol for a shorter period (hours), mono-deuteration became evident from a triplet of the group with a characteristic coupling constant of J = 2.0 Hz [Hesse *et al.*, 1997]. The original singlet decreased in intensity and new signals corresponding to CH_2D and CHD_2 appeared at high-field, while all other signals remained unchanged. The time-dependent H/D exchange was observed in their mass and ^{1}H NMR spectra, which are displayed in Figure 4.11 and Figure 4.12

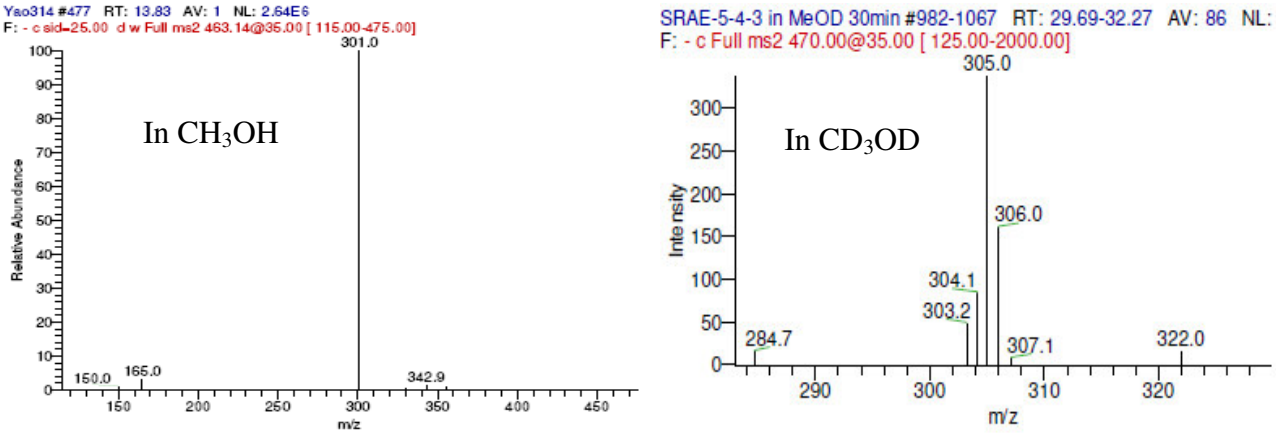

Figure 4.11 ESI-MS spectrum comparison of the aglycone of compound **1**

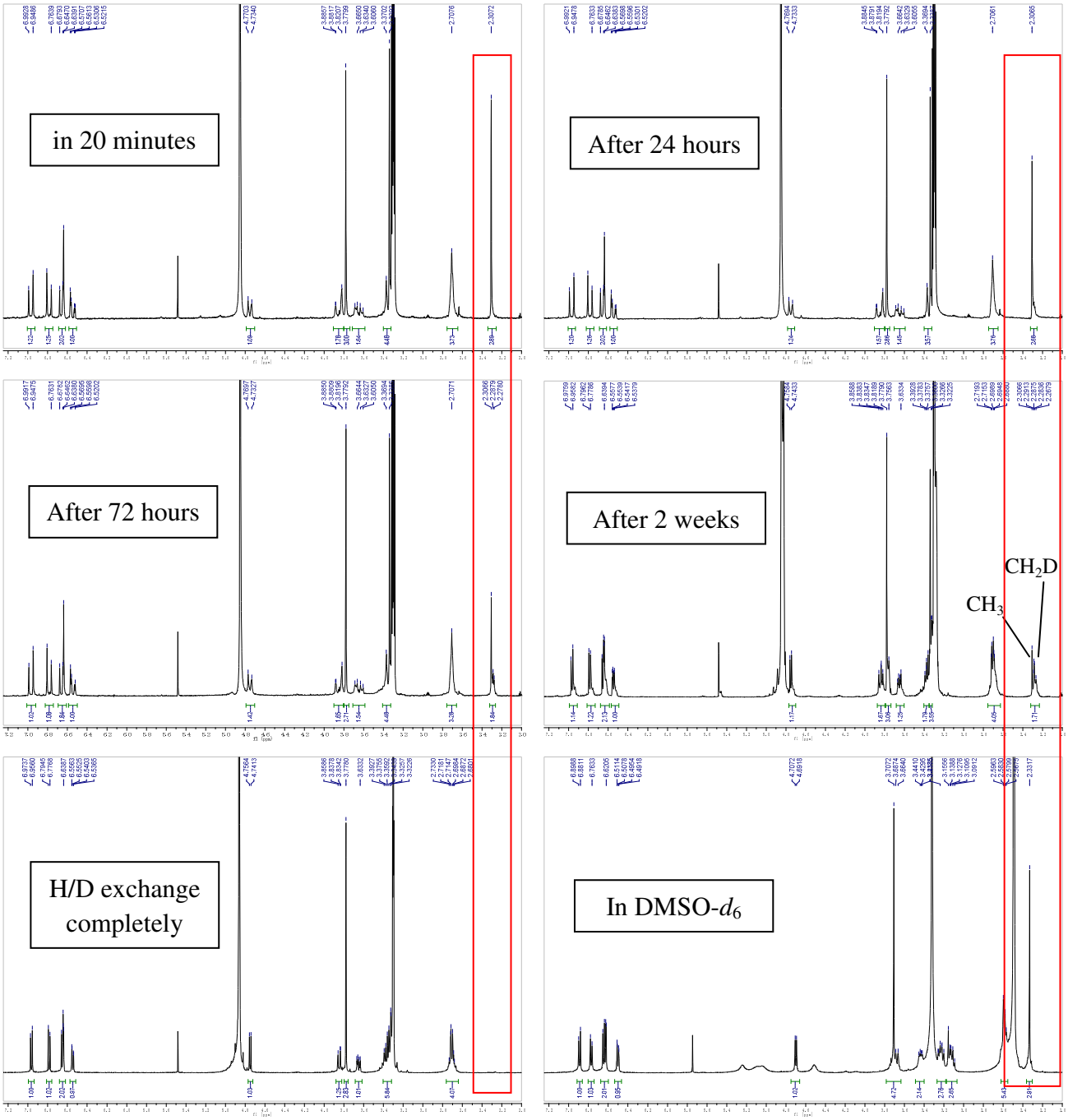

Figure 4.12 The time-dependent H/D exchange of ^{1}H NMR spectra for compound **1**

4.1.5. Structure–activity relationships of dihydrostilbenes and quinic acid derivatives in the antioxidant assay

According to the results of scorzodihydrostilbene A–E (**1**–**5**) and resveratrol, the well-known antioxidative stilbene, compounds **1** and **5** were more active than resveratrol or compounds **2**–**4**. Methoxy substitution at the *ortho* position relative to an OH group (C-4′) of the phenol moiety as found for **1** and **5** induced an increase in the scavenging reaction. The electron-donating methoxy group allows stabilization of the resulting aryloxy radical through electron delocalization after hydrogen donation by the OH group [Rice-Evans *et al.*, 1996]. The structure–activity relationships of the phenolic compounds were also comfirmed by theoretical studies, which indicated that the O–H bond dissociation enthalpy (BDE) value is reduced by an *ortho* substitution of a methoxy group, and the weaker the OH bond, the faster the reaction with free radicals [Wright *et al.*, 2001; Ordoudi *et al.*, 2006].

The caffeoyl quinic acid congeners were considerably more active than 5-*p*-coumaroylquinic acid, since phenolic compounds exhibits vicinal OH groups have a higher radical scavenging activity than monohydroxylated isomers (*p*-coumaric acid) [Rice-Evans *et al.*, 1996]. The antioxidant efficiency of chlorogenic acid was found to be weaker than those of the dicaffeoylquinic acids. 4,5-Dicaffeoyl-*epi*-quinic acid (**12**) and 3,5-dicaffeoyl-*epi*-quinic acid (**9**) exhibited slightly stronger antioxidant activities compared to 4,5-dicaffeoylquinic acid (**11**) and 3,5-dicaffeoylquinic acid (**8**), respectively. Macroantoin G presented similar IC_{50} values in DPPH assay when compared to 3,5-dicaffeoylquinic acid, thus methoxylation of the carboxyl group of the quinic acid moiety did not decrease the radical scavenging activity.

4.1.6. Structure–activity relationships of cytotoxicity of new dihydrostilbenes and their aglycones

Scorzodihydrostilbenes A–E (**1**–**5**) showed no cytotoxicity against either L5178Y or H4IIE cells. After hydrolysis, except for the aglycone of scorzodihydrostilbene A (ASDSA), none of other dihydrostilbene aglycones exhibited cytotoxicity in H4IIE cells which was assessed by neutral red assay. Even if those dihydrostilbenes or their aglycones were stimulated by TNF, there was still no significant suppresion of TNF-dependent NF-κB activation. However when ASDSA was stimulated with different concentrations of TNF, it enhanced TNF-mediated cytotoxicity against H4IIE cells in a dose-dependent manner, of which pretreatment of H4IIE cells with 20 μM ASDSA lead to a significant enhanced TNF-mediated cytotoxicity. The same experiment was determined for the aglycones of scorzodihydrostilbene B–E, but there was no difference in cytotoxicity as measured by neutral red assay. The aglycones showed stronger activity than glucosides, because they are lipophilic and pass easy through the cell membranes. Moreover ASDSA was more active than other aglycones, which was a result of the combination of a hydroxy function and its *ortho*-substituent methoxy group at C-4′ and C-3′ respectivly.

ASDSA was selected as the only active compound for further test. It induced a dose-dependent caspase 3/7 activation for the apoptotic potential. When H4IIE-SEAP cells with ASDSA were stimulated with 5 ng/ml TNF, the results were expressed as fold activity of the control and enhanced TNF-mediated cytotoxicity by inducing apoptotic cell death.

Isolated dihydrostilbene derivatives (**1**–**5**) did not show cytotoxicity as intense as the stilbene resveratrol. Nevertheless in the previous discussion, scorzodihydrostilbene A and E did show better antioxidant activity than resveratrol in DPPH assay. It has been reported that the majority of naturally ocurring antioxidants have cytotoxicity in vitro as known for resveratrol, flavonoids and carotenoids. It will be interesting to find out the mechanism and relationship of this.

4.2. Metabolites isolated from the Mongolian medicinal plant *Dianthus versicolor*

For the genus *Dianthus*, the majority of the reported secondary metabolites were saponins. However, the study for the cytotoxic fractions of *D. versicolor*, a plant growing in the same area as *S. radiata*, only yielded two lignans (**29** and **30**) and several triterpenes (**31**–**34**). The remainder fractions contained known triterpenes as shown by LC-MS and TLC analysis.

(–)-Matairesinol (**29**) and (–)-arctigenin (**30**) showed trivial activity inhibiting 24 protein kinases, and **30** exhibited slightly stronger activity than **29**. Nevertheless in the previous research, both lignans, especially **30**, have been reported to cause cell growth inhibition in human gastric adenocarcinoma cells and mouse hepatoma cells [Kang *et al.*, 2007], and to show antiproliferative activity [Matsumoto *et al.*, 2006]. Additionally, these two lignans as naturally occurring phytoestrogens have potential health benefits in man particularly against hormone-dependent diseases such as breast and prostate cancers and osteoporosis [Rowland *et al.*, 2003].

Lupeol (**31**) is found in many medicinal plants and has been investigated for its various pharmacological properties. In this study, lupeol exhibited moderate activity in the protein kinase inhibitory assays, but trifling activity against mouse lymphoma cell L5178Y. However, the compound has been shown to have strong anti-inflammatory and antimutagenic activity *in vitro* and *in vivo* [Geetha and Varalakshmi, 2001], and to inhibit the activities of protein kinases [Hasmeda *et al.*, 1999], serine proteases [Hodges *et al.*, 2003] and DNA topoisomerase II [Wada *et al.*, 2001]. Lupeol has also been reported to induce differentiation and to inhibit the cell growth of human leukemia [Aratanechemuge *et al.*, 2004] and prostate cancer cells [Saleem *et al.*, 2005], and mouse skin carcinogenesis [Saleem *et al.*, 2004], while it did not affect the growth of human melanoma cell lines [You *et al.*, 2003]. In conclusion, there are still a lot of work to be done for studying the potential selectivity and mechanism of different tumor cell lines.

4.3. Metabolites isolated from the medicinal plant *Psoralea corylifolia*

4.3.1. Biosynthetic relationships of isolated compounds from *P. corylifolia*

As a noted medicinal plant, *P. corylifolia* has been investigated extensively. However, in our study, sixteen prenylated flavonoids and three coumarins including two new ones were isolated. All of those are biosynthetically related compounds. The biosynthetic relationships are displayed in Figure 4.13–Figure 4.17.

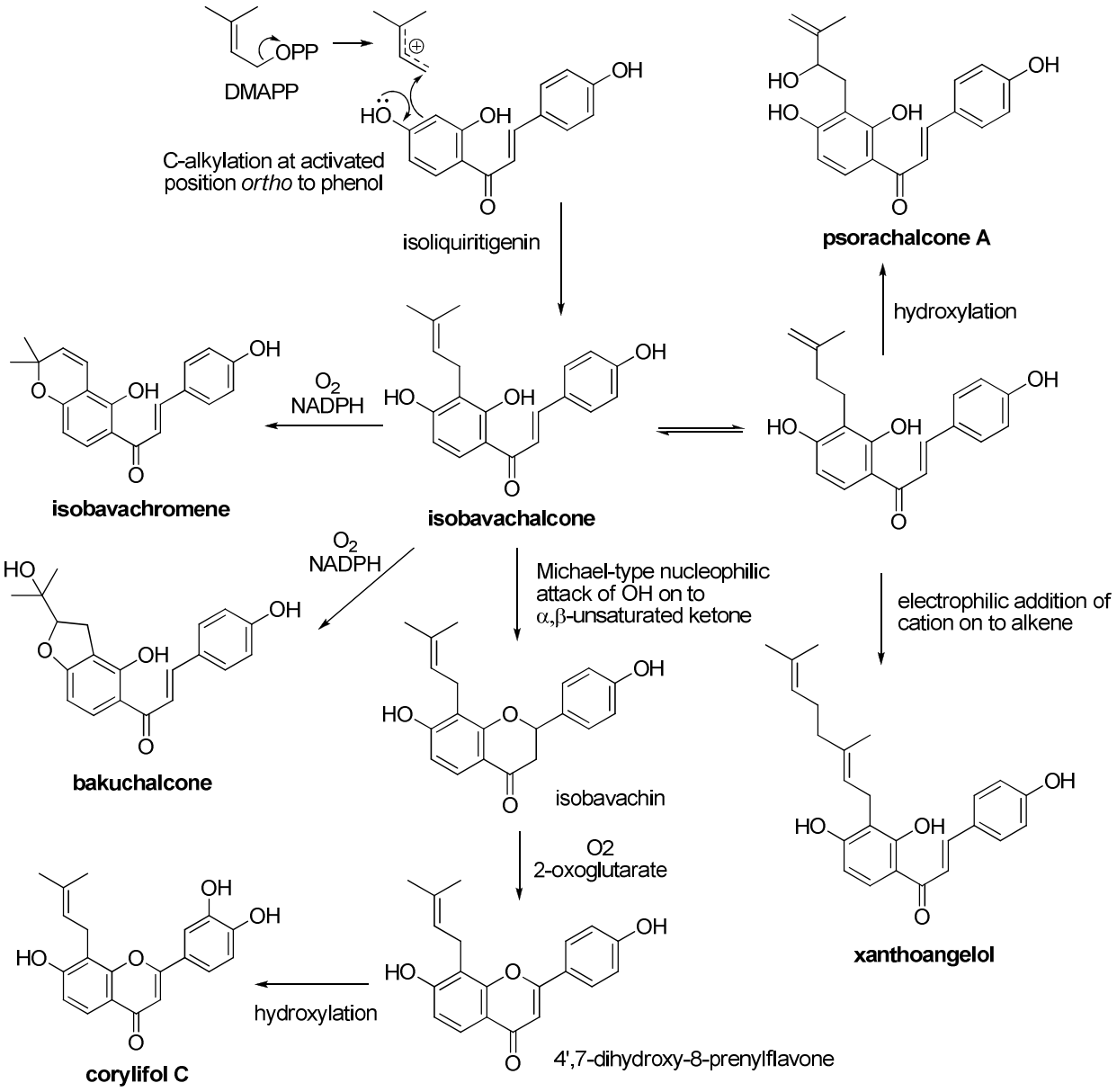

Figure 4.13 Biosynthetic relationship of isolated flavonoids

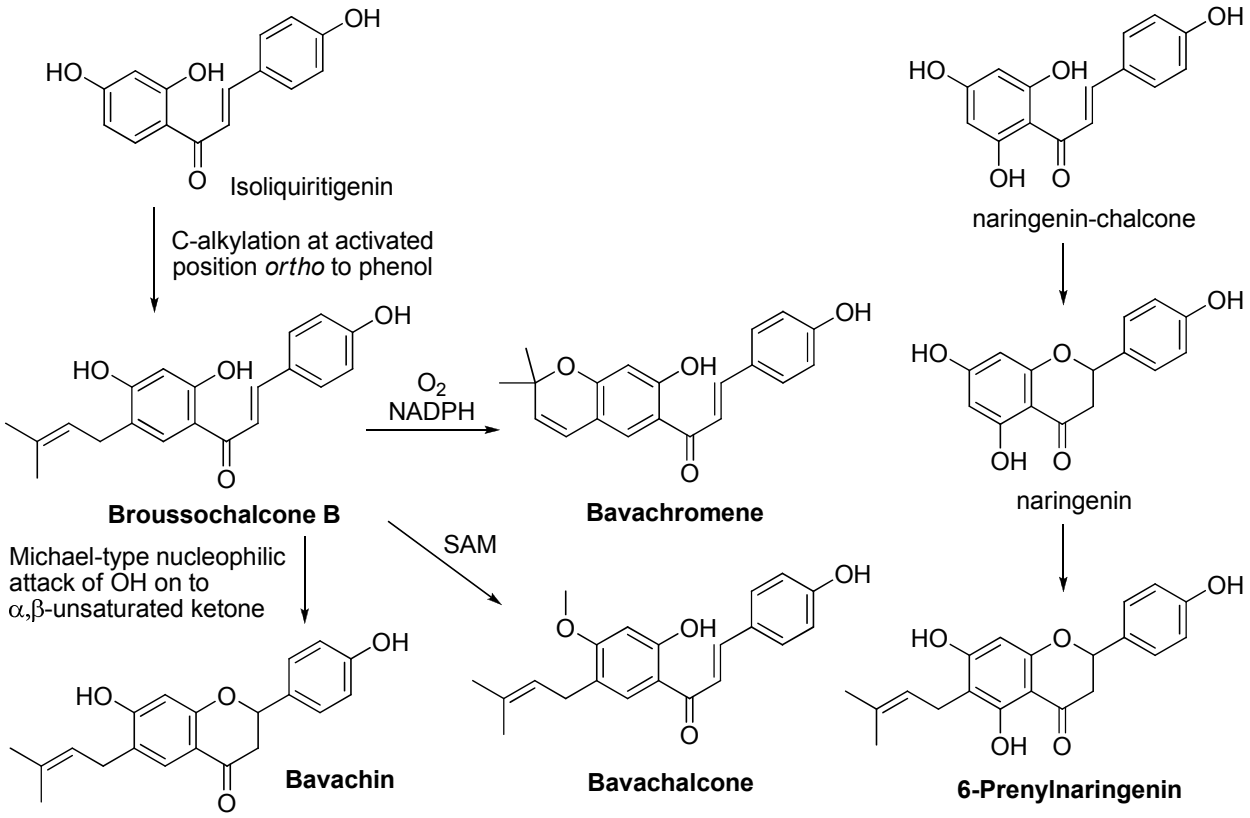

Figure 4.14 Biosynthetic relationship of isolated flavonoids

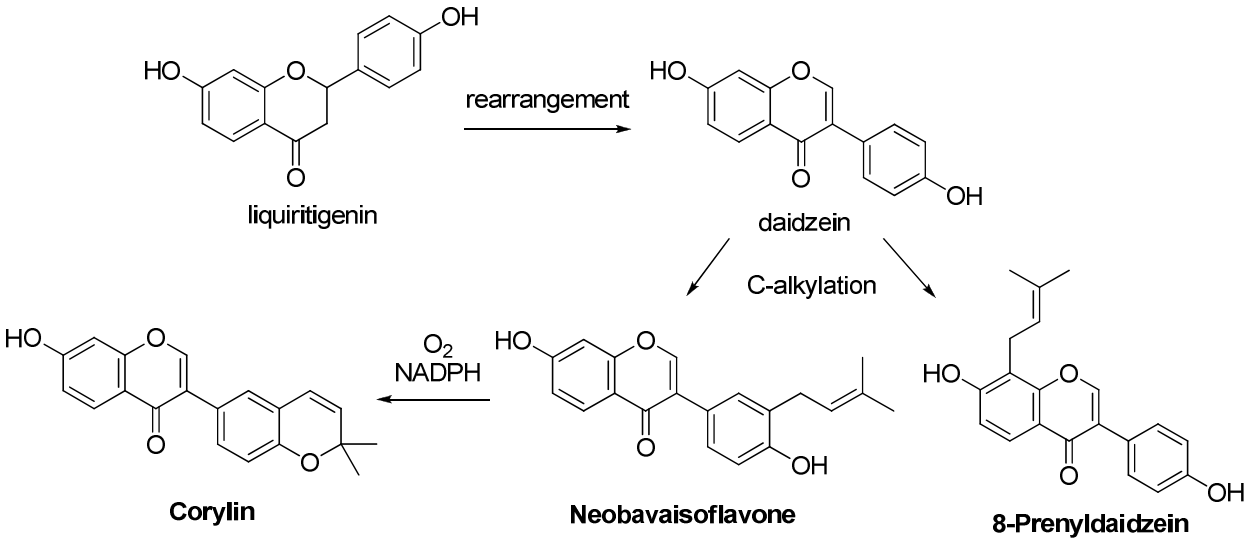

Figure 4.15 Biosynthetic relationship of isolated isoflavonoids

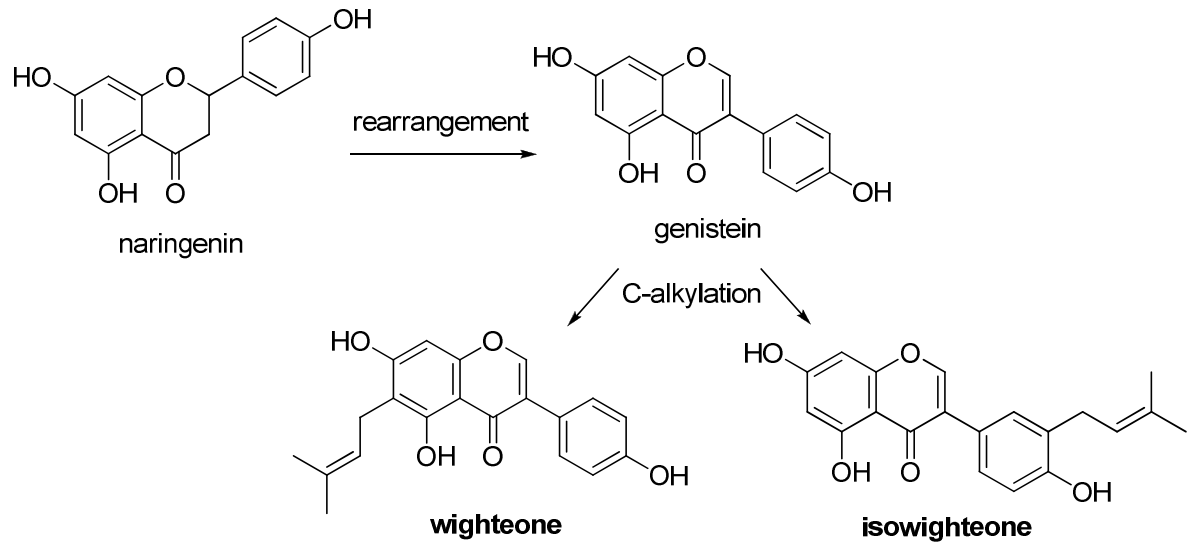

Figure 4.16 Biosynthetic relationship of isolated isoflavonoids

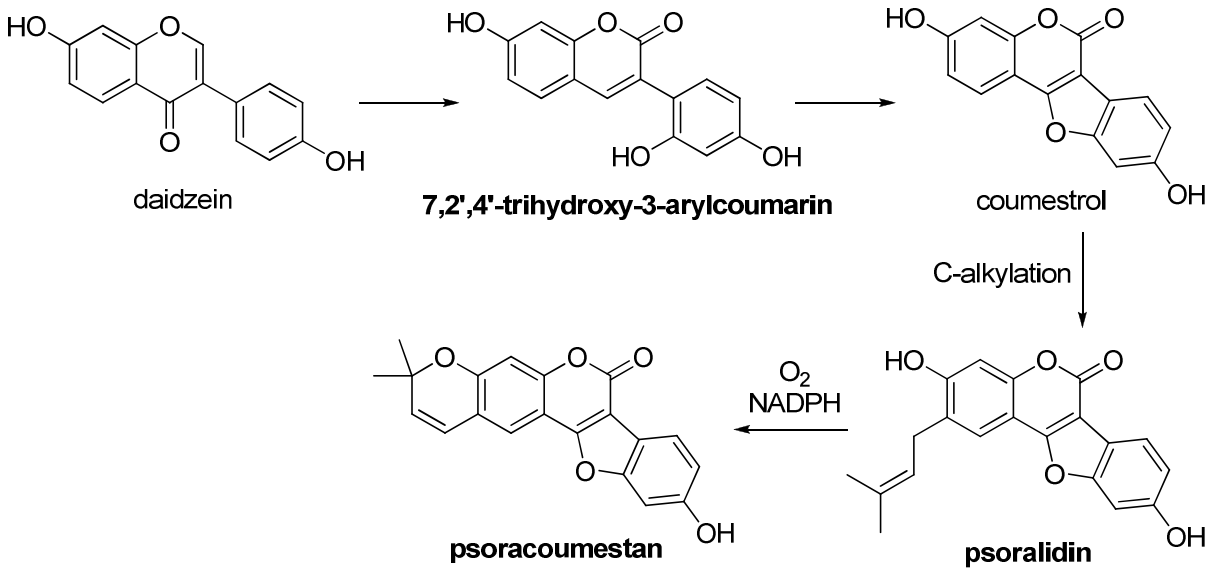

Figure 4.17 Biosynthetic relationship of isolated coumarins

4.3.2. Structure–activity relationships of the cytotoxic activity of the isolated compounds from *P. corylifolia*

Compound **42**, **45** and **55** were the most active ones, while **37**, **46** and **51** were also quite active. Moreover, compound **40**, **43**, **44**, **48** and **53** displayed mild cytotoxicity. When comparing the results of different classes of flavonoid derivatives (chalcone, flavone, flavanone and isoflavone), it was deduced that no direct correlation between the class of flavonoids and the intensity of the cytotoxicity could be observed. Compounds **42**–**46** showed relatively stronger activity, which indicated that the substituting position of prenyl moiety at C-6 on A-ring of chalcones and flavanones was important for activity. For flavanones (**45** and **46**) and isoflavones (**47**–**51**), OH groups at C-5 and C-7 enhanced the activity compared to the monosubstituted OH group at C-7. The formation of 2,2-dimethylchromene ring by a prenyl moiety and an *ortho* hydroxyl group also increased the cytotoxicity of the compound in most cases.

The activity of compound **51** and **55** increased approximately eight times with regard to caspase 3/7 compared to the blank, when incubated with 25 μM of them for 24 hours. Compound **36**, **40**, **43**, **45**, **46**, **48**, **50** and **52** raised the relative fluorescence units about three to five times. These results revealed that the above mentioned compounds affected caspase 3/7 activity to induce apoptotic cell death.

4.4. Structure–activity relationships of all tested compounds in the protein kinase assay

The 22 compounds showed different activities against the 24 protein kinases tested. None of the compounds inhibited all kinases to full extent. Compound **1**, **3**, **7**, **29**, **30**, **38**, **42** and **45**–**47** showed no significant inhibitory potency against any of the 24 protein kinases. Compound **2**, **8**, **9**, **25, 31**, **36**, **40**, **41**, **44**, **49**, **53** and **55** showed inhibition of $\geq$ 40% for at least one of the 24 kinases when tested at 1×10^{-6} g/mL, but they were still not active enough for further evaluation when applying the criteria of the industrial partner ProQinase.

Nevertheless among those compounds **8**, **9** and **41** were the most active ones when comparing the IC_{50} values of them to those of other tested compounds. It can be explained by the *ortho*-dihydroxy structure in the aromatic ring which confers high stability to the electrons through H-bond formation. **8** and **9** had even much smaller IC_{50} values than **41** as a result of a larger number of hydroxyl groups in the benzene ring compared to **41**.

For the flavonoid derivatives (**36**, **38**, **40**–**42**, **44**–**47** and **49**), compound **38,** the only one without prenyl group, showed the lowest activity suggesting that a substitution of prenyl group can improve the inhibiting activity. Compounds **36**, **40**, **41**, **44** and **49** were more active compared to the other derivatives. This observation indicated that the substituting position of the prenyl moiety at C-8 gave stronger inhibitory activity than the substituting position at either C-6 or C-3′. Compounds **45** and **46** exhibited less activity in comparison to other flavonoids which suggests that flavanones are not as active as flavones, chalcones or isoflavones in the protein kinase assay. The reason for that could be that the double bond between C-2 and C-3 in conjugation with the ketone function at C-4 is responsible for the electronic delocalization starting from the C ring of flavonoids [Leopoldini *et al.*, 2004].

In the three new dihydrostilbenes (**1**–**3**), **2** was the most active compound which is different to the antioxidant and cytotoxic results discussed above. The reason and mechanism are not clear, and more studies are necessary. Moreover, there was a big gap of activity from **7** to **8** or **9**. This was also dissimilar to the antioxidant and presumed results, however it was still acceptable.

5. Summary

Natural products, also known as secondary metabolites, have been the major sources of chemical diversity of starting materials for driving drug discovery over the past century. The vast majority of traditionally used crude drugs have been plant-derived extracts. However, only very few Mongolian medicinal plants nurtured by unique ecosystem of Mongolia have been studied phytochemically so far.

The subject of this study was the isolation and structural elucidation of the secondary metabolites from medicinal plants, followed by the evaluation of their pharmocological potential. Various modern chromatographic techniques were used for separation and purification of the natural products from the crude extract. The structures were unambiguously elucidated on the basis of one- and two-dimensional NMR and mass spectrometric data.

Two Mongolian medicinal plants (*Scorzonera radiata* and *Dianthus versicolor*) and one Chinese medicinal plant (*Psoralea corylifolia*) have been selected as biological sources in this study. The compounds that have been isolated and structurally elucidated from those plants are summarized in Table 5.1. Some of them showed promising biological activities and considered for further pharmacological studies.

5.1. *Scorzonera radiata*

The Mongolian medicinal plant *Scorzonera radiata* was collected in Ulaanbaatar region of Mongolia. Chromatographic separation of a crude extract obtained from aerial parts of the plant yielded five new dihydrostilbenes, two new flavonoids, one new quinic acid derivative, as well as twenty known compounds including eight quinic acid derivatives, four flavonoids, two coumarins, five simple benzoic acids, and one monoterpene glycoside. Scorzodihydrostilbene A–E and the isolated quinic acid derivatives exhibited antioxidative activity when analyzed in the DPPH assay. For scorzodihydrostilbene A and E the antioxidant activities were stronger than that of the well-known naturally occurring stilbene antioxidant resveratrol. However, none of those compounds showed

cytotoxicity inhibiting either tumour cells (H4IIE and L5178Y) or 24 selected protein kinases. After hydrolysis for the dihydrostilbene derivatives, the aglycone of scorzodihydrostilbene A (ASDSA) reduced cell viability in H4IIE rat hepatoma cells. Moreover, when ASDSA was stimulated with different concentrations of TNF-α, it significantly enhanced TNF-mediated cytotoxicity against H4IIE cells in a dose-dependent manner.

5.2. Dianthus versicolor

The medicinal plant *Dianthus versicolor* was collected in Ulaanbaatar region of Mongolia. The MeOH extract of the aerial parts of the plant was subjected with column chromatography to afford seven known compounds including two lignans, four triterpenes and one steroid. The tested compound showed moderate cytotoxic activity against L5178Y cells or 24 protein kinases.

5.3. *Psoralea corylifolia*

The seeds of plant *Psoralea corylifolia* were collected and extracted in China. The crude MeOH extract was separated chromatographically to obtain three coumarins including two new ones, 7,2′,4′-trihydroxy-3-arylcoumarin and psoracoumestan, sixteen known prenylated flavonoids and one meroterpene. The isolated compounds were evaluated for cytotoxic activity inhibiting H4IIE, Hct-116, and C6 cells lines, and for antioxidant capacity in TEAC assay. The structure–activity relationships were studied on the basis of these results. The active compounds were further investigated for their apoptotic and necrotic potential to understand the action mechanism. Additionally some selected compounds were also tested for their protein kinase inhibitory profiles.

Table 5.1 List of isolated compounds

Name	Structure	Source	Note
Scorzodihydrostilbene A (**1**)	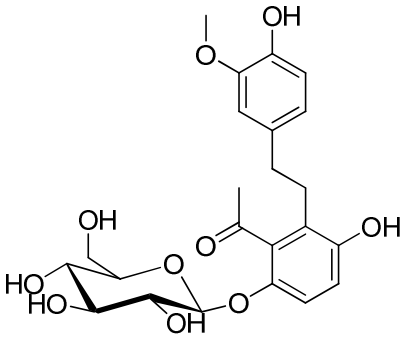	*Scorzonera radiata*	new
Scorzodihydrostilbene B (**2**)	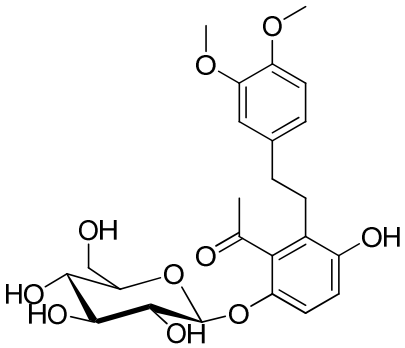	*Scorzonera radiata*	new
Scorzodihydrostilbene C (**3**)	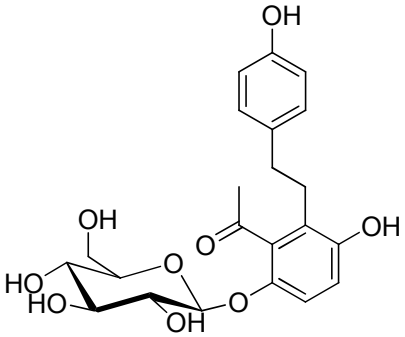	*Scorzonera radiata*	new
Scorzodihydrostilbene D (**4**)	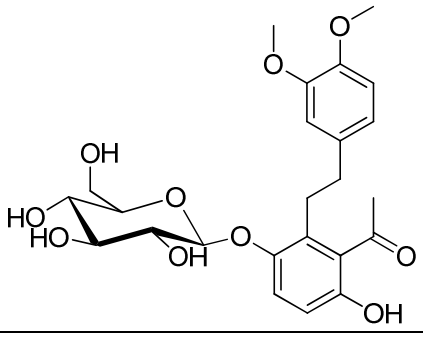	*Scorzonera radiata*	new

Scorzodihydrostilbene E (**5**)	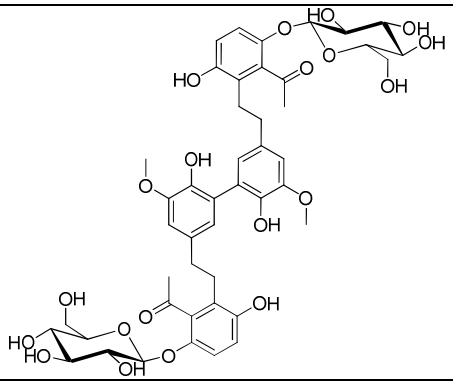	*Scorzonera radiata*	new
(−)-Quinic acid (**6**)	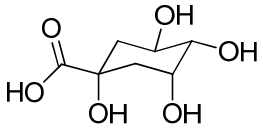	*Scorzonera radiata*	known
Chlorogenic acid (**7**)	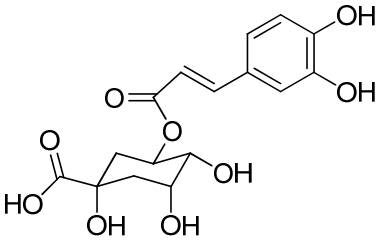	*Scorzonera radiata*	known
3,5-Dicaffeoylquinic acid (**8**)	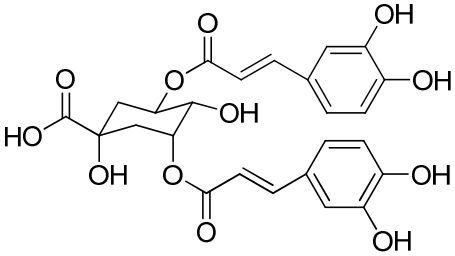	*Scorzonera radiata*	known
3,5-Dicaffeoyl-*epi*-quinic acid (**9**)	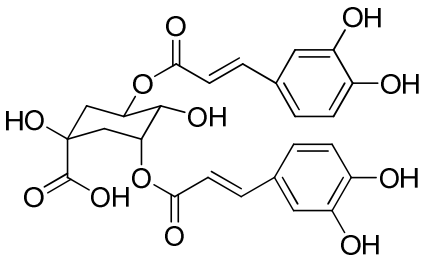	*Scorzonera radiata*	known
Macroantoin G (**10**)	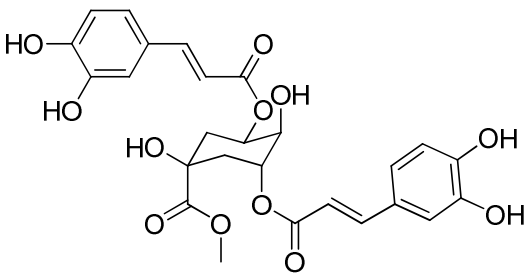	*Scorzonera radiata*	known

4,5-Dicaffeoylquinic acid (**11**)	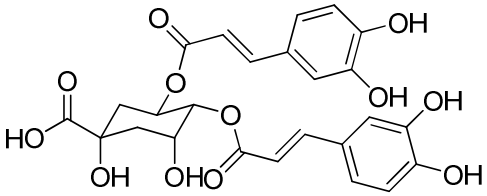	*Scorzonera radiata*	known
4,5-Dicaffeoyl-*epi*-quinic acid (**12**)	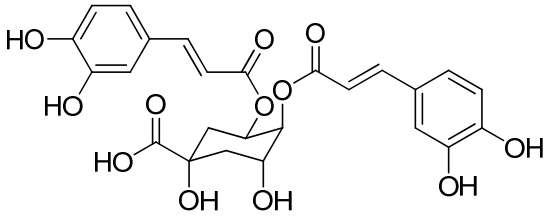	*Scorzonera radiata*	new
5-*p*-Coumaroylquinic acid (*trans*) (**13**)	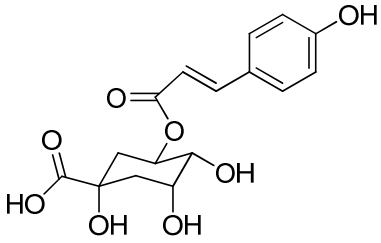	*Scorzonera radiata*	known
5-*p*-Coumaroylquinic acid (*cis*) (**14**)	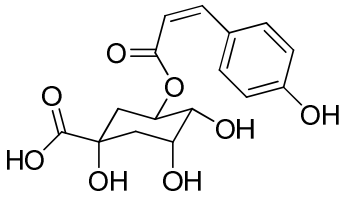	*Scorzonera radiata*	known
Isoorientin (**15**)	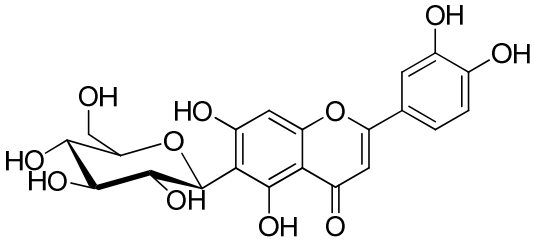	*Scorzonera radiata*	known
Scorzonerin A (**16**)	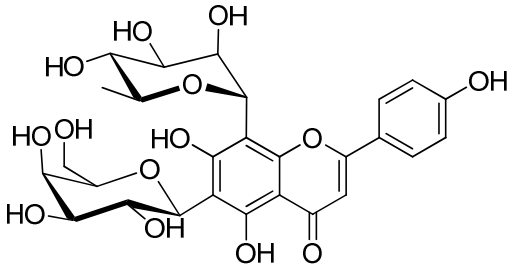	*Scorzonera radiata*	new

Scorzonerin B (**17**)	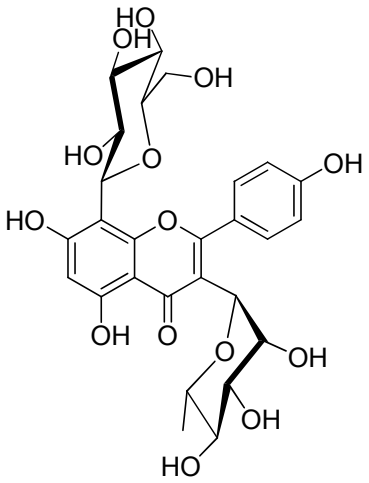	*Scorzonera radiata*	new
Kaempferol-3-rutinoside (**18**)	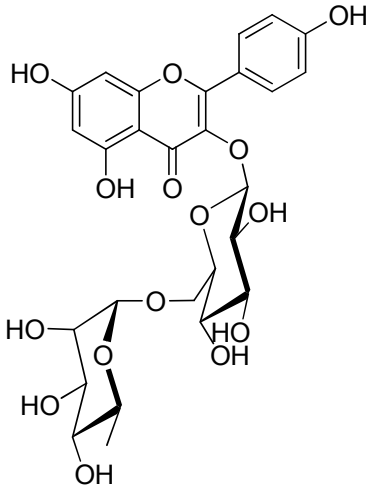	*Scorzonera radiata*	known
Rutin (**19**)	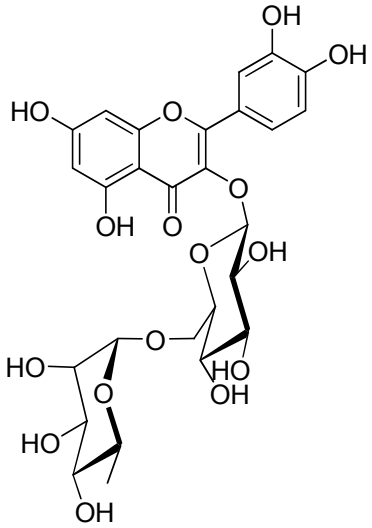	*Scorzonera radiata*	known
3,3',5,5',7-Pentahydroxyflavanone (**20**)	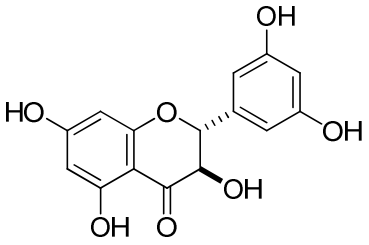	*Scorzonera radiata*	known

Umbelliferone (**21**)	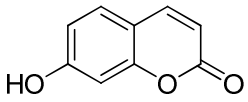	*Scorzonera radiata*	known
Skimmin (**22**)	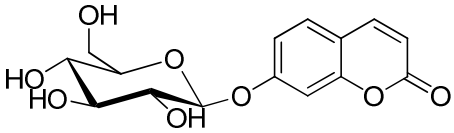	*Scorzonera radiata*	known
Piceol (**23**)	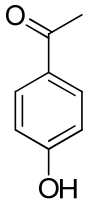	*Scorzonera radiata*	known
Piceoside (**24**)	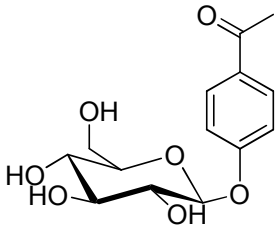	*Scorzonera radiata*	known
4-Hydroxybenzoic acid (**25**)	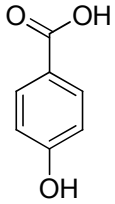	*Scorzonera radiata*	known
Arbutin (**26**)	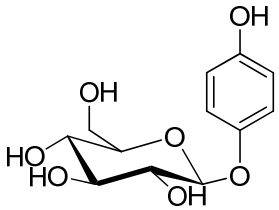	*Scorzonera radiata*	known
Lanceoloside A (**27**)	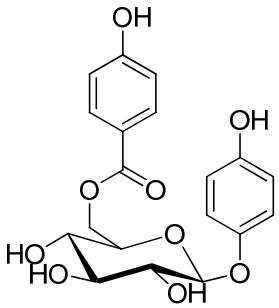	*Scorzonera radiata*	known
Staphylionoside D (**28**)	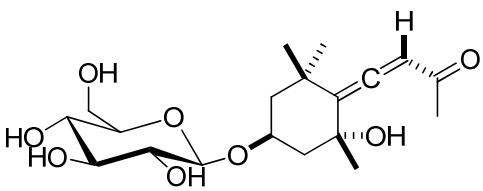	*Scorzonera radiata*	known

(−)-Matairesinol (**29**)	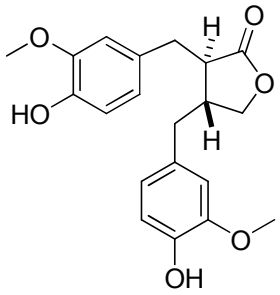	*Dianthus versicolor*	known
(−)Arctigenin (**30**)	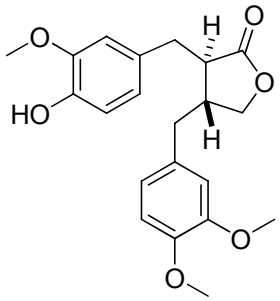	*Dianthus versicolor*	known
Lupeol (**31**)	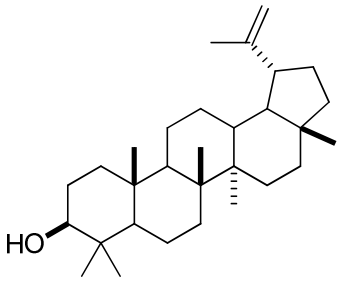	*Dianthus versicolor*	known
Taraxasterol (**32**)	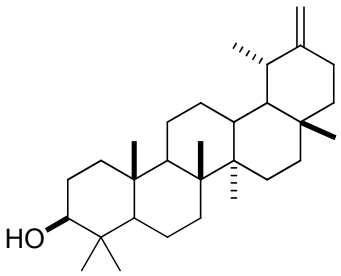	*Dianthus versicolor*	known
Pseudotaraxasterol (**33**)	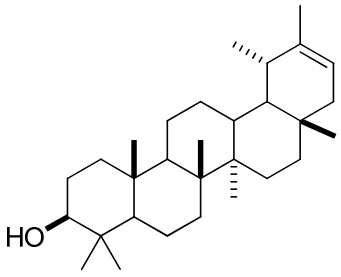	*Dianthus versicolor*	known
Ptiloepoxide (**34**)	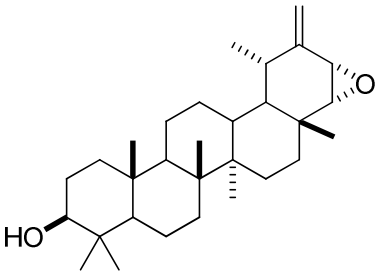	*Dianthus versicolor*	known

β-Sitosterol (**35**)	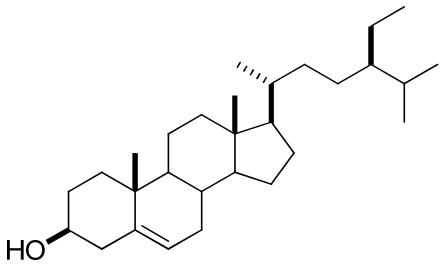	*Dianthus versicolor*	known
Isobavachalcone (**36**)	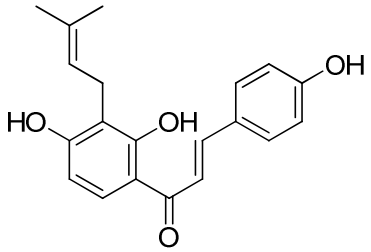	*Psoralea corylifolia*	known
Isobavachromene (**37**)	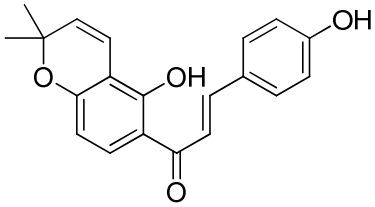	*Psoralea corylifolia*	known
Psorachalcone A (**38**)	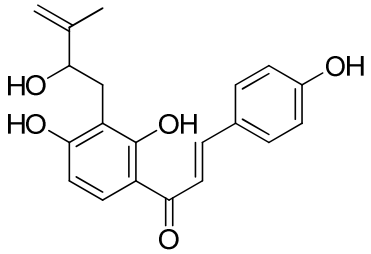	*Psoralea corylifolia*	known
Bakuchalcone (**39**)	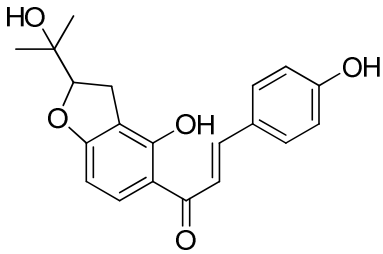	*Psoralea corylifolia*	known
Xanthoangelol (**40**)	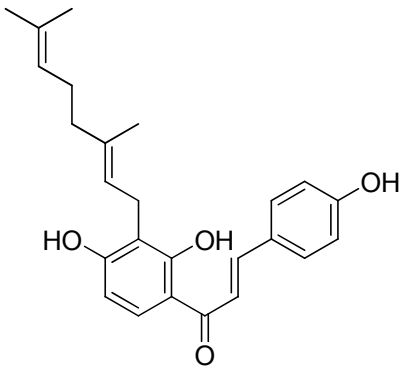	*Psoralea corylifolia*	known

Corylifol C (**41**)	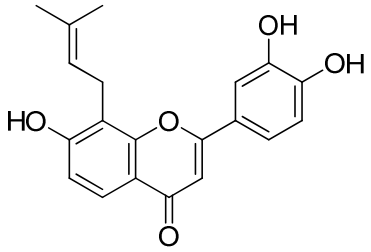	*Psoralea corylifolia*	known
Broussochalcone B (**42**)	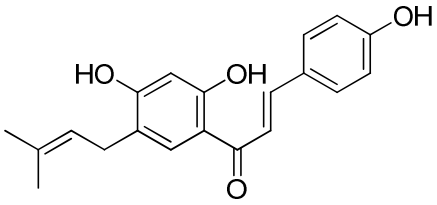	*Psoralea corylifolia*	known
Bavachromene (**43**)	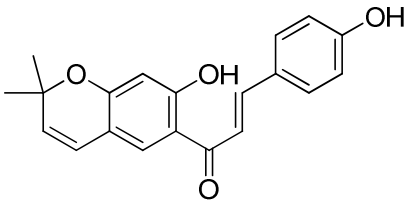	*Psoralea corylifolia*	known
Bavachalcone (**44**)	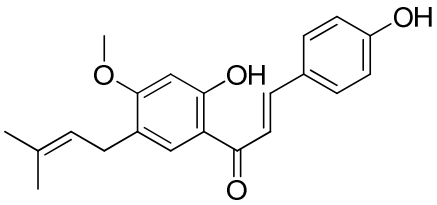	*Psoralea corylifolia*	known
Bavachin (**45**)	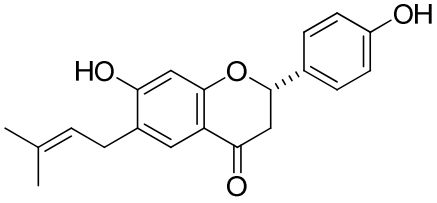	*Psoralea corylifolia*	known
6-Prenylnaringenin (**46**)	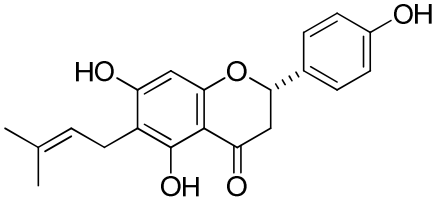	*Psoralea corylifolia*	known
Neobavaisoflavone (**47**)	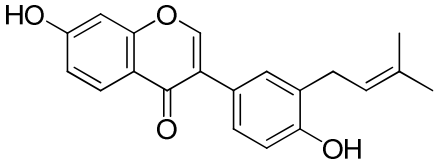	*Psoralea corylifolia*	known
Corylin (**48**)	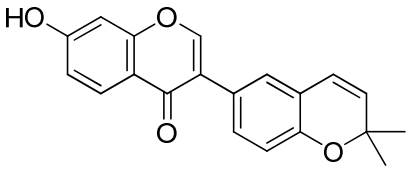	*Psoralea corylifolia*	known

8-Prenyldaidzein (**49**)	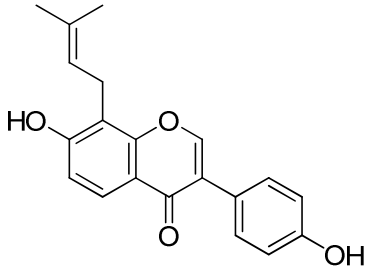	*Psoralea corylifolia*	known
Wighteone (**50**)	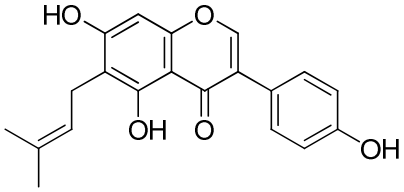	*Psoralea corylifolia*	known
Isowighteone (**51**)	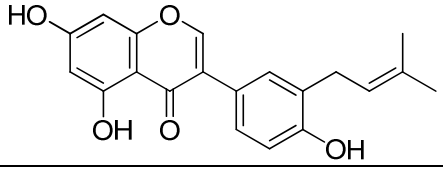	*Psoralea corylifolia*	known
7,2′,4′-Trihydroxy-3-arylc oumarin (**52**)	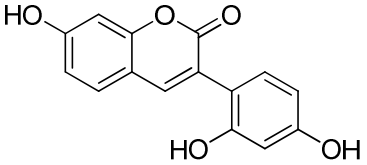	*Psoralea corylifolia*	new
Psoralidin (**53**)	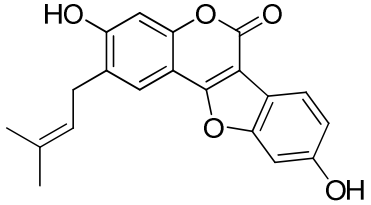	*Psoralea corylifolia*	known
Psoracoumestan (**54**)	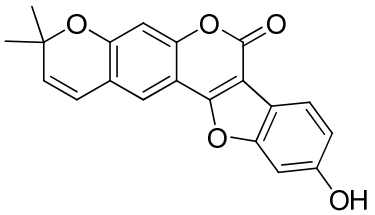	*Psoralea corylifolia*	new
Bakuchiol (**55**)	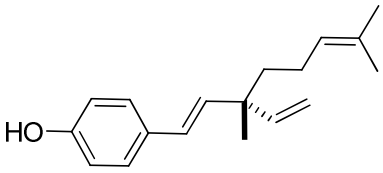	*Psoralea corylifolia*	known

6. References

Aratanechemuge, Y., Hibasami, H., Sanpin, K., Katsuzaki, H., Imai, K. and Komiya, T. (2004). Induction of apoptosis by lupeol isolated from mokumen (Gossampinus malabarica L. Merr) in human promyelotic leukemia HL-60 cells. *Oncol Rep*, **11**(2), 289-292.

Baba, K., Nakata, K., Taniguchi, M., Kido, T. and Kozawa, M. (1990). Chalcones from *Angelica keiskei*. *Phytochemistry*, **29**(12), 3907-3910.

Baur, J. A. and Sinclair, D. A. (2006). Therapeutic potential of resveratrol: the in vivo evidence. *Nat Rev Drug Discov*, **5**(6), 493-506.

Boguslavskaya, L. I., Dem'yanenko, S. I., Salam, D. K. and Soboleva, V. A. (1983). C-glycosides of *Dianthus versicolor*. *Chemistry of Natural Compounds*, **19**(6), 746-747.

Boldsaikhan, B. (2004). Encyclopedia of Mongolian medicinal plants. Ulaanbaatar, Mongolian University of Science & Technology, System Science Research Institute.

Bravo, L. (1998). Polyphenols: chemistry, dietary sources, metabolism, and nutritional significance. *Nutr Rev*, **56**(11), 317-333.

Bryanskii, O. V., Tolstikhina, V. V. and Semenov, A. A. (1992). A glycoside of syringaresinol from a tissue culture of Scorsonera hispanica. *Chemistry of Natural Compounds*, **25**(5), 519-520.

Bryanskii, O. V., Tolstikhina, V. V., Zinchenko, S. V. and Semenov, A. A. (1992). A sesquiterpene glucoside from cultivated cells of Scorzonera hispanica. *Chemistry of Natural Compounds*, **28**(6), 556-560.

Butler, M. S. (2004). The role of natural product chemistry in drug discovery. *J Nat Prod*, **67**(12), 2141-2153.

Carmichael, J., DeGraff, W. G., Gazdar, A. F., Minna, J. D. and Mitchell, J. B. (1987). Evaluation of a tetrazolium-based semiautomated colorimetric assay: assessment of radiosensitivity. *Cancer Res*, **47**(4), 943-946.

Carnat, A. P., Carnat, A., Fraisse, D., Lamaison, J. L., Heitz, A., Wylde, R. and Teulade, J. C. (1998). Violarvensin, a new flavone di-C-glycoside from Viola arvensis. *J Nat Prod*, **61**(2), 272-274.

Clark, A. M. (1996). Natural products as a resource for new drugs. *Pharm Res*, **13**(8), 1133-1144.

Clayden, J., Greeves, N., Warren, S. and Wothers, P. (2001). Organic Chemistry. Oxford, Oxford University Press.

Clifford, M. N. (1999). Chlorogenic acids and other cinnamates - nature, occurrence and dietary burden. *Journal of the Science of Food and Agriculture*, **79**(3), 362 - 372.

Cragg, G. M., Boyd, M. R., Cardellina II, J. H., Newman, D. J., Snader, K. M. and McCloud, T. G. (1994). Ethnobotany and the Search for New Drugs. Symposium proceedings. Fortaleza, Brazil, 30 November-2 December 1993. *Ciba Found Symp*, **185**, 1-280.

Cragg, G. M., Newman, D. J. and Snader, K. M. (1997). Natural products in drug discovery and development. *J Nat Prod*, **60**(1), 52-60.

D'Archivio, M., Filesi, C., Di Benedetto, R., Gargiulo, R., Giovannini, C. and Masella, R. (2007). Polyphenols, dietary sources and bioavailability. *Ann Ist Super Sanita*, **43**(4), 348-361.

Delmas, D., Lancon, A., Colin, D., Jannin, B. and Latruffe, N. (2006). Resveratrol as a chemopreventive agent: a promising molecule for fighting cancer. *Curr Drug Targets*, **7**(4), 423-442.

Dewick, P. M. (2001). Medicinal Natural Products a Biosynthetic Approach. Chichester, John Wiley & Sons.

Ding, L. S., Liang, Q. L. and Teng, Y. F. (1997). [Study on flavonoids in seeds of Hovenia dulcis]. *Yao Xue Xue Bao*, **32**(8), 600-602.

Dixon, R. A. (2001). Natural products and plant disease resistance. *Nature*, **411**, 843-847.

Dixon, R. A., Achnine, L., Kota, P., Liu, C., Reddy, M. S. S. and Wang, L. (2002). The phenylpropanoid pathway and plant defence—a genomics perspective. *Molecular Plant Pathology*, **3**(5), 371 - 390.

Dixon, R. A. and Paiva, N. L. (1995). Stress-Induced Phenylpropanoid Metabolism. *Plant Cell*, **7**, 1085–1097.

Eliel, E. L. and Ramirez, M. B. (1997). (-)-Quinic acid: configurational (stereochemical) descriptors. *Tetrahedron: Asymmetry*, **8**(21), 3551-3554.

ElSohly, H. N., Joshi, A. S., Nimrod, A. C., Walker, L. A. and Clark, A. M. (2001). Antifungal chalcones from Maclura tinctoria. *Planta Med*, **67**(1), 87-89.

Farnsworth, N. R., Akerele, O., Bingel, A. S., Soejarto, D. D. and Guo, Z. (1985). Medicinal plants in therapy. *Bull World Health Organ*, **63**(6), 965-981.

Flores-Parra, A., Gutiérrez-Avella, D. M., Contreras, R. and Khuong-Huu, F. (1989). ^{13}C and ^{1}H NMR investigations of quinic acid derivatives: Complete spectral assignment and elucidation of preferred conformations. *Magnetic Resonance in Chemistry*, **27**(6), 544 - 555.

Geetha, T. and Varalakshmi, P. (2001). Anti-inflammatory activity of lupeol and lupeol linoleate in rats. *J Ethnopharmacol*, **76**(1), 77-80.

Grubov, V. I. (1982). Key to the Vascular Plants of Mongolia. Leningrad, Nauka.

Grubov, V. I. (2001). Key to the vascular plants of Mongolia. Enfield (NH), USA, Science Publishers, Inc.

Gubanov, I. A. (1996). Conspectus of Flora of Outer Mongolia (Vascular Plants). Moscow, Valang Publ.

Gubanov, I. A. (1996). The conspectus of flora outer Mongolia (Vascular plants). Moscow, Valang.

Gupta, G. K., Suri, J. L., Gupta, B. K. and Dhar, K. L. (1982). Bakuchalcone, a dihydrofuranochalcone from the seeds of *Psoralea corylifolia*. *Phytochemistry*, **21**(8), 2149-2151.

Hakamatsuka, T., Ebizuka, Y. and Sankawa, U. (1991). Induced Isoflavonoids from Copper Chloride-treated Stems of *Pueraria lobata*. *Phytochemistry*, **30**(5), 1481-1482.

Harborne, J. B. and Williams, C. A. (2000). Advances in flavonoid research since 1992. *Phytochemistry*, **55**(6), 481-504.

Hasmeda, M., Kweifio-Okai, G., Macrides, T. and Polya, G. M. (1999). Selective inhibition of eukaryote protein kinases by anti-inflammatory triterpenoids. *Planta Med*, **65**(1), 14-18.

He, X. L. (2004). Study on the genus *Scorzonera* L. from China. *Journal of Hebei University (Natural Science Edition)*, **24**(1), 65 - 73.

Hesse, M., Meier, H. and Zeeh, B. (1997). Spectroscopic Methods in Organic Chemistry. Stuttgart, Georg Thieme Verlag.

Hikino, H., Ohsawa, T., Kiso, Y. and Oshima, Y. (1984). Analgesic and antihepatotoxic actions of dianosides, triterpenoid saponins of Dianthus superbus var. longicalycinus herbs. *Planta Med*, **50**(4), 353-355.

Hodges, L. D., Kweifio-Okai, G. and Macrides, T. A. (2003). Antiprotease effect of anti-inflammatory lupeol esters. *Mol Cell Biochem*, **252**(1-2), 97-101.

Jeong, S. H., Han, X. H., Hong, S. S., Hwang, J. S., Hwang, J. H., Lee, D., Lee, M. K., Ro, J. S. and Hwang, B. Y. (2006). Monoamine oxidase inhibitory coumarins from the aerial parts of Dictamnus albus. *Arch Pharm Res*, **29**(12), 1119-1124.

Kametani, S., Kojima-Yuasa, A., Kikuzaki, H., Kennedy, D. O., Honzawa, M. and Matsui-Yuasa, I. (2007). Chemical constituents of cape aloe and their synergistic growth-inhibiting effect on Ehrlich ascites tumor cells. *Biosci Biotechnol Biochem*, **71**(5), 1220-1229.

Kang, K., Lee, H. J., Kim, C. Y., Lee, S. B., Tunsag, J., Batsuren, D. and Nho, C. W. (2007). The chemopreventive effects of Saussurea salicifolia through induction of apoptosis and phase II detoxification enzyme. *Biol Pharm Bull*, **30**(12), 2352-2359.

Karikas, G. A., Euerby, M. R. and Waigh, R. D. (1987). Isolation of Piceoside from Arctostaphylos uva-ursi. *Planta Med*, **53**(3), 307-308.

Khalifa, T. I., Muhtadi, F. J. and Hassan, M. M. A. (1983). Rutin. *Analytical profiles of drug substances*, **12**, 623-639.

Khalil, A. T., Chang, F. R., Lee, Y. H., Chen, C. Y., Liaw, C. C., Ramesh, P., Yuan, S. S. and Wu, Y. C. (2003). Chemical constituents from the Hydrangea chinensis. *Arch Pharm Res*, **26**(1), 15-20.

Kim, H. J. and Lee, Y. S. (2005). Identification of new dicaffeoylquinic acids from Chrysanthemum morifolium and their antioxidant activities. *Planta Med*, **71**(9), 871-876.

Kinghorn, A. D. (2001). Pharmacognosy in the 21st century. *J Pharm Pharmacol*, **53**(2), 135-148.

Kinoshita, T., Ichinose, K., Takahashi, C., Ho, F. C., Wu, J. B. and Sankawa, U. (1990). Chemical Studies on Sophora tomentosa: the Isolation of a New Class of Isoflavonoid. *Chem Pharm Bull (Tokyo)*, **38**(10), 2756-2759.

KLETTER, C., GLASL, S., THALHAMMER, T. and NARANTUYA, S. (2008). Traditional Mongolian Medicine - A Potential for Drug Discovery. *Sci. Pharm.*, **76**(1), 49 - 63.

Kojima, H., Sato, N., Hatano, A. and Ogura, H. (1990). Sterol glucosides from *Prunella vulgaris*. *Phytochemistry*, **29**(7), 2351-2355.

Komatsu, M., Yokoe, I. and Shirataki, Y. (1981). Studies on the Constituents of *Sophora* Species. XIV. Constituents of the Root of *Sophora franchetiana* Dunn (1) *Chem Pharm Bull (Tokyo)*, **29**(2), 532-538.

Kong, J. M., Goh, N. K., Chia, L. S. and Chia, T. F. (2003). Recent advances in traditional plant drugs and orchids. *Acta Pharmacol Sin*, **24**(1), 7-21.

Kuć, J. (1995). Phytoalexins, Stress Metabolism, and Disease Resistance in Plants. *Annual Review of Phytopathology*, **33**, 275-297.

Kumazawa, T., Minatogawa, T., Matsuba, S., Sato, S. and Onodera, J. (2000). An effective synthesis of isoorientin: the regioselective synthesis of a 6-C-glucosylflavone. *Carbohydr Res*, **329**(3),

507-513.

Labbe, C., Faini, F., Coll, J. and Connolly, J. D. (1996). Bakuchiol Derivatives from the leaves of *Psoralea glandulosa*. *Phytochemistry*, **42**(5), 1299-1303.

Lee, M. H., Kim, J. Y. and Ryu, J. H. (2005). Prenylflavones from Psoralea corylifolia inhibit nitric oxide synthase expression through the inhibition of I-kappaB-alpha degradation in activated microglial cells. *Biol Pharm Bull*, **28**(12), 2253-2257.

Leopoldini, M., Pitarch, I. P., Russo, N. and Toscano, M. (2004). Structure, Conformation, and Electronic Properties of Apigenin, Luteolin, and Taxifolin Antioxidants. A First Principle Theoretical Study. *J. Phys. Chem. A*, **108**, 92-96.

Li, H., Koike, K. and Ohmoto, T. (1993). Dianchinenosides A and B, two new saponins from *Dianthus chinensis*. *J Nat Prod*, **56**(7), 1065-1070.

Li, H., Koike, K. and Ohmoto, T. (1994). Triterpenoid saponins from *Dianthus chinensis*. *Phytochemistry*, **35**(3), 751-756.

Li, J., Wu, Q. X., Shi, Y. P. and Zhu, Y. (2004). A new sesquiterpene lactone from *scorzonera austriaca*. *Chin. Chem. Lett.*, **15**(11), 1309-1310.

Ligaa, U. (1994). Medicinal plants of Mongolia used in Mongolian traditional medicine. Korea, KCA Press.

Ligaa, U. (1996). The Medicinal Plants from Mongolia Used in Mongolian Traditional Medicine. Ulaanbaatar, KSA Press.

Lin, L. C., Kuo, Y. C. and Chou, C. J. (1999). Immunomodulatory principles of Dichrocephala bicolor. *J Nat Prod*, **62**(3), 405-408.

Liu, G. X., Zhao, Y. Z., Liu, L. H. and Liu, D. Q. (2002). Analysis of floral ecological and geographical distribution of *scorzonera* genus in the Mongolian plateau. *Acta Prataculturae Sin*, **11**(2), 37-44.

Liu, G. X., ZHao, Y. Z. and Xu, J. (2001). Study on Classification and Ecology Geographical Distribution of Plants from the Genus *Scorzonera* in the Mongolian Plateau. *Grassland of China*, **23**(2), 12 - 18.

Liu, J. K. (2000). Prospect of the development of new natural drugs as foreshadowed by the R & D of the world 20 leading pharmaceutical corporations. *Chin Tradit Herb Drugs*, **31**(7), 481-487.

Lu, Y., Sun, Y., Foo, L. Y., McNabb, W. C. and Molan, A. L. (2000). Phenolic glycosides of forage legume Onobrychis viciifolia. *Phytochemistry*, **55**(1), 67-75.

Ma, L., Gu, Y. C., Luo, J. G., Wang, J. S., Huang, X. F. and Kong, L. Y. (2009). Triterpenoid Saponins from Dianthus versicolor. *J Nat Prod*.

Mabberley, D. J. (1997). The plant book (a portable dictionary of the vascular plants). Cambridge, Cambridge University Press

MacLeod, G. and Ames, J. M. (1991). Gas chromatography-mass spectrometry of the volatile components of cooked scorzonera. *Phytochemistry*, **30**(3), 883-888.

Malyschev, L. I. and Peschkova, G. A. (1979). Central sibirian flora novosibisk: Aedibs. Nauka Divisid Sibirica.

Manach, C., Scalbert, A., Morand, C., Remesy, C. and Jimenez, L. (2004). Polyphenols: food sources and bioavailability. *Am J Clin Nutr*, **79**(5), 727-747.

Marrugat, J., Covas, M. I., Fito, M., Schroder, H., Miro-Casas, E., Gimeno, E., Lopez-Sabater, M. C., de la Torre, R. and Farre, M. (2004). Effects of differing phenolic content in dietary olive oils on lipids and LDL oxidation--a randomized controlled trial. *Eur J Nutr*, **43**(3), 140-147.

Matsumoto, T., Hosono-Nishiyama, K. and Yamada, H. (2006). Antiproliferative and apoptotic effects of butyrolactone lignans from Arctium lappa on leukemic cells. *Planta Med*, **72**(3), 276-278.

Menichini, F., di Benedetto, R. and Delle Monache, F. (1996). A triterpene epoxide and a guaianolide from *Ptilostemmon gnaphaloides*. *Phytochemistry*, **41**(5), 1377-1379.

Menichini, F., Statti, G. and Delle, M. F. (1994). Flavonoid glycosides from Scorzonera columnae. *Fitoterapia*, **65**(6), 555-556.

Michels, G., Watjen, W., Weber, N., Niering, P., Chovolou, Y., Kampkotter, A., Proksch, P. and Kahl, R. (2006). Resveratrol induces apoptotic cell death in rat H4IIE hepatoma cells but necrosis in C6 glioma cells. *Toxicology*, **225**(2-3), 173-182.

Mosmann, T. (1983). Rapid colorimetric assay for cellular growth and survival: application to proliferation and cytotoxicity assays. *J Immunol Methods*, **65**(1-2), 55-63.

Newman, D. J., Cragg, G. M. and Snader, K. M. (2000). The influence of natural products upon drug discovery. *Nat Prod Rep*, **17**(3), 215-234.

Nkengfack, A. E., Kouam, J., Vouffo, T. W., Meyer, M., Tempesta, M. S. and Fomum, Z. T. (1994). An isoflavanone and a coumestan from *Erythrina sigmoidea*. *Phytochemistry*, **35**(2), 521-526.

Öksüz, S., Gören, N. and Ulubelen, A. (1990). Terpenoids from Scorzonera tomentosa. *Fitoterapia*,

61(1), 92-93

Ordoudi, S. A., Tsimidou, M. Z., Vafiadis, A. P. and Bakalbassis, E. G. (2006). Structure-DPPH* scavenging activity relationships: parallel study of catechol and guaiacol acid derivatives. *J Agric Food Chem*, **54**(16), 5763-5768.

Paraschos, S., Magiatis, P., Kalpoutzakis, E., Harvala, C. and Skaltsounis, A. L. (2001). Three new dihydroisocoumarins from the Greek endemic species Scorzonera cretica. *J Nat Prod*, **64**(12), 1585-1587.

Pauli, G. F., Poetsch, F. and Nahrstedt, A. (1998). Structure assignment of natural quinic acid derivatives using proton nuclear magnetic resonance techniques. *Phytochemical Analysis*, **9**(4), 177-185.

Pegnyemb, D. E., Messanga, B. B., Ghogomu, R., Sondengam, B. L., Martin, M. T. and Bodo, B. (1998). A new benzoylglucoside and a new prenylated isoflavone from lophira lanceolata. *J Nat Prod*, **61**(6), 801-803.

Perry, N. B., Benn, M. H., Foster, L. M., Routledge, A. and Weavers, R. T. (1996). The glycosidic precursor of (Z)-5-ethylidene-2(5H)-furanone in Halocarpus biformis juvenile foliage. *Phytochemistry*, **42**(2), 453-459.

Pezzuto, J. M. (1997). Plant-derived anticancer agents. *Biochem Pharmacol*, **53**(2), 121-133.

Pistelli, L., Spera, K., Flamini, G., Mele, S. and Morelli, I. (1996). Isoflavonoids and chalcones from *Anthyllis hermanniae*. *Phytochemistry*, **42**(5), 1455-1458.

Pouchert, C. (1992). Aldrich Library of ^{13}C and ^{1}H FT NMR Spectra, John Wiley & Sons.

Re, R., Pellegrini, N., Proteggente, A., Pannala, A., Yang, M. and Rice-Evans, C. (1999). Antioxidant activity applying an improved ABTS radical cation decolorization assay. *Free Radic Biol Med*, **26**(9-10), 1231-1237.

Reynolds, W. F., McLean, S. and Poplawski, J. (1986). Total Assignment of ^{13}C and ^{1}H Spectra of Three Isomeric Triterpenol Derivatives by 2D NMR: An Investigation of the Potential Utility of ^{1}H Chemical Shifts in Structural Investigations of Complex Natural Products. *Tetrahedron*, **42**(13), 3419-3428.

Rice-Evans, C. A., Miller, N. J. and Paganga, G. (1996). Structure-antioxidant activity relationships of flavonoids and phenolic acids. *Free Radic Biol Med*, **20**(7), 933-956.

Roupe, K. A., Remsberg, C. M., Yanez, J. A. and Davies, N. M. (2006). Pharmacometrics of stilbenes: seguing towards the clinic. *Curr Clin Pharmacol*, **1**(1), 81-101.

Rowland, I., Faughnan, M., Hoey, L., Wahala, K., Williamson, G. and Cassidy, A. (2003). Bioavailability of phyto-oestrogens. *Br J Nutr*, **89 Suppl 1**, S45-58.

Saleem, M., Afaq, F., Adhami, V. M. and Mukhtar, H. (2004). Lupeol modulates NF-kappaB and PI3K/Akt pathways and inhibits skin cancer in CD-1 mice. *Oncogene*, **23**(30), 5203-5214.

Saleem, M., Kim, H. J., Ali, M. S. and Lee, Y. S. (2005). An update on bioactive plant lignans. *Nat Prod Rep*, **22**(6), 696-716.

Saleem, M., Kweon, M. H., Yun, J. M., Adhami, V. M., Khan, N., Syed, D. N. and Mukhtar, H. (2005). A novel dietary triterpene Lupeol induces fas-mediated apoptotic death of androgen-sensitive prostate cancer cells and inhibits tumor growth in a xenograft model. *Cancer Res*, **65**(23), 11203-11213.

Samuelsson, G. (2004). Drugs of Natural Origin: a Textbook of Pharmacognosy, 5th. Stockholm, Swedish Pharmaceutical Press.

Sancher, C., Batkhuu, J. and Komatsu, K. (2003). Picture handbook of useful plants from Mongolia. Ulaanbaatar, KSA Press.

Sandermann Jr, H. (2004). Molecular ecotoxicology of plants. *Trends in Plant Science*, **9**(8), 406.

Sari, A., Zidorn, C., Ellmerer, E. P., Özgökçe, F., Ongania, K. H. and Stuppner, H. (2007). Phenolic Compounds from *Scorzonera tomentosa* L. *Helvetica Chimica Acta*, **90**(2), 311-317.

Saxena, V. K. and Bhadoria, B. K. (1990). 3'-prenyl-4'-methoxy-isoflavone-7-O-beta-D-(2"-O-p-coumaroyl) glucopyranoside, a novel phytoestrogen from Sopubia delphinifolia. *J Nat Prod*, **53**(1), 62-65.

Scalbert, A., Manach, C., Morand, C., Remesy, C. and Jimenez, L. (2005). Dietary polyphenols and the prevention of diseases. *Crit Rev Food Sci Nutr*, **45**(4), 287-306.

Scott, K. N. (1970). NMR parameters of biologically important aromatic acids I. benzoic acid and derivatives. *journal of magnetic resonance*, **2**, 361-376.

Slimestad, R., Fossen, T. and Verheul, M. J. (2008). The flavonoids of tomatoes. *J Agric Food Chem*, **56**(7), 2436-2441.

Solecka, D. (1997). Role of phenylpropanoid compounds in plant responses to different stress factors. *Acta Physiologiae Plantarum*, **19**(3), 257-268.

Stevens, J. F., Ivancic, M., Hsu, V. L. and Deinzer, M. L. (1997). Prenylflavonoids from *Humulus lupulus*. *Phytochemistry*, **44**(8), 1575-1585.

Tanaka, T., Iinuma, M., Asai, F., Ohyama, M. and Burandt, C. (1997). Flavonoids from The Root and Stem of Sophora tomentosa. *Phytochemistry*, **46**(8), 1431-1437.

Tolstikhina, V. V., Bryanskii, O. V., Syrchina, A. I. and Semenov, A. A. (1988). Chemical composition of a culture of tissue of Scorzonera hispanica. *Chemistry of Natural Compounds*, **24**(5), 655.

Tolstikhina, V. V. and Semenov, A. A. (1998). Minor metabolites of Scorzonera hispanica L. cell culture. *Rastitel'nye Resursy*, **34**(2), 77-80.

Tolstikhina, V. V., Semenov, A. A. and Ushakov, I. A. (1999). Minor furofuranoid lignans from cultivated cells of Scorzonera hispanica L. *Rastitel'nye Resursy*, **35**(1), 87-90.

Tomczyk, M., Gudej, J. and Sochacki, M. (2002). Flavonoids from Ficaria verna Huds. *Z Naturforsch [C]*, **57**(5-6), 440-444.

Tsevegsuren, N., Edrada, R., Lin, W., Ebel, R., Torre, C., Ortlepp, S., Wray, V. and Proksch, P. (2007). Biologically active natural products from Mongolian medicinal plants Scorzonera divaricata and Scorzonera pseudodivaricata. *J Nat Prod*, **70**(6), 962-967.

Tulin, T. G., Heywood, V. H., Burges, N. A., Moore, D. M., Valentine, D. H., Walters, S. M. and Webb, D. A. (1976). Flora Europaea. London, Cambridge University Press.

Ververidis, F., Trantas, E., Douglas, C., Vollmer, G., Kretzschmar, G. and Panopoulos, N. (2007). Biotechnology of flavonoids and other phenylpropanoid-derived natural products. Part I: Chemical diversity, impacts on plant biology and human health. *Biotechnol J*, **2**(10), 1214-1234.

Wada, S. I., Iida, A. and Tanaka, R. (2001). Triterpene constituents from the stem bark of Pinus luchuensis and their DNA topoisomerase II inhibitory effect. *Planta Med*, **67**(7), 659-664.

Wald, B., Wray, V., Galensa, R. and Herrmann, K. (1989). Malonated Flavonol Glycosides and 3,5-Dicaffeoylquinic acid from pears. *Phytochemistry*, **28**(2), 663-664.

Wall, M. E., Wani, M. C., Cook, C. E., Palmer, K. H., McPhail, A. T. and Sim, G. A. (1966). Plant Antitumor Agents. I. The Isolation and Structure of Camptothecin, a Novel Alkaloidal Leukemia and Tumor Inhibitor from *Camptotheca acuminata*. *J Am Chem Soc*, **88**(16), 3888 - 3890.

Wang, J., Shen, Y., He, H., Kang, W. and Hao, X. (2005). Norsesquiterpenoid and sesquiterpenoid glycosides from Evodia austrosinensis. *Planta Med*, **71**(1), 96-98.

Wang, Y., Edrada-Ebel, R., Tsevegsuren, N., Sendker, J., Braun, M., Wray, V., Lin, W. and Proksch, P. (2009). Dihydrostilbene derivatives from the Mongolian medicinal plant Scorzonera radiata. *J Nat Prod*, **72**(4), 671-675.

Worden, R. L., Savada, A. M. and Division, L. o. C. F. R. (1991). Mongolia: A Country Study (Area Handbook Series), Claitor's Law Books and Publishing Division.

Wright, J. S., Johnson, E. R. and DiLabio, G. A. (2001). Predicting the activity of phenolic antioxidants: theoretical method, analysis of substituent effects, and application to major families of antioxidants. *J Am Chem Soc*, **123**(6), 1173-1183.

Xie, L. H., Ahn, E. M., Akao, T., Abdel-Hafez, A. A., Nakamura, N. and Hattori, M. (2003). Transformation of arctiin to estrogenic and antiestrogenic substances by human intestinal bacteria. *Chem Pharm Bull (Tokyo)*, **51**(4), 378-384.

Yamamoto, Y. and Gaynor, R. B. (2001). Therapeutic potential of inhibition of the NF-kappaB pathway in the treatment of inflammation and cancer. *J Clin Invest*, **107**(2), 135-142.

Yang, Y. M., Hyun, J. W., Sung, M. S., Chung, H. S., Kim, B. K., Paik, W. H., Kang, S. S. and Park, J. G. (1996). The cytotoxicity of psoralidin from Psoralea corylifolia. *Planta Med*, **62**(4), 353-354.

Yin, S., Fan, C. Q., Wang, Y., Dong, L. and Yue, J. M. (2004). Antibacterial prenylflavone derivatives from Psoralea corylifolia, and their structure-activity relationship study. *Bioorg Med Chem*, **12**(16), 4387-4392.

You, Y. J., Nam, N. H., Kim, Y., Bae, K. H. and Ahn, B. Z. (2003). Antiangiogenic activity of lupeol from Bombax ceiba. *Phytother Res*, **17**(4), 341-344.

Youssef, D. and Frahm, A. W. (1995). Constituents of the Egyptian Centaurea scoparia. III. Phenolic constituents of the aerial parts. *Planta Med*, **61**(6), 570-573.

Yu, Q., Matsunami, K., Otsuka, H. and Takeda, Y. (2005). Staphylionosides A-K: megastigmane glucosides from the leaves of Staphylea bumalda DC. *Chem Pharm Bull (Tokyo)*, **53**(7), 800-807.

Zhang, W. D., Tam, H. T., Chen, W. S., Kong, D. Y., Li, H. T., Wang, Y. H. and Fouraste, I. (2000). Two new caffeoyl conjugation from Erigeron breviscapus. *J Asian Nat Prod Res*, **2**(4), 283-288.

Zidorn, C., Ellmerer-Müller, E. P. and Stuppner, H. (2000). Tyrolobibenzyls - Novel Secondary Metabolites from *Scorzonera humilis*. *Helvetica Chimica Acta*, **83**(11), 2920 - 2925.

Zidorn, C., Ellmerer-Muller, E. P. and Stuppner, H. (2000). Sesquiterpenoids from Scorzonera hispanica L. *Pharmazie*, **55**(7), 550-551.

Zidorn, C., Ellmerer, E. P., Sturm, S. and Stuppner, H. (2003). Tyrolobibenzyls E and F from Scorzonera humilis and distribution of caffeic acid derivatives, lignans and tyrolobibenzyls in European taxa of the subtribe Scorzonerinae (Lactuceae, Asteraceae). *Phytochemistry*, **63**(1), 61-67.

Zidorn, C., Petersen, B. O., Udovičić, V., Larsen, T. O., Duus, J. Ø., Rollinger, J. M., Ongania, K. H., Ellmerer, E. P. and Stuppner, H. (2005). Podospermic acid, 1,3,5-tri-O-(7,8-dihydrocaffeoyl)quinic acid from *Podospermum laciniatum* (Asteraceae). *Tetrahedron Letters*, **46**(8), 1291-1294.

Zidorn, C., Spitaler, R., Ellmerer-Muller, E. P., Perry, N. B., Gerhauser, C. and Stuppner, H. (2002). Structure of tyrolobibenzyl D and biological activity of tyrolobibenzyls from Scorzonera humilis. *Z Naturforsch [C]*, **57**(7-8), 614-619.

7. Abbreviations

$[\alpha]_D$	specific rotation at the sodium D-line
approx.	approximately
ASDSA	aglycone of scorzodihydrostilbene A
br	broad signal
CC	column chromatography
CoA	coenzyme A
COSY	correlation spectroscopy
d	doublet
DAD-HPLC	HPLC with diodenarray detector
dd	double of doublets
ddd	double double of doublets
DEPT	distortionless enhancement by polarization transfer
DMSO	dimethyl sulphoxide
DNA	deoxyribonucleic acid
DPPH	2,2-diphenyl-1-picrylhydrazyl
EC_{50}	half maximal effective concentration
e.g.	*exempli gratia* (for the sake of example)
EI	electron impact
ESI	electro spray ionization
et al.	*et alia* (and others)
EtOAc	ethyl acetate
FBS	fetal bovine serum
FCS	fetal calf serum
g	gram
H_2O	water
HCO_2H	formic acid
HMBC	heteronuclear multiple bond connectivity
HMQC	heteronuclear multiple quantum coherence
HPLC	high performance liquid chromatography
HRMS	high resolution mass spectroscopy
Hz	hertz
IC_{50}	half maximal inhibitory concentration
LC-MS	liquid chromatography-mass spectrometer
LDH	lactate dehydrogenase
M	molarity
m	multiplet
MeOD	deuterated methanol
MeOH	methanol
mg	milligram
MHz	megahertz
min	minute

mL	millilitre
MS	mass spectroscopy
MTT	3-(4,5-dimethylthiazol-2-yl)-2,5-diphenyltetrazolium bromide
m/*z*	mass per charge
μg	microgram
μL	microliter
MW	molecular weight
NADPH	nicotinamide adenine dinucleotide phosphate
n-BuOH	n-butanol
n.d.	not determined
NF-κB	nuclear factor kappa-light-chain-enhancer of activated B cells
ng	nanogram
nm	nanometer
NMR	nuclear magnetic resonance
NOE	Nuclear Overhauser Effect
ppm	part per million
q	quartet
ROESY	rotating frame overhauser enhancement spectroscopy
RP	reversed phase
s	singlet
SAM	S-adenosyl methionine
SDSA	scorzodihydrostilbene A
SEAP	pNF-κB-secreted embryonic alkaline phosphatase
Si	silica
t	triplet
TEAC	TROLOX equivalent antioxidative capacity
TFA	trifluoroacetic acid
TLC	thin layer chromatography
TNF	tumor necrosis factor
TOCSY	total correlation spectroscopy
UV	ultra-violet

Curriculum Vitae

Name:	Yao Wang
Date of birth:	18th March 1980
Nationality:	Chinese
Gender:	Male
Marital status:	Single
E-mail address:	wziyao@yahoo.com

Education

09/2005–07/2009	PhD in natural product chemistry Institute of Pharmaceutical Biology and Biotechnology, Heinrich-Heine University Düsseldorf, Germany
04/2005–08/2005	Practical study in marine natural products State Key Laboratory of Natural and Biomimetic Drugs, Peking University, P. R. China
08/2003–12/2004	Master of science in drug chemistry School of Chemistry, Newcastle University, United Kingdom
09/1998–07/2002	Bachelor of Engineering in Pharmacy School of Pharmacy, Wuhan Institute of Technology, P. R. China

Publication

- Wang, Y.; Edrada-Ebel, R.; Tsevegsuren, N.; Sendker, J.; Braun, M.; Wray, V.; Lin, W.; Proksch, P. *J. Nat. Prod.* **2009**, 72 (4), 671–675

- Liu, H.; Edrada-Ebel, R.; Ebel, R.; Wang, Y.; Schulz, B.; Draeger, S.; Müller, W. E. G.; Wray, V.; Lin, W.; Proksch, P. *J. Nat. Prod.* **2009** (published online)

- Wang, Y.; Edrada-Ebel, R.; Wray, V.; Sendker, J.; Duong, T. N.; Tsevegsuren, N.; Lin, W.; Proksch, P. *Phytochemistry* **2009** (submitted)

Conference

- Poster presentation in the 55th International Congress and Annual Meeting of the Society for Medicinal Plant Research, September 2007, Graz, Austria.

Working Experience

02/2008–06/2009	Research on active agents from marine microorganisms Bio-Mar GbR, Düsseldorf, Germany